

The copyright of this thesis vests in the author. No quotation from it or information derived from it is to be published without full acknowledgement of the source. The thesis is to be used for private study or non-commercial research purposes only.

Published by the University of Cape Town (UCT) in terms of the non-exclusive license granted to UCT by the author.

9

**BIRDS, MOLECULES, AND EVOLUTIONARY PATTERNS  
AMONG AFRICA'S ISLANDS IN THE SKY**

**Rauri Charles Kerr Bowie**

Thesis presented for the degree of

**DOCTOR OF PHILOSOPHY**

In the Percy FitzPatrick Institute of African Ornithology,

Department of Zoology,

UNIVERSITY OF CAPE TOWN

**Supervised by:**

*Associate Professor Timothy M. Crowe*

Percy FitzPatrick Institute, University of Cape Town

**Co-supervised by:**

*Professor Jon Fjeldså*

Zoological Museum, University of Copenhagen, Copenhagen

*Dr Shannon J. Hackett*

Field Museum of Natural History, Chicago

June 2003

**Declaration:****BIRDS, MOLECULES AND, EVOLUTIONARY PATTERNS AMONG  
AFRICA'S ISLANDS IN THE SKY****Candidate:**

Rauri Charles Kerr Bowie

I hereby,

- a) grant the University of Cape Town free license to reproduce the above thesis in whole or in part, for the purpose of research;
- b) declare that:
  - i) the above thesis is my own unaided work, both in concept and execution and that apart from the normal guidance of my supervisors, I have received no assistance except stated below:

Dr Paulette Bloomer kindly provided the cytochrome-b data used within Chapter 6 and, the late Dr Phillip Clancey summarized the morphological data presented in Table 1 of Chapter 6.

- ii) neither the substance nor any part of the above thesis has been submitted in the past, or is being submitted for a degree in the University or any other university

The thesis is presented by me for examination for the degree of PhD.

Signed by candidate
---------------------

Rauri C. K. Bowie

Date 25-01-2003

**This thesis is dedicated to my grandfather Desmond Bowie who would have been proud, to my family and grandparents whom are proud and just a little relieved, and to Verna who is proud, but mostly relieved. And to myself, who is just relieved.**

University of Cape Town



**“To look is something,  
To see what you look at is another,  
To understand what you see is another,  
To learn from what you understand is something else,  
But to act on what you learn is what really matters”**

**- Winston Churchill**

## Acknowledgements

I am grateful to the Tanzania Commission for Science and Technology, Kenyan Wildlife Service, the Western Cape Nature Conservation Board (South Africa), and the respective Wildlife Boards of Uganda, Malawi, Mozambique, Zambia and Zimbabwe for permission to collect and export specimens. I thank, in no particular order: David Moyer, Jacob Kiure, Malcolm Wilson, Peter Ryan, Steven Wamiti, Bernard Chege, Patrick Guichugi, Luca Borghesio, Matim de Melo, Luc Lens, Tom Smith, Collin Jackson, David Willard, Tom Gnoske, Steve Goodman, Ben Marks, Callan Cohen, Marc Herremans, Ben Warren, Pamela Beresford, Jon Fjelds  and Noam Leader for their help with collecting specimens. The American Museum of Natural History, Field Museum of Natural History, Natural History Museum of Louisiana State University, Museum of Zoology at the University of Michigan, Museum Victoria, Academy of Natural Sciences of Philadelphia, Zoological Museum of the University of Copenhagen, Barrick Museum at the University of Nevada Las Vegas and Museum National D'Histoire Naturelle are all thanked for providing tissues. I am grateful to the curators and collection managers at: The Museum of Natural History (Tring), Royal Museum for Central Africa, American Museum of Natural History, United States National Museums, National Museums of Kenya, Cincinnati Natural History Museum and the Durban Natural History Museum, for their help, interest and hospitality while visiting their collections. A very special note of thanks to all my friends and colleagues at the Field Museum of Natural History, both in the Zoology Department and the Pritzker Laboratory for Molecular Systematics - my visits were always a wonderful experience. Shannon and John, Gina and Jeff, I will always be in your debt and without your generosity in all matters, I would not where I am today. Please accept my deepest thanks. To everyone who has helped me over the years at UCT, too many of you to name, I sincerely thank you. A special thanks to Chris Tobler, Lionel Mansfield and Andrea Plos, who always did their best to solve my computer problems, as well as forward various documents to me in all kinds of strange places around the world. Peter Ryan, Phil Hockey, Pamela Beresford, Bob Cheke, Terry Oatley, Bryan Stuart, John Bates, Gary Voelker, Paulette Bloomer, Krystal Tolley, Claire Spottiswoode, Jose Tello and Luc Lens are thanked for commenting on various drafts of

chapters in this thesis. I thank the National Research Foundation (South Africa), the University of Cape Town Research Committee, the Danish Research Council, and the Skye Foundation and Charitable trust, for providing funding for this project. To Dr Neville Passmore, thank you for always being so patient with my often late reports and for all that you and the foundation have made possible. I thank my supervisors for letting me pursue my ideas and for always being willing to provide guidance when requested. A special thanks to my family and Verna, who never wavered in their support despite the long periods that I spent away from home. I am sure that I have forgotten many who deserve a special mention, if so, it was not intentional and I take this opportunity to wholeheartedly thank you for your help. Verna it is finally over! I promise!

University of Cape Town

## Abstract

One of the fundamental tenets of systematic biology is centred on gaining an understanding of how spatial distributions of populations relate to the process of speciation. Addressing this question is not easy, as exemplified by the debate on how divergence takes place in isolation. Two models have been proposed to explain how populations and ultimately species may form in allopatry: the vicariance model and dispersal. In recent years, the vicariance model has become the favoured alternative, with most biologists agreeing that it is necessary to first disprove vicariance before invoking dispersal. Yet, dispersal must take place because biotic assemblages do form on oceanic islands of volcanic origin. In addition, given the cyclical nature of many geological or climatological processes, accepting concordance in topologies between area-cladograms of two or more lineages as evidence that each lineage was temporally isolated by the same geographical or climatological barrier, i.e. vicariance, can be tenuous. Indeed, whereas taxa have single histories, areas can have multiple histories with respect to the component taxa of an area being considered. Thus, while there may be topological congruence in area-cladograms among several lineages that would suggest a shared history (vicariance), the temporal origins of these patterns may vary (dispersal or vicariance + dispersal).

One of the more puzzling features of African montane biogeography is that, despite the often-huge distances and unfavourable habitat between montane isolates, a large proportion of montane bird species reappear in even the most isolated forests. One of the great difficulties in trying to explain patterns of montane bird speciation in Africa has been to develop hypotheses that can adequately explain why some mountains or areas of endemism have taxa unique to them, whereas others share the same species, but different subspecies, and still others have for all intents and purpose the same species.

It is broadly accepted that during periods when the Northern Hemisphere was glaciated the African tropics became more arid, resulting in the reduction of montane and lowland forests. If forest bird communities have a history of fragmentation, how is the high number of avian taxa that are shared between disjunct montane groups explained? Diamond and Hamilton (1980) presented with this problem concluded that montane bird species that today show disjunct populations "have probably either flown from one area to the other or else once occurred in the intervening lowland forest". This presents one of the greatest

paradoxes of African biogeography as it seems extremely unlikely when we consider that nearly all studies of montane birds suggest limited dispersal and then mostly altitudinal, as well as natal philopatry. All putative montane refugia would have contained lowland forest, and therefore their associated avian communities, suggesting levels of completion between montane and lowland birds were not reduced.

Prigogine (1987) addressed this problem suggesting that, during wet periods, montane forest would have occurred at lower altitudes and gradually expanded to cover the tops of lower lying hills 600 to 900m above sea level. A number of montane isolates are connected by ancient fault lines or uplifted escarpments of lower lying hills. Following expansion of montane forest, characteristic montane species could have followed in a stepping-stone fashion. Later, with the onset of glacial conditions, the increased aridity would have caused the fragmentation and eventual disappearance of the forest corridors. Thus, previously widespread taxa became isolated within the different montane massifs they had reached. The central theme of Prigogine's models is that climatic fluctuations, especially recurrent glaciation periods over the last 3 million years have played an important role in the repeated fragmentation of the montane biome. Thus, the montane habitats of different mountains are likely to have experienced a complex pattern of fragmentation, ranging from being in contact with neighbours on a number of occasions to never having been directly in contact with other montane forest or afro-alpine vegetation.

Sunbirds are members of an Old World family (Nectariniidae) of small nectarivorous songbirds. Most species exhibit extreme plumage dimorphism with male sunbirds typically having bright metallic plumages. The family contains the largest genus (*Nectarinia*), which occurs throughout sub-Saharan Africa, the islands of the Indian Ocean, extending to Asia with one species reaching northern Australia. The highest species richness occurs within Africa, peaking in the montane highlands where up to 29 species can co-occur. Sunbirds thus provide an ideal model group with which to explore montane bird diversification patterns in Africa. The major disadvantage of using sunbirds as a model is that no robust phylogenetic hypothesis has been erected for the family, a necessity if monophyletic groups are to be delineated and thus appropriate biogeographical inferences made. To address this approximately 3000 bp of nucleotide data (mitochondrial and nuclear) was collected from 68 sunbird species representing 17 of the 18 currently recognised genera. Eleven to twelve

dispersal events were recovered using dispersal-variance analysis, with strong support for an Asian origin for the Nectariniidae, although at least one back-colonization from Africa to Asia, possibly via the Islands of the Indian Ocean has occurred more recently. With the exception of a back-colonization, dispersal events are restricted to within Asia or Africa, and a single vicariant origin for the African Nectariniidae is inferred. The resulting parsimony and Bayesian Inference topologies did not support recent taxonomic revisions of the Nectariniidae by Irwin (1999) or Cheke *et al.* 2001.

Based on the generated sunbird phylogeny, monophyletic lineages were selected with which to explore montane biogeography (Chapters 3-5 and 8). To test for hierarchical vicariance patterns in the context of historical biogeography, phylogeographic structure of two largely montane turdine species, the Olive Thrush, *Turdus olivaceus* (Chapters 6 and 7) and the Starred Robin, *Pogonocichla stellata* (Chapter 9) were also investigated. Results from these studies suggested that a number of taxa warranted elevation to full species status, and one newly discovered species of sunbird is described; *Nectarinia skyei* sp. nova. The validity of recognizing the Eastern Arc as a single area of endemism must be questioned given the significant genetic structure uncovered among diverse lineages of birds both in this thesis (Chapters 3 & 7), as well as by Mike Roy and co-authors for Greenbuls (Roy 1997, Roy *et al.* 1998, Roy *et al.* 2000). Consequently, the Eastern Arc is divided into four smaller areas of endemism, the northern Arc (Taita Hills, Pare and Usambara Mnts), the central Arc (Rubeho, Nguu and Nguru Mnts), the Uluguru Mnts and the southern Arc (Udzungwa Highlands), each of which has two or more endemic species restricted to them. Generating area-cladograms and estimating relative ages of divergence among adjacently distributed sister lineages suggests that most divergence took place well before the Pleistocene. Whereas, there is some spatial concordance among area-cladograms there is little temporal concordance between the times of divergence among sister taxa in adjacent areas; thus questioning the validity of a purely vicariance mechanism as an evolutionary model with which to explain montane bird distribution patterns in Africa.

The results of the population level analyses suggest that the ancestral ranges of the Starred Robin and Olive Sunbird were fragmented in response to aridification of Africa following the cooling of the Northern Hemisphere from about 2.8 myrs BP. With the retraction of the ice in the northern hemisphere, Africa entered a wetter phase in response to the greater influence of low-latitude

insolation forcing of the west and east African monsoons in relation to the Earth's Orbital precession. Increased precipitation may have provided the impetus for the more recently observed secondary contact between populations in the northern and south-central Eastern Arc, and between the Albertine Rift and Eastern Arc. Thus, even within species, there appears to be evidence of lineages being isolated in the same areas of endemism as uncovered for Double-collared Sunbirds (Chapters 3-5), the Olive Thrush (Chapter 7) as well as in Greenbuls (Roy 1997, Roy *et al.* 1998), but within a more recent temporal (Plio-Pleistocene) framework.

Combining results from phylogenetic and population level studies suggests that climatic cycling has had a profound influence on montane bird speciation in Africa. The results from this thesis suggest that there is deep genetic divergence between many clades (8-12%) of montane passerine birds in Africa, with some shallow divergence towards the tips (4-6%). For widespread species reciprocal monophyly has not been reached in some instances, but generally there is some support for the refuge idea that isolation (fragmentation) of montane forests has facilitated speciation. However, most speciation events happened well before the Pleistocene and therefore the Pleistocene Refugia Hypothesis is not appropriate as a model with which to explain patterns of montane bird diversification in Africa. Rather, both dispersal and vicariance have played important roles in shaping montane bird communities. Thus, a refugia type model does work, but only within the context of pulsed or cyclic expansion and contraction of montane forests., supported in this study by the consistent recovery of spatially structured areas of endemism, despite varying temporal dynamics. The main features of this pulsed speciation model in general conforms to that suggested by Prigogine (1987) although the temporal dimension is wider than he hypothesized. The above should be considered a working hypothesis as there are still too few phylogenies to determine the extent to which species-cladograms agree with area-cladograms. It is hoped that the data presented within this thesis will form a foundation on which better evolutionary models can be built.

## Contents

### Birds, molecules, and evolutionary patterns among Africa's islands in the sky

- Ch1:** General overview of African montane biogeography and scope of the thesis (30 pages)
- Ch2:** Systematics and biogeography of the sunbirds (Aves: Nectariniidae) of the world: Aves largest genus (*Nectarinia*) takes a tumble (60 pages)
- Ch3:** Systematics and biogeography of the Eastern Double-collared Sunbird (*Nectarinia mediocris*) species complex (42 pages)
- Ch4:** A revaluation of species boundaries within the *Nectarinia afra/chalybea* complex of Double-collared Sunbirds (43 pages)
- Ch5:** Description and affinities of a new member of the Greater Double-collared Sunbird complex (genus *Nectarinia*) discovered in the Eastern Arc Mountains of Tanzania (20 pages)
- Ch6:** The Karoo Thrush, *Turdus smithi* Bonaparte 1850, a southern African endemic (19 pages)
- Ch7:** Systematics of the Olive Thrush (*Turdus olivaceus*) species complex with special reference to the globally, critically-endangered Taita Thrush (26 pages)
- Ch8:** Molecular evolution in space and through time: mtDNA phylogeography of the Olive Sunbird (*Nectarinia olivacea/obscura*) throughout continental Africa (37 pages)
- Ch9:** The shifting roles of dispersal and vicariance in the evolution of African birds during the Plio-Pleistocene: phylogeography of a montane forest robin (*Pogonocichla stellata*) (43 pages)
- Ch10:** Synthesis: Climatic cycling and its putative influence on speciation among African montane birds (23 pages)
- Ch11:** Literature cited (27 pages)



## List of Tables

1.1	List of 298 Afrotropical montane bird species	1.13-21
1.2	Percentage of montane forest birds shared between areas of endemism	1.22
2.1	Individuals sequenced for the higher level sunbird phylogeny	2.36-37
2.2	Primers used for the higher level sunbird phylogeny	2.38
2.3	Nucleotide substitution model parameters	2.39
2.4	Description and position of indels located in Fib5	2.40
2.5	Average sequence divergence within and between sunbird genera	2.41
2.6	ILD test results for combining data partitions	2.42
2.7	Tests for monophyly of sunbird genera	2.43
3.1	Eastern Double-collared Sunbird morphometrics	3.23-25
3.2	Intraspecific morphological variation in <i>Nectarinia mediocris</i>	3.26-27
3.3	Principal and discriminant components for EDC species complex	3.28
3.4	Classification results from the discriminant analysis of the EDC species complex	3.29
3.5	Nucleotide substitution model parameters	3.30
4.1	Taxa sampled in the <i>Nectarinia afra/chalybea</i> complex	4.22-24
4.2	Pairwise sequence divergence among taxa in the <i>N. afra/chalybea</i> complex	4.25
4.3	Plumage variation among members of the <i>N. afra/chalybea</i> complex	4.26-27
4.4	Morphometrics for members of the <i>N. afra/chalybea</i> complex	4.28-34
4.5	Principal and discriminant components for <i>N. afra/chalybea</i> complex	4.35
4.6	Relative significance of subsets of the discriminant variables	4.36
4.7	Classification results from the discriminant analysis of the	4.37-38

	<i>N. afra/chalybea</i> complex	
5.1	Taxa sampled for molecular DNA analyses	5.14-15
5.2	Statistical comparisons of morphological traits between <i>N. whytei</i> and <i>N. skyei</i>	5.16
6.1	Plumage and morphological characters of <i>Turdus olivaceus</i>	6.12
6.2	Pairwise DNA sequence divergence values	6.13
6.3	Molecular characteristics of DNA data partitions analysed	6.14
7.1	Taxa sampled for molecular DNA analyses	7.14-17
7.2	Pairwise sequence divergence among taxa in the <i>Turdus olivaceus</i> complex	7.18
8.1	Summary of populations sampled for the Olive Sunbird	8.23-27
8.2	Interpretation of the results from the NCA analyses	8.28-29
8.3	Measures of selective neutrality for Olive Sunbird populations	8.30
9.1	Description of the major plumage and vocal characters among subspecies of the Starred Robin	9.27-28
9.2	Populations sampled for the Starred Robin	9.29-30
9.3	Genetic diversity within sampled Starred Robin populations	9.31-32
9.4	Average sequence divergence among subnetworks of Starred Robin haplotypes	9.33
9.5	Interpretation of the results from the NCA analyses	9.34
10.1	Summary of the spatial and temporal variance in speciation of sister lineages of five groups of taxa around the montane circle of Africa	10.15-16

## List of Figures

1.1	Distribution of African montane rainforest	1.23
1.2	Vegetation structure in relation to altitude on Africa's tall mountains	1.24
1.3	Models for divergence in isolation	1.25
1.4	Montane areas of endemism	1.26
1.5	Examples of distribution patterns	1.27
1.6	Putative dispersal corridors	1.28
1.7	Graphical depiction of Prigogine's (1987) montane speciation model	1.29
1.8	Utility of sunbirds a model group with which to investigate montane biogeography	1.30
2.1	Summary of the three major systematic arrangements that have been proposed for the Nectariniidae	2.47
2.2	Nucleotide base composition of gene regions sequenced	2.48
2.3	Levels of genetic variation among different gene regions	2.49
2.4	Nucleotide sequence saturation plots	2.50
2.5	Comparison of pairwise mitochondrial vs. nuclear sequence divergence	2.51
2.6	MP tree for the mitochondrial DNA data partition	2.52
2.7	BI tree for the mitochondrial DNA data partition	2.53
2.8	MP tree for the nuclear DNA data partition	2.54
2.9	BI tree for the nuclear DNA data partition	2.55
2.10	MP tree for the combined mitochondrial and nuclear DNA data partition	2.56
2.11	MP tree for the combined mitochondrial and nuclear DNA data partition	2.57
2.12	Ancestral area re-construction using dispersal-vicariance analysis	2.58
2.13	Comparison of split (posterior) probabilities with bootstrap support	2.59
2.14	Evolutionary history of the Nectariniidae	2.60
3.1	Distribution ranges of members of the Eastern Double-collared	3.32

	Sunbird species complex	
3.2	Bivariate plots of male EDC complex sunbird biometrics	3.33
3.3	Scatter plots of the principle component scores for the EDC complex	3.34
3.4	Plots of the discriminant function scores for the EDC complex	3.35
3.5	Mean sequence divergence within and between species in the EDC complex	3.36
3.6	Strict consensus of 88 MP trees for the EDC complex	3.38
3.7	ML tree of the EDC complex	3.39
4.1	Distribution ranges of members of the <i>Nectarinia afra/chalybea</i> species complex	4.39
4.2	MP tree of taxa in the <i>N. afra/chalybea</i> complex	4.40
4.3	ML tree of taxa in the <i>N. afra/chalybea</i> complex	4.41
4.4	Scatter plots of the principle component scores for the <i>N. afra/chalybea</i> complex	4.42
4.5	Plots of the discriminant function scores for the <i>N. afra/chalybea</i> complex	4.43
5.1	Sampling localities from which <i>N. skyei</i> has been collected	5.17
5.2	Box plot summaries of morphological variation	5.18
5.3	MP tree of taxa in the <i>N. afra/chalybea</i> complex including <i>N. skyei</i>	5.19
5.4	ML tree of taxa in the <i>N. afra/chalybea</i> complex including <i>N. skyei</i>	5.20
6.1	Distribution ranges for southern African <i>Turdus olivaceus</i>	6.15
6.2	Phylogenetic hypothesis for ND3	6.16
6.3	Phylogenetic hypothesis for cytb	6.17
6.4	Phylogenetic hypothesis using combined data (ND3 + cytb)	6.18
7.1	Distribution ranges for members of the <i>Turdus olivaceus</i> complex	7.20
7.2	MP phylogenetic hypothesis for members of the <i>T. olivaceus</i> complex	7.21
7.3	Saturation plots for ND3	7.22
7.4	Summary of MP analyses conducted under differential	7.23-24

	weighting of 3 <sup>rd</sup> position transitions	
7.5	ML phylogenetic hypothesis for members of the <i>T. olivaceus</i> complex	7.25
7.6	BI phylogenetic hypothesis for members of the <i>T. olivaceus</i> complex	7.26
8.1	Geographical distribution of <i>Nectarinia olivacea</i> & <i>N. obscura</i>	8.33
8.2	Nested-clade design for the 55 sampled haplotypes	8.34
8.3	Summary of the statistical results from the NCA analysis	8.35
8.4	Mismatch profiles for Olive Sunbird populations	8.36
8.5	Modified models and resulting mismatch profiles for selected population where secondary contact is suspected	8.37
9.1	Geographical distribution of Starred Robin populations	9.37
9.2	MP tree of the 58 haplotypes sampled from the Starred Robin	9.38
9.3	Statistical parsimony network and nested-clade design of the 58 haplotypes	9.39
9.4	Summary of the statistical results from the NCA analysis	9.40
9.5	Summary of the major demographic events identified by the NCA	9.41
9.6	Estimates of directional gene flow among regional populations	9.42
9.7	Mismatch profiles of Starred Robin populations	9.43
10.1	Summary of relationships in the EDC complex	10.17
10.2	Summary of relationships in the <i>N. afra/chalybea</i> complex	10.18
10.3	Summary of relationships among northern populations of the Olive Thrush	10.19
10.4	Summary of relationships among montane species of Greenbuls	10.20-21
10.5	Reciprocal monophyly or the lack thereof.	10.22
10.6	Summary of relationships in two montane species of <i>Cryptospiza</i>	10.23

# Chapter 1

## General overview of African montane biogeography and scope of the thesis

Two undeniable features can be attributed to tropical habitats: their high biodiversity and the dramatic threats to this biodiversity posed by humans. The richly forested montane habitats of Africa are scattered along a 5000 km chain of mountains running from the Ethiopian Plateau in the north to the South African coast. To the west, are isolated mountain chains in Angola and Cameroon (Fig. 1.1).

This discontinuous distribution of montane habitats is primarily a consequence of relief, as only a few isolated areas are high enough to meet the requirements that allow for montane conditions (low temperature and high precipitation) to develop. Some of these isolated habitats are within sight of each other, whereas others are separated by hundreds of kilometers. Yet, in nearly all cases, the intervening vegetation, ranging from evergreen lowland forest to sub-desert steppe, appears to form an effective barrier to dispersal for species whose breeding ranges are confined to these high altitude habitats (Dowsett 1986). Strengthening this isolation is habitat transformation by humans (Bennun & Njoroge 1999, Fjeldså 1999, Ryan *et al.* 1999, Balmford *et al.* 2001, Brooks *et al.* 2001, Dinesen *et al.* 2001). The montane habitats of Africa can thus be considered as ecological islands, detached from the landscape below by a 'sea' of clouds. They provide a fascinating system for testing a range of ecological and evolutionary.

### THE MONTANE HABITATS

The montane environment in Africa typically occurs above 1800m. As one moves south, latitude starts to compensate for altitude, enabling montane taxa to occur at sea level in South Africa (Fig 1.1). Montane environments consist of two broad ecological types, a lower lying forest-belt and a high afro-alpine zone, consisting of moorland and grassland (Hedberg 1986). On Africa's tallest

mountains, for example, Mount Kenya, Mt. Kilimanjaro and the Ruwenzori and Virungu Mountains, vegetation is stratified into distinct altitudinal zones: permanent glacial caps, afro-alpine moorlands and giant heathlands, a transitional zone of juniper woodland and bamboo and finally the montane forest itself (Fig. 1.1 & 1.2). White (1983) provides detailed descriptions of the flora characterizing each vegetation zone.

Physical conditions are extreme in these habitats. The thin air and often, cloudless sky let the upper slopes freeze by night and scorch by day. Consequently, it is rare to find tropical organisms that are able to survive this daily ordeal of sun and ice (Kingdon 1989). Despite these physiological constraints, whole communities have become adapted to these environments. The central theme of this thesis is to improve the understanding of the origins and conservation of these unique communities, from the perspective of the montane bird fauna.

## **THE MONTANE AVIFAUNA**

African montane habitats have characteristic avifaunas. A number of authors have compiled lists and provided distributional information for species typical of the montane zone (Moreau 1966; Hall & Moreau 1970; Snow 1978; Dowsett 1986). Most recently, Dowsett (1986) classified a species as being montane, only if it is confined as a breeding species to high altitude, or is so in at least two of the seven afro-tropical montane groups (see montane groups below). According to these criteria, 222 of the approximately 1600 breeding bird species recorded within the Afrotropical Region can be considered typical of montane environments. Of these, 160 are considered characteristic of montane forest while the remaining 62 are associated with the afro-alpine zone. Using the revised classification scheme of Sibley and Monroe (1990) and Monroe and Sibley (1993), as well as information for recently described montane species (Dinesen *et al.* 1994, Safford *et al.* 1995), the total number of species may be increased to 298 (Table 1.1). Furthermore, many montane isolates also support some of the rarest bird species in Africa, many of which have extremely limited ranges, and in some cases populations that are likely to total less than 2000 individuals (Collar & Andrew 1988; Collar & Stuart 1988, Birdlife International

2000). This makes further study of these communities a high conservation priority.

### **EVOLUTIONARY ORIGINS OF THE MONTANE BIRDS OF AFRICA.**

There are three broad classes of processes of speciation: sympatric, allopatric and parapatric models. Under sympatric speciation, reproductive divergence of two co-occurring forms takes place through the build-up of pre and post-zygotic barriers. Advocates of parapatric speciation emphasize the importance of ecological gradients. This model predicts that sister taxa should occupy different, but adjacent habitats (Smith *et al.* 1997). For example, birds in a savannah/forest mosaic will start to diverge morphologically due to directional or disruptive selection acting across the ecotone. However, this model presents a major conceptual difficulty. There are many different ecotones in nature, often spatially or temporally isolated. Thus, it has to be asked; why are there not many new species constantly arising (Moritz *et al.* 2000)? Further, it is difficult to apply this model to clades wholly endemic to one biome, such as the African lowland rainforest (Beresford 2002), or to envisage how an ecotone-dependent model would operate over large spatial scales, such as the African continent. Thus, especially for the isolated montane highlands of Africa, allopatric speciation, or divergence in isolation, remains the predominant mechanism to explain divergence among montane birds.

### **The shifting roles of vicariance and dispersal in biogeography**

How divergence takes place in isolation remains a subject of much debate. Two models have been proposed to explain how populations and ultimately species may form in allopatry: the vicariance model and dispersal. In recent years, the vicariance model has become the favoured alternative, with most biologists agreeing that it is necessary to first disprove vicariance before invoking dispersal (Zink *et al.* 2000). This has led to the formation of a number of different speciation models, such as the Pleistocene Refuge Model (for Africa, Moreau 1966, Diamond & Hamilton 1980, Crowe & Crowe 1982) and, the Montane Speciation Model (Fjelds  1995, Fjelds  & Lovett 1997, Roy 1997) among others (see Haffer 1997 and Moritz *et al.* 2000 for reviews).



Nevertheless, both models provide explanations for allopathic speciation. The key difference lies in the relative role of the barrier, which facilitates the initiation of divergence (Fig. 1.3). Under the vicariance model, the formation of the barrier creates the opportunity for divergence by fragmenting a once continuously distributed parental species. Through disruptive, directional selection, or drift, populations on either side of the barrier if separated for long-enough, speciate. Under the dispersalist model, individuals from the parent species traverse a pre-existing barrier (two oceanic islands would be a classic example). This dispersal is then interrupted by some mechanism and isolation develops with subsequent speciation. How do you choose between the models? In theory, this can be done relatively easily. Because vicariance is dependent on the formation of a barrier and not random dispersal across it, a range of taxa should show a common pattern of divergence across a barrier as its formation should have affected them all at the time at which the common barrier formed (Zink *et al.* 2000). Thus times of divergence among a range of taxa should be roughly concordant, subject to the level of polymorphism and effective polymorphism of the ancestral population.

### **The montane groups (areas of endemism)**

Mountains possessing a montane avifauna have traditionally been divided into six groups: (1) the Cameroon Highlands, (2) Angolan Highlands, (3) Eastern Arc-Malawi, (4) Albertine Rift, (5) Kenyan Highlands and (6) Ethiopian Highlands (after Moreau 1966, Fig. 1.4). Dowsett (1986), in his analysis of distributional patterns of afromontane birds retained Moreau's (1966) six groups, but added a seventh, southeastern Africa. Each of these montane groups has several endemic species (Table 1.1). They can thus be considered as classic 'areas of endemism', which by definition must be delimited by the congruent distribution of at least two endemic species (Nelson & Platnick 1981, Morrone & Crisci 1995).

One of the more puzzling features of African montane biogeography is that, despite the often huge distances and unfavourable habitat between montane isolates, a large proportion of montane bird species reappear in even the most isolated forests – a feature mirrored by mammals (Kingdon 1989; 1997)

butterflies (Carcasson 1964), dung beetles (Davis *et al.* 2001), spiders (Griswold 1991) and flora (White 1983, Dowsett-Lemaire & Dowsett 2001). By considering the number of montane species shared among these groups, useful insight can be gained about the relationships among the montane groups. Unfortunately, due to the isolation and small geographical extent of montane highlands, recent studies focusing on the distributional patterns of African birds using a 1 by 1 degree grid (e.g. de Klerk 1998, Williams *et al.* 1999, Burgess *et al.* 2000, de Klerk *et al.* 2002a, b), have been unable to elucidate relationships among Africa's montane highlands. The central problem being that at this scale (*ca.* 100 x 100km), many widespread non-montane taxa are included in the analyses, artificially making a 1 by 1 degree grid cell containing montane specialists more similar than it really is to its neighbours.

The most comprehensive analysis of montane bird distributional patterns to date is that of Dowsett (1986). Dowsett (1986) restricted his analyses to just montane forest specialists and calculated the coefficients of association (CA) using Simpson's (1960) index. This index considers both species abundance and the number of endemics present among the different montane groups. The CA between pairs of mountain groups varied from 21% (Cameroon Highlands and Ethiopian Highlands) to 89% (Angolan Highlands and Albertine Rift, Table 1.2). To place these findings in context, Dowsett (1986) evaluated the extent of intra-group variation (*i.e.* among neighbouring mountains). The CA among neighbouring mountains within both the Eastern Arc-Malawi and southeastern Africa groups was about 75%. Therefore, for the purposes of inter-group comparisons it seems plausible to assume that groups sharing at least 70% of their montane forest avifauna are closely related. Based on these premises, interesting relationships between groups become apparent (Table 1.2). For instance, the montane species of Angola appear to have little affinity with the species of southeastern Africa, but strong ties with the more distant Albertine Rift and Kenyan Highlands.

### **The paradox and the paradigm**

One of the great difficulties in trying to explain patterns of montane bird speciation in Africa is to develop a hypothesis, which can adequately explain

why some mountains or areas of endemism have taxa unique to them, whereas others share the same species, but different subspecies, and still others have for all intents and purposes the same species. For example, the warbler *Apalis cinerea* is disjunctly distributed throughout the Albertine Rift and Kenya highlands, reappearing as isolated populations in both the highlands of Angola and Cameroon, but is absent from the highlands of Ethiopia, the Eastern Arc, Malawi Rift, and the montane forests of southern Africa (Fig. 1.5). On the other hand, many species are endemic to one particular montane group. For instance, *Xenoperdix udzungwensis* is only known from two forests within the southern Eastern Arc Mountains of Tanzania (Dinesen *et al.* 1994, Fjelds  & Kiure in press). In other cases, the distributional range of apparently the same species, e.g. *Turdus olivaceus* spans some 5000 km running along the mountain chain from Ethiopia to South Africa. Still other taxa, e.g. *Nectarinia kilimensis*, are partly distributed along the Ethiopian-South Africa mountain chain, but with isolated populations in the highlands of Angola or Cameroon (Fig. 1.5).

How do you explain such a juxtaposition of distributional patterns? Chapin (1923, 1932) proposed that changes in temperature and rainfall regimes during the past, had permitted a great extension of montane forest, thus connecting montane areas now widely separated by lowland rainforest or savanna. L nnberg (1929) in particular developed the idea that present distributions of animals are the result of past climate changes. However, it was Moreau (1966), who first suggested a time frame for African montane bird speciation. On the evidence then available, Moreau (1966) suggested that Africa's isolated montane blocks would have been connected during glacial periods, where he hypothesized increased precipitation, coupled with a 5 C reduction in temperature (see also Moreau 1963) would have had the effect of lowering montane forest limits in the tropics from around 1800m to 700-500m, thus permitting a great expansion of montane forest. This would have allowed a free interchange between mountain blocks. During interglacials, higher temperature and reduced precipitation would have reduced the extent of montane forest and have lead to a contraction of the present montane forest islands. Thus, according to Moreau (1966), the present disjunctions of montane habitats and their associated taxa are a consequence of the fragmentation of a continuous range existing during glacials. Connectivity

between the montane blocks was considered to have lasted for at least 50 000 years and only to have ended with the start of the next interglacial period about 18 000 years before present (BP). Livingstone (1975) criticised this view and, based on palaeo-botanical evidence, concluded that prior to 12 000 BP the continent was much drier. Therefore, even if the temperatures were low enough to move montane forest boundaries to lower altitudes, the aridity was too severe to support forest. Thus, if montane forest expansion has occurred, according to Livingstone (1975) it has only done so within the last 18 000 BP – the opposite view to Moreau (1966).

Currently, in view of mounting evidence (reviewed by deMenocal 1995, Partridge *et al.* 1995), it is broadly accepted that during glaciation peaks the tropics became more arid. During the dry and cold glacials, montane forests were reduced, while lowland forests mostly disappeared, except in refugia (Livingston 1975, Hamilton 1976, Diamond & Hamilton 1980, Crowe & Crowe 1982, Mayr & O'Hare 1986, Meadows 1996, Hamilton *et al.* 2001). Accepting this, how do we explain the high number of avian taxa that are shared between montane groups?

Diamond and Hamilton (1980) presented with this problem concluded that montane bird species that today show disjunct populations “have probably either flown from one area to the other or else once occurred in the intervening lowland forest”. A central tenant to Diamond and Hamilton's (1980) explanation for montane disjunctions is centred on lowland forest penetrations by montane species when competition was reduced. This could have happened during the short period at the beginning of an interglacial when lowland forest, and by extension associated species would have been expanding rapidly from refugia. Accepting this interpretation to explain the discontinuous distribution patterns implies that montane birds would have had to have been either, very mobile or previously have shown a much wider tolerance of altitudinal range (Dowsett 1986). Additionally, Diamond and Hamilton's (1980) competitive exclusion theory seems inadequate as many of the important montane refugia (e.g. Albertine Rift, Cameroon-Gabon, see Prigogine 1987) also included lowland forest. Thus, there is no reason to assume that lowland species would not be present to first exploit

available niches that appeared with the expansion of the lowland forest. Consequently, rapid dispersal, possibly across huge distances, seems the more likely of Diamond and Hamilton's (1980) hypotheses. This presents one of the greatest paradoxes of African biogeography, as it seems extremely unlikely when we consider that nearly all studies of montane birds suggest limited dispersal and then mostly altitudinal, as well as natal philopatry (e.g. Dowsett 1982; 1985, Dowsett & Dowsett-Lemaire 1984, Dowsett-Lemaire 1983, 1988, 1989).

Recently, an alternative to the Pleistocene Refuge Model has been suggested (Fjelds  1995, Fjelds  & Lovett 1997, Roy 1997, Roy *et al.* 1997), the Montane Speciation Model. The central tenant of this hypothesis is that speciation takes place primarily in topographically complex places, where orographic moderation of the weather creates high eco-climatic stability on certain slopes and basins. Once sufficient population sizes and genetic diversity have accumulated, these 'younger species' are redistributed within the lowland rainforest, thereby erasing much of the historical biogeographic signal. Thus, under the Montane Speciation Model, the lowland forests acts as a 'museum' for old and relict species. However, as with the Pleistocene Refuge Model, the Montane Speciation Model cannot explain how montane species (the younger species) could of crossed lowland forests when humid and warm conditions prevailed, and then again become isolated on distant mountain ranges, nor how the same mountain can have a juxtaposition of relict taxa, allospecies, subspecies and representatives of morphologically similar populations.

### **An alternative model? – Prigogine's model of climatic cycling**

An abnormal relationship between montane and lowland forest exists on the East Usambara Mountains and on Mt. Cameroon (Moreau 1966). These mountains abut the east and west coasts of Africa respectively, and due to orographic rain and their equatorial position experience very high rainfall and humidity. On the East Usambara Mountains for example, montane birds occur as low as 900m (Moreau 1952), while on the southeastern face of Mt. Cameroon, where temperatures fall even lower, montane birds extend down to 600m (Prigogine 1987). Prigogine (1987) suggested that during wet periods, montane forest would have occurred a lower altitudes and gradually expanded to cover the tops

of lower lying hills 600 to 900m above sea level. A number of montane isolates are connected by ancient fault lines or uplifted escarpments of lower lying hills. For example, a series of hills connect the Albertine Rift with the Cameroon Highlands via the northern rim of the Congo basin (Fig. 1.6C). In East Africa, a series of hills separated by 20-30km lowland gaps, connects the crater highland of north-central Tanzania with the Udzungwa and Rubeho massifs of the southern Eastern Arc Mountains (Fig. 1.7A). Following expansion of montane forest, characteristic montane species could have followed in a stepping-stone fashion. Eventually, connections could be developed for instance between the Albertine Rift and the Cameroon Highlands via a series of populations occupying the hill-corridor running along the northern Congo basin. Later, with the onset of glacial conditions, the increased aridity would have caused the fragmentation and eventual disappearance of the forest corridors. Thus, previously widespread taxa became isolated within the different montane blocks they had reached.

The above model does well to explain connectivity between montane blocks. However, if we assume that the degree of morphological divergence of two isolated sister taxa is correlated with the length of the isolation, how can allospecies, subspecies and morphologically similar allopatric populations 'pile-up' in the same montane block? A simple solution was suggested by Prigogine (1987), for allospecies isolated on different mountain ranges he maintained that dispersal and subsequent isolation occurred further back in time than for subspecies, which in turn were isolated less recently than morphologically similar allopatric populations (Fig. 1.7).

The central theme of Prigogine's model (1987) is that climatic fluctuations, especially recurrent glaciation periods over the last 3 million years have played an important role in the repeated fragmentation of the montane biome. This idea is supported to an even greater extent with more recently collected palaeo-ecological data (reviewed by deMenocal 1995). Thus, the montane habitats of different mountains are likely to have experienced a complex pattern of fragmentation. These range from being in contact with neighbours on a number of occasions to never having been directly in contact with other montane forest or afro-alpine vegetation (e.g. Mount Kulal and Mount Marsabit in northern

Kenya). Patterns of connectivity have been further complicated by volcanic activity, which in East and central Africa has produced a juxtaposition of relatively young mountains (e.g. Mt. Kilimanjaro) embedded within a landscape of ancient mountains (e.g. The Aberdares) (Griffiths 1993, Partridge *et al.* 1995).

### **A time line**

The rapid development of molecular biology as a scientific discipline in the past decade has provided a rich data source and a diversity of analytical techniques that have enriched biogeographical analyses. Perhaps their most significant contribution is that molecular comparisons can provide a time dimension with which it is possible to tentatively date speciation events (Riddle 1996). If we accept a molecular clock, that is, for example in mitochondrial DNA (mtDNA) divergence accumulates at a roughly uniform and time dependant rate (at least for the same gene among closely related species) then we would expect sister species in different lineages separated by the same biological barrier to exhibit similar mtDNA distances.

Klicka and Zink (1997) used this argument to investigate the importance ascribed to the two most recent glacial cycles in North America, the Wisconsinian (beginning *ca.* 100 000 BP) and the Illinoian (*ca.* 250 000 BP) as the prevailing mechanism of avian speciation among North American passerine birds (e.g. Mengel 1970; Hubbard 1973). Klicka and Zink (1997) termed this model the Late Pleistocene Origins model (LPO). They compared mtDNA from 35 closely related species pairs of passerines, each postulated to have evolved within the framework of the LPO model. Assuming a molecular clock, calibrated to a rate of *ca.* 2% divergence per million years (Myr) the expected divergence between sister taxa under the LPO model should be no greater than 0.5%. Instead they found an average divergence of 5.1% ( $\pm 3\%$ ), which is a tenfold increase over that predicted from the LPO model. They concluded that speciation among the 35 sister species in general occurred much earlier than previously thought under the LPO model.

At all levels the use of molecular DNA sequence data in erecting phylogenetic hypothesis and application of the molecular clock is fundamentally changing perspectives on avian evolution, not only within the recent past as suggest by Klicka and Zink (1997, see above), but for intermediate and deeper nodes as well. Recent studies in African birds have inferred dates derived from molecular clocks, suggesting that ages of putative refuge species are much older than the Pleistocene, and instead are Pliocene to Miocene in age (Fjelds  1994, Roy *et al.* 2000, Beresford 2002). Similarly, recent molecular studies (Barker *et al.* 2002, Ericson *et al.* 2002), have given credence to Cracraft's (1973, 2001) original hypothesis, based on morphological data, of a vicariant origin for passerines birds, derived from the break-up of the cretaceous super-continent Gondwana. Various studies, based on molecular data suggest that the extant avian orders diverged in the early to mid Cretaceous (Sibley & Ahlquist 1990, Hedges *et al.* 1996, Cooper & Penny 1997, Cooper *et al.* 2001, van Tuinen & Hedges 2001). This is in conflict with the interpretation of the available fossil record, which suggests a Tertiary origin for all modern avian orders (Feduccia 1996). The utility of molecular data to provide a temporal perspective to phylogenetic hypotheses forms a critical part for testing between alternative speciation hypotheses for African montane birds and is the primary data medium used to erect and test hypotheses within this thesis.

## SUNBIRDS

The sunbirds (Nectariniidae), which includes Aves largest genus *Nectarinia* (Bock & Farrand 1980) have undergone a dramatic radiation in Africa, and encompass a large number of montane species (Table 1.1). This is best reflected by the similar distributional overlay of the 79 endemic sunbird species with the 298 characteristic montane species listed in Table 1.1. Centres of sunbird species richness coincide remarkably with general hotspots for montane bird richness (Fig. 1.8). Sunbirds thus provide an ideal model group with which to explore montane bird diversification patterns in Africa.

The major disadvantage of using sunbirds as a biogeographical model is that no robust phylogenetic hypothesis has been erected for the family. An understanding of phylogenetic relationships among species and clear delineation



of monophyletic groups is fundamental if appropriate biogeographical inferences are to be made. Consequently, in Chapter 2, nucleotide sequence data are used to infer a phylogeny for the family Nectariniidae. Based on this hypothesis, monophyletic lineages are selected with which to explore afro-montane biogeography (Chapters 3-5 and 8). Additionally, the phylogeny will be used in further studies (not part of this thesis) to explore the evolution of sexually dichromatism and ecological traits associated with nectarivory as a life-history strategy. To test for hierarchical vicariance patterns in the context of historical biogeography (*sensu* Nelson & Platnick 1981), phylogeographical structure of two largely montane turdine species, the Olive Thrush, *Turdus olivaceus* (Chapters 6 and 7) and the Starred Robin, *Pogonocichla stellata* (Chapter 9) are investigated. Chapter 10 provides a synthesis of the above chapters as well as relevant literature, with a view to determine the extent different data sets are congruent, and hence derived from a vicariant origin. Non-congruence would support a differential dispersal across pre-existing barriers, as a hypothesis with which to explain African montane bird distribution patterns.

**Table 1.1.** Taxonomic composition of the 298 Afrotropical montane birds encompassed under the following definition: the species should be wholly confined as a breeding bird to high altitude, greater than 1800m in most cases, except for southern Africa, where the species should be restricted to afro-montane forest or grassland in greater than 80% of its breeding range. This allows for the inclusion of both the southern African high altitude species and those species that behave as strictly high-altitude birds in a substantial part, but not all of their range. Key: F = Afro-montane Forest, NF = non-forest, including - Afroalpine moorland & grassland, F/NF, both habitats or a species of forest edge.

Family	Genus	Species	Habitat	Comments
1 Phasianidae	<i>Francolinus</i>	<i>erckelii</i>	NF	
2		<i>castaneicollis</i>	F	includes <i>atrifrons</i>
3		<i>jacksoni</i>	F	
4		<i>nobilis</i>	F	
5		<i>camerunensis</i>	F	
6		<i>swierstrai</i>	F	
7		<i>harwoodi</i>	NF	
8		<i>psilolaemus</i>	NF	
9		<i>levaillantii</i>	NF	
10	<i>Xenoperdix</i>	<i>udzungwensis</i>	F	
11 Anatidae	<i>Cyanochen</i>	<i>cyanopterus</i>	NF	
12 Indicatoridae	<i>Indicator</i>	<i>pumilio</i>	F	
13 Picidae	<i>Campethera</i>	<i>tullbergi</i>	F	includes <i>taeniolaema</i>
14	<i>Dendropicos</i>	<i>abyssinicus</i>	F/NF	
15		<i>griseocephalus</i>	F	sometimes lumped with <i>goertae</i>
16 Lybiidae	<i>Stactolaema</i>	<i>olivacea</i>	F	includes <i>woodwardi</i> - <i>woodwardi</i> sometimes placed in genus <i>Cryptolybia</i>
17	<i>Pogoniulus</i>	<i>leucomystax</i>	F	
18		<i>coryphaeus</i>	F	
19 Bucerotidae	<i>Ceratogymna</i>	<i>brevis</i>	F	often put into the genus <i>Bycanistes</i>
20 Trogonidae	<i>Apaloderma</i>	<i>vittatum</i>	F	
21 Meropidae	<i>Merops</i>	<i>oreobates</i>	F	
22 Cuculidae	<i>Cercococcyx</i>	<i>montanus</i>	F	
23 Psittacidae	<i>Poicephalus</i>	<i>flavifrons</i>	F	
24	<i>Agapornis</i>	<i>taranta</i>	F	
25 Apodidae	<i>Schoutedenapus</i>	<i>myoptilus</i>	F/NF	

26		<i>schoutedeni</i>	F/NF	
27	<i>Apus</i>	<i>niansae</i>	NF	
28	<i>Tachymarpis</i>	<i>aequatorialis</i>	NF	often placed in the genus <i>Apus</i>
29	<b>Musophagidae</b>	<i>leucotis</i>	F	<i>donaldsoni</i> treated as conspecific
30		<i>ruspolii</i>	F	
31		<i>hartlaubi</i>	F	
32		<i>bannermani</i>	F	
33		<i>livingstoni</i>	F	includes <i>chalcophus</i> but not <i>schalowi</i>
34	<i>Musophaga</i>	<i>johnstoni</i>	F	some place in <i>Tauraco</i> or <i>Ruwenzorornis</i>
35				
36	<b>Tytonidae</b>	<i>Phodilus</i>	<i>prigoginei</i>	F
37	<b>Strigidae</b>	<i>Bubo</i>	<i>capensis</i>	F/NF <i>mackinderi</i> is treated as conspecific
38			<i>vosseleri</i>	F often lumped with <i>poensis</i>
39	<i>Asio</i>	<i>abyssinicus</i>	F	often lumped with <i>otus</i>
40	<i>Glaucidium</i>	<i>albertinum</i>	F	
41	<b>Caprimulgidae</b>	<i>Caprimulgus</i>	<i>poliocephalus</i>	NF <i>guttifer</i> , <i>koesteri</i> & <i>ruwenzori</i> all treated as conspecific
42			<i>solala</i>	NF? only one specimen (described from a wing) therefore habitat unknown
43			<i>prigoginei</i>	F
44	<b>Columbidae</b>	<i>Columba</i>	<i>albitorques</i>	NF <i>iriditorques</i> superspecies, excluded
45			<i>arquatrix</i>	F
46			<i>sjostedti</i>	F
47			<i>delegorguei</i>	F
48			<i>larvata</i>	F
49	<i>Streptopelia</i>	<i>lugens</i>	F/NF	
50	<b>Rallidae</b>	<i>Sarothrura</i>	<i>ayresi</i>	NF
51			<i>affinis</i>	NF
52	<i>Rougetius</i>	<i>rougetii</i>	NF	
53	<b>Charadriidae</b>	<i>Vanellus</i>	<i>melanocephalus</i>	NF
54	<b>Accipitridae</b>	<i>Gypaetus</i>	<i>barbatus</i>	NF
55		<i>Accipiter</i>	<i>rufiventris</i>	F sometimes lumped with <i>A. nisus</i>
56		<i>Buteo</i>	<i>oreophilus</i>	F includes <i>trizonatus/tachardus</i>
57	<b>Threskiornithidae</b>	<i>Geronticus</i>	<i>calvus</i>	NF
58		<i>Bostrychia</i>	<i>carunculata</i>	NF
59	<b>Eurylaimidae</b>	<i>Pseudocalyptomena</i>	<i>graueri</i>	F
60	<b>Laniidae</b>	<i>Lanius</i>	<i>marwizi</i>	F often lumped with <i>collaris</i>

61	<b>Corvidae</b>	<i>Pyrrhocorax</i>	<i>pyrrhocorax</i>	NF	
62		<i>Corvus</i>	<i>crassirostris</i>	NF	
63			<i>albicollis</i>	NF	
64		<i>Oriolus</i>	<i>percivali</i>	F	often lumped with <i>larvatus</i>
65			<i>monacha</i>	F	
66			<i>chlorocephalus</i>	F	
67		<i>Coracina</i>	<i>caesia</i>	F	altitudinal <i>migrant</i>
68			<i>graueri</i>	F	
69		<i>Trochocercus</i>	<i>albonotata</i>	F	
70		<i>Trochocercus</i>	<i>albiventris</i>	F	
71		<i>Terpsiphone</i>	<i>bedfordi</i>	F	often lumped with <i>rufiventer</i>
72		<i>Laniarius</i>	<i>atroflavus</i>	F	
73			<i>poensis</i>	F	sometimes lumped with <i>fuellborni</i>
74			<i>fuellborni</i>	F	
75		<i>Telophorus</i>	<i>nigrifrons</i>	F	sometimes lumped with <i>multicolor</i>
76			<i>olivaceus</i>	F	
77			<i>kupeensis</i>	F	
78			<i>dohertyi</i>	F	
79		<i>Malaconotus</i>	<i>gladiator</i>	F	
80			<i>alius</i>	F	
81			<i>monteiri</i>	F	
82		<i>Prionops</i>	<i>alberti</i>	F	
83		<i>Batis</i>	<i>capensis</i>	F	
84			<i>diops</i>	F	sometimes lumped with <i>capensis</i>
85			<i>dimorpha</i>	F	often lumped with <i>capensis</i>
86			<i>margaritae</i>	F	often lumped with <i>capensis</i>
87			<i>mixta</i>	F	includes <i>ultima</i> , both often lumped with <i>capensis</i>
88	<b>Picathartidae</b>	<i>Chaetops</i>	<i>aurantius</i>	NF	
89			<i>frenatus</i>	NF	
90	<b>Muscicapidae</b>	<i>Monticola</i>	<i>explorator</i>	NF	
91		<i>Zoothera</i>	<i>tanganjicae</i>	F	sometimes lumped with <i>piaggiae</i>
92			<i>gurneyi</i>	F	
93			<i>piaggiae</i>	F	
94			<i>oberlaenderi</i>	F	

95	<i>Turdus</i>	<i>olivaceus</i>	F/NF	<i>oldeani</i> , <i>roehli</i> , <i>swynnertoni</i> , <i>abyssinicus</i> , <i>ludoviciae</i> , <i>helleri</i> , are treated as conspecific
96	<i>Alethe</i>	<i>poliophrys</i>	F	
97		<i>fuelleborni</i>	F	
98		<i>choloensis</i>	F	
99	<i>Dioptrornis</i>	<i>chocolatina</i>	F	often placed in the genus <i>Melaenornis</i>
100		<i>fischeri</i>	F	often lumped with <i>chocolatinus</i> - often in genus <i>Melaenornis</i>
101		<i>brunneus</i>	F	often lumped with <i>chocolatinus</i> - often in genus <i>Melaenornis</i>
102	<i>Melaenornis</i>	<i>ardesiacus</i>	F	
103	<i>Muscicapa</i>	<i>lendu</i>	F	
104		<i>itombwensis</i>	F	often lumped with <i>lendu</i>
105	<i>Pogonocichla</i>	<i>stellata</i>	F	
106	<i>Swynnertonia</i>	<i>swynnertoni</i>	F	
107	<i>Sheppardia</i>	<i>aequatorialis</i>	F	
108		<i>bocagei</i>	F	
109		<i>sharpei</i>	F	
110		<i>montana</i>	F	
111		<i>lowei</i>	F	
112		<i>gabela</i>	F	
113		<i>poensis</i>	F	often lumped with <i>bocagei</i>
114	<i>Cossypha</i>	<i>archeri</i>	F	pops assigned between <i>archeri</i> & <i>anomala</i> are often uncertain
115		<i>anomala</i>	F	<i>mbuluensis</i> , <i>albigularis</i> , <i>gurue</i> treated as conspecific
116		<i>semirufa</i>	F	
117		<i>caffra</i>	F/NF	
118		<i>dichroa</i>	F	
119		<i>isabellae</i>	F	
120		<i>roberti</i>	F	
121	<i>Xenocopsychus</i>	<i>ansorgei</i>	NF	
122	<i>Cercomela</i>	<i>sordida</i>	NF	
123		<i>dubia</i>	NF	
124	<i>Myrmecocichla</i>	<i>melaena</i>	NF	
125	<i>Thamnolaia</i>	<i>semirufa</i>	NF	
126		<i>cinnamomeiventris</i>	NF	includes <i>bambarae</i> , <i>albiscapulata</i>
127 Sturnidae	<i>Poeoptera</i>	<i>stuhlmanni</i>	F	
128		<i>kenricki</i>	F	

129	<i>Onychognathus</i>	<i>tenuirostris</i>	F/NF	
130		<i>walleri</i>	F	
131		<i>albirostris</i>	NF	
132	<i>Cinnyricinclus</i>	<i>sharpii</i>	F	
133		<i>femoralis</i>	F	
134	<b>Paridae</b>	<i>Parus</i>	<i>fasciiventer</i>	F
135			<i>leuconotus</i>	F/NF
136	<b>Hirundinidae</b>	<i>Hirundo</i>	<i>atrocaerulea</i>	NF long-distance migrant
137			<i>megaensis</i>	NF
138		<i>Psalidoprocne</i>	<i>fuliginosa</i>	F
139			<i>antinorii</i>	NF <i>blanfordi</i> is treated as conspecific
140	<b>Pycnonotidae</b>	<i>Andropadus</i>	<i>tephrolaemus</i>	F
141			<i>milanjensis</i>	F
142			<i>olivaceiceps</i>	F often lumped with <i>milanjensis</i>
143			<i>montanus</i>	F <i>roehli</i> considered conspecific
144			<i>masukuensis</i>	F
145			<i>kakamegae</i>	F often lumped with <i>masukuensis</i>
146			<i>nigriceps</i>	F
147			<i>chorigula</i>	F
148		<i>Chlorocichla</i>	<i>laetissima</i>	F
149			<i>prigoginei</i>	F sibling species of <i>laetissima</i>
150		<i>Phyllastrephus</i>	<i>placidus</i>	F often lumped with <i>cabanisi</i>
151			<i>flavostriatus</i>	F
152			<i>alfredi</i>	F often lumped with <i>flavostriatus</i>
153			<i>poensis</i>	F
154			<i>poliocephalus</i>	F sometimes lumped with <i>flavostriatus</i>
155			<i>cabanisi</i>	F much taxonomic confusion
156	<b>Cisticolidae</b>	<i>Cisticola</i>	<i>ayresii</i>	NF
157			<i>aberdare</i>	NF
158			<i>lais</i>	NF
159			<i>distinctus</i>	NF often lumped with <i>lais</i>
160			<i>njombe</i>	NF
161			<i>bodessa</i>	NF
162			<i>hunteri</i>	NF
163			<i>chubbi</i>	NF

164		<i>discolor</i>	NF	often lumped with <i>chubbi</i>
165		<i>nigriloris</i>	NF	
166		<i>robustus</i>	NF	
167		<i>angolensis</i>	NF	includes <i>awemba</i> , both are often lumped with <i>robustus</i>
168	<i>Prinia</i>	<i>leontica</i>	F	
169		<i>melanops</i>	NF	
170	<i>Oreophilais</i>	<i>robertsi</i>	F/NF	
171	<i>Urolais</i>	<i>epichlora</i>	F/NF	
172	<i>Apalis</i>	<i>jacksoni</i>	F	
173		<i>chariessa</i>	F	extinct in Kenya
174		<i>thoracica</i>	F	includes <i>griseiceps</i> , <i>fuscigularis</i> , <i>lynesi</i> , <i>murina</i> , <i>flavigularis</i> & <i>thoracica</i>
175		<i>cinerea</i>	F	
176		<i>argentea</i>	F	includes <i>eidos</i> , both sometimes lumped with <i>rufogularis</i>
177		<i>porphyrolaema</i>	F	
178		<i>chapini</i>	F	includes <i>strausae</i>
179		<i>bamendae</i>	F	
180		<i>chirindensis</i>	F	
181		<i>pulchra</i>	F	
182		<i>ruwenzorii</i>	F	
183		<i>karamojae</i>	F	
184		<i>personata</i>	F	
185		<i>goslingi</i>	F	
186		<i>alticola</i>	F	
187		<i>kaboboensis</i>	F	often lumped with <i>alticola</i>
188	<i>Eminia</i>	<i>lepida</i>	NF	
189	<b>Zosteropidae</b>	<i>Speirops</i>	F	sometimes lumped with <i>lugubris</i>
190		<i>Zosterops</i>	F	includes <i>kikuyuensis</i> , <i>winnifredae</i> , <i>silvanus</i> , <i>eurocricotus</i>
191	<b>Sylviidae</b>	<i>Bradypterus</i>	NF	includes <i>bangwaensis</i>
192		<i>victorini</i>	F/NF	
193		<i>cinnamomeus</i>	F/NF	
194		<i>barratti</i>	F	
195		<i>mariae</i>	F	includes <i>barakae</i>
196		<i>lopezi</i>	F	includes <i>camerunensis</i>
197		<i>sylvaticus</i>	F/NF	
198	<i>Scepomycter</i>	<i>winnifredae</i>	F	

199	<i>Chloropeta</i>	<i>similis</i>	F/NF	
200	<i>Orthotomus</i>	<i>moreaui</i>	F	
201		<i>metopias</i>	F	some place in the genus <i>Camaroptera</i>
202	<i>Poliolais</i>	<i>lopezi</i>	F	some place in <i>Camaroptera</i> or <i>Orthotomus</i>
203	<i>Graueria</i>	<i>vittata</i>	F	
204	<i>Sylvietta</i>	<i>leucophrys</i>	F	
205		<i>chapini</i>	F	often lumped with <i>leucophrys</i>
206	<i>Hemitesia</i>	<i>naumanni</i>	F	
207	<i>Phylloscopus</i>	<i>ruficapillus</i>	F	
208		<i>laetus</i>	F	
209		<i>herberti</i>	F	
210		<i>umbrovirens</i>	F	
211		<i>budongoensis</i>	F	
212	<i>Modulatrix</i>	<i>stictigula</i>	F	
213	<i>Arcanator</i>	<i>orostruthus</i>	F	sometimes put in <i>Modulatrix</i> or <i>Phyllastrephus</i> (Pycnonotidae)
214	<i>Illadopsis</i>	<i>pyrrhoptera</i>	F	
215		<i>abyssinica</i>	F	includes <i>stierlingi</i> , prob. be in <i>Pseudoalcippe</i>
216		<i>atriceps</i>	F	should prob. be in <i>Pseudoalcippe</i>
217	<i>Kakamega</i>	<i>poliothorax</i>	F	
218	<i>Turdoides</i>	<i>hypoleucus</i>	F/NF	
219	<i>Lioptilus</i>	<i>nigricapillus</i>	F	
220	<i>Kupeornis</i>	<i>rufocinctus</i>	F	montane if you consider <i>K. chapini</i> a separate species
221		<i>gilberti</i>	F	
222	<i>Parophasma</i>	<i>galinieri</i>	F	
223	<i>Sylvia</i>	<i>lugens</i>	NF	
224 <b>Alaudidae</b>	<i>Heteromira</i>	<i>ruddi</i>	NF	
225		<i>archeri</i>	NF	recently, 1996 recorded in Ethiopia
226	<i>Calandrella</i>	<i>erlangeri</i>	NF	some lump with <i>somalica</i>
227 <b>Nectariniidae</b>	<i>Promerops</i>	<i>gurneyi</i>	NF	sometimes lumped with <i>cafer</i>
228		<i>cafer</i>	NF	
229	<i>Anthreptes</i>	<i>rubritorques</i>	F	sometimes lumped with <i>rectirostris</i>
230		<i>pallidigaster</i>	F	recorded from the Udzungwas
231	<i>Nectarinia</i>	<i>ursulae</i>	F	
232		<i>afra</i>	NF	
233		<i>stuhlmanni</i>	F	often lumped with <i>afra</i>



234		<i>prigoginei</i>	F	often lumped with <i>afra</i>
235		<i>ludovicensis</i>	F	often lumped with <i>afra</i>
236		<i>preussi</i>	F	
237		<i>regia</i>	F	
238		<i>rockefelleri</i>	F/NF	
239		<i>mediocris</i>	F	
240		<i>loveridgei</i>	F	sometimes lumped with <i>mediocris</i>
241		<i>moreaui</i>	F	sometimes considered <i>mediocris</i> x <i>loveridgei</i>
242		<i>tacazze</i>	NF	
243		<i>purpureiventris</i>	F	
244		<i>kilimensis</i>	F/NF	includes <i>gadowi</i>
245		<i>bocagei</i>	F	
246		<i>reichenowi</i>	NF	
247		<i>famosa</i>	NF	
248		<i>johnstoni</i>	NF	
249		<i>violacea</i>	NF	
250		<i>oritis</i>	F	
251		<i>alinae</i>	F	
252		<i>rufipennis</i>	F	
253	Passeridae	<i>flavicollis</i>	NF	
254	Anthus	<i>crenatus</i>	NF	
255		<i>latistriatus</i>	NF	often lumped with <i>cinnamomeus</i>
256		<i>hoeschi</i>	NF	sometimes lumped with <i>editus</i>
257		<i>chloris</i>	NF	
258		<i>camaroonensis</i>	NF	often lumped with <i>cinnamomeus</i> or <i>novaeollandiae</i>
259		<i>sharpi</i>	NF	often placed in the genus <i>Macronyx</i>
260	Ploceus	<i>baglafecht</i>	NF	includes <i>emini</i> , <i>reichenowi</i> , <i>stuhlmanni</i>
261		<i>bertrandi</i>	F/NF	
262		<i>melanogaster</i>	F	
263		<i>alienus</i>	F	
264		<i>insignis</i>	F	
265		<i>bannermani</i>	F	
266		<i>nicolli</i>	F	
267		<i>aureonucha</i>	F	
268	Euplectes	<i>psammocromius</i>	NF	

269		<i>jacksoni</i>	NF	
270	<i>Nesocharis</i>	<i>shellei</i>	F	sometimes considered a race of <i>ansorgei</i>
271		<i>ansorgei</i>	NF	
272	<i>Pytilia</i>	<i>lineata</i>	NF	often considered conspecific with <i>phoenicoptera</i>
273	<i>Cryptospiza</i>	<i>reichenovii</i>	F	
274		<i>salvadorii</i>	F	
275		<i>shellei</i>	F	
276		<i>jacksoni</i>	F	
277	<i>Euschistospiza</i>	<i>cinereovinacea</i>	NF	
278	<i>Estrilda</i>	<i>ochrogaster</i>	NF	often considered conspecific with <i>paludicola</i>
279		<i>melanotis</i>	F/NF	
280		<i>kandti</i>	F	often lumped with <i>atricapilla</i>
281	<b>Fringillidae</b>	<i>canicollis</i>	NF	includes <i>flaivertex</i>
282	<i>Serinus</i>	<i>nigriceps</i>	NF	
283		<i>flavigula</i>	NF	
284		<i>totta</i>	NF	
285		<i>symondsi</i>	NF	sometimes considered a race of <i>totta</i>
286		<i>citrinelloides</i>	F/NF	
287		<i>hyposticus</i>	F/NF	often treated as race of <i>citrinelloides</i>
288		<i>frontalis</i>	F/NF	includes <i>kikuyuensis</i> , both often treated as race of <i>citrinelloides</i>
289		<i>scotops</i>	F	
290		<i>tristriatus</i>	NF	
291		<i>ankoberensis</i>	NF	sometimes considered a race of <i>menachensis</i> (Yemen Siskin)
292		<i>burtoni</i>	F/NF	
293		<i>melanochrous</i>	F/NF	often treated as a race of <i>burtoni</i>
294		<i>striolatus</i>	NF	
295		<i>whytii</i>	NF	often lumped with <i>striolatus</i>
296		<i>leucopterus</i>	NF	
297		<i>reichardi</i>	NF	often considered a race of <i>canicapillus</i>
298	<i>Linurgus</i>	<i>olivaceus</i>	F	

**Table 1.2.** Percentage of montane forest birds shared between areas of endemism (modified from Dowsett 1986).

Areas of endemism	1	2	3	4	5	6	7
	(48) <sup>1</sup>	(18)	(51)	(64)	(92)	(83)	(34)
1. Cameroon Highlands(37%) <sup>2</sup>	****	67	27	35	60	50	21
2. Angolan Highlands (6%)		****	56	72	89	78	28
3. Southeastern Africa (16%)			****	78	51	78	35
4. Eastern Arc-Malawi (8%)				****	62	87	53
5. Albertine Rift (29%)					****	71	65
6. Kenyan Highlands (5%)						****	74
7. Ethiopian Highlands (26%)							****

1 Figures in parentheses are the numbers of forest species recorded from each group.

2 Figures in parentheses are the percentages of forest species endemic to each group.

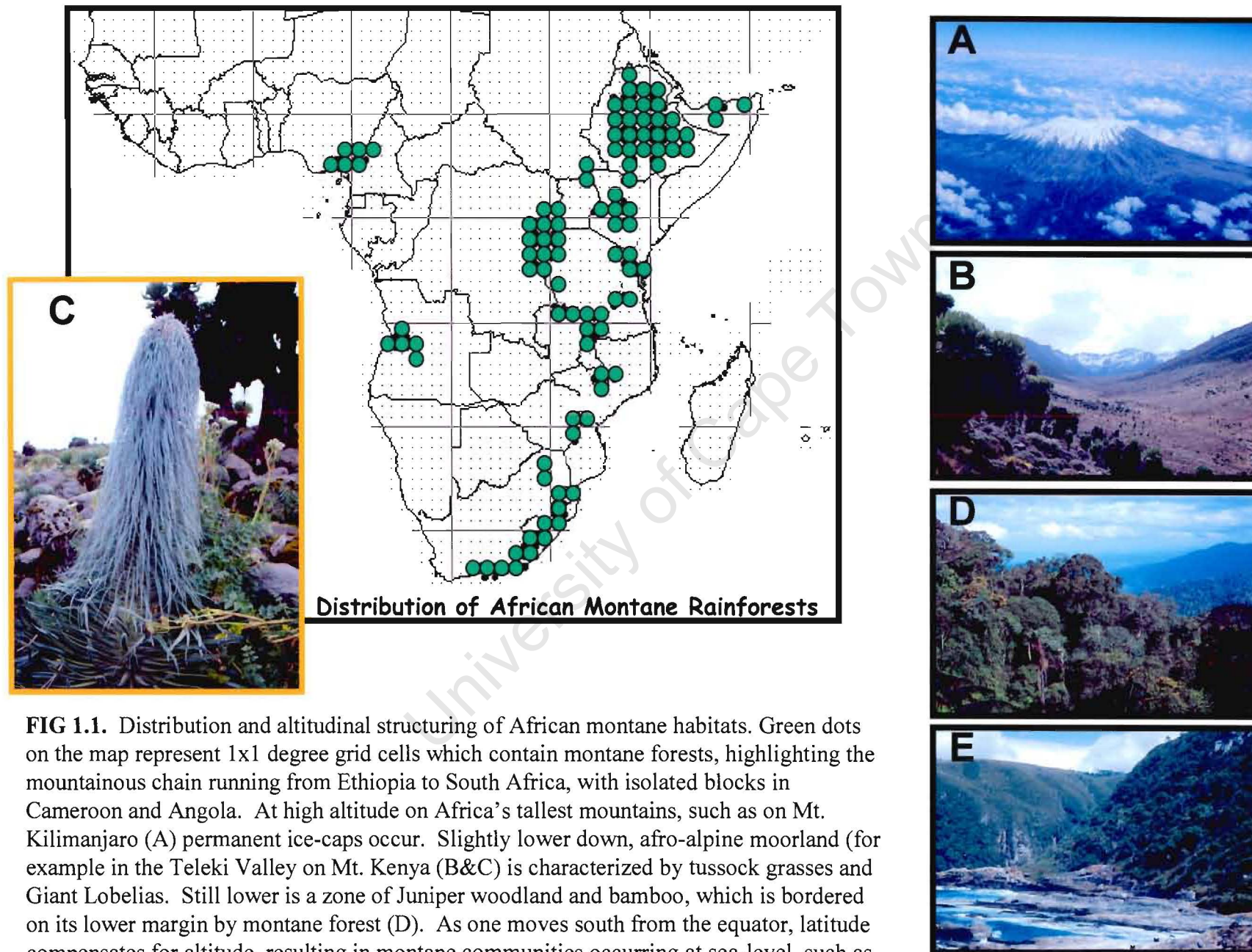


**FIG 1.1.** Distribution and altitudinal structuring of African montane habitats. Green dots on the map represent 1x1 degree grid cells which contain montane forests, highlighting the mountainous chain running from Ethiopia to South Africa, with isolated blocks in Cameroon and Angola. At high altitude on Africa's tallest mountains, such as on Mt. Kilimanjaro (A) permanent ice-caps occur. Slightly lower down, afro-alpine moorland (for example in the Teleki Valley on Mt. Kenya (B&C) is characterized by tussock grasses and Giant Lobelias. Still lower is a zone of Juniper woodland and bamboo, which is bordered on its lower margin by montane forest (D). As one moves south from the equator, latitude compensates for altitude, resulting in montane communities occurring at sea-level, such as at the mouth of the Storms River in South Africa (E).

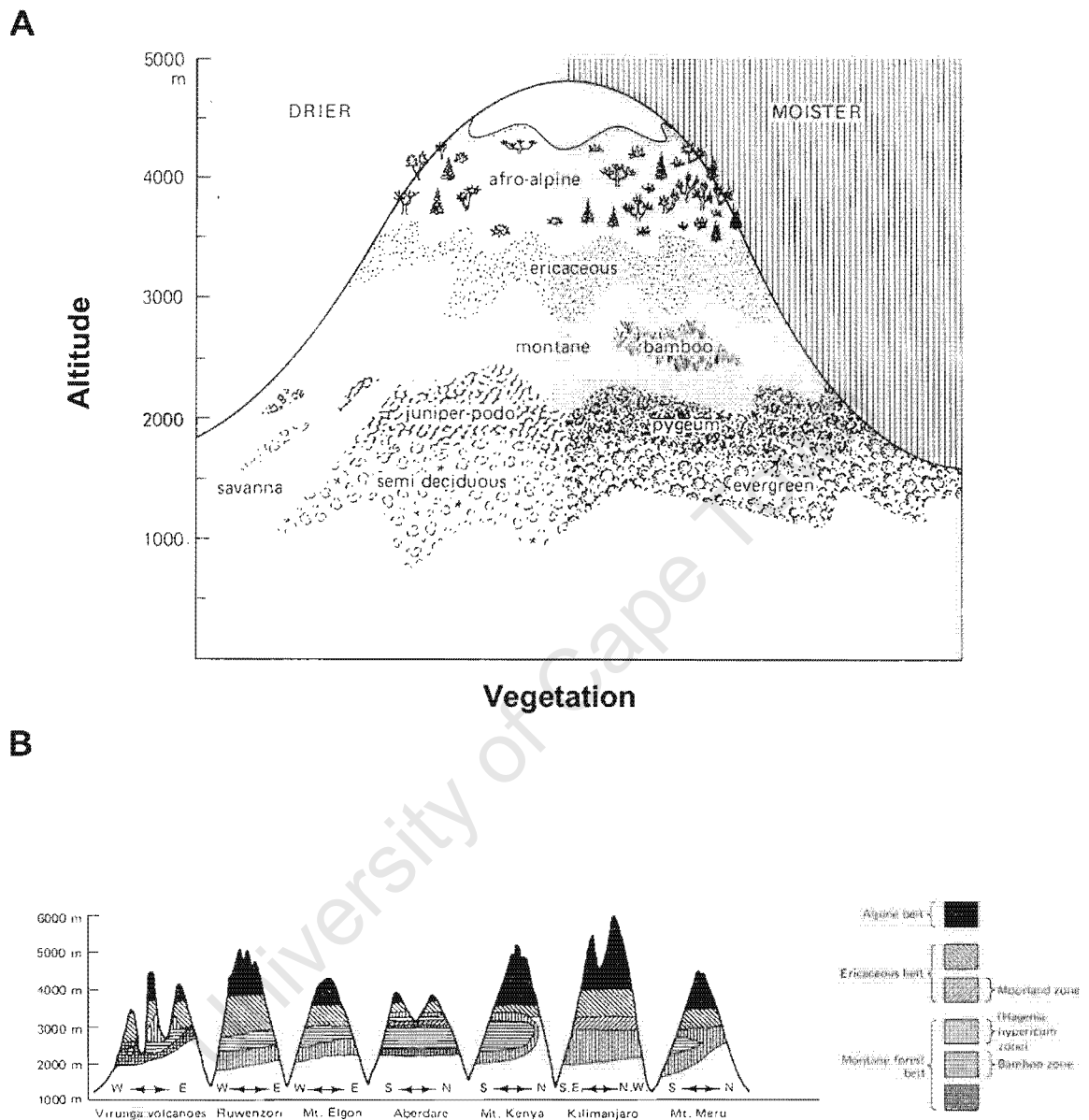
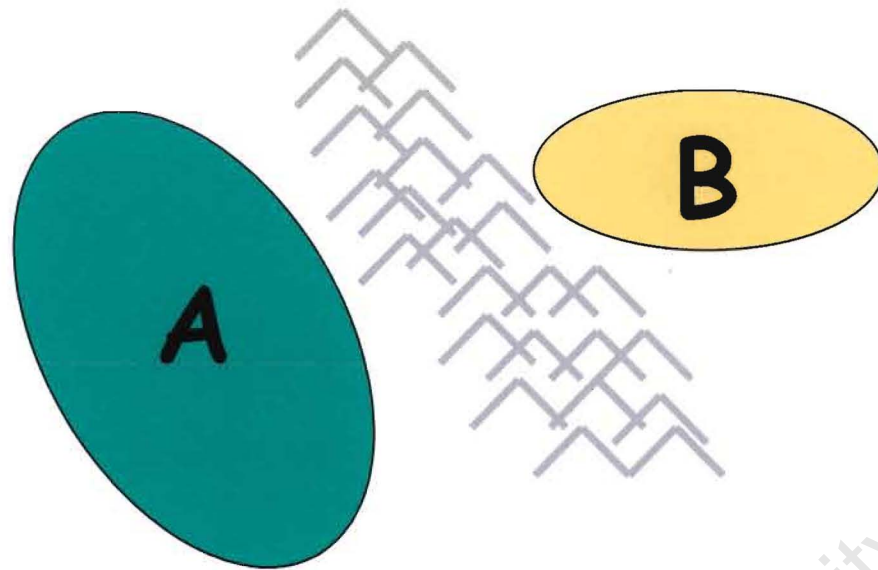


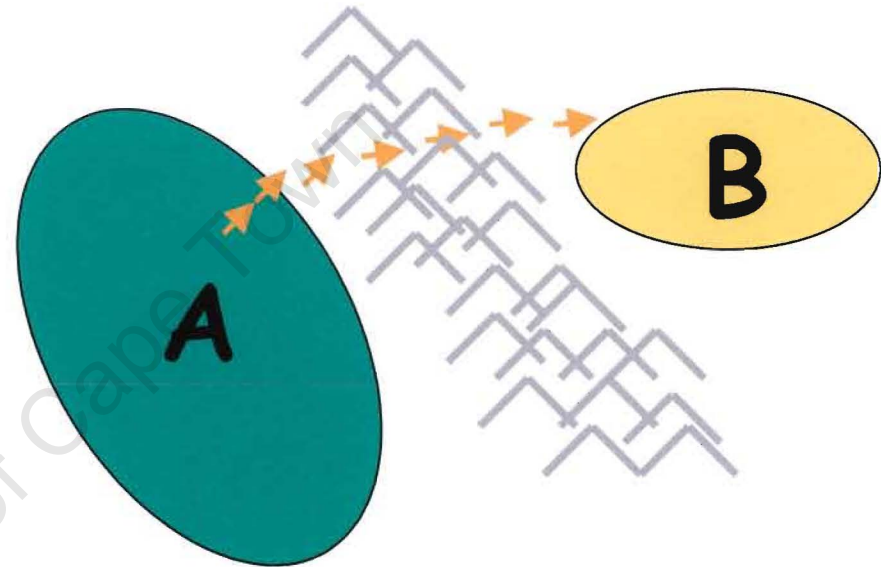
**FIG 1.2.** (A) Vegetation in relation to altitude on Africa's tallest mountains. (B) Schematic profiles of altitudinal zonation of vegetation on Africa's seven tallest mountains. Figures are after Kingdon (1989).

## Vicariance



Formation of the barrier  
induces isolation

## Dispersalist



Dispersal across an existing barrier with  
subsequent isolation

**FIG 1.3.** Graphical depiction of the alternative schools of thought on how divergence in isolation takes place



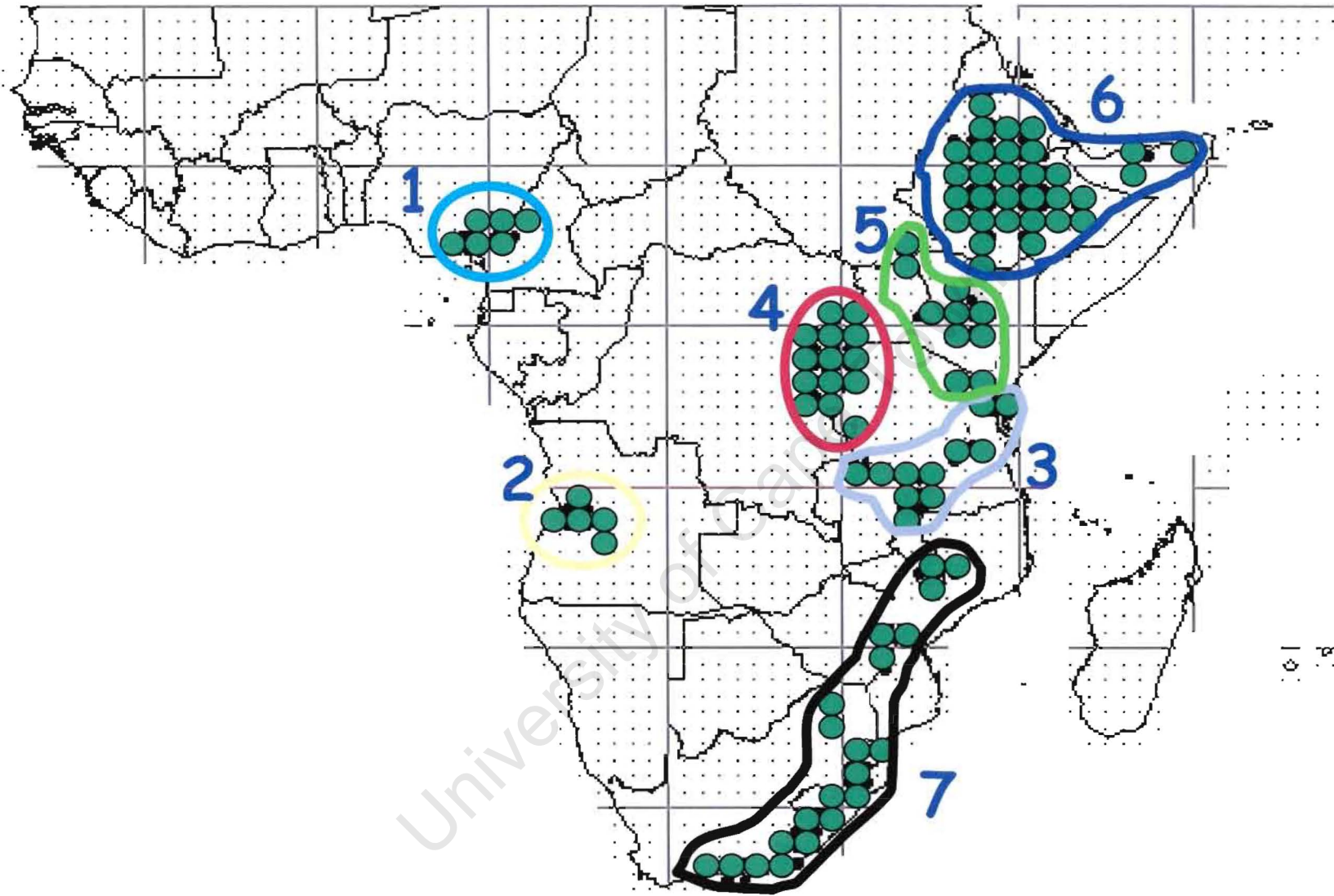


**FIG 1.4.** African montane areas of endemism for birds (after Moreau 1966, Dowsett 1986): (1) Cameroon Highlands, (2) Angolan Highlands, (3) Eastern Arc Mountains – Malawi, (4) Albertine Rift, (5) Kenyan Highlands, (6) Ethiopian Highlands and (7) Southeastern Africa.

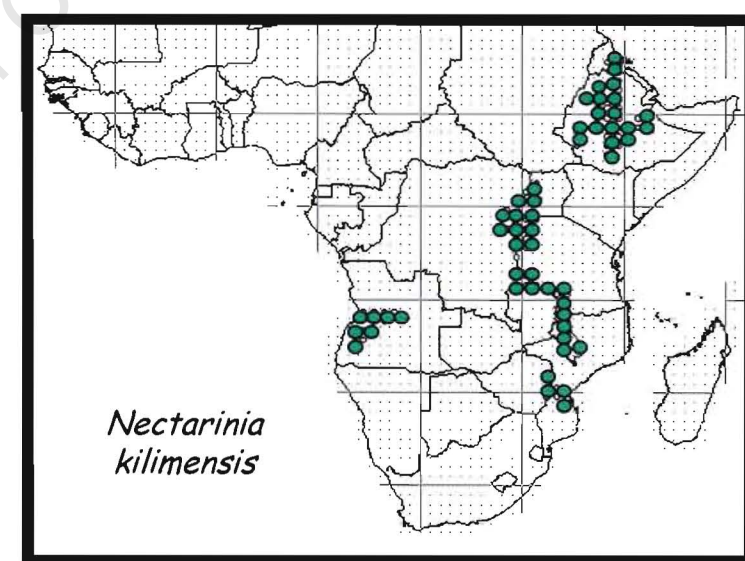
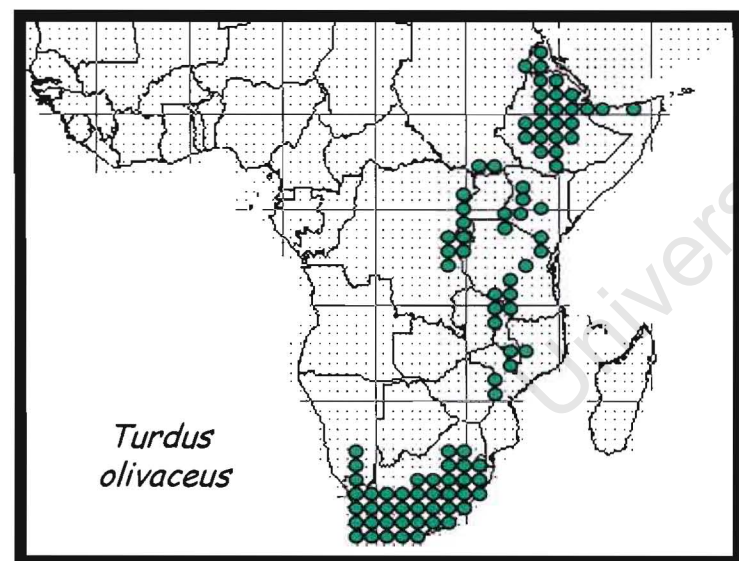
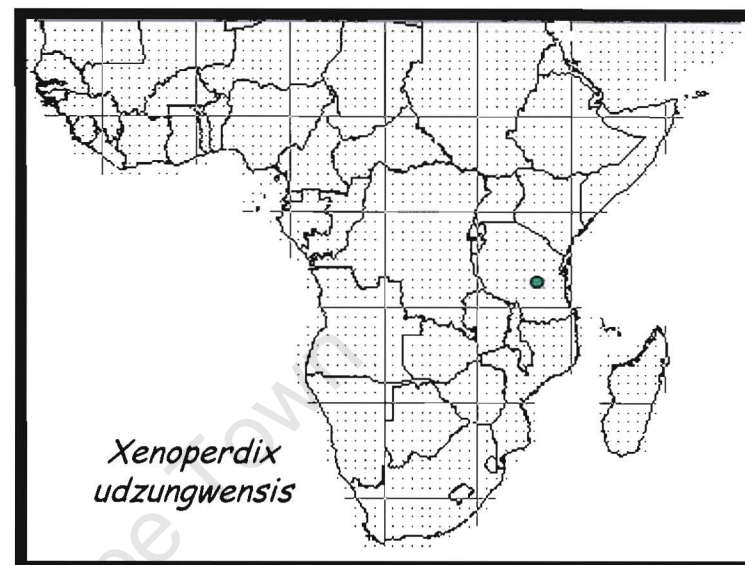
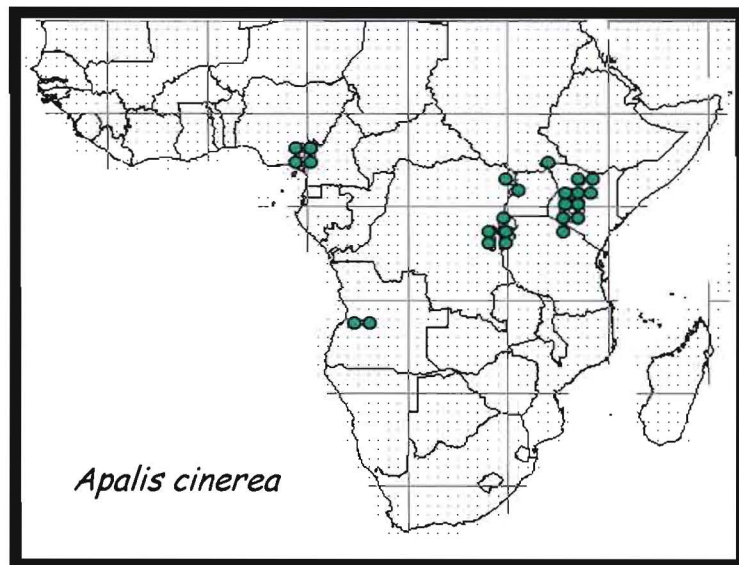
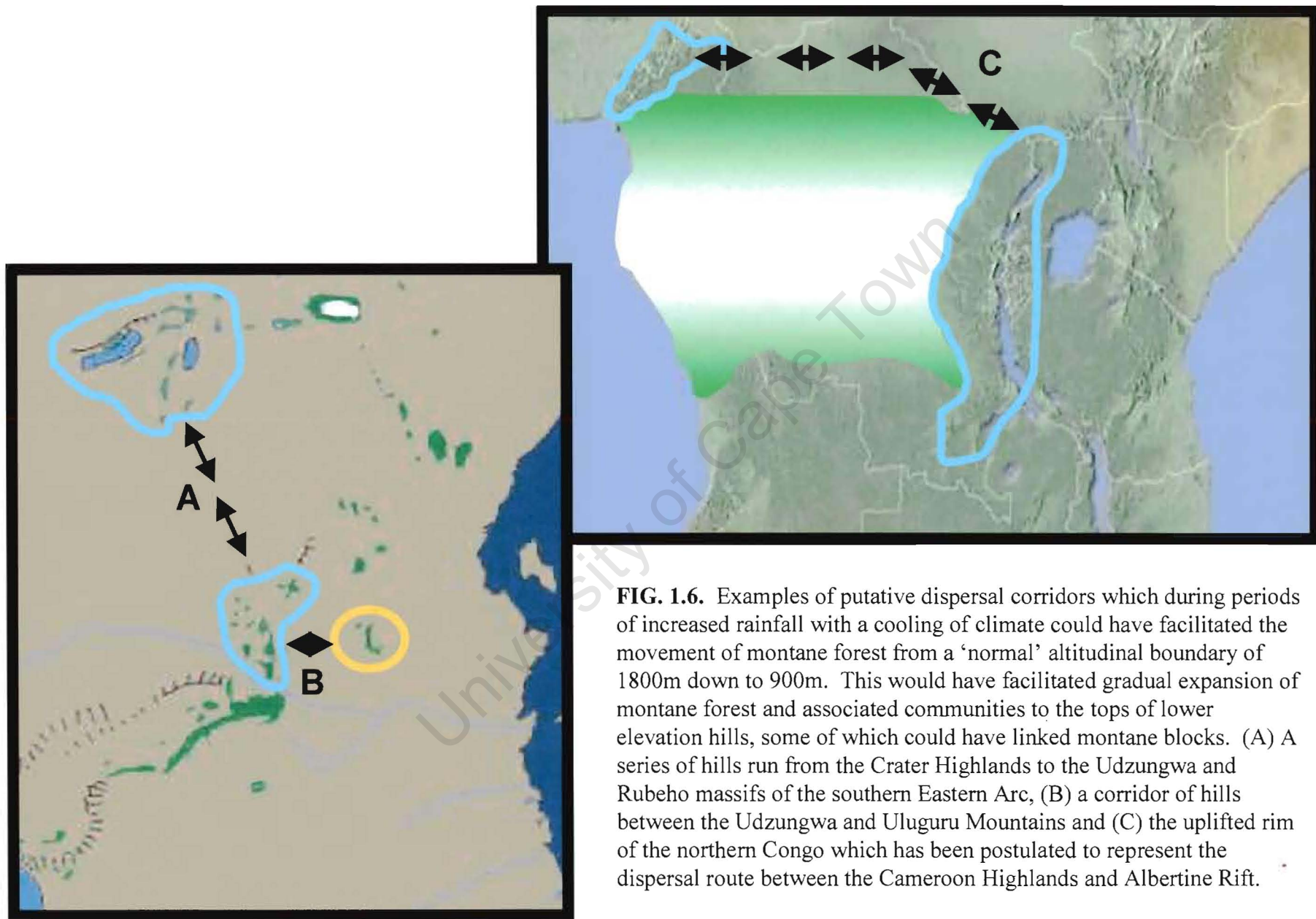
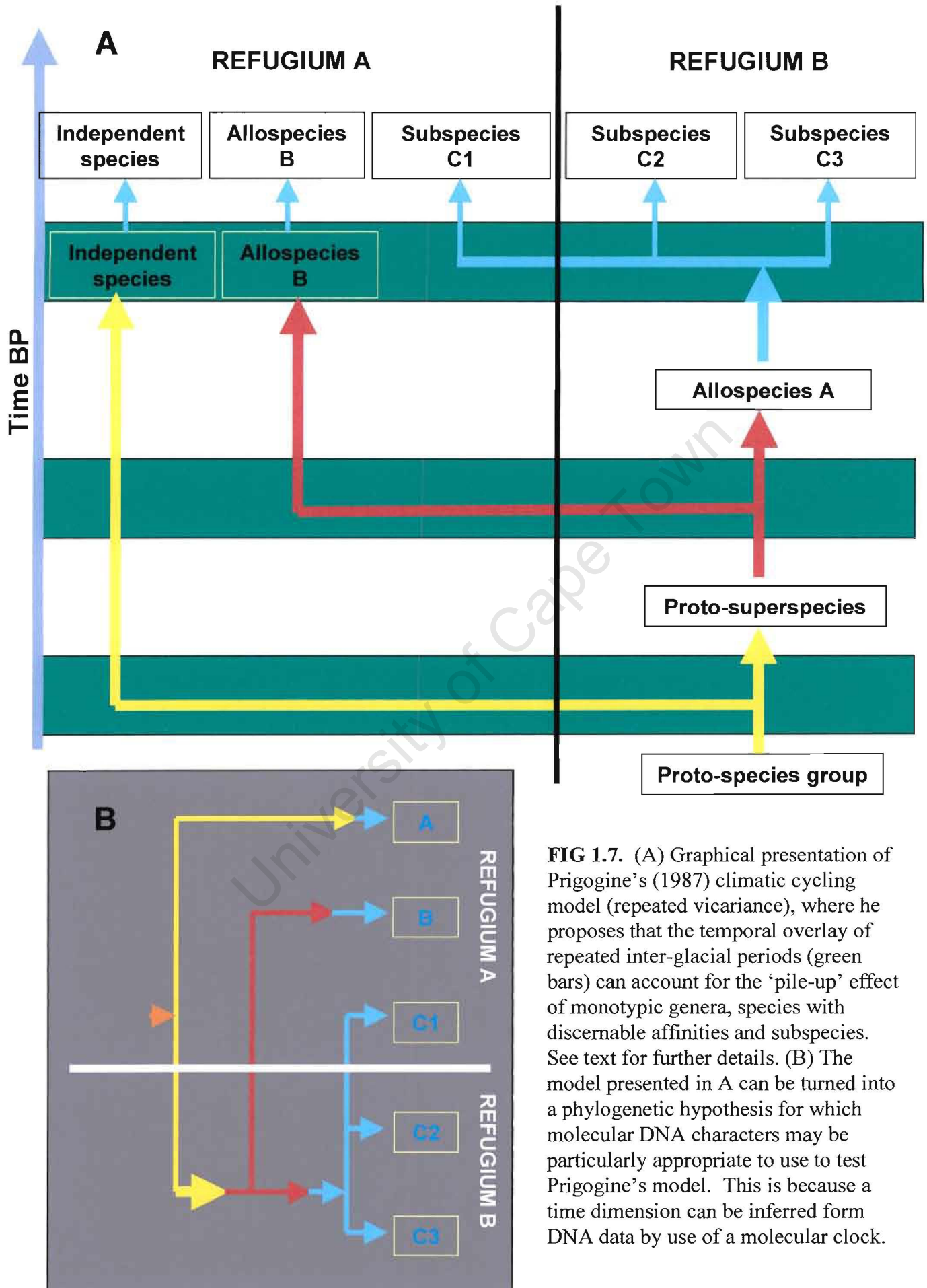


FIG 1.5. Patterns of distribution of four African montane birds.







**FIG 1.7.** (A) Graphical presentation of Prigogine's (1987) climatic cycling model (repeated vicariance), where he proposes that the temporal overlay of repeated inter-glacial periods (green bars) can account for the 'pile-up' effect of monotypic genera, species with discernable affinities and subspecies. See text for further details. (B) The model presented in A can be turned into a phylogenetic hypothesis for which molecular DNA characters may be particularly appropriate to use to test Prigogine's model. This is because a time dimension can be inferred from DNA data by use of a molecular clock.



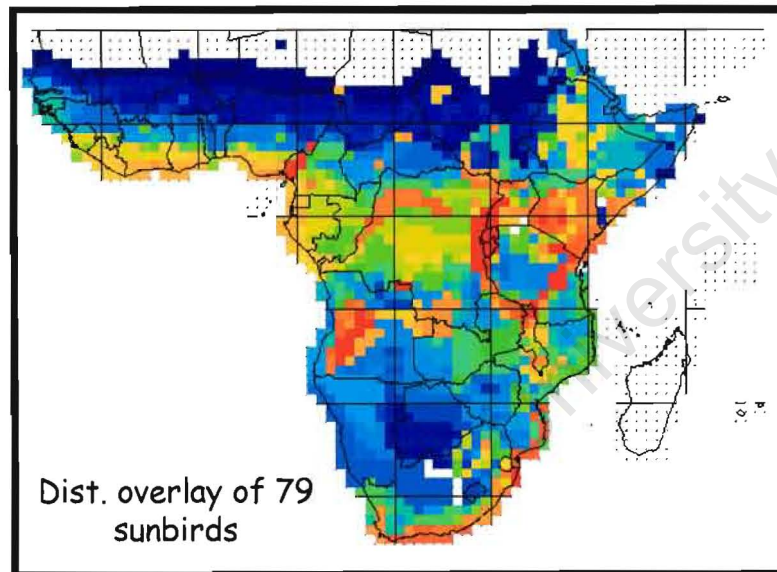
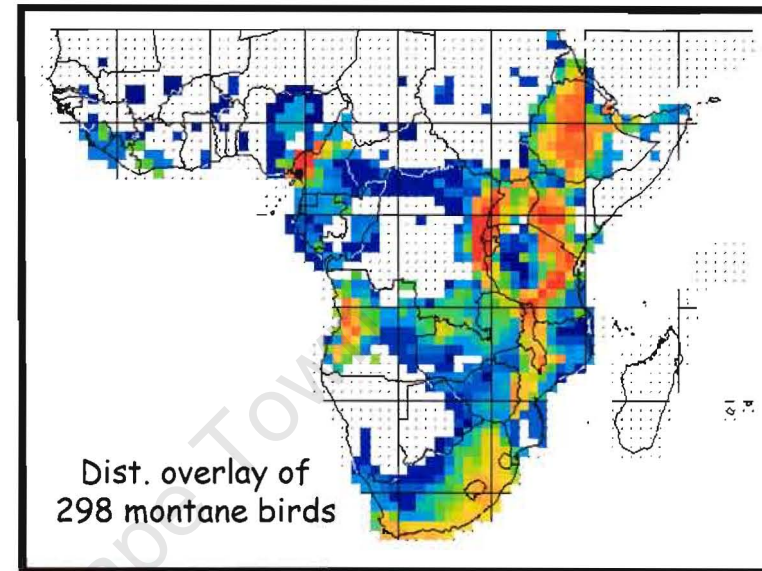
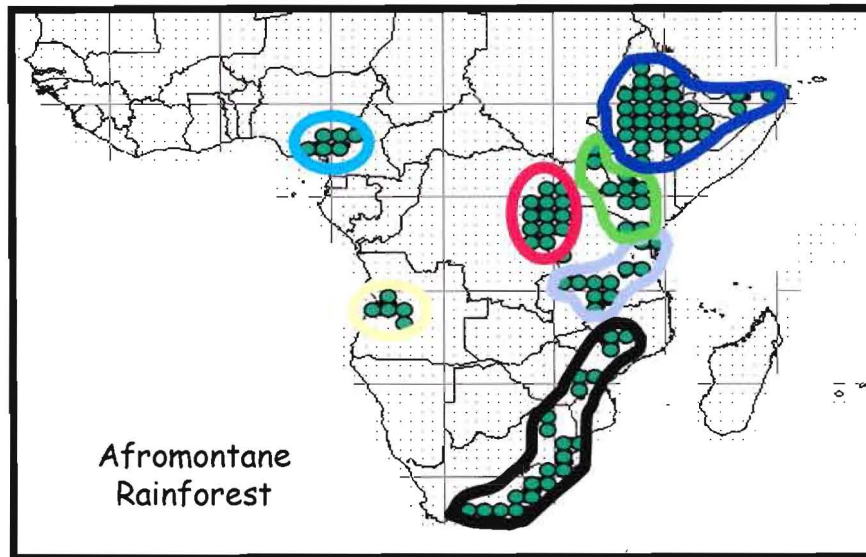


**FIG 1.8.** Utility of sunbirds (Nectariniidae) as model group with which to explore montane distributional patterns in Africa. As would be expected in the distributional overlay of the range distributions of 298 montane bird species (Table 1.1), areas of high species richness (yellow to red) closely match the seven demarcated areas of endemism. In a distributional overlay of the 79 species of African sunbirds, two of which are represented (A) *Nectarinia kilimensis* and (B) *Nectarinia reichenowi*, areas of high species richness closely matches that for montane birds in general.

## Chapter 2

### **Systematics and biogeography of the sunbirds (Aves: Nectariniidae) of the world: Aves largest genus (*Nectarinia*) takes a tumble**

#### **Summary**

Sunbirds are members of an Old World family (Nectariniidae) of small nectarivorous songbirds. Most species exhibit extreme plumage dimorphism with male sunbirds typically having bright metallic plumages. All members of the family have very similar skeletal structure and body plans. These similarities have made it difficult for any consensus to be established with regard to 1) the monophyly of the family, 2) the number of genera and 3) the taxonomic association among genera. Recent classification approaches have focused on bill variation as a key character and have considered plumage to be secondary when assigning species to genera. To address the above questions *ca.* 3000 bp of nucleotide data was collected from 68 sunbird species representing some 17 of the 18 currently recognised genera. A phylogeny of these taxa was constructed using both parsimony and Bayesian Inference algorithms. Parsimony and Bayesian Inference produced similar topologies for the mtDNA and nDNA datasets, as well as in the combined analyses. In general Bayesian trees were less resolved than the shortest trees obtained using parsimony. Posterior probabilities for clade splits greater than 95% ( $\alpha=0.05$ ) corresponded well with clades supported by bootstrap values of greater than 75%. Eleven to twelve dispersal events were recovered using dispersal-variance analysis. There is strong evidence for an Asian trans-Wallacean origin for the Nectariniidae. However, there is some evidence to suggest that a back-colonization from Africa to Asia, possibly via the Islands of the Indian Ocean has occurred more recently. With the exception of a back-colonization, dispersal events are restricted to within Asia or Africa, and a single vicariant origin for the African Nectariniidae is inferred. Very large sequence divergence values ( $>20\%$  for mtDNA and  $>6\%$  for nDNA) were recorded between the Asian gene *Arachnothera*, *Hypogramma*, *Dicaeum* and *Prionochilus*. Within African sunbirds, divergence among taxa

averaged between 9 and 17%, somewhat surprising for a group of birds, which are thought to have radiated during the Pleistocene. The results do not support recent taxonomic revisions of the Nectariniidae. Plumage characters may be more reliable than bill morphology when assigning species to a genus.

## INTRODUCTION

The recent paradigm shift towards supporting a Gondwana origin for passerine birds (Cracraft 1973, Hedges *et al.* 1996, Cracraft 2001, Barker *et al.* 2002, Ericson *et al.* 2002) has demanded a review of the current understanding of patterns of avian systematics and biogeography. The basis for much of this shift is associated with the use of molecular DNA which has provided novel characters from which phylogenetic hypotheses can be constructed (Barker *et al.* 2002, Ericson *et al.* 2002). Based on these hypotheses, it is increasingly apparent that the 'tapestry' of relationships among passerine birds, provided by Sibley and Alquist's (1990) DNA-DNA hybridisation data is in need of revision. One of the interesting hypotheses derived from using molecular markers to construct phylogenetic hypotheses for the origin of passerine birds, is that oscine passerines appear to have had their evolutionary origins in Australasia, and from there dispersed to colonize the globe (Barker *et al.* 2002, Ericson *et al.* 2002).

The sunbirds (Nectariniidae) are a group of small nectarivorous songbirds which provide an interesting model with which to test the hypothesis of an Australasian origin for oscine passerines. The Nectariniidae represent the basal branch of the Passeroidea radiation, which contains such well-known bird families as the Passeridae (includes weavers, sparrows, wagtails and pipits) and Fringillidae (includes buntings, honeycreepers, canaries and tanagers) (Barker *et al.* 2002). Sunbirds occur throughout sub-Saharan Africa, the islands of the Indian Ocean and extend across Asia and the Indonesian archipelago, with one species reaching northern Australia. Most sunbird species exhibit sexual dichromatism, with the males typically being larger and having bright metallic plumages. Sunbirds are primarily forest birds with many species having small to very small ranges. Furthermore, some species have adapted to a nectarivorous life-style in such diverse habitats, as semi-arid desert and montane heathland. Despite utilizing widely different habitats, sunbirds exhibit remarkable skeletal

uniformity (Farquhar *et al.* 1996), and have similar basic body plans. Structural similarity and corresponding lack of morphological characters, combined with highly unique and different plumages, has made it difficult for any consensus to be established on: the taxonomy, monophyly, phylogeny and biogeographic origins of the family.

If the flowerpeckers (*Prionochilus* & *Dicaeum*) are excluded from the Nectariniidae, as is well established by recognition of the Dicaeidae in many traditional classification schemes (Wetmore 1960, Rand 1967), then two-thirds of all sunbird species but none of the currently recognized genera are endemic to Africa. In contrast, three genera, *Arachnothera* (spiderhinters), *Aethopyga* (yellow-rumped sunbirds) and the Purple-naped Sunbird (*Hypogramma hypogrammicum*) are endemic to Asia-Australasia. The genera *Anthreptes* and *Nectarinia* are shared between Africa and Asia-Australasia. Mapping the distributions of these genera on to the phylogenetic topology obtained from Sibley and Alquist's (1990) DNA-DNA hybridisation analyses, suggests an Asian-Australasian origin for the family in support of the 'out of Australasia' hypothesis for the evolutionary origins of oscine passerines (Fig. 2.1). However, if the origins of the Nectariniidae lie in Asia-Australasia, how does one explain the incredible species endemism and morphological variation within the African Nectariniidae? Confronted with this problem, Irwin (1999) argued that the higher-level taxonomy of the Nectariniidae had been sorely neglected, undermining the recognition of evolutionary diversity within Africa. He 'rectified' this by using a phenetic approach to erect nine additional genera, bringing the total number of genera to 14, eight of which are restricted to Africa, four restricted to Asia-Australasia and two of which are shared. Irwin (1999) argues that the greater number of genera restricted to Africa, compared with Asia-Australasia provides support of an African centre of origin for the Nectariniidae. This is in direct contrast to the findings of Sibley and Alquist (1990). Which hypothesis is better supported is of fundamental importance to evaluating alternative hypotheses of oscine evolution.

This chapter has two key objectives. The first is to determine which sunbird taxa represent the deeper nodes within the Nectariniidae, so that the biogeographical

origins for the large and diverse assemblage of African sunbirds can be postulated. The second is to review the taxonomy of the Nectariniidae using a character based phylogenetic framework for the first time. Of particular interest is the validity of the split of what was the largest avian genus *Nectarinia* (Bock & Farrand 1980), into nine genera by Irwin (1999), whose classification has recently been adopted in 'Birds of Africa' (Vol. VI, ed. Fry & Keith 2001) and 'Sunbirds of the World' (Cheke *et al.* 2001).

To address these questions, three mitochondrial DNA (mtDNA) coding genes and a nuclear intron (nDNA) (total of 2722 base pairs) were sequenced from 68 ingroup species. The 68 species encompass all but one of the 18 genera recognised in recent arrangements of the Nectariniidae (Irwin 1999, Cheke *et al.* 2001, Mann 2002). The sugarbirds *Promerops*, are excluded from this study, as preliminary analyses place the two members of the genus well away from other members of the Nectariniidae (Bowie unpublished data). It will take much greater outgroup sampling, which is beyond the scope of this study, to resolve the phylogenetic affinities of *Promerops*.

The utility of two phylogenetic methods, parsimony (MP) and Bayesian inference (BI) are also compared. Search strategies implemented under MP attempt to find the best phylogenetic hypothesis based on the shortest number of steps (tree length). BI is fundamentally different, in that it does not attempt to obtain the optimal solution, but instead uses a Markov-Chain-Monte-Carlo (MCMC) methodology to sample phylogenetic trees in proportion to their posterior probability until the user defines a stopping point (Huelsenbeck *et al.* 2001, Lewis 2001). The BI analysis retains information about every tree and parameter visited during the search. The resulting distribution of trees can be examined to determine the posterior probabilities of branch-lengths, parameter estimates, and topology of clades; thus providing a time efficient model based approach to phylogenetic construction, particularly when large datasets are analysed as within this study.

### A brief review of sunbird taxonomy

Delacour (1944) was the first to revise the sunbirds as an entity, not adopting the earlier regional approaches of authors such as Shelley (1876-1880, 1900) for Africa. Using primarily bill and tongue characters, rather than plumage which he considered too variable to reliably delineate genera, he recognised 106 species in five genera: *Neodrepanis* (2 species), *Nectarinia* (66), *Anthreptes* (16), *Aethopyga* (13) and *Arachnothera* (9, Fig. 2.1). Subsequently, the Malagasy false-sunbirds (*Neodrepanis*) have been removed and are now classified within the family Philepittidae, and the Purple-naped Sunbird has been elevated to a distinct monotypic genus *Hypogramma* (Amadon 1951). Rand (1967) recognised 116 species and retained the basic five genera of Delacour (1944): *Anthreptes* (17 species), *Hypogramma* (1), *Nectarinia* (74), *Aethopyga* (14) and *Arachnothera* (10). Wolters (1977), in his revision of the family, made extensive use of plumage characters, recognising 97 species distributed among 25 genera. However, his classification has not been adopted in any major modern review.

Sibley and Alquist's (1990) studies based on DNA-DNA hybridisation recover the five genera of Delacour (1944) with modifications by Amadon (1951). However, they broaden the Nectariniidae to include the sugarbirds (genus *Promerops*), which they classify into one of two subfamilies, the Promeropinae. The second subfamily, the Nectariniinae is split into two tribes, the Dicaeini (flowerpeckers - which are traditionally classified within their own family the Dicaeidae and considered sister to the Nectariniidae), and the Nectariniini, which contains the traditional five genera attributed to the Nectariniidae. In their tribe Nectariniini, Sibley and Alquist (1990) added two additional species to *Anthreptes* and five more to *Nectarinia*, bringing sunbirds to a total of 122 species. One new species of *Aethopyga* has since been described (Kennedy *et al.* 1997). With a total of 79 species, the genus *Nectarinia* has for many years been considered the largest avian genus (Bock & Farrand 1980).

Irwin (1999), using a phenetic approach recently reviewed the classification of African sunbirds, and split *Nectarinia* into nine genera, eight of which are endemic to Africa. Irwin (1999) considers *Anthreptes* to be the most ancient genus because it possesses a short and unspecialised bill morphology. He also



modifies *Anthreptes* by separating *Anthreptes fraseri* into a monotypic genus *Deleornis*, in recognition of its warbler-like behaviour and insectivorous diet. *Anthreptes collaris*, *platyura*, *metallica* and *pallidigaster* are split and included in the resurrected genus *Hedydipna*.

Irwin (1999) considered the Asian-Australasian genera *Aethopyga*, *Arachnothera* and *Hypogramma* to be derived from an *Anthreptes/Deleornis*-like ancestor due to the curvature of the bill starting at the base of the skull and not from the cranial-facial slit, a character he orders as the primitive state. Although Irwin (1999) did not specifically construct a phenogram to suggest relationships among genera, he did state that the description of the genera follow a 'phyletic sequence'.

Therefore, I have attempted to construct a topological arrangement of the genera (Fig. 2.1). Irwin (1999) argues that with the adoption of his classification, more genera become endemic to Africa than Asia, and therefore, Africa should be considered the locale for the origin of the Nectariniidae. However, I believe that due to only a superficial consideration of the Asian-Australasian taxa by Irwin (1999), and the lack of a clear topology of relationships among genera, Irwin (1999) missed one of the key predictions of his revision. An overlay of distributional data on to the topology constructed in Figure 2.1 suggests that if Irwin's (1999) classification is adopted, then there must have been at least three colonisation or dispersal events between Africa and Asia. The first is needed to explain the placement of *Aethopyga*, *Arachnothera* and *Hypogramma*, the second to account for *Leptocoma*, which Irwin (1999), and Delacour (1944) consider to be derived from an *Chalcomitra*-like ancestor, and the third to explain the mixing of Asian-Australasian and African taxa belonging to the genus *Cinnirys*. Irwin (1999) does not mention the dispersal hypotheses underpinning his classification, which are in stark contrast to the findings of earlier authors (Delacour 1944; Rand 1967; Sibley & Alquist 1990) whose classifications of the Nectariniidae have in common three genera endemic to Asia-Australasia, all basal, with the remaining two genera shared between Asia-Australasia and Africa, suggesting that the African taxa are derived from an Asian-Australasian ancestor/s (Fig. 2.1).

## METHODS

### Taxon Sampling

Nucleotide sequence data was collected from 123 individuals representing 70 currently recognized species (68 ingroup) (Table 2.1). When possible, two individuals from each taxon were sequenced for each gene region. Photographic archives and/or voucher specimens are housed for each individual at the respective institutions listed in Table 2.1. *Corvus albus* and *Turdus abyssinicus* were chosen as outgroups, as they are oscines not closely related to the Nectariniidae (Barker *et al.* 2002).

### Laboratory procedures

DNA was extracted from frozen tissues or blood using a Puregene DNA isolation kit (Gentra Systems, Minneapolis, Minnesota) following the manufacturer's animal tissue protocols, but with an overnight Proteinase K digestion at 55°C. Three mtDNA genes, NADH2 (ND2), NADH3 (ND3) with flanking tRNAs (Glycine & Arginine) and ATPase 6 (ATP6), and one nuclear intron, Beta-Fibrinogen Intron 5 (Fib5), were PCR amplified under standard conditions (denaturation at 94°C, annealing at 50-54°C, and extension at 72°C) and the primers listed in Table 1.2. PCR products were electrophoresed on 1.5% low-melting point agarose gels (FMC Bioproducts), stained with ethidium bromide and visualized under UV light. Amplicons of the appropriate length were cut out of the gel and purified using the GELase™ Agarose gel-Digesting Preparation and the 'fast protocol' method (Epicentre Technologies, Madison, Wisconsin). The purified product was cycle-sequenced using Big Dye terminator chemistry (Applied Biosystems, Inc [ABI]). Cycle-sequencing reactions were precipitated with 3M ammonium acetate or 100% isopropanol, rinsed in 70% ethanol, dried and re-suspended in formamide-EDTA solution, and run on an ABI 377 or ABI 3100 automated DNA sequencer.

Sequences were always obtained from both strands of DNA with most gene regions being sequenced at least twice for each species. Nuclear copies (*numts*) of a number of mtDNA genes have been reported in birds (Arctander 1995,

Quinn 1997). The following precautions were taken in an attempt to avoid the amplification of *numts*. (1) Most DNA extracted and PCR amplified in this study was derived from tissue and not blood, which Quinn (1997) suggests is more prone to *numt* contamination. (2) Large fragments of the gene regions were PCR amplified even when internal primers were used for cycle-sequencing. (3) All mtDNA sequences were checked using the program Sequencher 3.0 (Gene Codes Corp), and aligned to the chicken (*Gallus gallus*) mtDNA sequence (Desjardins & Morais 1990) to check for the presence of any insertions or deletions characteristic of *numts*. (4) Sequences were translated into their amino acids and screened for termination codons. (5) Each mtDNA gene region was examined separately for deviation from 'normal' base composition. A few *numt* sequences were easily identified for ND3, but as a whole the lack of insertion or deletions, high Guanine biased base composition, and lack of termination codons, allows moderate confidence that nuclear pseudogenes were avoided. All intron sequences were screened for the presence of conserved exon sequences at both the 3' and 5' ends, to ensure that the whole intron was sequenced and that any length variation was due to the presence of insertions or deletions (indels).

When DNA sequence data are collected from nuclear genes two potential problems arise: (1) length variation between alleles, and (2) heterozygosity. When alleles differ due to an indel causing a frame shift in one allele relative to the other, it is not possible to sequence using standard techniques. To overcome this problem, PCR products from such individuals were cloned using the TOPO cloning kit (Invitron Inc.) and multiple clones (6 to 10) were cycle-sequenced. A total of 10 species were cloned. Most alleles differed by only 1 or 2 bp in length, the largest difference was a 16 bp insertion in one of the alleles of *Cinnyris. minulla* (both individuals). Both alleles were included in initial maximum parsimony analyses. In all instance the two alleles from a single individual clustered together with high bootstrap support. Consequently, the allele without the unique insertion or deletion was used in the final analyses. Bases which are heterozygous among alleles were easily detected by the presence of double-peaks in the chromatograms. These differences were represented in the alignment with ambiguity codes or as missing data.

## **Alignment**

Sequences for the mtDNA and nDNA data partitions were first aligned using Clustal X (Thompson *et al.* 1994). The initial alignment of FIB5 was edited by eye to minimize the number of gaps resulting from indels. Indels ranged from 1 bp to 201 bp, with a number of indels being shared among taxa. Because some of these indels were so large it was not possible to recode them as binary characters. Instead indels were treated as missing data in the MP analyses, and were mapped onto the obtained topologies to assess their utility for support of specific nodes within the phylogeny.

## **Analyses**

### ***Base composition***

The base composition for each gene region and various data combinations was estimated using Modeltest 3.06 (Posada & Crandall 1998). Because base composition has been shown to confound methods of phylogenetic inference (Collins *et al.* 1994, Swofford *et al.* 1996), homogeneity of nucleotide composition was analysed for each gene region and dataset combination using a chi-squared test of nucleotide frequencies across all taxa as implemented in PAUP\* version 10b (Swofford 2002).

### ***Testing congruence between data partitions***

The heterogeneity of different gene regions and dataset combinations were assed using the incongruence length difference test (ILD test, Farris *et al.* 1995), as implemented in PAUP\*. Invariant sites were removed, as suggested by Cunningham (1997), and 100 replicates were used for each test.

### ***Phylogenetic analyses of data partitions***

Data from each gene region was analysed separately to (1) assess the relative level of phylogenetic signal in each partition, (2) examine the effect of data saturation (homoplasy), and (3) explore the potential contribution of each data partition in combined analyses. All three mtDNA gene regions, individually and in combination, as well as the nuclear intron, were analysed using maximum parsimony (MP) as conducted with the Parsimony Ratchet (Nixon 1999). Search options for the MP ratchet were *ca.* 10 % of the characters for each data partition

were removed during each of 1000 random addition replicates with five trees were held at each iteration, and full tree-bisection-reconstruction (TBR) branch-swapping was implemented. The MP ratchet was conducted using NONA (Goloboff 1999) running under the WINCLADA interface (Nixon 1999-2002). For the mtDNA dataset combination (ND2, ND3 & ATP6) and the nuclear intron (Fib5), MP analyses were also carried out using heuristic searches with stepwise addition and 1000 random addition replicates as implemented in PAUP\*. Heuristic search parameters were: all characters unordered, uninformative characters excluded, TBR branch swapping, steepest descent option not in effect, zero branch lengths collapsed to polytomy, MULPARS option in effect, and topological constraints not enforced.

Saturation within each mtDNA gene region both individually and in combination was analysed by plotting transition (Ti) and transversion (Tv) differences between pairs of taxa against their Kimura-2-parameter distances (Kimura 1980). A dataset was considered saturated if the plot demonstrated, either (1) a levelling-off of the data points, or (2) ingroup comparisons were equal or greater than outgroup comparisons. To compare relative rates of substitution between the combined mtDNA data partition and Fib5, sequence divergence values for all pairwise comparisons for mtDNA were plotted against those for Fib5. A third order regression was fitted to these data and the derivative at the origin was derived as a heuristic estimate of the relative rate of substitution between the two data partitions (after Johnson & Clayton 2000).

For saturated data partitions MP analyses were conducted under several third position transition weighting schemes, to evaluate the sensitivity of tree topology to saturation. Nodal support for each gene region and dataset combination was estimated using 1000 bootstrap replicates (Felsenstein 1985), with one random addition replicate per iteration, and full TBR branch-swapping when using PAUP\*, or 5 random addition replicates per iteration, with full TBR when using NONA.

The computer program Mr Bayes 2.01a (Huelsenbeck & Ronquist 2001) was used to conduct a Bayesian approach to phylogenetic inference. Four

Metropolis-coupled MCMC chains (one cold and three heated chains) were run simultaneously to optimise efforts to find peaks in tree-space. To check that equilibrium had been reached, the fluctuating value of the log-likelihood was graphically monitored in Excel (Microsoft). This search strategy was repeated five times (four runs of 1 million generations and one run of 2 million generations), with each run beginning from a random tree. The General-Time-Reversible model of nucleotide substitution with a gamma distribution (estimated using four rate categories) and invariable sites (GTR + I + G) was used in the Bayesian analyses (model selected using Modeltest, Posada & Crandall 1998). A Dirichlet distribution was assumed for estimation of the base frequency parameters and an uninformative (flat) prior was used for the topology. Trees were sampled every 100 generations, resulting in a sample of 10001 or 20001 trees for the 1 million and 2 million generation runs, respectively. The number of cycles to discard (the burn-in) was estimated empirically from the log-likelihood plots.

### ***Combined evidence***

All data partitions were combined in a total evidence analysis. To assess the effects of saturation on tree topology, MP analyses were conducted using several third position transition weighting schemes for the mtDNA data partition. All intron characters were given the same weight as 3<sup>rd</sup> position transversions and first and second mtDNA codon positions. Heuristic searches with 1000 random addition replicates were conducted as described for the individual data partitions above. Nodal support was evaluated using 1000 bootstrap replicates for heuristic searches and the parsimony ratchet as described above. Bayesian analyses were conducted for the total evidence dataset as described for the data partitions, except that only three chains (one cold, two heated) were run due to memory constraints (even with 1.2 Giga-bites of RAM!). Seven runs, four of 1 million, two of 2 million and one of 5 million generations were conducted with a sampling frequency of every 100 generations.

### ***Ancestral areas***

To establish the centre of origin for the Nectariniidae, the fully resolved MP phylogeny (Fig. 2.10) was converted into an area cladogram. Because the

hypothesis being tested was whether the Nectariniidae have an Africa or Asian-Australasian centre of origin, only broad areas were defined. In accordance with its significance in avian biogeography, Wallace's Line (Wallace 1860, Mayr 1944, Keast 1981, White & Bruce 1986, Barker *et al.* 2002) was used to delimit the Australo-Papuan region referred to as (1) cis-Wallacea (Australia, New Zealand, New Guinea and the Indonesian Islands on the Australo-Papuan side of Wallace's Line as defined by Coates and Bishop (1977), from (2) trans-Wallacea, which refers to the rest of Indonesia and Asia (in this study); (3) Africa, the (4) Western Indian Ocean Islands were included as an area due to hypotheses that these islands are occupied by lineages of mixed Asian and African ancestry (Benson 1984, Louette 1992), and finally (5) the Levant, which is the extreme corner (Israel & Jordan) of the Mediterranean. Dispersal-vicariance analysis (DIVA, Ronquist 1996, 1997) was used to construct ancestral distributions on the phylogeny, and to estimate the number of dispersal events required to explain the present distribution patterns of the Nectariniidae (for more details see Voelker 1999a).

### ***Testing for monophyly***

Monophyly of different clades was tested using a BI approach. The number of times a split (node) is recovered is directly proportional to the posterior probability of that split. Thus in the BI analyses, the probability of support for the monophyly of clades of interest was assessed by filtering the post burn-in posterior distribution of trees. This approach is possible because the Markov chain has the useful property of sampling trees in proportion to their posterior probabilities (Lewis 2001). The Templeton (1983), and Kishino and Hasegawa (1989) tests were not used to compare competing topologies, because these tests have been shown to be statistically invalid if topologies have not been *a priori* defined (Goldman *et al.* 2000, Buckley *et al.* 2001), and the Shimodaira-Hasegawa test (Shimodaira & Hasegawa 1999) could not be used because a parsimony equivalent version of this test is not presently available.

## RESULTS

### Base composition and nucleotide model parameters

The base composition of the three mtDNA genes is typical of that for mtDNA in birds (Fig. 2.2; Hunt *et al.* 2001, Kirchman *et al.* 2001, Price & Lanyon 2002), with a deficiency of Guanine and Thymine relative to Adenine and Cytosine. In contrast, the composition of Fib5 is more homogeneous, with Cytosine in lowest abundance. Homogeneity of base composition across taxa was not rejected in either the mtDNA or nDNA datasets (mtDNA  $\chi^2=207$  *d.f.*=207 *P*=0.485; nDNA  $\chi^2=24.5$  *d.f.*=207 *P*=1.00). The marginal rates, proportion of invariable sites, and gamma shape parameter estimated from the 5 million generation BI run were very similar to those obtained from the hLRTs as implemented in Modeltest for the mtDNA and nDNA data partitions.

### Partition variability

The mtDNA and nDNA data partitions had similar numbers of variable sites, 57.2% and 51.5% respectively (Fig. 2.3). However, this variability was partitioned markedly differently; 50.1% of the sites within the mtDNA partition were parsimony informative (p-informative), compared with a more even split of 25.9% variable and 25.6% p-informative sites within the nDNA data partition (Fig. 2.3). A total of 21 indels (19 deletions and 2 insertions) were detected within the 609 bp Fib5 alignment. Only four of the deletions were shared among more than one taxon (Table 2.4).

Although sequence lengths differed among the three mtDNA genes analysed (ATP6, ND2 and ND3) it is nonetheless useful to compare relative levels of genetic variability among genes for different codon positions. The 3<sup>rd</sup> codon position sites of all three mtDNA genes were over 98% variable and over 96% p-informative (Fig. 2.3). In contrast, less than 18% of 2<sup>nd</sup> and 53% of 1<sup>st</sup> position sites were p-informative, respectively. For ND2, considerably more 1<sup>st</sup> codon position sites were p-informative relative to ATP6 and ND3 (52.6% vs. 36.4% and 35.0%).



### Saturation plots and sequence divergence

In all three mtDNA data partitions there is a clear levelling off for third position transitions, suggesting that these codon positions are saturated (Fig. 2.4). First and second position transitions, and for all codon positions transversions, appeared not to be saturated. Neither transitions nor transversions were saturated for the nDNA data partition (Fig. 2.4). Average pairwise Kimura-two-parameter (K2P) sequence divergence distances among currently recognised genera (Irwin 1999, Cheke *et al.* 2001) are summarised in Table 4.5. Comparison of pairwise sequence divergence values for the combined mtDNA data partition with those from the nDNA (Fig 2.5) indicated that mtDNA evolves approximately 8.4 times faster than Fib5.

### ILD tests

Incongruence length differences (ILD) tests were performed for each pairwise combination of data partitions to assess levels of heterogeneity among data partitions (Table 2.6). Tests between ND3 and the other two mtDNA data partitions, ATP6 and ND2, indicated that significant heterogeneity existed, most likely as a consequence of the small number of base pairs in ND3 compared with the other two mtDNA genes. Consequently, I did not consider it inappropriate to combine ND3 with ND2 and ATP6 into a larger mtDNA data partition. ILD tests between the FIB5 data and the mtDNA genes (separately and combined) did not indicate that significant heterogeneity existed among these data partitions (Table 2.6).

### Phylogenetic analyses of data partitions

Individual analyses of each equally-weighted mtDNA data partition using the parsimony ratchet recovered two equally most parsimonious trees for ND2 (not shown, length = 9993, CI = 0.15, RI = 0.34), five trees for ATP6 (not shown, length = 5442, CI = 0.15, RI = 0.31) and 35 trees for ND3 (not shown, length = 2910, CI = 0.17, RI = 0.36). Using the most recently suggest taxonomic arrangement for the Nectariniidae (Irwin 1999, Cheke *et al.* 2001, Mann 2002), in all three analyses the Asian genera *Dicaeum*, *Prionochilus*, *Hypogramma* and *Arachnothera* formed the basal clades of the Nectariniidae relative to the remaining ingroup taxa. In all but the ATP6 analysis, where *Chalcoparia* was

sister to *Anthobaphes*, *Aethopyga*, and *Leptocoma*; *Chalcoparia* and *Anthreptes malacensis* formed a clade sister to the large assemblage of African sunbirds. This larger assemblage includes only a single Asian-Australasian species, *Cinnyris jugularis*. Within the primarily African sunbird assemblage, there was limited consistency in inferred phylogenetic affinities among the three mtDNA partitions, perhaps not unexpected given the limited number of base pairs of each individual mtDNA gene region, and the small number of characters along deeper nodes. Therefore, instead of describing how the mtDNA partitions differ in great detail, emphasis is placed on interpreting results from combined analyses of the three mtDNA partitions (2113bp) and how these results contrast with the topologies inferred from analyses of the nDNA data partition.

Equally-weighted MP analysis of the combined mtDNA (ATP6, ND2 and ND2) dataset recovered two trees (not shown) of 10277 steps (CI = 0.206, RI = 0.356). The two trees differed in only the relative position of one terminal branch. When 3<sup>rd</sup> position transitions were down-weighted relative to 3<sup>rd</sup> position transversions by the empirical estimate of 3.6 times (3.6x, calculated using PAUP\* Swofford 2002), one most parsimonious tree was recovered of 21546.8 steps (CI = 0.230, RI = 0.434; Fig. 2.6). The deeper nodes of the equally-weighted and weighted topologies are generally similar, with *Dicaeum* and *Prionochilus* sister to *Hypogramma* and *Arachnothera* (Fig. 2.6, node A) although with poor support (<50% bootstrap). In the weighted MP analysis, *Hypogramma* clusters with *Arachnothera affinis* and *magna* (node B), and in the equally-weighted MP analysis with *Arachnothera longirostra* and *robusta*. In both cases, *Arachnothera* is rendered polyphyletic by *Hypogramma*. Three further clades of Asian-Australasian taxa (nodes C1-3) occur towards the base of the MP tree (Fig. 2.6). In the weighted analysis, *Leptocoma* (C1) is basal relative to *Chalcoparia* and *Anthreptes malacensis* (C2), which is sister to *Aethopyga* (C3), although with less than 50% bootstrap support. In the equally-weighted MP analysis, *Aethopyga* (C3) is basal relative to *Leptocoma* (C1) and *Chalcoparia* plus *Anthreptes malacensis* (C2), but still with low bootstrap support (<50%).

The African sunbirds plus one Asian-Australasian species (*Cinnyris jugularis*) form a single, large, well-supported (97%, 96% bootstrap for 3.6x and 0x,

respectively) assemblage (node D, Fig. 2.6). Within this primarily African assemblage of sunbirds, three major clades are apparent (nodes E1-3). The most basal clade (E1) consists of *Anabathmis reichenbachii*, *Anthobaphes violacea* and most members of the Double-collared group of *Cinnyris* (excludes *C. chloropygia*, *C. minulla* and *C. pulchella*). Terminal to node E1 is a clade (E2), which has *Hedydipna platura* basal relative to the three species belonging to the violet-backed group of *Anthreptes* (*A. longuemarei*, *neglectus* and *orientalis*). The remaining taxa form a large but diverse assemblage of sunbirds (E3), with members belonging to the genera *Anthreptes*, *Deleornis*, *Hedydipna*, *Dreptes*, *Cyanomitra*, *Chalcomitra*, *Nectarinia* and *Cinnyris*.

Within the large assemblage of primarily African sunbirds (node E3) a number of groups of taxa are consistently recovered in both the weighted and equally-weighted MP analyses. However, relationships among groups are poorly supported, and are largely either inconsistent among analyses, or unresolved. *Hedydipna collaris* and the Asian-Australasian *Cinnyris jugularis* form a well-supported (>80% bootstrap) clade (node F), which is sister to two weakly associated clades (<50%). The first, node G, comprises a mixed assemblage of *Dreptes thomensis*, *Chalcomitra balfouri* and, members of the White-bellied and Purple-banded groups of *Cinnyris*, *C. venusta* and *C. osea*, respectively. This clade is sister to an assemblage of Indian Ocean endemics (node H), with the exception of *fusca*, which is endemic to the arid west of southern Africa and is another member of the White-bellied group of *Cinnyris*.

The velvety sunbirds, genus *Chalcomitra*, are recovered (node I), but interestingly this genus appears to include the Indian Ocean endemic *Cinnyris notata*. A weak association (<50%) is suggested between *Chalcomitra* and the coppery sunbirds (node J), which themselves encompass a diversity of forms; three members of the genus *Nectarinia*, and three members of *Cinnyris*, which in turn each belong to a different subgroup – the Double-collared, Purple-banded and Miscellaneous groups of Cheke *et al.* (2001). The remaining two members of *Nectarinia*, the malachite sunbirds *N. famosa* and *N. johnstoni*, (node O) cluster with another large group of African sunbirds, containing *Cinnyris chloropygia*, *C. minulla* (node N) that have been traditionally considered part of

the Double-collared group of *Cinnyris* (Irwin 1999, Cheke *et al.* 2001), and the Blue-green Headed sunbirds, genus *Cyanomitra* (node M). The two west-central African 'green' sunbirds (node K) *Deleornis fraseri* and *Anthreptes seimundi*, which are split into different genera by Irwin (1999) based on bill-shape, parallel the plumage characters by clustering together with high bootstrap support (92%). Lastly, the suggested phylogenetic affinities of *Cyanomitra olivacea* with *Anthreptes reichenowi* (node L) and, *Cinnyris rufipennis* with node K, are unexpected based on analyses using plumage characters (Bowie unpublished data).

Doubling the down-weighting of 3<sup>rd</sup> position transitions relative to transversions (7x) recovered two MP trees of 36252 steps (CI = 0.241, RI = 0.459). The topology is almost identical to that obtained under the 3.6x 3<sup>rd</sup> position Ti/Tv weighting scheme (Fig. 2.6), with the exception that *Anthreptes malacensis* and *Chalcoparia* (node C2) become basal relative to *Leptocoma* (node C1) and *Aethopyga* (node C3), although bootstrap support remains less than 50%. The remaining nodes depicted in Figure 2.6 are recovered, but a large polytomy is formed among the African sunbirds (nodes F to O). Further down-weighting of 3<sup>rd</sup> position transitions (by 10x Ti/Tv) recovered the same two trees as in the 7x 3<sup>rd</sup> position Ti/Tv weighting scheme. No significant changes in bootstrap support were noted as down-weighting of 3<sup>rd</sup> position transitions was increased. The parsimony ratchet was used as an alternative MP search strategy to the more time-consuming heuristic search. A search with 1000 random addition replicates on the equally-weighted whole mtDNA dataset (2113bp) recovered one tree of 18727 steps (CI = 0.15, RI = 0.32, tree not shown), which had a topology similar to that obtained in the equally-weighted MP heuristic search. However, this tree is considerable longer than the two most parsimonious trees recovered of 10277 steps using a heuristic search (not shown).

For the BI analyses of the combined mtDNA the log-likelihood values of recorded topologies were plotted (not shown) and a burn-in value of 500 trees or 50 000 generations were extrapolated. The topologies and posterior probabilities (Fig. 2.7) obtained among the five BI runs for the mtDNA dataset were identical and did not differ when the search was run for 1 or 2 million generations. The

topology obtained from the BI analyses of the mtDNA data partition (Fig. 2.7) is generally similar to that from the 3.6x 3<sup>rd</sup> position Ti/Tv down-weighting MP tree, but less resolved among the large ‘African’ sunbird assemblage (nodes F to O). The only major difference among the deeper clades is that *Chalcoparia* (node C2a) now forms a clade basal relative to *Anthreptes malacensis* (node C2b), *Leptocoma* (C1) and *Aethopyga* (C3) although poorly supported with a posterior probability of 82%.

Analysis of FIB5 using a MP heuristic search quickly exceeded the maximum number of trees (110200) that could be stored in memory. An example of one of these trees is presented in Figure 2.8, which is identical to the strict consensus, with the exception that the two nodes marked with an X were collapsed. Using the parsimony ratchet, 556 trees of 915 steps (CI = 0.68, RI = 0.75) were recovered, a strict consensus of which has the same topology as the MP heuristic search. As for the mtDNA analyses, the nDNA tree recovers *Dicaeum* and *Prionochilus* at the base of the tree (node A), but differs from the mtDNA analyses in that *Hypogramma* (node B1) forms a clade on its own, and separate from *Arachnothera* (node B2 and B3), which in the strict consensus forms a trichotomy with *Chalcoparia* (node C2a). Again, as in the mtDNA analyses, *Anthreptes malacensis*, *Leptocoma* and *Aethopyga* (nodes C1, C2b and C3) form a clade sister to a large but poorly resolved African sunbird assemblage, which includes the Asian-Australasian *Cinnyris jugularis*. However, *Aethopyga* (nodes C3a and b) is rendered polyphyletic for the first time by the positioning of *Leptocoma* (node C1). Resolution is poor among the ‘African’ sunbird assemblage, however, the Double-collared group of sunbirds and *Anthobaphes* remain associated with high bootstrap support. One potentially important difference is that *Cinnyris jugularis* is no longer sister to *Anthreptes collaris* as in the mtDNA analyses, but clusters with the two endemic Indian Ocean sunbirds (*dussumeri* & *souimanga*), although with weak bootstrap support (51%). The BI analysis (Fig. 2.9) produced a similar topology with many nodes collapsed.

### Combined evidence

Because the ILD tests indicate no significant incongruence between the mtDNA and nDNA data partitions, these two partitions were combined in a ‘total

evidence dataset' for phylogenetic analyses. Down-weighting 3<sup>rd</sup> codon position transitions in the MP analysis by the empirical estimate of 3.6x recovered one tree of 23731.8 steps (CI = 0.270, RI = 0.452, Fig. 2.10). The topology is similar to that inferred for the mtDNA data partition on its own (Fig. 2.6), but with some notable exceptions. Nodes A and B are no longer sister and at the base of the tree, instead *Dicaeum* and *Prionochilus* (node A) form a clade basal relative to *Hypogramma* and *Arachnothera* (node B). As in the BI mtDNA analysis (Fig. 2.7) and the FIB5 MP analysis (Fig. 2.8), *Chalcoparia* (node C2a) is split from *Anthreptes malacensis* (node C2b) and basal relative to a clade containing *Anthreptes malacensis* (node C2b), *Leptocoma* (node C1), and a monophyletic *Aethopyga* (node C3). The primarily African assemblage of sunbirds (node D) is recovered with 100% bootstrap support, as are nodes E1 and E2.

Node E3 (a + b) encompasses the remaining African sunbirds as well as the Asian-Australasian *Cinnyris jugularis*. Nearly all the nodes (F to O) recovered in the mtDNA analyses are again recovered in the combined analysis, but relationships among the nodes differ. *Dreptes* is no longer sister to *Chalcomitra balfouri*, *Cinnyris osea* and *Cinn. venusta* (nodes G + H), but is now the most basal member of nodes G plus H. Nodes G plus H are also no longer sister to the velvety sunbirds (node I) and the coppery sunbirds (node J), but rather in the combined MP analysis, G plus H are sister to the West African 'green' sunbirds (node K). The velvety and coppery sunbirds (nodes I + J) remain associated, but are now sister to *Cinn. chloropygia* and *Cinn. minulla* (node N), which remain well separated from the other Double-collared sunbirds (*Cinnyris* in the clade defined by node E1). The blue-green headed sunbirds (*Cyanomitra*, node M) are now sister to the two malachite sunbirds (node O), with the Olive Sunbird, *Cyanomitra olivacea* apparently more closely related to the malachite sunbirds than to other members of *Cyanomitra*. Lastly *Cinn. rufipennis* and *Anthreptes reichenowi* cluster (<50% bootstrap support). This is an unlikely phylogenetic association, given the extent of morphological divergence between these two taxa. Further down-weighting of the 3<sup>rd</sup> positions recovers the same topology as described above for 3.6x Ti/Tv ratio. Bootstrap values are marginally higher among all nodes for the combined analyses relative to values obtained when analysing only the mtDNA or nDNA data partitions individually.

As for the individual mtDNA and nDNA data partitions, a burn-in value of 50 000 generations was empirically estimated for each of the seven BI runs, which included one long run of 5 million generations. The topology recovered (Fig. 2.11) is remarkable similar to the topology recovered from the weighted MP analyses (Fig. 2.10), with only a few differences. Within node A, the flowerpecker genera *Prionochilus* and *Dicaeum* remain polyphyletic, although the relative position of *Prionochilus maculatus* shifts. In the BI analyses, *Hypogramma* (node B1) no longer renders *Arachnothera* (B2) polyphyletic, and *Leptocoma* (node C1) is now sister to *Aethopyga* (C3) instead of *Anthreptes malacensis* (node C2b). Within the assemblage of primarily African sunbirds (node D) *Cinn. jugularis* is no longer sister to *Anthreptes collaris* as in the MP analyses (node F), but instead is basal relative to nodes G plus H. The West African 'green' sunbirds in the BI analyses (node K) are most closely related to the velvety (node I) and coppery sunbirds (node J), while in the MP analyses they are sister to nodes F, G and H. *Cinn. rufipennis* continues to shuffle around and is now basal relative to node K, whereas *Anthreptes reichenowi* is now sister to the Blue-green headed sunbirds (node M), the malachite sunbirds (node O) and *Cyanomitra olivacea*. Lastly, the two aberrant members of the Double-collared group of *Cinnyris* (node N) are sister to the velvety sunbirds (node I) in the BI analyses, but are sister to both the velvety and coppery sunbirds (nodes I and J) in the MP analyses.

### **Ancestral areas and intercontinental movements**

Results of the dispersal-vicariance analysis (DIVA) on the 3.6x weighted MP trees (Fig. 2.10) suggested that trans-Wallacea (see Methods for area definition) constitutes the most plausible centre of origin for the Nectariniidae (Fig. 2.12). In total, 11 dispersal events were inferred under the assumption that all five defined distributional areas could form part of the ancestral distribution (i.e. Gondwana). Because this is extremely unlikely to be true, given the trans-Wallacea origin hypothesis for the Passerida (Barker *et al.* 2002, Ericson *et al.* 2002), the number of ancestral areas was restricted to two (the minimum number allowed in DIVA). This analysis resulted in 12 dispersal events being inferred. Most dispersal events inferred corresponded to trans- or cis-Wallacean

movements, or dispersal from the African mainland to the western Indian Ocean Islands by two independent lineages, and dispersal via the Nile Valley to the Levant. However, there has also been a back-colonization (*Cinnyis jugularis*) from Africa to trans/cis-Wallacea.

### Testing for monophyly

The post burn-in posterior distribution of trees obtained in either a 2 million (mtDNA and nDNA, 19501 trees) or 5 million (combined, 49501 trees) generation search were filtered to determine the split (node) posterior probabilities of putative monophyletic lineages according to traditional (Delacour 1944, Sibley & Monroe 1990) and recently proposed (Irwin 1999, Cheke *et al.* 2001, Mann 2002) classification schemes for the Nectariniidae. In general results for the mtDNA, nDNA, and the two data sets combined were similar, and suggested that both traditional and recently proposed Nectarinid genera do not reflect monophyletic lineages (Table 2.7), with the possible exception of *Cyanomitra*. Analysis of the nDNA data partition on its own suggests that the four spiderhunters (*Arachnothera*) and five yellow-rumped sunbirds (*Aethopyga*) do not reflect monophyletic lineages, respectively. In contrast, the mtDNA and combined DNA analyses suggest that they do. Lastly, whereas in both the mtDNA and combined DNA analyses the monophyly of the white-bellied subgroup (*Cinn. venusta* and *fusca*) of *Cinnyris* is rejected, the nDNA partition does not reject monophyly.

## DISCUSSION

Four issues are touched upon in the discussion: (1) patterns of gene evolution, (2) the utility of BI as a method of phylogenetic reconstruction, (3) historical biogeography of the Nectariniidae and (4) the taxonomic implications of the molecular analyses.

### Patterns of gene evolution

A bias in base composition, with Cytosine and particularly Guanine being present in much lower quantities within the mtDNA genome is well documented in many avian families and orders (see Moore & DeFilippis 1997 for a review). All three mtDNA genes, ATP6, ND2 and ND3 conform to this general pattern of



mtDNA base composition in birds, strengthening the conclusion that base composition in mtDNA varies little among taxa. The nDNA Intron 5 of Beta-fibrinogen also has a biased base composition, being more Adenine/Thymine rich compared with the mtDNA. While no studies have yet been published reporting intron 5 sequences, the observed base composition is very similar to that obtained for Beta-Fibrinogen Intron 7 in woodpeckers (Prychitko & Moore 1997, Weibel & Moore 2001) and for non-coding nDNA sequences in general (Li & Graur 1991). Li and Graur (1991) have suggested that over 60% of all mutations that occur in non-coding regions of nDNA result in either an A or T substitution. Thus, it is not surprising that a non-coding sequence should become AT rich through the course of its evolution. This phenomenon has been reported for Fib7 in woodpeckers (Prychitko & Moore 1997), and also appears to be the case for Fib5 in the Nectariniidae (Table 2.3).

ND2 had the greatest number of variable sites and the largest percentage of parsimony informative sites, although ATP6 and ND3 had only marginally less (Fig. 2.3). The nDNA Fib5 intron had a similar number of variable sites as the mtDNA genes, but only about half as many parsimony informative sites (Fig. 2.3). A similar pattern has been reported in Columbiformes for Fib7 (Johnson & Clayton 2000). Of the 19 indels documented within this study, only four were parsimony informative (Table 2.4). A similar percentage, 4 of 23 indels, were reported to be parsimony informative within the woodpecker genus *Picoides* for the larger Fib7 (Weibel & Moore 2001). Although indels, particularly deletions, may be relatively abundant in large alignments of non-coding nDNA, their phylogenetic utility remains to be established.

In this study, the 201 bp deletion shared by the three violet-backed sunbirds of the genus *Anthreptes* (*longuemarei*, *orientalis* and *neglectus*) is strong support for their monophyly. Despite the deletion being treated as missing data in both the MP and BI analyses, the three taxa were always recovered as monophyletic, with one exception (BI of nDNA, Fig. 2.9). Mapping indels onto the combined MP and BI topologies suggests that homoplasy does exist. For example, a 35 bp deletion occurs in two of four members in node I, and two of six in node J (Figs

2.10 & 2.11), but in neither the BI or MP analyses do the taxa which have the indel form a monophyletic lineage.

The phylogenetic signal contained within each of the mtDNA genes are remarkable uniform when compared using either the consistency (CI) or retention indices (RI) (CI range 0.15-0.17, RI range 0.31-0.36), and combining the three partitions did not drastically alter these values (CI = 0.21, RI = 0.36). Both the CI and RI indices were considerably higher for the nDNA intron (CI = 0.68 RI = 0.75). In all three mtDNA data partitions the same groups of taxa formed the deeper nodes in the combined mtDNA and nDNA analyses, although branching order was not identical. However, the consensus MP topology for ND3 resulted in most of the African sunbird assemblage (nodes E1, E2 & E3) being unresolved, and the MP ATP6 and ND2 topologies differed dramatically. The combined mtDNA analysis recovered a topology that was more similar to the topology recovered from the combined mtDNA and nDNA data partitions (Fig. 2.10), particularly if saturation was accounted for by down-weighting 3<sup>rd</sup> position transitions (Fig. 2.6). The lack of consistency in the topological arrangements recovered from MP analyses of individual data partitions most likely is a consequence of short inter-nodes, and therefore it is not surprising that adding more base pairs improves resolution of phylogenetic affinities.

The nDNA data partition, while placing similar taxa towards the base of the tree, did not result in improved resolution of phylogenetic affinities at either the base of the tree or towards the tips where many terminal nodes were collapsed. In addition, bootstrap values were not significantly different from those obtained in the combined mtDNA analyses, and characters were fairly evenly distributed across the tree (Fig. 2.8). Reflecting the similarity in phylogenetic signal between the combined mtDNA and the nDNA data partitions, a partition-homogeneity test under MP using a heuristic search did not detect phylogenetic heterogeneity between the two data partitions. Although it is unusual for mtDNA and nDNA datasets to have similar levels of phylogenetic signal due to the relatively slower rate of substitution in nDNA, Johnson and Clayton (2000) and Weibel and Moore (2001) reported similar lack of heterogeneity between mtDNA genes and Fib7 in Columbiformes and Piciformes, respectively.

Contrasting relative rates of divergence between the combined mtDNA and nDNA data partitions for pairwise comparisons among taxa, the mtDNA molecule was estimated to evolve at approximately 8.4 times the rate of Fib5, which is in agreement with the typically higher mutation rate of vertebrate mtDNA (Brown *et al.* 1979, Avise 2000). The eight to nine-fold higher substitution rate for mtDNA vs. Fib5 in the Nectariniidae is similar to the estimated 5.6-fold increase in substitution rate for Cytochrome *b* relative to Fib7 in Columbiformes (Johnson & Clayton 2000).

### **Parsimony vs. Bayesian Inference, and bootstrap support vs. posterior probabilities**

In all instances down-weighting 3<sup>rd</sup> position transitions relative to transversions resulted in a MP tree which had a greater number of nodes resolved compared to the consensus of the posterior distribution of trees obtained during the BI analyses. The number of unresolved nodes in the BI analyses rapidly reduced as greater amounts of data were added (e.g. compare Figs 2.7 to 2.11).

For systematists, the most important potential benefits of using a BI approach to phylogenetics is the ability to estimate topology and concurrently gain estimates for clade support. Clade or split posterior probabilities are analogous to bootstrap support values, but differ in a number of fundamental ways, and should arguably not be compared directly. For example, clade probabilities are conditional on the data, whereas bootstrap values can only be computed by perturbing the data (Lewis 2001, Huelsenbeck *et al.* 2002). Bootstrapping asks the question “What range of variation would I expect if I had sampled a different set of nucleotides from the same distribution?” Split posterior probabilities address a different question, namely “What is the probability that this split (node) is present in the true tree given the data observed?” Split probabilities and bootstrap values thus provide answers to different, but related questions (Lewis 2001).

However, it has proved irresistible to scientists to attempt to compare posterior probabilities with bootstrap values, because the bootstrap (Felsenstein 1985) has

been a benchmark of statistical support for splits (nodes) for such a long time. Suzuki *et al.* (2002) recently used simulations of four hypothetical taxa to generate a 15 000 bp concatenated dataset. Analyses using this dataset suggested that the split posterior probability is excessively high as an indicator of statistical confidence, and that the bootstrap is more appropriate. In contrast, Wilcox *et al.* (2002) using simulations of a 20 species snake dataset, suggests that the split posterior probability is a better indicator of statistical confidence than the bootstrap.

I compared split posterior probabilities from a 2 or 5 million generation BI run with bootstrap values obtained under MP from 1000 replicates for (1) the combined mtDNA dataset and (2) the 'total evidence' dataset (Fig. 2.13). Examining only splits in common between the MP and BI topologies, most (all data 33/38, mtDNA 38/41) of the BI posteriors probabilities greater than 95% corresponded with bootstrap values greater than 75%. Thus, the 95% confidence level does seem reliable, but is obviously higher than the bootstrap value. This is because the tree with the highest maximum likelihood (greatest posterior probability) or set of trees is visited again and again in the MCMC computation for the specified dataset. In comparison, the computation of bootstrap support is dependant on the original dataset being considered as a single evolutionary event with associated stochastic errors, and therefore the original set of nucleotide sequences is reshuffled with replacement (bootstrap-resampling) to evaluate the reliability of the original consensus topology (Lewis 2001). In only one case was the BI posterior probability greater than 95% and the bootstrap value less than 50% (Figs 2.10 & 2.11, node E1, between *stuhlmanni* and *regia*). Similarly, in only one case was a posterior probability less than 95%, and the bootstrap value greater than 75% (Figs 2.6 & 2.7, node E2).

### **Historical biogeography of the Nectariniidae**

An African centre of origin for the Nectariniidae would be difficult to explain in context of the recent hypothesised Australasian origins of oscine passeriform birds (Barker *et al.* 2002, Ericson *et al.* 2002). These authors hypothesize that oscine passerines have a cis-Wallacean origin, from which a founder event lead to the establishment of some ancestral species of the Passerida in trans-Wallacea,

but where? It would be most parsimonious to assume that Asia would be where most of the older Passerida lineages were established, and that colonization of Africa was secondary. Dispersal-vicariance analysis (DIVA) strongly supports a trans-Wallacea origin for the Nectariniidae (Fig. 2.12) in agreement with the above hypothesis. However, one common prediction of both the African (Irwin 1999) and Asian-Australasian (inferred from Sibley & Alquist 1990) centre of origin theories is that the African Nectariniidae do not reflect one single large radiation, due to multiple exchanges having occurred between Africa and Asia, which has led to the two continents independently sharing *Anthreptes* and *Nectarinia* (*Cinnyris* in Irwin 1999). The molecular phylogenetic hypotheses constructed in this study (Figs 2.6-2.11) and the DIVA (Fig. 2.12) support multiple Africa-Asia exchanges, but not as envisaged by the authors of previous revisions of the family (Delacour 1944, Sibley & Monroe 1990, Irwin 1999, Cheke *et al.* 2001). The Asian *Anthreptes* appear well separated from members of what is clearly a polyphyletic African ‘*Anthreptes*’, and *Leptocoma* is never recovered as sister to *Chalcomitra* (Figs 2.6-2.11). Instead, the Asian *Anthreptes*, *Leptocoma* and *Aethopyga* form a clade that is sister to a large clade of primarily African sunbirds. The split of Asian from African members of *Anthreptes*, and the hypothesised phylogenetic position of *Leptocoma*, suggest that the considerable species richness of African sunbirds may originate from a single colonization or vicariance event, and that the lack of support among many clades of African, may be a consequence of rapid radiation following isolation from Asia. Curiously, while the deeper nodes of the phylogeny are all restricted to Asian-Australasian taxa, the primarily African sunbird assemblage contains one sampled Asian species, *Cinnyris* (*Nectarinia*) *jugularis*. If the origins of the Nectariniidae really are Asian-Australasian as this and other studies (Sibley & Alquist 1990) have suggested, and the African sunbirds do stem from a single lineage, then *Cinnyris jugularis* must have reached Asia via a back-colonization from Africa, as is inferred using DIVA (Fig. 2.12).

*Cinnyris jugularis* is one of five species retained by Irwin (1999) and Cheke *et al.* (2001) in the large, but primarily African genus *Cinnyris*. *Cinnyris jugularis* has the largest range of any Asian-Australasian Nectarinid, and is the only sunbird species to reach Australia. The species has been linked in the past with

the sunbirds of the Indian Ocean Islands, which themselves have caused considerable uncertainty regarding their systematic placement. *Cinnyris dussumeri*, which is endemic to the Seychelles Islands, has been postulated by various authors to have either African or Asian affinities, leading to the Indian Ocean islands being hypothesised as ‘stepping-stones’ between Africa and Asia (Benson 1984, Sibley & Monroe 1990, Louette 1992).

Warren *et al.* (in press) recently reviewed the phylogeography of all species of western Indian Ocean sunbirds using mtDNA, and demonstrated that these taxa originated from two independent radiations; (1) the ancestor of the *Cinnyris souimanga* species complex colonized the Comoro Islands from the African mainland, and subsequently dispersed to the Seychelles Islands and Madagascar, and (2) *Cinnyris notata* colonized Madagascar from the African mainland, and subsequently dispersed to the Comoro Islands. An African mainland origin is inferred for both lineages of Indian Ocean sunbirds (route 3, Fig. 2.14b) and there is no support for association with the Asian-Australasian *Cinnyris jugularis*. The mtDNA results of this study, which has a much larger number of taxa, support the conclusions of Warren *et al.* (in press). However, if the nDNA data partition is analysed on its own, *Cinnyris jugularis* in both the MP (Fig. 2.8) and BI (Fig. 2.9) analyses is sister to the two representatives of the Indian Ocean sunbird lineages included within this study (although with only 51% bootstrap support). DIVA of the combined nucleotide dataset, supports independent colonisations of the Indian Ocean Islands from the mainland by the two major sunbird lineages (route 3, Fig. 2.14b). However, if the mtDNA is discounted, and the present day endemic radiation of Indian Ocean sunbirds is indeed sister to *Cinnyris jugularis*, the Indian Ocean Islands may well have facilitated a back-colonization to Asia from Africa (route 4a, Fig. 2.14b), after the initial (single) founding of African Nectarinids from Asia. Further studies of nDNA markers are needed if the apparent ambiguity between the results of the biogeographical history inferred from the mtDNA and nDNA data partitions is to be resolved.

This study is not the first to use molecular phylogenetic methods to investigate biotic interactions between Africa and Asia. Wilkinson *et al.* (2002) provided convincing evidence that the African tree-frog genus *Chiromantis* dispersed to

Africa from Asia. In contrast, Palkovacs *et al.* (2002) demonstrate that Giant Indian Ocean tortoises (*Dipsochelys*) are embedded within Malagasy tortoise lineages, and argue that Indian Ocean tortoises are derived from a common Malagasy ancestor and do not have close African or Asian affinities, but may have relictual affinities to Gondwana. However, systematic hypothesis of the origins of African shrews (Soricidae, Quéroutil *et al.* 2001), fruit-bats (Megachiroptera, Juste *et al.* 1999), pipits (Voelker 1999a & b) and wagtails (Voelker 2002) parallel sunbirds in that the systematic arrangement of genera/species as inferred from nucleotide sequence data suggests that there have been multiple biotic exchanges between Africa and Asia.

Although the many caveats for using a molecular clock should be acknowledged (see Arbogast *et al.* 2002) and nodes have not been dated using a molecular clock in the present study, a relatively high rate (4.6-6.4 % per myrs, compared to the 'standard' vertebrate mtDNA clock of 1.6 to 2% per myrs, Krajewski & King 1996, Friesen & Anderson 1999, Fleischer *et al.* 1998, Avise 2000) of nucleotide substitution would be necessary to bracket the African sunbird radiation within the Pleistocene. If a rate of 1.6% per million years divergence (Fleischer *et al.* 1998) is used as a proxy, then the major radiation of African sunbirds occurred 8-11 myrs BP. With the Indian Ocean islands being an unlikely dispersal route (route 1, in Fig 2.14a), and the only Mediterranean sunbird *Cinnyris osea* clearly having African origins (Fig. 2.12, route 5, Fig. 2.14b), dispersal across Europe and then subsequently dispersing across the Gibraltar land-bridge during the Late Miocene (route 3, Fig. 2.14a), as suggested for mammals by Steiniger *et al.* (1985, route 3 in Fig 2.14), also seems unlikely. Rather, as suggested for many groups of mammals (see Juste *et al.* 1999), a forest corridor that linked Africa with Asia during the Miocene may provide the most plausible hypothesis to explain how sunbirds arrived in Africa (route 1, Fig. 2.14b). The subsequent rise of mountains in the Middle-East, together with increased aridity and the opening of the Red Sea at the end of the Miocene, would have led to African and Indo-Australasian forests and their associated fauna (Cox & Moore 1993, Juste *et al.* 1999) becoming fragmented. The changes in climate beginning in the Early Pliocene would have restricted forest species but provided opportunities for dispersal for open habitat species (grasslands/shrublands/woodlands specialists).

This has been documented in pipits (genus *Anthus*, Voelker 1999a & b) and wagtails (genus *Motacilla*, Voelker 2002), for which multiple invasions (16 & 26 dispersal events for *Anthus* and *Motacilla*, respectively) from Asia to Africa, expansions to Europe, and back-colonisations to Asia, have been inferred. In contrast, DIVA infers 11-12 dispersal events among the Nectariniidae taxa included within this study, and most of these are associated with either trans to cis-Wallacean movements, or dispersal from the African mainland to the Levant (route 5, Fig. 2.14b) and the western Indian Ocean Islands (route 3, Fig. 2.14b).

One major difference between sunbirds and pipits are their habitat requirements, sunbirds are primarily forest species, whereas pipits occupy open grassland and shrubland. Since fragmentation of the Asia-Africa 'forest corridor', and aridification of the Middle-East and northern Africa, there has been ample suitable habitat available for species of open habitats, and the Middle-East appears to have provided a corridor for pipit (and wagtail) dispersal into Africa from Asia, and vice versa. The maintenance of an aridified Middle-East has persisted since the Pliocene, and consequently it is not surprising that multiple dispersal events for open habitat species such as pipits have occurred between Africa and Asia. In summary, both vicariance (initial African colonization of Africa by forest corridor and subsequent fragmentation, route 1 Fig. 2.14b) and dispersal (back colonization to Asia from Africa (route 4a or 4b, Fig. 2.14b), dispersal from African mainland to the Levant (route 5, Fig. 2.14b) and Indian Ocean Islands (route 3, Fig. 2.14b)) appear to have played important roles in shaping the evolutionary history of the Nectariniidae.

### **Taxonomic implications of the molecular analyses**

#### ***Dicaeum* and *Prionochilus***

The flowerpeckers are traditionally divided into two genera *Dicaeum* and *Prionochilus* and are placed by some authors (Wetmore 1960, Rand 1967) within their own family, the Dicaeidae. The flowerpeckers differ fundamentally from the spiderhunters and sunbirds by having all ten primaries relative long, compared to the 10<sup>th</sup> primary being considerably reduced in size in all other Nectarinids. Within the flowerpeckers the two genera are not well defined, and it is not surprising that in this study neither genus was recovered as monophyletic,



as there is no single morphological character or even combination of characters, which can be used to consistently distinguish *Dicaeum* from *Prionochilus*. Cheke *et al.* (2001) describe four different tongue morphologies for *Dicaeum*, members of which were included in this study: (1) *agile* and *bicolor*, (2) *melanoxanthum*, (3) *nigrilore* and (4) *aeneum*. At least in the case of group 1, tongue morphology, if compared to either the mtDNA, nDNA or combined DNA analyses for MP or BI, is plesiomorphic. In addition, the phylogenetic affinities among the flowerpeckers in this study do not appear to corroborate any clearly discernable plumage patterns within either of the two genera. I suggest that before *Dicaeum* and *Prionochilus* are revised, additional taxa should be sequenced to improve the extent to which morphologically diverse forms are represented within the phylogeny.

### ***Hypogramma* and *Arachnothera***

The Purple-naped Sunbird *Hypogramma hypogrammicum* has one of the most aberrant plumages of all Nectarinids. The sexes are dimorphic, with the male having tufts of purple-blue feathers on the nape, lower back, rump and upper tail-coverts, characters found in no other Nectarinid. The female lacks metallic plumage. The throat, breast and upper belly are heavily streaked dark olive, reminiscent of the plumage pattern in *Arachnothera*, although the spiderhunters are almost twice the size, have large robust bills instead of a long thin and curved bill, and both sexes lack metallic plumage. The tongue structure also differs between *Hypogramma* and *Arachnothera*. *Hypogramma* has a unique tongue structure. The tongue is rolled in at the edges to form two tubes for most of its length, the distal 20% being split centrally with the inner edge deeply fimbriated, and at the tip each half of the tongue splits again to form a quadrifid brush-tip (Gill 1971, Cheke *et al.* 2001). In contrast, *Arachnothera* has a long tongue rolled to form a complete tube for most of its length, with two lateral splits near the tip, which are again rolled to form two tubes (Cheke *et al.* 2001).

Given the unique morphological structures associated with *Hypogramma* it is surprising that in the MP analyses (Fig. 2.6 & 2.10) *Hypogramma* renders *Arachnothera* polyphyletic. Analyses of the nDNA data partition (Fig. 2.8 & 2.9) or BI analysis of the combined data partitions (Fig. 2.11) suggest that

*Hypogramma* is a deep node possibly sister to *Arachnothera*. Pairwise sequence divergence distances for both the mtDNA and nDNA data partitions (Table 2.5) suggest that *Hypogramma* is not closely related to any other nectarinid lineage (>20% mtDNA, >6% nDNA). The spiderhunters *Arachnothera* similarly are distantly related to all other nectarinid lineages (>19% mtDNA, >5% nDNA), and probably speciated in the Miocene given the extraordinary average pairwise sequence divergence of the four members of the genus sequenced (18.6% for mtDNA and 4.5% for nDNA, Table 2.5). These divergences are similar to or greater than divergences between the flowerpeckers (*Dicaeum* and *Prionochilus*), which are often classified in their own family the Dicaeidae, and the ‘typical sunbirds’: *Aethopyga*, *Chalcoparia*, *Leptocoma*, *Anthreptes*, *Deleornis*, *Hedydipna*, *Anabathmis*, *Anthobaphes*, *Nectarinia*, *Chalcomitra*, *Cyanomitra*, *Dreptes* and *Cinnyris*.

### ***Chalcoparia***

The split of *Chalcoparia singalensis* from *Anthreptes* by Mann (2002) appears to be well founded. In both the combined MP and BI analyses this taxon forms a clade sister to all the remaining sunbirds. *Chalcoparia* has a unique horny plate on the tongue (Mann 2002), which is most similar to some flowerpeckers, and the lower bill lacks the serrations found in all other sunbirds.

### ***Aethopyga***

The yellow-rumped sunbirds, so named because the male almost invariably and female frequently have a contrasting yellow patch of varying size on the lower back and rump, form a monophyletic assemblage, which is either sister to *Leptocoma* (BI, Fig. 2.11) or to *Leptocoma* plus *Anthreptes malacensis* (MP, Fig. 2.10). Members of *Aethopyga* share a common tongue morphology, a flat terminal lobe between two semi-circular lobes (Scharnke 1932, Cheke *et al.* 2001). All species lack pectoral tufts, but all have much elongated and ‘fluffy’ feather tufts at the sides of the lower back.

### ***Leptocoma***

With the major revision of the Nectariniidae by Delacour (1944), *Leptocoma* became synonymised within a greatly expanded *Nectarinia*, until Cheke *et al.*

(2001) resurrected the genus. Delacour (1944), however, did retain *Leptocoma* as a subgenus of *Nectarinia*, and due to a shared velvet-like plumage on the upperparts considered *Leptocoma* to be “certainly related to the Africa [subgenus] *Chalcomitra*”. The results of both the MP and BI combined DNA analyses strongly support the recognition of *Leptocoma* as a valid genus, although it is not closely related to *Chalcomitra*. Instead, as suggested by Wolters (1977), *Leptocoma* has close affinities to Asian members of the genus *Anthreptes*, as well as to *Aethopyga*.

### **Asian ‘*Anthreptes*’**

The genus *Anthreptes* is characterised by possessing what is thought to be an ancestral bill morphology; the bill is typically wedge-shaped, straight proximally with the distal curvature formed principally by the tapering and downward attenuation of the culmen (Irwin 1993). The emphasis placed on bill morphology, especially in a nectarivore where bill morphology may be expected to be plastic, appears to be due to Delacour (1944), who considered bill characters more ‘reliable’ than plumage characters. This notion has been perpetuated ever since, and as a consequence *Anthreptes* has for many years been a ‘dumping ground’ for short-billed sunbirds from both Africa and Asia. The results from the molecular analyses strongly demonstrate that the nominate for the genus, *Anthreptes malacensis*, is well separated from African members of the genus, which in turn are polyphyletic within the African sunbird assemblage. It will be interesting in the future to determine if the two other Asian *Anthreptes* species, *A. rhodalaema* and *A. simplex* are also well separated from African ‘*Anthreptes*’ (tissues at present are lacking).

### **African sunbird assemblage**

The ‘African’ sunbird assemblage currently contains 79 species restricted to Africa, *Cinnyris jugularis*, and most likely the other four Asian members of the genus *Cinnyris*, not sampled in this study: *Cinn. buettikoferi*, *solaris*, *lotenius* and *asiaticus*. Recently, Irwin (1999) split *Nectarinia*, which was Aves largest genus (Bock & Farrand 1980), into nine additional genera (Fig. 2.1). Both MP and BI analyses for both the mtDNA and nDNA data partitions, or in combined DNA analyses, suggest that the traditional genera *Nectarinia* and *Anthreptes* are

polyphyletic, as are many of Irwin's proposed genera: *Anthreptes*, *Hedydipna*, *Chalcomitra*, *Cyanomitra* and *Nectarinia*. This result is further supported by constraint analyses using the Bayesian posterior distribution of trees (Table 2.12), where only monophyly of *Cyanomitra* could not be outright rejected.

The deepest nodes within the African sunbird assemblage contain most members of the Double-collared group of *Cinnyris* (*C. chloropygia*, *C. minulla* and *C. pulchella* are excluded) as well as *Anthobaphes violacea* and *Anabathmis reichenbachii* (node E1). This is followed by the violet-backed sunbirds traditionally considered part of *Anthreptes* and the Pygmy Sunbird (node E2) assigned by Irwin (1999) to *Hedydipna*. Terminal to E1 and E2, node E3 encompasses the remaining members of the African Nectariniidae as well as the Asian-Australasian *Cinnyris jugularis*. That many of Irwin's (1999) proposed genera are not monophyletic is not to say that some of these genera do not have merit, only that their limits are not well defined. For instance, three of the four members of *Chalcomitra* go together (Node I), but *Chalcomitra* appears to include the Indian Ocean endemic *Cinnyris notata*, a result perhaps not to surprising considering the heavy throat, breast and belly streaking in female *Cinn. notata*, a character typical of female *Chalcomitra*. Similarly, the four Blue-green headed sunbirds group (node M) with high support, but the rather morphologically aberrant Olive Sunbird *Cyanomitra olivacea* appears to be more closely related to the two Malacite sunbirds (node O), which in turn are well separated from the other members of *Nectarinia* (Node J).

Although the inherent subjectivity of categories above species should be recognized, it is clear based on the results of this study that the Nectariniidae is in need of a new classification system if monophyletic lineages are to be reflected. Whether this new classification scheme should return many members of the 'African' sunbird assemblage to one large genus *Nectarinia*, or if additional genera, many which would be monotypic should be recognised, is a subject of future debate. It is at present beyond the scope of this chapter to provide a comprehensive revised classification for members of the 'African' sunbird assemblage, and before doing this it will be necessary to both include additional

morphologically diverse members of the of the African sunbird assemblage in the molecular analyses. This is at present being undertaken.

University of Cape Town

**Table 2.1.** Species, museum voucher numbers and country of origin for individuals sequenced for three mtDNA (ATP6, ND2, ND3) and one nDNA (Fib5) gene region in this study. \* Not sequenced. Source: FMNH, Field Museum of Natural History; LSUMNS, Natural History Museum, Louisiana State University; UMMZ, University of Michigan Museum of Zoology; ANSP, Academy of Natural Sciences of Philadelphia; AMNH, American Museum of Natural History; MV, Museum Victoria; ZMUC, Zoological Museum, University of Copenhagen; MNHN, Museum National D'Histoire Naturelle; SAN, San Francisco State University.

Species	Source	Country	ATP6	ND3	ND2	Fib5
<i>Corvus albus</i>	FMNH396806	Ghana	X	X	X	X
<i>Turdus olivaceus</i>	FMNH356763	Tanzania	X	X	X	X
<i>Prionochilus olivaceus</i>	FMNH357587	Philippine Islands	X	X	X	X
	FMNH357589	Philippine Islands	X	X	*	X
<i>Prionochilus maculatus</i>	LSUMNS B36382	Malaysia	X	X	X	X
<i>Dicaeum aeneum</i>	AMNH23441	Solomon Islands	X	X	X	X
<i>Dicaeum agile</i>	LSUMNS B7927	Zoo/Captive	X	X	X	X
<i>Dicaeum anthonyi</i>	FMNH357602	Philippine Islands	X	X	X	X
	FMNH429296	Philippine Islands	X	X	*	*
<i>Dicaeum bicolor</i>	FMNH357606	Philippine Islands	X	X	X	X
<i>Dicaeum hirundinaceum</i>	MV B460	Australia	X	X	X	X
	MV W012	Australia	X	X	*	X
<i>Dicaeum melanoxanthum</i>	MNHN 18-42	China	X	X	X	X
	AMNH23295	Nepal	X	X	*	*
<i>Dicaeum nigrilore</i>	FMNH357596	Philippine Islands	X	X	X	*
<i>Dicaeum pectorale</i>	MV E579	New Guinea	X	X	X	X
	MV E376	New Guinea	X	X	*	X
<i>Hypogramma hypogrammicum</i>	LSUMNS B36403	Malaysia	X	X	X	X
	ANSP1197	Malaysia	X	X	*	*
<i>Arachnothera affinis</i>	LSUMNS B36416	Malaysia	X	X	X	X
	ANSP1187	Malaysia	X	X	*	*
<i>Arachnothera longirostra</i>	LSUMNS B36307	Malaysia	X	X	X	X
<i>Arachnothera magna</i>	MNHN 14-33	China	X	X	X	X
	AMNH833202	Vietnam	X	X	*	X
<i>Arachnothera robusta</i>	LSUMNS B36483	Malaysia	X	X	X	X
<i>Chalcoparia singalensis</i>	ANSP1321	Malaysia	X	X	X	X
	MNHN 5-39	Laos	X	X	*	X
<i>Aethopyga boltoni</i>	FMNH357630	Philippine Islands	X	X	*	X
	FMNH357631	Philippine Islands	X	X	X	X
<i>Aethopyga gouldiae</i>	MNHN 18-71	China	X	X	X	X
<i>Aethopyga nipalensis</i>	AMNH831365	Nepal	X	X	X	X
<i>Aethopyga primigenius</i>	FMNH357624	Philippine Islands	X	X	*	X
	FMNH357626	Philippine Islands	X	X	X	X
<i>Aethopyga siparaja</i>	FMNH345063	Philippine Islands	X	X	X	X
	AMNH833200	Vietnam	X	X	*	*
<i>Anthreptes longuemarei</i>	ZMUC O5945	Tanzania	X	X	X	X
<i>Anthreptes malacensis</i>	FMNH358538	Philippine Islands	X	X	*	X
	LSUMNS B23362	Malaysia	X	X	X	X
<i>Anthreptes neglectus</i>	FMNH356805	Tanzania	X	X	X	X
	ZMUC JK05-110601	Tanzania	X	X	X	X
<i>Anthreptes orientalis</i>	Rauri Bowie (04)	Kenya	X	X	X	X
	Rauri Bowie (11)	Kenya	X	X	X	X
<i>Anthreptes reichenowi</i>	Rauri Bowie (03)	Kenya	X	X	X	X
<i>Anthreptes seimundi</i>	AMNH831872	Central African Rep.	X	X	X	X
<i>Deleormis fraseri</i> <sup>1</sup>	AMNH832201	Central African Rep.	X	X	X	X
	FMNH396702	Ghana	X	X	*	X
<i>Hedydipna collaris</i>	FMNH346553	Burundi	X	X	X	X
	AMNH831876	Central African Rep.	X	X	*	*
<i>Hedydipna platara</i>	FMNH396706	Ghana	X	X	X	X
	FMNH396707	Ghana	X	X	*	X
<i>Anabathmis reichenbachii</i>	LSUMNS B27124	Cameroon	X	X	*	X
	LSUMNS B27180	Cameroon	X	X	X	X
<i>Dreptes thomensis</i>	Univ. of Aberdeen	Sao Tome Island	X	X	X	X
	Univ. of Aberdeen	Sao Tome Island	X	X	X	X
<i>Anthobaphes violacea</i>	Rauri Bowie (Bred1)	South Africa	X	X	X	X
	Rauri Bowie (W40023)	South Africa	X	X	X	X
<i>Cyanomitra alinae</i>	FMNH355996	Uganda	X	X	X	*
	FMNH358148	Burundi	X	X	*	X
<i>Cyanomitra cyanolaema</i>	Rauri Bowie (09)	Uganda	X	X	X	X
	FMNH396720	Ghana	X	X	*	*

<i>Cyanomita olivacea</i> <sup>2</sup>	AMNH24926	Central African Rep.	X	X	X	X
	FMNH346568	Uganda	X	X	*	X
<i>Cyanomitra oritis</i>	SAN99-22	Cameroon	X	X	*	*
	SAN99-34	Cameroon	X	X	X	X
<i>Cyanomitra verticalis</i>	FMNH346602	Burundi	X	X	*	*
	LSUMNS B27139	Cameroon	X	X	X	X
<i>Chalcomitra adelberti</i>	FMNH396730	Ghana	X	X	*	X
	FMNH396731	Ghana	X	X	X	X
<i>Chalcomitra balfouri</i>	Ben Warren 294a	Socotra Island	X	X	X	X
<i>Chalcomitra rubescens</i>	AMNH832205	Central African Rep.	X	X	X	X
<i>Chalcomitra senegalensis</i>	FMNH396721	Ghana	X	X	X	X
<i>Leptocoma sericea</i>	MV E648	New Guinea	X	X	X	X
	MV E550	New Guinea	X	X	*	X
<i>Leptocoma sperata</i>	FMNH345061	Philippine Islands	X	X	X	*
	FMNH358544	Philippine Islands	X	X	*	X
<i>Nectarinia famosa</i>	Rauri Bowie (Bred1)	South Africa	X	X	X	X
	FMNH385279	Uganda	X	X	*	*
<i>Nectarinia johnstoni</i>	FMNH385289	Uganda	X	X	X	*
	Rauri Bowie (X86081)	Kenya	X	X	*	*
<i>Nectarinia kilimensis</i>	FMNH385298	Uganda	X	X	X	X
	Rauri Bowie (06)	Kenya	X	X	*	X
<i>Nectarinia purpureiventris</i>	FMNH356303	Uganda	X	X	*	X
	FMNH356306	Uganda	X	X	X	X
<i>Nectarinia tacazze</i>	Rauri Bowie (X86076)	Kenya	X	X	*	*
	Rauri Bowie (X86077)	Kenya	X	X	X	*
<i>Cinnyris chalybea</i>	Rauri Bowie (Gamoegas1)	South Africa	X	X	*	*
	Rauri Bowie (Kirst3)	South Africa	X	X	X	*
<i>Cinnyris chloropygia</i>	FMNH385274	Uganda	X	X	*	*
	AMNH832204	Central African Rep.	X	X	X	*
<i>Cinnyris cuprea</i>	Rauri Bowie (07)	Uganda	X	X	*	X
	FMNH396732	Ghana	X	X	X	*
<i>Cinnyris dussumieri</i>	Ben Warren A-S16a	Seychelles Islands	X	X	X	X
	Ben Warren A-S26c	Seychelles Islands	X	X	X	X
<i>Cinnyris fusca</i>	Rauri Bowie (RB#1)	South Africa	X	X	X	X
<i>Cinnyris jugularis</i>	MV C002	New Guinea	X	X	X	X
	MV JCW071	Australia	X	X	X	X
<i>Cinnyris loveridgei</i>	ZMUCO4922	Tanzania	X	X	X	X
	ZMUCO4088	Tanzania	X	X	X	X
<i>Cinnyris mariquensis</i>	Rauri Bowie (RB#1)	South Africa	X	X	X	X
<i>Cinnyris mediocris</i>	FMNH356820	Tanzania	X	X	X	X
	ZMUC JK01-250401	Tanzania	X	X	X	X
<i>Cinnyris minulla</i>	FMNH DW-5092	Central African Rep.	X	X	*	X
	Rauri Bowie (RB#1)	Uganda	X	X	X	X
<i>Cinnyris notata</i>	FMNH345978	Madagascar	X	X	*	*
	FMNH345979	Madagascar	X	X	X	X
<i>Cinnyris osea</i>	Rauri Bowie (RB#1)	Israel	X	X	X	X
<i>Cinnyris pulchella</i>	UMMZ232422	Cameroon	X	X	X	X
	FMNH396735	Ghana	X	X	X	*
<i>Cinnyris regia</i>	FMNH346631	Burundi	X	X	*	X
	FMNH356179	Uganda	X	X	X	X
<i>Cinnyris reichenowi (preussi)</i>	FMNH358155	Burundi	X	X	X	X
	FMNH346608	Burundi	X	X	*	X
<i>Cinnyris rufipennis</i>	ZMUC07162	Tanzania	X	X	X	X
	ZMUC07189	Tanzania	X	X	X	X
<i>Cinnyris souimanga</i>	FMNH352966	Madagascar	X	X	X	X
	FMNH352967	Madagascar	X	X	*	X
<i>Cinnyris stuhlmanni</i>	FMNH356096	Uganda	X	X	X	X
	FMNH356109	Uganda	X	X	X	X
<i>Cinnyris venusta</i>	UMMZ232421	Cameroon	X	X	*	X
	FMNH356088	Uganda	X	X	X	*

(1) *Deleornis fraseri* and *auxillaris* are considered conspecific in this study.

(2) *Cyanomitra olivacea* and *obscura* are considered conspecific in this study.

**Table 2.2.** Primers used in this study.

Gene Region	Primer	Sequence (5'-3')	Source
ATP6	A8PWL	CCTGAACCTGACCATGAAC	<a href="http://nmg.si.edu/bermlab/primers">http://nmg.si.edu/bermlab/primers</a>
	CO3HMH	CATGGGCTGGGGTCRACATGTG	<a href="http://nmg.si.edu/bermlab/primers">http://nmg.si.edu/bermlab/primers</a>
ND3	ND3-L10755	GACTTCCAATCTTTAAAATCTGG	Prizker Lab, Field Museum
	ND3-H11151	GATTGTGTGAGCCGAAATCAAC	Prizker Lab, Field Museum
ND2	TrpC	CGGACTTTAGCAGAACTAAGAG	<a href="http://nmg.si.edu/bermlab/primers">http://nmg.si.edu/bermlab/primers</a>
	Lmet	TATCGGGCCCATAACCCGAATAT	Prizker Lab, Field Museum
	Lsun	CGAAAATGATGGTTCAACYCCTTCC	This study
	THH	GAGAGATGGAGGAAAAGGCTAGG	Prizker Lab, Field Museum
	L5575	AAACTAGGACTAGTGCCATTCCA	Prizker Lab, Field Museum
	H5578	CCTTGAAGCACTTCTGGGAATCAGA	Prizker Lab, Field Museum
	L5560	GCAATTTCAATTAACTAGG	Prizker Lab, Field Museum
	LSUNint	TGATTCCCAGAAAGTACTYCAAGG	This study
	HSUNint	TTGTGTTTGGTTTAGTCCYATTC	This study



**Table 2.3.** Nucleotide substitution model parameters calculated using Hierarchical Likelihood Ratio Test using Modeltest (Posada & Crandall 1998) and marginal probabilities of model parameters from a 2 million generation (minus 50 000 generation Burn-in) BI run.

Hierarchical Likelihood Ratio Tests						Marginal Probabilities	
Rates	ATP6	ND2	ND3	mtDNA	FIB5	mtDNA	FIB5
R(a) [A-C]	0.08	0.23	0.23	0.13	1.00	0.15	1.29
R(b) [A-G]	6.57	9.31	8.74	7.20	3.13	8.12	3.21
R(c) [A-T]	0.20	0.25	0.40	0.23	0.67	0.25	0.64
R(d) [C-G]	0.18	0.18	0.50	0.18	0.67	0.20	1.26
R(e) [C-T]	4.99	4.13	8.74	4.31	3.13	4.93	4.35
R(f) [G-T]	1.00	1.00	1.00	1.00	1.00	1.00	1.00
Gamma shape (alpha)	0.45	0.72	0.59	0.60	2.54	0.56	5.03
Prop. Invariable sites	0.42	0.36	0.42	0.40	0.0	0.38	0.06
Model	GTR+I+G	GTR+I+G	TVM+I+G	GTR+I+G	K81uf+G	GTR+I+G	GTR+I+G

**Table 2.4.** Description and position of indels located in Beta-Fibrinogen Intron-5 among the Nectariniidae taxa included within this study. Preference numbers 1-4 refer to indels, which are shared by more than one species.

<i>Dicaeum agile</i>	2 bp del pos. 118-119
<i>Dicaeum aeneum</i>	6 bp del pos. 369-374
<i>Dicaeum melanoxanthum</i>	1 bp del pos. 590
<i>Hypogramma hypogrammicum</i>	2 bp del pos. 438-439, 5 bp del pos. 528-531
<i>Arachnothera longirostra</i>	1 bp del pos. 127, 4 bp del pos. 130-133
<i>Arachnothera magna</i>	1 bp del pos. 288
<i>Chalcoparia singalensis</i>	2 bp del pos. 248-249
<i>Aethopyga gouldiae</i>	13 bp del pos. 140-152
<i>Aethopyga siparaja</i>	18 bp insert pos. 338-355
<i>Anthreptes malacensis</i>	7 bp del pos. 68-74
<i>Anthreptes longuemarei</i>	<sup>1</sup> 201 bp del pos. 282-483
<i>Anthreptes neglectus</i>	<sup>1</sup> 201 bp del pos. 282-483
<i>Anthreptes orientalis</i>	<sup>1</sup> 201 bp del pos. 282-483
<i>Cyanomitra oritis</i>	<sup>4</sup> 12 bp del pos. 545-556
<i>Cyanomitra verticalis</i>	<sup>4</sup> 12 bp del pos. 545-556
<i>Chalcomitra adelberti</i>	<sup>2</sup> 35 bp del pos. 453-488
<i>Chalcomitra balfouri</i>	1 bp del pos. 363
<i>Chalcomitra senegalensis</i>	24 bp del pos. 204-227, 9 bp del pos. 572-580
<i>Nectarinia kilimensis</i>	<sup>2</sup> 35 bp del pos. 453-488
<i>Nectarinia purpureiventris</i>	<sup>2</sup> 35 bp del pos. 453-488
<i>Cinnyris dussumieri</i>	<sup>3</sup> 1 bp del pos. 493
<i>Cinnyris jugularis</i>	<sup>3</sup> 1 bp del pos. 493
<i>Cinnyris minulla</i>	16 bp insert pos. 31-46, <sup>2</sup> 35 bp del pos. 453-488
<i>Cinnyris notata</i>	<sup>2</sup> 35 bp del pos. 453-488
<i>Cinnyris pulchella</i>	<sup>2</sup> 35 bp del pos. 453-488
<i>Cinnyris reichenowi (preussi)</i>	5 bp del pos. 244-248
<i>Cinnyris souimanga</i>	<sup>3</sup> 1 bp del pos. 493

All taxa had a 0-2bp variable deletion at position 85-87 which was excluded from analyses.

**Table 2.5.** Average sequence divergence within and between the recently recognized genera of the Nectariniidae (Irwin 1999, Cheke et al. 2001, Mann 2002), as well as divergence between the Nectariniidae and outgroup taxa. Mitochondrial sequence divergence values for the combined mtDNA data partition (ATP6, ND2 & ND3) are below the diagonal, nuclear (Fib5) sequence divergence values are above the diagonal and the diagonal itself is the within genus nDNA/mtDNA sequence divergence. \*\*\* Designates a monotypic genus or that there was no within genus sequence divergence.

	1	2	3	4	5	6	7	8	9	10	11	12	13	14	15	16	17	18	19	20
1. <i>Corvus</i>	***	13.2	9.2	10.0	10.5	10.9	11.6	11.4	10.8	12.1	10.9	10.7	11.4	10.9	10.0	10.7	10.8	11.3	11.9	11.0
2. <i>Turdus</i>	26.6	***	9.8	10.3	10.1	9.2	10.3	9.9	9.6	10.2	9.7	9.5	9.9	9.6	9.6	9.5	9.9	10.2	11.2	10.5
3. <i>Prionochilus</i>	22.4	24.4	4.4/17.7	5.1	6.7	6.9	7.5	7.6	6.9	7.4	6.9	6.7	7.3	7.1	6.7	6.5	7.0	7.5	8.3	6.9
4. <i>Dicaeum</i>	23.2	24.9	16.7	4.2/15.9	7.5	7.5	8.3	8.4	7.7	8.0	7.6	7.5	8.1	7.9	7.4	7.4	7.6	8.2	9.0	7.7
5. <i>Chalcoparia</i>	22.7	25.4	19.5	20.4	***	4.0	5.2	4.7	4.1	6.8	4.0	3.8	4.4	4.3	4.0	4.6	3.9	4.6	5.7	5.8
6. <i>Deleornis</i>	24.8	24.1	21.1	21.4	18.4	***	4.0	2.3	2.0	6.5	1.6	2.0	2.2	2.1	1.7	3.4	1.8	2.4	4.2	5.3
7. <i>Anthreptes</i> <sup>a</sup>	22.7	24.3	21.0	21.3	17.1	19.1	***	4.7	4.3	8.4	4.2	4.4	4.2	4.6	4.2	4.0	4.1	4.8	5.1	6.5
8. <i>Anthreptes</i> <sup>b</sup>	24.3	25.5	21.5	22.2	16.0	15.6	19.2	1.8/11.6	2.2	7.9	2.0	1.8	2.4	2.7	2.3	3.6	1.8	3.0	5.0	6.4
9. <i>Hedydipna</i>	23.4	25.1	21.2	20.7	17.4	15.6	18.3	15.3	2.2/15.4	6.9	2.0	2.2	2.3	2.3	2.0	3.6	1.9	2.6	4.6	5.5
10. <i>Hypogramma</i>	23.7	27.5	22.7	22.3	21.8	20.4	23.0	22.3	21.2	***	6.3	6.7	7.2	7.2	6.8	7.1	7.1	7.3	8.4	7.5
11. <i>Anabathmis</i>	22.7	22.2	20.0	20.0	17.1	15.8	16.6	14.7	15.1	21.1	***	2.0	2.2	2.1	1.7	3.4	1.8	2.4	4.4	5.4
12. <i>Dreptes</i>	22.2	23.0	20.9	20.6	16.8	14.3	17.5	15.4	14.7	21.5	15.2	***	2.3	2.2	2.1	3.6	2.0	2.5	4.6	5.4
13. <i>Anthobaphes</i>	24.0	25.2	19.9	21.1	17.0	18.1	19.2	16	16.6	20.6	14.6	17.2	***	2.3	2.2	3.6	2.0	2.6	4.9	5.5
14. <i>Cyanomitra</i>	23.2	23.8	19.9	20.1	17.2	15.0	17.8	14.8	14.5	20.4	14.1	14.4	15.8	1.4/12.2	2.0	3.7	1.9	2.5	4.8	5.7
15. <i>Chalcomitra</i>	23.2	23.9	20.2	20.3	16.6	15.4	18.2	14.7	14.6	20.9	15.0	13.7	16.1	13.6	1.5/11.0	3.4	1.7	2.4	4.4	5.5
16. <i>Leptocoma</i>	23.9	23.5	19.7	21.1	17.1	17.2	17.3	17.6	16.9	20.9	17.6	15.6	17.9	16.3	16.6	1.4/14.2	3.4	4.2	3.7	5.7
17. <i>Nectarinia</i>	23.3	23.0	20.1	20.6	16.7	14.0	17.0	14.7	14.5	20.3	14.1	14.1	16.0	13.4	13.0	15.9	1.4/11.7	2.2	4.5	5.7
18. <i>Cinnyris</i>	23.8	24.1	20.4	20.5	17.7	15.7	18.3	15.9	15.3	21.1	14.8	14.8	16.2	14.2	14.1	17.1	14.1	3.0/14.6	5.1	6.0
19. <i>Aethopyga</i>	22.8	24.1	20.1	21.0	17.4	17.5	17.4	18.9	17.7	21.3	16.4	17.0	18.2	17.0	16.4	16.7	16.5	17.3	4.2/14.1	6.6
20. <i>Arachnothera</i>	24.0	25.8	21.5	21.0	19.5	21.1	20.5	20	20.3	21.0	20.0	20.5	20.8	19.6	20.1	20.1	19.9	20.3	20.7	4.5/18.6

a & b, The genus *Anthreptes* is divided to reflect taxa which are restricted to Asia-Australasia and Africa respectively.

**Table 2.6.** Results of the ILD tests on pairwise combinations of different data partitions. Mitochondrial genes are ATP6, ND2 and ND3 and the nDNA is comprised of Beta-Fibrinogen Intron 5. \* Values significant at  $\alpha = 0.05$

	ATP6	ND2	ND3	mtDNA
ATP6				
ND2	0.100			
ND3	0.010*	0.002*		
nDNA	0.940	0.960	0.990	0.960

University of Cape Town

**Table 2.7.** Tests for support of putative monophyletic lineages according to traditional (Delacour 1944, Sibley & Monroe 1990) and recently proposed (Irwin 1999, Cheke *et al.* 2001, Mann 2002) classification schemes for the Nectariniidae. *Leptocoma* is excluded from the test below due to being recovered as a monophyletic lineage in all phylogenetic analyses.

Node	mtDNA	nDNA	mtDNA + nDNA
<b>Traditional classification</b>			
<i>Dicaeum</i>	$P = 0.013$	$P < 0.001$	$P < 0.001$
<i>Prionochilus</i>	$P = 0.028$	$P < 0.001$	$P < 0.001$
<i>Arachnothera</i>	$P = 0.160$	$P = 0.029$	$P = 0.805$
<i>Aethopyga</i>	$P = 1.000$	$P = 0.032$	$P = 1.000$
<i>Anthreptes</i>	$P < 0.001$	$P < 0.001$	$P < 0.001$
<i>Nectarinia</i>	$P < 0.001$	$P < 0.001$	$P < 0.001$
<b>Irwin (1999) classification<sup>1</sup></b>			
African <i>Anthreptes</i>	$P < 0.001$	$P < 0.001$	$P < 0.001$
<i>Hedydipna</i>	$P < 0.001$	$P = 0.044$	$P < 0.001$
<i>Cyanomitra</i>	$P = 0.038$	$P = 0.353$	$P = 0.056$
<i>Chalcomitra</i>	$P < 0.001$	$P < 0.001$	$P < 0.001$
<i>Nectarinia</i>	$P < 0.001$	$P < 0.001$	$P < 0.001$
<i>Cinnyris</i>	$P < 0.001$	$P < 0.001$	$P < 0.001$
Double-banded group <sup>2</sup>	$P < 0.001$	$P < 0.001$	$P < 0.001$
Purple-banded group <sup>2</sup>	$P < 0.001$	$P < 0.001$	$P < 0.001$
White-bellied group <sup>2</sup>	$P < 0.001$	$P = 0.336$	$P < 0.001$

1. Irwin (1999) did not examine Asian members of the genus *Anthreptes*.

2. Three of six subgroups of *Cinnyris* recognized by Irwin (1999) and Cheke *et al.* (2001).

## FIGURE LEGENDS

**FIG. 2.1.** Summary of the three major systematic arrangements that have been proposed for the Nectariniidae with the continental distributions of genera highlighted. The False-Malagasy Sunbirds (*Neodrepanis*: Philipettidae) used to be considered part of the Nectariniidae, but are now well established as one of the Old World suboscine lineages.

**FIG. 2.2.** Nucleotide base composition of the various gene regions and data combinations analysed.

**FIG. 2.3.** Levels of genetic variation for different data combinations and codon positions within the mtDNA protein coding genes

**FIG. 2.4.** Nucleotide sequence saturation plots for transition and transversions for each mtDNA and nDNA data partition. Red represent third positions, purple second and blue first positions.

**FIG. 2.5.** Sequence divergence for the combined mtDNA dataset (ND2, ND3 and ATP6) versus nDNA divergence for each pairwise comparison of taxa. Mitochondrial DNA was estimated to be evolving 8.4 times faster than Fib5.

**FIG. 2.6.** Single MP tree obtained (Length = 21546.8, CI = 0.230, RI = 0.434) from a 3.6x 3<sup>rd</sup> position transition down-weighting of the combined mtDNA data partition (ND2, ND3, ATP6, 2113 bp). Labels on the node refer to specific clades mentioned in the text. Values below the nodes indicate bootstrap support from 1000 replicates. Continental distribution patterns are highlighted, Aus – Australasia.

**FIG. 2.7.** Consensus topology of the posterior distribution (minus the burn-in) of trees sampled using four Markov chains in a 2 million generation BI run of the combined mtDNA data partition using the substitution model listed in Table 2.3. Values below the nodes are split (posterior) probabilities of clade support ( $\alpha \leq 0.05$  when  $P \geq 95$ ).

**FIG. 2.8.** One of 110200 MP trees obtained from a MP heuristic search of the nDNA Beta-Fibrinogen Intron 5 data partition (609 bp aligned). The branches indicated with an

X, collapse in a strict consensus topology. Values above the branches refer to branch lengths and below the branches indicate bootstrap support from 1000 replicates.

**FIG. 2.9.** Consensus topology of the posterior distribution (minus the burn-in) of trees sampled using four Markov chains in a 2 million generation BI run of the nDNA FIB5 data partition, using the substitution model listed in Table 2.3. Values below the nodes are split (posterior) probabilities of clade support ( $\alpha \leq 0.05$  when  $P \geq 95$ ).

**FIG. 2.10.** Single MP tree obtained (Length = 23731.8, CI = 0.270, RI = 0.452) from a  $3.6 \times 3^{\text{rd}}$  position transition down-weighting of the combined mtDNA (ND2, ND3, ATP6, 2113 bp) and nDNA (Fib5, 609 bp) data partitions. Values below the nodes indicate bootstrap support from 1000 replicates.

**FIG. 2.11.** Consensus topology of the posterior distribution (minus the burn-in) of trees sampled using three Markov chains in a 5 million generation BI run of the combined mtDNA and nDNA data partitions, under the substitution model listed in Table 2.3. Values below the nodes are split (posterior) probabilities of clade support ( $\alpha \leq 0.05$  when  $P \geq 95$ ).

**FIG. 2.12.** Ancestral area reconstruction for the Nectariniidae taxa included within this study. Eleven to 12 dispersal events are required to explain the present distributional patterns of the Nectariniidae, and a trans-Wallacean (Asian) origin for the family was inferred.

**FIG. 2.13.** Comparison of the split (posterior) probabilities from a 2 (mtDNA) or 5 million (mtDNA & nDNA) generation BI run with bootstrap values obtained under MP from 1000 replicates for (A) the combined mtDNA dataset and (2) the 'combined evidence' dataset.

**FIG. 2.14.** (A) The three alternate dispersal routes for invasion of Africa by an ancestrally trans-Wallacean distributed Nectarinid; route 1, across the Indian Ocean via stepping stone islands, route 2; via a Miocene forest corridor linking southeast Asia with Africa through the Middle-East, and route 3, across central Asia to Europe and from there across the

Gibraltar Bridge which existed during the late Miocene to Africa. (B) The major intercontinental and continent to island colonisations inferred for the Nectariniidae: (1) invasion of Africa by dispersal (diffusion) along the hypothesized Miocene forest corridor, with the ancestral African sunbird assemblage becoming isolated from Asia-Australasia when the corridor fragmented in response to increased aridification in the Early Pliocene, (2) Early radiation of Asian-Australasian Nectarinid lineages, (3) two independent dispersals from the African mainland to colonize the Indian Ocean Islands, (4) alternative routes for back-colonization of *Cinnyris jugularis* from Africa to Asia-Australasia, (5) dispersal of *Cinnyris osea* to the Levant via the Nile Valley, and (6) secondary radiation in Asia of an African derived back-colonization.



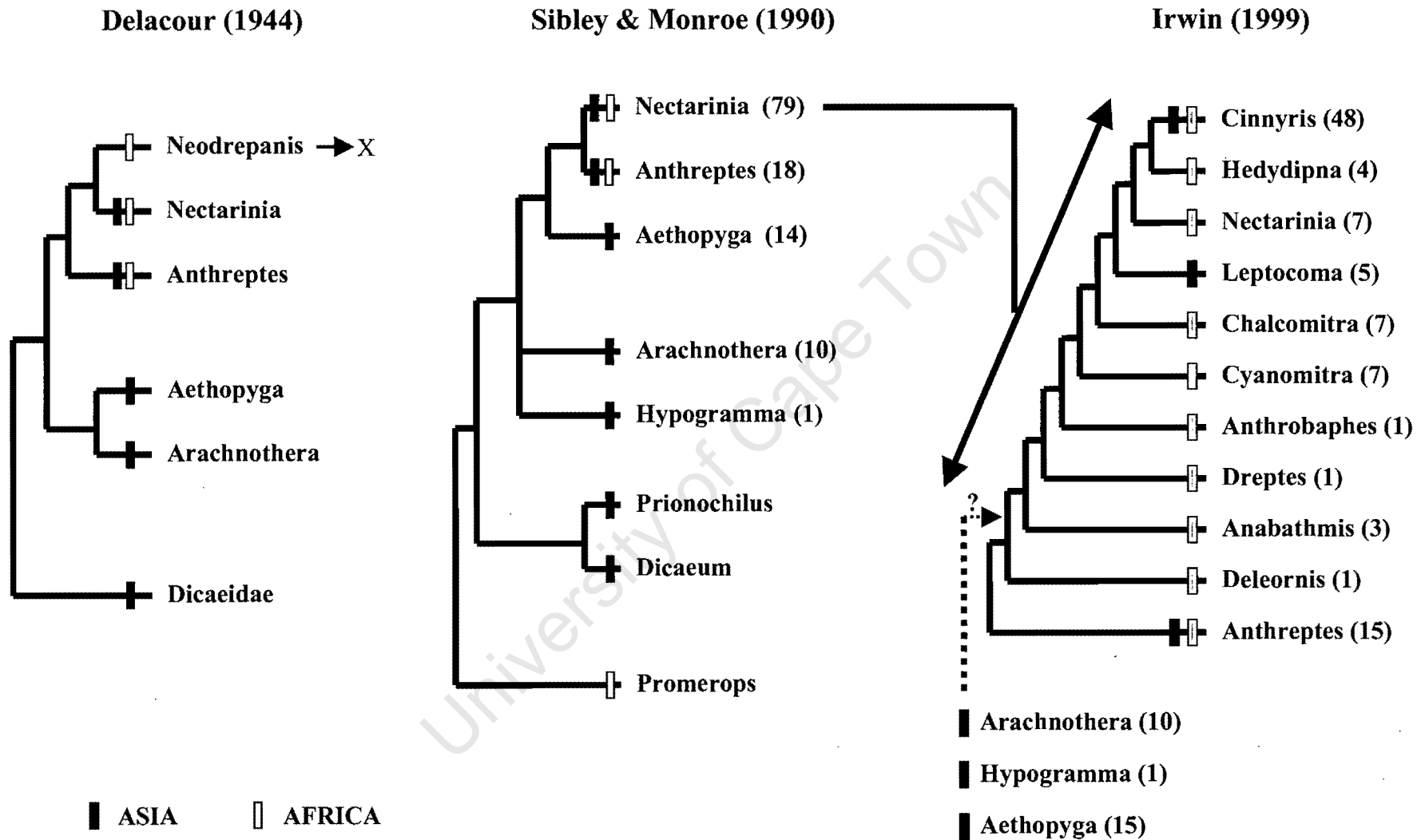
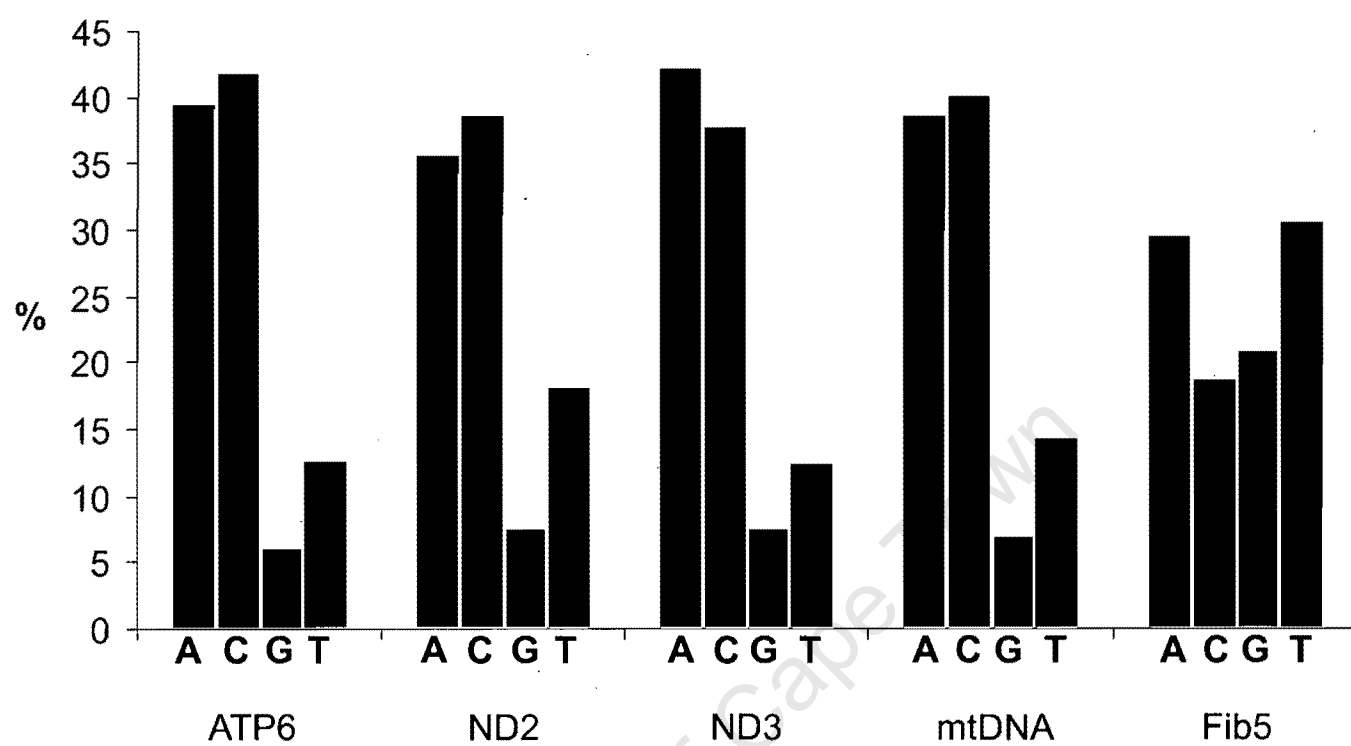
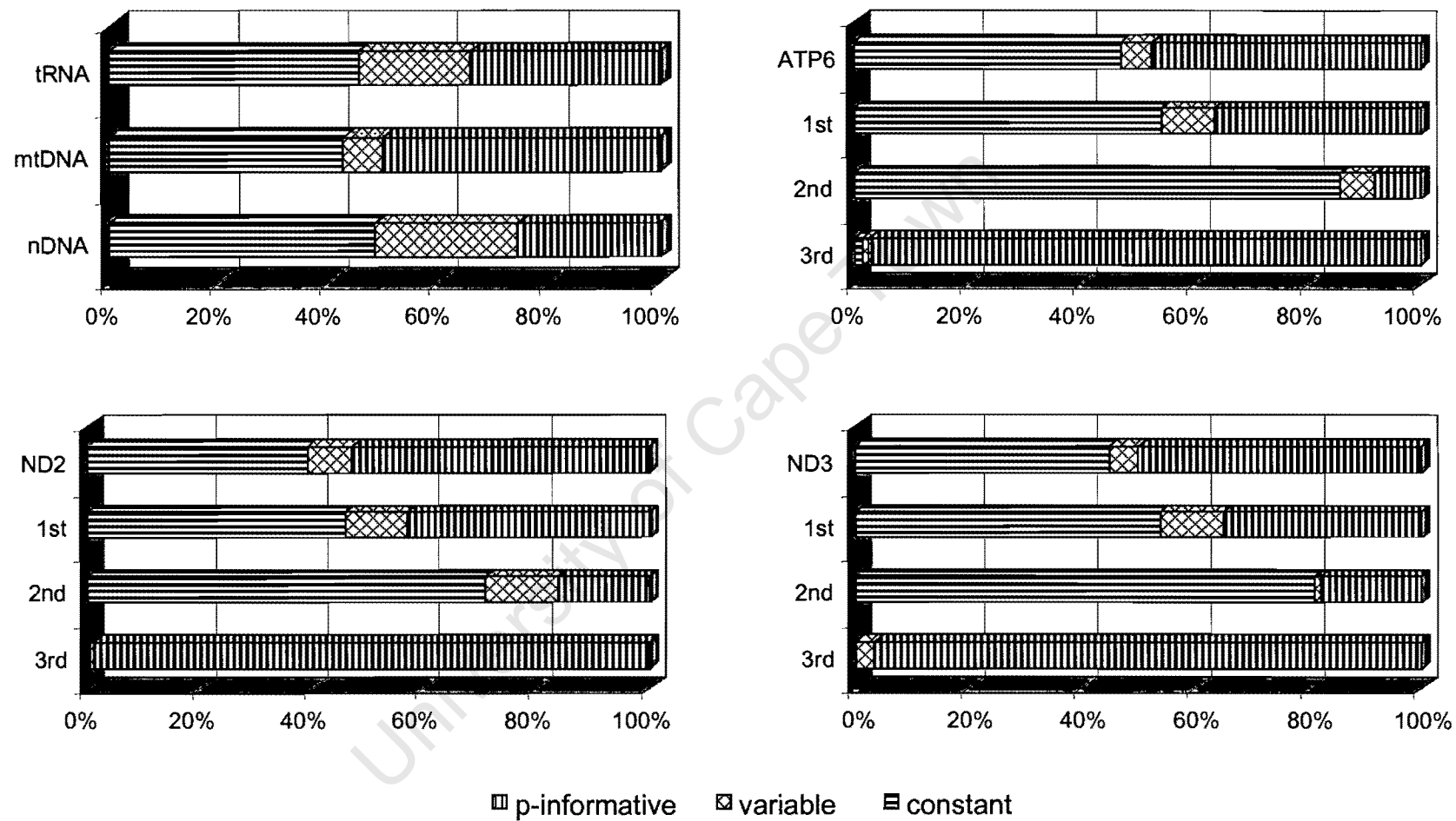


FIG 2.1

**FIG 2.2**



**FIG 2.3**

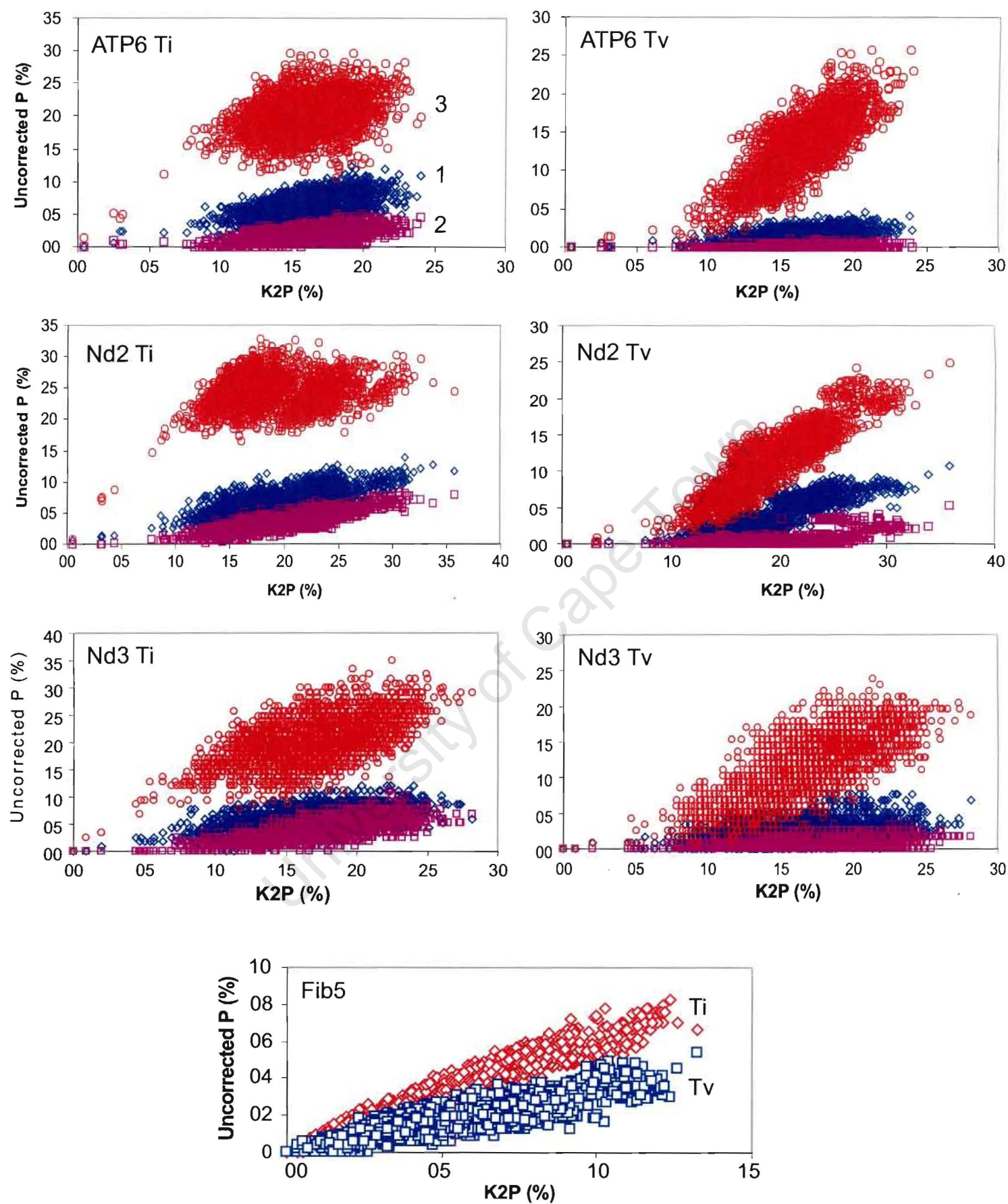


FIG 2.4

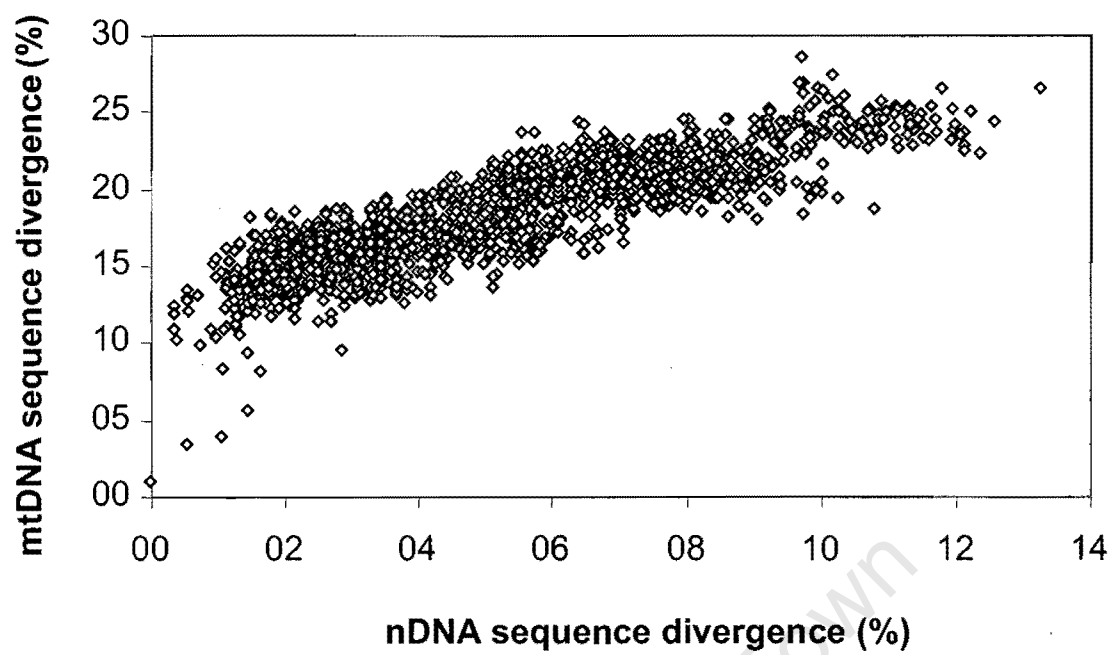


FIG 2.5

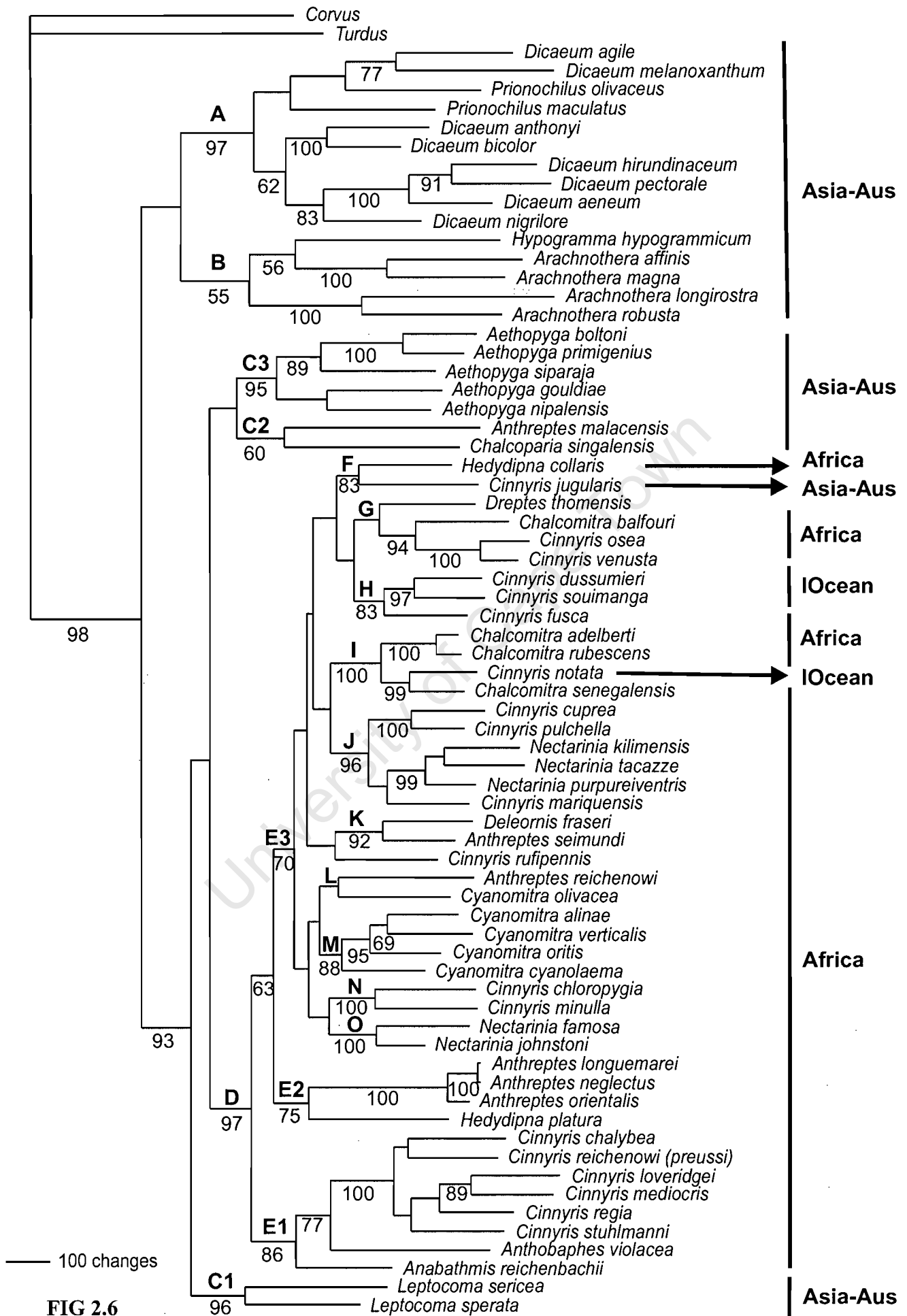


FIG 2.6

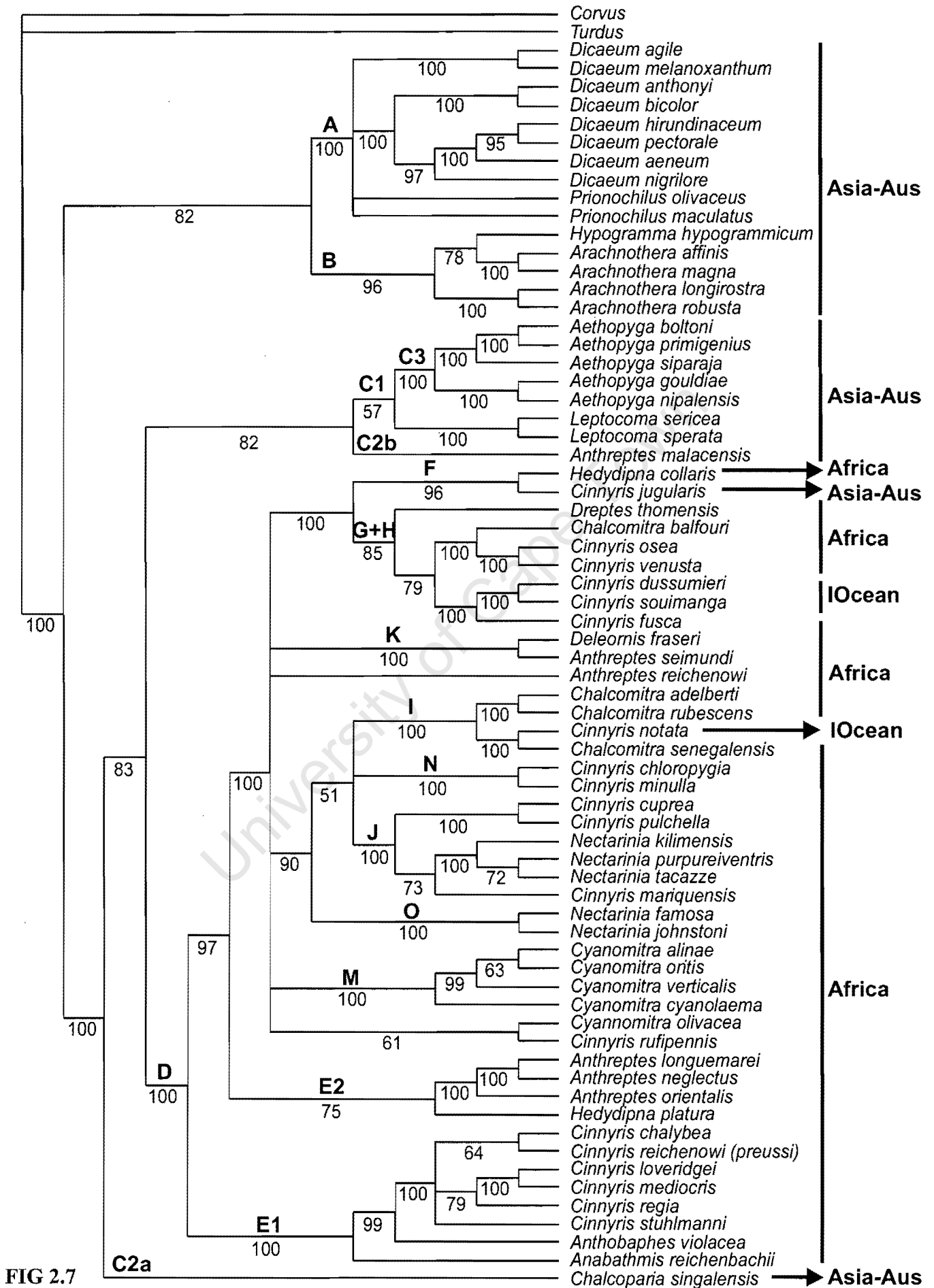


FIG 2.7

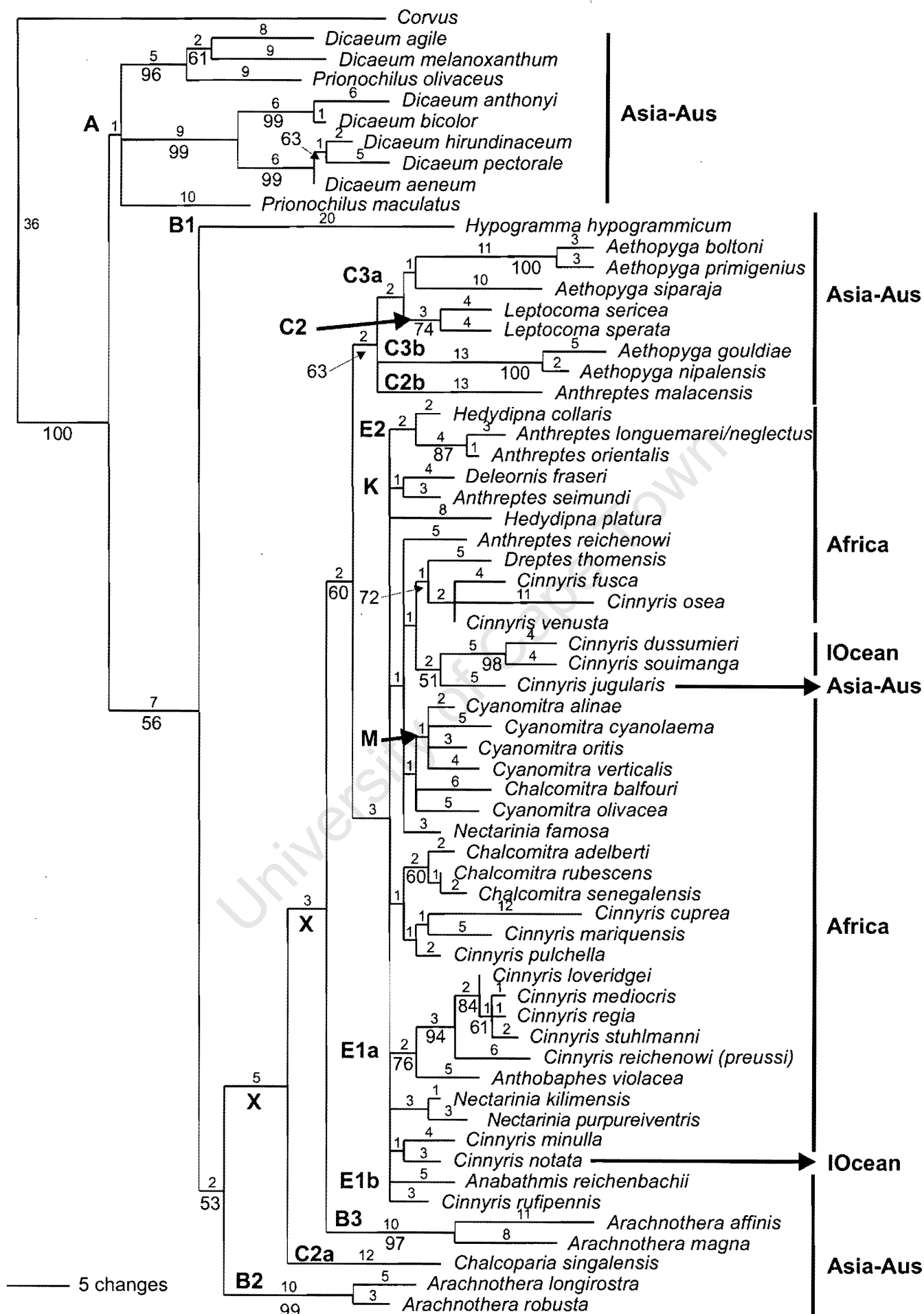


FIG 2.8



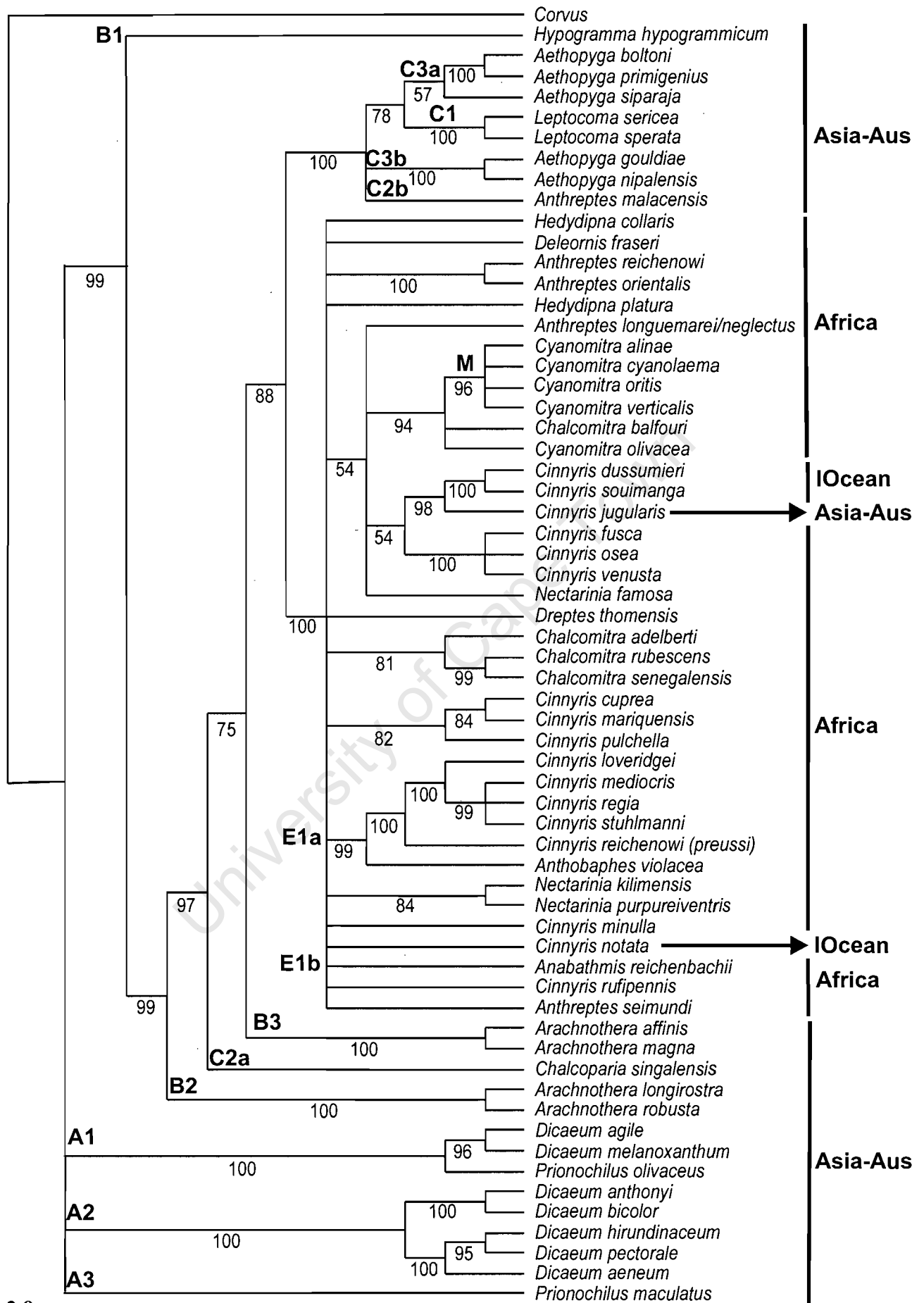
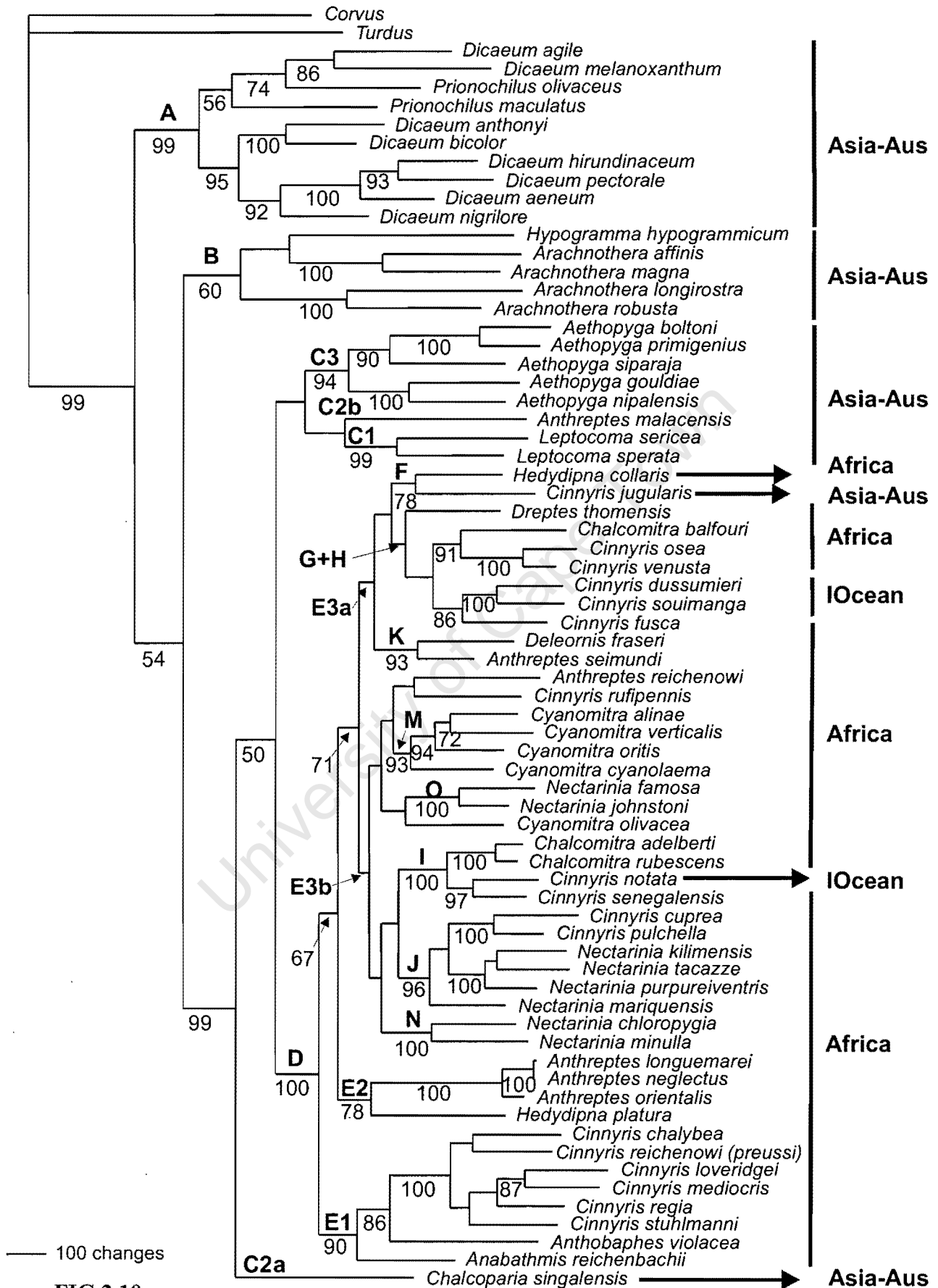


FIG 2.9



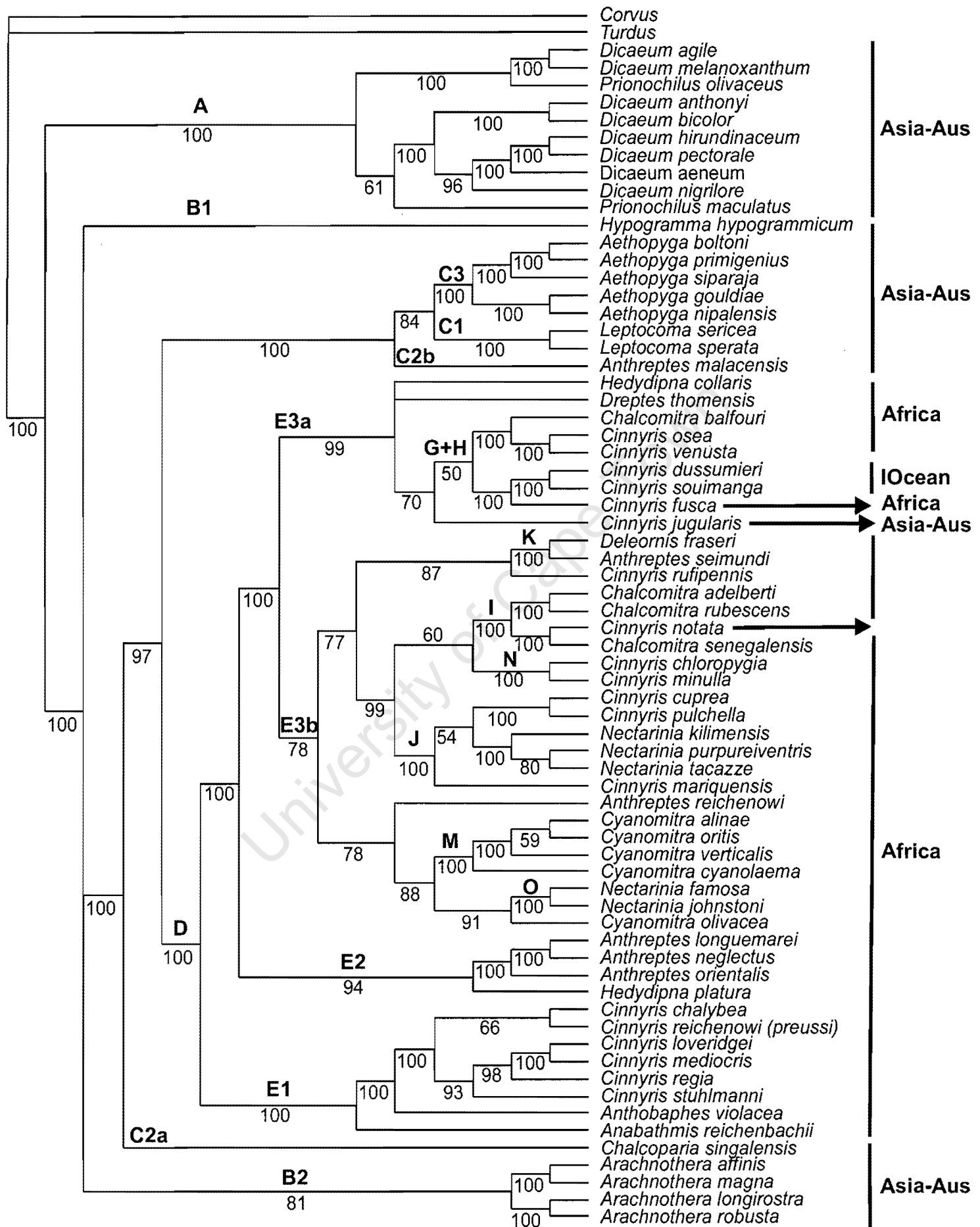


FIG 2.11

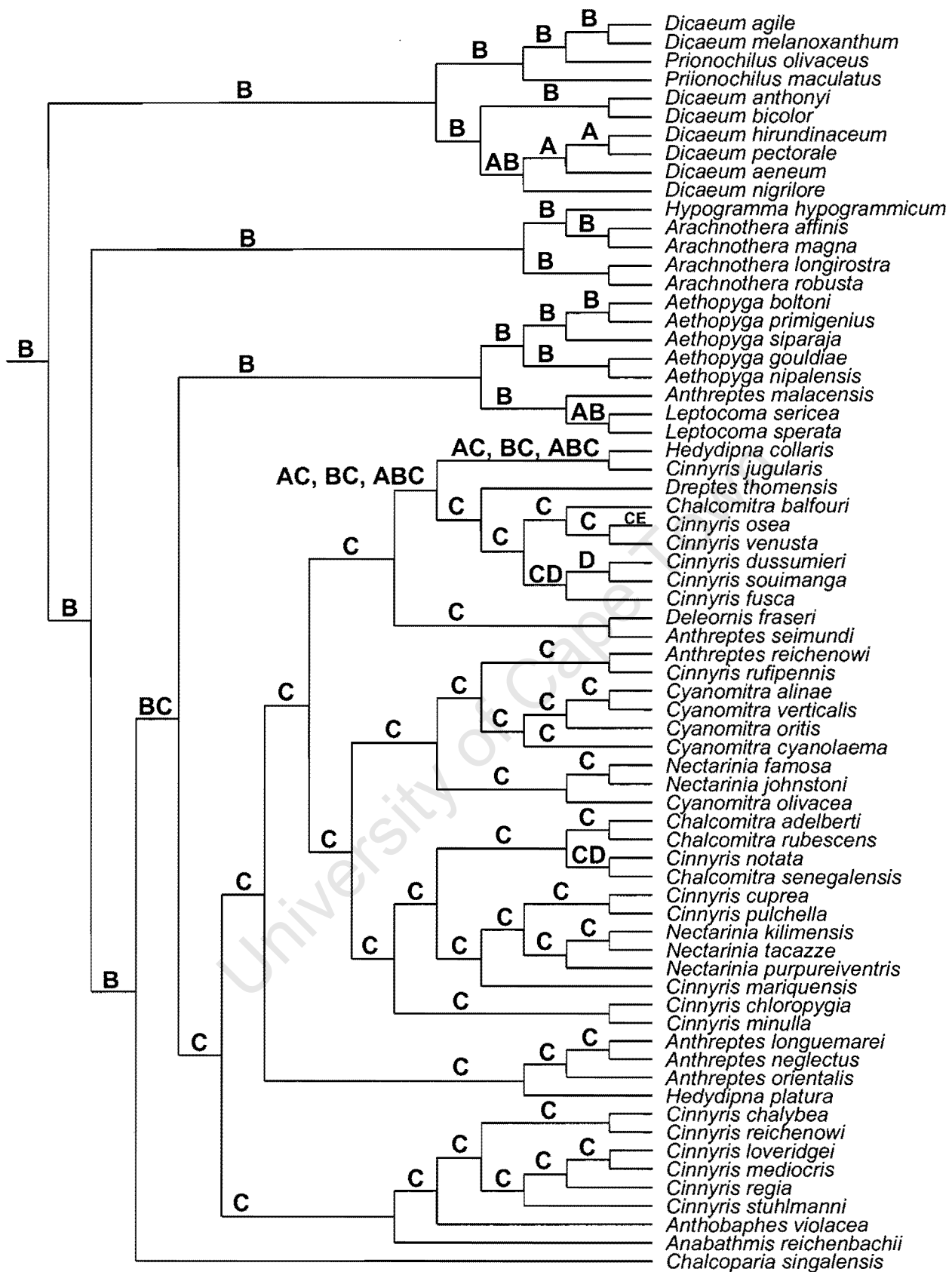


FIG 2.12

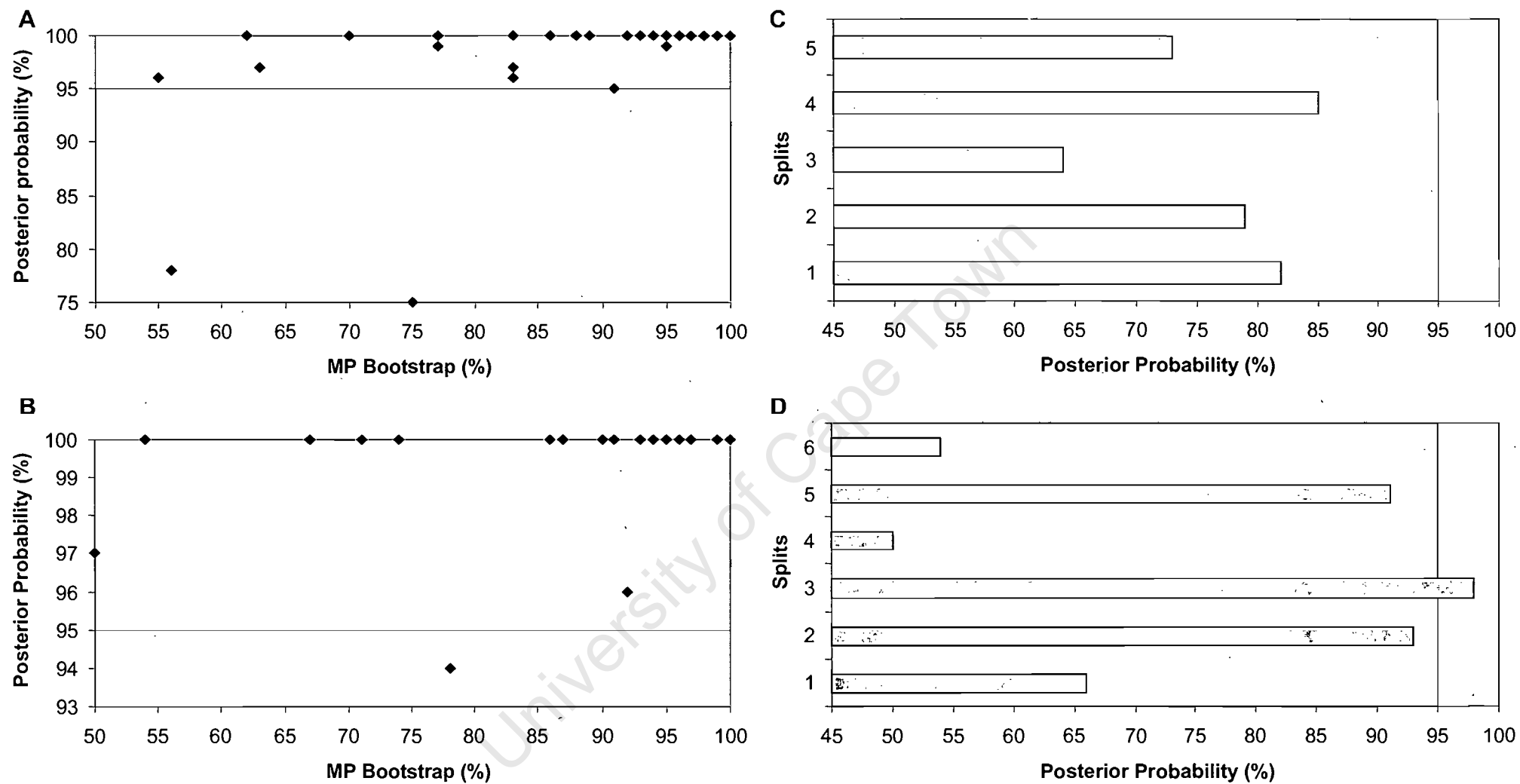


FIG 2.13

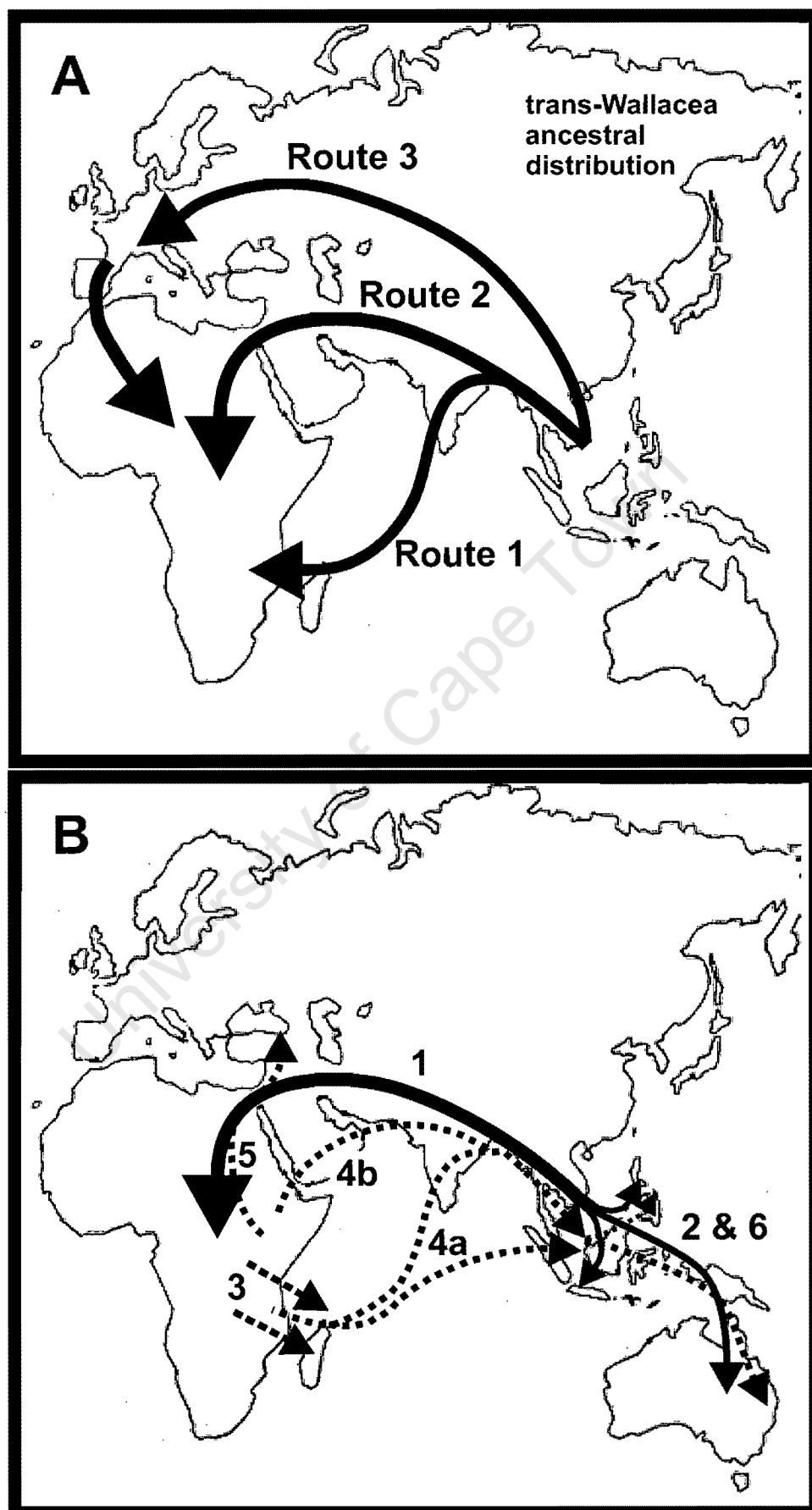


FIG 2.14

## Chapter 3

### Systematics and biogeography of the Eastern Double-collared Sunbird (*Nectarinia mediocris*) species complex

#### Summary

The Double-collared Sunbirds of the Eastern Arc Mountains of Tanzania and southeastern Kenya are characterized by regional variation in morphology and plumage that has resulted in considerable dispute over their taxonomic status and the delineation of range boundaries. It has been suggested that Moreau's Sunbird (*Nectarinia moreaui*) is an atypical phenotype that has arisen from a hybridization event between the more widely distributed Eastern Double-collared Sunbird (EDC, *N. mediocris*) and the narrowly distributed Loveridge's Sunbird (*N. loveridgei*). A discriminant analysis of six standard morphological characters indicates that Moreau's Sunbird is intermediate in shape and size between EDC and Loveridge's Sunbird. There is greater overlap between female Moreau's and EDC than between males, whereas Loveridge's shows little overlap with the other taxa. However, discreet plumage characters separate all three taxa. Molecular analyses of 728 bp of mtDNA (NADH3 & Control Region) suggests that Moreau's Sunbird is a valid taxon and the sister species to Loveridge's Sunbird. Sequence divergence (~5%) between these two taxa suggests they diverged prior to the onset of the Pleistocene epoch. EDC haplotypes can be divided into three distinct clades, separated from each other by substantial genetic divergence (~8-10% sequence divergence). I propose that each of these three clades warrant species status and erect the following three taxa *N. mediocris* Shelley 1855, *N. usambaricus* Gröte 1922 and *N. fuelleborni* Reichenow 1899. Finally, a biogeographical hypothesis of speciation events within the *N. mediocris* species complex is proposed.

## INTRODUCTION

The Eastern Arc Mountains form a long crescent of isolated crystalline massifs that run from the Taita Hills in southeastern Kenya to the Udzungwa Mountains in Tanzania (Fig. 3.1; Lovett & Wasser 1993). These mountains are biogeographically complex and exhibit high species endemism, a feature that has been attributed to persistent humidity since the Tertiary on some mountain escarpments facing the Indian Ocean (Fjeldså & Lovett 1997; Burgess *et al.* 1998).

Ten species of birds are considered to be endemic to the Eastern Arc Mountains (Burgess *et al.* 1998), and a further three species may be added if taxonomic suggestions concerning the avifauna of the Taita Hills (Brooks *et al.* 1998) are accepted. Of the 10, four species are sunbirds (Nectariniidae), with three of the species traditionally being included within the double-collared complex of sunbirds (Hall & Moreau 1970; Jensen 1983). Recent revisions of the family suggest that the Rufous-winged Sunbird (*Nectarinia rufipennis*) is not closely related to other double-collared sunbirds (Irwin 1999, Cheke *et al.* 2001, Chapter 2) as suggested in the original species description (Jensen 1983). The remaining two endemic species, Loveridge's Sunbird (*N. loveridgei*) and Moreau's Sunbird (*N. moreaui*), form a species complex with the Eastern Double-collared Sunbird (*N. mediocris*), which is more widely but disjunctly distributed in montane East Africa.

In general, double-collared sunbirds are difficult to identify, (at least from illustrations in currently available fieldguides), although several populations are diagnosable when carefully examined. This applies to those of the Eastern Double-Collared complex discussed in this chapter. The female of *N. moreaui* is olive above and olive-yellow below as in *N. mediocris*, lacking the distinct aniline yellow of *N. loveridgei*. Male *N. moreaui* have an olive rump, not a metallic green one as in *N. mediocris*, and the underparts of *N. moreaui* are intermediate between *N. mediocris* and *N. loveridgei*. The males of all three taxa have distinct chest bands. In *N. moreaui*, the scarlet-band is confined to the upper breast as in *N. mediocris*, whereas in *N. loveridgei*, scarlet is confined to the centre of the breast with the lower breast and abdomen an intergradation



between orange and ochre. All three taxa have yellow pectoral tufts, which in *N. mediocris* are small and pale, and in *N. moreaui* and *N. loveridgei* are large and bright yellow. Bordering the tufts, *N. moreaui* has a yellow wash to the sides of the breast and abdomen, features more in common with *N. loveridgei*, in which the yellow patches grade into analine yellow underparts. This apparent mixing of plumage characters has resulted in some dispute over the taxonomic status of *N. moreaui* and the delineation of range boundaries among the three taxa. It has been suggested that *N. moreaui* is an atypical phenotype that has arisen in the central Eastern Arc by hybridization between *N. mediocris* and *N. loveridgei* (Hall & Moreau 1970, Stuart & van der Willigen 1980).

Recent consensus has been to recognize *N. moreaui* as a southern Eastern Arc Mountain endemic restricted to the Nguru, Ukaguru, Rubeho, and Uvidunda Mountains (Fig. 3.1, Burgess *et al.* 1998, Birdlife International 2000, Cheke *et al.* 2001, but see Stevenson & Fanshaw 2002) and Mwanihana Forest on the eastern escarpment of the Udzungwa Mountains (Stuart *et al.* 1987, Evans & Anderson 1993). *Nectarinia loveridgei* is endemic to the Uluguru Mountains. These two forms displace the more widespread *N. mediocris*, which therefore has a disjunct distribution with two subspecies in the north/east and two in the south/west. The nominate, *N. m. mediocris*, occupies the highlands of Kenya extending south to the crater highlands of Tanzania, Mount Kilimanjaro and the North Pare Mountains. *Nectarinia m. usambaricus* is restricted to the Taita Hills, the South Pare and West and East Usambara Mountains. *Nectarinia m. fuelleborni* is described from the mountains of southwestern Tanzania, ranging from the Udzungwa highlands to Karonga in the extreme north of Lake Malawi and further west to northeastern Zambia, with local populations along the Rukwa Rift. *Nectarinia m. bensoni* occupies Malawi (except the extreme north) and the mountains of northern Mozambique.

During recent fieldwork in southeastern Tanzania, new localities were added to the documented distribution of *N. moreaui*, the Ndundulu and Nyumbanitu Mountains in the eastern part of the Udzungwa Highlands (Dinesen *et al.* 2001), Image Forest, which is a northern outlier of that highland, and Mangalisa and Wota Mts, which are fault-blocks isolated slightly west of the Rubeho Mountains

(this chapter). Specimens recently collected from these localities (vouchers deposited at the Zoological Museum, Copenhagen) were assigned to *N. moreaui* as opposed to *N. mediocris* (based on discrete plumage characters, see results), which was previously thought to occupy these mountain ranges (Fjeldså & Rabøl 1995).

In this chapter, I seek to (1) resolve phylogenetic relationships within the *N. mediocris* species complex, specifically the taxonomic status of *N. moreaui* and (2), further investigate the apparent replacement of *N. mediocris* by *N. moreaui* in the northern Udzungwa Highlands. I first quantify and describe morphometric and plumage characters among *N. mediocris*, *N. moreaui* and *N. loveridgei*, to evaluate the postulated hybrid origin of *N. moreaui* (Stuart & van der Willigen (1980). Secondly, I use DNA sequence data from two rapidly evolving regions of the mitochondrial genome, NADH dehydrogenase subunit 3 and domain-I of the control region to assess phylogenetic relationships among the three putative taxa. These genes have highly conserved flanking regions that facilitate primer design and have a relatively faster rate of evolution than the mtDNA genome as a whole, and are therefore excellent markers for resolving questions at the species–population interface (Baker & Marshall 1997, Chesser 1999, 2000).

## **MATERIALS AND METHODS**

### **Morphometrics**

RCKB measured 155 birds from currently recognized species (Table 3.1): 144 were from specimens housed in the collections of The Natural History Museum (Tring, UK), American Museum of Natural History, United States National Museum, Zoological Museum of Copenhagen, National Museums of Kenya and the Durban Natural History Museum; 11 birds were measured in the field. Wing-length (flattened cord, from the carpal joint to the tip of the longest primary feather) was measured to the nearest 0.5mm using a wing rule. The remaining measurements were made with digital Vernier calipers to the nearest 0.1mm); culmen length (chord length from notch on the skull to the tip of the upper mandible), upper mandible length (from the distal edge of the nares to the tip of the upper mandible), bill-depth (depth in the vertical plane at the anterior edge of the nares), bill-width (width in the horizontal plane at the anterior edge of the

nares) and the length of the longest and shortest tail feathers (from the base of the pygostyle to the tip of either the central or outer rectrix. For all individuals moult was scored for both the wing and tail to help eliminate spurious results. Culmen length and upper mandible length were correlated ( $R^2 = 0.91$ ,  $P < 0.001$ ). Upper mandible length was preferred because of improved repeatability. Where age, using standard criteria (% skull ossification) was not recorded for museum specimens, bill and plumage characters (yellow-orange gape, body moult towards sexually mature plumage in the males or presence/absence of a brood patch in females in relation to congeners from the same populations which are breeding) were used to identify juveniles. All juvenile birds were excluded from the analyses.

### **Morphological analyses**

Morphological measurements were log-transformed ( $\log x+1$ ) to reduce variance between characters. Differences in univariate measures between species were tested using one-way ANOVA with Student-Newman-Keuls tests to identify which taxa grouped together (Zar 1996). Principal component analysis (PCA) was used to summarize morphological variation. PCA was performed on individuals and only principal components (PCs) with eigenvalues greater than one were extracted from the correlation matrix. The factor matrix was rotated using the varimax method to optimize variable loadings. The resulting rotated factor matrix was used to determine which of the original variables were most highly correlated with the PCs.

A discriminant analysis (DA), which utilized the original log-transformed morphological data as input variables, was used to examine differences in the group centroids (the multivariate means) of each taxon. DA was also used to reclassify each individual sunbird into one of the three putative species. The adequacy of the reclassification was determined by the percentage of correct classifications, assuming that there was an equal probability (33%) of being classified into any one of the three groups by chance alone. Rates of classification substantially greater than 33% for any taxon would suggest that the discriminant functions have utility for predicting group membership, although a reclassification of 100% would be necessary to consider morphological

measurements diagnostic at the species level. Classification rates were also cross-validated by classifying each individual sunbird based on the functions derived from all the remaining individuals in the analysis other than itself (essentially a jackknife function).

Plumage pattern and color was scored from 155 birds (Male  $n = 101$ , Female  $n = 54$ ; Table 3.1). Plumage *colours* were matched to known color standards (Ridgway 1912) to help objectively define *colours* across specimens. For all male specimens, the widths (defined along the chin to tail axis) of the metallic violet/blue and red/orange chest bands were measured to the nearest millimetre using digital Vernier callipers.

### Sampling for molecular analyses

Samples for *N. mediocris* were collected from 10 localities (three in Kenya, six in Tanzania and one in northern Mozambique), for *N. moreaui* from eight localities in Tanzania and *N. loveridgei* from several localities in the Uluguru Mountains in Tanzania (Fig. 3.1, Appendix 3.1).

To assess the monophyly of the *N. mediocris* species complex samples from all other double-collared sunbirds were included (as defined by Irwin 1999, Fry 2000, Cheke *et al.* 2001) for which tissue was available. Species analyzed were: *N. chloropygia* (Olive-bellied Sunbird), *N. minulla* (Tiny Sunbird), *N. regia* (Regal Sunbird), *N. chalybea* (Southern Double-collared Sunbird), *N. afra* (Greater Double-collared Sunbird) and *N. preussi* (Northern Double-collared Sunbird). The entire phylogenetic assemblage was rooted on *N. rufipennis* (Rufous-winged Sunbird), which is endemic to the Udzungwa Mountains and is thought to belong to the ‘maroon’ group of sunbirds (Irwin 1999, Cheke *et al.* 2001).

### Laboratory procedures

DNA was extracted from frozen tissues or blood using a Puregene DNA isolation kit (Gentra Systems, Minneapolis, Minnesota) following the manufacturer’s animal tissue protocols, but with an overnight proteinase K digestion at 50°C. Fragments of CR1 (390bp; F: 5’-CTTCATGCTTTACAGGGTTAT-3’; R-5’-

TAGCTCGGTTCTCGTGAG-3') and ND3 with flanking tRNAs (Glycine & Arginine; primers reported in Chesser 1999) were PCR amplified using standard conditions (denaturation at 94°C, annealing at 50-54°C, and extension at 72°C). PCR products were electrophoresed on 1.5% low-melting point agarose gels (FMC Bioproducts) stained with Ethidium bromide and visualized under UV light. Amplicons of the appropriate length were cut out of the gel and purified using the GELase™ Agarose gel-Digesting Preparation and the 'fast protocol' method (Epicentre Technologies, Madison, Wisconsin). The purified product was cycle-sequenced using Big Dye terminator chemistry (Applied Biosystems, Inc [ABI]). Cycle-sequencing reactions were precipitated with 3M ammonium acetate or 100% isopropanol, rinsed in ethanol, dried and re-suspended in formamide-EDTA solution and run on an ABI 377 or ABI 3100 automated DNA sequencer.

Sequences were obtained from both strands of DNA for all the outgroup taxa and 20 ingroup taxa (3-4 per taxon). For the remaining individuals, only the forward strand was sequenced. All sequences were checked using the program Sequencher 3.0 (Gene Codes Corp), and for ND3 aligned to the chicken (*Gallus gallus*) mtDNA sequence (Desjardins & Morais 1990) to test for the presence of any insertions or deletions. Control region haplotypes were easily aligned by eye.

### **Molecular analyses**

Phylogenetic analyses were performed using two approaches: maximum parsimony (MP) and maximum likelihood (ML). Parsimony analyses, using PAUP\*4.0b8 (Swofford 1998) were conducted using the heuristic search option, implementing stepwise addition with 100 random addition replicates (Maddison 1991). Transitions often accumulate at higher rates than transversions; MP analyses were conducted under several heuristic and empirically determined transition:transversion (Ti:Tv) weighting schemes to evaluate the sensitivity of tree topology to saturation. The search parameters for all MP analyses were: all characters unordered; equal weighting; uninformative characters excluded; TBR branch swapping; steepest descent option not in effect; zero branch lengths collapsed to polytomy; MULPARS option in effect; and topological constraints

not enforced. Two methods of clade support were calculated in the MP analyses. Bootstrap support (Felsenstein 1985) was estimated using 1000 bootstrap replicates (Farris *et al.* 1996).

For maximum likelihood analyses, the dataset was initially analyzed using Modeltest 3.06b (Posada & Crandall 1998) to help ascertain the substitution model that best described the dataset. The models of nucleotide substitution identified were incorporated in PAUP\* 4.0b8 for ML analyses using a full heuristic search with 100 random addition replicates and search parameters as described for the MP analyses. Clade support was estimated using 100 bootstrap replicates.

PAUP\*4.08b was used to compute partition homogeneity tests (1000 replicates with uninformative characters removed) to determine if data from the different genes suggested different phylogenetic signals. Likelihood ratio tests were used to test for rate heterogeneity among lineages (Huelsenbeck *et al.* 1996).

## RESULTS

### **Do morphological differences support a hybrid origin for *N. moreau*?**

Male sunbirds averaged larger than females in linear dimensions for every measurement (Table 3.1). As a consequence, morphological comparisons were restricted to single-sex groups. Of the three putative species, *N. moreau* displayed the greatest degree of sexual dimorphism for most of the traits measured. Sexual dimorphism was greatest for bill-length (ranges 7.3-15.7% within species) and maximum tail-length (7.9-15.6%), and was least marked in bill-width (1.1-3.9%, Table 3.1). *Nectarinia loveridgei* was the largest of the three species in all traits, except tail-length. In general, *N. moreau* is larger than *N. mediocris sensu lato* although there is overlap in most morphometric characters between the two putative species (Table 3.1; Fig. 3.2).

Within *N. mediocris* there is some size variation. For both sexes, *N. m. mediocris* has a significantly smaller bill than the other three subspecies (Table 3.2). For wing-length, male *bensoni* were slightly larger than either *mediocris* or *fuelleborni* and, much larger than *usambaricus*. Similarly, *bensoni*, *mediocris*

and *fuelleborni* have considerably longer tails than *usambaricus*. For most traits (wing, max. bill-length, bill-depth, tail max. and min.), *N. m. usambaricus* most closely resembles *N. moreau* in linear dimensions.

Breast coloration in all taxa is characterized by variation in two distinct bands, a narrow blue/violet and broad scarlet band, which border an iridescent green throat. *Nectarinia m. mediocris* had a significantly broader violet band compared with the other subspecies. Both of the northern subspecies, *N. m. mediocris* and *N. m. usambaricus* have significantly narrower scarlet chest bands than either *N. m. bensoni* or *N. m. fuelleborni* (Table 3.2). *Nectarinia moreau* and *N. loveridgei* have significantly wider scarlet chest bands than *N. mediocris* (Tables 3.1 & 3.2). *Nectarinia moreau* has larger yellow pectoral tufts than *N. mediocris*, but it was not possible to quantitatively measure this trait.

For both sexes, the first two principal components (PCs), had eigenvalues greater than one and accounted for 79% of the total variation (Table 3.3). Principal component loadings on PC1 were positive and strongly correlated with bill characters and wing-length. The tail measures were strongly correlated with PC2 (Table 3.3).

The scatterplots (Fig. 3.3) show that these variables are related differently in the three putative species and appear not to vary in a clinal fashion. For both sexes, *N. loveridgei* had the largest values on PC1 indicating that it is relatively larger in bill-length, width and depth, as well as wing-length. *Nectarinia mediocris* had the opposite pattern, whereas *N. moreau* was intermediate in morphotype, with females being more similar to same-sex *N. mediocris* than males (Fig. 3.3). PC2 could not readily discriminate between the three putative species, suggesting that variation in tail-length is a poor character by which to discriminate among the three taxa.

Once specimens have been assigned *a priori* to taxa, in this case using plumage characters (see below), a discriminant function analysis on the six morphological characters can be used to assess overlap among species. For both sexes, there were significant differences among the putative species when both discriminant

functions were considered (M: Wilks'  $\Lambda = 0.156$ ,  $P < 0.001$ ; F: Wilks'  $\Lambda = 0.119$ ,  $P < 0.001$ ), but only for males after DF1 was removed (M: Wilks'  $\Lambda = 0.804$ ,  $P < 0.001$ ; F: Wilks'  $\Lambda = 855$ ,  $P = 0.179$ ), suggesting that the three putative species can be distinguished using morphometrics.

Scatterplots show that the largest degree of separation among the species is along DF1 (Fig. 3.4), and is primarily due to differences in bill dimensions rather than either wing or tail measures (Table 3.3). For both males and females, *N. loveridgei* is readily distinguishable, whereas *N. mediocris* and *N. moreaui* show overlap. *A posteriori* classification, correctly classified 83.3% of females and 92.1% of males using morphometric data (Table 3.4). These values were slightly reduced in the cross-validated classification results where 79.6% of females and 89.1% of males were correctly classified. No female and only two males of *N. loveridgei* were incorrectly identified as *N. moreaui* (Table 3.4). Greater confusion existed when re-classifying *N. moreaui* and *N. mediocris*, than with *N. loveridgei* (Table 3.4).

### **Description of plumage differences between the taxa**

Despite the morphological overlap among taxa (see above), they can all be distinguished by discreet plumage characters. The most important of these are: size and colour of pectoral tufts, belly and tail coverts colours of males, and the color of the wing-panels in both sexes. However, separation of *N. m. fuelleborni* from *N. m. bensoni* is difficult because it was not possible to examine sufficient specimens to accurately place the slight darkening of the belly on *bensoni* in geographical context. The plumage descriptions below follow the colour standards and nomenclature of Ridgway (1912).

#### *Nectarinia mediocris mediocris*

In the adult male, head, neck, lesser wing-coverts, mantle, back and rump are metallic cossack green with a golden tone and bluish wash towards the tips of the feathers. The upper tail coverts are metallic methyl blue; wings are blackish-brown with olive-yellow edges to the primaries; tail is graduated, blackish-brown with T6 and the distal part of T5 having white inner edges and tips; chin and



throat, same as upper head and cheeks, this is bordered by a narrow methyl blue band across the chest and a broad grenadine red band across the breast; large lemon-yellow pectoral tufts on the sides of the chest; and belly to the vent is light olive-yellow. The adult female is olive-green above; wings are more brown as opposed to black in the male, with the olive edges to the primaries more distinct; T6 has a white tip and inner and outer edge; tail as in the male; olive-yellow chest, belly and vent; and the flanks and throat are darker olive.

*Nectarinia mediocris usambaricus*

The adult male differs from *N. m. mediocris* in having a narrower grenadine red breast band (Table 3.2) and the upper tail coverts are violet not metallic methyl blue. The belly is pyrite-yellow with a grey wash. The female has a slightly deeper olive throat.

*Nectarinia mediocris fuelleborni*

The adult male differs from *N. m. mediocris* and resembles *N. m. usambaricus* in having violet upper tail coverts, but differs from both previous taxa as the belly to vent are olive-green with almost no trace of yellow. In some individuals there is a definite brownish wash (tawny-olive to snuff brown) on the lower belly. The female is generally darker olive than in either of the above taxa.

*Nectarinia mediocris bensoni*

The adult male differs from *N. m. mediocris* in having violet upper tail coverts, and is different from all the above taxa in having the belly to vent more dusky olive-green, with almost no trace of yellow. The female is darker than either *N. m. mediocris* or *N. m. usambaricus*, but cannot be distinguished from *N. m. fuelleborni*

*Nectarinia moreaui*

The adult male differs from *N. m. mediocris* in having the upper tail coverts violet, rump plain olive, pectoral tufts are strontium yellow and large, extending the whole breadth of the red chest band, which is more scarlet than the grenadine red in *N. m. mediocris*. Thus, the breast ornament appears as a broad scarlet patch between two large yellow patches, rather than as a more orange-red band

separating small pale yellow patches as in *N. mediocris*; a difference that is not apparent in field-guide illustrations. The belly to vent is dark olive-yellow. The female is very similar to the preceding taxa, but more greyish-olive than in *N. m. mediocris*. The edges of the primaries are olive-ochre, but are not as broad as in *N. loveridgei*.

#### *Nectarinia loveridgei*

The adult male differs from *N. m. mediocris* in having the upper tail coverts violet; the neck, lesser wing-coverlets, mantle, back and the rump is metallic green. It differs from all the above taxa in that the upper wing is blackish with the secondaries, tertials and primary coverts being edged in olive, forming a distinctive wing-panel. Below: chin to the upper breast is metallic green like head, bordered below by a band of deep violet; the chest band is orange-ochre and is restricted to the centre of the lower breast, bordered on the sides by warm olive-yellow, grading into an aniline yellow belly and vent; and the pectoral tufts are large, as in *N. moreaui*, but more olive-ochre than strontium yellow. The female has an olive-grey head, contrasting with an olive-green back. Below, the chin is pale olive-grey, with the breast and belly olive-yellow.

### **Molecular Data**

#### **Genotypic Variation**

Compared with the homologous amino acid sequences for the chicken, sunbirds exhibit no insertions in ND3 as found for some other birds (Mindell *et al.* 1998). For CR1, six indels were identified, but these were easily incorporated into the alignment. The molecular characteristics of the mtDNA genes and gene regions used in this study are summarized in Table 3.5.

One of the striking results of this study is the high sequence variability in ND3 among apparently closely related sunbirds. In this study, ND3 not only had a higher percentage of variable sites than CR1 (37.9% vs. 24.7%), but more sites were also parsimony informative (30% vs. 19.2%; Table 3.5), an unexpected finding considering that ND3 is protein coding whereas the control region of the mtDNA genome is not.

Analysis of the full mtDNA dataset (728bp), identified 39 haplotypes among the 47 ingroup individuals sequenced. The haplotypes were distributed among the taxa as follows: *N. mediocris* ( $n = 15$ ), *N. moreau* ( $n = 21$ ) and *N. loveridgei* ( $n = 3$ ). Sequence divergence within *N. moreau* (av. 0.74, range 0.0 to 2.6) and *N. loveridgei* (av. 0.30, range 0.0 to 0.55) were low. In contrast, divergence among *N. mediocris* haplotypes was large (av. 8.67, range 7.17 to 10.04). Distances between sunbirds within the *N. mediocris* species complex compared to other double-collared sunbirds varied between 7.32 and 16.86, and compared to the outgroup *N. rufipennis* ranged from 12.48 to 15.19 (Fig. 3.5).

### Phylogenetic analyses

Results from the partition-homogeneity-test (1000 replicates) between ND3 with flanking regions and CR1 indicate that there is a significant difference in phylogenetic signal between the two mtDNA regions considered ( $P = 0.034$ ). The datasets were therefore analysed independently as well as in combination.

The two most parsimonious trees were obtained using a heuristic search for ND3, compared with 729 for the CR1 dataset (Table 3.5). The CR1 dataset, on its own failed to resolve relationships among *N. moreau*, *N. loveridgei* and *N. mediocris* (Table 3.5). In contrast, ND3 resolves relationships within the *N. mediocris* species complex with high bootstrap and jackknife support (Table 3.5, Fig. 3.6). The poor resolution of the CR1 dataset could be explained by one of three hypotheses: (1) the control region within the Nectariniidae mutates at a slower rate than ND3; (2) the control region is mutating at a very high rate and homoplasy is making phylogenetic reconstruction difficult; and (3) the control region sequences amplified in this study could all be from a nuclear copy of the mtDNA, which has been reported in other bird species (Quinn 1992, Sorenson & Fleischer 1996). Resolving which of the above hypothesis is correct is beyond the scope of this chapter, and is currently being further researched. However, preliminary analyses suggest that much of the conflict between the CR1 and ND3 datasets could be due to differential distribution of phylogenetically informative characters (Bowie unpublished data). In ND3, within clade haplotype diversity is reduced relative to CR1, but inter-clade variability is high. These differences could explain the significant conflicting signal in the datasets detected using the

partition-homogeneity test. Combining the two datasets did not alter the topology obtained from analysing the ND3 dataset alone. Therefore, I report below only the results for the analysis of the combined datasets.

Equally-weighted maximum parsimony analyses of the 728bp dataset (169 parsimony informative characters) yielded 88 equally short trees (Fig. 3.6;  $L = 458$ ,  $CI = 0.557$ ,  $RI = 0.843$ ). These trees differed from each other with respect to relationships among individuals within taxa, and the relationships among outgroup double-collared sunbirds relative to members of the *N. mediocris* species complex. Bootstrap and jackknife support is high (100% and 65% respectively) for the monophyly of the ingroup (*N. mediocris*, *N. moreaui* and *N. loveridgei*), although the sister taxon to the complex remains unresolved (possibly *N. preussi*, Fig. 3.6). Weighted parsimony analyses that down-weight third position transitions by a factor of 5:1 relative to transversions found 126 most parsimonious trees, the consensus topology of which is the same as in the equally-weighted tree (Fig. 3.6). Under greater weighting schemes, such as 10:1 down-weighting of third position transitions over transversions, 88 most parsimonious trees were obtained, with *N. afra*, *N. preussi* and *N. chalybea* forming a clade, which is sister to the *N. mediocris* complex. In all analyses, *Nectarinia chloropygia* and *N. minulla* cluster near the base of the tree rooted on *N. rufipennis*. Preliminary results from a larger phylogenetic study (Chapter 2) suggest that *N. chloropygia* and *N. minulla* are not members of the ‘classical’ double-collared sunbirds as defined by Irwin (1999) and Cheke *et al.* (2001).

To facilitate time-efficient maximum likelihood (ML) analysis, the dataset was pruned to 27 individuals. Identical haplotypes, and in clades with many haplotypes a few haplotypes differing by one point mutation relative to others were removed. However, multiple representatives of all haplotype clades were retained. Modeltest 3.06 was used to conduct log-likelihood ratio tests (LRTs) and calculate the Akaike Information Criterion (AIC). The two methods selected different models; LRTs selected a K80 with invariable sites (I) and gamma shape parameter ( $\Gamma$ ) model of nucleotide substitution; whereas the AIC criteria selected a HKY + I +  $\Gamma$  model of nucleotide substitution. The more parameter rich model

(HKY + I +  $\Gamma$ ) was used for ML analyses as it has been suggested that models of DNA substitution should be as realistic as possible to reduce the possibility of making a type I error (false rejection of the null hypothesis; Huelsenbeck *et al.* 1996). Parameters for the model are reported in Table 3.5. ML analyses recovered one tree of length  $-\ln 3107.6$  (Fig. 3.7). The topology of the ingroup is consistent with maximum parsimony (Fig. 3.6).

Analyses of the individuals included in this study suggest that both *N. moreau* and *N. loveridgei* are reciprocally monophyletic and sister to each other. In contrast, the populations traditionally classified as *N. mediocris* form a paraphyletic group with lineages that are sister to the two before-mentioned species, and basal relative to all these. The clustering of birds from the Ndundulu Mountains and Image Forest within *N. moreau* (indicated by \* in Figs 3.6 & 3.7) supports my field notes and those of others (Stuart *et al.* 1987; Evans & Anderson 1993), which suggest that the northeastern reaches of the Udzungwa Highlands is occupied by *N. moreau* and not *N. mediocris*. *Nectarinia moreau* is split into two clades; Clade A of birds from the Nguru Mountains, which are isolated from the rest by 30km of lowland savanna; and Clade B of individuals from the Ukaguru, Rubeho, Mangalisa, Uvidundu and northeastern Udzungwa mountains, which are separated by narrow but very deep (*ca* 2000m) lowland gaps. *Nectarinia mediocris* is split into three clades: Clade C of birds from the Udzungwa Highlands and Mozambique; Clade D of birds from the Usambara and South Pare mountains and Clade E of birds from the Kenyan highlands.

A log-likelihood ratio test of clock-like evolution using the same dataset as for the ML analyses did not reject a molecular clock ( $\chi^2 = 25.1$ , d.f. = 25, ns). This suggests that rates of evolution were not significantly different among the lineages in our tree and therefore that a molecular clock can be used to roughly estimate relative divergence dates.

## DISCUSSION

This study has four significant findings: (1) The mtDNA gene NADH subunit 3 can be highly informative in discriminating among closely related species, (2)

*Nectarinia moreau* is reciprocally monophyletic according to analyses of the mtDNA data partition, (3) *N. mediocris* is paraphyletic, with deep sequence divergence between clades suggesting an extended period of isolation, and (4) taxa can be separated by discrete plumage characters, but overlap somewhat in body dimensions.

#### **Taxonomic status of *Nectarinia moreau***

Hall & Moreau (1970) stated that: ‘It is doubtful if these [plumage] differences justify the specific recognition of *moreau*’ and, suggested that *N. moreau* could be ranked as either a subspecies of *N. mediocris* or *N. loveridgei*. Stuart and van der Willigen (1980) extended Hall and Moreau’s (1970) argument, but provided an explicit evolutionary hypothesis to explain the intermediate phenotype of *N. moreau*. They suggested *N. moreau* to be a stabilized hybrid species having arisen from interspecific hybridization between *N. mediocris* and *N. loveridgei*.

Support for *N. moreau* being an intermediate phenotype between *N. loveridgei* and *N. mediocris* is suggested by an overlap between *N. mediocris* and *N. moreau* in body dimensions. In plumage, it is acknowledged that *N. moreau* shares plumage characters with both *N. mediocris* and *N. loveridgei*. However, discrete plumage characters distinguish all three taxa, but the mtDNA results offer the strongest evidence to support recognizing *N. moreau* as a valid species. None of the 21 *N. moreau* haplotypes identified in this study were found in either *N. loveridgei* or *N. mediocris*. The confirmation that *N. moreau* occurs in the northern Udzungwa mountain complex, in the Ndundulu Mountains and Image Forest (Fig. 3.1) suggests that secondary contact between *N. moreau* and *N. mediocris* may take place. I do not have any direct evidence, but the Kisinga-Rugero Forest is separated from the south Image Forest by only 20km and from the Ndundulu Mountains by 55km, a distance, which is much less than that between some *N. moreau* populations (Fig. 3.1).

If hybridization takes place, this does not seem to result in the breakdown of the genetic integrity of the populations in the Udzungwa Highlands. The visual, focal and behavioural cues, with *N. moreau* being a bird of forest interior as opposed to *N. m. fuelleborni*, which is more typical of forest edges and small

fragments, may be sufficient to assure assortative mate recognition and prevent hybridization and genetic introgression. Additional fieldwork is required to explore this putative contact zone. This combined morphological and molecular approach demonstrates that morphological similarities may depend upon similar ecological requirements and/or mate recognition cues and, may not necessarily correlate with genetic relatedness or structure.

As to the evolutionary origins of *N. moreaui*, reciprocal monophyly does not exclude the possibility of a hybrid origin. Analyses of the ND3 dataset suggest that sufficient time has elapsed for mtDNA lineage sorting to have been completed. In analyses of sequence data from nuclear DNA markers (in this case Beta-Fibrinogen Intron 5) that have slower mutation rates and therefore slower coalescent times than mtDNA (Avice 2000), *N. moreaui* and *N. loveridgei* have identical sequences and differ from *N. mediocris* at 3 of 569 base pairs (0.5% divergence) (two individuals sequenced for each species, Bowie unpublished data). Therefore, until primers for PCR-amplifying more rapidly-evolving nuclear markers (e.g. microsatellites or AFLPs) are available, the phylogenetic hypothesis described here based on mtDNA provides the most robust data with which to evaluate the taxonomic status and origin of *N. moreaui*. The high support for a sister relationship with *N. loveridgei* and the relatively basal position of *N. mediocris* does suggest that a hybrid origin is unlikely and that colonization/isolation and subsequent genetic drift may provide a more plausible hypothesis for the origins of *N. moreaui* (and *N. loveridgei*).

### **Taxonomy of polytypic *Nectarinia mediocris***

Although morphological characters are arguably the most commonly used evidence in identifying and delineating species, revisions are sometimes necessary as more data become available and species concepts change. The ease with which molecular data can be gathered has seen a rapid increase in the number of studies examining avian species boundaries. Frequently, such studies result in taxonomic splitting (e.g., García-Moreno & Fjeldså 1999; Roy *et al.* 1998; Ryan *et al.* 1998, Ryan & Bloomer 1999).

Molecular phylogenetic analyses (Figs 3.6 & 3.7) revealed deeply divergent mtDNA lineages in populations of *N. mediocris* from different geographic regions. Populations from Kenya (*N. m. mediocris*) differ greatly those occurring in populations from the South Pare Mountains and Western Usambara Mountains in northeastern Tanzania (*N. m. usambaricus*), and populations from the southern Udzungwa Highlands (*N. m. fuelleborni*) and northern Mozambique (*N. m. bensoni*). Sequence divergence between these taxa range from 8 to 10%, which is considerable when compared with a 4-5% divergence in mtDNA between *N. moreaui* and *N. loveridgei* (Fig. 3.5).

The geographical variation in morphology has been documented in *N. mediocris* for many years via the recognition of trinomials (subspecies; *N. m. mediocris*, *usambaricus*, *fuelleborni* and *bensoni*.) These taxa occupy naturally fragmented habitats and are spatially distributed as a series of loosely connected allopatric populations. Under the biological species concept allopatric populations, which show some (but limited) phenotypic variation have traditionally been lumped into single taxon (e.g. Paynter & Mayr 1967, Hall & Moreau 1970). This study demonstrates that despite some overlap in body dimensions among taxa, discreet plumage characters can be identified for each taxon, which correlate with geographically structured genetic variation. This study also suggests that three of the currently recognized subspecies of *N. mediocris* be elevated to species status: *N. mediocris* Shelley 1885, *N. usambaricus* Gröte 1922 and *N. fuelleborni* Reichenow 1899. *Nectarinia m. bensoni* Williams 1953, is for now included with *N. m. fuelleborni* as they cluster in the mtDNA analyses. The small, but geographically widespread sample sizes in the morphological analyses were deemed insufficient to determine if the slight darkening of the belly in male *bensoni* is a discrete character or forms part of a cline in *fuelleborni*. These results may change when additional samples from important unsampled populations from northeastern Zambia, Malawi and Mozambique are collected.

### **Biogeography of the *Nectarinia mediocris* species complex**

The inclusion of multiple members of the double-collared sunbirds as outgroups supports the monophyly of the *N. mediocris* species complex, even though *N. mediocris* is paraphyletic. Analyses in this study do not conclusively identify



which double-collared sunbird is the closest relative to the *N. mediocris* species complex, but weighted parsimony analyses suggest that it is most likely to be *N. preussi* and not *N. regia* as suggested by Hall and Moreau (1970). *Nectarinia preussi* is disjunctly distributed, occurring as a series of isolated populations in the Cameroon Mountains, the Albertine Rift Mountains and in western to central Kenya (Cheke *et al.* 2001). *Nectarinia mediocris* and *N. preussi* marginally overlap in the southern Aberdares (Zimmerman *et al.* 1999).

Below I outline biogeographic hypotheses and tentatively date speciation events using the estimate of Fleischer *et al.* (1998) of 1.6% divergence per million years for mtDNA. This calibration is based on Kimura's (1980) gamma-corrected two-parameter distances for cytochrome *b* calculated for Hawaiian honeycreepers (Fringillinae). I use this rate since it is based on a songbird family and the honeycreepers are nectivorous and similar in body size to the old-world sunbirds (Nectariniidae). It should be noted that Fleischer *et al.* (1998) calculated this rate for *cytb* and not ND3, the mtDNA coding gene used in this study. Within the Nectariniidae, ND3 is probably evolving at a faster rate than the background mtDNA rate (Price & Lanyon 2002). To bracket estimates of divergence times we also calibrated divergence dates using the 'standard' 2% divergence per million years used for many biogeographic studies of birds and mammals (see Avise 2000 and Klicka & Zink 1997 for further discussion).

*Nectarinia usambaricus* and *N. mediocris* form a clade at the base of the tree (Fig. 3.6 & 3.7), suggesting that the divergence between birds from Kenya and northeastern Tanzania arose as a consequence of genetic drift, following the split of an ancestral species by vicariance some 8-6 million years (myrs) before present (BP) in the upper Pliocene. This is significant, because it pre-dates the Pleistocene by 3-5 myrs, and the late Pleistocene period characterized large-amplitude climatic change by 5-7 myrs (Kennett 1995). Mount Kilimanjaro and the Chyulu Hills formed during the Pleistocene, creating juxtaposition of young mountains between the more ancient crystalline blocks of the Eastern Arc Mountains and the eroded granitic formations of the central Kenyan Highlands and crater highlands (Griffiths 1993). This has important bearings on the present study as it suggests that the close proximity of *N. mediocris* and *N. usambaricus*,

with only the 35 km gap between the North Pare and South Pare mountains separating them, is secondary. *Nectarinia mediocris* may have been isolated in either the crater highlands or the central Kenyan highlands and during the last million years may have expanded its range to encompass northeastern Tanzania. Birds within the Usambara and South Pare hills have probably been isolated for a long period, and these areas may well form important refugia due to their relative climatic stability (Fjelds  & Lovett 1997; Burgess *et al.* 1998; Cordeiro 1998).

The origins of *N. fuelleborni* are more difficult to hypothesize. This species is placed between *N. mediocris*/*N. usambaricus* and *N. moreau*/*N. loveridgei* in the phylogeny (Fig. 3.6 & 3.7), suggesting a divergence from a *N. mediocris* or *N. usambaricus* ancestor around the Miocene/Pliocene transition. The derived position of *N. loveridgei* and *N. moreau* relative to *N. fuelleborni* suggests that an ancient barrier to gene flow existed between the Usambara and Nguru Mountains in eastern Tanzania. A series of moderately high hills, representing a southern extension of the formation of the Eastern Rift system form potential “stepping-stones” between the crater highlands to the Image/Wota/Rubeho Mountains, and may have been an important historical conduit for genetic exchange. Birds from the crater highlands (presently occupied by *N. mediocris*) may have temporarily been established on these hills extending into the Udzungwa Highlands and from there they could have colonized the Rukwa and Malawi Rifts. The onset of climatic change, specifically a glacial period, would have caused the interior of Tanzania to become even more arid than it is at present (Livingstone 1993). This could have lead to the loss of the hill-top forest fragments connecting the crater highlands with the southern Eastern Arc Mountains, resulting in the subsequent extinction of the populations of sunbird inhabiting these hills. This would have isolated the ancestral *N. fuelleborni*/*N. moreau*/*N. loveridgei* in the southern Eastern Arc. An alternate explanation is long-distance dispersal between the crater highlands/northern Eastern Arc and the southern Eastern Arc Mountains.

A series of low-lying hills (including Malundwe Forest) form potential “stepping-stones” between the Uvidundu and Uluguru Mountains, whereas the Nguru Mountains are separated from the Ukaguru Mountains by a lowland gap

of 30km. It seems likely that the ancestral *N. fuelleborni*/*N. moreaui*/*N. loveridgei* occupied the central and southern reaches of the Eastern Arc and, with the increased climatic instability through the Pliocene and Pleistocene (Kennett 1995), *N. loveridgei*, *N. moreaui* and *N. fuelleborni* were isolated by vicariance, and diversified due to genetic drift. Haplotypes of birds from the Nguru Mountains form a clade that is 1.5-2.5% divergent from the rest of *N. moreaui* haplotypes. This split across a 30km lowland gap suggest that genetic exchange may be limited between the large and genetically diverse *N. moreaui* population occupying the Ukaguru, Rubeho, Uvidundu and Udzungwa Highlands, and the small population supported in the less geographically extensive Nguru Mountains. *Nectarinia fuelleborni* was possibly isolated in the convection rainfall zone near the Malawi Rift, west of the broad, semi-arid plateau of the western Udzungwa Highland, suggesting that its parapatric contact with *N. moreaui* is secondary.

### Conservation implications

Recognizing *N. moreaui* as a distinct species and confirming the presence of this species in the northern Udzungwa Highlands has conservation implications. *Nectarinia moreaui* is restricted to the montane inselbergs of the south-central Eastern Arc Mountains and is therefore a range-restricted endemic to Tanzania. Although abundant at recorded localities and willing to enter secondary-growth thickets in disturbed forest (Jon Fjeldså personal observation), the naturally patchy distribution of its range and the susceptibility of montane rainforests to transformation, makes this a species of conservation concern and efforts should be made to improve our very rudimentary understanding of its life history attributes. Although most forests seem to persist well under present-day management, many highlands have been severally damaged by large fires, as suggested by the large areas of montane grassland with dense patches of second-growth forest only 4-5m tall in some parts of the Rubeho Mountains.

The identification of cryptic species has become a focal point of conservation genetics as biologists have begun to realize that conservation efforts can only be effective if managers know what they are managing. An important result of the present study is the paraphyletic distribution of mtDNA haplotypes in *N.*

*mediocris*. The three unique *N. mediocris* mtDNA lineages can be identified by discreet plumage characters and warrant elevation to species status. However, additional geographically important populations need to be studied both in the field and the laboratory to accurately delineate species boundaries. Nuclear DNA markers could be explored and, if possible, behavioural data in the form of vocalizations should be gathered to further document the distinctiveness of the taxa in question.

**Table 3.1.** Mean sizes and sexual dimorphism (proportional greater size of males relative to females) of species in the *Nectarinia mediocris* species complex. Significant differences between species were tested using one-way ANOVA with Newman-Keuls tests used to identify which taxa differed. \* Designates a male specific character.

Measure	Males		Females		Dimorphism
Taxa ( <i>n</i> , males, Females)	Mean	s.d.	Mean	s.d.	(%)
Wing-length (mm)					
<i>N. loveridgei</i> (19, 9)	58.2	1.7	55.2	1.1	5.2
<i>N. mediocris</i> (75, 37)	54.9	1.6	50.8	1.4	7.5
<i>N. moreaui</i> (7, 8)	54.5	2.4	50.6	0.7	7.2
	$F_{2,98} = 30.5, P < 0.001; \text{lov} > \text{med} = \text{mor}$		$F_{2,51} = 43.5, P < 0.001; \text{lov} > \text{med} = \text{mor}$		
Culman-length (mm)					
<i>N. loveridgei</i> (17, 7)	26.6	1.0	24.7	0.7	7.1
<i>N. mediocris</i> (72, 33)	21.3	1.5	19.8	1.0	7.0
<i>N. moreaui</i> (6, 8)	24.6	0.7	21.0	0.7	14.6
	$F_{2,92} = 105.6, P < 0.001; \text{lov} > \text{mor} > \text{med}$		$F_{2,45} = 82.6, P < 0.001; \text{lov} > \text{mor} > \text{med}$		
Bill-length (mm)					
<i>N. loveridgei</i> (17, 7)	23.2	0.7	21.1	0.6	9.1
<i>N. mediocris</i> (72, 33)	17.9	1.3	16.6	0.8	7.3
<i>N. moreaui</i> (6, 8)	21.0	0.4	17.7	0.4	15.7
	$F_{2,92} = 150.6, P < 0.001; \text{lov} > \text{mor} > \text{med}$		$F_{2,45} = 111.1, P < 0.001; \text{lov} > \text{mor} > \text{med}$		

Bill-width (mm)

<i>N. loveridgei</i> (18, 7)	3.61	0.16	3.57	0.18	1.1
<i>N. mediocris</i> (73, 36)	3.15	0.19	3.07	0.16	2.5
<i>N. moreaui</i> (5, 8)	3.35	0.08	3.22	0.08	3.9

$F_{2,93} = 47.4, P < 0.001; \text{lov} > \text{mor} > \text{med}$

$F_{2,48} = 31.1, P < 0.001; \text{lov} > \text{mor} > \text{med}$

Bill-depth (mm)

<i>N. loveridgei</i> (18, 6)	3.05	0.13	2.97	0.11	2.6
<i>N. mediocris</i> (72, 36)	2.67	0.17	2.59	0.19	3.0
<i>N. moreaui</i> (5, 6)	2.90	0.17	2.7	0.25	6.9

$F_{2,92} = 42.0, P < 0.001; \text{lov} > \text{mor} > \text{med}$

$F_{2,45} = 11.7, P < 0.001; \text{lov} > \text{mor} = \text{med}$

Max tail-length (mm)

<i>N. loveridgei</i> (18, 8)	37.8	2.5	33.7	1.8	10.8
<i>N. mediocris</i> (71, 37)	40.3	3.1	34.0	2.6	15.6
<i>N. moreaui</i> (7, 8)	34.7	3.1	32.0	1.8	7.9

$F_{2,93} = 13.8, P < 0.001; \text{lov} > \text{mor} > \text{med}$

$F_{2,50} = 2.2, \text{ns}$

Min tail-length (mm)

<i>N. loveridgei</i> (18, 8)	30.5	2.6	28.2	2.4	7.5
<i>N. mediocris</i> (71, 37)	32.8	2.9	28.7	2.5	12.5
<i>N. moreaui</i> (7, 8)	29.4	2.8	27.3	1.3	7.1

$F_{2,93} = 7.6, P = 0.001; \text{med} > \text{lov} = \text{mor}$

$F_{2,50} = 1.4, \text{ns}$

\*Violet breast-band width (mm)

<i>N. loveridgei</i> (16)	3.30	0.85	—	—	—
<i>N. mediocris</i> (64)	3.16	0.81	—	—	—
<i>N. moreaui</i> (4)	2.27	0.26	—	—	—

$F_{2,81} = 2.6$ , ns

\*Scarlet breast-band width (mm)

<i>N. loveridgei</i> (18)	18.6	2.3	—	—	—
<i>N. mediocris</i> (73)	11.7	2.2	—	—	—
<i>N. moreaui</i> (4)	16.4	3.5	—	—	—

$F_{2,92} = 68.7$ ;  $P < 0.001$ ; lov > mor > med

**Table 3.2.** Intraspecific morphological variation in *Nectarinia mediocris*. Significant differences between subspecies were tested using 1 x ANOVA, with Newman-Keuls tests to identify which taxa differed. Only significant results are reported.

MALE (n)	Mean	s.d.
Wing-length (mm)		
<i>N. m. bensoni</i> (10)	55.9	1.7
<i>N. m. fuelleborni</i> (6)	54.3	1.4
<i>N. m. mediocris</i> (53)	55.0	1.5
<i>N. m. usambaricus</i> (6)	52.8	1.4
$F_{3,71} = 5.3, P < 0.002$ ; ben = med = fuel > usamb		
Bill-length (mm)		
<i>N. m. bensoni</i> (10)	19.3	0.9
<i>N. m. fuelleborni</i> (6)	19.4	0.9
<i>N. m. mediocris</i> (53)	17.3	0.8
<i>N. m. usambaricus</i> (6)	19.6	1.2
$F_{3,71} = 29.8, P < 0.001$ ; usamb = fuel = ben > med		
Max tail-length (mm)		
<i>N. m. bensoni</i> (10)	40.6	2.2
<i>N. m. fuelleborni</i> (6)	38.7	3.1
<i>N. m. mediocris</i> (53)	41.2	2.5
<i>N. m. usambaricus</i> (6)	34.5	2.2
$F_{3,71} = 13.8, P < 0.001$ ; med = ben = fuel > usamb		
Min tail-length (mm)		
<i>N. m. bensoni</i> (10)	33.4	1.5
<i>N. m. fuelleborni</i> (6)	30.4	2.1
<i>N. m. mediocris</i> (53)	33.6	2.6
<i>N. m. usambaricus</i> (6)	28.4	1.7
$F_{3,71} = 10.6, P < 0.001$ ; med = ben > fuel = usamb		
Violet breast-band width (mm)		
<i>N. m. bensoni</i> (10)	2.7	0.56
<i>N. m. fuelleborni</i> (6)	2.1	0.29
<i>N. m. mediocris</i> (52)	3.4	0.68



*N. m. usambaricus* (6)

2.7

0.50

 $F_{3,70} = 11.4, P < 0.001$ ; med > ben = usamb > fuel

Scarlet breast-band width (mm)

*N. m. bensoni* (10)

14.3

2.4

*N. m. fuelleborni* (6)

14.2

2.0

*N. m. mediocris* (52)

11.1

1.6

*N. m. usambaricus* (6)

9.6

2.0

 $F_{3,70} = 15.9, P < 0.001$ ; ben = fuel > usamb = medFEMALE (n)

Bill-length (mm)

*N. m. bensoni* (4)

17.4

0.9

*N. m. fuelleborni* (5)

17.4

0.4

*N. m. mediocris* (27)

16.3

0.6

*N. m. usambaricus* (1)

17.1

—

 $*F_{2,32} = 9.5, P < 0.001$ ; fuel = ben > med

---

\*For females *N. m. usambaricus* is excluded from ANOVA as  $n = 1$

**Table 3.3.** Loadings of original variables (rotated factor matrix) on principal (PCs) and discriminant components (DA) for three species of sunbird belonging to the *Nectarinia mediocris* species complex. Only the highest loadings for each PC and DA are shown. Eigenvalues and percentage variation associated with each PC are given, as well the total variation summarized by the PCs and DA (\*).

	PC1	PC2	DA1	DA2
Measurement	Loading	Loading	Loading	Loading
<b>Female</b>				
Bill-length	0.939		0.863	
Bill-width	0.847		0.481	
Bill-depth	0.826			0.347
Wing-length	0.756			0.774
Max tail-length		0.959		0.694
Min tail-length		0.941		0.447
Eigenvalue	2.86	1.93	6.21	0.17
% Variation	47.6	32.1 (79.7)*	97.3	2.79 (100)*
<b>Male</b>				
Bill-length	0.850		0.826	
Bill-width	0.810		0.454	
Bill-depth	0.785		0.463	
Wing-length	0.765			0.629
Max tail-length		0.934		0.781
Min tail-length		0.930		0.424
Eigenvalue	2.64	2.13	4.15	0.24
% Variation	43.9	35.4 (79.4)*	94.5	5.5 (100)*

**Table 3.4.** Classification results from the discriminant analysis of three sunbird species from the *Nectarinia mediocris* complex. The column on the left indicates the original group while the top row indicates the predicted group. The percentage of sunbirds classified into a group are given, with the absolute number of sunbirds in parentheses. Correct classifications are italicised.

	Males			Females		
	<i>loveridgei</i>	<i>mediocris</i>	<i>moreau</i>	<i>loveridgei</i>	<i>mediocris</i>	<i>moreau</i>
<b>Original count</b>						
<i>N. loveridgei</i>	94.7% (18)	0% (0)	5.3% (1)	100% (9)	0% (0)	0% (0)
<i>N. mediocris</i>	0% (0)	90.7% (68)	9.3% (7)	0% (0)	78.4% (29)	21.6% (8)
<i>N. moreau</i>	0% (0)	0% (0)	100% (7)	0% (0)	12.5% (1)	87.5% (7)
<b>Cross-validated count</b>						
<i>N. loveridgei</i>	89.5% (17)	0% (0)	10.5% (2)	100% (9)	0% (0)	0% (0)
<i>N. mediocris</i>	0% (0)	88.0% (66)	12% (9)	0% (0)	78.4% (29)	21.6% (8)
<i>N. moreau</i>	0% (0)	0% (0)	100% (7)	0% (0)	37.5% (3)	62.5% (5)

**Table 3.5.** Molecular characterization of the mitochondrial genes and gene regions used in this study and a summary of tree statistics for each gene or gene region analysed using maximum parsimony. Total data set is part of NADH Dehydrogenase Subunit 3 (10789-11126, 338bp, ND3), Domain-I of the Control Region (366bp, CR1) and 24bp of tRNA-Arginine. \* Designates categories for which values were calculated using the program Modeltest 3.06 (Pasada & Crandall 1998).

	ND3	CR1	Total data set
<b>Nucleotide Composition*</b>			
A	28.73%	26.83%	27.19%
C	41.01%	14.83%	26.75%
G	11.46%	30.42%	21.13%
T	18.80%	27.91%	24.93%
<b>Percent Variable Sites</b>			
	128 (37.9%)	92 (24.7%)	213 (29.1%)
<b>Percent Parsimony Informative Sites</b>			
	98 (30.0%)	71 (19.2%)	162 (22.1%)
<b>Ts/Tv Ratio*</b>			
	10.57	4.18	6.09
<b>Alpha Value*</b>			
	N/A	0.5945	0.8281
<b>Proportion of Invariable Sites*</b>			
	0.6030	0.6264	0.5452
<b>Maximum Parsimony (Indels Included)</b>			
No. of MP trees	2	729	88
Tree Length	259	210	458
CI	0.602	0.543	0.557
RI	0.878	0.803	0.843

**FIG 3.1.** The montane rainforests of east and central Africa. The Eastern Arc Mountains are labelled by capital letters. Range distributions for taxa belonging to the *N. mediocris* complex are circled by polygons A to F. Populations sampled for molecular analyses are as follows: *Nectarinia mediocris mediocris*, (1) Mount Kenya, (2) Karisia Hills, (3) Mount Kulal; *N. m. usambaricus*, (4) Mount Shengena, (5) Mazumbai, (6) Ambangulu, (7) Magamba; *N. m. fuelleborni*, (8) Kisinga-Rugero, (9) Udzungwa Scarp Forest; *N. m. bensoni*, (10) Mount Namuli; *N. moreaui*, (11) Nguru Mnts, (12) Chonwe of Uvidunda Mnts, (13) Mamirwa, (14) Magalisa, (15) Mafimero, (16) Uquiwa, (17) Image, (18) Ndundulu Mnts and for *N. loveridgei* (19) Uluguru Mnts (see Appendix 3.1 for further details).

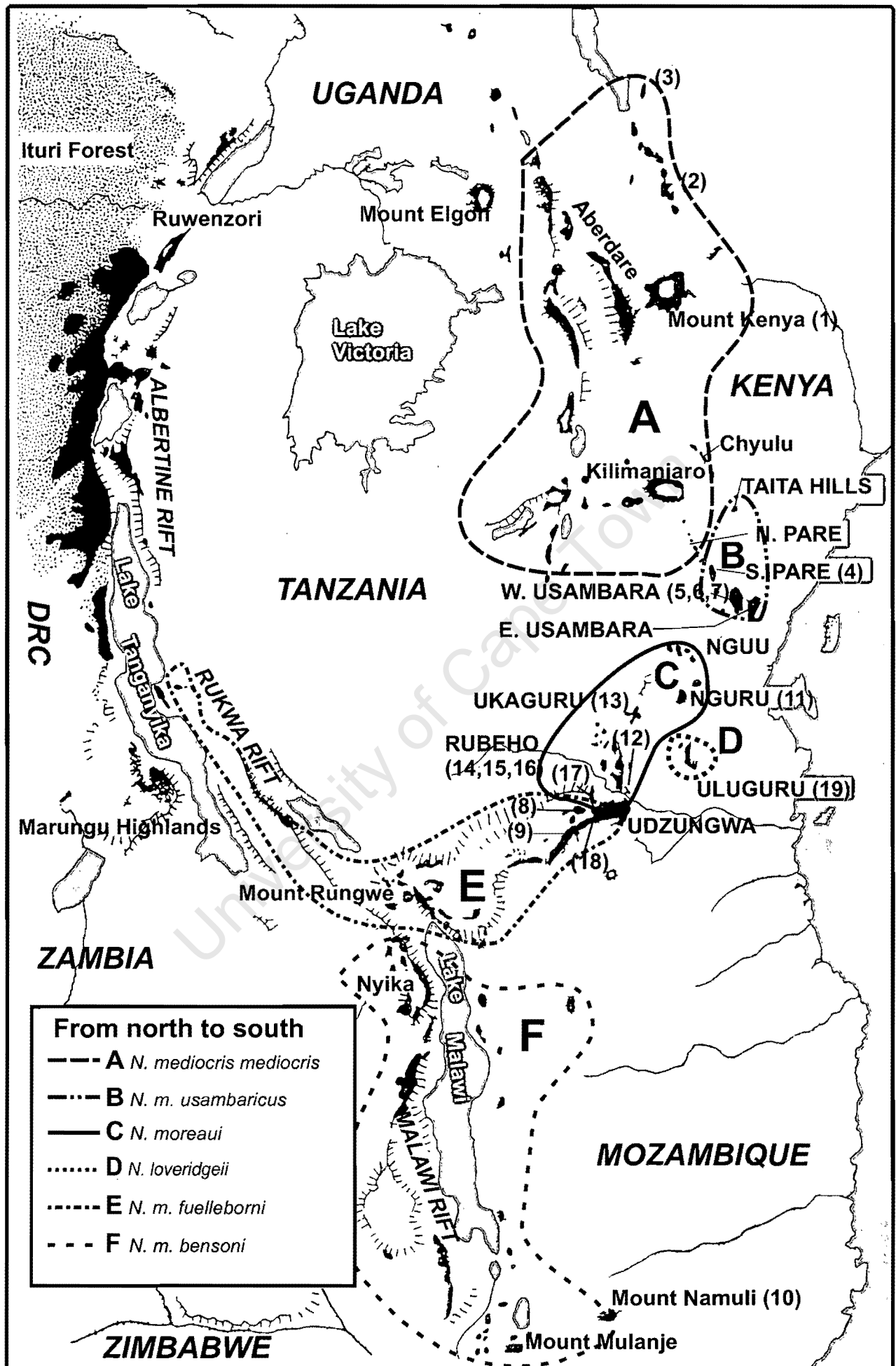
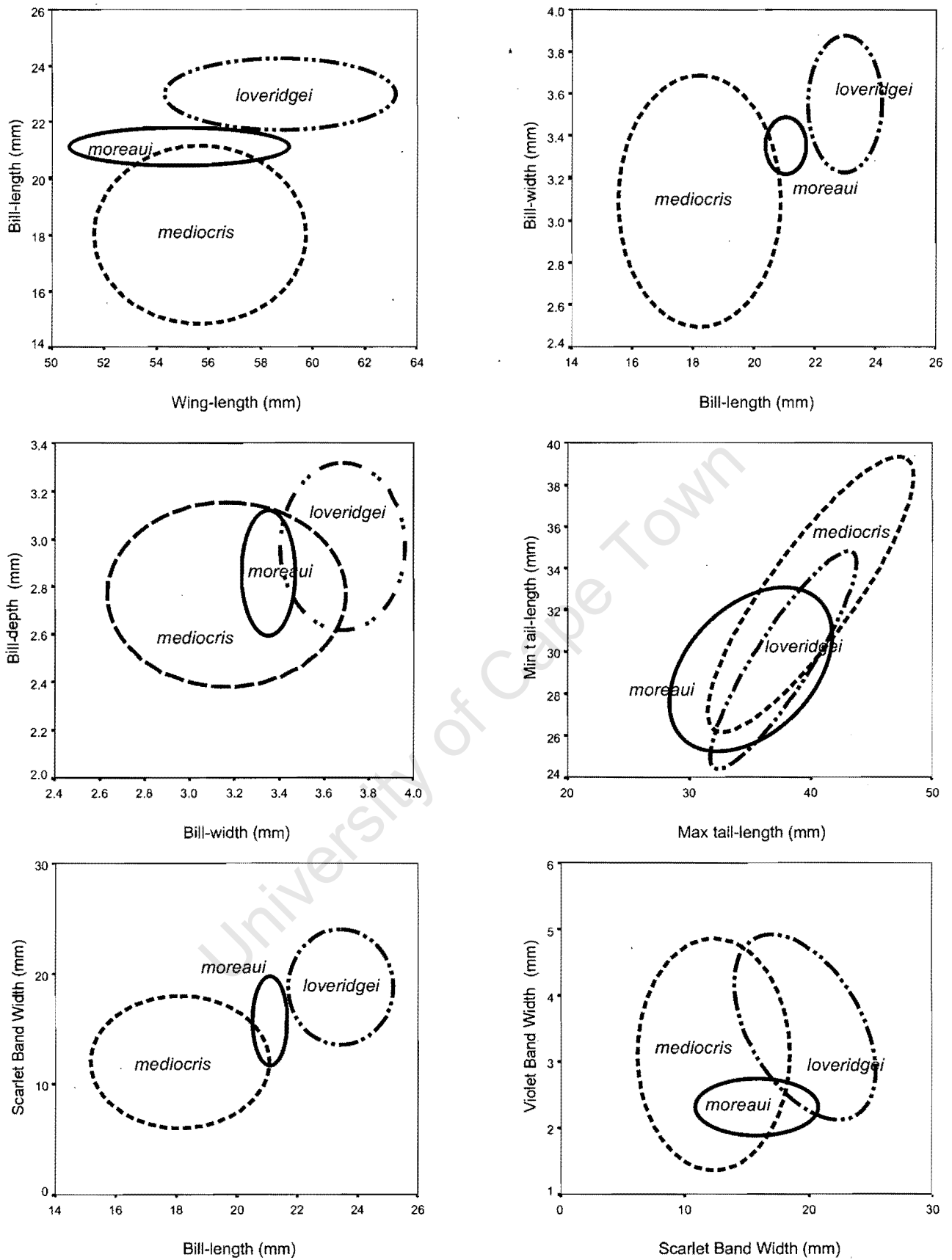
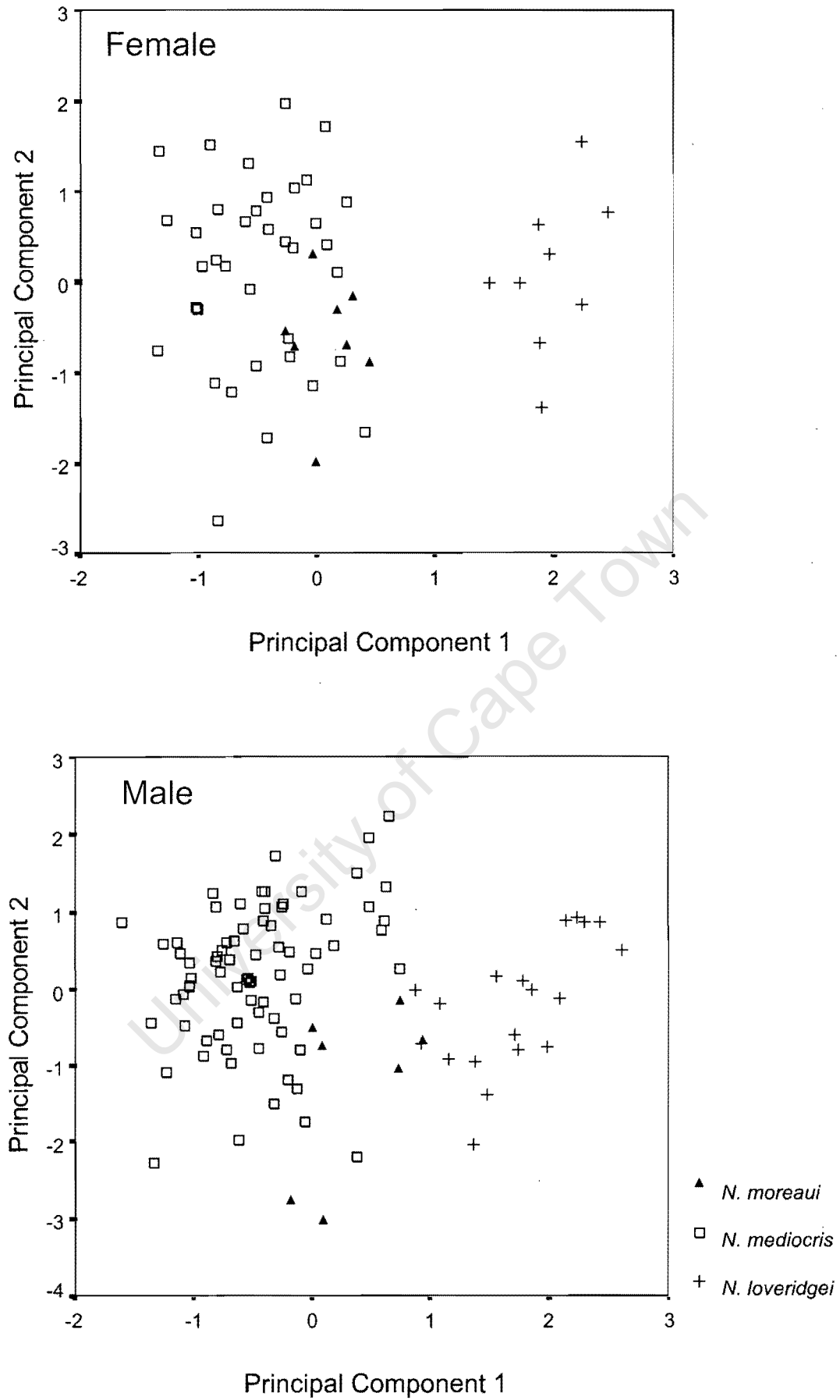


FIG 3.1



**FIG 3.2.** Bivariate plots of male sunbird biometrics. Polygons encompass 95% of individuals measured ( $n = 75, 19$  and  $7$  for *Nectarinia mediocris*, *N. loveridgei* and *N. moreaui*, respectively).



**FIG 3.3.** Scatter plots of the principal component scores derived from six morphological measures for the *Nectarinia mediocris* species complex separated by sex.



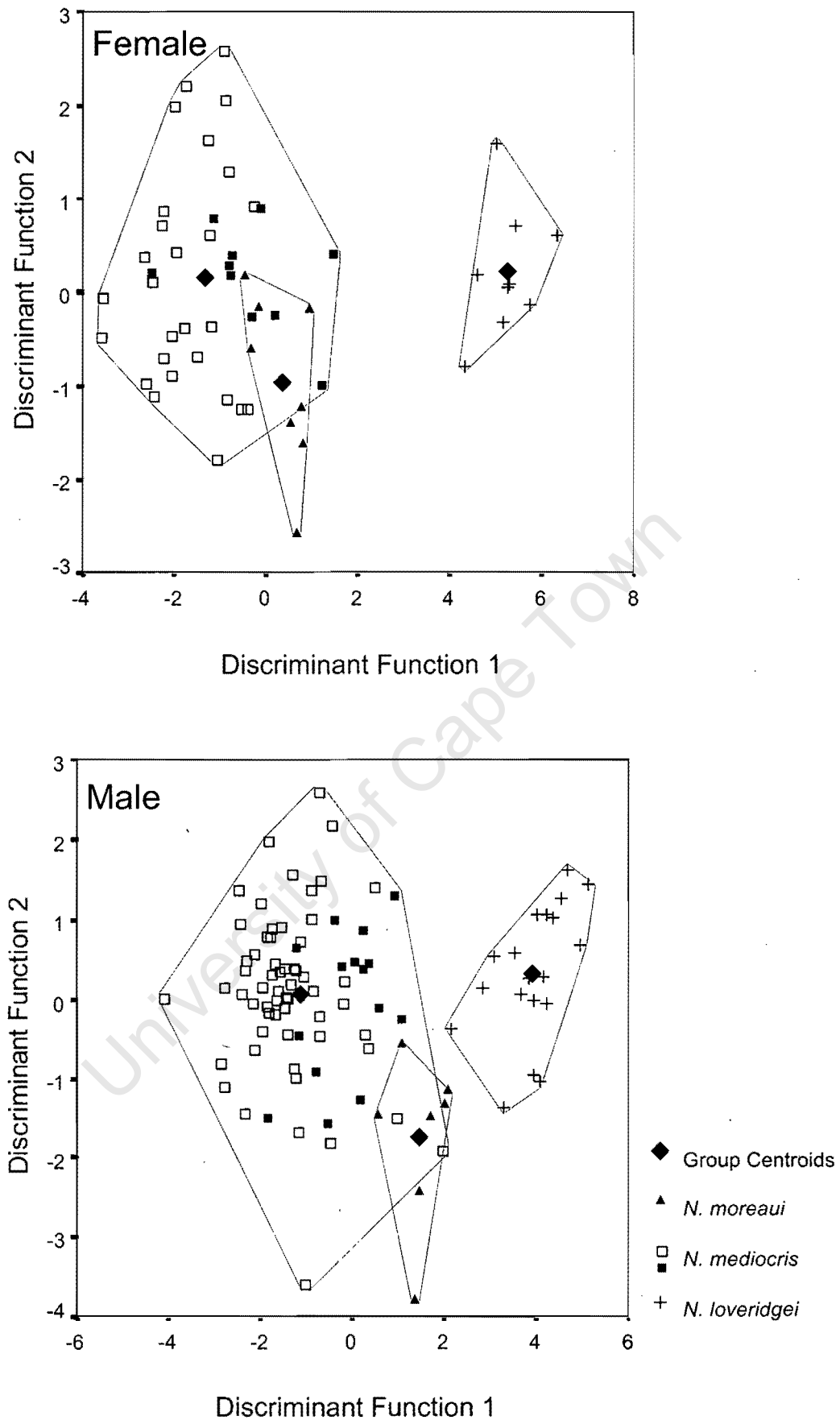


**FIG 3.4.** Discriminant function scores for sunbirds belonging to the *Nectarinia mediocris* species complex separated by sex. Group centroids for each species are indicated. Lines were plotted around each group to aid visualisation. Solid squares highlight *Nectarinia mediocris fuelleborni* and *N. m. bensoni*, the apparent sister taxon to *N. loveridgei* and *N. moreaui* (see Fig. 3.6 & 3.7).

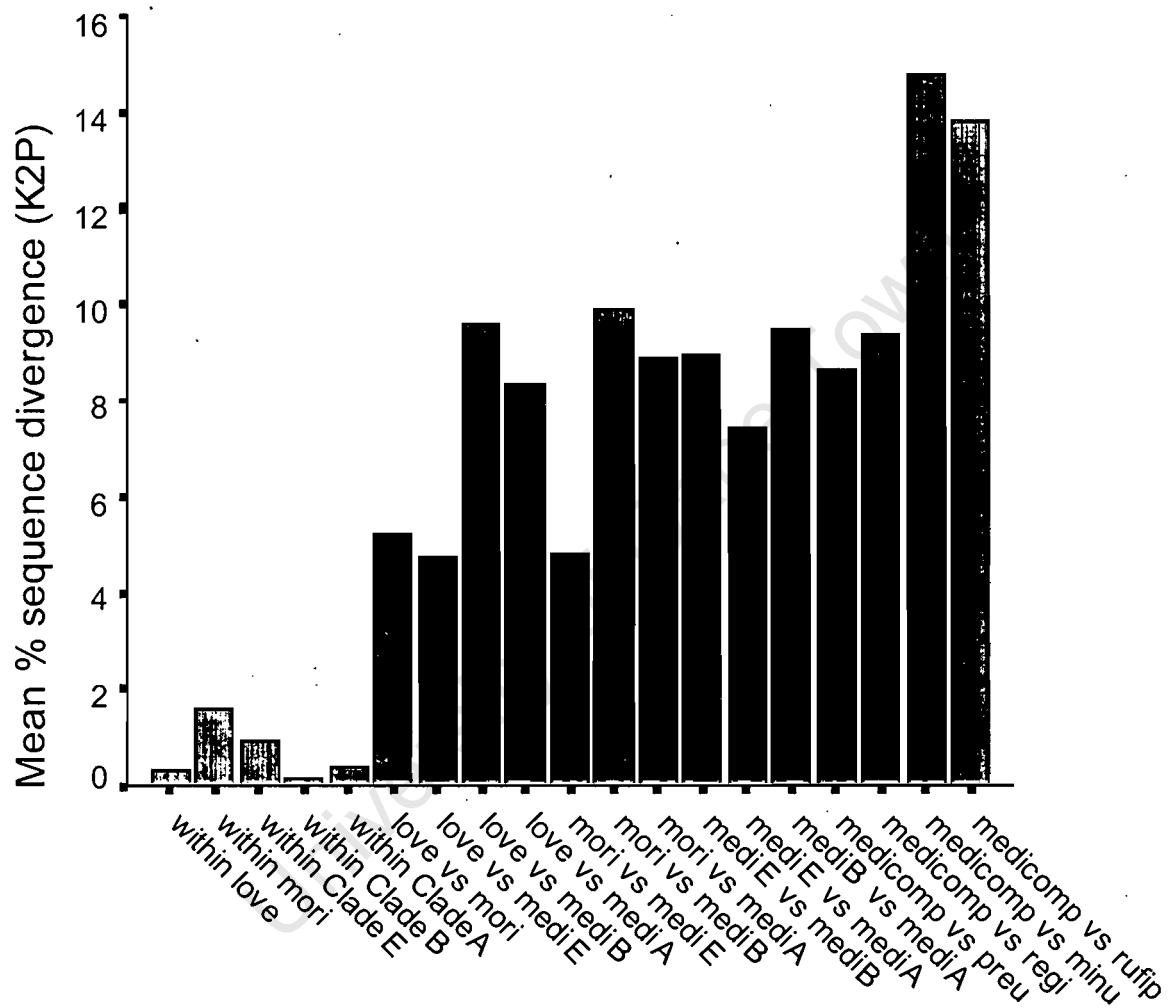
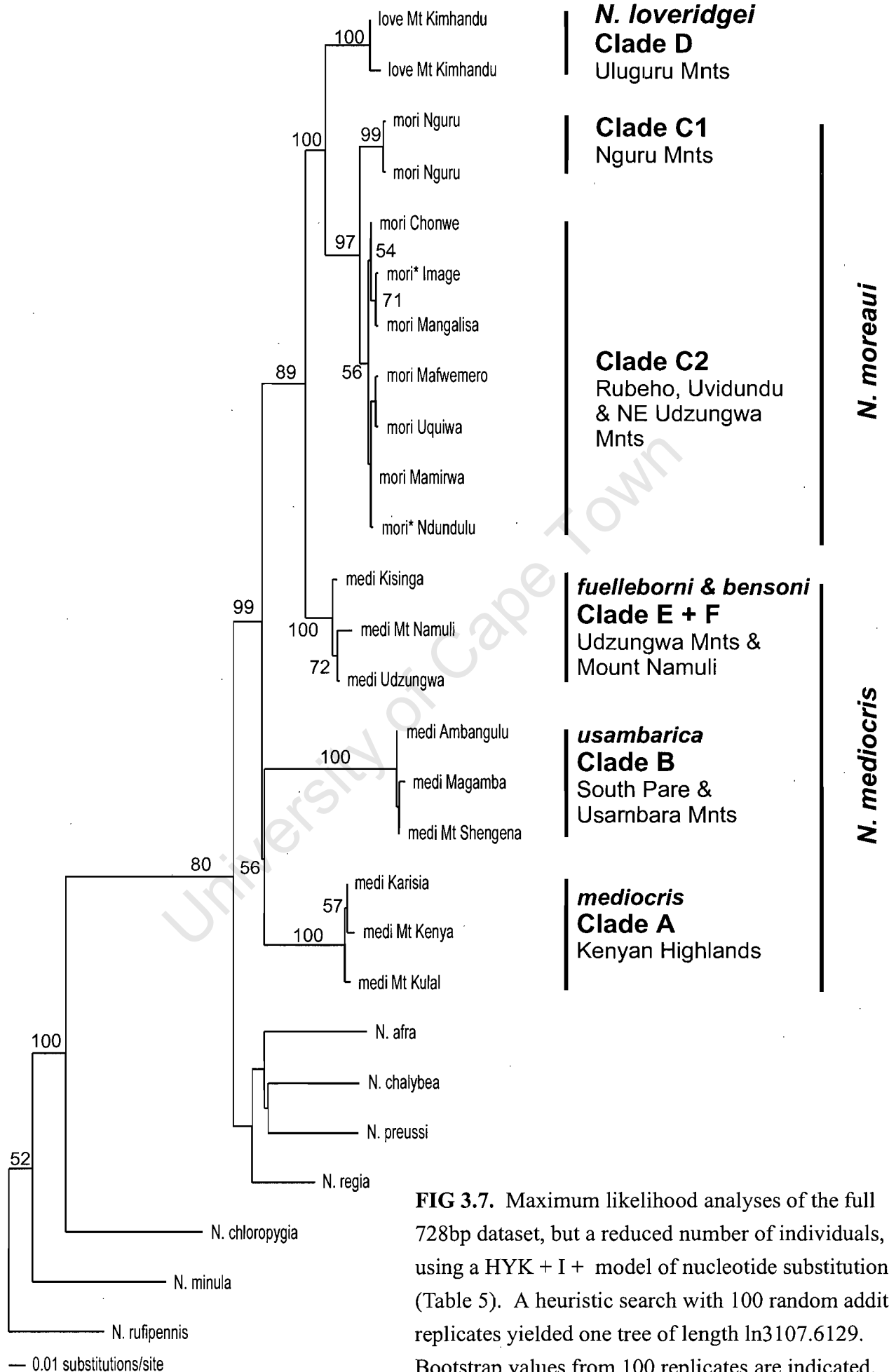


**FIG 3.5.** Mean sequence divergence (Kimura 2-parameter) within and between groups. Divergence values are low within *N. loveridgei* (love) and *N. moreaui* (mori), but large within *N. mediocris* (medi) reflecting the presence of three genetically distinct clades (Fig. 3.6 & 3.7).

**FIG 3.6.** Strict consensus tree of 88 most parsimonious trees obtained from the analysis of the entire 728bp mtDNA dataset using a heuristic search with 100 random addition replicates ( $L = 458$ ,  $CI = 0.557$ ,  $RI = 0.843$ ; Table 5). Values above the branches are bootstrap values for nodes with  $>50\%$  support and below the branches are parsimony jackknife values with a cut point of 50%. \*Indicates individuals from the NE Udzungwa Highlands populations sampled; their clustering with *N. moreaui* confirms the putative assignment of these individuals to this species instead of *N. mediocris* using plumage characteristics.

University of Cape Town

FIG 3.6



**Appendix 3.1.** Summary of species and populations analysed in this study. \*Indicates populations from the Ndundulu Mountains and Image Forest, which we assigned to *Nectarinia moreau* in place of *N. mediocris* which is traditionally thought to occupy these localities. \*\*Refers to the locality of voucher specimens: ZMUC – Zoological Museum of the University of Copenhagen, AMNH – American Museum of Natural History and FMNH – The Field Museum of Natural History.

Species	Sample No.	Locality	Source**
<b><u>Outgroups</u></b>			
<i>N. rufipennis</i>	07162	Udzungwa Mnts., Iringa District, Tanzania	ZMUC
<i>N. chloropygius</i>	832204	Dzanga-Sangha Forest Reserve, Central African Republic	AMNH
<i>N. minullus</i>	RB00002	Queen Elizabeth National Park, Uganda	Malcolm Wilson
<i>N. regius</i>	346631	Muramuya, Burundi	FMNH
<i>N. afra</i>	Hackerville	Hackerville, Southern Cape, South Africa	Rauri Bowie
<i>N. chalybea</i>	Kirst3	Kirstenbosch, Cape Town, South Africa	Rauri Bowie
<i>N. preussi</i>	358155	Cibitoke, Burundi	FMNH
<b><u>Mediocris complex</u></b>			
<i>N. mediocris mediocris</i>	NR296	Mount Kulal, E. Turkana, Kenya	ZMUC
	NR299	Mount Kulal, E. Turkana, Kenya	ZMUC
	T43038	Naro Moro, Mount Kenya, Kenya	Rauri Bowie
	T43065	Naro Moro, Mount Kenya, Kenya	Rauri Bowie
	T43080	Naro Moro, Mount Kenya, Kenya	Rauri Bowie
	LB10-131099	Karissia Hills, E. Maralal, Kenya	ZMUC

<i>N. mediocris usambaricus</i>	JK01-260401	Mount Shengena, S. Pare Mnts., Tanzania	ZMUC
	JK01-250401	Mount Shengena, S. Pare Mnts., Tanzania	ZMUC
	O4399	Mazumbai, W. Usambara Mnts., Tanzania	ZMUC
	JK04-201099	Magamba, W. Usambara Mnts., Tanzania	ZMUC
	JK06-201099	Magamba, W. Usambara Mnts., Tanzania	ZMUC
	356820	Ambangulu, W. Usambara Mnts., Tanzania	FMNH
<i>N. mediocris fuelleborni</i>	O3050	Kisinga-Rugero, Iringa District, Tanzania	ZMUC
	O3048	Kisinga-Rugero, Iringa District, Tanzania	ZMUC
	O7202	Udzungwa Scarp Forest, Tanzania	ZMUC
<i>N. mediocris bensoni</i>	AF48719	Mount Namuli, N. Mozambique	Peter Ryan
<i>N. moreaui</i>	O2958	*Ndundulu Mnts., Iringa District, Tanzania	ZMUC
	O2910	*Ndundulu Mnts., Iringa District, Tanzania	ZMUC
	O3035	*Ndundulu Mnts., Iringa District, Tanzania	ZMUC
	O3033	*Ndundulu Mnts., Iringa District, Tanzania	ZMUC
	JK09-070100	*Image Forest, Iringa District, Tanzania	ZMUC
	JK09-060100	*Image Forest, Iringa District, Tanzania	ZMUC
	JK06-080100	*Image Forest, Iringa District, Tanzania	ZMUC
	JK02-070100	*Image Forest, Iringa District, Tanzania	ZMUC
	JK05-231299	Magalisa Forest, Rubeho Mnts., Tanzania	ZMUC
	JK29-201299	Magalisa Forest, Rubeho Mnts., Tanzania	ZMUC
	JK14-120300	Mafimero Forest, Rubeho Mnts., Tanzania	ZMUC

	JK13-230200	Mafimero Forest, Rubeho Mnts., Tanzania	ZMUC
	JK04-271200	Mafimero Forest, Rubeho Mnts., Tanzania	ZMUC
	JK12-280300	Mafimero Forest, Rubeho Mnts., Tanzania	ZMUC
	JK11-260200	Mafimero Forest, Rubeho Mnts., Tanzania	ZMUC
	O3919	Uquiwa Forest, Rubeho Mnts., Tanzania	ZMUC
	O3931	Uquiwa Forest, Rubeho Mnts., Tanzania	ZMUC
	O3938	Uquiwa Forest, Rubeho Mnts., Tanzania	ZMUC
	JK03-230600	Mamirwa Forest, Ukaguru Mnts, Tanzania	ZMUC
	JK10-210600	Mamirwa Forest, Ukaguru Mnts, Tanzania	ZMUC
	JK12-130600	Mamirwa Forest, Ukaguru Mnts, Tanzania	ZMUC
	DCM02-250897	Chonwe Forest, Uvidundu Mnts, Tanzania	ZMUC
	DCM02-271197	Chonwe Forest, Uvidundu Mnts, Tanzania	ZMUC
	DCM07-261197	Chonwe Forest, Uvidundu Mnts, Tanzania	ZMUC
	JK03-241197	Chonwe Forest, Uvidundu Mnts, Tanzania	ZMUC
	JK04-241197	Chonwe Forest, Uvidundu Mnts, Tanzania	ZMUC
	S2389	Nguru Mnts, Tanzania	ZMUC
<i>N. loveridgei</i>	O4922	Kimhandu, Uluguru Mnts., Tanzania	ZMUC
	O4682	Kimhandu, Uluguru Mnts., Tanzania	ZMUC
	O4088	Kimhandu, Uluguru Mnts., Tanzania	ZMUC
	O4656	Kimhandu, Uluguru Mnts., Tanzania	ZMUC

---



## Chapter 4

### A revaluation of species boundaries within the *Nectarinia afra/chalybea* complex of Double-collared Sunbirds

#### Summary

Few groups of birds have generated as much taxonomic confusion and debate than has the delineation of species boundaries among the Double-collared Sunbirds. These sunbirds form a complex of morphologically similar forms for which it has proved difficult to find diagnostic characters. In an attempt to readdress delineation of species boundaries two complementary approaches were taken. (1) Plumage characters were scored, and nine morphological measurements were taken from 367 individuals, representing all taxa within the *N. afra/chalybea* complex. (2) I analysed mitochondrial DNA (NADH3) sequences from 54 individuals representing all but two of the presently recognised taxa in the species complex. Molecular phylogenetic hypotheses of species boundaries roughly correspond to existing species designations, with some important exceptions. *Nectarinia afra* appears to be more closely related to *N. manoensis* than to other members of the *N. afra/chalybea* complex. Mitochondrial sequence divergence between *manoensis* and *pinto*i (6.6%) is nearly as great as between *manoensis* and *afra* (7-8%), whereas despite the pronounced morphological differences, *manoensis* and *amicorum* have essentially identical mtDNA sequences (0.2%). The present study places *graueri* and *chapini* close to *stuhlmanni*, and suggests that these three taxa have only recently (<1 myrs BP) diverged. In contrast, *afra* and *manoensis*, *manoensis* and *pinto*i, and *stuhlmanni*, *ludovicensis* and *whytei*, diverged from each other well before the onset of the Pleistocene (>2.5 myrs BP). Based on the recovery of geographically structured monophyletic lineages, and the recognition of diagnostic plumage and morphometric characters, it is suggested that *whytei* and *pinto*i be accorded full species rank. A number of other evolutionary lineages (*amicorum*, and *subalaris*) were also identified, which with additional data may lead to these taxa gaining species rank.

## INTRODUCTION

Within Africa, few groups of birds have generated as much taxonomic confusion and debate than that on the delineation of species boundaries among the Double-collared Sunbirds (*Nectarinia afra/chalybea* species complex). These sunbirds form a complex of morphologically similar forms, in which the males have a metallic Cossack green head, back, wing-coverts, chin and throat, with the lower border of the throat edged by a narrow band of blue or violet, boarded posteriorly by a broader breast band of varying shades of scarlet-red to ochre. Their lateral pectoral tufts that flank the edges of the breast are yellow and vary in size and colour intensity. There is extensive variation in body dimensions as well as in the colouration of the belly and vent, grading from analine yellow to dark-grey. Females lack metallic plumage and pectoral tufts. Consequently, they appear relatively plain and homogeneous, varying from olive-green to grey, although forms differ somewhat in the edging of the primaries, amount of streaking on the throat and breast, and in body dimensions.

The most recent consensus with respect to Double-collared Sunbird systematics (Fry 2000, Cheke *et al.* 2001) has been to divide the taxa into three superspecies, the Greater Double-collared Sunbirds, *N. afra/N. ludovicensis/N. stuhlmanni*, the Lesser Double-collared Sunbirds, *N. chalybea/N. manoensis* and the Eastern Double-collared Sunbird complex, *N. mediocris/N. moreaui/N. loveridgei*, as well as several independent species, *N. preussi*, *N. regia*, *N. rockefelleri*, *N. neergardi*, *N. chloropygia*, *N. minulla* and *N. pulchella*. In Chapter 2, it was demonstrated that *N. chloropygia*, *N. minulla* and *N. pulchella* are unrelated to the other Double-collared sunbirds. With the exclusion of the three latter, no less than 14-15 taxa (including subspecies) are recognised by Fry (2000) and Cheke *et al.* (2001), respectively.

The major problem in assigning species rank within this group is the difficulty in readily identifying diagnostic characters for one taxon that are not to some extent present in another, often widely allopatric taxon (Clancey & Irwin 1978). Thus, strictly phenetic approaches have failed to delineate species boundaries consistently. This is best exemplified in a recent study of the species boundaries within the Eastern Double-collared Sunbird complex (Chapter 3). A

combination of morphological and molecular approaches, were used to demonstrate that species diversity within the *N. mediocris* complex had been greatly underestimated. What was thought to be two or three species has increased to five: *N. mediocris*, *N. usambaricus*, *N. moreaui*, *N. loveridgei* and *N. fuelleborni*. The deep genetic divergences detected among these taxa, for example a 9-11% sequence divergence between *N. mediocris* and *N. usambaricus*, suggest that the separation between these previously considered conspecific taxa occurred well before the onset of the Pleistocene.

In this chapter, the species limits among the series of taxa which have long been associated with the two widespread polytypic species, the Greater Double-collared Sunbird (*N. afra* complex: *afra*, *saliens*, *stuhlmanni*, *chapini*, *graueri*, *ludovicensis* and *whytei*) and the Lesser or Southern Double-collared Sunbird (*N. chalybea* complex: *chalybea*, *subalaris*, *manoensis*, *pintoi*, *amicorum* and *prigoginei*) are re-evaluated. Both species complexes are wide-ranging, occurring from southern South Africa to Angola, Malawi, southern Tanzania and the Albertine Rift (Fig. 4.1). The *N. chalybea* complex on the whole consists of taxa widely distributed in the lowlands of central and eastern southern Africa. In contrast, taxa within the *N. afra* complex north of the Limpopo River, are restricted to the upper edge of montane forest on isolated montane massifs, often widely separated from each other. Many localized members of the complex were successfully amplified from small skin fragments derived from museum study specimens. Museums are now more important than ever and their collections, together with improvements in molecular systematic techniques, are unlocking a new frontier in avian evolutionary biology. In addition, to mtDNA sequence data, plumage characters are summarised and nine morphological measurements assessed in context of the mtDNA results.

### **Taxonomic history**

The core of the taxonomic dispute about these sunbirds has centred round the association of the Albertine Rift and Angolan highland montane forms with the otherwise endemic South African species, *N. afra*. This problem can be traced back to 1908 when Neumann related the Double-collared sunbirds of central Africa with southern Africa, by describing *Cinnyris afra graueri* from the Kivu

volcanoes in the Albertine Rift. Sclater (1930: 693-696) provided the first complete revision of members of the Double-collared complex. He considered *N. afra* to be endemic to South Africa, but included *ludovicensis* and *graueri* (considering *schubotzi* Reichenow 1908 a synonym) with another southern African species *N. chalybea*. The Ruwenzori taxon, *stuhlmanni*, was placed with a third species, *N. reichenowi* (= *N. preussi*). Grant and Mackworth-Praed (1943: 9-10) argued that neither *stuhlmanni* nor *ludovicensis* was related to *reichenowi* (= *preussi*) or *chalybea*, but still united *graueri* with *afra*.

Benson (1949: 19) described *C. afer* (= *afra*) *whytei* from the Nyika Plateau in northern Malawi, and regarded *whytei* to be most similar to *graueri* and *ludovicensis*. Paterson (1954) challenged Benson's placement of *whytei*, arguing that *whytei* is a montane form of *chalybea*. Benson (1954: 95-96) presented a counterargument to Paterson (1954) and *whytei* has remained closely allied with *graueri* and *ludovicensis* since. In the 1950s, two additional taxa were described. Prigogine (1952: 412) described *C. afer chapini* from Mount Mohi, Kivu, lying to the west and north of the distribution of *graueri*. Chapin (1954: 250) considered *chapini* to be morphologically intermediate, especially in bill-length between *stuhlmanni* and *graueri*. Macdonald (1958: 7-9), while reviewing the taxonomic status of *manoensis*, then synonymised with *chalybea*, proposed that the birds from the Marungu Highlands were closer to *graueri* and *whytei*, than *manoensis* or *chalybea*, and thus suggested the name *C. afer prigoginei* for this isolated montane population. Clancey (1962: 188) split the southern African populations of *N. afra* into two taxa, the south coast *afra afra* and east coast *afra saliens*.

The 1970s saw a renewed discussion of species limits within the *N. afra/N. chalybea* species complex, with the collection in April 1970 of specimens from an isolated population of Double-collared sunbirds by T.B. Oatley and K.L. Tinley on Mount Gorongosa in central Mozambique. Clancey (1970:27) described this population as *N. afra amicorum*. Clancey and Irwin (1978), in their revision of the *N. afra/N. chalybea* complex, considered *amicorum* as a subspecies of *manoensis*, which also included the short-billed *pinto* from northern Angola and Zambia. Clancey and Irwin (1978) therefore proposed the

following classification scheme: *N. afra* (with subspecies *afra* and *saliens*), *N. chalybea* (*chalybea*, *albilateralis*, *subalaris* and *capricornensis*), *N. manoensis* (*manoensis*, *pinto* and *amicorum*), *N. ludovicensis* (*ludovicensis*, *whytei*, *prigoginei*, *chapini*, and *graueri*) and *N. stuhlmanni*. Prigogine (1979) generally agreed with Clancey and Irwin (1978) but, after a more comprehensive examination of available specimens from the Albertine Rift, suggested that *schubotzi* be recognised and that *chapini*, *graueri* and *schubotzi* have closer affinities to *N. stuhlmanni* than to *N. ludovicensis*. The races *whytei* and *prigoginei* were retained as subspecies of *N. ludovicensis*. Benson and Prigogine (1981) in a detailed study of all available samples of sunbirds from the Marungu Highlands suggested that *prigoginei* warranted species rank, but hypothesised that was probably of hybrid origin between *stuhlmanni* and *mediocris*. Fry (2000) followed Prigogine's (1979) modified sequence of Clancey and Irwin (1978), with the exception that *N. chalybea capricornensis* is treated as a synonym of *N. chalybea subalaris*. Cheke *et al.* (2001) follow Fry (2000) overall, but they follow Benson and Prigogine (1981) in elevating *prigoginei* to full species rank, and they consider *albilateralis* a synonym of *N. chalybea*.

## METHODS

### Sampling for molecular analyses

A total of 54 individuals from 19 taxa were analysed in this study. All members of the *N. afra/chalybea* complex with the exception of *N. prigoginei* and *N. afra saliens*, for which samples were not available, were included in this study.

Because many of the taxa are from isolated mountains, only a few fresh tissue were available, therefore small toe-pad samples from museum skins were used as a source from which DNA could be extracted. Details of the taxa collected, population localities and institutions holding vouchers are listed in Table 4.1. The entire Double-collared complex was rooted with *N. violacea*, the putative sister taxon (Chapter 2).

### Laboratory procedures

For the taxa where fresh tissue/blood was available, DNA was extracted using the Puregene Kit (Gentra Systems, Minneapolis, Minnesota). The mitochondrial NADH subunit 3 gene with flanking tRNAs (Glycine and Arginine) was PCR

amplified from fresh tissue and cycle-sequenced as described in Chapter 3. DNA was also extracted from small skin-scrapes collected from the feet of museum skins using the DNAeasy Kit (Qiagen Inc.), with slight modifications of the manufacturer's protocol. These were as follows: (1) the toe-pad was first washed using a vortex in 100% EtOH, drained and washed in 70% EtOH, drained and washed in dH<sub>2</sub>O, drained and allowed to soak for up to an hour in dH<sub>2</sub>O. These steps help to remove any surface contamination that may have resulted from the handling of the museum specimen over many years. (2) A small amount of tissue was minced with a scalpel blade and placed in the manufacturer's extraction buffer with the supplied Proteinase K. Samples were incubated for 3-4 days with an additional 20ul of Proteinase K (20mg/ml) being added every day. The long extraction period is needed to completely break down the tough skin sampled from the foot. (3) Once digested the extraction protocol follows the manufacturer's protocol with three exceptions, (A) the elution buffer is pre-warmed to 70°C, (B) only 80ul elution buffer was used for elution and (C) the elution buffer (80ul) was incubated on the column membrane at 70°C for 10 minutes before spinning through to facilitate binding and, thereby increase the amount of DNA eluted. The DNA extraction was carried out in a separate room from where normal template DNA was stored, as well as in an air flow-through hood. Multiple extraction blanks were also used at all stages, and some individuals were extracted several times. These extra precautionary steps are necessary to minimise the risk of contamination.

PCR amplification of the toe-pad derived DNA made use of three different primer combinations that broke the 395bp ND3 fragment into smaller parts to increase the likelihood of successful PCR amplification. The primer combinations were as follows: (1) ND3-L (5'-GACTTCCAATCTTTAAAATCTGG-3') / ND3-H2 (5'-GAAGAATCGGATGGAGAATGG-3') 191bp, (2) ND3-L1 (ACTATCTCCCTACGAATGCGG-3') / ND3-H1 (5'-ATTGTAGTTGAGTGGCTCATG-3') 148bp and (3) ND3-L2 (5'-CTCCTATTTCGACCTAGAAATCGC-3') / ND3-H (5'-GATTTGTTGAGCCGAAATCAAC-3') 185bp. The PCR cocktail for amplification of each fragment from toe-pads used 2ul of undiluted template

DNA mixed with standard reagents, with the exception that 0.3ul of AmpliTag Gold (PE Biosystems INC) and 4ul BSA (10mg/ml) were added for each 25ul reaction. DNA was amplified using the following protocol; an initial denaturation at 95°C for 10 minutes, followed by 35-40 cycles of denaturation at 95°C for 30s, annealing at 52°C for 30s, and extension at 72°C for 50s, and lastly a final extension step of 5 minutes at 72°C. PCR products were electrophoresed on 1.5% low-melting point agarose gels (FMC Bioproducts) stained with ethidium bromide and visualized under UV light. Amplicons of the appropriate length were cut out of the gel and purified using the GELase™ Agarose gel-Digesting Preparation and the 'fast protocol' method (Epicentre Technologies, Madison, Wisconsin). The purified products were cycle-sequenced using Big Dye terminator chemistry (Applied Biosystems, Inc [ABI]). Cycle-sequencing reactions were precipitated with 3M ammonium acetate or 100% isopropanol, rinsed in ethanol, dried and re-suspended in formamide-EDTA solution and run on an ABI 377 or ABI 3100 automated DNA sequencer.

Sequences were obtained from both strands of DNA for each individual and some individuals were sequenced several times if any base ambiguity was encountered. All sequences were checked using the program Sequencher 3.0 (Gene Codes Corp) and aligned to the chicken (*Gallus gallus*) mtDNA sequence (Desjardins & Morais 1990) to test for the presence of any insertions or deletions.

### **Molecular analyses**

Phylogenetic analyses of the DNA sequences were performed using two approaches: maximum parsimony (MP) and maximum likelihood (ML). MP analyses, using PAUP\*4.0b10 (Swofford 2002) were conducted using the heuristic search option, implementing stepwise addition with 1000 random addition replicates, and TBR branch swapping. Due to transitions often accumulating at higher rates than transversions; MP analyses were conducted under several transition:transversion (ts:tv) weighting schemes for 3<sup>rd</sup> codon positions to evaluate the sensitivity of the tree topology to saturation.

Modeltest 3.06b (Posada & Crandall 1998) was used to help ascertain the substitution model that best described the dataset. The parameters estimated from Modeltest were entered into PAUP\* and attempts were made to establish if the model could be simplified by eliminating extraneous parameters. This model was used to conduct a ML analysis using PAUP\*. Clade support for both the MP and ML analyses were estimated using 500 and 100 bootstrap replicates, respectively. Likelihood ratio tests were used to test for rate heterogeneity (molecular clock) among lineages (Huelsenbeck *et al.* 1996).

### **Morphometrics**

RCKB measured 367 adult birds from currently recognized taxa (Table 4.4, Male = 273, Female = 94, *schubotzi* was synonymised with *graueri*): 322 were from specimens housed in the collections of The Natural History Museum, The Royal Museum for Central Africa, American Museum of Natural History, United States National Museum, Field Museum of Natural History, Zoological Museum of Copenhagen, National Museums of Kenya and the Durban Natural History Museum; 45 birds were measured in the field, 22 for *N. a. afra* and 23 for *N. c. chalybea*. The following measurements were taken: wing-length, upper mandible length, bill-depth, bill-width and, the length of the longest and shortest tail feathers as described in Chapter 3. Tarsus length, from tibiotarsal joint to distal undivided scute was also measured. For all individuals moult was scored for both the wing and tail to help eliminate spurious results.

### **Morphological analyses**

Morphological measurements were log-transformed ( $\log x+1$ ) to reduce variance between characters. Differences in univariate measures between species were tested using one-way ANOVA with Student-Newman-Keuls tests to identify which taxa grouped together (Zar 1996). Principle components (PC) and discriminant analyses (DA) were performed as in Chapter 3.

Plumage pattern and colour was scored from all 367 birds from which measurements were taken. Plumage colours were matched to published colour standards (Ridgway 1912) to help objectively define colours across specimens. For all male specimens, the widths (defined along the chin to tail axis) of the



metallic violet/blue and red/orange chest bands were measured to the nearest 0.1mm using digital Vernier callipers.

## RESULTS

### Genotypic variation

A total of 395 bp of mtDNA was amplified from the 19 taxa and 54 individuals included within this study. Of these, 157 sites (39.7%) were variable and 139 (35.2%) were parsimony informative. There were 14 amino acid changes within ND3. Pairwise Kimura-two-parameter sequence divergence distances among all taxa are summarised in Table 4.2.

### Phylogenetic analyses

The removal of identical sequences from the dataset reduced the number of individuals from 54 to 45. Equally-weighted maximum parsimony (MP) analyses of this ND3 dataset yielded 70 most parsimonious trees of 307 steps (CI = 0.541, RI = 0.681). A strict consensus of these trees rendered most of the basal nodes unresolved. However, several lineages were recovered: (1) *afra*, (2) *pintoi*, (3) *manoensis* and *amicorum*, (4) *stuhlmanni*, *graueri* and *chapini*, which were sister to (5) *whytei*, (6) *chalybea* and *subalaris*, and (7) *moreaui*, *loveridgei* and *fuelleborni*, which are sister to a polytomy containing *ludovicensis*, *mediocris* and *usambaricus*. In addition, *chapini* and *graueri* were not reciprocally monophyletic. MP analyses that down-weight third position transitions by the empirical estimate of 11:1 relative to transversions, recovered 10 equally short trees (length = 1108, CI = 0.646, RI = 0.744) the consensus topology of which is the same as depicted among taxa in Figure 4.2. The same 10 trees were recovered if 3<sup>rd</sup> codon positions transitions relative to transversions (Ti/Tv) are down-weight by half the empirical estimate (5x, length = 680, CI = 0.609, RI = 0.718).

In both weighted MP analyses, the same lineages as described above for the equally-weighted (0x) MP analyses were recovered, but now relationships among the lineages could be inferred, although with less than 50% bootstrap support. In summary, *afra*, *pintoi*, *amicorum* and *manoensis* were sister to *whytei*, *stuhlmanni*, *graueri* and *chapini*; *chalybea* and *subalaris* were sister to *preussi*;

*fuelleborni*, *moreaui*, *loveridgei*, *mediocris*, and *usambaricus* were sister to *ludovicensis*. In all analyses *graueri* and *chapini* were not reciprocally monophyletic.

To facilitate time-efficient maximum likelihood (ML) analysis, the dataset was pruned to 23 individuals by limiting the dataset to one representative per taxon, except for *graueri* and *chapini*, for which I wanted to further explore the lack of reciprocal monophyly suggested in the MP analyses. Modeltest 3.06 selected a HKY model of nucleotide substitution with invariable sites (I) and gamma shape parameter ( $\Gamma$ ). Base composition was biased with a deficiency of guanine (G = 11.7%, A = 31.1%, C = 37.4%, and T = 19.9%), characteristic of mtDNA. The Ti/Tv ratio was estimated to be 11:1, I = 0.587 and  $\Gamma$  = 10.54. ML analyses recovered one tree of length  $-\ln 1884.65$  (Fig. 4.3), the topology of which is consistent with the weighted MP analyses (Fig. 4.2), except that *pintoi* is no longer sister to *afra*, but is now sister to *manoensis/amicorum*. Bootstrap support was above 50% for the support of (1) *whytei* as sister to *stuhlmanni*, *graueri* and *chapini*, (2) that this clade is sister to *afra*, *pintoi*, *amicorum* and *manoensis*, (3) *stuhlmanni* as sister to *graueri* and *chapini*, (4) *manoensis* and *amicorum* are sister to *pintoi*, (5) *ludovicensis* as the putative basal member of the *mediocris* complex, (6) *chalybea* and *subalaris* as sister taxa and (7) that *N. regia* is basal relative to other members of the ingroup. As in the MP analyses *graueri* and *chapini* were not reciprocally monophyletic.

A log-likelihood ratio test of clock-like evolution using the same dataset as for the ML analyses did not reject a molecular clock ( $\chi^2 = 20.4$ , *d.f.* = 21, ns). This suggests that rates of evolution were not significantly different among the lineages in the phylogeny and that a molecular clock can be used to roughly estimate relative divergence dates.

### Plumage

The male members of the *N. afra/chalybea* complex differ in both the presence/absence of metallic plumage on parts of the body and the specific shading. These characters are summarized in Table 4.3.

Females lack metallic plumage and are generally drab. The most pronounced differences are in the colour of the face, rump and belly. *Afra* and *saliens* are very similar, both having a deep olive head with an olive-green back, rump and tail-coverts. The throat and breast are light olive-grey with faint olive-green streaking, the belly, dull olive-yellow. *Saliens* is lighter above and more yellow on the belly than *afra*. *Stuhlmanni*, resembles *afra* and *saliens* by having deep olive-green upperparts, but the lores and ear-patches are dark olive-grey, and the primaries are edged pale olive-yellow. The underparts in *stuhlmanni* are olive-grey with faint streaking on the throat. The belly is pale olive-grey with a slight yellowing towards the centre. *Graueri* and *chapini* are similar to *stuhlmanni*, but differ in body dimensions (see below). *Ludovicensis* and *whytei* are greyer on the upperparts and in both taxa there is a slightly accentuated pale buff superciliary stripe. The throat and breast are pale-grey with the belly having a slight olive-yellow tinge. *Whytei* has a much darker throat and upper breast, and duller, but more yellow belly, than *ludovicensis*.

*Prigoginei* is uniformly olive and not grey with dark brown wings edged olive-green. The throat is dark olive with black streaking contrasting with a pale olive-belly that is more yellow towards the crissium and on the flanks. Specimens assigned to *manoensis* are greyish-brown above, with a yellow wash on the rump. The throat is brownish-grey, grading into pale-grey below with slight yellow overtones towards the centre. Those attributed to *pinto* have upperparts as in *manoensis*, but the underparts are much more strongly washed yellow. Those attributed to *amicorum* are much darker than *manoensis* or *pinto*, the upperparts and wing being dark olive and the underparts dusky-brown. In *chalybea*, the head is olive-green with the rest of the upperparts olive-yellow. The throat and breast are olive-grey becoming more olive towards the centre of the belly. Those attributed to *subalaris* are similar to *chalybea*, but darker olive above and below.

### Morphometrics

Male sunbirds were larger than females in linear dimensions for every measurement except bill-width and breadth, at the base of the nares (Table 4.4).

Sexual dimorphism was most pronounced in the length of the tail, wing and bill, with males on average 13.5%, 8.3%, and 8.1% larger in these variables than females. As a consequence, morphological comparisons were restricted to single-sex groups.

Multivariate analysis of the morphological characters confirmed that there are differences between the taxa. In both sexes, the communalities from the principal components analyses (PC) associated with the tarsus and minimum tail-length, and the blue-violet upper breast band of males were below 0.6. As a consequence these measures were excluded from the final PC analyses to help reduce the amount of 'noise' in the dataset. For both sexes, the first two principle components (PCs) had eigenvalues greater than one and accounted for 75% and 73% of the total variation for males and females, respectively (Table 4.5). Principal component loadings in males were positive and strongly correlated with wing and tail-length on PC1, and with bill characters on PC2. PC loading for females were as for males, except that the axes were reversed (Table 4.5).

In the PC scatterplots (Fig. 4.4) seven primary groups of taxonomic association were distinguished. (1) For both sexes *afra* and *saliens* (*Nectarinia afra*, Fig. 4.2) are diagnostic by having the longest bills (>26mm male, >24mm female, Table 4.4), relatively large tails, wings and lower breast band. *Afra* and *saliens* are morphologically similar, overlapping in morphospace (Fig. 4.4), although *saliens* has a significantly longer wing (see 1-way ANOVA, Table 4.4). (2) Three of the four taxa from the Albertine Rift, *stuhlmanni*, *graueri* and *chapini* cluster together (*N. stuhlmanni*, Fig. 4.2). These taxa are diagnostic for males by having the longest tails (>52mm), relatively long wings, and a broad lower breast patch. Females overlap slightly with *afra* and *amicorum* in wing-length (Fig. 4.4). For both sexes, *stuhlmanni*, *chapini* and *graueri* are diagnostically different from each other in bill characters; *stuhlmanni* has a significantly larger bill than *chapini*, which has a significantly larger bill than *graueri* (Table 4.4), hence the wide morphospace occupied along the y-axis in the scatterplots (Fig. 4.4). (3) *Ludovicensis* and *whytei* (*N. ludovicensis*, Fig. 4.2) overlap with the above Albertine Rift taxa in morphospace (Fig. 4.4), although both *ludovicensis* and

*whytei* can be distinguished from *stuhlmanni*, *chapini* and *graueri* by their much shorter tails. In males, *ludovicensis* has a significantly larger wing, bill, lower breast band, but smaller tail than *whytei*. For females, the trend is similar, but only significant for wing-length (Table 4.4). (4) The fourth Albertine Rift taxon, *prigoginei*, is separated from the remaining Albertine Rift taxa by its small size (Fig. 4.4, Table 4.4).

(5) On the other end of the scale, for both sexes *chalybea* and *subalaris* (*N. chalybea*, Fig. 4.4) are diagnostically smaller than other members of the *N. afra/chalybea* complex in wing-length (male <57mm, female <53mm), but have average sized bills and tails (Table 4.4). *Subalaris* has a lower breast band approximately twice the size of in *chalybea*, a significantly larger bill and slightly longer wing and tail (Table 4.4). (6) The two miombo woodland taxa, *manoensis* and *pintoii* (*N. manoensis*, Fig. 4.2) are more difficult to place. These two taxa are morphologically intermediate between the larger members of the complex (groups 1-3 above) and the smaller *chalybea* and *subalaris*. Key diagnosable characters separating *manoensis* and *pintoii* from all the taxa above, are the short tail-length (both sexes <42mm), reduced sexual dimorphism in tail-length (Table 4.4), and the uncharacteristically square shape of the tail; max/min tail ratio of  $1.08 \pm 0.05$  in *manoensis* and  $1.07 \pm 0.04$  in *pintoii*, relative to the more graduated shape (Av.  $1.19 \pm 0.09$ ) in the other taxa (excluding *amicorum*) of the complex. *Manoensis* has a significantly longer bill than *pintoii*, with *manoensis* being generally larger in wing and tail-length (Table 4.4).

(7) The last member of the *manoensis* complex is *amicorum* (*N. manoensis*, Fig. 4.2) from Mt. Gorongosa in central Mozambique. The three male specimens measured cluster in morphospace close to the other southern African taxa *afra* and *saliens*. The single female specimen examined, falls in the middle of the morphospace occupied by *afra* and *saliens* (Fig. 4.4). *Amicorum* has a square shaped tail (max/min ratio, Av.  $1.11 \pm 0.03$ ) as in *manoensis* and *pintoii*, but for both sexes *amicorum* is much larger in all dimensions than *manoensis* or *pintoii*, but smaller than *afra* or *saliens* (Table 4.4).

Once specimens had been assigned *a priori* to taxa, in this case using plumage characters and distributional data (Table 4.3, Fig. 4.1), a discriminant function analysis on the morphological characters was used to assess overlap among the taxa in multidimensional morphospace. Analysing the raw log (x+1) transformed data matrix, six and five discriminant functions were extracted for males and females, respectively (Table 4.5). The first two DCs explained 88.7% and 94.8% of the morphological variation in males and females, respectively. For both sexes there were significant differences among the taxa when subgroups of the DCs were considered, suggesting that the taxa can be distinguished using morphometrics (Table 4.6). Scatterplots of the first two DCs (Fig 4.5) resulted in the same seven clusters of taxa identified in the PC analyses (Fig. 4.4, see above).

In the *a posteriori* classification 86.5% of males and 83.5% of females were correctly reclassified (Table 4.7). These values were slightly reduced in the cross-validated classification results where 79.5% of males and 74.1% of females were correctly classified. In general, the classification results recovered the seven lineages of taxonomic association first identified in the PC analyses. In both sexes, most incorrect reclassifications occurred within groups, with the exception of groups 2-4, *stuhlmanni*, *graueri*, *chapini*, *prigoginei*, *ludovicensis* and *whytei*, where much confusion occurred in assigning species status on morphometric data. For these taxa, reclassifications should be restricted to diagnostic traits only.

## DISCUSSION

The lineages recovered in both the weighted MP and ML analyses (Figs 4.2 & 4.3) roughly correspond to existing species boundaries with some important exceptions. *Nectarinia afra* appears to be more closely related to *N. manoensis sensu lato* (includes *pinto*i and *amicorum*) than to the other traditional members of the Greater Double-collared Sunbird complex, *N. stuhlmanni* from the Albertine Rift and *N. ludovicensis sensu lato*, disjunctly distributed within the Angolan Highlands and the high plateaus of northern Malawi and eastern Zambia. Although *afra* and *manoensis* differ in size, with *afra* being larger, both are species of rather open woodland habitat. *Nectarinia afra* prefers valley

bushveld, tall scrubland and coastal plains, actively avoiding forest (Skead 1967). *Nectarinia manoensis* is primarily a bird of open miombo woodland, but will enter riverine woodland, gardens and parks (Cheke *et al.* 2001).

A deep divergence exists between *afra* and *manoensis* (6.8-8.1%). If an estimate of 1.6% sequence divergence per million years (Fleischer *et al.* 1998) is used as a proxy with which to date nodes in the absence of a fossil record, a divergence in excess of four million years before present (BP) is inferred. Thus, a vicariance or dispersal event must have occurred well before the onset of the Pleistocene 2.5 myrs BP (deMenocal 1995) and appears to have initiated divergence between these taxa. An analysis of plumage characters lends further support to *afra* and *manoensis sensu lato* being sister taxa: *afra* and *manoensis* are the only taxa in the *N. afra/chalybea* complex where males do not have a metallic coloured rump (although some individuals of *N. chalybea* from arid western South Africa also lack metallic plumage on the rump). Instead the rump is olive-brown, being paler in *manoensis sensu lato* than *afra* (Table 4.3).

Although *afra* and *manoensis sensu lato* differ remarkably in size, *amicorum* (*N. manoensis*, Figs 4.2 & 4.3) provides something of a link. *Amicorum* is unusual as it appears to have shifted its habitat from open woodland to montane heathland on Mt. Gorongosa to which it is endemic (Clancey 1970). More remarkably though, is the dramatic shift in body dimensions that has accompanied this ecological shift. Whereas *amicorum* retains the short square tail typical of *manoensis sensu lato*, it is much larger than *manoensis* or *pinto* in body dimensions. In the PC and DC plots (Figs 4.4 & 4.5) *amicorum* clusters close to, or with *afra*. The low genetic divergence 0.00-0.52% between *manoensis* and *amicorum* suggests that the divergence between these two taxa has taken place very recently in geological time (<350 000 years BP), and that lineage sorting is not yet complete. Consequently, the observed morphological changes in body size must have also occurred very rapidly, either in response to genetic drift, directional selection or disruptive selection.

Given the pronounced and diagnostic linear dimensions of *amicorum* relative to other members of the *N. afra/chalybea* complex, should *amicorum* be accorded

full species rank? This is an important question, as according *amicorum* full species rank would make *amicorum* Mozambique's second endemic bird, thereby potentially increasing ecotourism opportunities and revenue for local communities. However, for an objective conservation priority analysis it is essential that taxonomic rank is based strictly on biological evidence. It is clear that on purely molecular genetic grounds *amicorum* and *manoensis manoensis* are essentially identical. Should this precluded species recognition of *amicorum* solely on the basis of morphological divergence, particularly if selection has been strong, which may be the case in *amicorum*? This is because there is no reason that the rate of mutation at protein-coding or neutral genetic markers should reflect morphological divergence if directional selection is operating. In male plumage traits, *amicorum* differs from *manoensis manoensis*, but shares with *pinto* a lack of metallic violet-blue on the tail coverlets (Table 4.3).

Under a purely phylogenetic species concept (Cracraft 1983), the changes in body dimensions and the unique plumage traits attributed to *amicorum* would be sufficient to elevate it to species rank. Proponents of more traditional approaches to taxonomy consider *amicorum* a subspecies or incipient species of *N. manoensis*. However, describing subspecies as a means to designate isolated sublineages that may evolve into full species (e.g. Mayr 1942) has the unavoidable problem of requiring knowledge of the future (Frost *et al.* 1992, Burbrink *et al.* 2000). Thus, subspecies have no real taxonomic meaning if they are used to represent arbitrary degrees of morphological divergence or incipient species (Burbrink *et al.* 2000). Consequently, this approach should not be adopted. However, the major caveat with according *amicorum* species rank based purely on morphological grounds is that the material examined in making such a decision should be derived from a representative sample of the population. With only three males and one female ever having been collected from Mt. Gorongoza (all examined in this study) it is difficult to argue that these individuals are a representative sample. Thus, morphological values may change and plumage polymorphisms may be detected.

Cases are known (e.g. among Darwin's Finches) where significant morphological change has evolved within a few decades in response to selection,



with no evidence to suggest that such changes are irreversible or will lead to reproductive barriers. Another explanation for the discord between mtDNA and morphology may be that *amicorum* is a stabilized hybrid between *manoensis* (mother) and *afra* (father). This would account for the similarity in mtDNA shared between *amicorum* and *manoensis*, and the intermediate body dimensions of *amicorum* between *afra* and *manoensis*. However, this explanation is unlikely to give the present distribution of *afra*, which is restricted to south of the Limpopo River in southern Africa (Fig. 4.1). Use of a nuclear marker will be essential to test alternative hypotheses of the evolutionary origins of *amicorum*. With greater sampling efforts on Mt. Gorongosa and surrounding populations of *manoensis* it will be possible to not only better quantify morphological and plumage traits but, also to model the extent to which genetic exchange takes place or has taken place between Mt. Gorongosa and surrounding populations of *manoensis* (and *afra*?). It is suggested that for now *amicorum* remain a subspecies (= polymorphic population) of *N. manoensis*. However, emphasis should be placed on a return expedition to Mt. Gorongosa with the objective of collecting additional specimens of *amicorum* to better evaluate morphological characters and also to provide tissues to facilitate further molecular analyses.

Differences between *manoensis* and *pinto*i include a lack of metallic colour on the tail-coverlets in *pinto*i, pale olive-brown flanks in *manoensis* versus pale-grey flanks and belly, with extensive yellow intrusions towards the centre of the belly in *pinto*i (Table 4.3; and see Clancey & Irwin 1978). Both *manoensis* and *pinto*i are similar in size, although *manoensis* is generally larger and has a significantly longer bill (Table 4.4). The mtDNA dataset suggests that *manoensis* and *amicorum* are sister to *pinto*i. However, the 6.6% divergence between these taxa is nearly as great as between *manoensis sensu lato* and *afra* (6.8-8.1%). Using a calibration of 1.6% per myrs, suggests that *manoensis* and *pinto*i split from an ancestral stock well before the Pleistocene *ca.* four myrs BP.

The ability to diagnose *pinto*i from *manoensis* accurately using plumage, morphometric or DNA characters strongly argues that *pinto*i warrants full species rank. However, it is well documented that *manoensis* and *pinto*i freely interbreed where their respective ranges meet around Lake Malawi (Macdonald 1958,

Clancey & Irwin 1978). Currently, the extent or width of this area of hybridisation has not been documented. The deep genetic divergence between *manoensis* and *pinto* suggest that they were isolated for a long period of time and probably have come into secondary contact only recently. As a phylogenetic species concept (Cracraft 1983) is adopted here, it is suggested that *pinto* be accorded species rank.

*Nectarinia stuhlmanni* is well separated from *N. afra* and *N. ludovicensis*, both genetically (8.8% and 9.6% sequence divergence, respectively), in plumage traits (Table 4.3) and in linear dimensions (Table 4.4). This is in agreement with recent revisions of the *N. afra/chalybea* complex (Clancey & Irwin 1978, Prigogine 1979, Fry 2000 and Cheke *et al.* 2001), which have accorded *stuhlmanni* species rank. Contrary to Clancey and Irwin (1978) and in agreement with Prigogine (1979), *graueri* and *chapini* share more recent ancestry with *stuhlmanni* than with *ludovicensis*; 1.6% and 1.34% sequence divergence to *stuhlmanni*, and 10.1% and 10.2% sequence divergence to *ludovicensis*, respectively. All three taxa, *stuhlmanni*, *graueri* and *chapini* have similar sized tails, which are significantly longer than in any other member of the *N. afra/chalybea* complex.

*Graueri* and *chapini* were untied with *ludovicensis* by Clancey and Irwin (1978) based on all three taxa having similar sized bills relative to the much greater bill length in *stuhlmanni*. The close association between *stuhlmanni*, *graueri* and *chapini* suggested by the mtDNA results, implies that the considerable differences observed in bill dimensions have arisen relatively recently (<1 myrs BP). Phenotypic plasticity in bill shape, particularly length is further supposed by *chapini* having a significantly longer bill with respect to *graueri*, despite neither taxon being reciprocally monophyletic (Fig. 4.2). Designating species rank to each of the morphologically diverse taxa of the Albertine Rift area is perhaps premature, as the lack of clear geographically structured clades despite phenotypes appearing geographically structured could be a consequence of: (1) recent divergence among phenotypic lineages with not enough time having past for mtDNA lineage coalescence to have occurred, (2) ancestral mtDNA polymorphism and (3) recent recurrent gene flow, with strong phenotype

selection. Until the geographical basis of nucleotide and phenotype variation within Albertine rift populations is better understood it is suggested that *graueri* and *chapini* remain subspecies of *stuhlmanni*. *Nectarinia prigoginei* is much smaller than the other Albertine Rift forms and is the only member of the *N. afra/chalybea* complex that lacks metallic plumage on the lesser wing-coverts. I agree with Benson and Prigogine (1981) that *prigoginei* warrants species rank although the hypothesised hybrid origin remains to be demonstrated.

The third member of the *N. afra* complex traditionally recognised is *N. ludovicensis*, disjunctly distributed within the Angolan Highlands and on Nyika Plateau in northern Malawi. The mtDNA phylogenies (Figs 4.2 & 4.3) suggests that *N. ludovicensis* is not monophyletic. *Whytei* appears to be sister to *N. stuhlmanni* (including *graueri* and *chapini*), although these taxa are separated by a sequence divergence of 6.6% (*ca.* 4 myrs BP), suggesting that they have been isolated since before the onset of the Pleistocene. *Ludovicensis* in the MP and ML analyses forms the basal member of the Eastern Double-collared Sunbird complex (*N. mediocris*, *usambaricus*, *fuellborni*, *moreaui* and *loveridgei*, Figs 4.2 & 4.3), although with poor bootstrap support. Thus, this result should be interpreted with caution and additional data should be collected to better determine the phylogenetic affinities of *ludovicensis*. Regardless, *ludovicensis* and *whytei* are separated by 11.42%, reciprocally monophyletic, and each has discreet morphological characters. Consequently, it is suggested that *whytei* be accorded full species rank: *Nectarinia whytei* Benson 1949.

The last remaining members of the *N. afra/chalybea* complex to consider are *chalybea* and *subalaris*, traditionally classified under *N. chalybea* (Fig. 4.2). Aside from a weakly supported affinity (55% bootstrap support in the MP analysis, Fig. 4.2) with *N. preussi*, *chalybea* and *subalaris* form an independent lineage, with no clear evolutionary affinities to those mentioned above. Both taxa are significantly smaller than other members of the *N. afra/chalybea* complex (Table 4.4). The relatively deep genetic divergence (2.6%) detected between *chalybea* and *subalaris* is something of a surprise. Despite differences between the taxa, with *subalaris* having a much broader lower breast band and longer bill, there is no clear break in distribution between *chalybea* and *subalaris*

(Lloyd & Craig 1989). The relatively large genetic divergence may result from isolation by distance across southern Africa, or the two taxa may have been separated from each other in the past and recently come into secondary contact. Additional sampling and data collection will have to be conducted to separate the above hypotheses. It is suggested that *chalybea* and *subalaris* should remain united as one species, *N. chalybea*.

The remaining lineages offer no real surprises; the *N. mediocris* complex remains monophyletic with relationships among species as described in Chapter 3. The evolutionary affinities of *N. preussi* remain uncertain, and *N. regia* endemic to the Albertine Rift appears to be the most basal member of the Double-collared sunbirds sampled in this study.

Clancey and Irwin (1978) provide the only existing hypothesis on the evolutionary history of the *N. afra/chalybea* complex. They note that most of the taxa within the *N. afra/chalybea* complex are of tropical distribution in the highlands of central Africa, and propose that most of these forms diverged during the glacial-cycling of the Pleistocene, suggesting that only recently (Holocene) was the ancestral range of *whytei*, *ludovicensis* and *graueri* fragmented, leading to the present polytypic taxa. Clancey and Irwin (1978) considered *stuhlmanni* to be monotypic with uncertain evolutionary affinities. The present study places *graueri* and *chapini* close to *stuhlmanni* and suggests that these three taxa have only recently (<1myrs BP) diverged. In contrast, *stuhlmanni*, *ludovicensis* and *whytei* diverged well before the onset of the Pleistocene (>2.5 myrs BP), as appears to be the case for a growing number of studies investigating speciation in montane African birds (e.g. Roy *et al.* 2002, Chapter 3).

Clancey and Irwin (1978), further hypothesized that there has been a double colonization of Double-collared sunbirds from central/eastern Africa to South Africa, with one lineage leading to *N. afra* and the other *N. chalybea*, which is of great antiquity. Certainly the sequence divergences between *N. afra* and *N. chalybea* do suggest that these taxa have had a relatively long evolutionary history in South Africa, with *N. manoensis* more closely related to *N. afra* than *N. chalybea*. Unfortunately the short mtDNA (395bp) fragment sequenced

proved insufficient to resolve relationships among the major lineages, *N. afra* and *N. manoensis*, *N. whytei* and *N. stuhlmanni*, *N. ludovicensis*, *N. preussi*, *N. regia* and the *N. mediocris* species complex with any degree of confidence. More data, including tissue samples from museum specimens, are needed to resolve relationships and test such interesting hypotheses as a double colonization of South Africa by members of the *N. afra/chalybea* complex. In addition, where as this study has suggested that *whytei* and *pintoii* be accorded full species rank, a number other evolutionary lineages (*amicorum*, and *subalaris*) were also been identified, which with future study of unsampled geographically important populations may lead to these taxa gaining species rank.

**Table 4.1.** Summary of taxa analysed in this study. \*\*Refers to the locality of voucher specimens: FitzPatrick – Percy FitzPatrick Institute, University of Cape Town, ZMUC – Zoological Museum of the University of Copenhagen, AMNH – American Museum of Natural History, FMNH – The Field Museum of Natural History, NMK – National Museums of Kenya and, RMCA – Royal Museum for Central Africa. For most blood samples a photographic slide of the bird is available.

Species		Sample No.	Locality	Tissue	Source**
<i>N. violacea</i>	<i>violacea</i> (1)	Bred1	Overberg, South Africa	Muscle	FitzPatrick
	<i>violacea</i> (2)	X50407	Cape Point, South Africa	Blood	FitzPatrick
<i>N. regia</i>	<i>kivuensis</i> (1)	346631	Muramuya, Burundi	Muscle	FMNH
	<i>kivuensis</i> (2)	346628	Muramuya, Burundi	Muscle	FMNH
<i>N. preussi</i>	<i>preussi</i> (1)	358155	Cibitoke, Burundi	Muscle	FMNH
	<i>preussi</i> (2)	T43091	Aberdares, Kenya	Blood	FitzPatrick
<i>N. afra</i>	<i>afra</i> (1)	Hack_T	Hackerville, Southern Cape, South Africa	Muscle	FitzPatrick
	<i>afra</i> (2)	GA05613	Grootvadersbosch, South Africa	Blood	FitzPatrick
	<i>afra</i> (3)	W50962	Storms River Village, South Africa	Blood	FitzPatrick
<i>N. stuhlmanni</i>	<i>stuhlmanni</i> (1)	356109	Mubuku Valley, Ruwenzori Mnts, Uganda	Muscle	FMNH
	<i>stuhlmanni</i> (2)	356096	Mubuku Valley, Ruwenzori Mnts, Uganda	Muscle	FMNH
	<i>stuhlmanni</i> (3)	356127	Mubuku Valley, Ruwenzori Mnts, Uganda	Muscle	FMNH
	<i>stuhlmanni</i> (4)	O7409	Mubuku Valley, Ruwenzori Mnts, Uganda	Blood	ZMUC
	<i>stuhlmanni</i> (5)	O7322	Mubuku Valley, Ruwenzori Mnts, Uganda	Blood	ZMUC
	<i>graueri</i> (1)	10067	Mt. Mahavura, Rwanda	Toe-pad	NMK

	<i>graueri</i> (2)	10065	Mt. Mahavura, Rwanda	Toe-pad	NMK
	<i>graueri</i> (3)	10068	Mt. Mahavura, Rwanda	Toe-pad	NMK
	<i>graueri</i> (4)	346605	Muramuya, Burundi	Toe-pad	FMNH
	<i>graueri</i> (5)	350903	Kayanza, Burundi	Toe-pad	FMNH
	<i>chapini</i> (1)	77-22-A-211	Mabono, Demo. Republic of Congo	Toe-pad	RMCA
	<i>chapini</i> (2)	8596	Kilumba, Demo. Republic of Congo	Toe-pad	RMCA
	<i>chapini</i> (3)	8906	Mt. Kabobo, Demo. Republic of Congo	Toe-pad	RMCA
	<i>chapini</i> (4)	89213	Mt. Kabobo, Demo. Republic of Congo	Toe-pad	RMCA
<i>N. ludovicensis</i>	<i>ludovicensis</i> (1)	225649	Huambo, Angola	Toe-pad	FMNH
	<i>ludovicensis</i> (2)	225641	Huambo, Angola	Toe-pad	FMNH
	<i>whytei</i> (1)	W40023	Nyika Plateau, Northern Malawi	Blood	FitzPatrick
	<i>whytei</i> (2)	206331	Chiri River, Zambia	Toe-pad	FMNH
	<i>whytei</i> (3)	206332	Chiri River, Zambia	Toe-pad	FMNH
<i>N. manoensis</i>	<i>manoensis</i> (1)	17349	Matopus, Zimbabwe	Toe-pad	DMNH
	<i>manoensis</i> (2)	28803	Mt. Selinda, Zimbabwe	Toe-pad	DMNH
	<i>amicorum</i> (1)	26037	Mt. Gorongosa, Central Mozambique	Toe-pad	DMNH
	<i>amicorum</i> (2)	26038	Mt. Gorongosa, Central Mozambique	Toe-pad	DMNH
	<i>pintoi</i> (1)	206336	Mzimba, Malawi	Toe-pad	FMNH
	<i>pintoi</i> (2)	206338	Chingola, Zambia	Toe-pad	FMNH
	<i>pintoi</i> (3)	225635	Huila, Angola	Toe-pad	FMNH

	<i>pintoi</i> (4)	92717	Kasaji, Demo. Republic of Congo	Toe-pad	RMCA
	<i>pintoi</i> (5)	92792	Kasaji, Demo. Republic of Congo	Toe-pad	RMCA
<i>N. chalybea</i>	<i>chalybea</i> (1)	Kirst3	Cape Town, South Africa	Muscle	FitzPatrick
	<i>chalybea</i> (2)	Gamoegas	Gomoegas, South Africa	Tissue	FitzPatrick
	<i>chalybea</i> (3)	W50939	Knysna, South Africa	Blood	FitzPatrick
	<i>chalybea</i> (4)	W50946	Knysna, South Africa	Blood	FitzPatrick
	<i>chalybea</i> (5)	W50356	Knysna, South Africa	Blood	FitzPatrick
	<i>subalaris</i> (1)	390160	Boston, South Africa	Tissue	FMNH
	<i>subalaris</i> (2)	KZN1	Pietermaritzberg, South Africa	Blood	FitzPatrick
<i>N. mediocris</i>	<i>mediocris</i> (1)	T43038	Naro Moro, Mount Kenya, Kenya	Blood	FitzPatrick
	<i>mediocris</i> (2)	LB10-131099	Karissia Hills, Eastern Maralal, Kenya	Blood	ZMUC
<i>N. usambaricus</i>	<i>usambaricus</i> (1)	JK06-201099	Magamba, W. Usambara Mnts., Tanzania	Tissue	ZMUC
	<i>usambaricus</i> (2)	JK01_250401	Mt. Shengena, South Pare Mnts, Tanzania	Blood	ZMUC
<i>N. fuelleborni</i>	<i>fuelleborni</i> (1)	AF48719	Mount Namuli, Northern Mozambique	Blood	FitzPatrick
	<i>fuelleborni</i> (2)	O3050	Kisinga-Rugero, Iringa District, Tanzania	Blood	ZMUC
<i>N. moreaui</i>	<i>moreaui</i> (1)	JF03-241197	Chonwe Forest, Uvidundu Mnts, Tanzania	Blood	ZMUC
	<i>moreaui</i> (2)	JK04-271200	Mafimero Forest, Rubeho Mnts., Tanzania	Muscle	ZMUC
<i>N. loveridgei</i>	<i>loveridgei</i> (1)	O4088	Kimhandu, Uluguru Mnts., Tanzania	Muscle	ZMUC
	<i>loveridgei</i> (2)	O4656	Kimhandu, Uluguru Mnts., Tanzania	Muscle	ZMUC



**Table 4.2.** Pairwise estimates of Kimura-2 parameter nucleotide sequence divergence (%) between taxa of Double-collared Sunbirds (*Nectarinia* spp.) Values below the diagonal are the average pairwise Kimura-2-parameter distance (%) between taxa and, above the diagonal are standard deviations.

	<i>afr</i>	<i>stu</i>	<i>gra</i>	<i>cha</i>	<i>lud</i>	<i>why</i>	<i>man</i>	<i>pin</i>	<i>ami</i>	<i>chy</i>	<i>sub</i>	<i>med</i>	<i>usa</i>	<i>fue</i>	<i>mor</i>	<i>lov</i>	<i>pre</i>	<i>reg</i>	<i>vio</i>
<i>afra</i>		0.36	0.25	0.61	0.37	0.28	0.32	0.38	0.32	0.22	0.21	0.16	0.50	0.37	0.30	0.19	0.21	0.25	0.42
<i>stuhlmanni</i>	8.84		0.01	0.26	0.16	0.11	0.33	0.58	0.33	0.32	0.27	0.33	0.29	0.30	0.28	0.01	0.30	0.21	0.28
<i>graueri</i>	9.74	1.59		0.62	0.23	0.01	0.18	0.56	0.18	0.27	0.01	0.02	0.24	0.29	0.46	0.01	0.01	0.00	0.24
<i>chapini</i>	9.80	1.34	0.78		0.60	0.34	0.45	0.67	0.45	0.49	0.43	0.51	0.89	0.55	0.58	0.35	0.42	0.46	0.54
<i>ludovicensis</i>	11.08	9.60	10.17	10.24		0.15	0.25	0.22	0.25	0.31	0.18	0.19	0.50	0.32	0.41	0.24	0.18	0.24	0.27
<i>whytei</i>	11.87	6.59	7.27	6.87	11.42		0.23	0.49	0.23	0.27	0.04	0.04	0.47	0.30	0.36	0.01	0.14	0.12	0.23
<i>manoensis</i>	6.83	8.41	8.98	9.17	10.32	10.82		6.62	0.02	0.29	0.27	0.20	0.52	0.21	0.40	0.25	0.28	0.18	0.26
<i>pintoi</i>	8.07	10.55	11.27	11.27	11.22	11.72	6.62		0.50	0.54	0.52	0.32	0.30	0.30	0.60	0.20	0.47	0.69	0.41
<i>amicorum</i>	6.83	8.41	8.98	9.17	10.32	10.82	0.02	6.62		0.29	0.27	0.20	0.52	0.21	0.40	0.25	0.28	0.18	0.26
<i>chalybea</i>	11.93	11.35	11.30	11.41	11.31	12.82	8.97	10.26	8.97		0.16	0.31	0.41	0.29	0.53	0.28	0.16	0.29	0.26
<i>subalaris</i>	10.56	10.38	10.99	11.14	9.80	11.83	8.17	9.37	8.17	2.61		0.20	0.28	0.22	0.46	0.00	0.11	0.45	0.31
<i>mediocris</i>	13.83	12.39	13.36	13.16	10.76	12.54	13.47	14.39	13.47	11.16	10.77		0.43	0.11	0.21	0.14	0.02	0.04	0.30
<i>usambaricus</i>	14.52	12.35	12.32	12.14	12.09	14.11	14.14	14.11	14.14	14.89	13.76	11.80		0.32	0.25	0.29	0.48	0.45	0.59
<i>fuelleborni</i>	8.78	8.92	9.65	9.94	9.77	10.87	10.55	12.10	10.55	11.44	9.66	9.73	10.38		0.07	0.04	0.37	0.26	0.83
<i>moreaui</i>	12.65	14.31	15.32	15.12	13.33	14.94	14.02	14.85	14.02	13.35	12.26	12.54	13.22	5.84		0.03	0.29	0.23	0.45
<i>loveridgei</i>	12.06	12.29	12.31	12.29	12.42	13.91	12.40	13.44	12.40	12.61	11.53	12.51	11.47	5.19	6.42			0.00	0.25
<i>preussi</i>	11.85	12.29	9.42	9.57	10.42	10.62	9.08	11.32	9.08	9.24	7.46	11.92	14.28	9.20	11.46	12.56		0.03	0.28
<i>regia</i>	8.13	9.37	10.04	10.04	9.65	10.49	8.02	9.41	8.02	8.62	7.23	10.32	14.71	9.00	10.51	11.27	7.83		0.16
<i>violacea</i>	15.96	15.02	15.40	15.51	15.32	15.29	14.07	14.73	14.07	13.55	12.86	15.58	17.51	13.97	18.06	15.75	13.12	11.78	

**Table 4.3.** Description of the major variations in male plumage among the different members of the *N. afra/chalybea* complex.

	<b>Rump</b>	<b>Lesser coverts</b>	<b>Tail coverlets</b>	<b>Upper breast band</b>	<b>Lower breast band</b>	<b>Flanks</b>	<b>Belly</b>
<i>afra</i>	olive-brown	metallic green	Haye's blue	Haye's blue	deep scarlet	dark olive	citrine-drab
<i>saliens</i>	olive-brown	metallic green	Haye's blue	Haye's blue	orange-scarlet	light Ecu olive	light Ecu olive
<i>stuhlmanni</i>	metallic green	metallic green	violet-blue	violet	deep scarlet	dark olive	dark olive-grey
<i>graueri</i>	metallic green	metallic green	violet-blue	violet	orange-red	dark grey	dark grey
<i>chapini</i>	metallic green	metallic green	violet-blue	violet	deep scarlet	dark grey	dark grey
<i>prigoginei</i>	metallic blue	dark brown	blueish-purple	blueish-purple	dark red	olive-yellow	Olive yellow, to light grey
<i>ludovicensis</i>	metallic green	metallic green	Paris blue	Paris blue with slight violet intrusions	dull orange-scarlet	dark olive-grey	dark olive-grey
<i>whytei</i>	metallic green	metallic green	methvl blue	methvl blue with almost no violet	scarlet-red	dark olive-grey	dark olive-grey
<i>manoensis</i>	pale olive-brown	metallic green	violet-blue	violet-blue	scarlet	pale olive- brown	pale olive-brown
<i>pintoi</i>	pale olive- brown	metallic green	olive-grey	violet-blue	scarlet	pale grey	pale grey, more yellow towards centre of lower

							belly
<i>amicorum</i>	pale olive-brown	metallic green	olive-brown	violet	scarlet	olive-brown	olive-brown
<i>chalybea</i>	metallic green*	metallic green	blue	Paris blue with violet bases to feathers	dark red	light olive-grey with yellow	olive-grey, more yellow towards centre of lower belly
<i>subalaris</i>	metallic green	metallic green	blue	as in <i>chalybea</i>	scarlet-red	olive-grey with yellow	Dark olive-grey

---

\* In some populations in the arid western parts of South Africa the rump is plain olive-brown.

**Table 4.4.** Mean sizes and sexual dimorphism (proportional greater size of males relative to females) of species in the *N afra/chalybea* complex. Significant differences between species were tested using one-way ANOVA with Newman-keuls tests used to identify which taxa differed. \* Designates a male specific character.

Measure	Males		Females		Dimorphism
Taxa (n, males, Females)	Mean	SD	Mean	SD	(%)
<b>Wing-length (mm)</b>					
<i>afra</i> (25, 18)	64.5	2.9	58.8	1.8	
<i>saliens</i> (20,6)	66.8	1.7	61.5	1.0	
<i>stuhlmanni</i> (8,2)	66.5	1.4	63.0	2.8	
<i>graueri</i> (78, 30)	65.3	1.6	59.8	1.2	
<i>chapini</i> (39, 8)	66.2	2.6	60.7	1.9	
<i>prigoginei</i> (4,2)	62.8	1.9	59.2	1.7	
<i>ludovicensis</i> (25, 12)	65.8	1.5	57.5	1.5	
<i>whytei</i> (12, 2)	62.2	1.5	56.5	0.7	
<i>manoensis</i> (12, 7)	61.2	1.8	56.6	1.4	
<i>pintoi</i> (8, 0)	60.3	1.5	—	—	
<i>amicorum</i> (3,1)	64	1.7	58.5	—	
<i>chalybea</i> (27, 2)	54.9	1.8	50.2	0.3	
<i>subalaris</i> (8, 7)	56.1	1.5	51	1.5	

$F_{12, 256} = 77.2, P < 0.001;$

chy = sub < pin = man = why = pri < ami <  
 afr = gra = lud = cha = stu < sal

$F_{10, 85} = 32.8, P < 0.001;$

chy = sub < why = man < lud = afr = pri <  
 gra = cha = sal < stu

**Bill-length (mm)**

<i>afra</i> (25, 18)	26.8	0.6	25.2	0.9
<i>saliens</i> (19,6)	27.3	0.8	24.4	0.7
<i>stuhlmanni</i> (8,2)	24.5	0.8	23.1	1.1
<i>graueri</i> (58, 23)	17.8	0.8	17.1	1.1
<i>chapini</i> (37, 8)	20.9	1.4	20.0	1.4
<i>prigoginei</i> (4,2)	18.5	0.7	18.0	0.7
<i>ludovicensis</i> (23, 11)	18.8	0.8	17.0	0.6
<i>whytei</i> (8, 2)	17.5	0.4	16.2	0.4
<i>manoensis</i> (12, 7)	20.3	1.6	18.1	1.5
<i>pintoi</i> (8, 0)	18.4	0.8	—	—
<i>amicorum</i> (3,1)	24.3	0.5	21.6	—
<i>chalybea</i> (28, 1)	20.1	1.1	16.7	—
<i>subalaris</i> (8, 6)	21.6	0.8	19.1	0.7

$$F_{12, 228} = 226.2, P < 0.001;$$

why = gra = pin = pri = lud < chy = man =  
cha < sub < ami = stu < afra = sal

$$F_{10, 76} = 90.9, P < 0.001;$$

why = chy = lud < gra = pri = man < sub  
= cha < stu < sal = afra

**Bill-width (mm)**

<i>afra</i> (25, 18)	3.61	0.23	3.48	0.11
<i>saliens</i> (19,6)	3.68	0.17	3.54	0.23
<i>stuhlmanni</i> (8,2)	3.24	0.20	3.27	0.23
<i>graueri</i> (71, 25)	3.01	0.27	3.21	0.19

<i>chapini</i> (38, 8)	3.42	0.28	3.21	0.19
<i>prigoginei</i> (4,2)	3.33	0.23	3.19	0.04
<i>ludovicensis</i> (25, 11)	3.24	0.24	3.11	0.28
<i>whytei</i> (8, 2)	3.27	0.17	3.10	0.07
<i>manoensis</i> (12, 6)	3.14	0.34	3.14	0.48
<i>pintoi</i> (8, 0)	3.16	0.15	—	—
<i>amicorum</i> (3,1)	3.65	0.20	3.75	—
<i>chalybea</i> (28, 1)	2.99	0.25	3.06	—
<i>subalaris</i> (8, 6)	3.15	0.24	2.88	0.28

$F_{12, 243} = 19.1, P < 0.001;$

$F_{10, 77} = 10.3, P < 0.001;$

chy = gra < man = sub = pin = stu = lud =  
why = pri < cha < afr = ami = sal

gra = sub < chy = why = lud = man = pri  
= cha = stu < afr = sal

#### Bill-depth (mm)

<i>afra</i> (25, 18)	3.06	0.25	2.96	0.24
<i>saliens</i> (19,6)	3.25	0.14	3.23	0.15
<i>stuhlmanni</i> (8,2)	3.05	0.28	2.76	0.16
<i>graueri</i> (67, 25)	2.79	0.20	2.72	0.15
<i>chapini</i> (38, 8)	2.99	0.23	2.90	0.11
<i>prigoginei</i> (4,2)	2.90	0.13	2.93	0.15
<i>ludovicensis</i> (24, 11)	2.95	0.24	2.86	0.16
<i>whytei</i> (8, 2)	2.76	0.18	2.65	0.02
<i>manoensis</i> (12, 6)	2.96	0.25	2.86	0.25

<i>pintoi</i> (7, 0)	2.83	0.30	—	—
<i>amicorum</i> (3,1)	3.00	0.14	2.99	—
<i>chalybea</i> (28, 1)	2.53	0.15	2.42	—
<i>subalaris</i> (8, 6)	2.65	0.19	2.74	0.08

$F_{12, 238} = 16.8, P < 0.001;$

$F_{10, 77} = 6.6, P < 0.001;$

chy = sub < why = gra = pin = pri < lud =  
man = cha = ami = stu = afr < sal

chy < why = gra = sub = stu < man = lud  
= cha = pri = afr < sal

#### Max tail-length (mm)

<i>afra</i> (24, 18)	51.4	3.2	44.5	3.8
<i>saliens</i> (20,6)	49.3	2.6	42.7	4.4
<i>stuhlmanni</i> (7,2)	55.4	2.9	43.7	1.8
<i>graueri</i> (76, 28)	53.1	3.4	43.2	2.1
<i>chapini</i> (38, 6)	53.4	3.9	43.5	2.8
<i>prigoginei</i> (4,2)	46.5	1.9	41.0	0.1
<i>ludovicensis</i> (24, 12)	46.5	3.6	39.7	1.3
<i>whytei</i> (12, 2)	50.2	2.8	42.1	1.4
<i>manoensis</i> (12, 7)	38.9	4.4	37.4	3.7
<i>pintoi</i> (8, 0)	36.5	2.5	—	—
<i>amicorum</i> (3,1)	47.9	3.0	45.5	—
<i>chalybea</i> (26, 2)	43.0	2.2	38.0	2.3
<i>subalaris</i> (7, 7)	44.7	1.8	38.3	2.3

$F_{12, 248} = 47.7, P < 0.001;$ 
 $F_{10, 81} = 6.5, P < 0.001;$   
 pin = man < chy = sub = pri = lud < ami = man = chy < sub = lud = pro = why = sal  
 sal = why = afr < gra = cha = stu = gra = cha = stu < afr

**Min tail-length (mm)**

<i>afra</i> (24, 18)	45.3	2.6	38.3	9.3
<i>saliens</i> (20,6)	43.7	2.6	39.0	4.7
<i>stuhlmanni</i> (6,2)	44.1	2.7	37.6	0.4
<i>graueri</i> (69, 26)	42.1	3.2	36.7	2.0
<i>chapini</i> (38, 6)	42.3	3.5	36.7	3.6
<i>prigoginei</i> (4,1)	38.5	1.5	36.7	
<i>ludovicensis</i> (22, 11)	40.5	3.2	35.8	1.2
<i>whytei</i> (12, 2)	41.6	2.0	35.3	0.8
<i>manoensis</i> (11, 6)	36.4	3.5	35.3	4.6
<i>pintoi</i> (8, 0)	34.2	2.9	—	—
<i>amicorum</i> (3,1)	43.6	2.3	39.3	—
<i>chalybea</i> (26, 2)	38.1	2.3	33.2	4.5
<i>subalaris</i> (7, 7)	38.0	2.2	35.1	2.2

$F_{12, 248} = 15.7, P < 0.001;$ 
 $F_{10, 77} = 0.6, ns;$   
 pin = man < sub = chy = pri < lud = why < gra = cha < ami = sal = stu < afr

**Tarsus (mm)**

*afra* (24, 18)  
*saliens* (20,6)



*stuhlmanni* (7,2)  
*graueri* (76, 28)  
*chapini* (38, 6)  
*prigoginei* (4,2)  
*ludovicensis* (24, 12)  
*whytei* (12, 2)  
*manoensis* (12, 7)  
*pintoi* (8, 0)  
*amicorum* (3,1)  
*chalybea* (26, 2)  
*subalaris* (7, 7)

$F_{2,93} = 7.6, P = 0.001; \text{med} > \text{lov} = \text{mor}$

$F_{2,50} = 1.4, \text{ns}$

**\*Violet breast-band width (mm)**

<i>afra</i> (25)	3.80	0.45
<i>saliens</i> (20)	3.49	0.81
<i>stuhlmanni</i> (8)	4.8	0.59
<i>graueri</i> (74)	4.51	0.83
<i>chapini</i> (31)	4.43	0.58
<i>prigoginei</i> (4)	1.49	0.21
<i>ludovicensis</i> (25)	3.96	0.78
<i>whytei</i> (12)	4.42	0.54
<i>manoensis</i> (12)	2.98	0.80
<i>pintoi</i> (8)	3.13	0.38

<i>amicorum</i> (3)	3.24	0.40
<i>chalybea</i> (26)	3.07	0.62
<i>subalaris</i> (8)	2.89	0.56

$$F_{12, 241} = 17.5, P < 0.001;$$

pri < sub = man = chy = pin = ami = sal =  
afr < lud < why = cha < gra < stu

**\*Scarlet breast-band width (mm)**

<i>afra</i> (25)	21.1	2.7
<i>saliens</i> (20)	19.3	1.8
<i>stuhlmanni</i> (8)	21.3	2.5
<i>graueri</i> (74)	18.7	2.2
<i>chapini</i> (31)	19.3	2.6
<i>prigoginei</i> (4)	9.5	1.3
<i>ludovicensis</i> (25)	21.9	2.8
<i>whytei</i> (12)	15.5	2.1
<i>manoensis</i> (12)	10.4	2.0
<i>pintoi</i> (8)	10.7	2.7
<i>amicorum</i> (3)	13.2	2.6
<i>chalybea</i> (26)	7.4	1.4
<i>subalaris</i> (8)	14.2	2.5

$$F_{12, 245} = 82.7, P < 0.001;$$

chy < pri = man = pin < ami = sub = why <  
gra = sal = cha = afr = stu < lud

**Table 4.5.** Loadings of log (x+1) transformed morphological measures (rotated factor matrix) on principal (PCs) and discriminant components (DA). Eigenvalues and percentage variation associated with each PC and DC are given, as well as the total variation summarized by the PCs. The largest loadings for each axis are highlighted in bold. Total variation summarized by the DCs sums to 100%.

Measurement	PC1	PC2	DA1	DA2	DA3	DA4	DA5	DA6
<b>Male</b>								
Bill-length	0.01	<b>0.87</b>	<b>-0.74</b>	0.66	0.08	0.09	0.01	-0.10
Bill-width	0.11	<b>0.86</b>	-0.14	0.25	-0.10	0.20	<b>0.92</b>	-0.17
Bill-depth	0.36	<b>0.72</b>	-0.07	0.30	-0.25	0.30	0.16	<b>0.85</b>
Wing-length	<b>0.87</b>	0.24	0.24	0.62	-0.17	<b>0.63</b>	-0.27	-0.25
Max. tail-length	<b>0.85</b>	0.03	0.19	0.40	<b>0.84</b>	0.28	-0.5	0.15
L. Breast Band	<b>0.88</b>	0.24	0.25	<b>0.77</b>	0.09	-0.57	0.08	0.02
<b>Eigenvalue</b>	<b>3.0</b>	<b>1.5</b>	<b>13.1</b>	<b>8.3</b>	<b>2.0</b>	<b>0.5</b>	<b>0.2</b>	<b>0.02</b>
<b>% Variation</b>	<b>50.5</b>	<b>25.0 (75.5*)</b>	<b>54.4</b>	<b>34.3</b>	<b>8.3</b>	<b>2.2</b>	<b>0.8</b>	<b>0.1</b>
<b>Female</b>								
Bill-length	<b>0.86</b>	0.23	<b>0.96</b>	0.29	-0.06	0.08	0.01	
Bill-width	<b>0.85</b>	0.09	0.26	0.12	0.49	0.65	-0.51	
Bill-depth	<b>0.79</b>	0.06	0.18	0.15	<b>0.68</b>	0.02	<b>0.70</b>	
Wing-length	0.15	<b>0.85</b>	0.03	<b>0.99</b>	-0.01	-0.04	0.13	
Max tail-length	0.10	<b>0.89</b>	0.08	0.34	-0.57	<b>0.67</b>	0.32	
<b>Eigenvalue</b>	<b>2.4</b>	<b>1.3</b>	<b>13.6</b>	<b>3.7</b>	<b>0.6</b>	<b>0.2</b>	<b>0.1</b>	
<b>% Variation</b>	<b>48.7</b>	<b>24.9 (73.7*)</b>	<b>74.6</b>	<b>20.2</b>	<b>3.5</b>	<b>1.0</b>	<b>0.7</b>	

**Table 4.6.** Relative significance of subsets of the discriminant variables.

Test of Function(s)	Wilks' Lambda	Chi-squared	df	P
<b>Male</b>				
1 through 6	0.001	1439	72	<0.001
2 through 6	0.19	861	55	<0.001
3 through 6	0.180	374	40	<0.001
4 through 6	0.537	135	27	<0.001
5 through 6	0.819	43.7	16	<0.001
6	0.980	4.5	7	0.727
<b>Female</b>				
1 through 5	0.007	378	55	<0.001
2 through 5	0.098	175	40	<0.001
3 through 5	0.457	59	27	<0.001
4 through 5	0.746	22	16	0.140
5	0.887	9	7	0.246

**Table 4.7.** Classification results from the discriminant analysis of members of the *N. afra/chalybea* complex. The column on the left indicates the original group, whereas the top row indicates the predicted group for each sex separately. The percentage individuals reclassified for each taxon are given along with the absolute number of individuals in parentheses. Correct reclassifications are in bold along the diagonal.

	Group 1		Group 2			Group 4	Group 3		Group 6		Group 7	Group 5	
	<i>afra</i>	<i>sal</i>	<i>stu</i>	<i>gra</i>	<i>cha</i>	<i>pri</i>	<i>lud</i>	<i>why</i>	<i>man</i>	<i>pin</i>	<i>ami</i>	<i>chy</i>	<i>sub</i>
<b>Male</b>													
<i>afra</i>	<b>84(21)</b>	4(16)	0	0	0	0	0	0	0	0	0	0	0
<i>saliens</i>	25(5)	<b>75(15)</b>	0	0	0	0	0	0	0	0	0	0	0
<i>stuhlmanni</i>	0	0	<b>86(6)</b>	0	14(1)	0	0	0	0	0	0	0	0
<i>graueri</i>	0	0	0	<b>92(50)</b>	2(1)	0	2(1)	4(2)	0	0	0	0	0
<i>chapini</i>	0	0	0	13(4)	<b>80(24)</b>	3(1)	0	3(1)	0	0	0	0	0
<i>prigoginei</i>	0	0	0	0	0	<b>100(4)</b>	0	0	0	0	0	0	0
<i>ludovicensis</i>	0	0	0	14(3)	0	0	<b>81(17)</b>	5(1)	0	0	0	0	0
<i>whytei</i>	0	0	0	25(3)	0	0	0	<b>75(9)</b>	0	0	0	0	0
<i>manoensis</i>	0	0	0	0	0	0	0	0	<b>83(10)</b>	17(2)	0	0	0
<i>pintoi</i>	0	0	0	0	0	0	0	0	12(1)	<b>88(7)</b>	0	0	0
<i>amicorum</i>	0	0	0	0	0	0	0	0	0	0	<b>100(3)</b>	0	0
<i>chalybea</i>	0	0	0	0	0	0	0	0	0	0	0	<b>96(25)</b>	4(1)
<i>subalaris</i>	0	0	0	0	0	0	0	0	0	0	0	0	<b>100(7)</b>

**Female**

<i>afra</i>	<b>83(17)</b>	17(3)	0	0	0	0	0	0	0	0	0	0	0
<i>saliens</i>	33(2)	<b>67(4)</b>	0	0	0	0	0	0	0	0	0	0	0
<i>stuhlmanni</i>	0	0	<b>100(2)</b>	0	0	0	0	0	0	0	0	0	0
<i>graueri</i>	0	0	0	<b>88(21)</b>	8(2)	0	4(1)	0	0	0	0	0	0
<i>chapini</i>	0	0	17(1)	0	<b>67(4)</b>	0	17(1)	0	0	0	0	0	0
<i>prigoginei</i>	0	0	0	0	0	<b>50(1)</b>	50(1)	0	0	0	0	0	0
<i>ludovicensis</i>	0	0	0	9(1)	0	0	<b>91(10)</b>	0	0	0	0	0	0
<i>whytei</i>	0	0	0	0	0	0	50(1)	<b>50(1)</b>	0	0	0	0	0
<i>manoensis</i>	0	0	0	0	17(1)	0	0	0	<b>83(5)</b>	0	0	0	0
<i>pintoi</i>	0	0	0	0	0	0	0	0	—	0	0	0	0
<i>amicorum</i>	0	0	0	0	0	0	0	0	0	0	<b>100(1)</b>	0	0
<i>chalybea</i>	0	0	0	0	0	0	0	0	0	0	0	<b>100(1)</b>	0
<i>subalaris</i>	0	0	0	0	0	0	0	0	0	0	0	0	<b>100(6)</b>

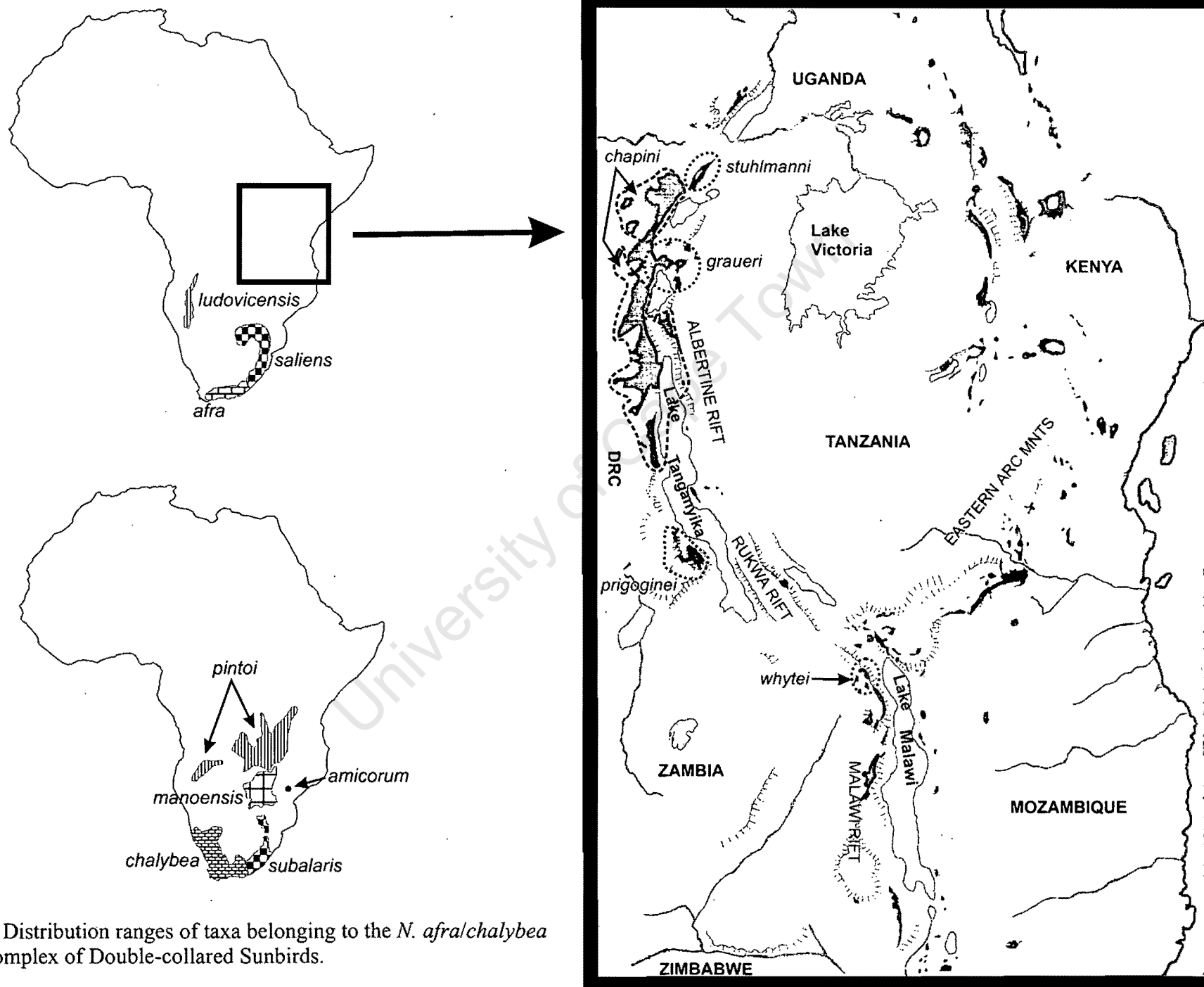


**FIG 4.1.** Distribution ranges of taxa belonging to the *N. afra/chalybea* species complex of Double-collared Sunbirds.

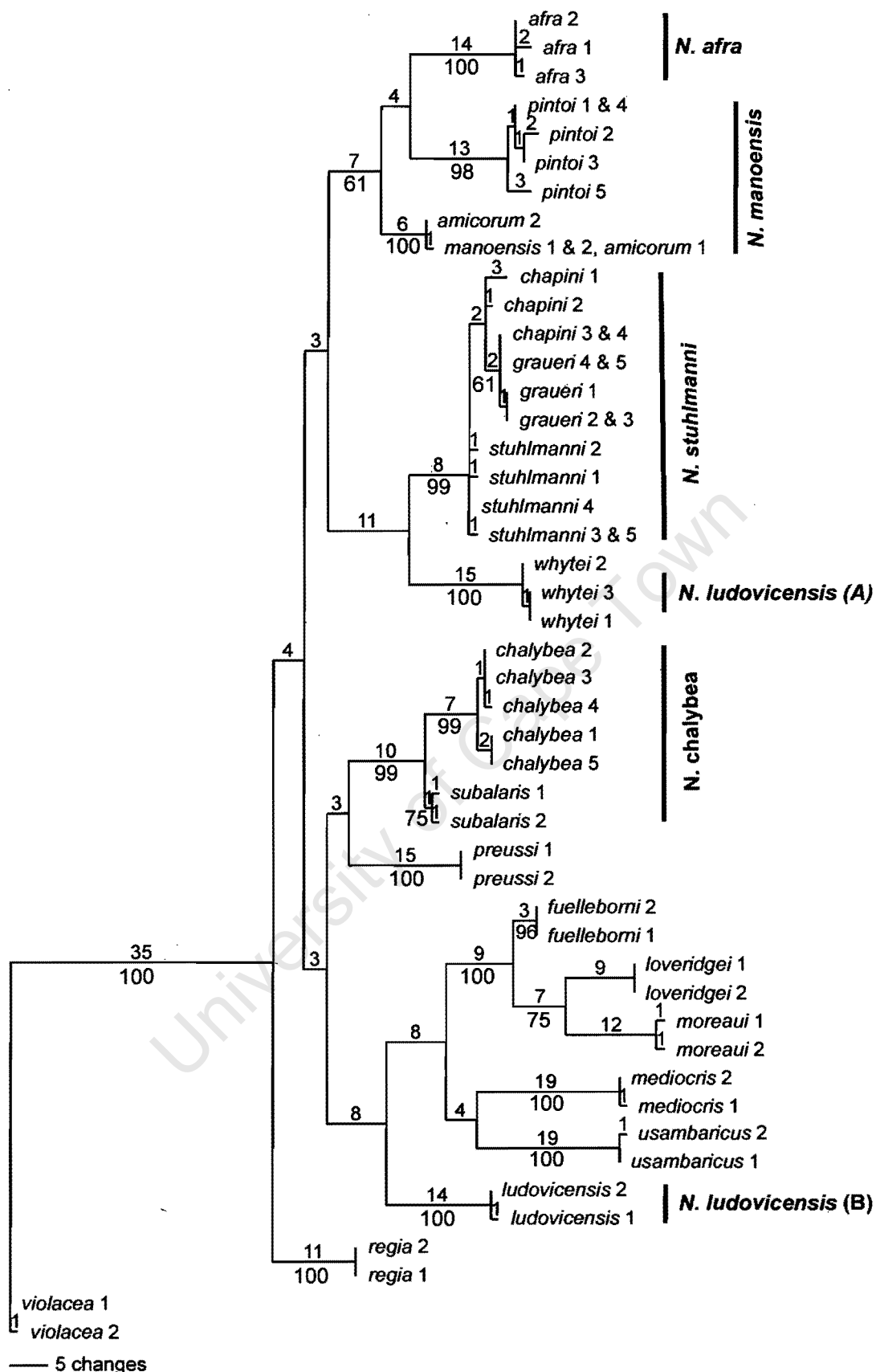


**FIG 4.2.** Empirically weighted (11:1 transitions to transversions in the 3<sup>rd</sup> codon position) maximum parsimony analyses of the 54 individuals sequenced yielded 10 MP trees of 1108 steps. The strict consensus has the same topology as this example of an unweighted MP tree. Currently recognised taxa belonging to the *N. afra/chalybea* complex of Double-collared Sunbirds are indicated. Numbers above branches are node lengths, below branches are bootstrap values from 500 replicates.



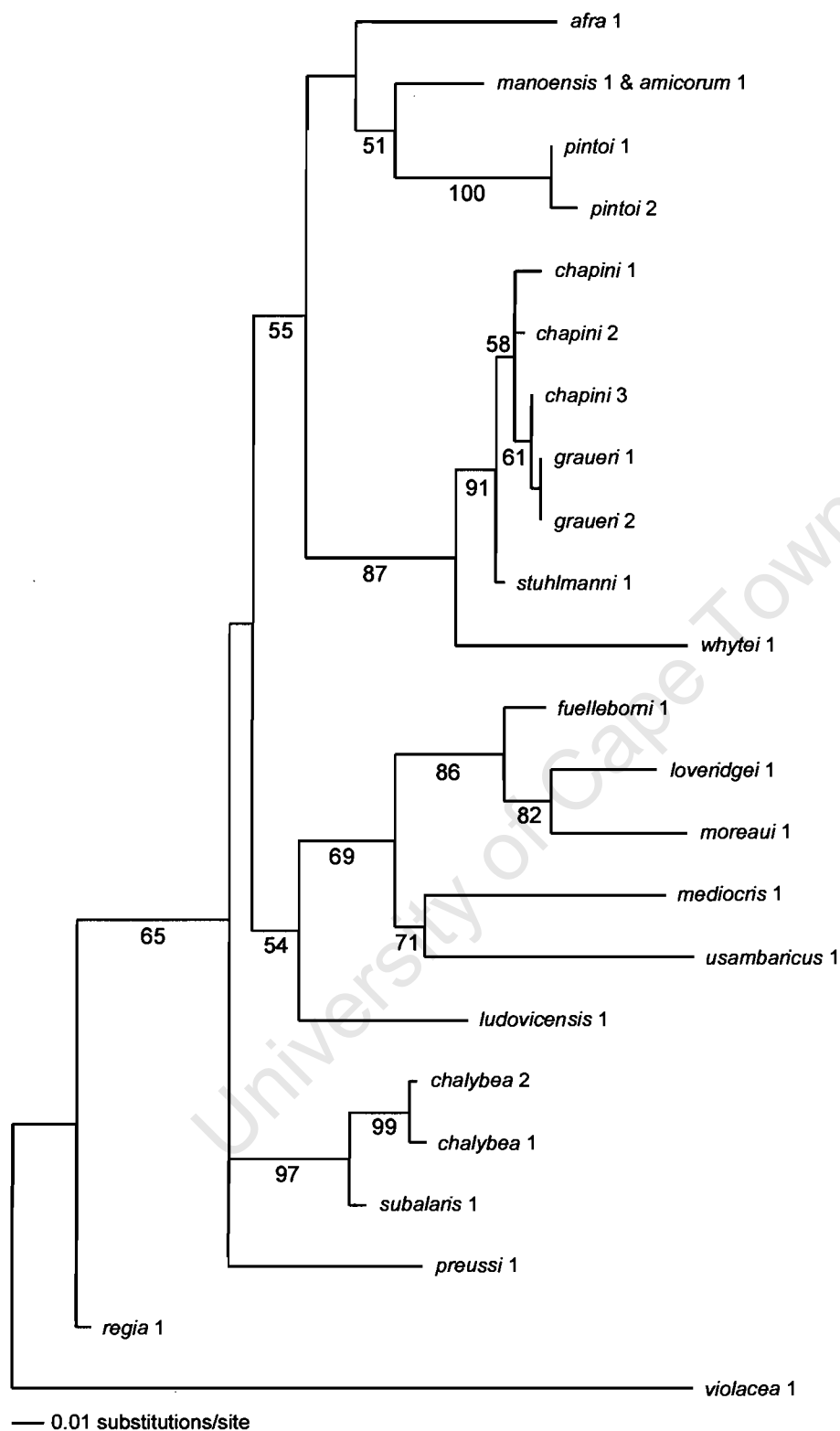


**FIG 4.3.** Maximum likelihood analysis of the full 395bp dataset, but with a reduced number of individuals ( $n=23$ ), using an HYK + I + model of nucleotide substitution (see text for parameters). A heuristic search with 100 random addition replicates yielded one tree of length  $\ln 1884.65$ . Bootstrap values from 100 replicates are indicated.

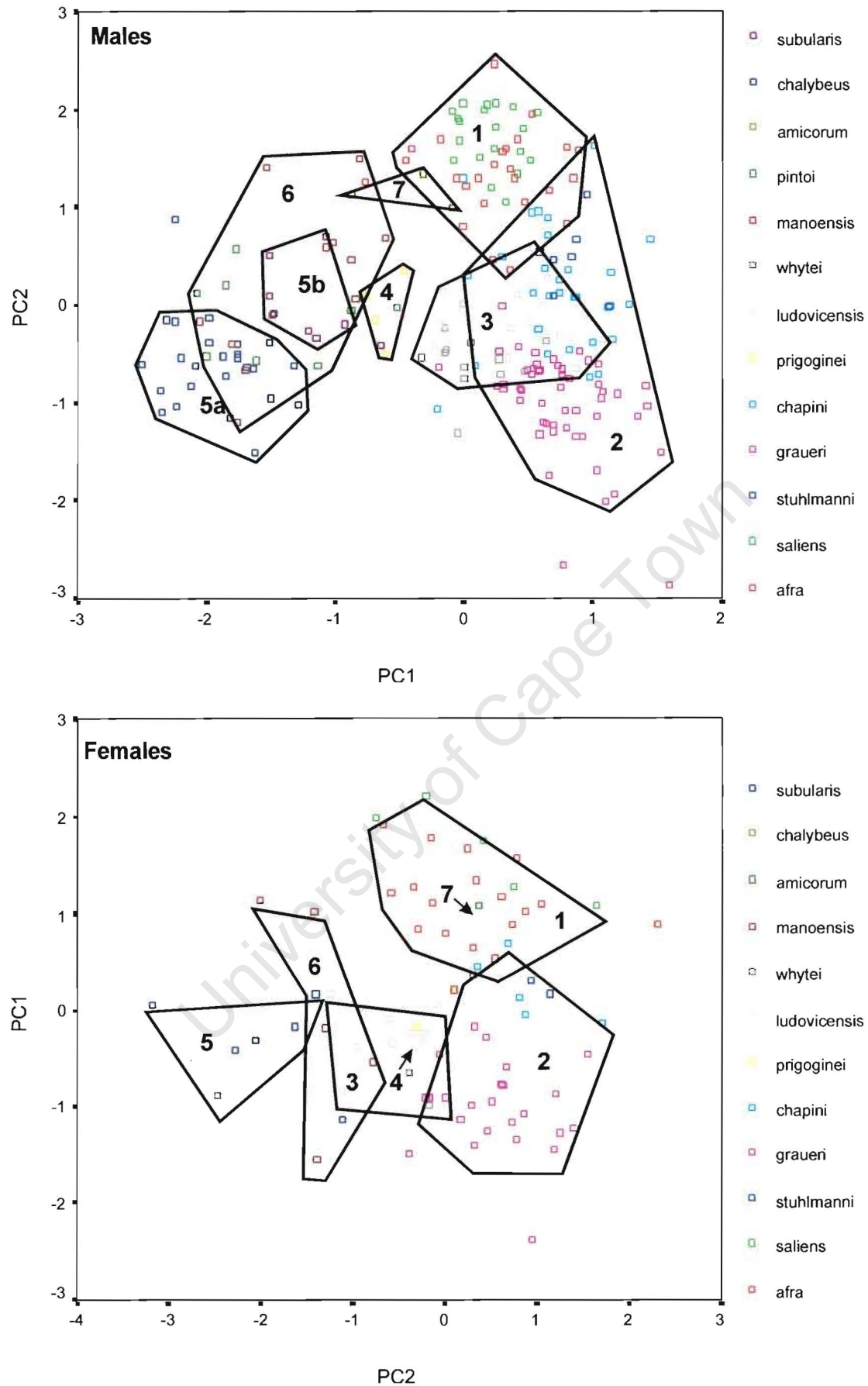


**FIG 4.4.** Scatter plots of the principal component scores derived from six morphological measures for the *N. afra/chalybea* species complex separated by sex. Lines represent 95% confidence polygons. Groups are: (1) *afra* and *saliens*, (2) *stuhlmanni*, *graueri* and *chapini*, (3) *ludovicensis* and *whytei*, (4) *prigoginei*, (5a) *chalybea*, (5b) *subularis*, (6) *manoensis* and *pintoi* and, (7) *amicorum*.

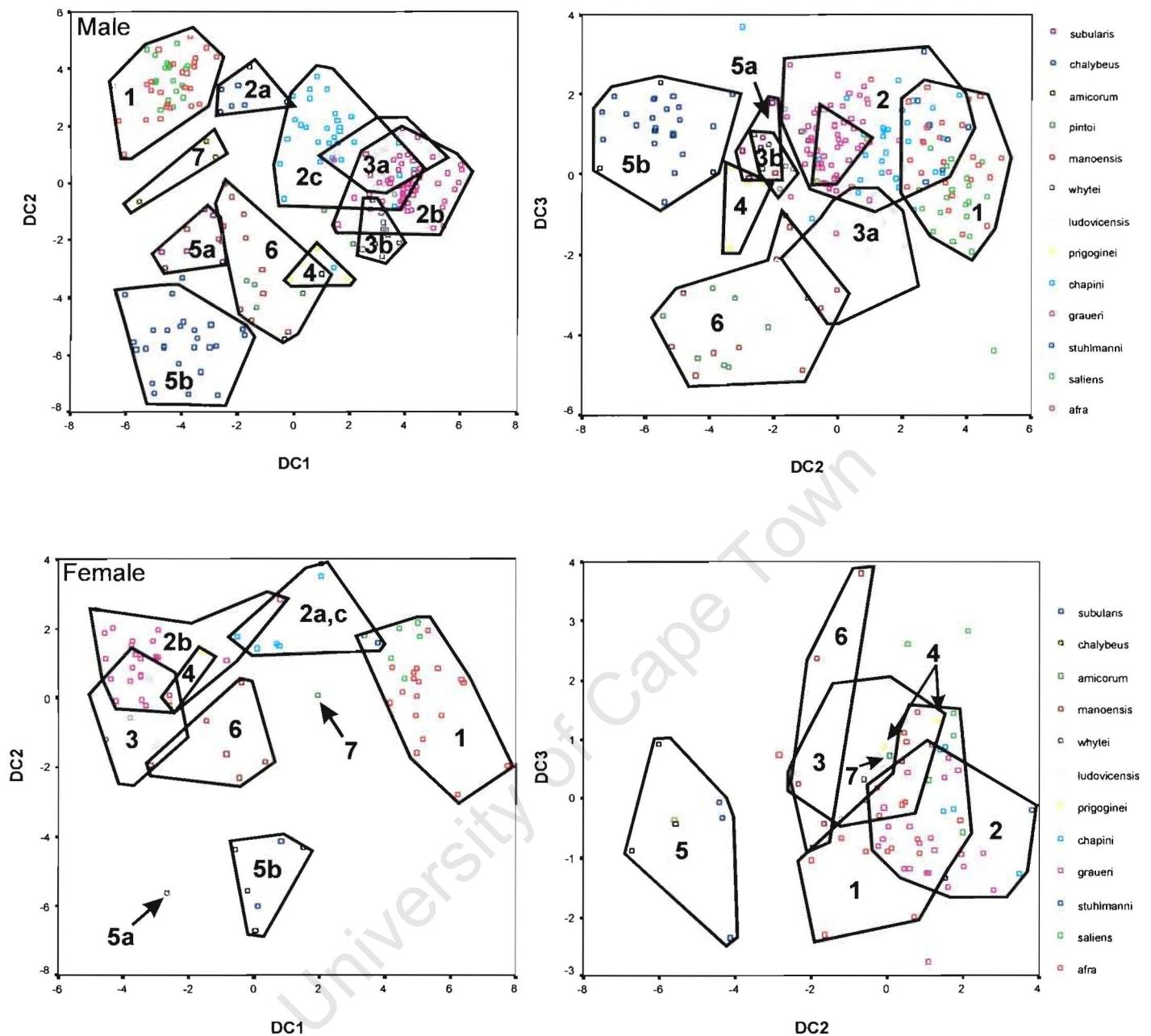


**FIG 4.5.** Discriminant function scores for sunbirds belonging to the *N. afra/chalybea* species complex separated by sex. Lines represent 95% confidence polygons. Groups are as in Fig. 4.4.

**DISCLAIMER:** This chapter is not to be considered as published in the sense of the International Code for Zoological Nomenclature, and statements herein are not herewith made available for purposes of zoological nomenclature

Thus, the new scientific name proposed herein is not to be used in any form (including fieldguides) without the express permission of the author of this work. The reason for this is that an additional 18 specimens have become available, which the author was not able to examine at the time of submission of this thesis. These specimens may have important implications with respect to the taxonomic status of the taxon described herein. Please wait until this chapter is published in a scientific peer reviewed journal.

## Chapter 5

### **Description and affinities of a new member of the Greater Double-Collared Sunbird complex (genus *Nectarinia*) discovered in the Eastern Arc Mountains of Tanzania**

#### **Summary**

The discovery of a new member of the *Nectarinia afra* complex (Aves: Nectariniidae) from the Eastern Arc Mountains, Tanzania and East Africa is documented. Phylogenetic relationships and taxonomic rank were assessed based on mtDNA sequence data and nine morphological characters. This new taxon has close affinities with *N. whytei* from Nyika Plateau in Malawi, although it has a significantly shorter tail, longer tarsus and broader blue/violet upper breast-band. The taxon is formally described as *N. skyei* species nova. *Skyei* has

been recorded above 1500m in scrub on the forest/grassland ecotone in the Rubeho and Ukaguru Mountains and probably has a very restricted range. This taxon is threatened by the effects of human settlement and agriculture.

## INTRODUCTION

The Eastern Arc Mountains of Tanzania (Fig. 5.1) have in recent years become known as a centre of high biological endemism (Lovett & Wasser 1993, Burgess *et al.* 1998) and form one of the global hotspots for conservation. Many of the components of this assemblage of mountain blocks are thought to be ancient, in some cases in excess of 7 million years old (Griffiths 1993, Partridge *et al.* 1995). In addition, it is highly likely that many of these mountains have been forested for considerable periods of time and remained so due to the local persistence of evergreen forest on mountain scarps that are under direct climatic influence from the Indian Ocean (Griffiths 1993, Partridge *et al.* 1995). Endemic species comprise some ancient relict forms that show highly nested distributions with peak aggregates in the Usambaras (at the coast) and the eastern scarp of the Udzungwa Highland (Cordeiro 1998). However, the Eastern Arc is also an area of recent diversification as isolation has alternated with opportunities for dispersal and (re)colonisation (Fjelds  & Lovett 1997, Chapter 3).

The Eastern Arc Mountains are ancient granitic and gneissic fault blocks isolated by savannah plains. Some of the savannah gaps are wide, but the biologically unique eastern scarp of the Udzungwa (Iringa) Highland is only separated by a narrow wooded gorge from the Rubeho Mountains to the northeast (Fig. 5.1). These extensive mountain complexes at 1500-2500m are separated by the narrow Great Ruaha Gorge, which widens into a rain shadow basin with extensive arid *Acacia* and *Adansonia* woodlands on the northwestern side of the mountains. The highlands to the north and east of the "barrier" are ornithologically largely unexplored, apart from a brief survey to Uquiwa forest in the Rubeho Mountains (Fjelds  *et al.* 1998) and, there has been a few short visits by the botanist Jon Lovett and butterfly collectors T.C.E. Congdon and Jan Kielland.

In order to improve the knowledge about this area, several ornithological surveys were undertaken from 1999-2002 by Jon Fjelds , Jacob Kiure and others, to

document avifaunal differences between the eastern Udzungwa Highlands, Image Forest (a northern projection of the Udzungwa Highland), the Mangalisa Plateau (isolated within the Ruaha Basin) and the Uvidundas and Rubeho Mountains to the east (Fig. 5.1).

A number of interesting biological discoveries were made, both in terms of replacements and species distributions extending right across the gap. A new population of Udzungwa Forest Partridge (*Xenoperdix udzungwensis*) was discovered (Fjeldså & Kuire in press). Further, a new species of Akalet (*Sheppardia* spp.) was discovered, which proved to be fairly abundant in the Rubeho Mountains (Fig. 5.1). Moreau's Sunbird (*Nectarinia moreaui*) was found to inhabit humid forest, displacing the Eastern Double-collared Sunbird (*N. mediocris*) from the eastern part of the Udzungwa Highlands (Chapter 3). A sunbird, which was first mistaken for an Eastern Double-collared was found along the eastern edges of forests inhabited by Moreau's Sunbird in the woodland/grassland ecotone. However, as material was collected and phylogenetic relationships were investigated, it became clear that this is a new member in this complicated group (see Chapters 3 and 4). This discovery comes less than 20 years after the unique Rufous-winged Sunbird (*N. rufipennis*) was discovered in the Udzungwa Highlands (Jensen 1983). This new population is described as a new species:

***Nectarinia skyei* sp. nova**

**(Skye's Double-collared Sunbird)**

#### **HOLOTYPE**

Male specimen, ZMUC 93.057 of the Zoological Museum of the University of Copenhagen (Field No. JK01-31032000). Collected 31 March 2000, at 2100m elevation on Chugu Hill, in Mafwemiro Forest, in the Rubeho Mountains, Tanzania (06°49'08"S; 36°34'02"E). Tissue samples are deposited with the ZMUC. Slight wear on the remiges and rectrices suggests that the bird had not recently moulted.

## PARATYPES

Two male specimens, ZMUC 93.056 and 93.129 of the Zoological Museum of the University of Copenhagen (Field Nos. JK02-31032000 and JK01-17052000, respectively) are included in the type series. Tissue samples are deposited with the ZMUC. ZMUC 93.056 was collected from Mafwemiro Forest on the same day as the holotype, while ZMUC 93.129 was collected from Ukwiva Forest (7°48'S, 36°37'48"E) also in the Rubeho Mountains two months later, 17 May 2000. This second bird collected from Mafwemiro Forest also had slight wear on the remiges and rectrices, suggesting that the bird had not recently moulted. The first three primaries had been replaced and the fourth primary was in moult for the bird collected from Ukwiva Forest. Both the secondaries and rectrices had significant wear, suggesting they were to still moult. No body moult on the head, back, rump, throat, breast or belly was visible.

## ETYMOLOGY

The scientific and vernacular name, acknowledge the contributions of the Skye Foundation to the education of African students, particularly in systematics.

## DESCRIPTION OF THE HOLOTYPE

Colours with initial capital letters refer to Ridgway (1912).

### Male upperparts

The head, scapulars, back, rump and lesser and median wing-coverts are metallic Cossack Green with golden overtones. The tail coverts are Dark Violet at the base of the feather, becoming Paris Blue towards the tips. The tail rectrices and wing remiges are Dark Dusty Brown. The primaries are narrowly edged on their outer margin with Olive. The outer three tail rectrices are narrowly tipped in White, most prominently on the outer retrix. The tail is graduated.

### Male face and underparts

The forehead, cheeks, malar and throat, as for the upperparts are metallic Cossack Green with golden overtones. The lores are black. The narrow upper chest band is metallic Methyl Blue at the tips of the feathers with dark violet at the base. The broad lower chest band is Scarlet-Red, bordered with large Pale

Lemon-yellow pectoral tufts. Underwings are Pale Grey. Belly and flanks are light Olive-grey with Olive Buff towards the vent. The crissium is Olive-grey.

#### **Male bare parts**

Iris dark-brown. Bill and feet are black.

#### **Female**

To date it has not been possible to net a female specimen and therefore procure a voucher. However, observations in the field indicate that the female has typical Greater Double-collared Sunbird characters; lack of metallic plumage and pectoral tufts with upper and underparts brownish-grey, with the centre of the lower belly paler and more olive-yellow.

#### **Measurement of type**

Wing-length (flattened chord, from the carpal joint to the tip of the longest primary feather) is 61.5mm. The remaining measurements were made with digital Vernier callipers to the nearest 0.1mm. Culmen length, chord length from notch on the skull to the tip of the upper mandible is 22.16mm. Upper mandible length, from the distal edge of the nares to the tip of the upper mandible is 19.04mm. Bill-depth, depth in the vertical plane at the anterior edge of the nares and bill-width, width in the horizontal plane at the anterior edge of the nares are 2.92mm and 3.25mm, respectively. The length of the longest and shortest tail feathers from the base of the pygostyle to the tip of either the central or outer rectrices are 46.89mm and 39.03mm, respectively. Tarsus, from tibiotarsal joint to distal undivided scute is 15.85mm.

#### **INDIVIDUAL VARIATION**

All three male specimens collected were similar in plumage (described above). Morphometric results are summarized in Figure 5.2, but there was little intraspecific variation in size.

#### **DIAGNOSIS**

Double-collared Sunbirds (*Nectarinia* spp.) form a complex of morphologically similar forms in which the males have the upperparts metallic Cossack green,



with the throat edged posteriorly by a narrow upper-breast band of blue or violet, boarded by a lower-breast band of varying shades of scarlet-red to ochre. Lateral pectoral tufts of varying size and shades of yellow border the edges of the breast. Belly and vent colouration grades from analine yellow to dark grey. Extensive variation exists in body dimensions.

Until recently, three species of Double-collared Sunbird were recognised as occurring within the Eastern Arc Mountains of Tanzania: *N. mediocris*, *N. moreaui* and *N. loveridgei*. They are closely related to one other and form the *N. mediocris* species complex (Chapter 3). Bowie (Chapter 3) recently revised species boundaries among these taxa and suggested that a further two species be recognised, *N. fuelleborni* and *N. usambaricus*. *Nectarinia moreaui* overlaps with *N. skyei* in geographical distribution, but differs dramatically in that the adult male has upper tail coverts completely violet, strontium yellow pectoral tufts that are exceptionally broad, and a belly to vent that is dark olive-yellow. In addition, there is a marked size difference, with *N. moreaui* in general being considerable smaller (e.g. male *moreaui*: wing  $54.5 \pm 2.4$ mm, tail-length  $34.7 \pm 3.1$ mm; *skyei*: wing  $61.3 \pm 0.29$ mm, tail-length  $44.1 \pm 2.77$ mm) except in exposed bill-length (*moreaui*:  $21.0 \pm 0.4$ mm, *skyei*  $18.2 \pm 0.74$ mm).

The above disparity in wing and tail length between *N. moreaui* and *skyei* is typical of differences between the Eastern Double-collared Sunbird species complex (*N. mediocris* complex, Chapter 3) and the Greater Double-collared Sunbird species complex (*N. afra* complex, Chapter 4). In addition, *skyei* has all the diagnostic plumage characters of the Greater Double-collared Sunbird complex: pale olive-grey belly, pale lemon-yellow pectoral tufts, methyl blue with violet bases to the feathers of the tail coverts and upper-breast band, and a broad scarlet-red lower-breast band. Thus, *skyei* can with confidence be considered the first representative of the Greater Double-collared Sunbird species complex discovered with the Eastern Arc Mountains, Tanzania and East Africa.

The closest geographical member of the Greater Double-Collared Sunbird complex to *N. skyei* is *N. whytei*, from Nyika Plateau in northern Malawi, which

until recently was considered a subspecies of *N. ludovicensis* from the Angolan Highlands (Chapter 4). Both in plumage and body dimensions *skyei* resembles *N. whytei* more than any other member of the Greater Double-collared Sunbird complex. The male *N. whytei* has head to scapulars and rump plus chin and throat metallic Cossack Green with golden overtones. Upper tail coverts and narrow upper-breast band Methyl Blue with Violet bases to the feathers, a broad Scarlet lower-breast band and Pale Lemon-yellow pectoral tufts. The tail is Black with a slight blue gloss. The remiges are Dark Brown, narrowly edged in Olive. The belly, extending to the vent and flanks, is Dark Olive-grey (colours follow Ridgway 1912).

### DISTRIBUTION

Found on the eastern fringe of Mafwemiro and Ukwiva forests of the Rubeho Mountains and in the Ukaguru Mountains (6°12'S, 36°48'E). Also observed in Image Forest Reserve (7°22'15"-33'15"S, 36°08'15"-12'25"E), which covers a huge mountain ridge at an elevation of 2454 m, called Selebu or Selegu on some maps. The ridge extends north from the northeastern corner of the Udzungwa Highlands (Fig. 5.1). Found along forest edges in the extreme north and northeast of Mangalisa Forest (7°9'S, 36°25'12"E), a large mesa-like highland in the northeastern part of the Great Ruaha Basin, close to the Rubeho Mountains although separated from them by arid lowland habitat, which is now densely populated. Expected to also occur on wooded mountaintops north of the Ruaha Basin and the northern plateaus of the Ukaguru group.

### MOLECULAR DATA AND PHYLOGENETIC ANALYSIS

DNA was extracted, PCR amplified for the mitochondrial DNA NADH subunit 3 gene with flanking tRNAs and cycle-sequenced as described in (Chapter 4).

Sequences were obtained from both strands of DNA for two individuals of *skyei* and aligned with the taxa listed in Table 5.1. Phylogenetic analyses of the DNA sequences were performed using maximum parsimony and maximum likelihood as implemented in PAUP\*4.0b10 (Swofford 2002). The tree was rooted with *N. violacea*, which is thought to be the closet relative to the Double-collared Sunbird complex (Chapter 2).

A total of 395 base pairs (bp) were amplified from the ND3 gene (351bp) with flanking tRNAs (Glycine and Arginine, combined 44bp). Of the 395 characters, 253 (64%) were constant, 39 (10%) variable and 103 (26%) parsimony informative. There were 14 amino acid changes within ND3.

Equally-weighted maximum parsimony analysis (MP), implementing stepwise addition with 1000 random addition replicates, and TBR branch-swapping, yielded 70 trees of 307 steps, one of which is illustrated in Figure 5.3 (CI = 0.541, RI = 0.681). A strict consensus of these trees resulted in relationships among species being largely unresolved; *skyei* clustered with *whytei* (100% bootstrap support) and *skyei* and *whytei* in turn were sister to *stuhlmanni* (includes *graueri* and *chapini*) from the Albertine Rift (91% bootstrap support). *Skyei* and *whytei* differ from each other by 1 to 2 mutations (0.26–0.52%) and from *stuhlmanni* by 25 to 27 mutations (6.5 – 7.1%)

Because transitions often accumulate at higher rates than transversions, MP analyses were conducted using different weighting schemes to evaluate the sensitivity of tree topology to possible saturation. The empirical Ti/Tv rate calculated was 11 to 1. Using this weighting scheme, 10 trees of 1108 steps were recovered (CI = 0.646, RI = 0.744). The strict consensus of these trees has identical topology to Figure 5.3, with the exception that relationships within *N. stuhlmanni* were unresolved, once more *skyei* grouped with high bootstrap support with *N. whytei* (100%). With a Ti/Tv ratio half that of the empirical value (5 to 1), the same 10 trees were obtained (Length = 680, CI = 0.609, RI = 0.718).

Modeltest 3.06b (Posada & Crandall 1998) was used to help ascertain the nucleotide substitution model that best described the data. Modeltest suggested a TVM model with invariable sites and equal rates. This model was further optimised using PAUP\* and an additional parameter eliminated without significant changes in the likelihood score. Model parameters: Base composition, A (30.8%), C (37.7%), G (11.8%) and T (19.6%); rates are all 1.0 except A to G and C to T which are 25.0; I = 0.6027. Using the above model parameters generated one tree (Fig. 5.4) of length  $-\ln 1901.7$ . The topology is

identical to the weighted MP trees, as are levels of support. Again *skyei* clusters with high bootstrap support (100%) with *N. whytei*, and together are sister to *N. stuhlmanni* (92% bootstrap support).

### MORPHOMETRIC COMPARISONS WITH *NECTARINIA WHYTEI*

Twelve male specimens of *N. whytei* were compared with three specimens of the type series of *skyei* for the nine morphological measures (see measurement of type). The two taxa were similar in size for wing-length, bill-length, bill-width, bill-height and the width of the scarlet chest band (Fig. 5.2, Table 5.2). *Skyei* has a significantly shorter tail than *whytei* (<48 mm), a significantly longer tarsus (> 15.5 mm) and a significantly broader violet/blue chest band (> 5.5 mm) (Table 5.2, Fig. 5.2).

### ECOLOGY

Recorded from 1700-2200 m along the eastern and northern parts of large undulating montane highlands in central Tanzania. These habitats are rather nutrient-poor with light brown sandy soils over gneiss and quartzites. High orographic rainfall occurs on the eastern scarps probably supplemented with mist precipitation. Precipitation from mist is expectedly to be most frequent in the Udzungwa Highlands. Based on the distribution and abundance of 'old man's beard' *Usnea* on *Podocarpus* trees some high plateaus in partial rain shadow may also be strongly influenced by mist. The dry season occurs from June to November.

Towards the eastern edge of the montane forest typical trees are: *Mangalisa* (Jon Lovett, 1984, unpublished data, Lovett & Congdon 1989) *Aningeria adolfi-friedericii*, *Albizia gummifera*, *Bersema abyssinica*, *Cassipourea melosana*, *Craibia brevicaudata*, *Cussonia spicata*, *Dais cotinifolia*, *Dombeya torrida*, *Euclea divinorum*, *Lepidiotrichilia volkensii*, *Maesa lanceolata*, *Myrica salicifolia*, *Manilkaria* cf. *discolor*, *Mastroxylon aethiopicum*, *Neoboutonia macrocalyx*, *Nuxia congesta*, *Ochna holstii*, *Olea capensis*, *Olinia rochetiana*, *Parinari excelsa*, *Peddiea fischeri*, *Podocarpus falcatus* and *latifolius*, *Rapanea melanophloeus*, *Rawsonia lucida*, *Syzygium guineense*, *Tecomaria capensis*, *Trichocladus ellipticus* and *Zimmermannia stipularis*; Image (Lovett & Congdon

1989): *Acokanthera laevigata*, *Aphloia theiformis*, *Cussonia spicata*, *Maesa lanceolata*, *Myrica salicifolia*, *Nuxia congesta*, *Lasianthus kilimandscharicus*, *Pavetta kymbilensis*, *Rawsonia reticulata* and *Ziziphus*, while larger trees comprise *Bersama abyssinica*, *Croton macrostachyus*, *Ekebergia capensis*, *Ixora scheffleri*, *Podocarpus latifolius*, *Prunus africana*, *Rapanea melanophloeos*, *Sysygium cordatum* and *Zanthoxylum* sp. (Lovett & Congdon 1990, Lovett & Minja 1990, Ruffo 1991).

The habitat fringing the forest contains mostly small patches of varying tree composition in a matrix of heathland, pastureland and small fields. The tree line extends into deeper gorges and along streams, grading into heathland with *Protea*, *Myrica* and *Erica*. This, in turn, grades into *Brachystegia spiciformis*/*Uapaca kirkiana* woodland with taller grass (*Themeda triandra*). *Nectarinia skyei* appears to be most abundant along the edges of the montane forest and the transition zone between heathland and semi-evergreen woodlands, prominent on the eastern slopes of the Mangalisa Plateau. In the Rubeho Mountains *skyei* occurs on the west edge of Ukwiwa Forest where open wooded, *Pterocarpus* etc, grades to dry montane (secondary) forest with a tree composition containing species listed above (see also Lovett & Pócs 1993). Mafwemiro is an extensive montane forest at 1700-2100 m, some of it heavily disturbed with shambas (tribal homes) located inside the forest edge, but other parts are apparently virgin forest with the surrounding land wooded with *Brachystegia* and *Acacia*. The Ukaguru Mountains are dominated by large high plateaus, which are sparsely wooded and stony.

## DISCUSSION

### Taxonomic rank and biogeography

In this paper, it is suggested that the newly discovered population of Double-collared Sunbird, *skyei*, which belongs to the *N. afra* species complex, be accorded species status. From both molecular DNA sequence data (Fig. 5.3) and plumage characters, it is clear that *whytei* and *skyei* are sister taxa. Discrete and diagnosable differences do exist in body dimensions, with *skyei* having a shorter tail, broader blue/violet breast band and longer tarsus than *whytei* (Table 5.2), despite only limited sequence divergence (0.26-0.52%, no fixed differences).

Under the framework of a phylogenetic species concept (Cracraft 1983) these diagnosable morphological character differences are sufficient to elevate *skyei* to full species rank (see Klicka et al. 1999 for a similar example in the Timberline Sparrow). Proponents of more traditional approaches to taxonomy may consider *skyei* a subspecies or incipient species of *N. whytei*. However, describing subspecies as a means to designate isolated sublineages that may evolve into full species (e.g. Mayr 1942) has the unavoidable problem of requiring knowledge of the future (Frost et al. 1992, Burbrink et al. 2000). Thus, subspecies have no real taxonomic meaning if they are used to represent arbitrary degrees of morphological divergence or incipient species (Burbrink et al. 2000). Consequently, this approach is not adopted.

The low genetic divergence between *whytei* and *skyei* haplotypes, 1-2 mutations (0.26-0.52% sequence divergence) suggests a recent separation between the two taxa. An old vicariance event ca. 3-4 million years before present is thought to have resulted in the isolation and subsequent speciation of *N. stuhlmanni* (includes *graueri* and *chapini*) from the Albertine Rift and *N. whytei* from northern Malawi (Chapter 4). The low sequence divergence between *whytei* and *skyei* suggests a recent origin of one or the other population, suggesting that either the Eastern Arc was recently colonised from northern Malawi or *vice versa*.

One important caveat of the above is that the documentation of diagnosable differences between *whytei* and *skyei* is based on only three individuals, all male. Thus, this chapter should be considered a working hypothesis, and additional individuals, especially females should be collected to provide a more comprehensive sample of the population, in order to determine if the characters reported here are close to the population mean or represent a biased sample of the population.

### Ecology

Based on initial field observations, *skyei* appears to prefer scrub and secondary growth often associated with the forest/grassland ecotone at altitudes of greater than 1500m. *Skyei* has not been recorded in montane forest, which is occupied

by *N. moreaui*. These habitat preferences are similar to those recorded for *whytei* on Nyika Plateau in Malawi. Above 1900 on Nyika, *whytei* is common in scrub and secondary growth 1.5 to 3-4m tall where it feeds on the nectar of several forest-edge plants (Dowsett-Lemaire 1989). Of the montane isolates of the *N. afra* complex, *whytei* is relatively well studied and has not been seen to penetrate forest (Benson 1949, Dowsett-Lemaire 1988, 1989). The close affinities between *whytei* and *skyei* suggest that the basic ecological data known for *whytei* may be applicable to *skyei*, for which almost nothing is as yet, known. However, any extrapolation of ecology or behaviour should be interpreted with caution until verified in the field.

*Nectarinia whytei* starts to breed on Nyika in February (Dowsett-Lemaire 1989), lays a single egg, but is able to double or triple brood (Dowsett-Lemaire 1988). Pairs are monogamous with the male actively defending food resources in relatively small territories, 0.1-0.5 ha. The female builds the nest, often making use of material from previous nests, and feeds the chick. The male may on occasion help feed the chick, but assumes a more active role in provisioning once the chick has fledged. Colour-ringed territorial males were resident year round (Dowsett-Lemaire 1988, 1989), suggesting the species does not attitudinally migrate in the winter months.

The two *skyei* specimens collected from Mafwemiro forest in March had slightly worn (sw) flight and tail feathers. The one individual collected from Ukwiva Forest in May had started to moult the primaries (P1-4 new, P5 moulting, P6-10 old). Twelve specimens were examined for moult in *whytei* (Bowie unpublished data), five birds taken in January had worn (w) to sw flight and tail feathers, two in June, very worn (vw) flight and tail feathers, and for both specimens taken in October moult was already well advanced with P7 and P8 just having been dropped in one individual, and P9 and P10 in the other. The tail feathers were also actively moulting. The three birds taken in November had nearly completed primary moult, with moulting of secondary flight feathers being well advanced. Tail moult had been completed in one of the two individuals. Unfortunately, no specimens were collected during the months February to May or July to August, or December. It is likely that moult in *skyei* (at least in one individual) may start

in April/May before the onset of moult in *whytei*, sometime between July and October.

### **Conservation implications**

This new taxon, although fairly common, does not occur in high densities locally. This is because the zone it inhabits is also the most densely human populated part of the highland. Relatively few individuals were seen in Image and Mangalisa Forests, where only small evergreen thickets occur. However, in the Rubeho Mountains where there are fairly large tracts of habitat, it has been observed in greater numbers. Potentially, this new taxon could occur in the outlying massifs northeast of the Rubeho Mountains (Fig. 5.1), which have semi-evergreen patches on their highest peaks, although some of these massifs are far up in the arid interior. These areas should be a priority for future survey work. In view of its tiny, fragmented range, *N. skyei* is a taxon of some conservation concern.

Habitat destruction resulting from human settlement and agriculture at the eastern edge of the humid forest zone are major threats. Whereas clearing inside the forest, which is especially prevalent in the northern parts of Mangalisa Forest may create some new edge habitats favoured by *N. skyei*, after a relatively short period of time village areas tend to become devoid of suitable trees or thickets, which are either cleared for firewood and/or slash-and-burn grazing. A landuse policy that implements a moderate use of burning, would support the maintenance of a patchwork of woodland and small evergreen thickets near the eastern fringe of the humid zone where human pressure is most intense. The northern Rubeho and Ukaguru Mountains appear to be more sparsely populated, probably due to their extensive stony plateaus with scattered bushes and tiny woodlots. These areas may act as a core refuge for *N. skyei*.



**Table 5.1.** Summary of the taxa for which mtDNA was analysed in this study. \*\*Refers to the locality of voucher specimens: FitzPatrick – Percy FitzPatrick Institute, University of Cape Town, ZMUC – Zoological Museum of the University of Copenhagen, FMNH – The Field Museum of Natural History, NMK – National Museums of Kenya and, RMCA – Royal Museum for Central Africa. For most blood samples a photographic slide of the bird is available.

Species		Sample No.	Locality	Tissue	Source**
<i>N. violacea</i>	<i>violacea</i>	Bred1	Overberg, South Africa	Muscle	FitzPatrick
<i>N. regia</i>	<i>kivuensis</i>	346631	Muramuya, Burundi	Muscle	FMNH
<i>N. preussi</i>	<i>preussi</i>	358155	Cibitoke, Burundi	Muscle	FMNH
<i>N. afra</i>	<i>afra</i>	Hack_Te	Hackerville, Southern Cape, South Africa	Muscle	FitzPatrick
<i>N. stuhlmanni</i>	<i>stuhlmanni</i>	356109	Mubuku Valley, Ruwenzori Mnts, Uganda	Muscle	FMNH
	<i>graueri</i> (1)	10067	Mt. Mahavura, Rwanda	Toe-pad	NMK
	<i>graueri</i> (2)	10065	Mt. Mahavura, Rwanda	Toe-pad	NMK
	<i>chapini</i> (1)	77-22-A-211	Mabono, Demo. Republic of Congo	Toe-pad	RMCA
	<i>chapini</i> (2)	8596	Kilumba, Demo. Republic of Congo	Toe-pad	RMCA
	<i>chapini</i> (3)	8906	Mt. Kabobo, Demo. Republic of Congo	Toe-pad	RMCA
<i>N. ludovicensis</i>	<i>ludovicensis</i>	225649	Huambo, Angola	Toe-pad	FMNH
	<i>whytei</i>	W40023	Nyika Plateau, Northern Malawi	Blood	FitzPatrick
<i>N. manoensis</i>	<i>manoensis</i>	28803	Mt. Selinda, Zimbabwe	Toe-pad	DMNH
	<i>pintoi</i> (1)	206336	Mzimba, Malawi	Toe-pad	FMNH
	<i>pintoi</i> (2)	206338	Chingola, Zambia	Toe-pad	FMNH

<i>N. chalybea</i>	<i>chalybea</i> (1)	Kirst3	Cape Town, South Africa	Muscle	FitzPatrick
	<i>chalybea</i> (2)	Gamoegas	Gomoegas, South Africa	Tissue	FitzPatrick
	<i>subalaris</i>	390160	Boston, South Africa	Tissue	FMNH
<i>N. mediocris</i>	<i>mediocris</i>	T43038	Mt. Kenya, Kenya	Blood	FitzPatrick
<i>N. usambaricus</i>	<i>usambaricus</i>	JK06-201099	Magamba, W. Usambara Mnts., Tanzania	Tissue	ZMUC
<i>N. fuelleborni</i>	<i>fuelleborni</i>	AF48719	Mount Namuli, Northern Mozambique	Blood	FitzPatrick
<i>N. moreaui</i>	<i>moreaui</i>	JF03-241197	Chonwe Forest, Uvidundu Mnts, Tanzania	Blood	ZMUC
<i>N. loveridgei</i>	<i>loveridgei</i>	O4088	Kimhandu, Uluguru Mnts., Tanzania	Muscle	ZMUC
<i>nova</i>	<i>skyei</i> (1)	93.056	Mafwemiro Forest, Rubeho Mnts., Tanzania	Muscle	ZMUC
<i>nova</i>	<i>skyei</i> (2)	93.057	Mafwemiro Forest, Rubeho Mnts., Tanzania	Muscle	ZMUC

**Table 5.2.** Independent t-tests comparing variation in nine morphological traits between male *whytei* and *skyei*.

Variable		<i>n</i>	mean	STD	<i>t</i>	df	<i>P</i> (2-tailed)
Wing-length	<i>whytei</i>	12	62.2	1.50	0.980	13	0.345
	<i>skyei</i>	3	61.3	0.29			
Bill-length	<i>whytei</i>	8	17.6	0.45	-1.724	9	0.119
	<i>skyei</i>	3	18.2	0.74			
Bill-width	<i>whytei</i>	7	3.3	0.17	1.280	8	0.236
	<i>skyei</i>	3	3.1	0.12			
Bill-height	<i>whytei</i>	8	2.8	0.18	-0.454	8	0.662
	<i>skyei</i>	2	2.8	0.13			
Max. Tail	<i>whytei</i>	12	50.2	2.78	3.381	13	0.005
	<i>skyei</i>	3	44.1	2.77			
Min. Tail	<i>whytei</i>	12	41.6	1.96	3.094	13	0.009
	<i>skyei</i>	3	37.7	1.90			
Tarsus	<i>whytei</i>	12	15.0	0.37	-3.435	13	0.004
	<i>skyei</i>	3	15.8	0.13			
Violet/Blue Band	<i>whytei</i>	12	4.4	0.54	-2.923	13	0.012
	<i>skyei</i>	3	5.4	0.15			
Scarlet Band	<i>whytei</i>	12	15.5	2.1	0.575	13	0.573
	<i>skyei</i>	3	14.8	1.4			

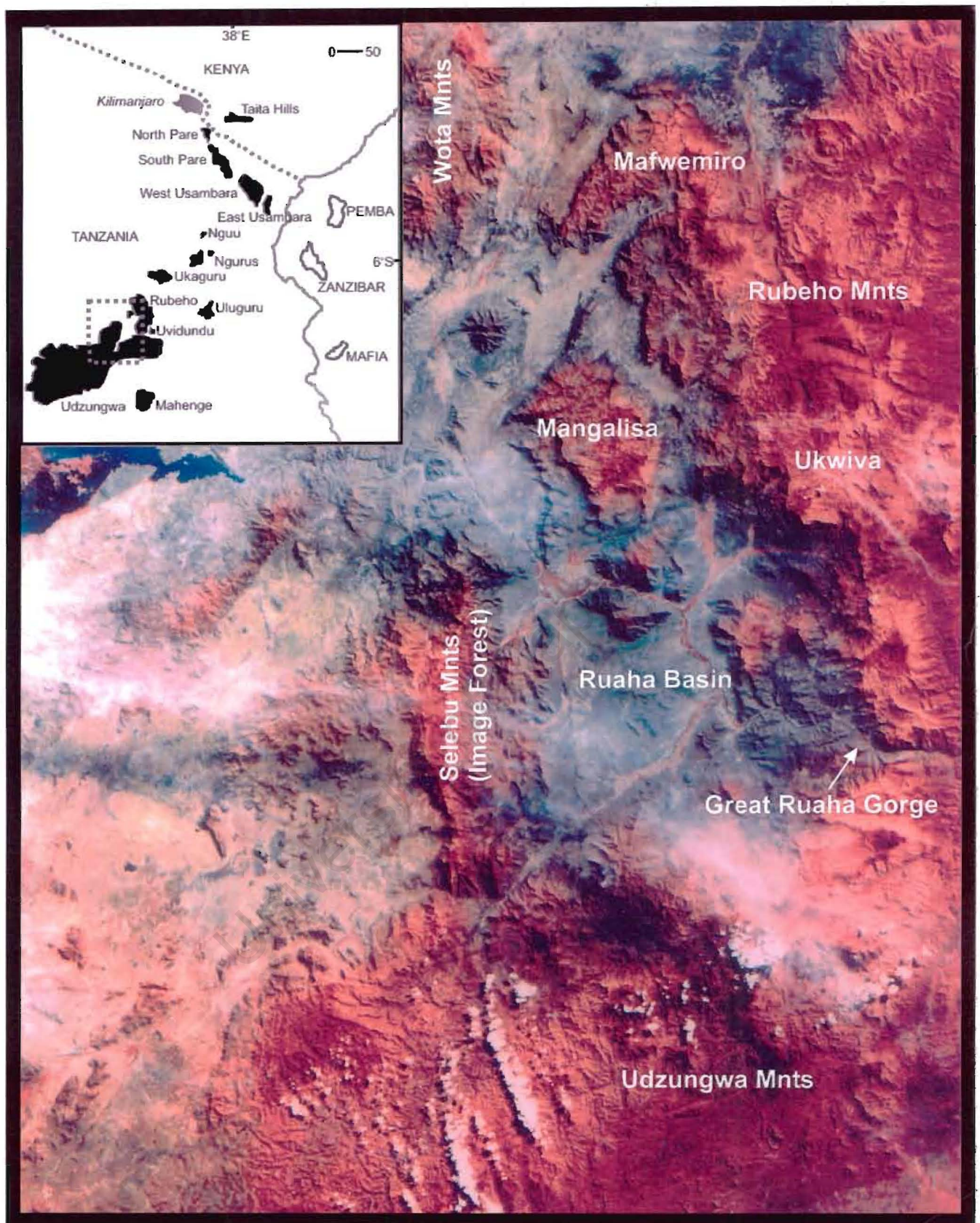


**FIG 5.1.** Sampling localities from which *skyei* has been collected to date in the Udzungwa and Rubeho Mountains of south-central Tanzania. On the satellite image montane forest is shaded reddish-brown.

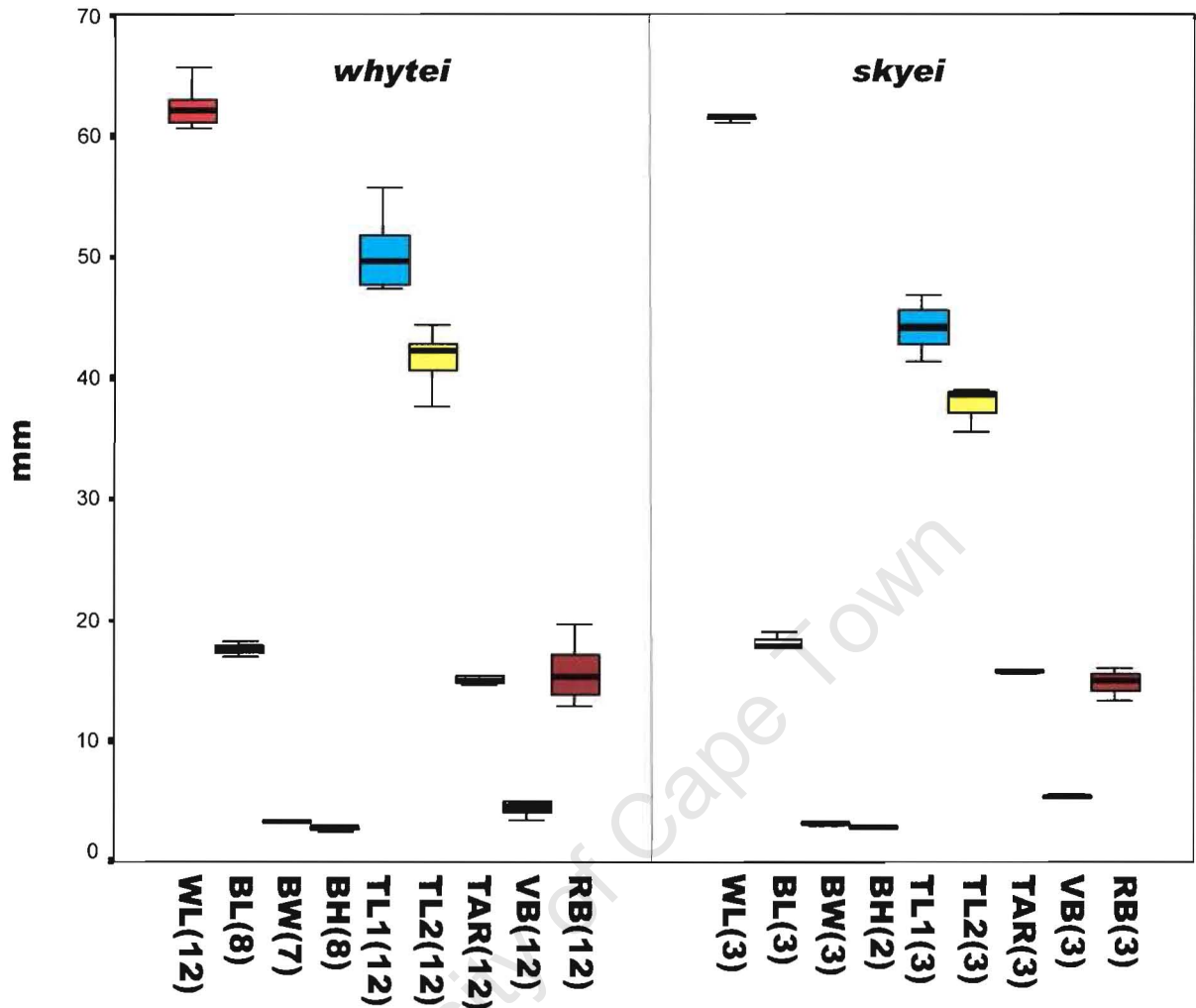


**FIG. 5.2.** Box plot (mean and standard deviation) summaries of the nine morphological measurements taken from male *whytei* and *skyei* specimens. Key: WL = wing-length, BL = bill-length, BW = bill-width, BH = bill-height, TL1 = max. tail-length, TL2 = min. tail-length, TAR = tarsus, VB = violet/blue upper breast band, RB = scarlet-red lower breast band. Numbers in parentheses refer to sample sizes.





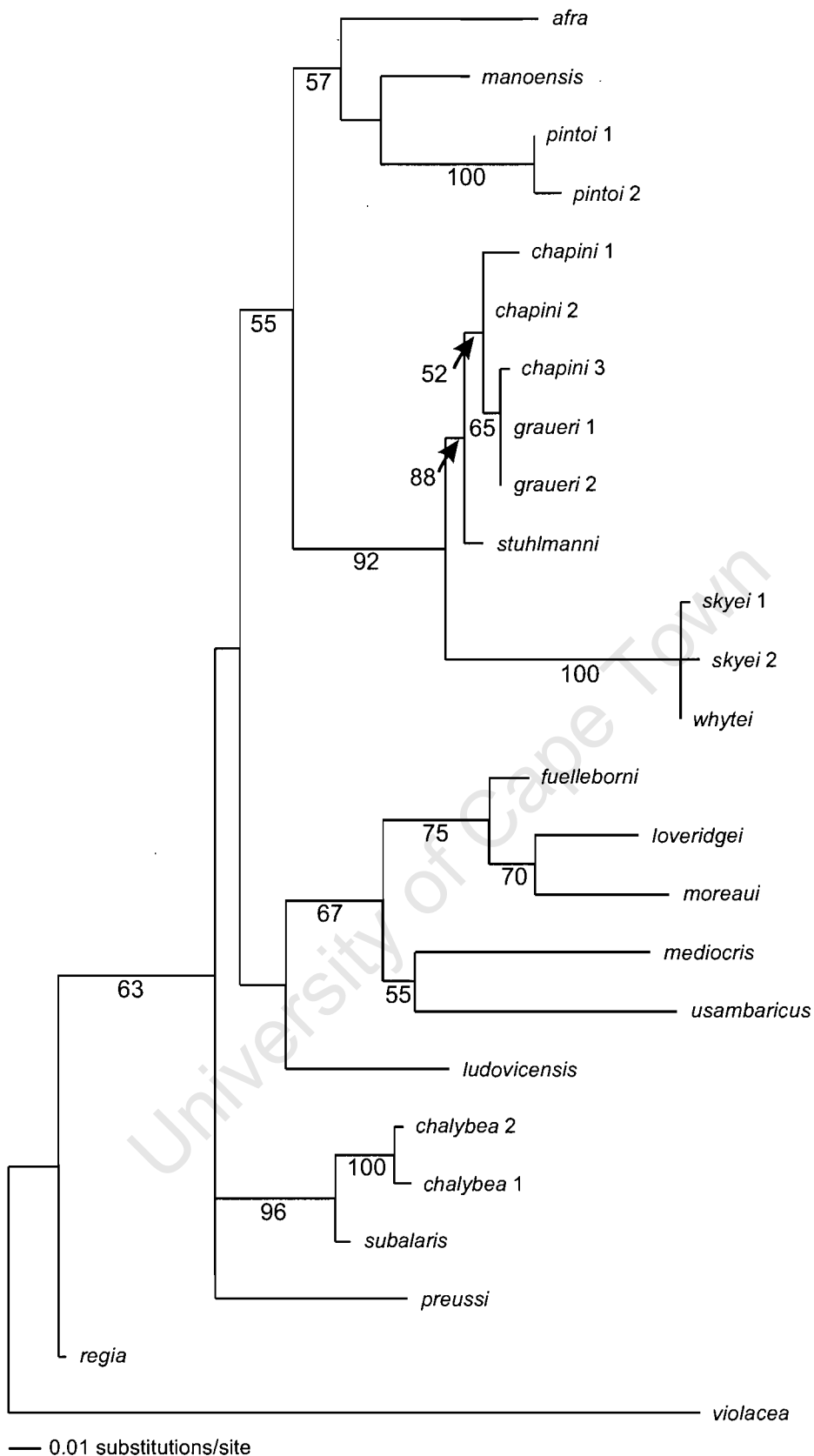


**FIG 5.4.** Phylogenetic relationships among members of the *N. afra* complex of Double-collared Sunbirds derived using maximum likelihood. A model of nucleotide substitution with invariable sites and equal rates among sites was used, and recovered one tree of length  $-\ln 1907.7$ . Branch lengths are proportional to the number of mutations along them. Values below branches are bootstrap values from 1000 replicates.

## Chapter 6

### The Karoo Thrush, *Turdus smithi* Bonaparte 1850, a southern African endemic

#### Summary

The Olive Thrush (*Turdus olivaceus*) species complex is characterized by striking geographical phenotypic variation. Recent consensus has been to recognise three assemblages (1) the *olivaceus* group restricted to southern Africa, (2) the *swynnertoni* group of the Zimbabwean and southern Malawi highlands and (3) the *abyssinicus* group of the montane highlands of eastern and central Africa. I re-examined the status of taxa in the *olivaceus* group of southern Africa, with specific reference to the central-western taxon *T. o. smithi* using both morphological and molecular evidence. Sequence divergence between *T. o. smithi* and other members of the *olivaceus* group averages 3.5% for the cytochrome-*b* gene and 4-4.5% for the NADH subunit 3 gene of the mitochondrial DNA. There is also both morphological (biometric and plumage) and molecular support for the recognition of *T. smithi* as a separate species', the common name of which we suggest should be, Karoo Thrush.

#### INTRODUCTION

The binomen *Turdus smithi* Bonaparte was proposed in 1850 to replace the pre-occupied *Merula obscura* Smith 1836, described from material collected in the interior of north-central South Africa towards the headwaters of the Orange River during Andrew Smith's exploratory expedition of 1834. Currently, the form is viewed as a well-differentiated subspecies of the widespread Olive Thrush *Turdus olivaceus* Linnaeus 1766, described from birds collected from the Cape of Good Hope, South Africa. *Turdus o. smithi* is one of five southern African forms recognised in *T. olivaceus*, following Clancey's (1982) revision. A sixth subspecies - the geographically remote *T. o. swynnertoni* Bannerman 1913: Chirinda Forest, Mt Selinda, Chipinga district, eastern Zimbabwe, is usually treated as part of *T. olivaceus*, but is assigned to a different assemblage, the 'swynnertoni' group. This assemblage extends from the Zimbabwean highlands



to central Malawi. Further north in Malawi and around the montane circle of central and eastern Africa birds are classified in the ‘*abyssinicus*’ group (Hall & Moreau 1970, Keith *et al.* 1992, Clement & Hathway 2000). The morphological gap separating the *olivaceus*, *swynnertoni* and *abyssinicus* assemblages remains a matter of uncertainty, the main difference seemingly being one of size.

In sharp contrast to other subspecies in the *T. olivaceus* complex, which are ecologically restricted to forest in southern and eastern Africa, *T. o. smithi* inhabits arid Karoo shrublands; especially riverine *Acacia* stands and associated scrubby growth. Its range extends from the Orange River basin of southern Namibia and northwestern South Africa, through the Karoo and country to its immediate east, i.e. into more mesic parts of the eastern continental plateau. In parts of its range, it has adapted well to life in parks and gardens. In the southern and eastern periphery of its range it impinges on its forest-based sister taxa, but with no evidence of either morphological intergradation or hybridization. In effect, *T. o. smithi*, with its type-locality Philippolis in the southwestern Free State (Macdonald 1957), is the most widely distributed subspecies of the Olive Thrush.

This chapter focuses on resolving relationships within the southern African taxa of the *T. olivaceus* complex, Hall and Moreau’s (1970) ‘*olivaceus*’ group. In an attempt to resolve the above relations use is made of DNA sequence data from two protein-coding regions of the mitochondrial genome (mtDNA), NADH dehydrogenase subunit 3 (ND3) and cytochrome-*b* (cytb). This is combined with a morphological and behavioural re-assessment of the taxonomic status of *T. o. smithi* relative to its southern African congeners.

## METHODS

### Morphometrics and Plumage

An unpublished dataset of plumage characters and measurements collected by Phillip Clancey from 103 birds derived from the collections of the Durban Natural Science Museum, the National Museum (Bloemfontein) and the East London Museum was analysed. In addition, locality records were noted from the Natural History Museum (Tring), United States National Museum and the Field

Museum of Natural History. Wing-length (flattened cord, from the carpal joint to the tip of the longest primary feather) and tail length (from the base of the pygostyle to the edge of the longest rectrix) were measured to the nearest 0.5mm using a wing-rule. Differences in univariate measures between species were tested using paired t-tests (Zar 1996). Plumage colours were matched to known colour standards (Ridgway 1912) to help objectively define colours across specimens. The localities of specimens examined are listed in Appendix 6.1.

### Population sampling for DNA analyses

The mtDNA data analysed in this chapter was generated in two different laboratories during independent studies and only combined at a later stage (Cytochrome-*b* data was provided by Dr Paulette Bloomer, Univ. of Pretoria). Hence, whereas localities are the same between data sets, individual birds are not necessarily so. For the ND3 data set, individuals were sampled from the following taxa and populations: *T. o. olivaceus*, Cape Town (1 individual), Grootvadersbosch Forest (1); *T. o. transvaalensis*, Dullstroom (2); *T. o. pondoensis*, Himeville (2), Boston, Natal (FMNH 390135 & 390136), *T. o. smithi*, Kimberley (MBM 5877, 7881 to 7883), Pretoria (1) and *T. o. abyssinicus* sampled from Kenya's Gatamaiyu (1) and Karuru Forests (1). For the cytochrome-*b* dataset: *T. o. olivaceus*, Cape Town (2), *T. o. transvaalensis*, Dullstroom (1); *T. o. pondoensis*, Himeville (1), *T. o. smithi*, Kimberley (1), Pretoria (1), Beaufort West (3) and *T. o. abyssinicus* sampled from Karuru Forest in Kenya (1). Both datasets were rooted using the Kurricane Thrush *T. libonyanus*, a basal member of the *T. olivaceus* complex (Keith *et al.* 1992).

### Laboratory procedures

DNA was extracted from frozen tissues or blood using either of two methods: (1) a Puregene DNA isolation kit (Gentra Systems, Minneapolis, Minnesota) following the manufacturer's animal tissue protocols, but with an overnight proteinase K digestion at 50°C, or (2) samples were digested overnight (50mM Tris, pH7.6, 100mM NaCl, 1mM EDTA, pH8.0, 0.5% SDS, 1mg/ml Proteinase K, 0.1g mg/ml RNase A) and purified using a phenol/chloroform/isoamylalcohol extraction, with the DNA precipitated overnight at -20 °C using 1/10 volume of 2M ammoniumacetate and 2.5 volumes

100% EtOH. Pellets were washed with 70% EtOH and DNA eluted in sterile distilled water.

The entire ND3 mtDNA gene (351bp) with flanking tRNAs (Glycine & Arginine) (395bp; F: 5'-GACTTCCAATCTTTAAAATCTGG-3'; R: 5'-GATTTGTTGAGCCGAAATCAAC-3') was PCR amplified using standard conditions (denaturation at 94°C, annealing at 50-52°C, and extension at 72°C). A 675bp portion of the 5' end of the mtDNA cytb gene was PCR amplified using primers L14990 (shortened L14841 of Kocher *et al.* 1989) and H15696 (H15547 of Edwards *et al.* 1991) using the conditions described in Ryan *et al.* (1998). PCR products were electrophoresed on 1.5% or 2% low-melting point agarose gels (FMC Bioproducts) stained with ethidium bromide and visualized under UV light. Amplicons of the appropriate length were cut out of the gel and purified using the GELase™ Agarose gel-Digesting Preparation and the 'fast protocol' method (Epicentre Technologies, Madison, Wisconsin) or the QIAEX I (Qiagen Inc.) gel extraction set.

Purified cytb PCR products were sequenced using four sequencing primers, L14990, H15696, L15245 (modification of CB4a-L of Palumbi *et al.* 1991) and H15245 (CBINT of Avise *et al.* 1994). Both the heavy and the light strands were sequenced using the T7 DNA polymerase (Sequenase version 2, United States Biochemical) and alpha 32P dATP labelling. Single stranded DNA was generated using streptavidin-coated Dynabeads (Dyna) and biotinylated external primers, electrophoresed on 6% polyacrylimide gels, transferred to Whatman paper and visualised on Hyperfilm-MP (Amersham) X-ray film. The purified ND3 PCR products were cycle-sequenced using Big Dye terminator chemistry (Applied Biosystems, Inc [ABI]) and the PCR primers. Cycle-sequencing reactions were precipitated with 3M ammonium acetate or 100% isopropanol, rinsed in ethanol, dried and re-suspended in formamide-EDTA solution and run on an ABI 377 or ABI 3100 automated DNA sequencer. Sequences were checked using the program Sequencher 3.0 (Gene Codes Corp), and aligned to the chicken (*Gallus gallus*) mtDNA sequence (Desjardins & Morais 1990) to test for the presence of any insertions or deletions.

### **Molecular analyses**

Sequence divergence distances between individuals were estimated for both ND3 and cytb using the Kimura-2-parameter model of nucleotide substitution in PAUP\*4.0b10 (Swofford 2002). Phylogenetic analyses of the DNA sequences were performed using two approaches: maximum parsimony (MP) and maximum likelihood (ML). Parsimony analyses, using PAUP\*4.0b10 (Swofford 2002) were conducted using the heuristic search option, implementing stepwise addition with 100 random addition replicates (Maddison 1991), or using the branch and bound search algorithm. Transitions often accumulate at higher rates than transversions; MP analyses were conducted under several transition: transversion (Ti:Tv) weighting schemes to evaluate the sensitivity of tree topology to possible positional saturation. The search parameters for all MP analyses were: all characters unordered, equal weighting, uninformative characters excluded, TBR branch swapping, steepest descent option not in effect, zero branch lengths collapsed to polytomy, MULPARS option in effect, and topological constraints not enforced.

Two methods of clade support were calculated in the MP analyses. Bootstrap support (Felsenstein 1985) was estimated using 1000 bootstrap replicates. Parsimony jackknife values were calculated for 1000 replicates and a cut point of 50%. Parsimony jackknife randomly removes approximately one-third of the characters, calculates the most parsimonious tree based on this smaller subset, repeating this procedure  $n$  (in this case 1000) times. Each clade is given a parsimony jackknife value, which represents the percentage of replicates in which the particular clade was recovered (Farris *et al.* 1996).

The data set was analysed using Modeltest 3.06b (Posada & Crandall 1998) to help ascertain the substitution model that best described the dataset. The parameters estimated from Modeltest were entered into PAUP\* 4.0b10 and attempts were made to establish if the model could be simplified by eliminating extraneous parameters. ML analyses were conducted using a full heuristic search with 100 random addition replicates and search parameters as described for the MP analyses. Clade support was estimated using 500 bootstrap replicates.

PAUP\*4.010b was used to compute partition homogeneity tests (1000 replicates with uninformative characters removed) to determine if data from the two genes suggested different phylogenetic signals.

## RESULTS

### Morphological considerations

Compared with nominate *T. o. olivaceus*, which is distributed to the immediate south of *T. o. smithi*, the latter was on average significantly larger for both wing and tail measurements (Table 6.1; wing:  $t_{0.05(2), 58} = 8.64$ ,  $P < 0.001$ , also significantly different for tail-length and for both measures from all the other taxa). However, there is nearly complete overlap, except with *T. o. transvaalensis* in both wing and tail measures. Thus, the biological significance of this size variation remains to be established. In plumage characters *T. o. smithi* differs widely from the other southern African subspecies (Table 6.1). This is described by Clancey (1982) as follows: "Dorsum somewhat browner, less greenish-grey than in nominate *T. olivaceus* (near hair brown, Ridgway 1912). Below: forethroat dusky (dark olive-drab), not white, the dark streaking finer; entire breast, sides and flanks about drab grey, the ventral orange much duller and restricted to the centre of the extreme lower breast and belly".

During the course of a re-examination of skins PAC ascertained that the populations lying to the northeast of those of the Karoo of the Cape Province are on the whole slightly differentiated over the ventral surfaces, having the ground of the throat whiter than in karroid birds, with rather heavier and darker shaft-streaking. The lower throat is also not quite so extensively invaded by drab from the breast, while the lower breast and belly in most eastern birds are distinctly less reddish and more buffy. The under tail-coverts are also more sharply wedged apically with buffish white. As a satisfactory delimitation of the ranges of the two could not be arrived at on the basis of the limited fresh eastern material available, PAC decided not to split the western and eastern populations, confining present consideration to an assessment of the possible specific status of *T. o. smithi*.

### Genotypic variation

A total of 1058bp were amplified; 383bp from the ND3 gene with flanking tRNAs - and 675bp from cytb. For ND3, 56 sites (15.96%) were variable, and 53 (15.10%) were parsimony informative. Within ND3, first, second and third positions varied greatly in their variability: 9 first position sites (16.07% of the variable sites), 7 second position sites (12.50%) and 40 third position sites (71.43%), were variable. Three sites (9.4%) were variable among the 32bp of tRNA sequenced. Of the 675bp of cytb sequenced, 88 sites (13.8%) were variable, and 65 (9.5%) were parsimony informative: 11 (1.6%) first, no second and 77 (11.41%) third positions were variable, and 8 (1.19%) first and 57 third (8.44%) positions were parsimony informative.

Sequence divergence between *T. o. smithi* and the other members of 'olivaceus' group ranged between 4.16-4.47% for ND3 and 3.38-3.54% for cytb (Table 6.2). Divergence values between *T. o. olivaceus*, *T. o. transvaalensis* and *T. o. pondoensis* were low for both ND3 (0.0 – 0.29%) and cytb (0.15 – 1.21%). Divergence values between members of the 'olivaceus' group and *T. o. abyssinicus* are over twice as large (ND3 Av = 9.63%, Cytb Av = 8.34%) as between the most divergent members within the 'olivaceus' group and similar to divergence values between *T. olivaceus* and the outgroup *T. libonyanus* (ND3 Av = 11.28%, Cytb Av = 8.42%; Table 6.2). There were no amino acid changes between *T. o. smithi* and other members of the 'olivaceus' group for cytb, but there were three amino acid changes between these taxa for ND3.

### Phylogenetic analyses

The partition-homogeneity-test (1000 replicates) between ND3 with flanking regions and cytb indicated that there is no significant difference in phylogenetic signal between the two mtDNA regions considered ( $P > 0.1$ ). The data sets were analysed independently as well as in combination.

Unweighted maximum parsimony analyses (MP) of the 17 individuals in the ND3 data set (56 parsimony informative characters) yielded one tree of 71 steps (CI = 0.859, RI = 0.933; Fig. 6.2). ML analyses using an HKY model of nuclear

substitution (for parameters see Table 6.3) recovered one tree of length  $-\ln 852.81$ , the topology of which is consistent with the MP tree (Fig. 6.2). Bootstrap and jackknife support is high in both the MP and ML analyses for *T. o. smithi* forming a clade, sister to the other southern African members of the ‘*olivaceus*’ group.

Unweighted MP analyses of the 12 individuals in the cytb data set (65 parsimony informative characters) yielded four equally short trees ( $L = 109$ ,  $CI = 0.853$ ,  $RI = 0.895$ ; Fig. 6.3, Table 6.3). These trees differed from each other with respect to relationships among individuals within *T. o. smithi*. ML analyses using an HKY + gamma + invariable sites model of nuclear substitution (for parameters see Table 6.3) recovered one tree of length  $-\ln 1446.64$ . The topology of the consensus MP tree and the ML tree was identical to that obtained for ND3 (Fig. 6.2), supporting a clear split between *T. o. smithi* and the remaining members of the ‘*olivaceus*’ group.

In combined analyses of both data sets (66 parsimony informative characters) yielded one MP tree ( $L = 173$ ,  $CI = 0.861$ ,  $RI = 0.747$ , Fig. 6.4, Table 6.3), as did the ML analyses ( $-\ln 2215.24$ , Table 6.3). The MP and ML tree topologies were identical and supported the results obtained in the independent dataset analyses (above). Weighted parsimony analyses that down-weighted transitions by empirical estimates for each gene region (21x for ND3 and 9x for cytb, Table 6.3) relative to transversions did not alter the topology obtained and only marginally changed the bootstrap and jackknife values obtained in either the ND3, cytb or combined analyses.

The main features of the above analyses are: (1) a sister relationship between *T. o. smithi* and the remaining members of the ‘*olivaceus*’ group of the Olive Thrush – *T. o. olivaceus*, *T. o. pondoensis* and *T. o. transvaalensis*, (2) a deep divergence between the ‘*olivaceus*’ and ‘*abyssinicus*’ assemblages within the Olive Thrush.

## DISCUSSION

### *Turdus smithi* as a southern African endemic?

Both morphological (plumage and morphometric data) and molecular data (1058bp of mtDNA) was collected to evaluate the taxonomic status of *smithi*. Body dimensions and plumage characters suggest *T. smithi* to be distinct. *Turdus smithi* is generally darker and duller than its forest congeners, which are more extensively orange-coloured mid-ventrally. Furthermore, the mtDNA sequence divergence data presented here provide a strong case for considering *T. smithi* to be a separate species and none of the haplotypes for either gene region identified in this study were found in nominate *T. olivaceus sensu lato*. This suggests that *T. smithi* may be reciprocally monophyletic with respect to *T. olivaceus*. In summary, although there is some overlap in body dimensions between *T. smithi* and *T. olivaceus sensu lato*, analysis of plumage characters and mtDNA haplotypes, supports the recognition of *T. smithi* as a species endemic to southern Africa.

### Range, ecological, behavioural and biogeographical considerations

Populations of *T. smithi* range from the mid- and lower reaches of the Great Fish River of Namibia (from about Mariental), south to the lower Olifants River and east to the Great Fish River of the eastern Cape, and the central and southern Transvaal (south of 24° 30' S., and to 29° 30' E.), and in the northern Cape to Barkley West and the lower Vaal River (Fig. 6.1). The range as broadly defined encompasses three major habitats recognized by Maclean (1985): desert, semi-desert and Karoo, with the average annual rainfall ranging from almost zero to *ca.* 500 mm. The species is well suited to the moderately mesic conditions provided by urban development, particularly in the east of the range, in contrast to populations at the mouth of the Orange River in the southern Namib (as at Brandkaros and Alexander Bay), which occupy desert.

To the south and east, *T. smithi* is replaced in areas supporting evergreen forest and nowadays commercial *Eucalyptus* plantations and gardens by four subspecies: nominate *T. o. olivaceus*, *T. o. culminans*, *T. o. transvaalensis* and in eastern Natal *T. o. pondoensis* (Fig 6.1). All four of the subspecies differ from *T.*



*smithi* in having a whiter and more heavily streaked forethroat and with the mid-ventral plane more extensively and brighter orange-buff (Clancey 1982).

*Turdus smithi* fills a close comparable role to the Blackbird, *Turdus merula* (basically a forest thrush) in western Europe, feeding terrestrially, often fully exposed to view, along the moist banks of irrigation furrows and the edges of shrubberies in gardens. Unlike the contiguous forest forms, it is moderately gregarious and less shy. Hockey *et al.* (1989) have drawn attention to its communal roosting behaviour, as observed in the Calvinia district in the far western Cape.

In the western Cape, Olive Thrushes, including *T. smithi*, breed almost throughout the year, records peaking from August to November. In the case of Transvaal birds, which also include elements of *T. smithi*, such nest from August through to March, with their peak from September to January (Kemp *et al.* 1985). *Turdus smithi* appears to be sedentary as no specimens applicable to it were found in museum collections from beyond the limits determined for it.

A re-examination of a reasonably comprehensive panel of specimens collected since the early 1950s failed to detect any evidence of direct hybridization between *T. smithi* and its parapatric congeners (*T. o. olivaceus*, *T. o. culminans* and *T. o. transvaalensis*); though the finding of typical examples of nominate *T. o. olivaceus* from the interior of the eastern Cape (Campher's Poort, Steytlerville, 25 Sept. 1954; Rust en Vrede, 9 Sept. 1965; Cradock, 18 April 1955; Murraysburg, 14 Nov. 1956), and of *T. o. transvaalensis* in the Orange Free State (Kirkenberg, at 28° 27' S. 29° 15' E. dated 18 Nov. 1976) does suggest that these forest-edge taxa are capable of spreading at the expense of *T. smithi* into habitats, such as gardens, orchards and commercial timber plantations. Such expansion is seemingly an outcome of the local introduction of suitable habitat resulting from the spread of European-style urbanization and agricultural methods since early colonial times.

## CONCLUSIONS

Both morphological (plumage and morphometric data) and molecular data (1058bp of mtDNA) suggest that *smithi* warrants specific status. Furthermore, none of the haplotypes for either gene region identified in this study were found in nominate *T. olivaceus sensu lato* and PAC failed to find any evidence of intergradation or hybridization between *T. smithi* and *T. olivaceus* in the specimens he examined. Body dimensions and plumage characters (Table 6.1) also support the distinctiveness of *T. smithi*. Since the core of this species' range encompasses the Karoo Biome, we suggest that the common name of this southern African endemic bird be the Karoo Thrush.

University of Cape Town

**Table 6.1.** Plumage and morphological characters of the ‘*olivaceus*’ assemblage of the Olive Thrush *Turdus olivaceus*. Plumage colours were matched to known colour standards (Ridgway 1912).

Plumage		Wings		Tail
<i>smithi</i>	Upperparts browner, less greenish-grey than in nominate <i>T. olivaceus</i> . Below, forethroat dusky not white, with finer dark streaking. Upper and mid-breast, sides and flanks drab grey, the ventral orange is duller and restricted to the extreme lower breast and belly. Vent is light orange and the eye-ring is pale yellow.	<i>n</i>	33	27
		Range	119-133	92.5-102
		Mean	124.4	96.5
		SD	3.32	2.43
<i>olivaceus</i>	Upper-parts greyish Chaetura Drab. Below, forethroat is white, heavily streaked with black; breast olivaceous-buff with grey overlay; lower ventral surface pale olivaceous-orange, the flanks are washed with olive. Vent is white to pale orange and the eye-ring is bring orange.	<i>n</i>	27	27
		Range	120-128	87.5-103
		Mean	123.7	93.7
		SD	2.40	3.00
<i>pondoensis</i>	Differs from <i>T. o. olivaceus</i> in having the entire upperside, wings and tail suffused with brownish olive. On the underside the breast is darker and the rest of ventral surface is deeper and more saturated with orange (mars yellow).	<i>n</i>	16	16
		Range	125-133	90-104.5
		Mean	129.4	97.5
		SD	2.49	3.68
<i>culminas</i>	Differs from <i>T. o. pondoensis</i> in lacking the olive wash to the upper-parts, wings and tail and is like <i>T. o. olivaceus</i> in this regard. Below, the breast is darker with the orange of mid-venter deeper and less bright.	<i>n</i>	11	11
		Range	128-140	93.5-105
		Mean	133.4	99
		SD	3.76	4.18
<i>transvaalensis</i>	Upper-parts are tinged with olive, and on the ventral the orange is distinctly more ochreous and less reddish or brownish.	<i>n</i>	8	8
		Range	110.5-118	80-87.5
		Mean	114.4	84
		SD	3.25	2.41

**Table 6.2.** Pairwise estimates of Kimura-2 parameter nucleotide sequence divergence (%) between taxa within the ‘*olivaceus*’ assemblage of the Olive Thrush *Turdus olivaceus*. Values above the diagonal are sequence divergence values for cytb and below the diagonal for ND3.

	<i>olivaceus</i>	<i>pondoensis</i>	<i>transvaalensis</i>	<i>smithi</i> Pretoria	<i>smithi</i> Kimberley	<i>abyssinicus</i>	<i>libonyanus</i>
<i>olivaceus</i>		1.05	1.21	3.54	3.54	8.86	8.98
<i>pondoensis</i>	0.00		0.15	3.38	3.38	8.32	8.26
<i>transvaalensis</i>	0.29	0.00		3.53	3.53	8.13	8.07
<i>smithi</i> Pretoria	4.47	4.16	4.16		0.60	8.49	8.24
<i>smithi</i> Kimberley	4.16	3.85	3.85	0.29		8.14	8.59
<i>abyssinicus</i>	9.98	9.63	9.63	9.63	9.29		8.39
<i>libonyanus</i>	10.99	11.34	11.34	10.99	11.34	11.67	

**Table 6.3.** Molecular characterization of the mitochondrial genes analysed in this study. Total data set is the whole of NADH Dehydrogenase Subunit 3 (351bp, ND3), the first 675bp of cytochrome-*b* and 8bp of tRNA-Glycine and 24bp of tRNA-Arginine. \* Designates categories for which values were calculated using the program Modeltest 3.06 (Pasada & Crandall 1998).

	ND3	cytb	Total data set
<b>Nucleotide Composition*</b>			
A	27.73%	27.95%	27.67%
C	33.67%	34.49%	34.53%
G	15.43%	14.80%	14.94%
T	23.17%	22.76%	22.86%
<b>Variable Sites</b>			
	59 (16.8%)	88 (13.8%)	142 (13.4%)
<b>Parsimony Informative Sites</b>			
	56 (15.9%)	65 (9.5%)	66 (6.3%)
<b>Ts/Tv Ratio*</b>			
	21.13	9.23	31.54
<b>Alpha Value*</b>			
	Equal rates	Equal rates	Equal rates
<b>Proportion of Invariable Sites*</b>			
	0	0.81	0.83

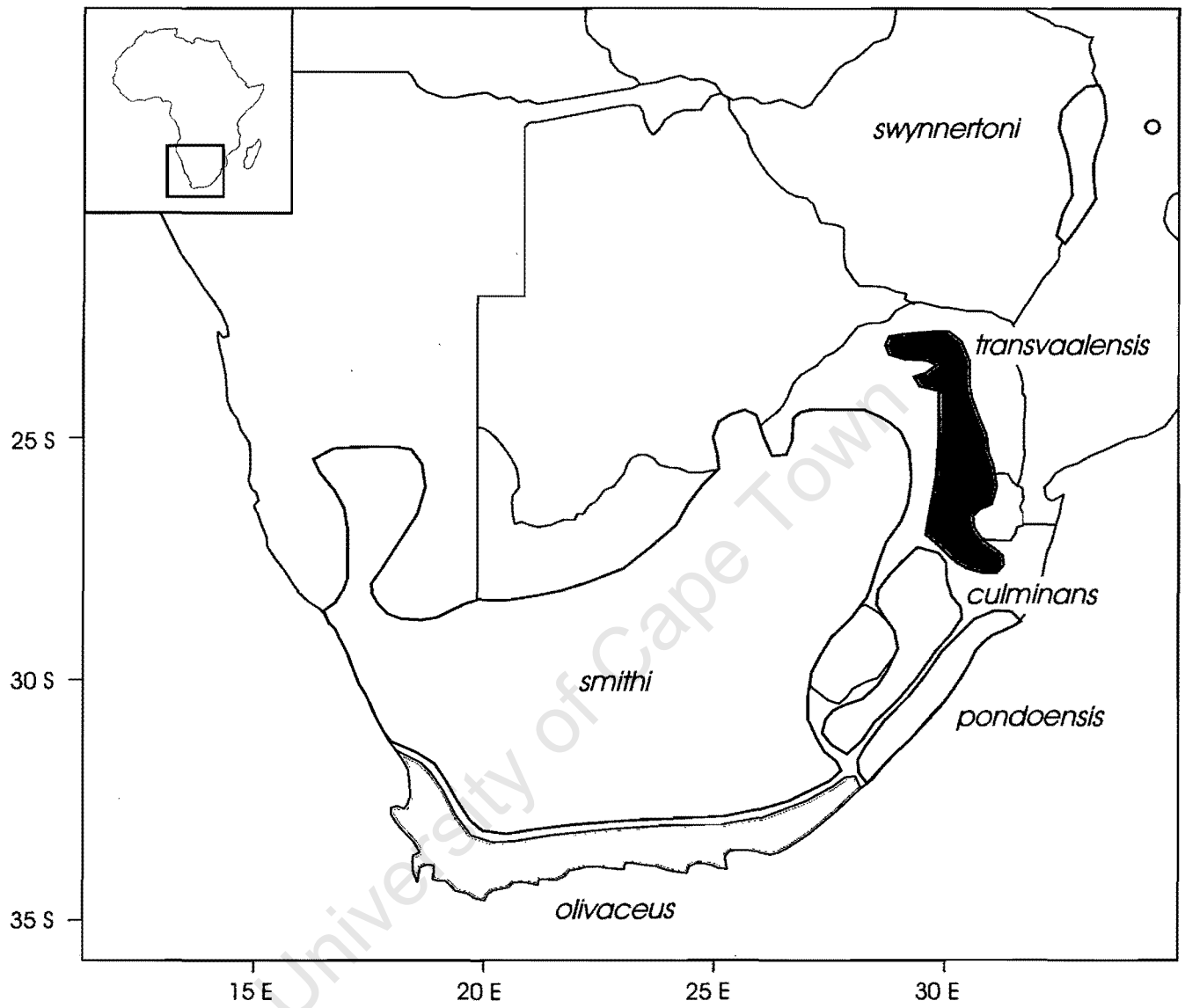


**FIG 6.1.** Distribution ranges of the southern African subspecies of Olive Thrush *Turdus olivaceus*.

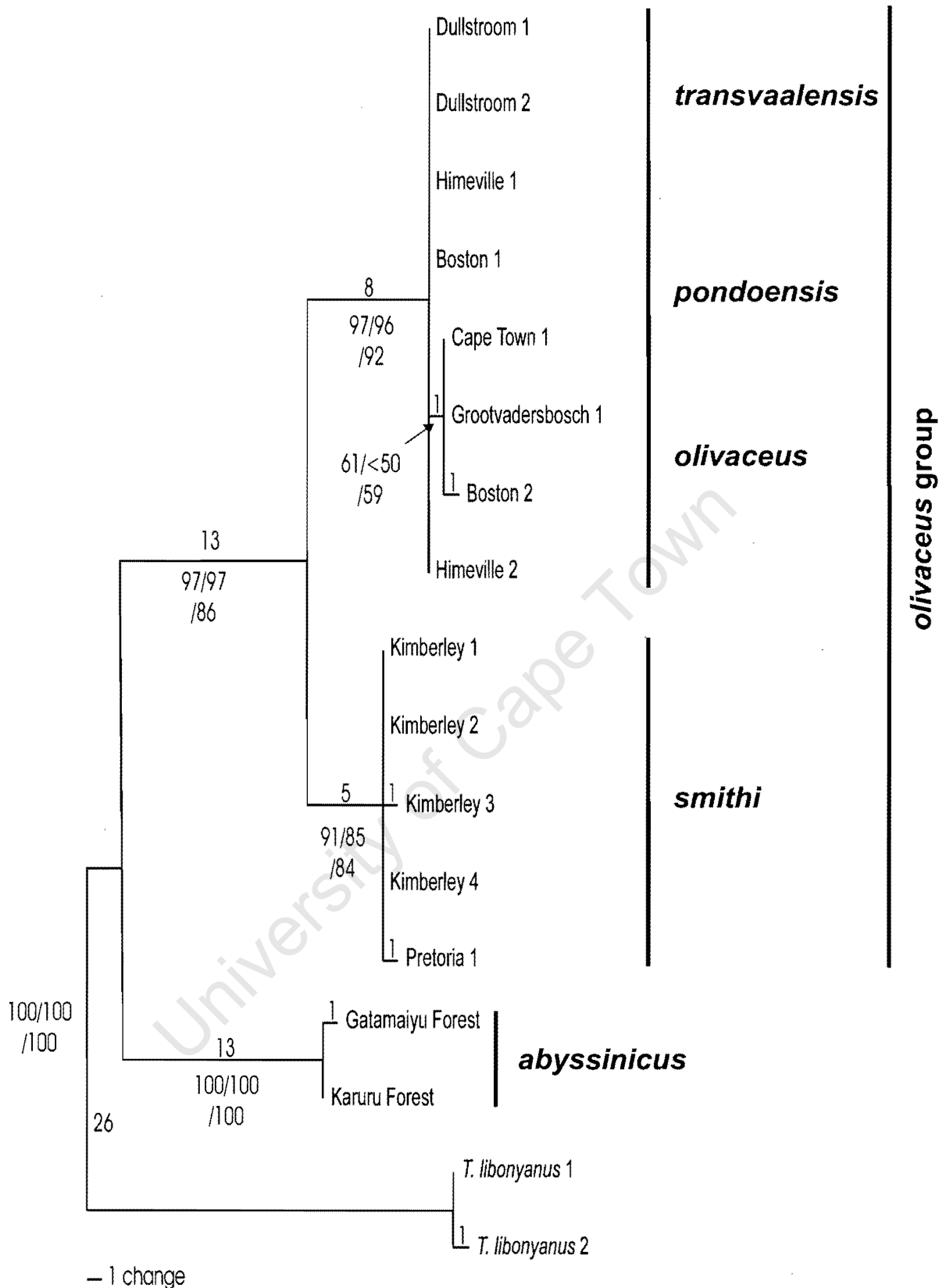


**FIG 6.2.** Phylogeny of members of the '*olivaceus*' assemblage of the Olive Thrush *Turdus olivaceus* using 383bp of ND3 and associated tRNA flanking regions. Maximum Parsimony analyses yielded 1 tree of length 71 depicted here. Maximum Likelihood analyses using an HKY model of nucleotide substitution yielded a tree score of -ln825.81 and, retained the topology of the MP tree. Numbers above branches are node lengths, below branches are bootstrap and jackknife values from 1000 iterations of a MP run, followed by a third value from 500 bootstrap iterations of a ML run.

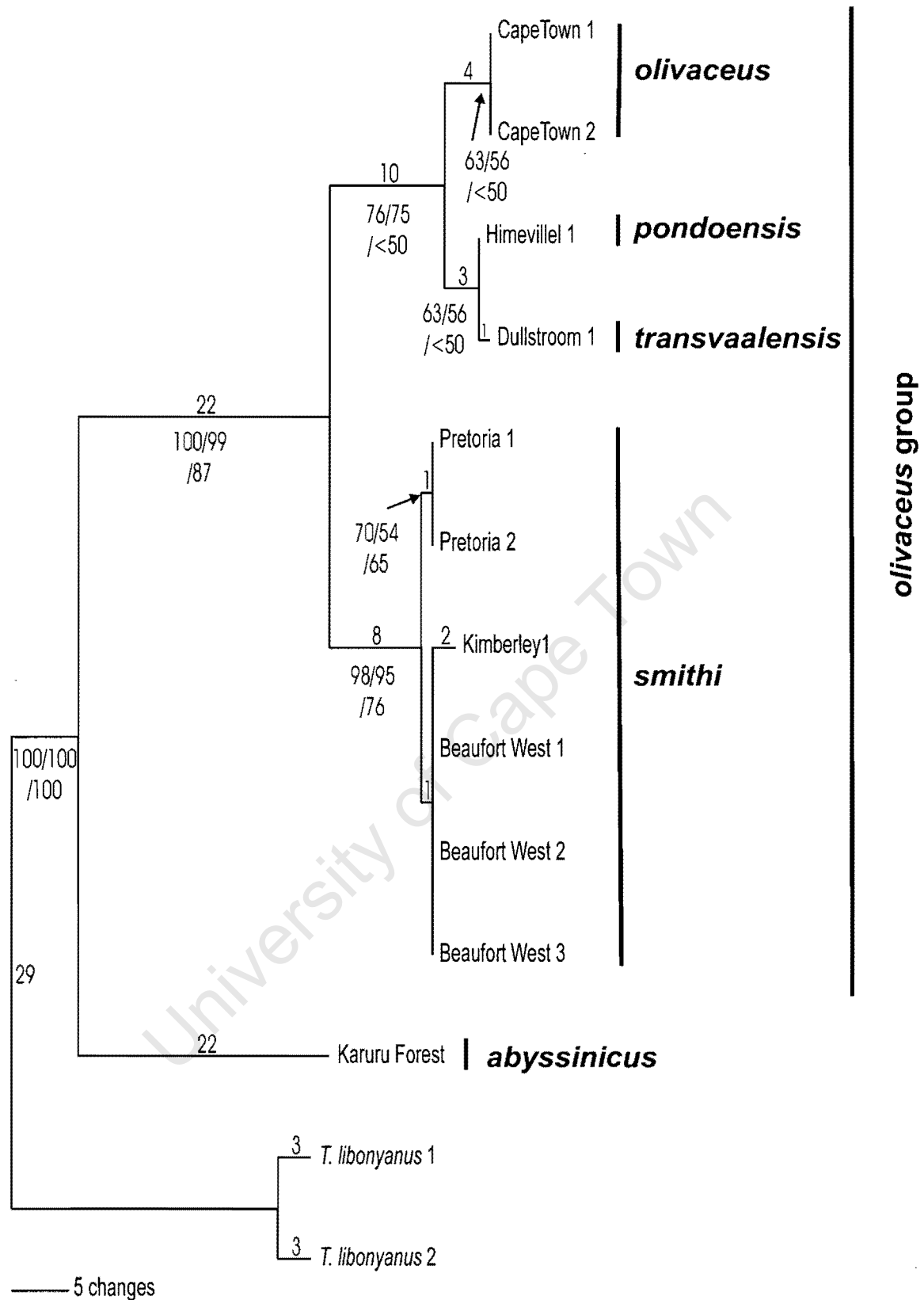


**FIG 6.3.** Phylogeny of members of the 'olivaceus' assemblage of the Olive Thrush *Turdus olivaceus* using 675bp of cytb. Maximum Parsimony analyses yielded 4 trees of length 109, one of which is depicted here. Maximum Likelihood analyses using an HKY + I + Gamma model of nucleotide substitution yielded a tree score of -ln1446.64 and, retained the topology of the strict consensus MP tree. Numbers above branches are node lengths, below branches are bootstrap and jackknife values from 1000 iterations of a MP run, followed by a third value from 500 bootstrap iterations of a ML run.



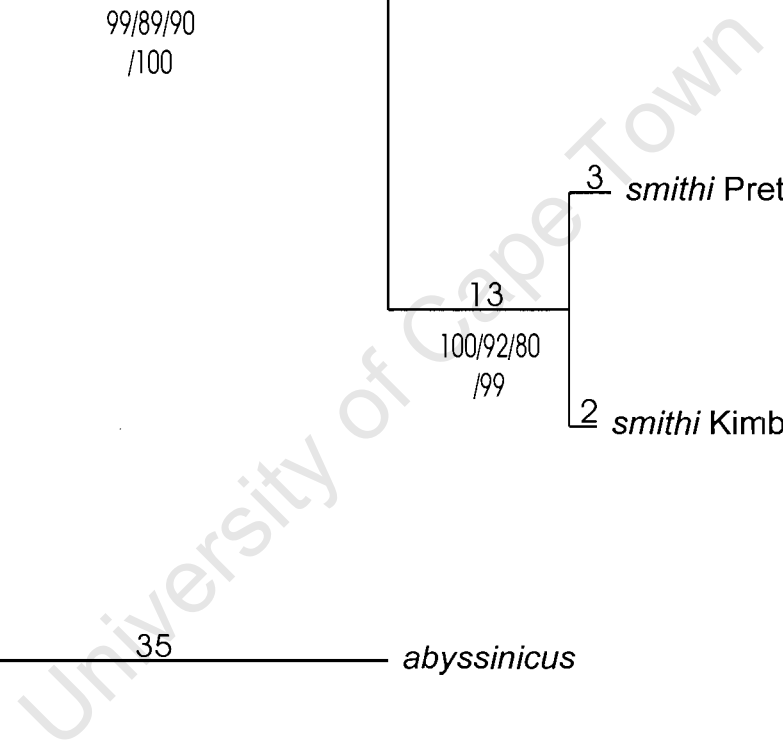


**FIG 6.4.** Phylogeny of members of the '*olivaceus*' assemblage of the Olive Thrush *Turdus olivaceus* using the combined ND3 and cytb dataset (1058bp). Maximum parsimony analyses yielded 1 tree (length 173 steps), as did the maximum likelihood analyses. Numbers above branches are node lengths, below branches are bootstrap values from 1000 iterations of a MP run under equal weighted and empirically estimated Ti/Tv weighting scheme for ND3 and cytb respectively (Table 6.3), followed by a fourth bootstrap value from 1000 iterations of a ML run.

**APPENDIX 6.1:** localities of specimens examined for *Turdus smithi* and co-occurring congeners

*Turdus smithi*

Alexander Bay, Brandkaros at the Orange River mouth, Garies, Karos Upington, Kuboes Richtersveld, Groblershoop, Pretoria, Prieska, Viools Drift on the lower Orange River, Vanrhynspas, Barkley West, Aliwal North, Steynsburg, Murraysburg, Sevenweekspoort near Laingsburg, Georgida, Willowmore, Cradock, Riverton, Vaal River north of Kimberley, 17km west of Aliwal North, Danebury, Dordrecht, Glen, Ladybrand, Nova (29° 14' S. 27° 22'E.), Pinekloof, Koppieskraal (28° 30' S. 27° 30' E.), Oranjekrag Orange River, Bloemfontein, Bishop's Glen.

*Turdus olivaceus olivaceus* from within the range of *T. smithi*

Cradock 18 April, 1955

Murrayburg 14 November, 1956

Rust en Vrede 9 September, 1965

Campher's Poort, Steytlerville 25 September, 1954.

*Turdus olivaceus transvaalensis* from within range of *T. smithi*

Kirkenberg 28° 27' S. 20° 15' E. 18 November, 1976.

## INTRODUCTION

For the best part of 40 years confusion has characterized the taxonomy of African thrushes in the genus *Turdus*. In particular, widespread disagreement has centred on the taxonomic status and species boundaries of the *Turdus olivaceus* species complex. Thrushes within this complex are characterised by having grey or olive-grey backs, underparts with varying amounts of matt orange, olive-grey and white, and streaking on the throat. Ripley (1964) recognised two species, the Northern Olive Thrush (*T. abyssinicus*) and the Southern Olive Thrush (*T. olivaceus*). Hall and Moreau (1970) retained Ripley's subspecific taxa, but lumped Southern and Northern Olive Thrush into one form (*T. olivaceus*), and reclassified some subspecies within the African Thrush (*T. pelios*). Hall and Moreau (1970) further included these two taxa in a superspecies with the Kurrucane Thrush (*T. libonyanus*), Bare-eyed Thrush (*T. tephronotus*) and the island dwelling Comoro (*T. bewsheri*) and the Gulf of Guinea Thrushs (*T. olivaceofuscus*) (Fig. 7.1). This means that the superspecies concept is extended to include not only geographically isolated representatives, but also some forms that are essentially sympatric, although segregated into different altitudinal zones.

*Turdus tephronotus* occupies coastal and semi-arid bushveld and scrub; *T. libonyanus*, Miombo woodlands in regions where 'olivaceus' inhabits evergreen forest at higher altitude. Based on the discovery that *T. pelios* has a continuous type of song with a short repetitive motif, quite unlike the brief rhythmical phrases of *T. olivaceus*, Dowsett and Dowsett-Lemaire (1980) suggested that *T. pelios* be considered a full species. Further, evidence supporting this suggestion is that *T. pelios* (with five subspecies; Clement & Hathway 2000) is confined to lowland evergreen forest (except on Mount Cameroon), and *T. olivaceus* to montane (high-altitude) rainforest, only invading drier country in western South Africa (Keith & Urban 1992, Dowsett & Dowsett-Lemaire 1993, Keith *et al.* 1997, Clement & Hathway 2000).

Recent taxonomic treatments of African thrushes (Sibley & Monroe 1990, Keith & Urban 1992, Dowsett & Dowsett-Lemaire 1993, Keith *et al.* 1997, Clement & Hathway 2000), have adopted the species boundaries suggested by Hall and

Moreau (1970) for *T. olivaceus* and *T. pelios*. Hall and Moreau (1970) used plumage characters to divide montane thrush populations into three groups: (1) the ‘*olivaceus*’ group in South Africa, characterized by underparts that are rich in orange with a slight olive-grey wash on the breast, and a white throat with well marked streaking; they include *smithi*, which extends into the drier parts of central and western South Africa, and has grey underparts and a dusky throat; (2) the ‘*swynnertoni*’ group extending from Zimbabwe to southern Malawi, which are similar to ‘*olivaceus*’, but are smaller and have a darker bill and; (3) the ‘*abyssinicus*’ group extending from northern Malawi through the Albertine Rift, Eastern Arc Mountains and the highlands of Kenyan and Ethiopia, characterised by having an olive-grey throat and breast (not white) with the rest of the underparts orange with some white around the vent.

Although most authors accept the taxonomic recommendations of Hall and Moreau (1970) in a broad sense, much debate has centred on the taxonomic status of thrush populations occupying the mountains on the Kenya-Tanzania border (Fig. 7.1). Most controversial is *helleri*, the Taita Thrush, classified as a globally, critically-endangered taxon by Birdlife International (Collar *et al.* 1994, Birdlife International 2000). This is (after the Somali Blackbird, *ludoviciae*) phenetically the most distinctive taxon among the montane forms of the ‘*abyssinicus*’ group, with a blackish head, dark grey breast and the remainder of the under-parts white, flanked in orange. Hall and Moreau (1970), Sibley and Monroe (1990), Keith and Urban (1992), Dowsett and Dowsett-Lemaire (1993), Keith *et al.* (1997) and Clement & Hathway (2000), all recognise the Taita Thrush as sub-specifically distinct, but include it within *T. olivaceus*. This is due to the existence of a ‘linking’ (clinal) taxon *roehli*, in the Pare and Usambara Mountains in northern Tanzania, which is duller and more olive than *helleri*, and forms a ‘clear link’ (Keith & Urban 1992; Dowsett & Dowsett-Lemarie 1993) between *helleri* and other neighbouring populations of the ‘*abyssinicus*’ group. Keith and Urban (1992) note that both taxa have orange underwing-coverts, otherwise a feature characterizing the austral ‘*olivaceus*’ group, and regard *helleri* and *roehli* as dull-coloured members of that complex.

The lumping of *helleri* in *olivaceus* has not found universal acceptance. Collar and Stuart (1985), Collar *et al.* (1994), Brooks *et al.* (1998a, b), Bennun and Njoroge (1999), Zimmerman *et al.* (1999), Galbusera *et al.* (2000), Birdlife International (2000), and Stevenson and Fanshawe (2002) have persisted with the recognition of *helleri* as a full species based on its distinct morphology, and have emphasised the need for immediate conservation action to be taken, due to its isolated distribution within the Taita Hills.

I investigate the phylogenetic relationships of taxa within the *T. olivaceus* species complex in an attempt to resolve some of the controversy surrounding species boundaries, particularly with respect the endangered Taita Thrush (*helleri*). Nucleotide sequence data from the NADH dehydrogenase subunit 3 gene (ND3) of the mitochondrial genome is used to help ascertain the phylogenetic relationships among the 15 taxa included in this study.

## METHODS

### Collection of samples

A total of 62 individuals from 15 taxa and 34 populations were analysed in this study. Unfortunately it was not possible to collect samples from the southern Albertine, Rukwa and Nyasa Rift areas, the crater highlands in Tanzania, or from Zimbabwe. Taxa collected, population localities, and institutions holding vouchers are listed in Table 7.1. The entire *T. olivaceus* complex was rooted on *Pogonocichla stellata* a member of the Muscicapinae, and two genera of the Sturnidae, *Lamprotornis* and *Onychognathus*, which together with the Mimidae are the sister group to the Turdidae (Sibley & Ahlquist 1990, Barker *et al.* 2002).

### Laboratory procedures

The same methods of DNA extraction and PCR amplification of the mitochondrial NADH subunit 3 gene with flanking tRNAs (Glycine and Arginine) as described in Chapter 3 were employed. PCR products were electrophoresed on 1.5% low-melting point agarose gels (FMC Bioproducts), stained with ethidium bromide and visualized under UV light. Amplicons of the appropriate length were cut out of the gel and purified using the GELase™

Agarose gel-Digesting Preparation and the 'fast protocol' method (Epicentre Technologies, Madison, Wisconsin). The purified products were cycle-sequenced using Big Dye terminator chemistry (Applied Biosystems, Inc [ABI]). Cycle-sequencing reactions were precipitated with 3M ammonium acetate or 100% isopropanol, rinsed in ethanol, dried and re-suspended in formamide-EDTA solution, and run on an ABI 377 or ABI 3100 automated DNA sequencer. Sequences were obtained from both strands of DNA for each individual, and some individuals were sequenced several times if any base ambiguity was encountered. All sequences were checked using the program Sequencher 3.0 (Gene Codes Corp) and aligned to the chicken (*Gallus gallus*) mtDNA sequence (Desjardins & Morais 1990) to test for the presence of any insertions or deletions, as well as to check that not stop-codons were present.

### **Phylogenetic analyses**

Parsimony analyses were conducted in PAUP\*4.0b10 (Swofford 2002) using a heuristic search, implementing stepwise addition with 1000 random addition replicates, and TBR branch-swapping. Because transitions often accumulate at higher rates than transversions, MP analyses were conducted under several heuristic and empirical 3<sup>rd</sup> position transition:transversion (ts:tv) weighting schemes to evaluate the sensitivity of tree topology to saturation. Two methods of clade support were calculated in the MP analyses. Bootstrap support (Felsenstein 1985) was estimated using 1000 bootstrap replicates. Parsimony jackknife (Farris *et al.* 1996) values were calculated for 1000 replicates, with one-third of the characters removed during each iteration. The dataset was analysed using Modeltest 3.06b (Posada & Crandall 1998) to help ascertain the substitution model that best described the dataset. The models of nucleotide substitution identified were incorporated in PAUP\* 4.0b10 for ML analyses using a full heuristic search with 100 random addition and TBR branch-swapping. Clade support was estimated using 50 bootstrap replicates.

Mr Bayes 2.01a (Huelsenbeck & Ronquist 2001) was used to conduct a Bayesian approach to phylogenetic inference. Four Metropolis-coupled MCMC chains (one cold and three heated chains) were run simultaneously to optimise efforts to find peaks in tree-space. To check that the log-likelihood distribution had

become stationary, the fluctuating value of the log-likelihood was graphically monitored. This search strategy was repeated six times (four runs of 1 million generations and two runs of 2 million generations), with each run beginning from a random tree. The General-time-reversible model of nucleotide substitution with gamma and proportion of invariable sites (GTR + I +  $\Gamma$ ) was used in the Bayesian analyses. A Dirichlet distribution was assumed for estimation of the base frequency parameters, and an uninformative (flat) prior was used for the topology. Trees were sampled every 50 generations, resulting in a sample of 20000 or 40000 for the 1 million and 2 million generation runs, respectively. The number of cycles to discard (the burn-in) was estimated empirically from the log-likelihood plots.

## RESULTS

### Sequence variation

Of the 383 base pairs (bp) sequenced, 139 sites (36.2%) were variable and 94 (24.5%) parsimony informative. Within ND3; 26 first position sites (19.2% of the variable sites), 17 second position sites (12.6%) and 92 third position sites (68.1%), were variable. Four (12.5%) sites were variable among the 32bp of tRNA sequenced. Excluding the outgroup taxa, the two starling genera (*Lamprotornis* & *Onychognathus*) and the muscicapid *Pogonocichla*, 87 sites (22.7%) were variable (15 first, 9 second & 63 third), and 80 (20.9%) of these were parsimony informative (12 first, 9 second & 59 third).

The three outgroup taxa all differed from members of the *T. olivaceus* complex by 16-22% sequence divergence. Within the *T. olivaceus* complex, *T. bewsheri* and *T. libonyanus* were on average, most divergent from other members of the complex (8-11%), but differed from each other by *ca* 6%. *Turdus olivaceofuscus* was well separated from all remaining members of the complex (6.5-9.5%), and approximately equidistant in divergence between the Olive Thrush '*olivaceus*' group and *T. pelios* (Table 7.2). Both the *olivaceus* and *abyssinicus* groups of the Olive Thrush sampled were 8.5-10% divergent from African Thrush, and 9-10% from each other. Sequence divergence within each of the '*olivaceus*' and '*abyssinicus*' groups was pronounced (Table 7.2), with the Taita Thrush differing

from other members of the *abyssinicus* group by 3-4.5%. Little or no variation existed between *olivaceus*, *pondoensis* and *transvaalensis*, or *abyssinicus*, *baraka* and *bambusicola* (Table 7.2).

### Phylogenetic analyses

Maximum Parsimony (MP) analyses of the unweighted data resulted in 36 most parsimonious trees (Length 291, CI = 0.608, RI = 0.887, topology as in Fig. 7.2). These trees varied primarily in the position of individuals within terminal taxa, with two exceptions. Firstly, in 30 of the 36 MP trees (83%), individuals from the southern Eastern Arc Mountains (*nyikae*) formed a clade basal relative to the birds from the Kenyan highlands (*abyssinicus*) and northern Albertine rift (*baraka* and *bambusicola*). Second, in 24 of 36 MP trees (67%) the birds from the Taita Hills (*helleri*) split into two clades. The first clade containing birds from the Taita Hills fragments Ngangao and Chawia, and the second birds from the largest fragment of remaining vegetation Mbololo (Taita 45-47 in Fig. 7.2).

Thrushes from the Taita Hills (*helleri*) and West Usambara Mountains (*roehli*) formed reciprocally monophyletic clades, both supported with high bootstrap (*helleri* 85%, *roehli* 99%) and jackknife support (*helleri* 81%, *roehli* 93%; Fig. 7.2). The relationship among thrushes from the crown clade *abyssinicus*, *nyikae*, *baraka* and *bambusicola* (Kenyan highlands, southern Eastern Arc Mnts and the northern Albertine Rift), *roehli* (Usambara & Pare Mountains) and *helleri* (Taita Hills) are more difficult to interpret with confidence, due to relatively low bootstrap and jackknife support of deeper nodes in the phylogeny. The consensus of the 36 MP trees, however (not shown but has the same topology as Fig. 7.2), suggests that *abyssinicus*, *baraka* and *bambusicola* form a clade which is sister to *helleri* and/or *roehli*.

Three other clades were identified: (1) Olive Thrushes from South Africa, with *smithi* split from the other southern African taxa (*olivaceus*, *pondoensis* and *transvaalensis*), grouping with the Gulf of Guinea Thrush (*T. olivaceofuscus*) although with weak bootstrap and jackknife support, (2) African Thrush (*T. pelios*) and (3) the Comoro and Kurricane Thrush (*T. bewsheri* & *T. libonyanus*) as putative sister taxa (at least based on the taxon sampling in this study).



However, relationships between the *abyssinicus* group, the *olivaceus* group, *T. olivaceofuscus* and *T. pelios* are poorly supported in MP analyses.

Saturation plots for ND3 (Fig. 7.3) indicate that only third position transitions appear to show the clear levelling off associated with saturation. This occurs by the 10% Kimura-2-parameter distance estimate. To take into account apparent saturation of third position transitions in ND3, step matrices were constructed that down-weighted 3<sup>rd</sup> position transitions over transversions by factors of 2, 5 and 10. Incrementally down-weighting 3<sup>rd</sup> position transitions resulted in a more fully resolved structure among taxa in the '*abyssinicus*' group. The remaining three clades identified in the equal-weighted analyses were recovered under all weighting schemes although their relative positions differed (Fig. 7.4). When 3<sup>rd</sup> position transitions are down-weighted to a greater degree, *T. olivaceofuscus* no longer clusters with the '*olivaceus*' group, but instead forms a fourth clade, and one individual of *T. pelios* from Lwiro splits from the remaining *T. pelios* to form a fifth clade. Incremental down-weighting of 3<sup>rd</sup> position transitions marginally improves support for nodes, but relationships between deeper nodes remain poorly supported.

To facilitate time-efficient maximum likelihood (ML) analysis the dataset was pruned to 41 individuals (identical haplotypes removed). Representatives of all clades were retained. Modeltest 3.06 was used to conduct log-likelihood ratio tests, which selected a TVM model of nucleotide substitution with gamma shape parameter ( $\Gamma$ ). Parameters for the model were as follows: base frequencies, A = 0.33, C = 0.34, G = 0.14 and T = 0.18; rate matrix, [A-C] = 0.8261, [A-G] = 12.2728, [A-T] = 0.2554, [C-G] = 0.3676, [C-T] = 12.2728 and [G-T] = 1.000; gamma shape parameter = 0.1688.

ML analyses recovered three trees of score  $-\ln 1846.31$ . The three trees differed only in the resolution of the two *T. bewsheri* individuals, in one tree they were fully resolved and basal relative to all other members of the *T. olivaceus* species complex included within this study, in another they were paraphyletic, but still basal relative to the ingroup and in the third tree they formed a polytomy at the

base of the ingroup. The topology of the consensus tree (Fig. 7.5) is similar to that obtained under weighted parsimony (Fig 7.2); recovering monophyletic ‘*abyssinicus*’ and ‘*olivaceus*’ groups. Relationships among deeper nodes remain poorly supported.

During each Bayesian Inference (BI) run, the Markov chains reached a stable negative log-likelihood score after *ca.* 25 000 generations. Therefore, only trees sampled after 25 000 generations ( $n = 19\,500$  or  $39\,500$  for the 1 million and 2 million generation runs, respectively) were used in determining the posterior probabilities of the model parameters, branch lengths and splits (nodes) within the tree. The marginal probabilities of the rate matrix were,  $[A-C] = 2.4032$ ,  $[A-G] = 45.1089$ ,  $[A-T] = 0.8157$ ,  $[C-G] = 1.8216$ ,  $[C-T] = 19.1304$  and  $[G-T] = 1.0000$ . The marginal probabilities of the nucleotide frequencies were  $A = 0.31$ ,  $C = 0.35$ ,  $G = 0.13$  and  $T = 0.21$ , and the marginal probability of the proportion of invariable sites was 0.5247, and the shape of the gamma parameter was 2.039. The consensus trees from each of the six Markov runs had identical topology (Fig. 7.6), and are similar to the best-fit ML tree when nodes with low bootstrap support are collapsed. The range of posterior probabilities for each clade obtained from the six Markov runs are shown above the branches in Figure 7.6. These values are not directly comparable to bootstrap values, but are instead probabilities (expressed as integers 1 to 100%). Therefore, if we are to accept significance at the 5% level, we might feel confident about relationships supported with a posterior probability of  $\geq 95\%$  (see Lewis 2001, Suzuki *et al.* 2002, Wilcox *et al.* 2002 and Chapter 2). A crown clade corresponding to the ‘*abyssinicus*’ group is supported. This clade together with the ‘*olivaceus*’ group, *T. pelios* and *T. olivaceofuscus* form a polytomy, and as in the ML analyses, *T. libonyanus* and *T. bewsheri* are no longer sister taxa (Fig. 7.6), but based on the currently sampling scheme (Table 7.1) have uncertain affinities.

The main features of the above analyses are: (1) support for the monophyly of the ‘*abyssinicus*’ group, with thrushes from (a) the Taita Hills (*helleri*), (b) the Usambara Mountains (*roehli*), and (c) the southern and central Eastern Arc Mountains (*nyikae*), and the Kenyan Highlands (*abyssinicus*) and the northern

Albertine rift (*baraka* and *bambusicola*) forming reciprocally monophyletic clades, (2) the '*olivaceus*' group with two clades (a) *smithi* from the arid shrublands of coastal and west-central South Africa and (b) the remaining forest and woodland taxa of northern, southern and eastern South Africa (*olivaceus*, *pondoensis* and *transvaalensis*), and (3) poorly supported resolution of deeper nodes.

## DISCUSSION

The genus *Turdus* is one of the largest and most widespread of all bird genera (Bock & Farrand 1980, Clement & Hathway 2000). Its cosmopolitan distribution combined with the great plumage diversity shown within the genus has made taxonomic treatments of many species difficult, and in some cases, has generated considerable debate. A major point of contention continues to centre on the taxonomic status of components of the Olive Thrush *T. olivaceus* complex (reviewed in the introduction). In these treatments all authors have recognised as full species the two island taxa in this complex, the Comoro Thrush (*T. bewsheri*) and Gulf of Guinea Thrush (*T. olivaceofuscus*), as well as the mainland Bare-eyed Thrush (*T. tephronotus*), so named due to its distinctive yellow eye-ring. In contrast, species limits among Kurricane (*T. libonyanus*), African (*T. pelios*) and Olive Thrush (*T. olivaceus*), have varied extensively (see Keith & Urban 1992, Clement & Hathway 2000 for reviews). Systematic hypotheses generated in this study from mtDNA analyses using various phylogenetic methodologies (MP, ML, BI, Fig. 7.2, 7.4-7.6) all suggest that *T. olivaceus* is polyphyletic. Southern African birds (*olivaceus*, *smithi*, *pondoensis* and *transvaalensis*) are split from all the more northern forms (*baraka*, *bambusicola*, *abyssinicus*, *helleri*, *roehli* and *nyikae*) by 8.5-10 % sequence divergence.

This result is not surprising. Traditionally, members of the '*abyssinicus*' group of eastern and central African birds were considered a distinct species, from the southern African taxa (White 1960, 1962a, b, Ripley 1964, Mackworth-Praed & Grant 1973 onwards). Phylogenetic analyses of mtDNA in this study strongly support the traditional classification of the Olive Thrush, with at least two of Hall and Moreau (1970) taxon groups being accorded species rank, *T. abyssinicus*

Gmelin 1789, the Northern or Mountain Olive Thrush, and *T. olivaceus* Linnaeus 1766, the Southern Olive Thrush.

### The *Turdus abyssinicus* group

The recognition of *T. abyssinicus* refuels the much-debated question of whether some of the more well-marked races of the ‘*abyssinicus*’ group, Taita Thrush (*helleri*), Somali Blackbird (*ludoviciae*) and the Yemen Thrush (*menachensis*), warrant full species rank (see Keith & Urban 1992, Clement & Hathway 2000 for a review of opinions). The Taita Hills endemic, *helleri* with its distinctive blackish head and breast is one of four divergent ‘subspecies’ which geographically separate central Kenyan birds (*abyssinicus*), from those of central Tanzania (*nyikae*, Fig. 7.1). The other ‘subspecies’ are: *deckeni* (breast is more grey than brown with orange on the belly), which extends from Longido to Monduli and occurs on Mount Kilimanjaro, *oldeani* (underparts are almost entirely grey with only a trace of orange on the belly and flanks) of the crater highlands of northern Tanzania, including Mt. Meru and Mt Hanang, and *roehli* (orange on belly infused with red and with a characteristic white centre) of the Pare and Usambara Mountains.

The controversy surrounding the taxonomic status of the most distinctive form *helleri*, stems from some authors (e.g. Keith & Urban 1992, Dowsett & Dowsett-Lemaire 1993) considering *roehli* to not only be intermediate in geography (Fig. 7.1), but also in plumage, with the white centre to the belly and reddish flanks suggestive of *helleri*, and the olive-grey head more like *nyikae*, which occupies the central and southern Eastern Arc. Consequently, most modern systematic treatments of African birds (Dowsett & Dowsett-Lemaire 1993, Keith *et al.* 1997), or the Turdidae (Keith & Urban 1992, Keith *et al.* 1997, Clement & Hathway 2000) have adopted the conservative approach of suggesting that these divergent races be considered part of the Olive Thrush, *T. olivaceus* (including *T. abyssinicus* itself).

The 12 individuals of *helleri*, always clustered together with high bootstrap and jackknife support (Figs 7.2, 7.4-7.6). Furthermore, reciprocal monophyly is observed for the five individuals from the two populations analysed for *roehli*,

which is 4.5% divergent from *helleri*, and 4% from *nyikae* (Table 7.2). All three analytical methods suggest that the geographically restricted *helleri* and *roehli* are phylogenetically basal relative to all other northern forms of the ‘*abyssinicus*’ group, suggesting that they may be relict populations. It is important to note that other forms that are morphologically fairly uniform and form a monophyletic group, have been able to spread to all montane forests in eastern Africa, even extending to the highlands of Ethiopia, and yet, the Taita (*helleri*) and Usambara-Pare Mountain (*roehli*) populations have maintained their genetic integrity, with no evidence to suggest introgression is or has taken place. The nucleotide sequence data gathered in this study are insufficient to provide a robust biogeographical hypothesis, but based on the resolved nodes in the ML and BI analyses (Figs 7.5-7.6) it suggests that *nyikae* is basal compared with Albertine rift populations (*baraka* and *bambusicola*) and the Kenyan Highlands (*abyssinicus*), which suggests that dispersal occurred northwards from the south-central Eastern Arc along the Rukwa/Albertine rifts, and thence to the Kenyan and the Ethiopia highlands.

Both *helleri* and *roehli* can be defined by discrete plumage characters (see Introduction, Clement & Hathway 2000) and are well-supported in all the molecular analyses, with no evidence of mtDNA introgression. Using either a biological (Mayr 1944) or phylogenetic (Cracraft 1983) species definition, both taxa warrant species rank: *Turdus helleri* Mearns 1913 the Taita Thrush, and *Turdus roehli* Reichenow 1905, for which the common name Usambara Thrush is suggested.

Further, the Taita Hills in southeastern Kenya are a series of isolated montane forests, geographically considered to be the northernmost range of the Eastern Arc Mountains. *Turdus helleri* occupies three of the remaining fragments; Chawia (ca 50 ha), Ngangao (92 ha) and the largest fragment Mbololo (ca 200 ha). A study of 155 individuals using microsatellite markers (Galbusera *et al.* 2000), suggested that all three remaining populations are genetically isolated, with the largest difference existing between populations in Mbololo and Chawia. With respect to mtDNA only two haplotypes were detected among the 12 individuals analysed. The two haplotypes differed from each other by only one

nucleotide substitution, with one haplotype restricted to Mbololo, whereas Chawia and Ngangao were genetically identical for mtDNA. The Mbololo massif is separated from the rest of the Taita Hills by a valley at about 900m (see Fig. 1 in Brooks *et al.* 1998a). Larger sample sizes are required for the mtDNA analyses if further inferences, for example sex biased dispersal are to be made.

Unfortunately, it was not possible to obtain samples from some important races; *deckeni* and *oldeani* of northern Tanzania, *ludoviciae* of Somali, *menachensis* of Yemen, and *swynnertoni* from Zimbabwe and Mt. Gorongosa, and *milanjensis* of northern Mozambique and southern Malawi. Until an ongoing study using tissues from museum specimens is completed, the taxonomic status of these taxa will remain uncertain, and the historical biogeography of this diverse complex of African thrushes speculative.

#### **The *Turdus olivaceus* group**

In a recent study using both morphological (plumage and biometric data) and molecular data (1058 bp of mtDNA), Bowie (Chapter 6) suggested that *smithi* warrants specific status. The present study with extensive sampling of northern taxa supports these conclusions, and suggests that *T. smithi* and *T. olivaceus* (including *transvaalensis*, *pondoensis* and *culminans*) are sister taxa.

**Table 7.1.** Taxa and populations of the *Turdus olivaceus* species complex analysed in this study. \*Refers to the locality of voucher specimens: ZMUC – Zoological Museum of the University of Copenhagen, FMNH – The Field Museum of Natural History, RMCA – Royal Museum for Central Africa, MBM - Barrik Museum at the University of Nevada Las Vegas, and the Percy FitzPatrick Institute, University of Cape Town.

Taxon		Inst./Indiv.*	Accession No.	Country	Locality
<i>T. libonyanus</i>	1	FitzPatrick	#61	South Africa	Tzaneen
	2	Peter Ryan	4A19951	Malawi	Mount Zomba
<i>T. bewsheri</i>	1	Ben Warren	GC150	Comoro Is.	Grande Comore
	2	Ben Warren	GC158	Comoro Is.	Grande Comore
	3	Ben Warren	GC190	Comoro Is.	Grande Comore
<i>T. olivaceofuscus</i>	1	Martim de Melo	#1	Rep. of Sao Tome & Principe Is.	Sao Tome
	2	Martim de Melo	#2	Rep. of Sao Tome & Principe Is.	Sao Tome
<i>T. pelios saturatus</i>	1	FMNH	396634	Ghana	Gonja Triange, 2km N of Buipe
	2	FMNH	396636	Ghana	Gonja Triange, 2km N of Buipe
<i>T. p. centralis</i>	1	ZMUC	RK16-280501	Demo. Rep. of the Congo	Lwiro
	2	FMNH	429758	Demo. Rep. of the Congo	Lwiro
	3	FMNH	385054	Uganda	Ngoto Swamp
<i>T. olivaceus olivaceus</i>	1	FitzPatrick	#31	South Africa	Cape Town
	2	Rauri Bowie	#2	South Africa	Grootvadersbosch
<i>T. o. pondoensis</i>	1	FitzPatrick	#1	South Africa	Himeville
	2	FitzPatrick	#65	South Africa	Himeville

	3	FMNH	390135	South Africa	Boston
	4	FMNH	390136	South Africa	Boston
<i>T. o. transvaalensis</i>	1	FitzPatrick	#1	South Africa	Dullstroom
	2	FitzPatrick	#2	South Africa	Dullstroom
<i>T. o. smithi</i>	1	MBM	5877	South Africa	Kimberely
	2	MBM	7881	South Africa	Kimberely
	3	FitzPatrick	#1	South Africa	Pretoria
<i>T. o. helleri</i>	1	Luc Lens	09	Kenya	Chawia, Taita Hills
	2	Luc Lens	20	Kenya	Chawia, Taita Hills
	3	Luc Lens	25	Kenya	Chawia, Taita Hills
	4	Luc Lens	27	Kenya	Chawia, Taita Hills
	5	Luc Lens	28	Kenya	Ngangao, Taita Hills
	6	Luc Lens	44	Kenya	Ngangao, Taita Hills
	7	Luc Lens	45	Kenya	Mbololo, Taita Hills
	8	Luc Lens	46	Kenya	Mbololo, Taita Hills
	9	Luc Lens	47	Kenya	Mbololo, Taita Hills
	10	Luc Lens	48	Kenya	Ngangao, Taita Hills
	11	Luc Lens	49	Kenya	Ngangao, Taita Hills
	12	Luc Lens	61	Kenya	Ngangao, Taita Hills



<i>T. o. roelhi</i>	1	ZMUC	JK01-201099	Tanzania	Magamba, W. Usambara Mnts
	2	ZMUC	JK06-221099	Tanzania	Magamba, W. Usambara Mnts
	3	ZMUC	JK02-241099	Tanzania	Magamba, W. Usambara Mnts
	4	FMNH	356763	Tanzania	Ambangulu, W. Usambara Mnts
	5	ZMUC	JK01-050601	Tanzania	Ambangulu, W. Usambara Mnts
<i>T. o. nyikae</i>	1	ZMUC	JK03-270700	Tanzania	Chamangani. Morogoro District
	2	ZMUC	O7828	Tanzania	Udzungwa Scarp Forest
	3	ZMUC	O7865	Tanzania	Udzungwa Scarp Forest
	4	ZMUC	DCM01-270697	Tanzania	Kungwe
	5	ZMUC	JK08-900600	Tanzania	Ukaguru Mnts
	6	ZMUC	O4644	Tanzania	Uluguru Mnts
<i>T. o. bambusicola</i>	1	FMNH	346414	Burundi	Teza, Muramuya District
<i>T. o. baraka</i>	1	FMNH	385051	Uganda	Echuya Forest Reserve, Kabale
	2	FMNH	385052	Uganda	Echuya Forest Reserve, Kabale
	3	FMNH	355653	Uganda	Nyabitaba, Ruwenzori Mnts
	4	FMNH	355655	Uganda	Nyabitaba, Ruwenzori Mnts
	5	FMNH	355659	Uganda	John Mate, Ruwenzori Mnts
	6	FMNH	355651	Uganda	Choha, Ruwenzori Mnts
	7	FMNH	355652	Uganda	Choha, Ruwenzori Mnts

<i>T. o. abyssinicus</i>	1	Rauri Bowie	BB0162	Kenya	Gatamaiyu Forest, S. Aberdares
	2	Rauri Bowie	BB0165	Kenya	Gatamaiyu Forest, S. Aberdares
	3	ZMUC	O5833	Kenya	Karisia Hill, N. Aberdares
	4	ZMUC	O8431	Kenya	Karisia Hill, N. Aberdares
	5	ZMUC	O8340	Kenya	Mount Kulal
	6	ZMUC	144	Kenya	Mount Marsibit
	7	Rauri Bowie	BB0157	Kenya	Mount Kenya
	8	FitzPatrick	#29	Kenya	Karuru Forest

---

**Table 7.2:** Average Kimura-2-Parameter divergence among African *Turdus* taxa sampled

	1	2	3	4	5	6	7	8	9	10	11	12	13	14	15	16	17
(1) <i>Onychognathus</i>																	
(2) <i>Lamprotornis</i>	0.197																
(3) <i>Pogonocichla</i>	0.219	0.195															
(4) <i>T. bewsheri</i>	0.196	0.168	0.176														
(5) <i>T. libonyanus</i>	0.211	0.203	0.200	0.058													
(6) <i>T. olivaceofuscus</i>	0.193	0.172	0.186	0.089	0.103												
(7) <i>T. pelios saturatus</i>	0.221	0.198	0.182	0.084	0.087	0.068											
(8) <i>T. pelios centralis</i>	0.203	0.173	0.169	0.073	0.095	0.077	0.038										
(9) <i>T. o. olivaceus</i>	0.218	0.202	0.186	0.103	0.103	0.084	0.100	0.105									
(10) <i>pondoensis</i>	0.214	0.206	0.182	0.106	0.106	0.081	0.097	0.103	0.003								
(11) <i>transvaalensis</i>	0.214	0.206	0.182	0.106	0.106	0.081	0.097	0.103	0.003	0.000							
(12) <i>smithi</i>	0.201	0.183	0.177	0.101	0.104	0.065	0.087	0.097	0.040	0.037							
(13) <i>helleri</i>	0.220	0.204	0.187	0.098	0.108	0.070	0.074	0.068	0.083	0.078	0.080						
(14) <i>roelhi</i>	0.215	0.195	0.200	0.103	0.106	0.098	0.087	0.078	0.091	0.094	0.094	0.091	0.045				
(15) <i>nyikae</i>	0.212	0.198	0.183	0.104	0.112	0.086	0.076	0.073	0.092	0.089	0.089	0.087	0.031	0.040			
(16) <i>abyssinicus</i>	0.210	0.209	0.192	0.113	0.117	0.095	0.085	0.096	0.098	0.095	0.095	0.094	0.032	0.042	0.026		
(17) <i>bambusicola</i>	0.203	0.203	0.193	0.106	0.109	0.088	0.081	0.073	0.091	0.088	0.088	0.087	0.031	0.035	0.025	0.003	
(18) <i>baraka</i>	0.211	0.206	0.189	0.107	0.108	0.094	0.080	0.095	0.096	0.093	0.093	0.092	0.031	0.036	0.022	0.006	0.005

## FIGURE LEGENDS

**FIG 7.1.** Distribution ranges of most of the taxa in the Olive Thrush *Turdus olivaceus* species complex (ranges of the Bare-eyed thrush *T. tephronotus* of arid Eastern Africa and the races *T. o. stromsi* and *bocagi* of Angola and central Africa are not depicted)

**FIG 7.2.** Phylogeny of members of the *Turdus olivaceus* species complex using 383 bp of ND3 and associated tRNA flanking regions. Maximum Parsimony analyses yielded 36 trees of 291 steps, one of which is depicted here. Numbers above branches are node lengths, below branches are bootstrap and jackknife values from 1000 iterations; here and in subsequent figures only values > 50% are reported.

**FIG 7.3.** Saturation plots for ND3 that relate Kimura-2-Parameter sequence divergence to changes due to transitions (A) and transversions (B) at first, second, and third codon positions.

**FIG 7.4.** Summary of topologies and bootstrap values (1000 iterations) obtained under different transition/transversion weighting schemes using the maximum parsimony optimality criteria.

**FIG 7.5.** Maximum likelihood analyses of the *Turdus olivaceus* species complex using a TVM +  $\Gamma$  model of nucleotide substitution. A heuristic search with 100 random addition replicates yielded three trees of length  $-\ln 1846.31$ . The consensus is depicted. Bootstrap values from 50 replicates are indicated.

**FIG. 7.6.** Topology obtained in each of the six Markov Chain Bayesian Inference analyses conducted. Values above the branches indicate the range of posterior probabilities recovered among the six BI runs (see text for details).

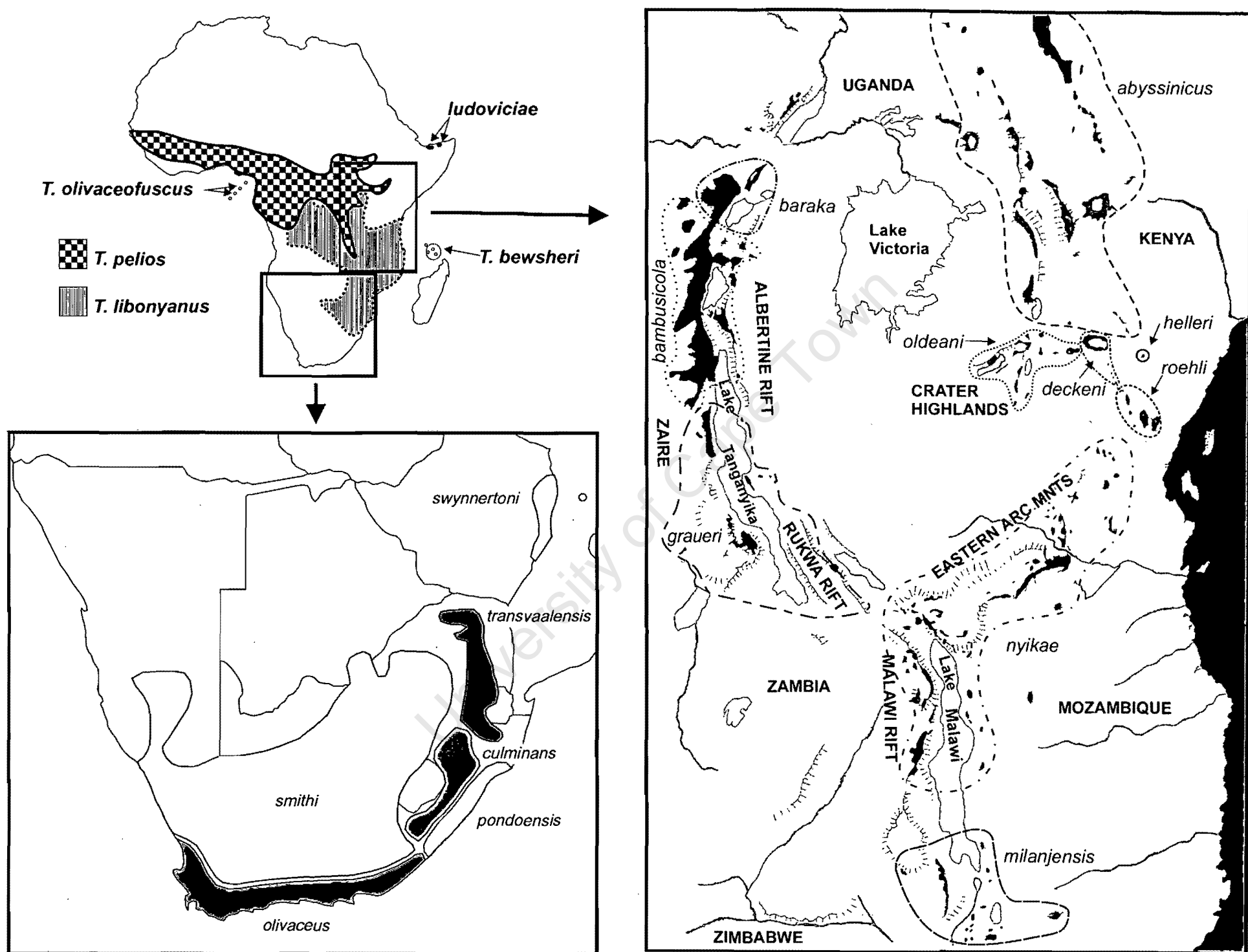


FIG 7.1

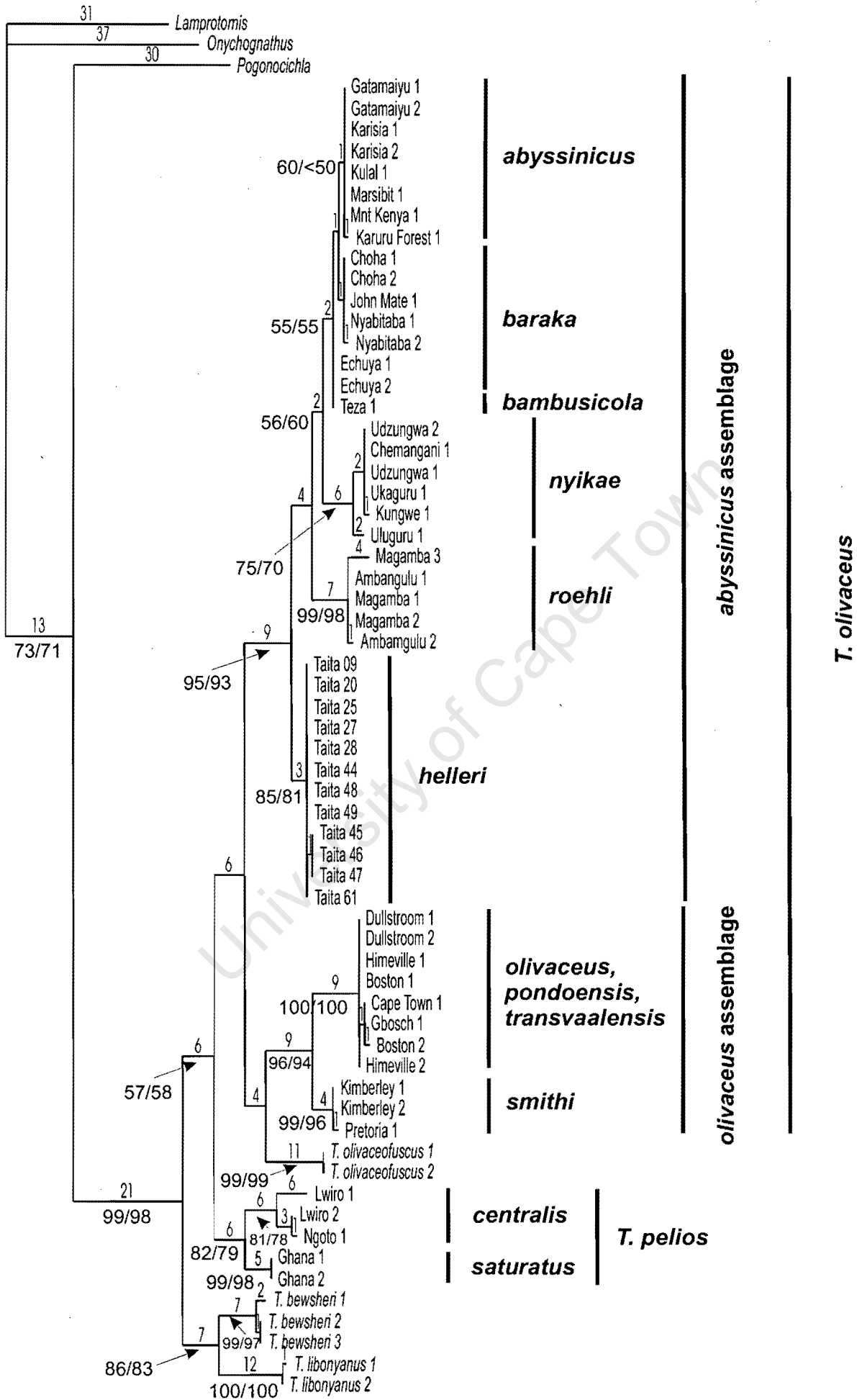


FIG 7.2

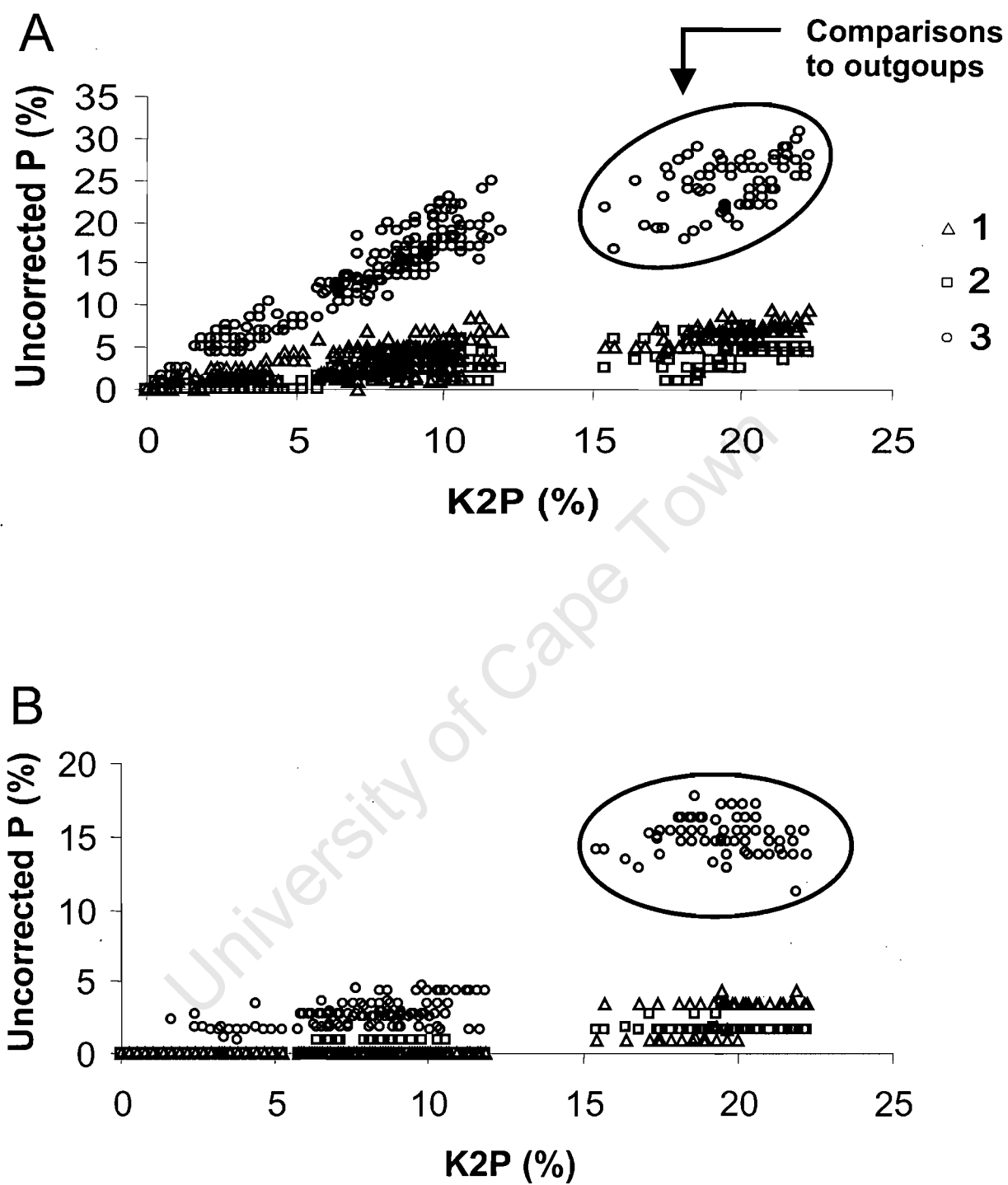


FIG 7.3

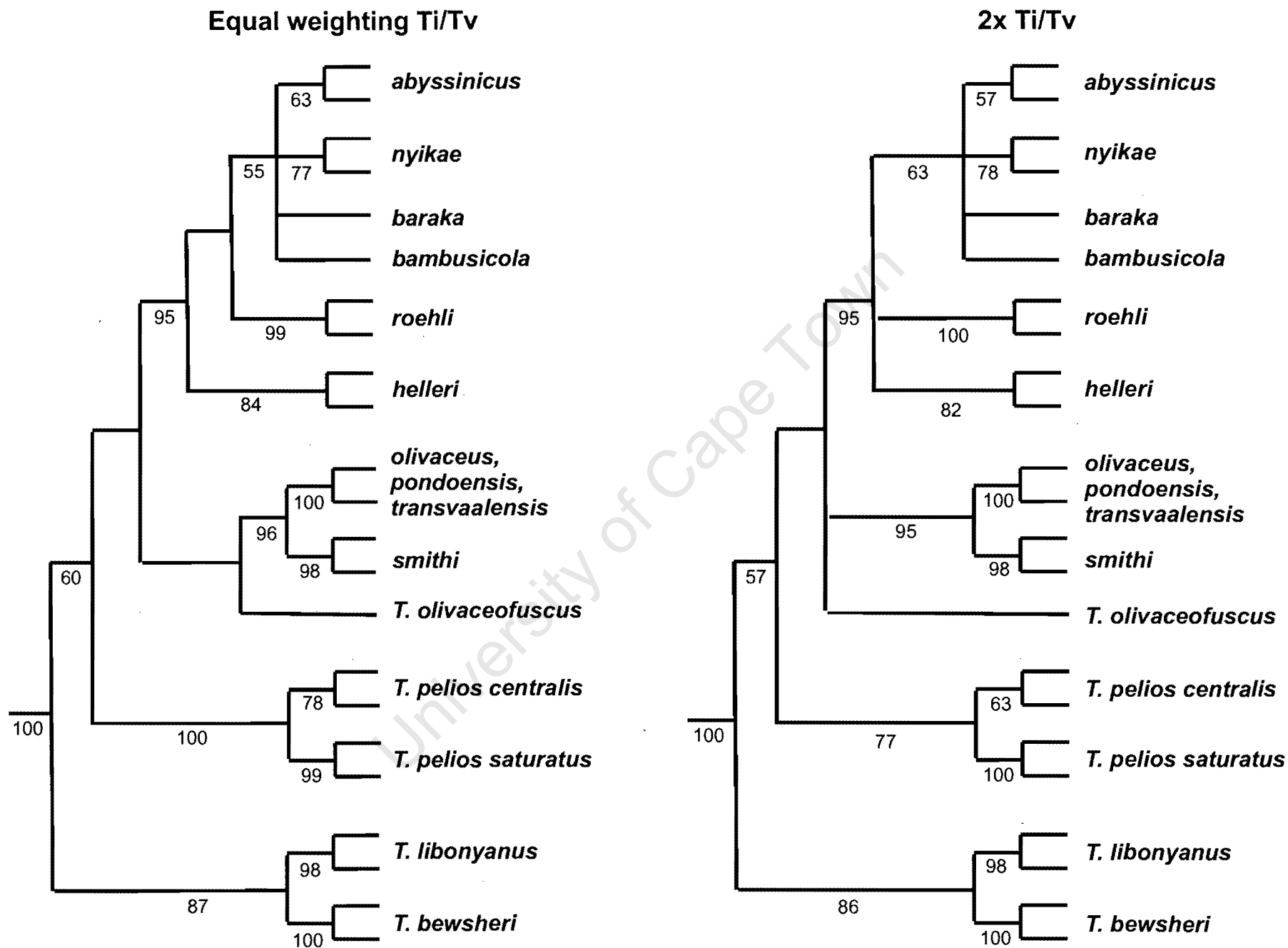
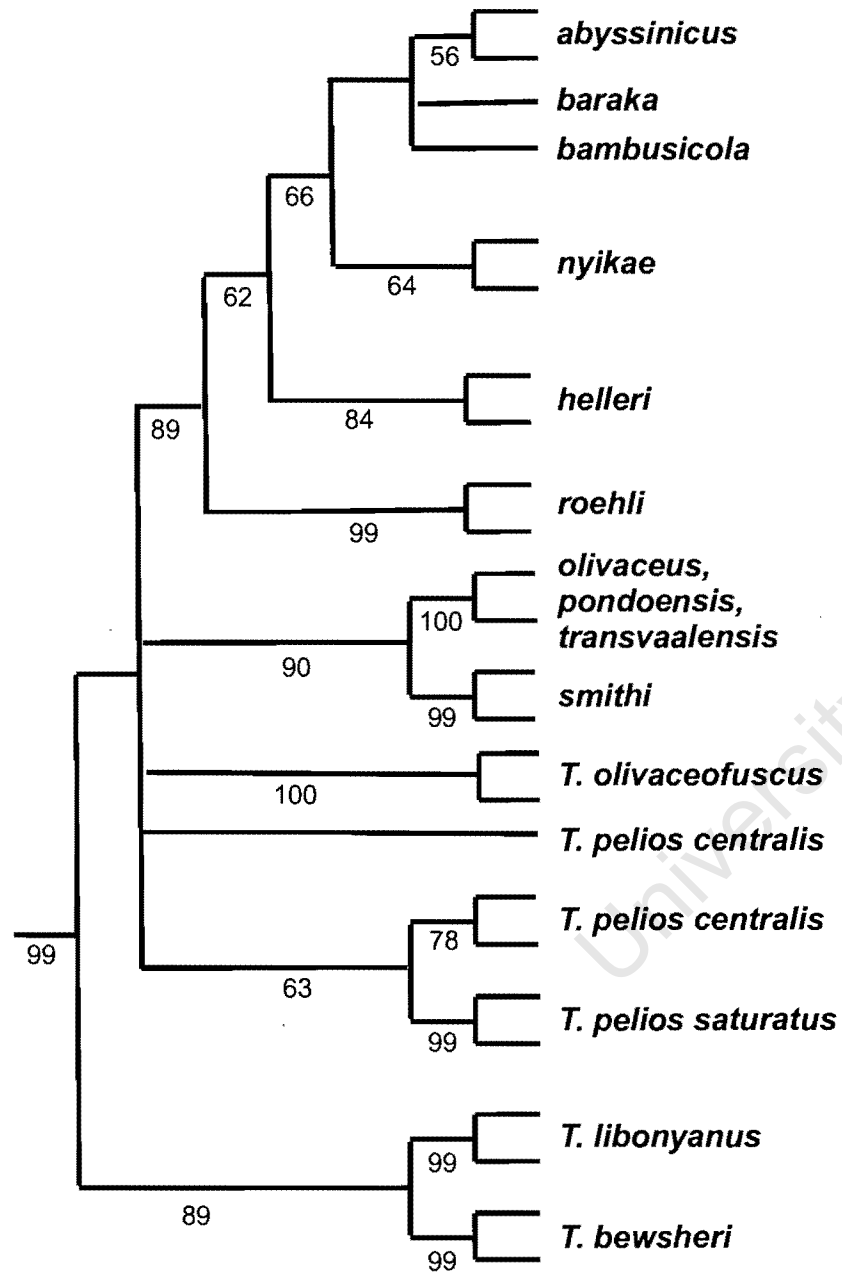


FIG 7.4a



5x Ti/Tv



10x Ti/Tv

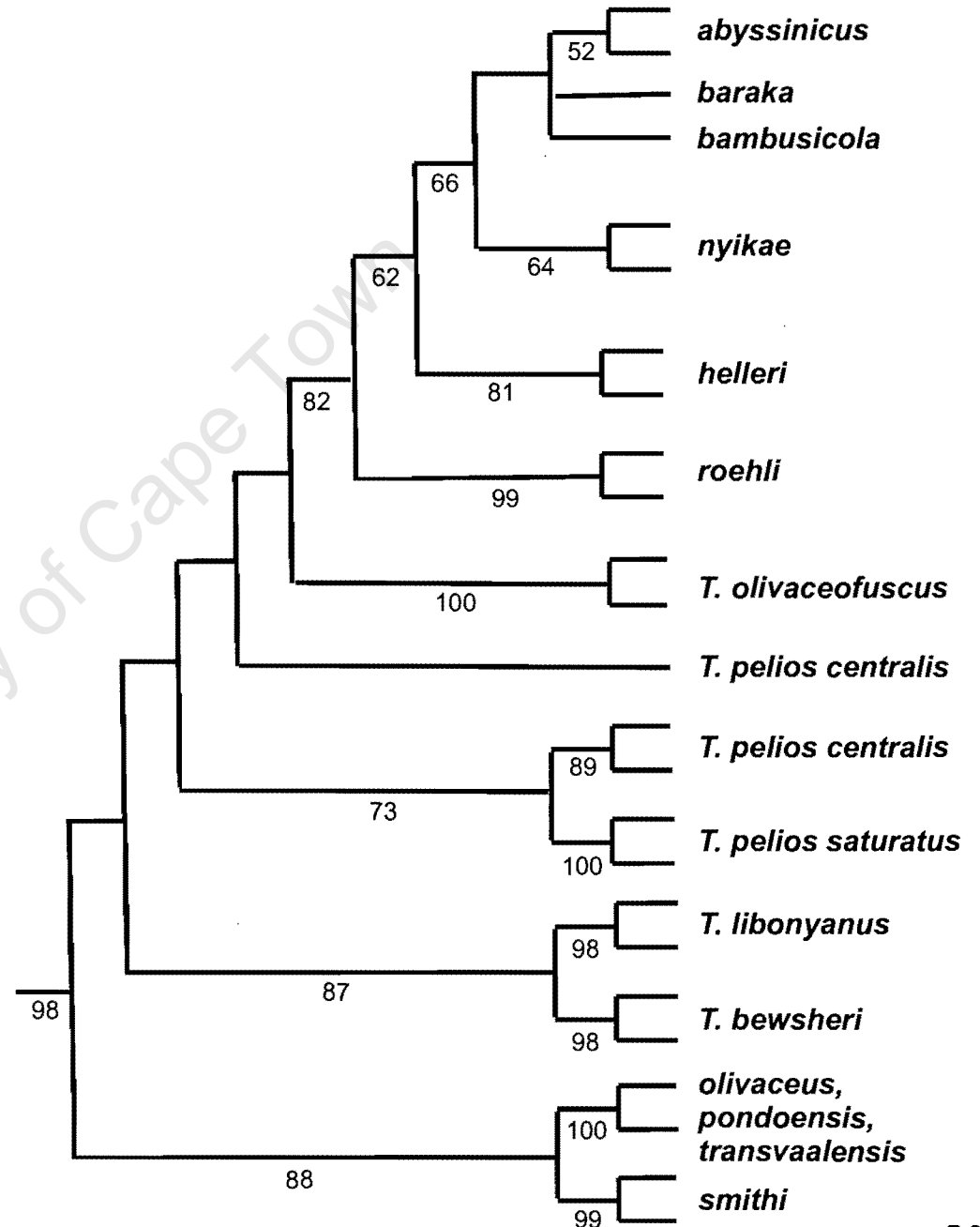


FIG 7.4b continue.

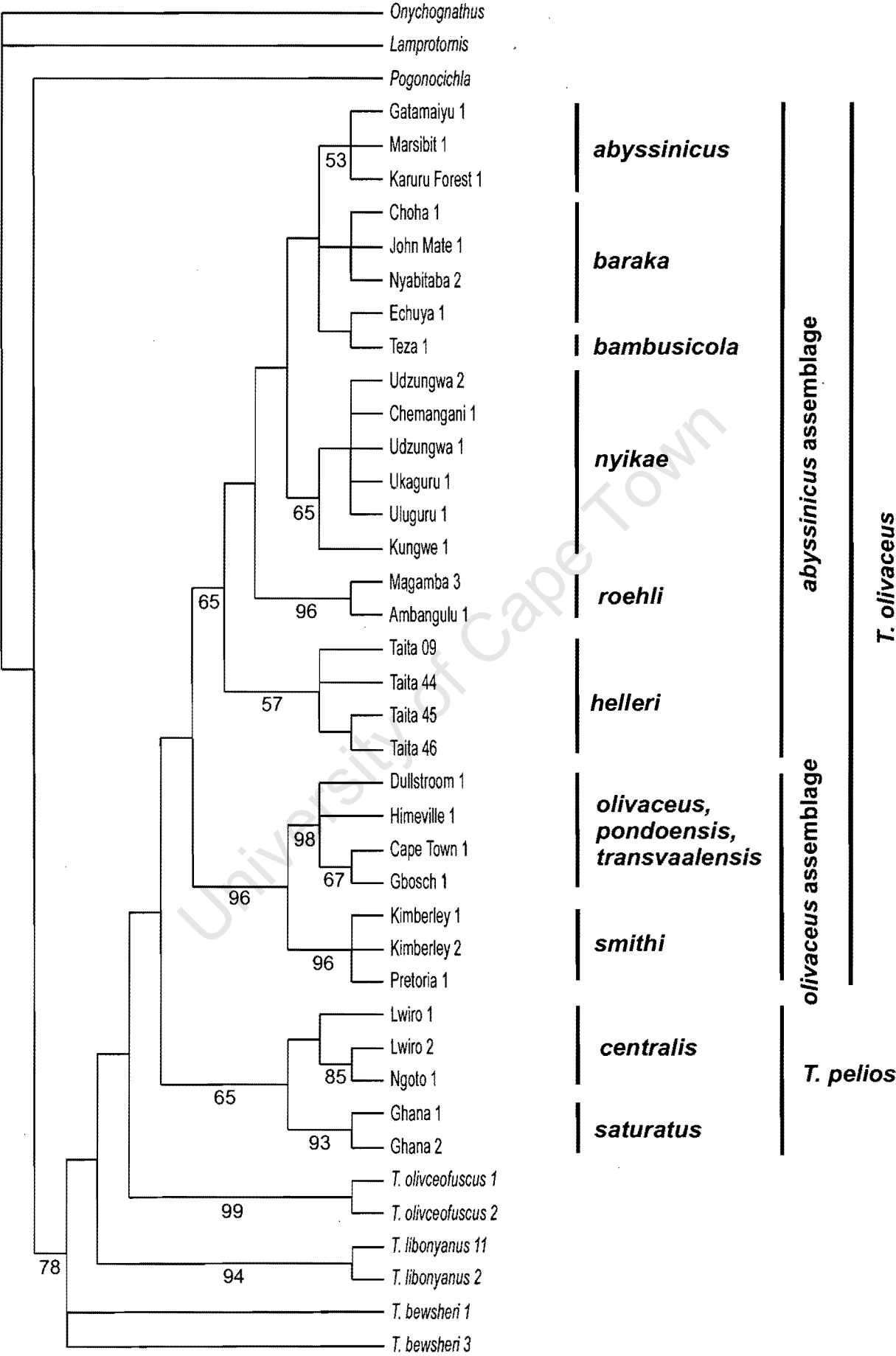


FIG 7.5

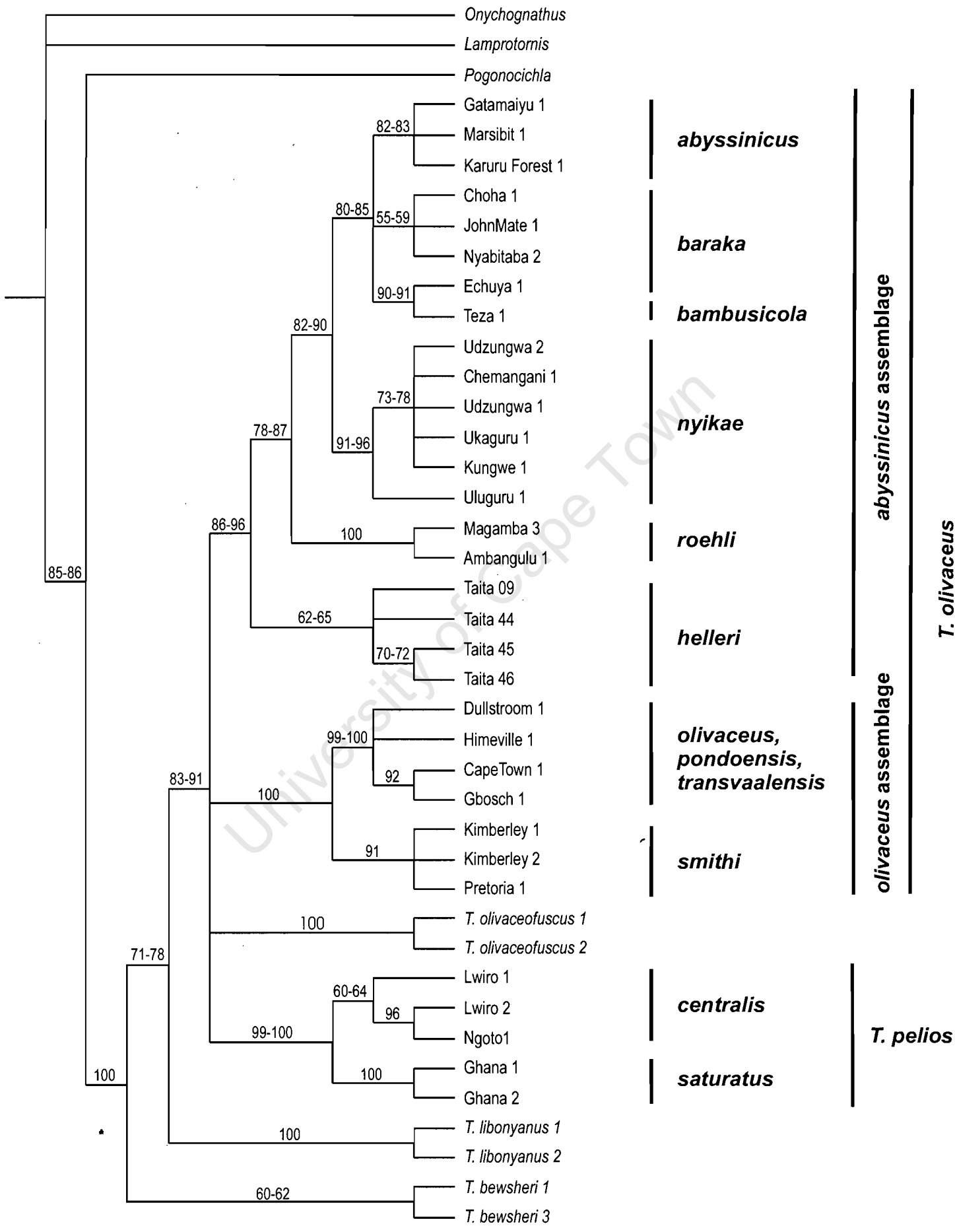


FIG 7.6

## Chapter 8

### **Molecular evolution in space and through time: mtDNA phylogeography of the Olive Sunbird (*Nectarinia olivacea/obscura*) throughout continental Africa**

#### **Summary**

The present study constitutes the first investigation of the phylogeographic structure of a forest bird distributed throughout the montane and lowland forest biomes of Africa. The key objective was to investigate the importance of Pleistocene climatic cycles on avian diversification across Africa. The Olive Sunbird is a relatively large polytypic sunbird widely distributed throughout evergreen, montane and coastal forests in Africa. Recently, it was split into two species, the Eastern Olive Sunbird *N. olivacea* and the Western Olive Sunbird *N. obscura*, based on the presence of large yellow pectoral tufts in female *N. olivacea*, which are absent in *N. obscura*. A 395 bp fragment of the mtDNA NADH subunit 3 gene with flanking tRNA sequences was obtained from 282 individuals, 196 from *N. olivacea* and 86 from *N. obscura*, respectively. Fifty-five haplotypes (19.5%) were identified. However, genetic divergence levels were low. Across some 9000 km, from Ghana in the northwest of Africa to KwaZulu-Natal in eastern South Africa, genetic divergence levels ranged from 1.0 to 2.4%. Neither currently recognized Olive Sunbird species was monophyletic using either parsimony or likelihood tree-building methods. Instead, genetic diversity within the *N. olivacea/obscura* complex was dominated by three star-like phylogenies linked to each other by a single mutational step and two subnetworks (IV and V) separated from the core star-like phylogenies (subnetworks I, II and III) by five to six mutational steps. The dominant evolutionary mechanism shaping genetic variation within the *N. olivacea/obscura* complex as identified by nested-clade analyses appears to be one of range expansion possibly out of East Africa associated with a period of forest expansion during the mid-Pleistocene, some 1.5-1.2 million years ago. Mismatch profiles suggested that secondary contact has occurred between eastern and western lineages within the Ufipa Escarpment and possibly Zimbabwe, as

well as between eastern lineages in the Kenyan Highlands and northern Eastern Arc Mnts.

## INTRODUCTION

The external forces which have shaped the flora and fauna of Africa differ significantly from those that shaped the biota of the other continents. The glaciations that scoured European and North American landscapes repeatedly during the Pleistocene (Hewitt 1996) were absent from Africa, and recession of the ice did not leave huge expanses open for re-colonization from putative refugia (deMenocal 1995). Nor has Africa been dramatically altered in shape as has South America by uplifting of mountain chains like the Andes or by marine incursions (Räsänen *et al.* 1995, see also Bates 2001). Nor is it like Asia, whose fauna must have been dramatically transformed when the Indian plate collided with the Eurasian plate, creating the Himalayas and releasing flora and fauna previously restricted to the Indian subcontinent (Bossuyt & Milinkovitch 2001). Still more recently Asia has experienced repeated links with the island archipelagos of Indonesia (Hall & Holloway 1998), which in turn have had only limited contact with Australia (Coates & Bishop 1997). Rather, Africa existed for perhaps the last 100 million years in much its present size and shape (Moreau 1966, Livingstone 1993).

Whereas the shape of the African land mass remained almost the same, the climate changed significantly and was particularly unstable in recent geological times. The closure of the Tethys Sea and geological uplift in central Africa (Partridge *et al.* 1995) resulted in aridification of much of northern and central Africa, and fragmentation of the extensive mid-Tertiary pan-African rainforest. Volcanism associated with uplift and rifting formed the Ethiopian and Kenya highlands, and over the last few million years has led to the formation of new landscapes, including Africa's great volcanoes, Mt. Kilimanjaro, Mt. Kenya, and Mt. Cameroon, and the troughs which so characterize Africa today, Lakes Albert, Kivu, Tanganyika, Malawi, and most recently Victoria (Griffiths 1993, Livingstone 1993, deMenocal 1995, Partridge *et al.* 1995, Seehausen 2002). Concurrently, huge ancient crystalline blocks were uplifted and tilted to form the Eastern Arc Mnts, which run from southern Kenya to the Makambako-Gap in

southwestern Tanzania, capturing the rain from the Indian Ocean and creating a rain-shadow on its leeward-side.

Long-term paleoclimatological data are scarce for Africa, but the most comprehensive dataset of wind-blown (eolian) dust in deep-sea drill-cores extending back *ca.* 5 million years (deMenocal 1995), suggest, together with pollen and sedimentation data (reviewed in Livingstone 1993, deMenocal 1995, Partridge *et al.* 1995, Maley 1996, 2001), that sub-Saharan Africa became much more arid during Pleistocene glacial periods. This increased aridity would have facilitated the expansion of the savanna and semi-arid biomes, and it has been postulated that isolation of forest refugia was a principal cause of speciation of forest birds (Diamond & Hamilton 1980, Crowe & Crowe 1982, Mayr & O'Hare 1986, deMenocal 1995, Partridge *et al.* 1995, Hamilton *et al.* 2001). The evidence from eolian dust deposition suggests that the pendulum swung towards forest and away from savanna on at least three occasions during the Plio-Pleistocene, viz. at 2.8, 1.7 and 1.0 million years before present, with intervening periods characterized by a series of cold and dry episodes (deMenocal 1995, Kennett 1995). In addition, African rainfall patterns are relatively unstable and have been documented to change over centuries and even from decade to decade over much of the continent (Nicholson 1994). However, certain areas, particularly montane highlands prone to orographic rain are thought to have had a more constant rainfall pattern which has helped maintain permanent forest cover (Servat *et al.* 1998; Fjelds  & Lovett 1996). Pleistocene climatic variation is often invoked to explain biogeographic patterns in Africa, but this is largely an *ad hoc* explanation with few supporting data. Forest refuges are inferred from current animal and plant distributions, and the role of general habitat contraction and expansion in shaping the regional species pool has never been critically assessed.

At all levels, the use of nucleotide sequence data in erecting phylogenetic hypothesis and application of molecular clocks to interpret their chronology, has changed perspectives on avian evolution. These changes are concerned not only within the recent past, as suggested by Klicka and Zink (1997) for North American birds and Garc a-Moreno and Fjelds  (2000) for Andean birds, but for

intermediate and deeper nodes as well. Recent studies of African birds suggest that the ages of divergence for groups of species once associated with putative lowland rainforest refuges predate the Pleistocene climatic cycles and instead many taxa are now thought to have diverged in the Miocene (Fjeldså 1994, Roy *et al.* 2000, Beresford 2002). In contrast, in broad analyses of vertebrate speciation, Avise and Walker (1998) and Avise *et al.* (1998) concluded that the Pleistocene had a considerable impact on the development of phylogeographic patterns within species and closely-knit species groups.

Among African birds, phylogeographic structure using DNA markers has only been studied in very few species, only one of which spans the whole continent, the Ostrich (*Struthio camelus*). In this arid-savanna species, Freitag and Robinson (1993) and Robinson and Matthee (1999) documented deep mitochondrial DNA (mtDNA) divisions between populations from eastern and northern African, but little between other African populations. A growing body of work on African savanna ungulates suggests complex phylogeographical structuring of Pleistocene age (e.g. Arctander *et al.* 1999, Nersting & Arctander 2001).

The present study constitutes the first investigation of the phylogeographic structure of a forest bird distributed throughout the montane and lowland forest biomes of Africa. Its key objective is to investigate the role of Pleistocene climatic cycles on avian diversification across Africa. It is critical that the temporal and spatial components of geographical structure be separated. Consequently, nested clade analysis (Templeton *et al.* 1987, Templeton *et al.* 1995, Templeton 1998), coupled with mismatch analyses (Rogers & Harpending 1992, Harpending *et al.* 1998), are used to investigate the phylogeographic structure in mtDNA of the Olive Sunbird (*Nectarinia olivacea/obscura*).

The Olive Sunbird is a relatively large polytypic sunbird widely distributed throughout evergreen, montane and coastal forests in Africa (Hall & Moreau 1970). Recently, it was split into two species, the Eastern Olive Sunbird *N. olivacea* Smith 1840 and the Western Olive Sunbird *N. obscura* Jardine 1843 (Clancey 1992-1993, Cheke *et al.* 2001). The basis for this split is the presence

or absence of large yellow pectoral tufts in females. Generally in sunbirds (Nectariniidae), the presence of lateral pectoral tufts is a male-specific sexual character that is erected during the mating display (Cheke *et al.* 2001). Populations east of 35° E in the north and 25° 30' in the south of the continent can be distinguished from those to the west as both the male and female bear pectoral tufts. In populations to the west, only males bear pectoral tufts (Fig. 8.1). Both complexes are polytypic for morphometric traits, with the eastern tufted *N. olivacea*, composed of six subspecies and the western species *N. obscura* with six or seven subspecies (Fry 2000, Cheke *et al.* 2001). The wide distribution, high number of subspecies and interesting polymorphism of a primarily male sexual character in females, makes the Olive Sunbird complex an interesting case study with which to explore African biogeography at the continental scale.

## METHODS

### Population sampling

Tissue or blood samples were collected from 282 individuals from across Africa. One hundred and ninety-six individuals from 49 populations, and 86 individuals from 18 populations were sampled for *N. olivacea* and *N. obscura*, respectively (Fig. 8.1, Table 8.1.)

### Laboratory procedures

DNA was extracted from frozen tissues or blood using a Puregene DNA isolation kit (Gentra Systems, Minneapolis, Minnesota) following the manufacturer's animal tissue protocols, but with an overnight proteinase K digestion at 55°C. The NADH dehydrogenase subunit 3 gene with flanking tRNAs (Glycine & Arginine; ND3-L10753 GACTTCCAATCTTTAAATCTGG, ND3-H11151 GATTTGTTGAGCCGAAATCAAC) was PCR amplified using standard conditions (30 cycles, denaturation at 94°C, annealing at 54°C, and extension at 72°C). PCR products were electrophoresed on 1.5% low-melting point agarose gels (FMC Bioproducts) stained with ethidium bromide and visualized under UV light. Amplicons of the appropriate length were cut out of the gel and purified using the GELase™ Agarose gel-Digesting Preparation and the 'fast protocol'



method (Epicentre Technologies, Madison, Wisconsin). The purified product was cycle-sequenced using Big Dye terminator chemistry (Applied Biosystems, Inc [ABI]). Cycle-sequencing reactions were precipitated with 3M ammonium acetate, rinsed in ethanol, dried and re-suspended in formamide-EDTA solution and run on an ABI 3100 automated DNA sequencer.

Sequences were obtained from both strands of DNA for each identified haplotype, as well as an additional 30 individuals (total 85 individuals). For the remaining individuals, only the forward strand was sequenced. All sequences were checked using the program Sequencher 3.0 (Gene Codes Corp) and aligned to the chicken (*Gallus gallus*) mtDNA sequence (Desjardins & Morais 1990) to test for the presence of any insertions, deletions or stop codons.

### **Phylogenetic analyses**

Phylogenetic analyses of the DNA sequences were performed using maximum parsimony (MP), and maximum likelihood (ML) algorithms. Parsimony analyses, using PAUP\*4.0b10 (Swofford 2002) were conducted using the heuristic search option, implementing stepwise addition with 100 random addition replicates and TBR branch swapping. ML analyses were performed using the quartet puzzling algorithm with 10 000 puzzling steps as implemented in PUZZLE (Strimmer & von Haeseler 1996). An HKY85 model of nucleotide substitution and a gamma-shaped distribution (estimated using four rate categories) were implemented to account for rate heterogeneity. All parameters were empirically estimated from the data using Modeltest 3.06b (Posada & Crandall 1998). Clade support for the MP and ML analyses was estimated using 1000 and 100 non-parametric bootstrap replicates, respectively.

### **Nested clade analyses (NCA)**

Since underlying assumptions of standard parsimony and maximum likelihood methods are often violated when analysing intraspecific datasets (see Crandall *et al.* 1994, Crandall & Templeton 1996 for reviews) the use of the Templeton, Crandall and Sing parsimony algorithm (TCS) and nested clade analysis (NCA, Templeton *et al.* 1992) in investigating phylogeographic structure was explored. TCS takes into account the problems of reconstructing relationships between

closely related species, or haplotypes within a species. NCA, attempts to separate the roles of recurrent forces such as gene flow from historical events such as fragmentation or range expansion events. This is achieved by overlaying the evolutionary relationships among the haplotypes upon a spatial landscape of the geographical distributions of haplotypes and clades (Templeton *et al.* 1995, Templeton 1998). By overlaying an evolutionary hypothesis (tree) on a spatial landscape, both space (geography) and time (tree) are integrated into a single analysis (Templeton 2002).

TCS version 1.01 (Clement *et al.* 2000) was first used to estimate the number of steps by which any two haplotypes can be separated from each other if spurious connections due to homoplasy (Templeton *et al.* 1992) are to be avoided. This estimated parsimony criterion, here referring to the minimum number of differences separating two individual sequences, rather than the global minimum tree length based on shared derived characters, was then used to infer a haplotype network using the programme TCS. The TCS-derived haplotype network was manually converted into a series of hierarchically nested clades using the rules in Templeton *et al.* (1987) and Templeton and Sing (1993).

Nested clade analyses quantify the spatial distributions of haplotypes and clades by calculating two distinct distances. The first is the clade distance ( $D_c$ ), which measures the geographical range of a clade by calculating the average distance that an individual bearing a haplotype from the clade of interest lies from the geographical center of all individuals bearing the haplotypes from the same clade. The second distance measure calculated is the nested clade distance ( $D_n$ ), which measures how a clade is geographically distributed relative to its closet relatives – the clades grouped together in the next hierarchically nested level. Additionally, the measures of average distance between the interior and tip clades within a nested group ( $I-T_c$ ), and the tip to interior distance for the nesting clade ( $I-T_n$ ) are estimated. Contrasts between clades within and among different nesting levels were used to discriminate between potential causes of geographical structuring of genetic variation following the revised version of the inference key published by Templeton *et al.* (1995) and Templeton (1998), which is available at: [http://bioag.byu.edu/zoology/crandall\\_lab](http://bioag.byu.edu/zoology/crandall_lab). Statistical measures of

significance were determined using the permutation procedure of Roff and Bentzen (1989) with 10 000 replicates. Calculation of clade distances and permutation testing were conducted using the program GEODIS 2.0 (Posada *et al.* 2000).

### **Mismatch distributions and tests of selective neutrality**

Pairwise mismatch differentiation of selected populations and regions, and two tests of selective neutrality, Tajima's D (Tajima 1989) and Fu's F test (Fu 1997) were calculated (1) to test whether populations are in mutation-drift equilibrium under an infinite sites model, and (2) as indicators of recent demographic change, which could have resulted from either population expansions or contraction (Rogers & Harpending 1992, Fu 1997, Harpending *et al.* 1998, Tolley *et al.* 2002). Both tests were implemented using Arlequin 2.0 (Schneider *et al.* 2000).

## **RESULTS**

### **Sequence variation**

A 395 bp fragment of the mtDNA NADH subunit 3 gene with flanking tRNA sequences was obtained from all 282 individuals. The aligned sequences were pruned at both the 5' and the 3' ends to ensure that the analyzed dataset comprised no missing data. This resulted in a final alignment of 383 characters per individual. Merging identical sequences yielded 55 unique haplotypes. The number of samples and frequency of haplotypes from localities sampled are summarized in Table 8.1. Sequence divergence between haplotypes was estimated using a Jukes-Cantor model of evolution. A divergence of 4% between haplotypes 32 and 53-55 (Ghana vs. central Kenya; *N. olivacea* vs. *N. obscura*) was the largest observed. The dataset was not saturated for any codon position (plots not presented).

### **Phylogenetic analyses**

Maximum parsimony analyses (MP) of the 55 sampled haplotypes rooted with *N. olivacea/obscura*'s putative closest relative, *N. famosa* (Bowie 2003), yielded 780 most parsimonious trees with a step length of 99 (CI = 0.788, RI = 0.833). Excluding, *N. famosa* 328 (85.6%) characters were constant, 33 (8.6%) were variable but parsimony uninformative and 22 (5.7%) were parsimony

informative. Modeltest supported a HKY with gamma shape parameter model of nucleotide substitution (HKY + G), which additional optimization failed to simplify. Estimates of base frequencies under this model were: (A) 30.3%, (C) 34.3%, (G) 13.5% and (T) 21.9%. The Ti/Tv ratio and gamma shape parameter were estimated to be 5.97 and 0.157 respectively. Both a strict consensus of the 780 parsimony trees and an analyses of 10 000 ML puzzling steps resulted in an unresolved pectinate topology for which no nodes had high bootstrap support (topologies not presented). Mapping the currently accepted classification scheme (Table 8.1) on to the poorly resolved topology suggests that neither of the two currently recognized species, *N. olivacea* or *N. obscura* are monophyletic, nor are at least eight of the subspecies.

### Haplotype network and nested design

Evaluation of the limits of statistical parsimony using TCS suggested that topologies connecting haplotypes by eight steps or fewer have a cumulative probability of greater than 95% of being correct. The inference of the haplotype network with the TCS program resulted in the network depicted in Figure 8.2a. Three star-like patterns (centrally located common ancestral haplotypes to which several more recently derived haplotypes are connected) are linked to each other by one mutational step, forming subnetworks I, II and III. Two additional subnetworks are depicted; IV connects to subnetwork II by six mutational steps (indicated by solid circles, which represent either unsampled or extinct haplotypes) and subnetwork V is ambiguously connected by 5 steps either to the interior of subnetwork III or to haplotype 5, a tip of subnetwork I. Two ambiguities are also present inside subnetwork II, and one in subnetwork III.

The criteria initially suggested by Crandall and Templeton (1993), and latter expanded by Crandall (1996, see also Castello & Templeton 1994) were used to resolve the above ambiguities. For example, haplotype 45 (black arrow in Fig. 8.2a) is one step away from haplotypes 44 and 46, but because haplotype 46 is interior (see Methods) and occurs with much greater frequency than haplotype 44 (12 vs. 2), haplotype 45 is more likely to be connected to haplotype 46. Haplotypes 42 and 43 (singletons, grey arrow in Fig. 8.2a) are joined to each other via an unsampled haplotype as well as to haplotype 2. Here, the problem

lies in deciding if subnetwork IV should be joined to subnetwork II via haplotype 42 or 43. However, because haplotypes 42 and 43 come from the same geographical locality, breaking the loop along either pathway will have no influence on the nested clade analyses (Templeton *et al.* 1987; Templeton & Sing 1993).

The ambiguous connection of subnetwork V to either I or III is more difficult to resolve. Using predictions based upon coalescence theory (Crandall & Templeton 1993, Castello & Templeton 1994, Crandall 1996) the connection between haplotype 3 and 15 (via four missing haps) was considered more likely than between 5 and 15. This is because haplotype 3, the interior node of subnetwork III, is more likely to be the ancestral haplotype. It occurs at high frequency (19%) and is connected to many low-frequency haplotypes. Haplotype 5, on the other hand has a frequency of 0.014%, which although high relative to most tips in the network (0.003%), is considerably less than the frequency of the interior haplotype 3. The two connections were, however, considered alternatively when performing the nested clade analysis.

Figure 8.2b shows the nested design inferred following the rules of Templeton *et al.* (1987) and Templeton and Sing (1993), with the preferred resolution of ambiguities. The alternative, linking haplotype 15 to haplotype 5 results in a different higher level nested structure: clade 1-1 and 1-7 form 3-1, clades 1-12, 1-13, 1-14 and 1-15 form 3-4, and 3-1 plus 3-2 form 4-1, and 3-3 plus 3-4 form 4-2, with all clades now nested within a 5-step clade (5-1).

### **Nested clade analyses**

Figure 8.3 presents the results of the nested clade analyses of geographic distances performed on the nested structure illustrated in Figure 8.2b using GEODIS 2.0. Table 8.2 summarizes the resulting inferences about population structure and history inferred from the statistical results of the GEODIS analyses of the preferred (Fig. 3) and alternative nesting structures using the most recent inference key. The dominant evolutionary mechanism shaping genetic variation within the *N. olivacea/obscura* complex as identified by the NCA is one of range expansion (Table 8.2). At higher (therefore older) nesting levels a fragmentation

event between the central Kenyan highlands and Mt. Namuli (northern Mozambique) was inferred. Analyses of the alternative network (subnetwork V connected to subnetwork I) resulted in very similar NCA inferences (Table 8.2). Results differed in that subnetwork V, restricted to the Vumba Mts in Zimbabwe, is now historically linked with the northern Eastern Arc Mts and the highlands of Malawi and Mozambique via a contiguous range expansion. However, this expansion remains nested within a range expansion incorporating central and western Africa (clade 4-1), as suggested when subnetwork V is connected to subnetwork III (preferred nesting structure, Fig. 8.2b, Table 8.2).

### Mismatch distributions

Significant negative values for Tajima's  $D$  and Fu's  $F$  tests indicate that observed haplotype frequencies within the defined populations deviate from mutation-drift equilibrium and the mismatch profile is unlikely to have resulted from selective neutrality associated with a long-term stable population size. As detected from the NCA, the above tests and mismatch profiles suggest recent demographic changes within the geographical range of *N. olivacea/obscura* (Table 8.3).

Nucleotide pairwise differentiation profiles or mismatch distribution plots for various hierarchical clusters of populations are summarized in Figure 8.4. Unimodal, bell-shaped mismatch profiles are assumed to be associated with a past episode of population growth following for example recent range expansion. The NCA suggested population expansion to be the predominant demographic factor shaping genetic variability in Olive Sunbirds (Fig. 8.3, Table 8.2). West Africa, the Albertine Rift and the Eastern Arc all have bell-shaped mismatch profiles and significant Tajima and Fu statistics (Fig. 8.4, Table 8.3), thus supporting a model of recent population growth following range expansion. The major peak of the Eastern Arc mismatch profile is skewed to the right relative to the West African and Albertine Rift profiles (Fig. 8.4). This suggests that Eastern Arc populations expanded earlier, and therefore *N. olivacea/obscura* has probably occurred within the Eastern Arc for a relatively longer period of time.

In four of the eight mismatch profiles, including the *N. olivacea/obscura* complex as a whole, multimodal profiles were detected. Multimodal mismatch

profiles can occur as a consequence of a large number of factors. For example, populations of constant size are expected to display multimodal patterns (Slatkin & Hudson 1991, Rogers & Harpending 1992, Harpending *et al.* 1998), but so can populations which encompass geographic sub-structuring in relation to restricted gene flow (Marjoram & Donnelly 1994), and multimodal patterns may also result from secondary contact between expanding fronts (Liebers *et al.* 2001).

In an attempt to gain insight into the underlying demographic basis of the observed multimodal mismatch profiles a series of modified models were run by removing specific haplotypes or groups of haplotypes (see Table 8.3 for specific modifications to the original model used to derive the mismatch profiles presented in Fig. 8.5). With the removal of the haplotypes restricted to the Kenyan Highlands (haplotypes 4, 52-55) and haplotype 51 from Mt. Namuli (NCA inferred fragmentation), the mismatch profile for the *N. olivacea/obscura* complex as a whole (all individuals in Fig. 8.5) follows a unimodal, bell-shaped distribution. This unimodal shape together with the highly significant *D* and *F* neutrality statistics supports a model of rapid population growth following range expansion (Fig. 8.5, Table 8.3). The removal of the West African core haplotype 3 from the Ufipa Escarpment in southwestern Tanzania reduces genetic variability among the remaining seven in this sample to zero (Ufipa Escarpment in Fig. 8.5). This suggests that the Ufipa population represents a recent colonization event, probably via contiguous range expansion from the southern Eastern Arc/Malawi Rift as suggested by the NCA. Thus, the Ufipa Escarpment forms an important point of secondary contact between the primarily west and central African lineage (subnetwork III) and the southern Eastern Arc lineage (subnetwork II, Figs 8.1 & 8.2a).

The removal of the core Kenyan highland haplotype 4 (subnetwork IV) from the Taita Hills reduces what was a multimodal mismatch distribution to a unimodal distribution (Taita Hills in Fig. 8.5) with close affinities to other populations within the northern Eastern Arc (subnetwork I). A similar result is achieved if haplotype 4 is removed from the North Pare Mnts sample. Here, as for the Ufipa Escarpment, it is likely that the multimodal mismatch profile is a consequence of secondary contact between two independent lineages that have expanded from

areas that have held populations for a long period of time: subnetwork I in the northern Eastern Arc and subnetwork IV in the Kenyan Highlands and volcanoes (Mt. Kilimanjaro, Meru and the Chyulu Hills) of Eastern Africa (Figs 8.1 & 8.2). Lastly, even with the removal of haplotype 51 from the collated southern highlands sample (Malawi + Mozambique), the mismatch profile remains multimodal (Malawi Rift in Fig. 8.5). This suggests that these populations may have remained at constant size for a long period of time (Slatkin & Hudson 1991, Rogers & Harpending 1992, Harpending *et al.* 1998) or that underlying geographic sub-structuring exists that is not detectable with the current sampling design (Marjoram & Donnelly 1994). More intensive sampling in this area will allow these hypotheses to be further explored.

## DISCUSSION

Fifty-five haplotypes (19.5%) were identified from the 282 individuals surveyed, suggesting that the small 383 bp fragment of mtDNA analyzed is sufficiently variable to permit phylogeographic analyses of the Olive Sunbird at the continental level. However, genetic divergence levels were low. Across some 9000 km, from Ghana in the northwest of Africa to KwaZulu-Natal in eastern South Africa, genetic divergence levels were of the order of 1.0 to 2.4%. Divergence levels were slightly greater between South Africa and the central highlands of Kenya (2.9%), and greatest between the central Kenyan Highlands and Ghana (4.0%). Neither currently recognized Olive Sunbird species, Eastern Olive Sunbird *Nectarinia olivacea* and Western Olive Sunbird *N. obscura*, was monophyletic using either MP or ML. Instead, genetic diversity within the *N. olivacea/obscura* complex was dominated by three star-like phylogenies (I, II and III, Fig. 8.2a), with II and III linked to I by single mutational steps, and two subnetworks (IV and V) separated from the core star-like phylogenies (I, II and III) by five to six mutational steps. A star-like pattern in which many rare (low frequency) haplotypes are connected to one common central haplotype (presumably ancestral, see Crandall & Templeton 1993) is usually regarded as indicative of a population having recently expanded in size from one or a small number of founders (Templeton *et al.* 1995). Subnetworks I, II and III conform well to this description.



The nested clade analyses (Figs 8.2b & 8.3) allow us to hypothesize a series of specific demographic events, which underlie the observed spatial and temporal structure of genetic variation in the *N. olivacea/obscura* complex (Table 8.2). The greatest haplotype diversity in the analyzed dataset resides within the Tanganyika-Malawi mountains of East Africa (24 of 55 haplotypes). This may suggest a long persistence of populations in this area. Within these mountains, three cases can be inferred of restricted gene flow leading to isolation by distance (clade 1-1, 1-12 and 2-1; tip clade has a significantly smaller  $D_c$  than interior clade, see Fig. 8.3), and one case of contiguous range expansion (clade 2-6; restricted range for the nested interior clade) (Table 8.2). Clade 1-1 encompasses subnetwork I which occurs at highest frequency within the northern Eastern Arc (Taita Hills, North and South Pare Mnts and the West and East Usambara Mnts) and the Malawi Rift area (Zomba Mnts) and northern Mozambique (Mt. Namuli). Clade 1-12 encompasses the core of subnetwork II, which occurs at highest frequency in the central and southern Eastern Arc Mnts (Uluguru, Rubeho, and Udzungwa Mnts) as well as on the Ufipa Escarpment of the Rukwa Rift in southwestern Tanzania and the Njesi Plateau of northern Mozambique. These two clades are united in clade 2-1. Subnetwork II also includes haplotype 46, which occurs at relatively high frequency (4%) and is connected to the core of subnetwork II (hap 2) by an internal haplotype cluster (haps 48,49 and 50, Fig. 8.2a), forming clade 2-6 (Fig. 8.2b). The NCA suggests that the genetic variation encompassed within clade 2-6 is derived from a contiguous range expansion and subsequent isolation (a contiguous range expansion is defined as a non-recurrent historical event, see Templeton 1998).

Examination of the spatial distribution of haplotypes 45-50 makes it difficult to identify a likely geographic origin for these haplotypes, as they are represented in low frequency from some 14 localities (Table 8.1). Many of these localities are coastal forests (e.g. Arabuko-Sokoke in Kenya, Gombero and Lulago in northeastern Tanzania and the Ruvu drainage in eastern Tanzania), as well as low-lying montane forest, e.g. Lutindi in the East Usambara Mnts. This suggests limited gene flow between coastal and highland forests in this region.

The age of a clade is the age of the oldest clade nested within it and tends to increase on average when going from one clade level to the next (Templeton *et al.* 1995). Thus, the non-recurrent historical range expansion detected by the NCA in clade 2-6 (clade 1-13 vs. 1-14, Fig. 8.3) may, to some extent, have become swamped by the recurrent restricted gene flow within the Eastern Arc Mnts. This provides a good example of the utility of NCA in being able to separate recurrent processes shaping population structure from population history. Clades 2-1 and 2-6, together with haplotypes 42 and 43 (clade 2-7) are combined in clade 3-1, where the inferred demographic event is again restricted gene flow with isolation by distance.

The detection of two distinct evolutionary lineages (subnetwork I & II, Fig. 8.1 & 8.2a) within the Eastern Arc Mnts for the Olive Sunbird is not without precedent. Bowie *et al.* (submitted), in an analysis of species boundaries within the Eastern Double-collared Sunbird (*N. mediocris*) species complex, detected five independent lineages within eastern Africa: *N. mediocris* from the Kenyan highlands, *N. usambaricus* restricted to the Taita, Pare and Usambara Mnts, *N. moreaui* in the Nguru, Ukaguru, Rubeho and northern Udzungwa Mnts, *N. loveridgei* endemic to the Uluguru Mnts and *N. fuelleborni* from the central Udzungwa highland to the Rukwa and Malawi Rift Mnts. *Nectarinia moreaui*, *N. loveridgei* and *N. fuelleborni* form the sister clade to *N. mediocris* and *N. usambaricus*, suggesting that the 100 km of low-lying savanna between the Usambara and Nguru Mnts, effectively separating the northern part of the Eastern Arc from the central and south mountain ranges, is an old barrier to gene flow. A similar subdivision is also seen in the mountain greenbul (*Andropadus tephrolaemus* group, see Roy *et al.* 1998).

In a broad analysis of distributional patterns of 28 forest species, most of which are endemic to the Eastern Arc, Cordeiro (1998) identified the Nguru, Nguu and Rubeho Mnts as being impoverished and distinctly nested (*sensu* Patterson 1987) montane communities within the Eastern Arc. This suggests that even for fairly mobile species, crossing the gap between the Nguru and Usambara Mnts is difficult, effectively restricting gene flow. Thus for the Olive Sunbird, a fairly mobile forest generalist (Cheke *et al.* 2001), it is perhaps surprising that two

distinct evolutionary lineages were detected within the Eastern Arc. Therefore, it seems likely that the Nguru-Usambara gap has and continues to act as a barrier to gene flow, effectively explaining the isolation by distance pattern detected by the NCA (Fig. 8.3, Table 8.2) and illustrated in Figure 8.1.

A contiguous range expansion was inferred from the NCA analysis (Fig. 8.3, Table 8.2) for clade 2-2 and is hypothesized to underlie the core of the star-like phylogeny representing subnetwork III (Fig. 8.2a). Clade 2-2 encompasses the largest geographic range of any 2-step clade, stretching from the Albertine Rift, west through the Congo to Gabon, Cameroon and up to Ghana, east to western Kenya, as well as south and east through Zambia to the Zimbabwe highlands and the coastal forests of eastern South Africa. Inclusion of relatively divergent haplotypes from Ghana (Clade 2-4) and the Zimbabwe highlands (clade 2-5) within clade 3-2 in the NCA analysis suggested a pattern of restricted gene flow with isolation by distance, although an expanding population model was supported by the mismatch (Fig. 8.4) and neutrality analyses (Table 8.3).

The limited divergence among haplotypes from Ghana to South Africa encompassed within subnetwork III (Fig. 8.2a) and clade 3-2 (Fig. 8.2b) has important implications for the understanding of evolutionary processes which have shaped avian diversification patterns within western and southern Africa. The work of Beresford (2002) and Beresford and Cracraft (1999) demonstrates that avian lineages endemic to the lowland forests which stretches from the Albertine Rift in central Africa, west to Gabon and Cameroon and up through Nigeria across the Dahomey gap to Ghana and further west, have a complex genetic structure and have probably been subject to repeated vicariance events extending well back into the upper Tertiary. Others have interpreted the nested pattern of species richness and endemism in the Guinea-Congo forest region as reflecting isolation in forest refuges during “glacial periods” (e.g. Moreau 1966, Diamond & Hamilton 1980, Crowe & Crowe 1982, Prigogine 1987, Hamilton *et al.* 2001). It is thus surprising that in the present study no genetic structure was found among populations of *N. olivacea/obscura* from Ghana to northwestern Kenya. One possible explanation could be that the mitochondrial marker we used (ND3) does not provide sufficient mutational resolution to detect such

structure. However, a more likely explanation may be that because the Olive Sunbird inhabits a wide range of evergreen vegetation (such as forest edge, second-growth, riparian thickets and dense parts of woodland savanna), like most other forest birds with a similar wide range, and unlike the interior forest species studied by Beresford (2002) and Beresford and Cracraft (1999), the Olive Sunbird may be more prone to dispersal. Lens *et al.* (2002) in a long-term mark-recapture study of forest bird movements among habitat fragments in the Taita Hills demonstrated that of the seven species studied the Olive Sunbird was most prone to moving among habitat fragments.

The NCA (Fig. 8.3, Table 8.2) suggests that a contiguous population expansion, probably from the Albertine Rift westwards to western and northwestern Africa, underlies the genetic pattern observed. The largest divergence value within subnetwork III is 2.4%. Using the 2.0% per million years calibration of Shields and Wilson (1987) (also reported by Wood & Krajewski 1996, Friesen & Anderson 1997), this places the maximum age of the expansion event at approximately 1.2 million years before present (BP), and the Kimura 2-parameter calibration value of 1.6% per million years, derived from Fleischer *et al.* (1998), dates the divergence to roughly 1.5 million BP.

deMenocal (1995), summarizing knowledge about climate change in Africa over the last *ca.* 5 million years, found marked peaks in eolian dust deposition in deep sea cores at 2.8, 1.7 and 1.0 million years BP, suggestive of a cooler and a more arid climate. Between 3 and 0.8 myrs BP African climate was characterized by high-frequency, but low-amplitude cycles (deMenocal 1995, Kennett 1995), which would most likely have coincided with high forest-dynamics, when forest (at least outside the main Guinea-Congolian forest tract) was repeatedly expanding and contracting, thus providing frequent opportunities for expansion of forest-edge/thicket species such as the Olive Sunbird.

Curiously, NCA and the structure of subnetwork III suggest that the range expansion into West Africa also comprised a southward expansion incorporating the woodlands of Zambia, the currently isolated forests of the Zimbabwe highlands, and coastal South Africa (Fig. 8.2b and 8.3, Table 8.2). This suggests that southern Africa had strong links with the fauna of West Africa 1.2 to 1.5

million years BP. Such a connection is supported by evidence from marine pollen records, which document a southern expansion of West African vegetation zones during the Plio-Pleistocene (Dupont & Hoogheemstra 1989).

Subnetwork IV is restricted to the central Kenyan highlands, but includes the volcanic Chyulu Hills in southeastern Kenya, Mt. Meru and Mt. Kilimanjaro in northeastern Tanzania, as well as one isolated haplotype from Mt. Namuli in northern Mozambique. The null hypothesis of no geographical associations within the nesting clade cannot be rejected for any 1-step or 2-step clades in the NCA analysis (Fig. 8.3). However, the small cluster of rare haplotypes surrounding haplotype 4 (Fig. 8.2a) suggests that with more intensive sampling of the central Kenyan and crater highlands (Fig. 8.1) a range expansion event may be detected. This is likely considering the geological history of eastern Africa. The volcanoes of Mt. Meru and Mt. Kilimanjaro are estimated to be at most 1 million years old, and may be considerably younger (Griffiths 1993), and the Chyulu Hills may be no more than 40 000 years old (Moreau 1966). All three of these localities are closely linked with haplotypes detected within the Aberdares of the central Kenyan Highlands (hap. 4), suggesting colonization from the central Kenyan Highlands. Indeed, the mismatch distribution strongly suggests a recent range expansion (Table 8.3, Fig. 8.4). Still further support is provided by the detection of haplotype 4 (interior) within the Taita Hills, which geomorphologically forms the northern-most extreme of the Eastern Arc Mnts (Griffiths 1993). The Taita Hills do contain a high frequency of haplotypes characteristic of the northeastern Eastern Arc (subnetwork I, Fig. 8.2). However, three individuals from the 19 sampled had a genotype characteristic of the Kenyan highlands. This suggests secondary contact between the Kenyan highland lineage (subnetwork IV) and the northern Eastern Arc lineage (subnetwork I). This is further support by the clear bimodal shape of the mismatch distribution (Fig. 8.4) and non-significant neutrality tests (Table 8.3), which with the removal of the Kenyan highland haplotypes assumes a unimodal distribution (Fig. 8.5). A similar secondary contact occurs in the North Pare Mnts, where one individual sampled from Mt. Dido had a typical Kenyan Highland mtDNA genotype (Table 8.1).

At the 3-step clade level a fragmentation event is inferred within clade 3-3, suggesting that haplotype 51 from Mt. Namuli represents a historical connection between the Kenyan Highlands and the highlands of northern Mozambique. Furthermore Mt. Zomba shares greater affinities with subnetwork I, which is primarily restricted to the northern Eastern Arc (Taita, Pare and Usambara Mnts), than with the geographically more proximate southern Eastern Arc (Nguru, Rubeho, Uluguru and Udzungwa Mnts), which forms the core of subnetwork II (Fig. 8.2). These disjunctions are difficult to explain, but the NCA (Fig. 8.3, Table 8.2) and multimodal mismatch profiles (Figs 8.4 & 8.5, Table 8.3) suggests they reflect old population fragmentation. The Long-billed Apalis '*Apalis*' *moreaui*, which has uncertain evolutionary affinities and whose placement in *Apalis* is controversial (Sibley & Monroe 1990), has two relictual populations, one within the East Usambara Mnts and one on the Njesi Plateau. Similarly the understory Dapplethroat (*Arcanator orostruthus*) and Swynnerton's Robin (*Swynnertonia swynnertoni*) have widely sundered populations, with *Arcanator* occupying forest on the East Usambara, Udzungwa Scarp and Mt. Namuli, and *Swynnertonia* the East Usambara, Udzungwa highlands, Zimbabwe highlands and central Mozambique. These widely separated populations of apparently highly sedentary species suggest a long and complex pattern of origin, now also reflected within the higher (and therefore older) nested clades of the *N. olivacea/obscura* complex. Whether these disjunct populations have a common vicariant origin remains to be established.

#### **Gene-tree versus species tree, or morphology versus molecules**

The species status of *N. olivacea* and *N. obscura* rests on the assumption that the presence of pectoral tufts in females is a diagnostic, autapomorphy of eastern birds (Clancey 1992-1993). This split remains controversial and is exemplified by the debate over the taxonomic assignment of Olive Sunbirds on Zanzibar Island off the east coast of Africa. Female Olive Sunbirds on Zanzibar are thought not to be tufted, and therefore related to central and western African populations, which are also not tufted, as opposed to the tufted, but geographically more proximate east and southern African populations. This represents a remarkable geographical discontinuity, so pronounced that Fry (2000) places the Zanzibar population (subspecies *granti*) with tufted *N. olivacea*

purely on the grounds of geographical proximity. Hence, whereas Fry (2000) splits *N. olivacea/obscura*, he renders *N. olivacea* polyphyletic by including *granti* in *N. olivacea* instead of *N. obscura*.

Cheke *et al.* (2001) elaborate on this by addressing Pakenham's (1979) observation that some doubt remains about the absence/presence of tufts in female *granti*. Cheke *et al.* (2001) argue that the main source of doubt originates from a non-breeding tufted female collected on Zanzibar (NHM1929.6.27.87) classified as *granti* by the collector (J. H. Vaughan), which they regard as a representative of the mainland subspecies, *changamwensis*. This would make *granti* and *changamwensis* (and by extension *N. olivacea* and *N. obscura*) sympatric on Zanzibar. They argue that the case for sympatry on Zanzibar is further supported by the presence of another bird (NHM1947.5.62) which, while unsexed by the collector (R.H.W. Pakenham), has a fully ossified skull (and is therefore adult), is tufted, and can be considered a female *changamwensis* due to its throat coloration and anterior nostril width. Much rests on the assumption that the two birds above were accurately sexed using meristic data. Purely on this basis, a convincing argument can be made that more collecting with accurate sexing is urgently needed to support sympatry between *granti* and *changamwensis* on Zanzibar, and by extension to provide convincing evidence for splitting *N. olivacea/obscura*.

In this study, the South African haplotypes from tufted female populations group with those of western and central African populations of non-tufted females (subnetwork III, Fig. 8.2a). In addition, the Ufipa Escarpment population (where females are thought to lack tufts) has a mixture of southern Eastern Arc haplotypes (subnetwork II) derived from tufted female populations and western haplotypes (subnetwork III) characteristic of populations with non-tufted females. This suggests that either the split between *N. olivacea/obscura* is not valid and the presence/absence of a yellow tuft in females is a polymorphism (possibly under selection) or that the mtDNA gene-tree is decoupled from the species tree.

The decoupling of a gene-tree from a species tree may result from different evolutionary processes, e.g. vicariance, dispersal, directional selection and hybridization acting at different points through time and space. Thus, the presence of yellow pectoral tufts in female *N. olivacea* but not *N. obscura* may be under directional selection and may be evolving faster than the neutral mtDNA marker investigated. Consequently, the mtDNA gene-tree may reflect historical rather than ongoing population-level processes (Templeton *et al.* 1995, Templeton 1998). Alternatively, the reverse may be true, whereby evolutionary processes such as hybridization and lineage introgression may be swamping historical structure (Grant & Grant 1995). The NCA results indicate that multiple range expansions underpin much of the observed genetic structure within *N. olivacea/obscura*, and the mismatch profiles suggest that secondary contact has occurred between eastern and western lineages within the Ufipa Escarpment (II and III) and possibly Zimbabwe (alternative network, Table 8.2), as well as between eastern lineages in the Kenyan Highlands and northern Eastern Arc (Subnetworks IV and I). However, whereas hybridization seems likely, this cannot explain why within the Ufipa Escarpment or Zimbabwe, tufted females are unknown despite the presence of mtDNA genotypes characteristic of populations containing tufted females. One possible explanation is that the development of a sexual display tuft in females is a recently acquired trait of eastern populations, which is acting as a marker of female fitness. In a mating system where females are competing for male attention, pectoral tufts may be under directional selection and the mixture of characteristic ‘tufted’ and ‘non-tufted’ genotypes on the Ufipa Escarpment may reflect the extremities of a selective sweep on tufts in females with origins in eastern or southern Africa. Theory suggests that mutual ornamentation is expected when sex roles are similar (for example in year-round territories, with biparental care, as expected in eastern African rainforests with a predictable rainfall pattern), as well as when females are competing due to either competition for males or for resources among themselves (see Amundsen 2000) or with other sunbird species. Which of the above hypotheses underlie the evolutionary basis for the presence/absence of lateral yellow pectoral tufts in female Olive Sunbirds cannot be answered using the data in this study and awaits a more detailed study of mating systems and inheritance of pectoral tufts in ‘*N. olivacea*’ and ‘*N. obscura*’.



**Table 8.1.** Taxonomic classification, sampling localities, geographical coordinates, sample size and haplotypes identified at each sampling locality. \* Source codes: FMNH = Field Museum of Natural History, ZMUC = Zoological Museum of the University of Copenhagen, LSUMZ = Museum of Louisiana State University, MNHN = Muséum National d'Histoire Naturelle, AMNH = American Museum of Natural History, FITZ = Percy FitzPatrick Institute of African Ornithology, Lens = Luc Lens, University of Ghent.

<b>Taxon</b>	<b>Locality</b>	<b>Region</b>	<b>Country</b>	<b>Coordinates</b>	<b>n</b>	<b>Source*</b>	<b>Haplotypes</b>
<i>Nectarinia obscura</i>							
<i>cephaelis</i>	Assin-Foso	Central	Ghana	05.33N, 01.22W	11	FMNH	3(7) 22(1) 25(1) 31[1] 32[1]
<i>cephaelis</i>	SW Ghana	South-western	Ghana	05.00N, 01.00W	4	ZMUC	3(4)
<i>cephaelis</i>	Above Etome	Central Highlands	Cameroon	04.02N, 09.07E	2	LSUMZ	3(1) 28[1]
<i>cephaelis</i>	Nditam	Central Highlands	Cameroon	04.00N, 09.00E	1	MNHN	22(1)
<i>cephaelis</i>	Doussala	Ogooue-Maritime	Gabon	02.28S, 10.48E	3	FMNH	3(2) 22(1)
<i>cephaelis</i>	Dzanga-Sangha	Sangha-Mbaéré	Central Afr. Rep.	02.92N, 16.25E	1	AMNH	3(1)
<i>ragazzii</i>	Mambasa	Haut-Zaire	Demo. Rep. Congo	01.00N, 28.58E	4	FMNH	3(3) 19(1)
<i>ragazzii</i>	Lwero	Kivu	Demo. Rep. Congo	02.17S, 29.72E	5	ZMUC	3(5)
<i>ragazzii</i>	Nteko	Kisoro	Uganda	01.03S, 29.62E	4	FMNH	3(1) 24[1] 25(2)
<i>ragazzii</i>	Nyabyeye	Masindi	Uganda	01.67S, 31.54E	2	FMNH	3(1) 21[1]
<i>ragazzii</i>	Ngoto	Kabale	Uganda	00.88S, 29.73E	6	FMNH	3(6)
<i>ragazzii</i>	Sese Island	Lake Victoria	Uganda	01.00S, 32.00E	1	FMNH	3(1)
<i>ragazzii</i>	Toro Game	Kabale	Uganda	01.08S, 30.42E	24	ZMUC	3(19) 20[2] 26[1]

	Res.						29[1] 30 [1]
<i>ragazzii</i>	Queen Elizabeth	Kabale	Uganda	01.20S, 30.50E	2	ZMUC	3(2)
<i>ragazzii</i>	Kakamega	Western Kenya	Kenya	00.17N, 34.53E	1	FITZ	56 [1]
<i>ragazzii</i>	Mbizi	Tabora	Tanzania	07.90S; 31.70E	8	ZMUC	2(7) 3(1)
<i>ragazzii</i>	Kifugila	Northern	Zambia	09.31S, 29.05E	4	FITZ	23[2] 27[2]
<i>sclateri</i>	Mnt. Vumba	E. Highlands	Zimbabwe	19.00S, 32.50E	3	FITZ	15[1] 16[1] 17[1]
<u><i>Nectarinia olivacea</i></u>							
<i>neglecta</i>	Gatamaiyu	Aberdares	Kenya	00.93S, 36.67E	4	FITZ	4(2) 52[1] 55[1]
<i>neglecta</i>	Chyulu Hills	Chyulu	Kenya	02.58S, 37.83E	10	FITZ	4(9) 54[1]
<i>neglecta</i>	Kahe	Moshi	Tanzania	03.50S, 37.40E	1	ZMUC	4(1)
<i>neglecta</i>	Simba	Mt. Kilimanjaro	Tanzania	03.10S, 37.40E	2	ZMUC	4(1) 53[1]
<i>neglecta</i>	Laikinoi	Mt. Meru	Tanzania	03.20S, 36.70E	1	ZMUC	4(1)
<i>changamwensis</i>	Taita Hills	Taita	Kenya	03.42S, 38.33E	19	Lens	1(11) 4(3) 5[4] 11[1]
<i>changamwensis</i>	Arabuko-Sokoke	Malindi	Kenya	03.33S, 39.92E	10	FITZ, ZMUC	1(8) 2(1) 46(1)
<i>changamwensis</i>	Mt. Kindoroko	North Pare	Tanzania	03.73S, 37.65E	2	ZMUC	1(2)
<i>changamwensis</i>	Mt. Dido	North Pare	Tanzania	03.80S, 37.60E	2	ZMUC	2(1) 4(1)
<i>changamwensis</i>	Ngofi	North Pare	Tanzania	03.75S, 37.50E	1	ZMUC	2(1)

<i>changamwensis</i>	Mt. Shengena	South Pare	Tanzania	04.30S, 37.90E	1	ZMUC	1(1)
<i>changamwensis</i>	Mafi Hill	Tanga	Tanzania	04.93S, 38.15E	10	ZMUC	1(9) 2(1)
<i>changamwensis</i>	Gombero	Tanga	Tanzania	04.97S, 39.00E	9	ZMUC	1(5) 8(1) 13[1] 46(2)
<i>changamwensis</i>	Lulago	Tanga	Tanzania	05.62S, 37.46E	8	ZMUC	1(3) 2(1) 8(2) 46(2)
<i>changamwensis</i>	Pindirola	Tanga	Tanzania	09.33S, 29.33E	1	ZMUC	2(1)
<i>changamwensis</i>	Mazumbai	West Usambara	Tanzania	04.80S, 38.50E	1	ZMUC	2(1)
<i>changamwensis</i>	Ambangulu	West Usambara	Tanzania	05.00S, 38.42E	1	FMNH	2(1)
<i>changamwensis</i>	Magamba	West Usambara	Tanzania	04.70s, 38.30E	1	ZMUC	1(1)
<i>changamwensis</i>	Kambai	East Usambara	Tanzania	05.00S, 38.67E	1	ZMUC	7[1]
<i>changamwensis</i>	Amani	East Usambara	Tanzania	05.10S, 38.60E	3	ZMUC	1(2) 6[1]
<i>changamwensis</i>	Lutindi	East Usambara	Tanzania	05.10S, 28.40E	1	ZMUC	45[1]
<i>alfredi</i>	Mhonda	Nguru	Tanzania	06.12S, 37.53E	4	ZMUC	1(1) 9(1) 46(2)
<i>alfredi</i>	Mt Kanga	E of the Nguru	Tanzania	06.00S, 37.70E	1	ZMUC	1 (1)
<i>alfredi</i>	Mamirwa	Ukaguru	Tanzania	06.20S, 36.80E	3	ZMUC	1(2) 2(1)
<i>alfredi</i>	Madizini	Morogoro	Tanzania	07.20S, 36.77E	5	ZMUC	1(1) 2(3) 50(1)
<i>alfredi</i>	Ukwiva	Rubeho	Tanzania	07.08S, 36.63E	5	ZMUC	1(1) 2(3) 50(1)
<i>alfredi</i>	Magalisa	Rubeho	Tanzania	07.15S, 36.42E	2	ZMUC	2(2)
<i>alfredi</i>	Mafwemiro	Rubeho	Tanzania	06.83S, 36.57E	3	ZMUC	2(2) 10(1)
<i>alfredi</i>	Chamanyani	Morogoro	Tanzania	07.00S, 36.50E	3	ZMUC	2(2) 46(1)

<i>alfredi</i>	Matundu	Morogoro	Tanzania	08.09S, 36.23E	3	ZMUC	2(1) 38(1) 49(1)
<i>alfredi</i>	Kilombero	Mbeye	Tanzania	08.20S, 36.20E	1	ZMUC	49(1)
<i>alfredi</i>	Mahenge	Mahenge	Tanzania	08.70S, 36.78E	3	ZMUC	37[1] 40[1]41[1]
<i>alfredi</i>	Selous	Selous	Tanzania	09.00S, 38.00E	1	ZMUC	2(1)
<i>alfredi</i>	Tegetero	Uluguru	Tanzania	06.09S, 37.70E	9	ZMUC	1(4) 2(4) 47[1]
<i>alfredi</i>	Kungwe	Uluguru	Tanzania	06.87S, 37.92E	6	ZMUC	1(1) 2(4) 44(1)
<i>alfredi</i>	Ngambaula	Uluguru	Tanzania	06.50S, 37.80	2	ZMUC	2(1) 48[1]
<i>alfredi</i>	Kawemba	Iringa	Tanzania	07.80S, 35.80E	2	ZMUC	34[2]
<i>alfredi</i>	Ndundulu	Iringa	Tanzania	07.50S, 36.25E	3	ZMUC	2(2) 38(1)
<i>alfredi</i>	Kihansi-Gorge	Iringa	Tanzania	08.40S, 36.30E	4	ZMUC	2(1) 33[1] 42(1) 43[1]
<i>alfredi</i>	Kitemele	Iringa	Tanzania	08.16S, 36.03E	11	ZMUC	1(1) 2(9) 46(1)
<i>alfredi</i>	Udzungwa	Iringa	Tanzania	08.20S, 35.70E	7	ZMUC	2(6) 35[1]
<i>alfredi</i>	Uhafiwa	Iringa	Tanzania	08.05S, 35.50E	15	ZMUC	2(11) 36[2] 46(1) 50(1)
<i>alfredi</i>	Mnt. Zomba	Mt. Zomba	Malawi	15.40S, 35.30E	2	FITZ	1(1) 10(1)
<i>alfredi</i>	Mnt. Namuli	Mt. Namuli	Mozambique	15.30S, 37.00E	5	FITZ	1(3) 39[1] 51[1]
<i>alfredi</i>	Mnt. Jesi	Mt. Jesi	Mozambique	13.00S, 35.00E	1	FITZ	44(1)
<i>olivacina</i>	Rondo Plateau	Lindi	Tanzania	10.12S, 39.17E	1	ZMUC	1(1)
<i>olivacina</i>	Ruvu	Lindi	Tanzania	07.00S, 37.17E	1	ZMUC	14[1]

<i>olivacina</i>	Ruvu South	Lindi	Tanzania	07.00S, 37.67E	3	ZMUC	2(1) 46(2)
<i>olivacea</i>	Maltino	Kwazulu-Natal	South Africa	29.00S, 30.50E	1	FITZ	18[1]

---

University of Cape Town

**Table 8.2.** Interpretation of the results of Figure 8.3 using the inference key of Templeton *et al.* (1995) and Templeton (1998). The most recent version of the key is available from [http://bioag.byu.edu/zoology/crandall\\_lab](http://bioag.byu.edu/zoology/crandall_lab). Demographic inferences are presented both for the preferred nested structure (8.2b) as well as the alternate nesting structure (subnetwork V linked to hap. 5, Fig. 8.2a). One step clades remain the same for both nesting structures. \* Reference is made relative to labelled star-like phylogenies in Figure 8.2a.

Clade	Structure*	Chain of inference	<u>Geographical distribution</u>	Demographic event inferred
<b><u>Preferred nested structure</u></b>				
1-1	Core of subnetwork I	1-2-3-4-NO	Eastern Arc, Malawi & Mozambique	Restricted gene flow with isolation by distance
1-12	Core of subnetwork II	1-2-11-17-4-NO	Eastern Arc, Malawi & Mozambique	Restricted gene flow with isolation by distance
2-1	Core of subnetworks I & II	1-2-11-17-4-NO	Eastern Arc, Malawi & Mozambique	Restricted gene flow with isolation by distance
2-2	Core of subnetwork III	1-2-11-12-NO	West Africa to Albertine Rift, down through Zambia to Zimbabwe and South Africa	Contiguous range expansion
2-6	Haps 45-50	1-2-11-12-NO	Mainly Kenyan & Tanzanian lowland forests	Contiguous range expansion
3-1	Whole of subnetworks I & II	1-2-11-17-4-NO	Kenya, Eastern Arc & highlands of Malawi, Mozambique to Zimbabwe	Restricted gene flow with isolation by distance
3-2	Whole of subnetworks III & V	1-2-11-17-4-NO	West Africa to Albertine Rift, down through Zambia to Zimbabwe and South Africa	Restricted gene flow with isolation by distance
3-3	Whole of subnetwork IV	1-2-3-4-9-NO	Kenya plus Mt. Namuli	Past fragmentation

Total	subnetworks I to V	1-2-11-12-NO	African continent	Contiguous range expansion
<b><u>Alternative nested structure</u></b>				
2-2	Core of subnetwork III	1-2-11-12-NO	West Africa to Albertine Rift, down through Zambia to Zimbabwe and South Africa	Contiguous range expansion
2-6	Haps 45-50	1-2-11-12-NO	Mainly Kenyan & Tanzanian lowland forests	Contiguous range expansion
3-1	Whole of subnetworks I & V	1-2-11-12-NO	Northern Eastern Arc, Malawi, Mozambique and Zimbabwe	Contiguous range expansion
3-3	Whole of subnetwork IV	1-2-3-4-9-NO	Kenya plus Mt. Namuli	Past fragmentation
3-4	Whole of subnetwork II	1-2-3-4-NO	Southern Eastern Arc, Malawi and Mozambique	Restricted gene flow with isolation by distance
4-1	Whole of subnetworks I, III & V	1-2-11-12-NO	West Africa to the Albertine Rift, down through Zambia to Zimbabwe and South Africa, and the northern Eastern Arc	Contiguous range expansion
4-2	Whole of subnetworks II & IV	1-2-11-12-YES	Kenya, southern Eastern Arc and highlands of Malawi and Mozambique	Long distance dispersal or contiguous range expansion
Total	subnetworks I to V	1-2-3-4-NO	African continent	Restricted gene flow with isolation by distance

**Table 8.3.** Measures of selective neutrality (Tajima's  $D$  and Fu's  $F$ ) and significant values based on 10 000 permutations for various groupings of populations of the *Nectarinia olivacea/obscura* complex using two different models (see text for details of models). Significant negative values indicate populations out of equilibrium, suggesting they have recently undergone recent demographic changes.

Categories	Original model				Modified model				Model modifications
	$D$	( $P$ )	$F$	( $P$ )	$D$	( $P$ )	$F$	( $P$ )	
All individuals	-1.9	0.003	-26.1	0.000	-2.3	0.000	-27.5	0.000	remove haps 4, 51-55
Kenyan Highlands	-1.9	0.005	-2.7	0.003	—	—	—	—	—
Western Africa	-1.6	0.041	-1.7	0.098	—	—	—	—	—
Albertine Rift	-2.1	0.001	-8.2	0.000	—	—	—	—	—
Eastern Arc	-2.0	0.003	-19.4	0.000	—	—	—	—	—
Mbizi Highlands	-1.3	0.099	0.7	0.487	N/A	N/A	N/A	N/A	remove hap. 3
Southern Highlands	-1.4	0.066	-0.1	0.447	-0.9	0.260	-0.9	0.150	remove hap. 51
Taita Hills	-0.0	0.539	3.2	0.925	-0.3	0.370	-0.3	0.290	remove hap. 4
N/A Neutrality tests are no longer applicable as there is now only one haplotype in the population.									



**FIGURE LEGENDS**

**FIG 8.1.** (A) Geographical distribution of *Nectarinia olivacea* and *N. obscura*. Circled islands are *N. obscura*. (B) Map, with montane circle enlarged showing the major regions sampled. Bar charts represent the frequency with which haplotypes from each of the five subnetworks in Figure 8.2a are present in each region.

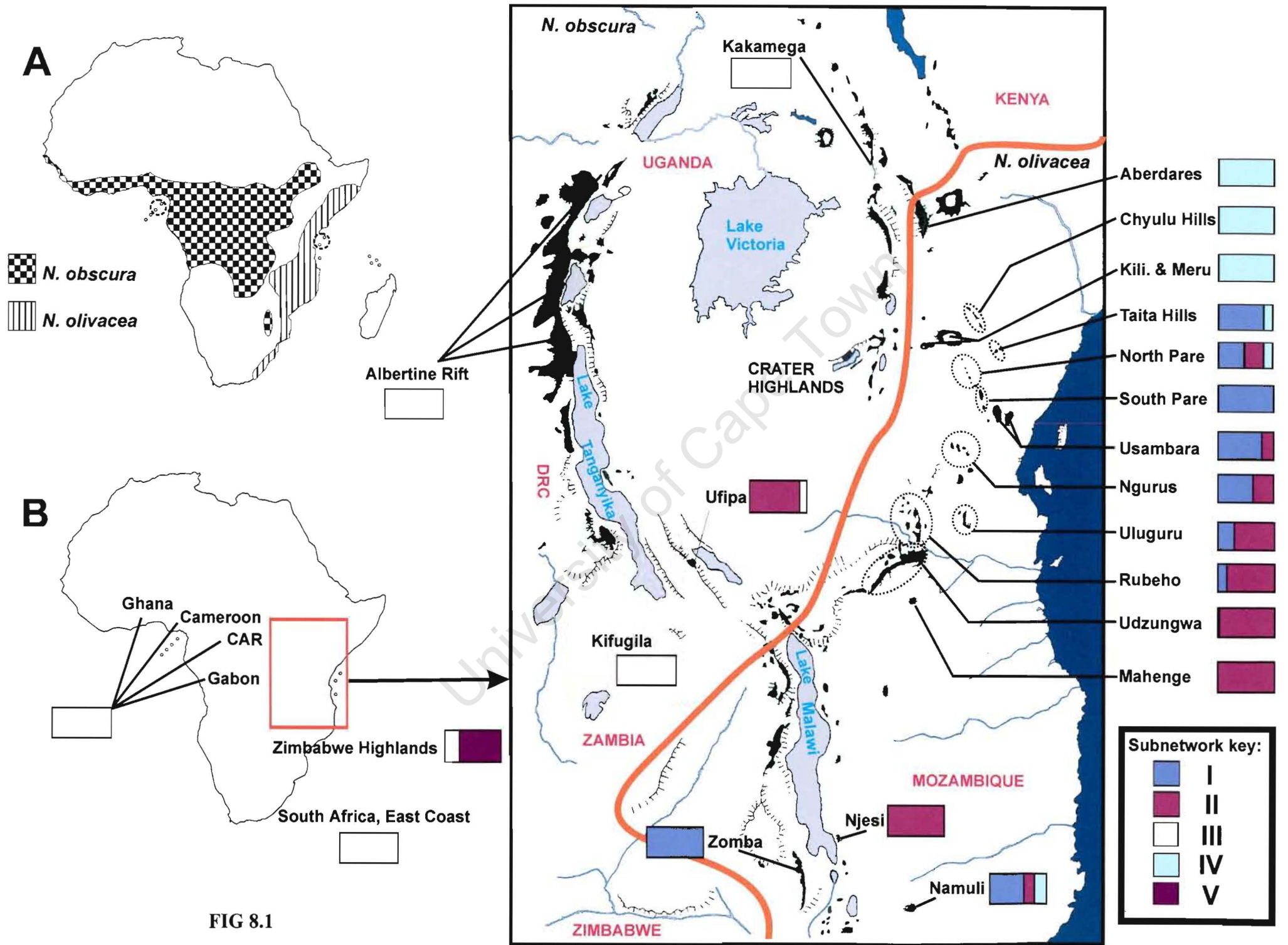
**FIG 8.2(a).** Statistical parsimony network for the 55 haplotypes of *N. olivacea/obscura* sampled. Each line in the network represents one mutational step. The five haplotypes with highest frequency are represented within circles, the area which is proportional to the frequency with which the haplotype was sampled. Empty haplotypes represent intermediate haplotypes that are necessary to link all observed haplotypes to the network. The intermediate haplotypes are either unsampled or have become extinct. Dotted lines and arrows point to ambiguities within the network, where there is more one parsimonious way to make a connection. Five subnetworks can be identified (I-V). Subnetworks II and III are connected to subnetwork I by a single step, IV is connected to II by 6 steps and V to I or III, by 6 steps. The frequency and geographical association of each of the subnetworks is illustrated in Fig. 8.1. **(2b).** The preferred resolution of the ambiguities for the haplotype network in Fig. 8.2a, with associated nested design (A) 1-step clades (B) 2-step and higher level clades, used for statistical analyses (see text).

**FIG 8.3.** Summary of the statistical results of the nested clade analysis of geographical distances for the 55 mtDNA haplotypes of *N. olivacea/obscura*. Haplotype numbers are the same as those on Table 8.1 and Figure 8.2. An I or t next to a haplotype number corresponds is designation as an interior or tip, respectively. Haplotypes nested in 1-step clades are grouped in boxes as represented in Fig. 8.2a. Higher level clades are represented as one moves down the figure. In each box, the clade distance ( $D_c$ ) and nested clade distance ( $D_n$ ) calculated for each clade within the nested group is shown, as well as the average difference in distances between interior and tip clades for  $D_c$  and  $D_n$  ( $[Int-Tip]_c$ ) and ( $[Int-tip]_n$ ), respectively. Significantly small or large distances (at  $\alpha=0.05$ ) are underlined and characterised by s or L, respectively.

**FIG 8.4.** Mismatch profiles for selected geographical categories. The histogram represents the observed distribution and the line the expected Poisson distribution for a growing population under the same mean.

**FIG 8.5.** Mismatch profiles for the modified model parameters (see Table 8.3) for selected geographical categories. The histogram represents the observed distribution and the line the expected distribution for a growing population under the same mean.

University of Cape Town



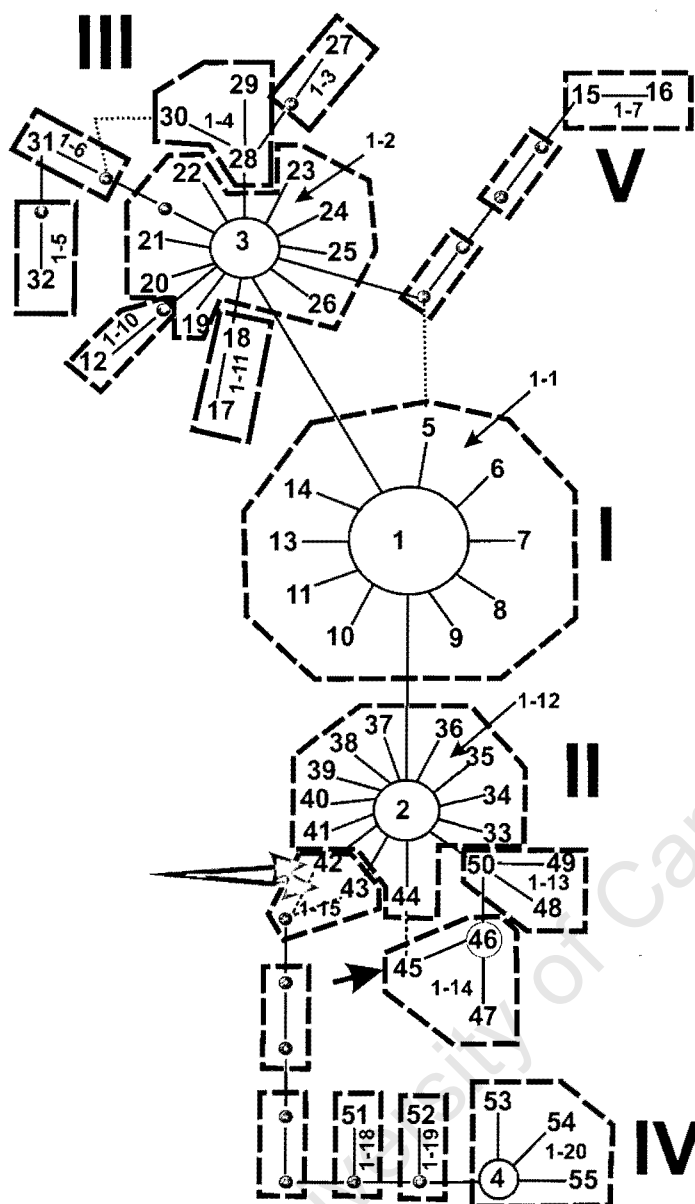
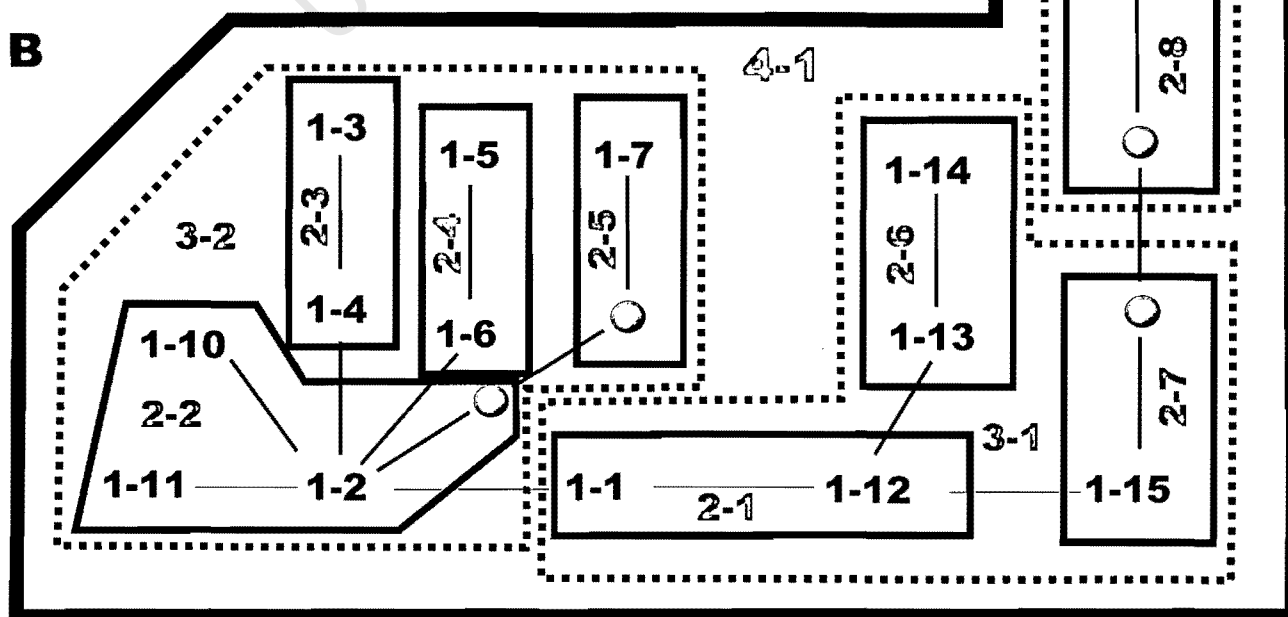
**A****B**

FIG 8.2

0-step	1i	5i	6i	7i	8i	9i	10i	11i	13i	14i	2i	3i	34i	35i	36i	37i	38i	39i	40i	41i	44i
Dc	366	0	0	0	0	0	338	0	0	0	263	0	0	0	0	0	48	0	0	0	82
Dn	367	355	180	180	180	97	790	355	180	81	291	80	80	80	80	47s	128	750L	47s	47s	498
(Int-Tip)c																					
(Int-Tip)n																					
1-step					1-1i											1-12i					
Dc					356											291					
Dn					425L											298					
(Int-Tip)c																					
(Int-Tip)n																					
2-step																					
Dc																					
Dn																					
(Int-Tip)c																					
(Int-Tip)n																					
3-step																					
Dc																					
Dn																					
(Int-Tip)c																					
(Int-Tip)n																					
0-step	48i	49i	50i		45i	46i	47i		42	43	3i	19i	20i	21i	22i	23i	24i	25i	26i		12
Dc	0	9	34		0	122	0				1977	0	0	0	348	0	0	1678	0		
Dn	217	25	82		167	125	26				2024	2125	2125	2125	2310	2243	2125	1721	2125		
(Int-Tip)c																					
(Int-Tip)n																					
1-step	1-13i				1-14i										1-2i					1-10i	
Dc	40s				121										2082s					0	
Dn	120				135										2224					1926	
(Int-Tip)c																					
(Int-Tip)n																					
2-step					2-6i																
Dc					127s																
Dn					131s																
(Int-Tip)c																					
(Int-Tip)n																					
3-step																					
Dc																					
Dn																					
(Int-Tip)c																					
(Int-Tip)n																					
0-step	17i	18i		27	28i	29i	30i		31	32	15	16		4i	53i	54i	55i		52		51
Dc	0	0			0	0	0							100	0	0	0				
Dn	282	847			1044	3584	3584							104	86	53	191				
(Int-Tip)c																					
(Int-Tip)n																					
1-step	1-11i				1-3i		1-4i														
Dc	423				0		1617														
Dn	2587				990		3131														
(Int-Tip)c																					
(Int-Tip)n																					
2-step					2-3i		2-4i														
Dc					1560		0														
Dn					1598		2721														
(Int-Tip)c																					
(Int-Tip)n																					
3-step																					
Dc																					
Dn																					
(Int-Tip)c																					
(Int-Tip)n																					

FIG 8.3

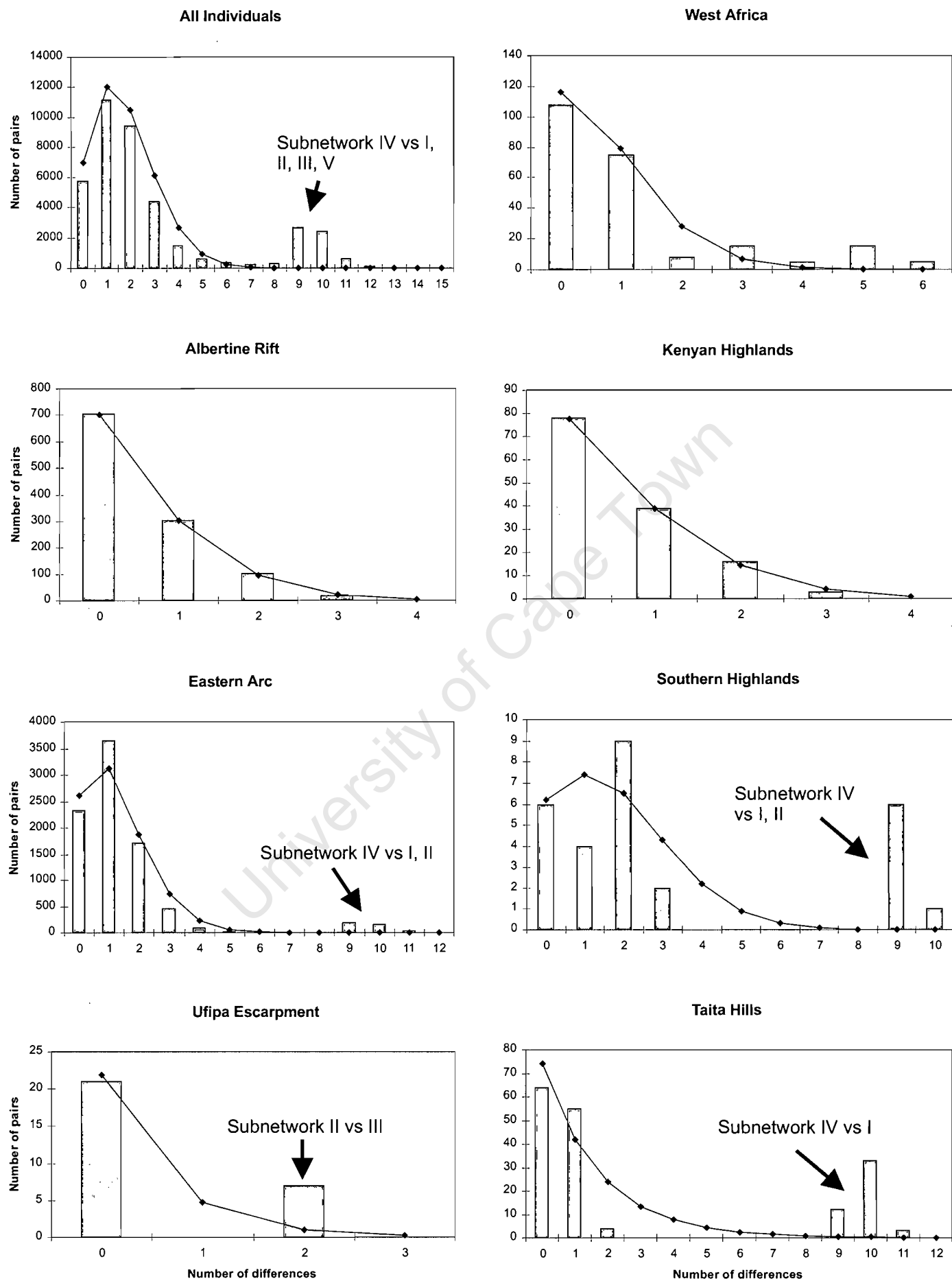


FIG 8.4

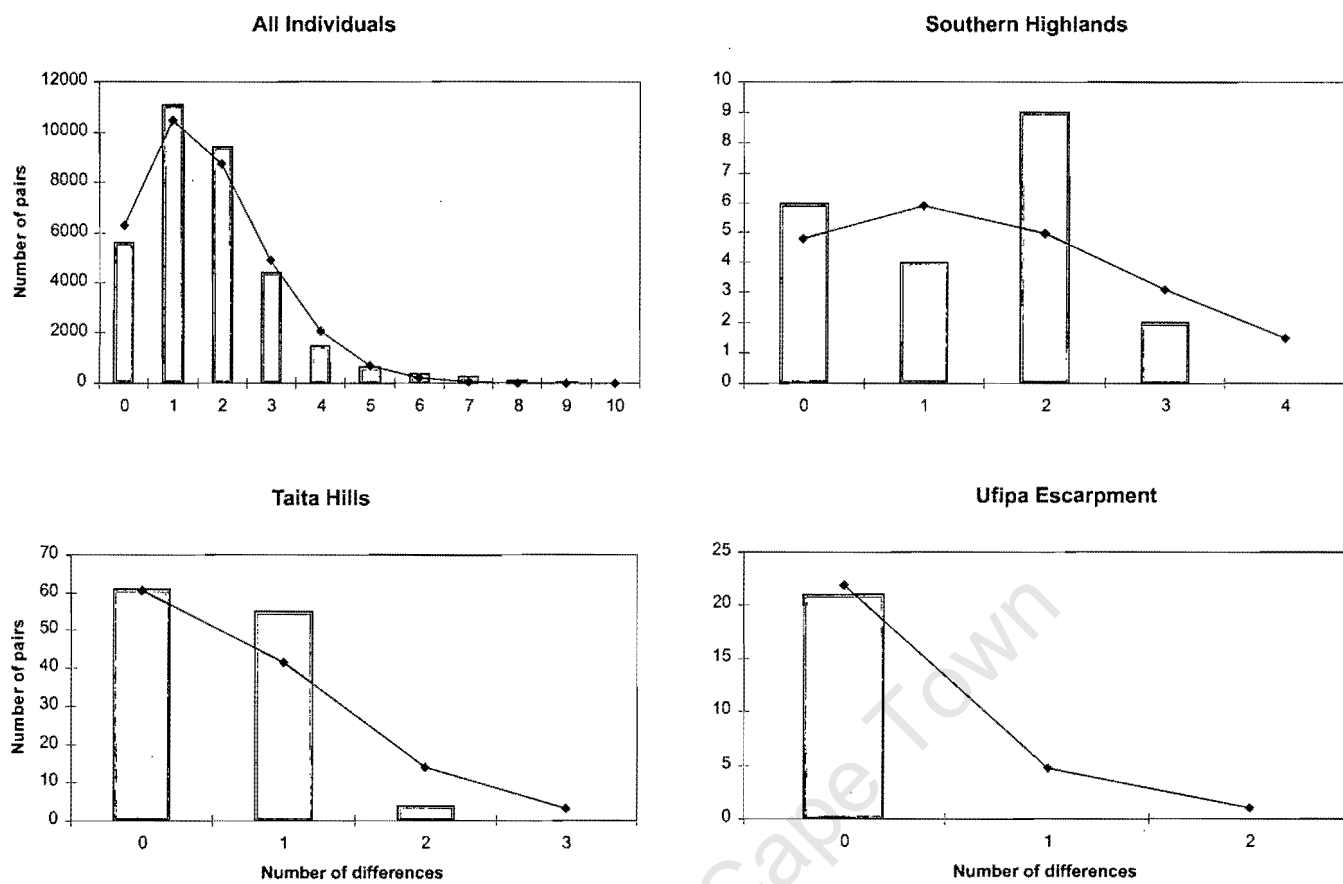


FIG 8.5

## Chapter 9

### **The shifting roles of dispersal and vicariance in the evolution of African birds during the Plio-Pleistocene: phylogeography of a montane forest robin (*Pogonocichla stellata*)**

#### **Summary**

Whereas many studies have documented the effect of ice-ages on the evolutionary history of Northern Hemisphere flora and fauna, this study is the first to investigate how the indirect aridification of Africa caused by global cooling in response to Northern Hemisphere glacial cycles has influenced the evolutionary history of an African montane bird. Mitochondrial DNA sequences from the NADH Dehydrogenase subunit 3 gene were collected from 283 individual Starred Robins. To separate historical process (e.g. vicariance) from recurrent processes (e.g. gene flow), a hierarchical analytical structure was followed. First a phylogeny of the identified haplotypes was constructed. This was followed by an investigation of geographical and demographic structure using a combination of nested-clade and mismatch analyses, and finally coalescent modelling was used to refine results from the above analyses and to estimate directional gene flow among geographical regions. Genetic structure and diversity within populations of the Starred Robin distributed around the montane circle of Africa appears to have been initiated by an ancient vicariance event(s), that led to the formation of four major ancestral populations: (1) Kenyan Highlands, (2) Albertine Rift, (3) northern Eastern Arc and (4) south-central Eastern Arc and/or the Malawi Rift. These isolates appear to have had a protracted history, with range expansions and long distance dispersal facilitating colonization of the isolated montane mountains of arid northern Kenya, young volcanoes adjacent to northern isolates of the Eastern Arc, and a southwards expansion into the central Albertine Rift from the Ruwenzori Mountains. This fragmentation of the ancestral range of the Starred Robin appears to have occurred in response to the successive aridification of Africa following the cooling of the Northern Hemisphere from about 2.8 myrs BP. With the retraction of the ice in the northern hemisphere, Africa entered a wetter phase in



response to the greater influence of low-latitude insolation forcing of the west and east African monsoons in relation to the Earth's Orbital precession. Increased precipitation may have provided the impetus for the more recently observed secondary contact between populations in the northern and south-central Eastern Arc, and between the Albertine Rift and Eastern Arc.

## INTRODUCTION

During the last decade, many studies have emphasized the influence of repeated Pleistocene glaciations on the evolution of the Northern Hemisphere faunas (e.g. Hewitt 1996, 2000, Klicka & Zink 1997, 2000, Taberlet *et al.* 1998, Branco *et al.* 2002, Pfenninger & Posada 2002). Few studies though have attempted to link the high-latitude climatic perturbations of the Pleistocene with the formation of species or major phylogenetic lineages within species in Africa, or other lower-latitude continents.

Deep-sea core records of African climatic variability suggest that prior to 2.8 myrs BP, African climate was regulated by low-latitude insolation forcing of the East and West Africa monsoon climate at periodicities corresponding to orbital precession (deMenocal 1995). A considerable body of evidence has now accumulated (reviewed by deMenocal 1995, Partridge *et al.* 1995) that suggests that changes in the orbital precession periodicity near 2.8, 1.7 and 1.0 myrs BP caused the development of periodically cooler and drier conditions in Africa. These changes are thought to have been initiated with the onset of bipolar glaciation 2.8 myrs BP. Subsequent remote forcing from the cold North Atlantic sea-surface temperatures shifted the dominant mode of variation in orbital precession, consequently triggering a shift towards more arid conditions in Africa (deMenocal 1995). These changes in African climate are coincident with a shift to more arid and open vegetation conditions, that in-turn have been linked to major steps in the evolution of African hominids (deMenocal 1995, Partridge *et al.* 1995, Vrba 1999, Templeton 2002) and bovids (Vrba 1985). This suggests that some Pliocene (Plio)-Pleistocene speciation events in Africa may have been climatically driven.

The present-day highly disjunct distribution pattern of African montane rainforests presents some difficult problems to biogeography. Indeed, one of the most puzzling features of African biogeography is that despite the often-huge distances and unfavourable habitat between montane isolates, a large proportion of montane species reappear in even the most isolated forests (birds: Moreau 1966, Diamond & Hamilton 1980, Prigogine 1987, mammals: Kingdon 1989, 1997, butterflies Carcasson 1964; spiders Griswold 1991, and flora White 1983, Dowsett-Lemaire & Dowsett 2001).

The key to addressing the above problem is centred on inferring the timing of the past changes in the extent of montane forest. Our improved understanding of African climate during the Plio-Pleistocene and apparent correlation with speciation patterns observed in the fossil record of African arid-adapted species assemblages, suggests that the periodical aridification of Africa as a consequence of changes in Northern Hemisphere climate has had a profound influence on the formation of species and phylogenetic lineages in Africa. It seems logical to assume that if the aridification of the Africa continent favoured arid-adapted species, montane forest species must have been disadvantaged as suitable habitat was reduced, and distributions became fragmented. Investigation of the influence of the aridification of Africa continent peaking at 2.8, 1.7 and 1.0 myrs BP (deMenocal 1995) on the distributional patterns of montane species may help to resolve the intriguing puzzle of how montane “islands” can have species unique to them, while others share the same species, but different sub-species, and still others have for all intent and purposes the same species, despite their wide geographic separation.

Montane forest birds in Africa are typically either: (1) sedentary and do not tend to disperse more than a few kilometres from their natal sites; or (2) exhibit altitudinal movements in the cold non-breeding season, returning to montane forest to breed (Chapin 1923, 1932, 1954, Dowsett 1982, 1985, Dowsett & Dowsett-Lemaire 1984, Dowsett-Lemaire 1983, 1988, 1989, Moreau 1966, Oatley & Tinley 1987). The Starred Robin with its many subspecies (Moreau 1951, Oatley & Arnott 1998), interesting plumage and vocal polymorphisms (see below), and documented altitudinal migrations (Moreau 1951, Oatley & Arnott

1998), provides an interesting model organism to investigate the influence of climatic perturbations on the genetic structure and diversity of a widely distributed African montane bird. In this chapter I investigate the phylogeographic structure, genetic variability and extent of gene flow within populations of Starred Robins among five broad geographical regions that encompass the montane circle of Africa: 1) Kenyan Highlands, 2) Albertine Rift, 3) northern Eastern Arc, 4) central and southern Eastern Arc and, 5) the Ufipa Plateau and Malawi Rift (Fig. 9.1).

Mitochondrial DNA nucleotide sequences for the coding protein NADH Dehydrogenase subunit 3 were collected from 283 individual birds. To separate historical process (e.g. vicariance) from recurrent processes (e.g. gene flow), a hierarchical analytical structure was followed. First a phylogeny of the identified haplotypes was constructed. Then I used nested clade and mismatch analyses to investigate phylogeography and demographic structure, and finally, I used coalescent modelling to estimate directional gene flow among regions.

### **The Starred Robin**

The Starred Robin (*Pogonocichla stellata*) is a small brightly coloured forest robin, which typically breeds in montane forest between 2500 and 3300m (Oatley & Arnott 1998). In the adult male and female the head and throat are deep grey-blue, the upperparts olive, underparts bright yellow and the tail patterned black and yellow. The species is named after the white 'stars' on the head (supraloral spots). A black-rimmed white spot occurs at the lower edge of the dark throat, but is rarely displayed. The species is distributed in montane evergreen forest extending from the Imatong Mountains in southern Sudan and Mount Kulal (ca. 4°N) in Kenya, southwards across the eastern and central parts of the continent. In South Africa where latitude compensates for altitude, the Starred Robin reaches sea level at ca. 34°S.

Altitudinal migration by this species is widespread. In many areas this is probably partial, with the breeding birds remaining resident for most of the year and non-breeding birds, subadults and occasionally juveniles dispersing (Dowsett 1982, Oatley 1982a,b, Oatley & Arnott 1998). This is especially prevalent in the

dry season when the distribution of non-breeding birds extends to lowland forest, often adjacent to the montane forest, but also to coastal forest such as the Pugu Hills and other forest in the Zanzibar-Inhambane region (Oatley & Arnott 1998, N. Baker unpublished data, RCK Bowie unpublished data). Mark-recapture studies on Starred Robins from Nyika Plateau in northern Malawi (Dowsett 1982) revealed that females preferentially move away from the Plateau during the coldest months of the year (April to August), whereas males tend to remain at the breeding territory. Thus, altitudinal migration probably varies across geography. How far from the breeding territory altitudinal movements take individuals is largely unknown. In most instances, it is likely to be only short distances (several kilometres, Oatley & Arnott 1998), but some birds are strongly suspected to have dispersed hundreds of kilometres (Oatley & Arnott 1998, M.P.S. Irwin *in litt.*).

Despite these movements, the Starred Robin is discontinuously distributed in the highlands of Africa apparently with a complex population structure as some 15 subspecies having been recognised (Oatley & Arnott 1998). In this chapter, I follow Moreau (1951) and recognise nine subspecies (Fig. 9.1). The Starred Robin is unique among robins, in having two distinct immature plumages: 1) A spangled or mottled juvenile plumage, with the feathers having yellow centres and black margins (in its brightest form), and which may be moulted after 3 months and (2) A subadult plumage that has the entire upperparts olive-green and underparts dull yellow with some olive-grey markings. This 'olive' subadult plumage is retained, at least in southern African populations, for 12 months until the next annual moult (Moreau 1951, Dowsett 1982, Oatley 1982b,c).

Geographical variation is marked in the juvenile, subadult and adult plumages, a full description of which is provided by Moreau (1951) and summarized in Table 9.1. Interestingly, not all populations appear to retain juvenile and subadult plumages, leading to the suggestion that for some population's juveniles may moult directly from a spangled to an adult plumage (Dowsett 1982, Oatley & Arnott 1998). For both the spangled and olive plumages, there is a decline in the degree of contrast and extent of mottling as you move away from the equator towards the south coast of South Africa. Populations from the subspecies

*macarthurii*, *helleri*, *guttifer* (Oatley *in litt.*) and *orientalis* southwards seem to always pass through the olive subadult plumage stage, whereas *keniensis* rarely develops a full olive-plumage and, *ruwenzorii* is intermediate (Table 9.1).

The extent of yellow on the rump and tail-coverts becomes more restricted from the equator southwards, as does the extent of black intrusions in the tail (Table 9.1). The pattern in wing colouration does not follow the general north-south trend as described above. *Pogonocichla s. orientalis*, which is geographically central, has the edges of the adult primaries and secondaries trimmed olive-grey. In both populations north and south of *orientalis* the wing is edged blue-grey (Table 9.1). Based on plumage differences in the adult and juvenile as well as the 'presence/absence' of an olive subadult plumage, Starred Robin populations can be divided into two groups. Birds from southern African, Malawi, Mozambique and central and western Tanzania (*stellata*, *transvaalensis* and *orientalis*) tend to have one general plumage pattern and populations (*ruwenzorii*, *elgonensis*, *keniensis*, *guttifer*, *macarthurii* and *helleri*) close to the equator another. Two somewhat different groupings are supported by vocal data. One group possesses a simple piping call (*ruwenzorii*, *keniensis*, *guttifer*, *orientalis* and *stellata*) and the other has a complex piping call (*macarthurii*, *helleri* and *transvaalensis*). The call structure of *elgonensis* is at present undescribed (Oatley & Arnott 1998).

## METHODS

### Population sampling

Tissue or blood samples were collected from 283 individuals from 58 sites representing 30 populations distributed around the montane circle of Africa (Table 9.2, Fig. 9.1). Due to relatively small sample sizes, sites in the same mountain range were pooled and assumed to be from the same population. Of the seven northern montane subspecies recognised by Moreau (1951), six were sampled in this study: *keniensis* (= *intensa* + *pallidiflava*), *ruwenzorii*, *guttifer*, *macarthurii*, *helleri* and *orientalis*. Unfortunately no samples of *elgonensis* from Mt. Elgon were obtained.

### Laboratory procedures

DNA was extracted, PCR amplified for ND3 with flanking tRNAs and cycle-sequenced as described in Chapter 3. Sequences were obtained from both strands of DNA for each identified haplotype, as well as from an additional 65 individuals (total 123 individuals), to double-check that nucleotide basis were consistently correctly called. For the remaining individuals, only the forward strand was sequenced. All sequences were checked using the program Sequencher 3.0 (Gene Codes Corp) and aligned to the chicken (*Gallus gallus*) mtDNA sequence (Desjardins & Morais 1990) to test for the presence of any insertions, deletions or stop codons.

### Phylogenetic analyses

Phylogenetic analyses of the DNA sequences were performed using parsimony (MP) conducted using the Ratchet (Nixon 1999). Search options for the MP ratchet were: 10% of the characters in the ND3 data partition were removed during each of 10 000 random addition replicates, five trees were held for each iteration, and full tree-bisection-reconstruction (TBR) branch-swapping was implemented. The MP ratchet was conducted using NONA (Goloboff 1999) running under the WINCLADA interface (Nixon 1999-2002). Clade support for the MP analysis was estimated using 1000 nonparametric bootstrap replicates (Felsenstein 1985).

Due to the problems associated with constructing intraspecific phylogenies (see Posada & Crandall 2001) a statistical parsimony network among the 58 haplotypes was constructed using the program TCS ver. 1.01 (Clement *et al.* 2000). The statistical parsimony algorithm estimates the number of steps any two haplotypes can be separated from each other if spurious connections due to homoplasy are to be avoided (Templeton *et al.* 1992) and joins these by minimizing the number of differences separating two individual sequences, rather than as in traditional parsimony which tries to find the global minimum number of steps with which all nodes in the topology can be joined.

### **Nested clade analyses (NCA)**

The Templeton, Crandall and Sing parsimony algorithm (nested clade analysis, NCA, Templeton *et al.* 1992) was used as an objective statistical approach to infer the population history of *Pogonocichla*. The method first attempts to reject the null hypothesis of no association between haplotype variation and geographical position. The significant patterns are then interpreted using explicit criteria (Templeton *et al.* 1995, 1998), which include an assessment of sampling design, with the objective of separating the roles of recurrent forces such as gene flow from historical events such as fragmentation or range expansion. This is achieved by overlaying the evolutionary relationships among the haplotypes (phylogenetic tree/network) upon a spatial landscape (geography) of the geographical distributions of haplotypes and clades, thus integrating both time and space into a single analysis (Templeton 2002).

The TCS-derived statistical parsimony network was manually converted into a series of hierarchically-nested clades using the rules in Templeton *et al.* (1987) and Templeton and Sing (1993). NCA quantifies the spatial distributions of haplotypes and clades by calculating three distances; (1) the clade distance ( $D_c$ ), which measures the geographical range of a clade by calculating the average distance that an individual bearing a haplotype from the clade of interest lies from the geographical center of the clade, relative to all other individuals bearing haplotypes from the same clade; (2) the nested clade distance ( $D_n$ ), which measures how a clade is geographically distributed relative to its closet relatives – the clades grouped together in the next hierarchical nested level; lastly (3) the average distance between the interior and tip clades within a nested group ( $(I-T)_c$ ), and the tip to interior distance for the nesting clade ( $(I-T)_n$ ) are estimated.

Contrasts between clades within and among different nesting levels were used to make inferences about potential causes of geographical structure of genetic variation following the revised version of the inference key published by Templeton *et al.* (1995) and Templeton (1998), also available at:

[http://bioag.byu.edu/zoology/crandall\\_lab](http://bioag.byu.edu/zoology/crandall_lab). Statistical measures of significance were determined using the permutation procedure of Roff and Bentzen (1989) with 10 000 replicates. Calculation of clade distances and permutation testing were conducted using the program GEODIS 2.0 (Posada *et al.* 2000).

### Coalescence Analyses

Whereas NCA does provide a powerful analytical tool with which to infer population history, it does not allow for the estimation of parameters of interest such as gene flow among populations. Recent advances, based on the coalescent approach (Kingman 1982) have made it possible to obtain directional maximum-likelihood estimates of gene flow among populations while taking into account population structure and demographic processes (Beerli & Felsenstein 1999, 2001). These novel analytical methods overcome the limitations imposed by traditional population genetic models, which usually rely on the biologically unrealistic assumptions of equal population sizes and symmetrical migration rates among populations. Thus, the coalescent-based methods likely provide more robust estimates of migration parameters than traditional  $F_{ST}$  based methods (Bossart & Prowell 1998, Beerli & Felsenstein 1999).

There are inherent difficulties in unravelling the evolutionary history of a species that has extensive intraspecific genetic structure among a series of allopatric populations. Forest-dwelling species such as the Starred Robin that are distributed around the montane circle of Africa clearly fall into this category. Therefore, coalescent-based estimates of gene flow were used to: (1) seek support of inferences made using NCA and (2) determine estimates of migration rates between populations. Ideally, one should estimate all relevant parameters for the migration model, along with their likelihood's, but this is currently computationally not feasible. Pooling individuals into larger regional populations based on geography is a reasonable solution to circumvent computational difficulties, as well as to help resolve problems with estimating migration rates from small sample sizes (Pfenninger & Posada 2002). Populations were pooled into five 'regional' populations, representing montane areas of endemism as follows: (1) Kenyan Highlands (pops 7 to 10, Table 9.2), (2) Albertine Rift (pops 1 to 6), (3) Northern Eastern Arc (pops 11 to 17), (4) Southern and Central Eastern Arc (pops 18 to 25) and (5) the Ufipa Plateau and Malawi Rift (pops 26 to 30).



Even for five populations when long Markov-Chain-Monti-Carlo (MCMC) runs are implemented, computational time can be considerable (weeks). To make effective use of access to two 20-processor computer clusters available for these analyses I decided to split the estimation procedure into several steps. First, a fully constrained migration parameter model was estimated, where only neighbouring populations exchanged migrants. Second, the five regional populations were divided into all possible combinations of groups of three populations and a fully resolved migration model was estimated for each of these couplets. Third, the information on relative migration rates from these triplet models was synthesised. Where there was consensus that no gene flow was taking place among triplets with pairs of populations in common, parameters between these population pairs were set to zero in a migration matrix. This matrix, with user defined zero migration between some population pairs, the partial-constraints model, was subsequently used to simultaneously estimate all remaining parameters among the five regional populations. The above approach has the added advantage that by eliminating parameters from the model, the statistical power with which the remaining parameters are estimated is increased. Peter Beerli kindly provided a parallel version of Migrate, which together with the standard Unix version (Beerli & Felsenstein 1999, 2001) was used to estimate the above model on the 20-processor clusters.

For each migration analysis (the full constraints model, population triplets and the partial constraints model), two analytical runs were conducted, an initial short run, followed by a second longer run. For both runs, the starting values of the population mutation parameter and the ratio between the immigration rate and the respective population and mutation rate per generation were estimated from  $F_{ST}$  values (Beerli & Felsenstein 1999). For the long-run (short-run values in parentheses) 10 short-chains, each with a total of 100 000 (10 000) generations and a sampling increment of 1000 (500) generations, and three long-chains each with a total of 1000 000 (100 000) generations and a sampling increment of 10 000 (5000) generations were run twice. For both the short and long runs, the first 10 000 genealogies were discarded (the burn-in). An adaptive heating scheme with four chains and a swapping interval of one was used. For the other settings, default values were implemented.

### Mismatch distributions

Pairwise mismatch distributions using individuals from within selected populations and regions were calculated as indicators of recent demographic change, which could have resulted from either population expansion or contraction (Rogers & Harpending 1992, Harpending *et al.* 1998). Tests were implemented using Arlequin 2.0 (Schneider *et al.* 2000).

## RESULTS

### Genetic Diversity

A 395 bp fragment of the mtDNA coding ND3 gene with flanking tRNA sequences was amplified from 283 individuals representing six subspecies of the Starred Robin (*Pogonocichla stellata*). The aligned sequences were pruned at both the 5' and the 3' ends to remove missing data from the analysed dataset. This resulted in a final alignment of 383 bp per individual. Merging identical sequences yielded 58 unique haplotypes (Table 9.2.) The number of substitutions between haplotypes ranged from 1 to 17 (uncorrected P, 0.26% to 5.9%). A divergence of 6.3% (Kimura-2-parameter) between haplotypes 32 and 50 from Kahe Hill at the foot of Mount Kilimanjaro (Tanzania) and Choha in the Ruwenzori Mountains (Uganda) was the largest observed in the present dataset.

Haplotype and nucleotide diversity were generally high within populations, with each biogeographical region having some populations with a comparatively high number of nucleotide differences from others within the same region. (1) Within the Albertine Rift, Mambasa (population 1), the Ruwenzori Mountains (pop. 2), and Echuya Forest (pop. 3), exhibited high nucleotide diversity despite relatively small sample sizes (Table 9.3). Nucleotide diversity in Toro (Pop. 4) was more than 2.5 times greater than for any other sampled population, due to the presence of haplotypes characteristic of both the Albertine Rift and the northern Eastern Arc being present at the same frequency (Table 9.3, Fig. 9.1). (2) Mount Nyiru (pop. 8) and Mt. Kenya (pop. 10) had relatively high nucleotide diversity levels within the Kenyan Highlands. In contrast, 13 individuals from Mt. Kulal (pop. 7) all had the same haplotype. (3) The Pare (pops. 13 & 14) and Usambara Mountains (pops 16 & 17) were genetically most diverse within the northern

Eastern Arc, and (4) within the southern and central Eastern Arc the Udzungwa Highlands (pop. 15) harboured the greatest nucleotide diversity. On the whole, the southern populations of Starred Robin on Mount Zomba (pop. 30) and Namuli (pop. 29) in the Malawi Rift and Mozambique highlands, respectively, were as genetically diverse as populations from other regions around the montane circle. For the number of individuals sequenced, the Ufipa Plateau (pop. 26) was genetically impoverished relative to the neighbouring Udzungwa Highlands.

### Phylogenetic relationships among the haplotypes

Parsimony analyses (MP) of the 58 sampled haplotypes rooted with *Sheppardia sharpei* and *Stiphrornis erythrothorax*, two other members of the African Robin assemblage (Irwin & Clancey 1974), yielded 154 most parsimonious trees with a length of 294 steps (CI = 0.61, RI = 0.79, Fig. 9.2). Among the 383 bp analysed, 288 sites were constant, 41 (10.7%) sites were variable but parsimony uninformative and 54 (14.1%) sites were parsimony informative.

In the MP analyses, very few nodes had greater than 50% bootstrap support. However, a few clusters of haplotypes were identified. (1) Eighteen haplotypes from the distribution of *orientalis* with a few individuals from the adjacent range of *helleri* in the North and South Pare mountains (Fig. 9.1, Table 9.2). (2) Two clades of haplotypes, (a) haplotype 32 from Kahe, a hill with ground water forest situated between Mt. Kilimanjaro and the Pare Mountains, (b) 13 haplotypes from SE Kenya and NE Tanzania that include *macarthuri* restricted to the Chyulu Hills, Kenya, (pop. 11) for which all four individuals sampled had hap25. Most of the remaining 12 haplotypes are found in the Taita Hills, Pare Mountains and Mt. Kilimanjaro. However, the most common haplotype sampled in this clade, hap2, is found disjunctly from Toro in the Albertine Rift (Uganda), and from Mt. Zomba (Malawi) and Mt. Namuli (Mozambique). Both Mt. Kilimanjaro and Mt. Meru (Tanzania) had hap35, which is closely allied with members of clade II in the trees. Thus, the range of *guttifer* appears to include Mt. Meru (at least according to the genetic data) but with a sample size of one from Mt. Meru, it is difficult to make any definitive conclusions, especially when considering that specimens from Mt. Meru are usually ascribed to *keniensis*

(Moreau 1951, Keith *et al.* 1992). Excluding the Mt. Meru haplotype the birds from the Kenyan highlands (*keniensis*) form a monophyletic clade (clade III). Two haplotypes (hap4 & 45) were detected among the 16 individuals sampled from the Ufipa Plateau (clade IV). The most common of these, hap 4, was found at low frequency in both populations of the central and northern parts of the Eastern Arc. Lastly, clades V, VI and VII are collectively from the Albertine Rift, and constitute the northern half of the range of the taxon *ruwenzorii*.

The largest average Kimura-2-parameter (Kimura 1980) divergence value (4.33%) among the seven haplotype clusters (Fig. 9.2) is between Clade V (Ruwenzori Mountains and SW Uganda) and the northeastern Arc (Clade II, Table 9.4). The lowest (0.77%) is between the Ufipa Plateau (Clade IV) and the geographically adjacent south-central Eastern Arc (Clade I). It is notable that diversity within the Kenyan Highlands (Clade III, *keniensis*) is almost double that for any other regional population. This is due to Mt. Nyiru at the southern end of Lake Turkana having two divergent haplotypes (Hap 42 & 43). Divergence values between populations within the Albertine Rift (Clades V-VII, *ruwenzorii*) are greater (2.41-3.54%) than, between the Kenyan Highlands and the Eastern Arc (2.79-286%), or between the northern and southern Eastern Arc (1.85%).

### **Statistical parsimony network and nested design**

Evaluation of the limits of statistical parsimony suggest that topologies connecting haplotypes by eight steps or fewer have a cumulative probability of greater than 95% of being connected in a parsimonious fashion (i.e. without homoplasy). The inference of the haplotype network with the TCS program resulted in the network depicted in Figure 9.3. The network can be broken into seven subnetworks, which match those recovered in Figure 9.2. Haplotypes are distributed within (I) the southern Eastern Arc and Malawi Rift, (II) northern Eastern Arc, Chyulu Hills, Mt. Kilimanjaro and Mt. Meru, (III) Kenyan Highlands, (IV) Ufipa Plateau, (V) Ruwenzori Mountains, northern Kabale and mountains on the southwestern side of Lake Edward, (VI) Kibira National Park and (VII) the Virunga Highlands. Several mutational steps indicated by solid circles, which represent either unsampled or extinct haplotypes separate the

subnetworks from each other. Subnetworks I and II, are characterized by a star-like pattern, where the centrally located common 'ancestral' haplotype (IV) (Crandall & Templeton 1993) is connected to several more recently derived haplotypes. Subnetwork V is ambiguously connected to subnetworks I, III and VI (broken lines in Fig. 9.3). Subnetwork I can be connected to subnetwork II in two alternate ways and there is an internal loop between haplotypes 47 and 49 within subnetwork V. These ambiguities result from the presence of more than one parsimonious connection of a haplotype to the rest of the network.

In the final nested design, it makes little difference how subnetwork I and II are connected, or how the loop within subnetwork V is resolved, as alternative nested designs do not change any of the inferred results in the NCA analyses. More difficult to resolve is how to link subnetwork V to the remaining network. The MP analysis (Fig. 9.2) suggests that all three subnetworks (V, VI and VII), which include haplotypes from the Albertine Rift form a monophyletic clade, which is sister to the Kenyan Highlands (III). Thus, I connect subnetwork V to VI, Kibira National Park due to being within the same montane area of endemism and because of hypothesised phylogenetic affinities (Fig. 9.2). Strictly applying the nesting rules of Templeton *et al.* (1987) and Templeton and Sing (1993) results in the following higher level nesting structure [(3-1 + 3-2) (3-3 + 3-4) (3-5 + 3-6)] which form three 4-step clades in the final 5-step cladogram. This nesting structure however, splits the Albertine Rift into two discreet groups, clade 3-4 (subnetwork VII from the Virunga Volcanoes) is united with the Kenyan Highlands, to the exclusion of the remaining Albertine Rift clades. This does not agree with the putative relationships among the different haplotypes (Fig. 9.2), where all haplotypes from the Albertine Rift form one monophyletic clade. As a result I repeated the NCA analyses using a simplified nesting structure [(3-1 + 3-2 + 3-3) (3-4 + 3-5 + 3-6)], which united the Kenyan Highlands with the Eastern Arc and Malawi Rift, but also united the three Albertine Rift subnetworks (V-VII) into a single 4-step clade. This is hereafter referred to as the preferred nesting structure.

### **Nested clade analyses and inferred population history**

Figure 9.4 presents the results of the nested clade analyses of geographical distances performed on the nested structure illustrated in Figure 9.3 using GEODIS 2.0. Table 9.5 summarizes the resulting inferences about population structure and history inferred from the statistical results of the GEODIS analyses. The inferred population history underlying intraspecific genetic structure in the Starred Robin is dominated by the interaction of expansion events (dispersal - contiguous range expansion, isolation by distance) and contraction events (vicariance - fragmentation), which have occurred repeatedly (at multiple nested levels) during the Pleistocene (Table 9.5, divergence calibrated using the 1.6% sequence divergence per million years of Fleischer *et al.* 1998). In Figure 9.5, I graphically summarise the phylogeographic patterns uncovered by the NCA.

For all significant geographically structured nesting levels, genetic diversity in Starred Robin populations from the south-central Eastern Arc and Malawi rift (subnetworks I and IV, clades, 2-1 and 1-1) appear to be driven by restricted gene flow with isolation by distance, or contiguous range expansion (Table 9.5). These evolutionary mechanisms are not opposed because both indicate an expansion of the ancestral range containing the observed haplotypes. Two fragmentation events are also inferred. The more recent one (clade 1-7) separates the volcanic Chyulu Hills (Hap 25) from the rest of the northern Eastern Arc (subnetwork II), and the older (clade 3-2) infers a fragmentation between the high volcanoes of Mt. Kilimanjaro and Meru, from the montane highlands of the Eastern Arc. At the 4-step clade level, two fragmentation or isolation events were inferred, the first leading to the separation of the Kenyan Highlands from the northern Eastern Arc. The second, splitting the Eastern Arc into a northern and south-central cluster of mountains (Fig. 9.5).

Within the Kenyan Highlands (subnetwork III, clade 3-3) a relatively deep intraspecific genetic divergence (1.5%) exists between haplotypes from Mt. Nyiru and the central Kenyan Highlands, Mt. Kenya, the Aberdares and hills in eastern Maralal. At present, it is not possible to conclusively determine which of the two lineages are older, and thus interior-tip status cannot be determined. However, if clade 3-3 is rooted on either lineage (by making it an interior) then a

contiguous range expansion is recovered, although whether this occurred from the central Kenyan Highlands to Mt. Nyiru or *vice versa* is unknown. At lower levels (Clade 1-17) restricted gene flow with some long distance dispersal was inferred between the central Kenyan Highlands, Mt. Kenya and Mt. Kulal. Three subnetworks of haplotypes occur within the Albertine Rift (V, VI & VII). Their evolutionary origins depend on how the higher-level clades are nested. Under the preferred nesting structure with two 4-step clades [(3-1 + 3-2 + 3-3) (3-4 + 3-5 + 3-6)], an old contiguous range expansion is inferred within the Albertine Rift, possibly from the Ruwenzori Mountains southwards (clade 4-2). If three 4-step clades are used [(3-1 + 3-2) (3-3 + 3-4) (3-5 + 3-6)] then haplotypes from the Virunga Volcanoes are nested with clade 3-3 from the Kenyan Highlands. In this alternate network, both clades 3-3 and 3-4 are interiors and, as such, this results in an inconclusive outcome due to the inability to determine interior/tip status. However, if clade 3-3, which has the higher outgroup probability (Castelloe & Templeton 1994) is made an interior, then a contiguous range expansion from the Kenyan Highlands to the Virunga Volcanoes is inferred. For clade 4-3 (3-5 + 3-6), a contiguous range expansion between the northern (Mambasa, Ruwenzori and Toro) and the highlands on the eastern sides of Lakes Albert and Kivu (Kibira) is inferred.

Finally, the inference for the total cladogram (5-step clade) in either the preferred network (clades 4-1 & 4-2) or alternate network (clades 4-1, 4-2 and 4-3), suggest that past fragmentation (vicariance) between the Albertine Rift, Kenyan Highlands, and north and south-central Eastern Arc has historically shaped genetic variation among Starred Robin populations distributed around the montane circle of Africa (Table 9.5, Fig. 9.5).

### **Coalescent modelling of gene flow**

For the long and short runs (see Methods), similar results were obtained although the 95% confidence limits in the long-run were smaller. In the full constraints model, where gene flow was limited to only neighbouring populations, no discernible gene flow was detected between the Kenyan Highlands and Albertine Rift, or between the Kenyan Highlands and the northern Eastern Arc including surrounding volcanoes, Mt. Kilimanjaro, Mt. Meru and the Chyulu Hills. A

small amount of gene flow ( $4nm < 1$ ) was inferred between the northern, and the central and southern parts of the Eastern Arc, with a slight asymmetry from south to north. Similarly, a slight trickle ( $4nm = 1.3$ ) from the Albertine Rift to the Ufipa Plateau and Malawi Rift was detected but only in one direction.

Considerable gene flow occurs between the central and southern Eastern Arc, and the Ufipa Plateau and highlands of Malawi and northern Mozambique with a strong asymmetry from the Eastern Arc towards the more southerly populations (Fig. 9.6).

Couplets of three populations each, for all possible combinations among the five regions analyses were used to help develop a more complex, but realistic, model of gene flow among Starred Robin populations distributed around the montane circle of Africa. As in the full constraints model, results suggested that no, or negligible gene flow occurred between (1) the Kenyan Highlands and the Albertine Rift, (2) between the Kenyan Highlands and the southern and central Eastern Arc, Ufipa Plateau and Malawi Rift, (3) between the Albertine Rift, Ufipa Plateau and the Malawi Rift. In the partial constraints model the above migration parameters were set to zero (no gene flow), allowing the parameters to be estimated within the final model to be reduced from 25 to 17.

Coalescent analyses of the partial constraints model produced results among neighbouring populations as described above, but provided a few additional insights. (1) A small amount of gene flow was inferred to occur between the Albertine Rift and the southern Eastern Arc, with gene flow being slightly biased from the Eastern Arc towards the Albertine Rift ( $4nm = 1.0$  vs.  $0.13$ , Fig. 9.6). (2) Gene flow is asymmetrically biased from the central and southern Eastern Arc towards the northern Eastern Arc, with negligible gene flow from north to south. (3) There is considerable genetic exchange between the northern Eastern Arc and surrounding volcanoes, with the highlands of Malawi and Northern Mozambique. A strong asymmetrical bias exists from north to south (Fig. 9.6).

### **Mismatch Distributions**

Nucleotide pairwise differentiation profiles or mismatch distribution plots for various regional populations of the Starred Robin are summarized in Figure 9.7.



Unimodal, bell-shaped mismatch profiles are usually associated with a past episode of population growth following a range expansion. The south-central Eastern Arc and Kenyan Highlands, Ufipa Plateau and Malawi Rift all have characteristic bell-shaped curves suggestive of relatively recent population expansion. In contrast, the northern populations of the Eastern Arc and surrounding volcanoes have something of an intermediate pattern reflecting a more ancient range expansion, a result concordant with both the NCA analysis and the spatially complex positioning of taxa (*guttifer*, *macarthuri* and *helleri*) in this geographically and topographically complex region.

Multi-modal mismatch profiles can occur as a consequence of a large number of factors. For example, populations of constant size are expected to display multimodal patterns (Slatkin & Hudson 1991, Rodgers & Harpending 1992, Harpending *et al.* 1998), but so can populations, which encompass geographic sub-structuring in relation to restricted gene flow (Marjoram & Donnelly 1994), and multimodal patterns may also result from secondary contact between expanding fronts (Pfenninger & Posada 2002). One or more of these factors are certainly operating within the Albertine Rift to give the very strange profile depicted (Figure 9.7). Both traditional parsimony (Fig. 9.2) and statistical parsimony (Fig. 9.3) reveal three divergent subnetworks of haplotypes (V, VI & VII) within the Albertine Rift, confirming substructure. This is further complicated by the immigration of migrants from the northern Eastern Arc to the central Albertine Rift (Fig. 9.6). Therefore secondary contact also appears to have played a role in generating the aberrant mismatch pattern of the Albertine Rift when considered as a whole. At the 4-step clade level of the NCA analysis a contiguous range expansion from the Ruwenzori Mountains was inferred. Inferences made at higher NCA clade steps tend to be older (Crandall & Templeton 1993). This conclusion is strongly supported by the mismatch profile for the Ruwenzori Mountains (Fig. 9.7), which reflects traces of an ancient range expansion in what is now most probably a stable population.

## DISCUSSION

The Starred Robin in the southern parts of its distribution is an altitudinal migrant, with females leaving breeding territories in winter and males tending to

remain resident year round (Moreau 1951, 1966, Irwin 1971, Dowsett 1982, Oatley 1982a,b,c, Oatley & Arnott 1998). Irwin (*in litt*) and Oatley & Arnott (1998) recount the capture of a bird by a cat in a Harare garden (Zimbabwe) in December 1995, which appeared to belong to the more northerly subspecies *orientalis*, rather than to the geographically closer *transvaalensis*. Thus, some individuals do appear to disperse over hundreds of kilometres as opposed to a partial movement to the nearest low-altitude forest. Dowsett (1982) stresses that just because a bird does disperse away from its breeding territory, and even if it were to form part of a mixed flocks with other 'subspecies' in the non-breeding season, there is no reason to suppose that a high level of genetic structure cannot be maintained if natal philopatry is high. Indeed, this has been suggested to be the case for many Northern Hemisphere arctic breeding birds (Baker *et al.* 1994, Liebeers *et al.* 2001), and may well apply to the Starred Robin given the relatively large number of subspecies described. Dowsett (1982), based on limited mark-recapture records of Starred Robin populations from Nyika Plateau, suggests that there is some evidence that juvenile Starred Robins return to their natal sites. However, Oatley (1982b) in an intensive mark-recapture study of Starred Robin populations in KwaZulu-Natal South Africa, established that juvenile or subadult Starred Robins dispersed away from their birthplace and seldom returned. Immigrants from other populations move into forests at the onset of the subsequent breeding season and recruit into any vacant territories in the local population.

One important difference between the interpretations on Starred Robin philopatry by Dowsett (1982) and Oatley (1982b) is spatial scale. Dowsett (1982) was, in general, referring to philopatry in the context of juvenile birds recruiting into populations within the same geographical region (Nyika Plateau). In contrast, Oatley (1982b) was referring to recruitment into a specific forest population within a broader geographical region. Given the possibility of natal philopatry and recognition of extensive plumage and vocal variation by the description of a relatively large number of subspecies (Table 9.1), it is not surprising that the most ancient demographic event detected by the NCA (5-step clade) is one of historical fragmentation (vicariance) of the ancestral range into at least three broad geographical regions, 1) Kenyan Highlands, 2) Albertine Rift and 3) the

Eastern Arc. This was probably followed relatively quickly by isolation of the northern Eastern Arc from the south-central Arc. However, because of secondary contact (see below) it is not possible to determine exactly where the barrier formed, or for how long it persisted.

Although a maximum of *ca.* 6% divergence was detected among the 58 sampled haplotypes, due to lineage sorting it may be more appropriate to use average sequence divergence values among these three regions to infer the putative age of the fragmentation of the ancestral range of the Starred Robin. Using a calibrated rate of 1.6% divergence per million years (myrs, Fleischer *et al.* 1998) this suggests that fragmentation of the ancestral range of the Starred Robin took place between 2.7 and 1.8 myrs BP. This would have led to the isolation of present day *ruwenzorii* in the Albertine Rift, *keniensis* within the Kenyan Highlands, *orientalis* in the south-central Eastern Arc and Malawi Rifts, and *helleri* in the northern Eastern Arc. These dates are noteworthy as they correspond to the ending of a relatively stable Pliocene in Africa (deMenocal 1995) when montane forest was thought to have been well established.

Between 2.8 and 1 myrs BP high-latitude Northern Hemisphere climate started to oscillate between moderate glacial and interglacial extremes at a 41 kys (thousand years) orbital tilt periodicity (reviewed by deMenocal 1995, Partridge *et al.* 1995). Abundant evidence now exists (reviewed by deMenocal 1995, Partridge *et al.* 1995) that suggests that these changes in orbital tilt periodicity altered global circulation patterns and caused Africa to become more arid. This would have induced contraction of montane forest and putatively initiated the formation of the highly disjunct distribution pattern of montane forest that we see today. It is worth noting that the observed estimates for divergence dates would have to have been overestimated by 50% or more, if the fragmentation of the ancestral range of the Starred Robin was to be associated with the large-amplitude 100 kys cycles of the mid-Pleistocene that started *ca.* 0.8 myrs BP (deMenocal 1995, Kennart 1995, Partridge *et al.* 1995, Rutherford & D'Hondt 2000). Furthermore, the divergence estimate above would need to be inaccurate by an order of magnitude, if the observed genetic structure within the Starred Robin was purely a consequence of the most recent glacial maximal. Thus, as has been

demonstrated among closely related species (Zink & Slowinski 1995, Klicka & Zink 1997, Roy *et al.* 1998, Roy *et al.* 2000, Chapter 3, 4, & 7) and now within a species (this study), the high amplitude glacial cycling of the upper Pleistocene, for so long a paradigm as an evolutionary mechanism underpinning avian speciation, is questionable.

A more protracted history of isolation of Starred Robin populations is probably accurate, especially given the high genetic diversity (Table 9.3) and mismatch profiles (Fig. 9.7) observed within each of the major biogeographical regions: Albertine Rift, Kenyan Highlands, northern Eastern Arc and, south-central Eastern Arc and Malawi Rift. This is not to say that the high amplitude glacial cycling of the upper Pleistocene has not played an important role in shaping genetic structure and diversity in bird populations (see Avise & Walker 1998, Avise *et al.* 1998), only that these climatic perturbations had less of an influence on avian speciation than had been emphasised in the past (e.g. Moreau 1966, Diamond & Hamilton 1980). In the Starred Robin a number of important demographic events have occurred subsequent to the fragmentation of its ancestral range around the montane circle of Africa.

The central Kenyan Highlands form a large north-south extension on either side of the eastern Rift. Just to the east of the ancient Aberdare Mountains lies the relatively young volcano Mt. Kenya, and further north are a series of isolated massifs in semi-arid desert with montane forest restricted to just their tops. These northern outliers of the Kenyan Highlands, Mt. Nyiru, Mt. Kulal and Mt. Marsibit with their impoverished avian faunas, due to their arid surroundings, are not likely to have ever been in direct contact with other mountains (Moreau 1966, Dowsett 1985). The impoverishment of their forest avian communities can thus be explained by the need for long-distance colonization, which given their small size and isolation, is probably rare. The NCA suggests that the evolution of both the Starred Robin populations on Mt. Kenya and Mt. Kulal has arisen as a consequence of restricted gene flow, but with some long distance dispersal, a scenario that matches the *a priori* predictions given the spatial composition of the environment. The founding number on Mt. Kulal was most likely small (and not unexpectedly), given that all 13 birds sampled had the same haplotype (hap 37,

Table 9.2). The Starred Robin has never been recorded on Mt. Marsibit, a high massif, like Mt. Kulal with only forest on its extreme upper margin in a matrix of semi-arid desert (Moreau 1951, 1966, Friedmann & Stager 1969, Diamond & Keith 1980, Lewis & Pomeroy 1989, L. Borghesio *in litt.*). This is despite there being apparently suitable habitat and the dispersal potential of the Starred Robin (Dowsett 1982).

At southern terminus of Lake Turkana and slightly closer to the northern margin of the Aberdares, Mt. Nyiru occurs. Two divergent haplotypes (Hap 42 & 43) from four birds were recovered from this massif (Table 9.3). NCA suggests that the diversity of the Starred Robin community on Mt. Nyiru has evolved from a contiguous range expansion, or isolation by distance between it and the central Kenyan Highlands, although due to not being able to determine interior-tip status (see Methods) the direction of these expansion events cannot at present be determined. Whatever the specific mechanism or direction, the expansion event is likely to be much older than the expansion of *keniensis* to Mt. Kenya and Mt. Kulal given the higher clade level (3-step vs. 1-step).

An ancient (4-step clade) contiguous range expansion, possibly from the Ruwenzori Mountains towards the central Albertine Rift is similarly inferred if the preferred simplified nesting structure is used. In the alternative nesting structure, subnetwork VII groups with III in clade 4-2, while the remaining two Albertine Rift subnetworks V and VI are united in clade 4-3. Under this nesting structure two contiguous range expansions are inferred, the first from the Ruwenzori Mountains southwards, and the second from the Kenyan Highlands to the Virunga Mountains. This implies that after fragmentation of the ancestral range of the Starred Robin, which isolated some populations within the Albertine Rift, a secondary colonization from the Kenyan Islands to the central Albertine Rift may have occurred. In either case it is clear that the evolutionary history of Starred Robin populations within the Albertine Rift is complex. Indeed, one of the most unexpected finding of this study was the detection of three distinct subnetworks of haplotypes (Figs 9.1-9.3) within the Albertine Rift, which apart from a brief note by Clancey (1972) has always been considered one taxon *Pogonocichla s. ruwenzorii*. The spatial sampling in this study is too poor to

accurately delimit subnetwork boundaries within the Albertine Rift and will be the focus of a future study. A comprehensive re-examination of specimens from this area of endemism is certainly warranted in light of the extensive genetic structure detected. An expansion from the northern parts of the Albertine Rift to some extent may explain why the species reaches Mt. Kobobo on the western side of Lake Tanganyika (Dowsett 1982), but has failed to be detected in the Marungu Highlands (Dowsett & Prigogine 1974), although these highlands are still relatively unexplored due to war.

Northeastern Tanzania and SE Kenya have a spatially complex distribution of Starred Robin subspecies in accordance with the juxtaposition of old and young mountains. *Pogonocichla s. helleri* is located in the Taita Hills and Pare Mountains, which represent the most northerly extent of the Eastern Arc. Just to the north of the Taita Hills, *macarthurii* is restricted to the very young volcanic Chyulu Hills and to the west *guttifer* is confined to the relatively young Mt. Kilimanjaro, although this study suggests that the population on Mt. Meru is *guttifer* and not *keniensis*. On the basis of nature and extent of the gaps between (1) Mt. Kilimanjaro and Mt. Meru, (2) Mt. Meru and the Crater Highlands, and (3) Mt. Kilimanjaro and the North Pare Mountains it is reasonable to assume that the closest relationship (and most recently maintained gene flow) for Starred Robin populations in NE Tanzania occurs between Mt. Kilimanjaro and Mt. Meru, since the 7000 ft (2135 m) contours of the two mountains are only 45 km apart and separated by comparatively moist tableland at about 800-1000 m. By contrast, the Pangani valley in gap 3 and the rift in gap 2 is hot, dry acacia scrub with only very localized ground water forest. As little as 250 years ago the gap between Mt. Kilimanjaro and Mt. Meru may have been sufficiently wooded to allow easy passage to dispersing Starred Robins, and it is historically recorded that clearing of forest for agriculture only reached the 1600 m contour on Meru in 1830. Currently Starred Robins are common in secondary forest and fringing scrub at 1440 m on SW Mt. Kilimanjaro foothills, in line of sight with Mt. Meru (T.B. Oatley *in litt.*). These populations, with the possible exception of *guttifer* (which differs from *keniensis* in only the saturation of colour) all have discreet plumage differences (Moreau 1951, Dowsett 1982, Table 9.1). In addition, *helleri* and *macarthurii* are reported to have a complex piping call, whereas

*keniensis*, *guttifer*, *orientalis* and *ruwenzorii* have a more simple structure to their calls (Dowsett 1982, Oatley & Arnott 1998).

The NCA analysis suggest that the isolation of *helleri* and *guttifer* (clades 4-1 and 3-2 respectively) is much more ancient than the isolation of *macarthurii* in the Chyulu Hills. This result is consistent with the geology of the region, where Mt. Kilimanjaro is thought to be around 1 myrs in age, and the Chyulu Hills possibly as recent as 40 000 yrs old (Moreau 1966, Griffiths 1993). Thus, dispersal from a more ancient ancestral *helleri* stock within the northern Eastern Arc, to the younger volcanic mountains to the north and west, with subsequent isolation, does provide a plausible hypothesis for the evolution of *guttifer* and *macarthurii*. Both these taxa from Mt. Kilimanjaro and the Chyulu Hills, respectively, have unique haplotypes (Table 9.3). However, coalescent modelling of gene flow (Fig. 9.6) and the mismatch distributions (Fig. 9.7) reveal that extensive 'secondary' contact is taking place between *helleri* and *orientalis* in both the northern Eastern Arc, and southern parts of the Malawi Rift. This is an unexpected finding, given the documented differences in both plumage and song reported between these taxa (Moreau 1951, Dowsett 1982, Oatley & Arnott 1998). It is possible that the mixing of haplotypes characteristic of *helleri* (subnetwork II) and *orientalis* (subnetwork II) could be due to incomplete lineage sorting (Avise 2000), but because coalescent methods of modelling gene flow take into consideration genetic structure and demography (Beerli & Felsenstein 1999, 2001), a more plausible explanation would be secondary contact and therefore introgression.

Examination of gene flow estimates reveals that an asymmetrical relationship exists within the Eastern Arc, with *orientalis* from the south-central Eastern Arc dispersing across the wide arid-lowland savannah gap separating the Nguru Mountains from the northern Usambara and Pare Mountains. In contrast, there is negligible gene flow from the northern Eastern Arc into the central or southern Arc. However, extensive gene flow appears to be taking place between the northern Eastern Arc, and the more distant Malawi Rift and highlands of northern Mozambique. This is unexpected, but it is possible that dispersal between these areas could take place via coastal forests in Tanzania, and birds

have been recorded in the Pugu Hills, as well as along the Zanzibar-Inhambane coastal zone (N. Baker unpublished data, RCK Bowie unpublished data J. Fjeldså unpublished data). Coalescent modelling of gene flow supports the results of the NCA in that the Kenyan Highlands (*keniensis*) are isolated from remaining Starred Robin populations, but also suggests that limited gene flow takes place between the Albertine Rift (*ruwenzorii*) and the Eastern Arc (*helleri* and *orientalis*). Thus, this appears to be a second case of secondary contact. Dowsett (1982) reports that *orientalis* along with southern African populations of the Starred Robin tend to be more migratory in nature than taxa further north. In both the case of secondary contact with *helleri*, and with *ruwenzorii*, gene flow tends to be asymmetrical in favour of *orientalis* dispersing.

## CONCLUSIONS

Genetic structure and diversity within populations of the Starred Robin distributed around the montane circle of Africa appears to have been initiated by an ancient vicariance event(s), that led to the formation of four major ancestral populations: (1) Kenyan Highlands, (2) Albertine Rift, (3) northern Eastern Arc and (4) south-central Eastern Arc and/or the Malawi Rift. These isolates appear to have had a protracted history, with range expansions and long distance dispersal facilitating colonization of the isolated montane mountains of arid northern Kenya, young volcanoes adjacent to northern isolates of the Eastern Arc, and a southwards expansion into the central Albertine Rift from the Ruwenzori Mountains. This fragmentation of the ancestral range of the Starred Robin appears to have occurred in response to the successive aridification of Africa following the cooling of the Northern Hemisphere from about 2.8 myrs BP. With the retraction of the ice in the northern hemisphere, Africa entered a wetter phase in response to the greater influence of low-latitude insolation forcing of the west and east African monsoons in relation to the Earth's Orbital precession. Increased precipitation may have provided the impetus for the more recently observed secondary contact between populations in the northern and south-central Eastern Arc, and between the Albertine Rift and Eastern Arc.

Whereas many studies have documented the effect of ice-ages on the evolutionary history of Northern Hemisphere fauna (e.g. Hewitt 1996, Branco *et*



*al.* 2002, Pfenninger & Posada 2002), this study is the first to investigate how the indirect aridification of Africa caused by global cooling in response to Northern Hemisphere glacial cycles has influenced the evolutionary history of an African montane bird.

University of Cape Town

**Table 9.1.** Description of the major characters separating the nine subspecies of the Starred Robin (*Pogonocichla stellata*) recognised by Moreau (1951) and Dowsett (1982).

Subspecies	Adult Plumage			Spangled plumage; Degree of contrast	Olive plumage; Degree of mottling	Plumage sequence; Occurrence of olive stages	Piping-call
	Edges of remiges	Rump & upper Tail-coverts	Tail-feather Pattern <sup>1</sup>				
1. <i>ruwenzori</i>	primaries blue-grey; secondaries olive	yellow	(1) distal half (2) 17-20mm	very high	heavy	Intermediate <sup>3</sup>	simple
2. <i>elgonensis</i>	blue-grey	yellow	(1) whole web (2) almost entire feather	very high	?	rare	unknown
3. <i>keniensis</i>	blue-grey	yellow	(1) whole web (2) 14-17mm	very high	?	rare	simple
4. <i>guttifer</i> <sup>2</sup>	blue-grey	yellow	(1) whole web (2) 14-17mm	very high	medium	common/intermediate <sup>4</sup>	simple
5. <i>macarthuri</i>	blue-grey	yellow	(1) distal third (2) <i>ca.</i> 10mm	high	heavy	common	complex
6. <i>helleri</i>	blue-grey with	yellow, but	(1) distal half	high	heavy	common	complex

	green wash	extent reduced	(2) 7-10mm				
7. <i>orientalis</i>	olive-grey	rump green, yellow- green tail coverts	(1) distal half (2) <i>ca.</i> 10mm	high	heavy	common	simple
8. <i>transvaalensis</i>	blue-grey, but coverts are edged white	green	(1) distal half (2) <i>ca.</i> 10mm	low	little	common	complex
9. <i>stellata</i>	blue-grey	green	(1) distal half (2) <i>ca.</i> 10mm	low	none	common	simple

1. The central pairs of feathers are black in all taxa, (1) the extent of black on the outer web of the next pair, and (2) depth of the extent black on the remaining feathers.

2. *Pogonocichla s. guttifer* differs from *keniensis* in being more saturated in colour

3. Juveniles in the Democratic Republic of the Congo and Rwanda have bright yellow (rather than drab yellow) in their tails, which suggests that a direct moult from a spangled to adult plumage may take place (Oatley & Arnott 1998).

4. Unpublished data on juvenile moult in *guttifer* was generously provided by T.B. Oatley (*in litt.*)

**Table 9.2.** Populations, geographical coordinates, sample size and haplotypes identified in each sampling locality. \* Source codes: FMNH = Field Museum of Natural History, ZMUC = Zoological Museum of the University of Copenhagen, FITZ = Percy FitzPatrick Institute of African Ornithology, Barrick = The Barrick Museum, University of Nevada.

#	Population	Country of origin	Geographical co-ordinates	n	Source*	Haplotypes
1	Mambasa	Uganda	01.00N, 28.58E	6	FMNH	5(3) 47[1] 48(2)
2	Ruwenzori Mnts	Uganda	00.25S, 30.00E	12	FMNH	5(5) 46[1] 48(1) 49(1) 50[1] 51[1] 52[1] 53(1)
3	Echuya Forest	Uganda	01.17S, 29.42E	3	FMNH	54[1] 55[1] 56(1)
4	Toro	Uganda	01.08S, 30.42E	4	ZMUC	1(1) 5(1) 12(1) 53(1)
5	Virunga Mnts	Rwanda	01.40S, 29.60E	2	RCKB	57[1] 58[1]
6	Kibira National Park	Burundi	01.97S, 29.34E	3	FMNH	56(3)
7	Mt. Kulal	Kenya	02.72N, 36.93E	13	ZMUC	37 (13)
8	Mt. Nyiru	Kenya	02.08N, 36.51E	4	ZMUC	43[3] 42[1]
9	Aberdare Mnts	Kenya	00.06N, 36.67E	24	ZMUC	3(14) 36[2] 38(2) 39[5] 41[1]
10	Mt. Kenya	Kenya	00.17S, 37.02E	4	RCKB	3(1) 40[2] 38(1)
11	Chyulu Hills	Kenya	02.58S, 37.83E	4	RCKB	25[4]
12	Taita Hills	Kenya	03.42S, 38.33E	10	LLENS	2(6) 23[1] 24[1] 26[1] 28[1]
13	North Pare Mnts	Tanzania	03.72S, 37.58E	13	ZMUC	1(2) 2(6) 4(1) 27(1) 31[1] 33[1] 34(1)
14	South Pare Mnts	Tanzania	04.26S, 37.83E	5	ZMUC	1(1) 2(3) 30[1]
15	Kilimanjaro district	Tanzania	03.27S, 37.17E	6	ZMUC	32[1] 35(5)
16	West Usambara	Tanzania	04.83S, 38.41E	18	ZMUC	1(2) 2(12) 4(1)

	Mnts					14[1] 27(1) 29[1]
17	East Usambara	Tanzania	05.00S, 38.58E	5	ZMUC	1(4) 2(1)
	Mnts					
18	Nguru Mnts	Tanzania	06.12S, 37.53E	1	ZMUC	1(1)
19	Ukaguru Mnts	Tanzania	06.35S, 36.88E	1	ZMUC	1(1)
20	Pugu Hills	Tanzania	06.88S, 39.08E	2	ZMUC	1(2)
21	Rubeho Mnts	Tanzania	07.02S, 36.54E	39	ZMUC	1(27) 2(2) 4(3) 7(4) 8[1] 18[2]
22	Morogoro	Tanzania	07.10S, 36.64E	16	ZMUC	1(13) 7(1) 16(1) 22[1]
23	Uvidundu Mnts	Tanzania	07.60S, 36.95E	3	ZMUC	1(2) 44[1]
24	Uluguru Mnts	Tanzania	06.73S, 37.46E	17	ZMUC	1(11) 7(2) 10(1) 13[1] 16(1) 20[1]
25	Udzungwa Highland	Tanzania	07.96S, 36.06E	30	ZMUC	1(20) 5(1) 6[1] 10(1) 11(1) 12(1) 15[1] 17[2] 21[1] 34(1)
26	Ufipa Plateau	Tanzania	07.90S; 31.70E	16	ZMUC	4(13) 45[3]
27	Mt. Rungwe	Tanzania	09.20S, 33.60E	3	ZMUC	1(3)
28	Mt. Njesi	Mozambique	13.00S, 35.00E	1	FITZ	1(1)
29	Mt. Namuli	Mozambique	15.30S, 37.00E	6	FITZ	1(3) 2(3)
30	Mt. Zomba	Malawi	15.40S, 35.30E	10	FITZ/ Barrick	1(5) 2(1) 9[1] 16(1) 19[2]

**Table 9.3.** Genetic diversity indices based on 383 bp of ND3 with flanking tRNAs for the 30 populations of Starred Robin (*Pogonocichla stellata*) sampled.

#		Haplotype Div.	Av. No. of Diffs	Nucleotide Div (x 10 <sup>3</sup> ).
1	Mambasa	0.73±0.15	1.9±1.3	5.1±3.8
2	Ruwenzori Mnts	0.85±0.10	2.7±1.5	7.0±4.5
3	Echuya Forest	1.0±0.27	2.7±1.9	7.0±6.2
4	Toro	1.0±0.18	7.3±4.3	19.1±13.6
5	Virunga Mnts	1.0±0.50	2.0±1.7	5.2±6.4
6	Kibira National Park	—	—	—
7	Mt. Kulal	—	—	—
8	Mt. Nyiru	0.50±0.26	2.0±1.4	5.2±4.4
9	Aberdare Mnts	0.63±0.09	0.8±0.6	2.2±1.8
10	Mt. Kenya	0.83±0.22	1.7±1.2	4.3±3.8
11	Chyulu Hills	—	—	—
12	Taita Hills	0.67±0.16	0.8±0.6	2.1±1.8
13	North Pare Mnts	0.79±0.11	2.6±1.5	6.8±4.4
14	South Pare Mnts	0.70±0.22	2.0±1.3	5.2±4.1
15	Kilimanjaro district	0.33±0.21	1.3±0.9	3.5±2.9
16	West Usambara Mnts	0.56±0.13	1.8±1.1	4.8±3.2
17	East Usambara Mnts	0.40±0.24	1.6±1.1	4.2±3.4
18	Nguru Mnts	—	—	—
19	Ukaguru Mnts	—	—	—
20	Pugu Hills	—	—	—
21	Rubeho Mnts	0.51±0.09	0.9±0.7	2.5±1.9
22	Morogoro	3.5±0.15	0.4±0.4	1.0±1.1
23	Uvidundu Mnts	0.67±0.31	1.3±1.1	3.5±3.6
24	Uluguru Mnts	0.59±0.13	0.7±0.5	1.8±1.6
25	Udzungwa Highland	0.56±0.11	1.6±1.0	4.3±2.9

9.32

26	Ufipa Plateau	$0.32 \pm 0.13$	$0.3 \pm 0.3$	$0.8 \pm 1.0$
27	Mt. Rungwe	—	—	—
28	Mt. Njesi	—	—	—
29	Mt. Namuli	$0.60 \pm 0.13$	$2.4 \pm 1.5$	$6.2 \pm 4.5$
30	Mt. Zomba	$0.76 \pm 0.13$	$1.5 \pm 1.0$	$4.1 \pm 3.0$

---

University of Cape Town

**Table 9.4.** Average sequence divergence (Kimura-2-Parameter, Kimura 1980) within (diagonal) and between haplotypes belonging to the seven subnetworks demarcated in Figure 9.2 (mean below diagonal, standard deviation above diagonal).

	I	II	III	IV	V	VI	VII
South/Central Eastern Arc & Malawi Rift (I)	0.60±0.18	0.36	0.54	0.19	0.38	0.58	0.33
Northern Eastern Arc (II)	1.85	0.87±0.42	0.51	0.35	0.60	0.60	0.24
Kenyan Highlands (III)	2.79	2.86	1.56±1.01	0.50	0.67	0.61	0.43
Ufipa Plateau (IV)	0.77	1.40	2.34	0.36±0.16	0.30	0.55	0.20
Ruwenzori Mountains & Kabale (V)	3.57	4.33	3.92	3.08	0.95±0.38	0.56	0.31
Kibira National Park (VI)	3.67	3.69	3.6	3.16	3.19	0.75±0.44	0.32
Virunga Highlands (VII)	3.15	3.22	2.96	2.74	3.54	2.41	0.55±0.0



**Table 9.5.** Interpretation of the results of Figure 9.4 using the most recent version of the nested clade inference key. Demographic inferences are presented both for the preferred nesting structure as well as the alternate nesting structure. One-step, 2-step and 3-step clades remain the same for both nesting structures. \*Abbreviations are: CRE, contiguous range expansion; IbD, restricted gene flow with isolation by distance and LDC, long distance colonization.

Clade	Chain of inference	Demographic event inferred*
<b>Preferred nested structure ((3.1 + 3.2+ 3.3) (3.4 + 3.5 + 3.6))</b>		
1-1	1-2-11-17-NO	Inconclusive outcome (CRE or IbD)
1-7	1-2-3-4-9-NO	Past Fragmentation
1-17	1-2-11-12-13-YES	Restricted Gene Flow with some LDC
2-1	1-2-11-17-4-NO	IbD
3-2	1-2-3-4-9-NO	Past Fragmentation
3-3	1-2-?	Inconclusive outcome (CRE or IbD)
4-1	1-2-3-5-15-NO	Past Fragmentation
4-2	1-2-11-12-NO	CRE
Total	1-2-3-5-15-NO	Past Fragmentation
<b>Alternate nested structure ((3.1 + 3.2) (3.3 + 3.4) (3.5 + 3.6))</b>		
4-1	1-2-11-12-NO	CRE
4-2	1-2-?	Inconclusive Outcome (CRE)
4-3	1-2-11-12-NO	CRE
Total	1-2-3-5-15-NO	Past Fragmentation

## FIGURE LEGENDS

**FIG 9.1.** Geographical distribution of the nine subspecies of Starred Robin and populations sampled from within the montane circle of Africa. Bar charts represent the frequency with which haplotypes from each of the seven subnetworks in Figures 9.2 and 9.3 are present in each region.

**FIG 9.2.** Strict consensus of 154 equal length trees ( $L = 294$ ,  $CI = 0.61$ ,  $RI = 0.79$ ) obtained using the parsimony ratchet. Seven clades of haplotypes were identified, which did not corroborate current subspecies boundaries. Values below the nodes represent bootstrap support from 1000.

**FIG 9.3.** Statistical parsimony network for the 58 Starred Robin haplotypes sampled with associated nested design, 1-step clades (black boxes), 2-step (blue boxes) and, 3-step clades (orange boxes) used for statistical analyses (see text). Each line in the network represents one mutational step. The five haplotypes with highest frequency are represented within circles, the area of which is proportional the frequency with which the haplotype was sampled. Empty haplotypes represent intermediate haplotypes that are necessary to link all observed haplotypes to the network. The intermediate haplotypes were either not sampled or have become extinct. Dotted lines point to ambiguities within the network, where there is more than one parsimonious way to make a connection. Seven subnetworks can be identified (I-VII), and are the same as those depicted in Figure 9.2.

**FIG 9.4.** Summary of the statistical results of the nested clade analysis of geographical distances for the 58 Starred Robin mtDNA haplotypes sampled. Haplotype numbers are the same as those in Table 9.2 and Figs 9.2 and 9.3. The symbols, I or t designate a haplotype or clade as an interior or tip, respectively. Haplotypes nested in 1-step clades are grouped in boxes as represented in Fig. 9.3. Higher level clades are designated as one moves down the figure. In each box, the clade distance ( $D_c$ ) and nested clade distance ( $D_n$ ) calculated for each clade within the nested group is shown, as well as the average difference in distances between interior and tip clades for  $D_c$  and  $D_n$  ( $[Int-Tip]_c$ ) and ( $[Int-$

tip[n]), respectively. Significantly small or large distances (at  $\alpha=0.05$ ) are underlined and characterised by s or L, respectively.

**FIG 9.5.** Summary of the major demographic events that were identified by the NCA on the preferred network as having shaped genetic diversity within the Starred Robin.

**FIG 9.6.** Estimated migration parameters for the full constraint and partial constraint models of gene flow. In the full constraint model of gene flow only neighbouring populations can exchange immigrants. The partial model of gene flow was generated by first analysing all possible combinations of 3-regional population triplets. Where gene flow was consistently negligible between two populations in all triplets bearing these populations, the parameters in the matrix were set to zero. This has the effect of reducing the number of parameters to estimate from 25 to 17, thereby increasing statistical power. Lines, which are dotted represent a migration rate of  $4nm < 0.5$ . Solid lines are proportional to the extent to which immigration between two populations is taking place. Regional populations are: (1) Kenyan Highlands, (2) Albertine Rift, (3) Northern Eastern Arc, (4) Southern Eastern Arc and (5) Ufipa Plateau and the Malawi Rift. See text for further details on model parameters.

**FIG 9.7.** Mismatch profiles for regional Starred Robin populations. Histograms represent the observed distribution and lines the expected Poisson distribution for a growing population under the same mean.

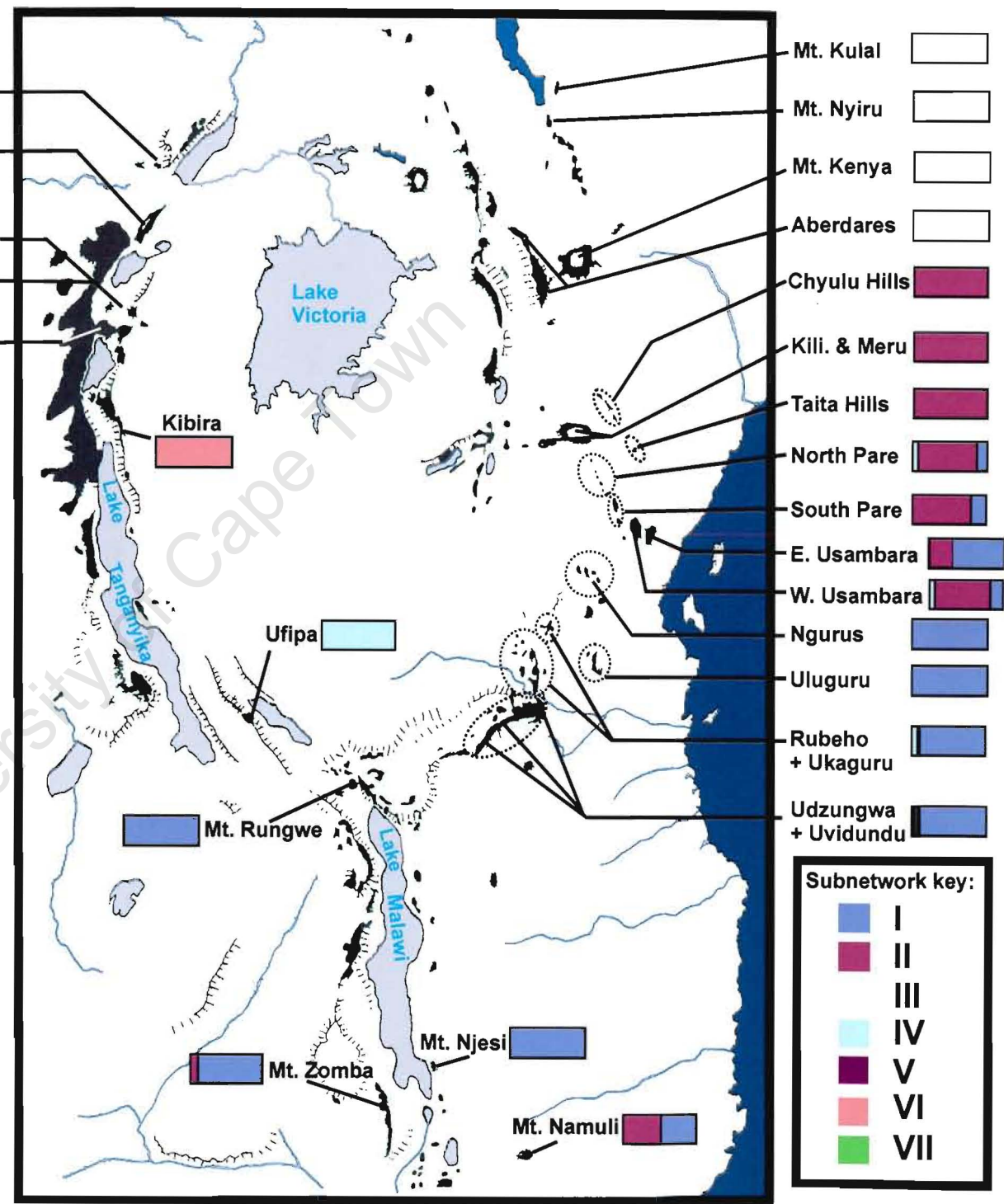
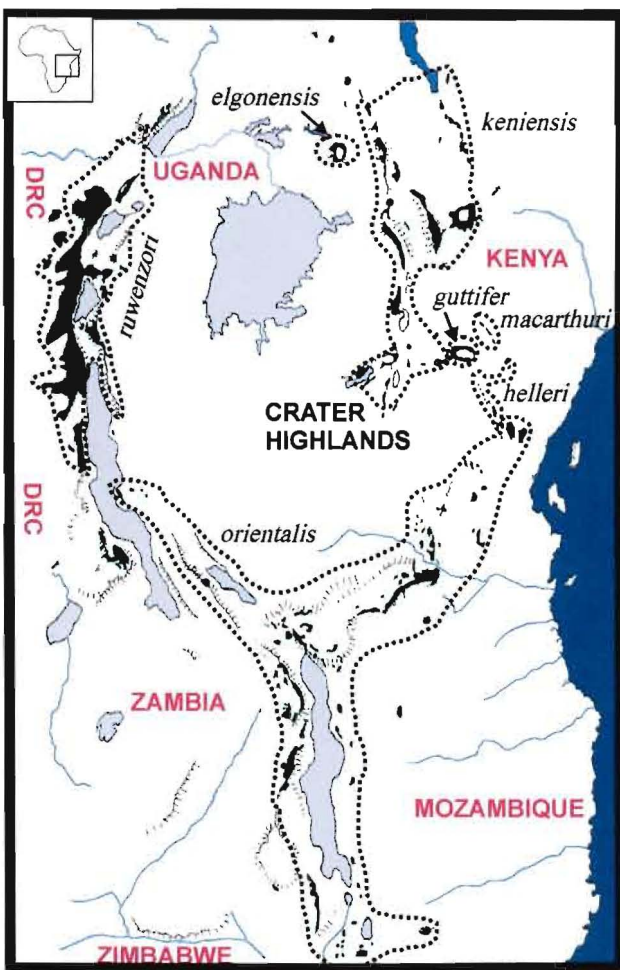
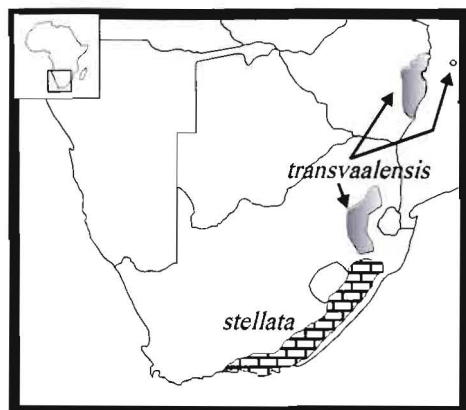


FIG 9.1

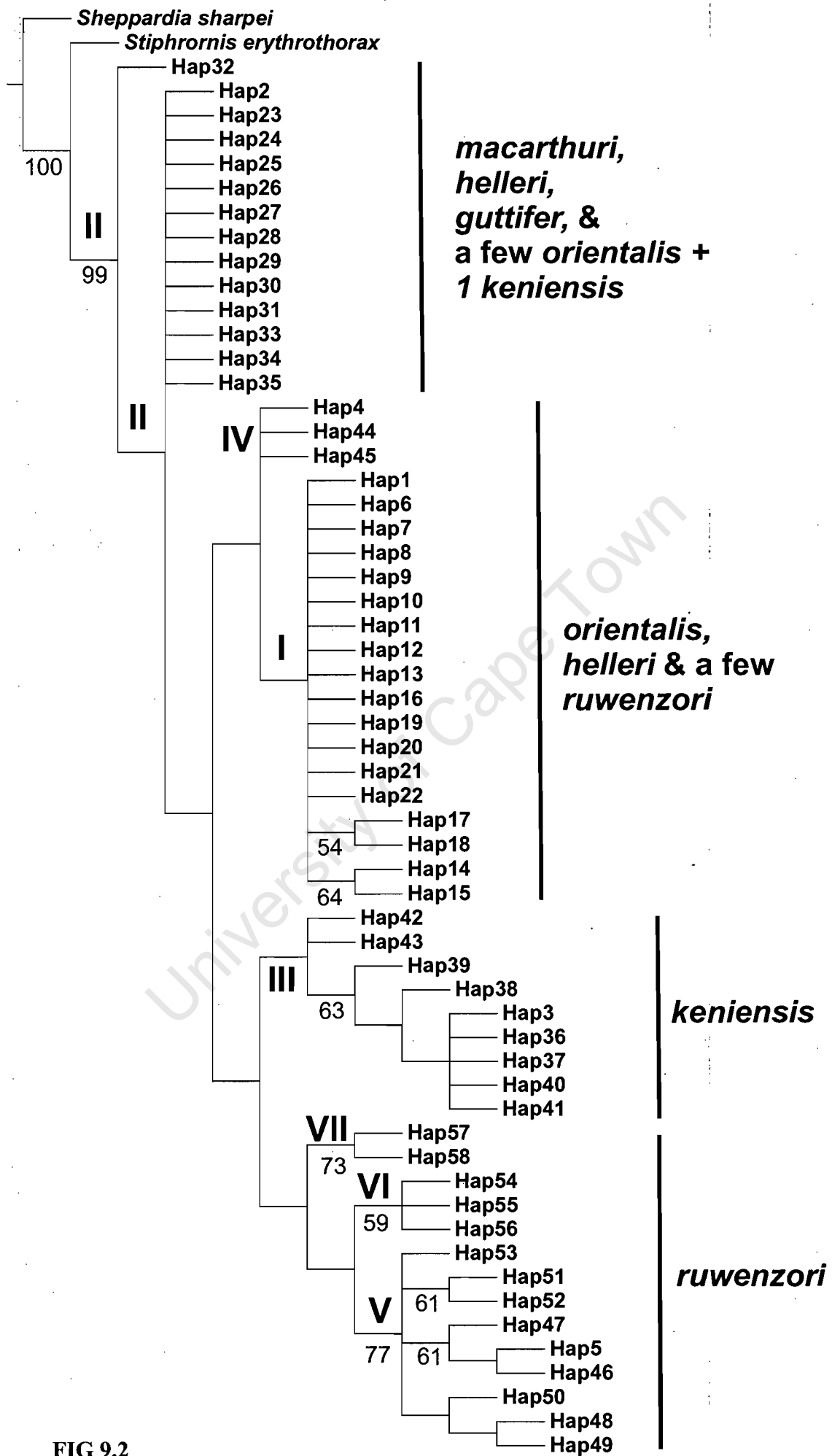


FIG 9.2

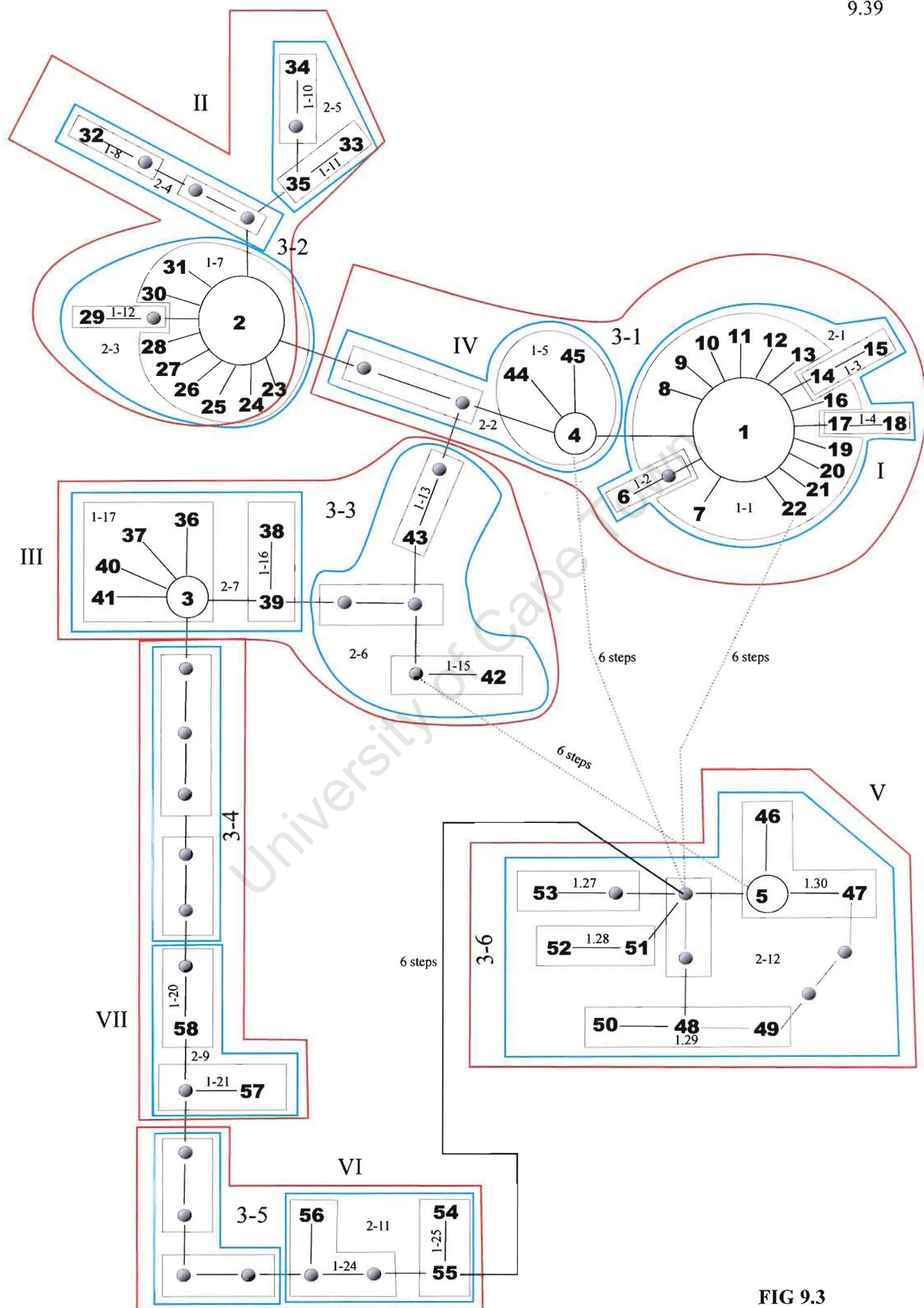


FIG 9.3



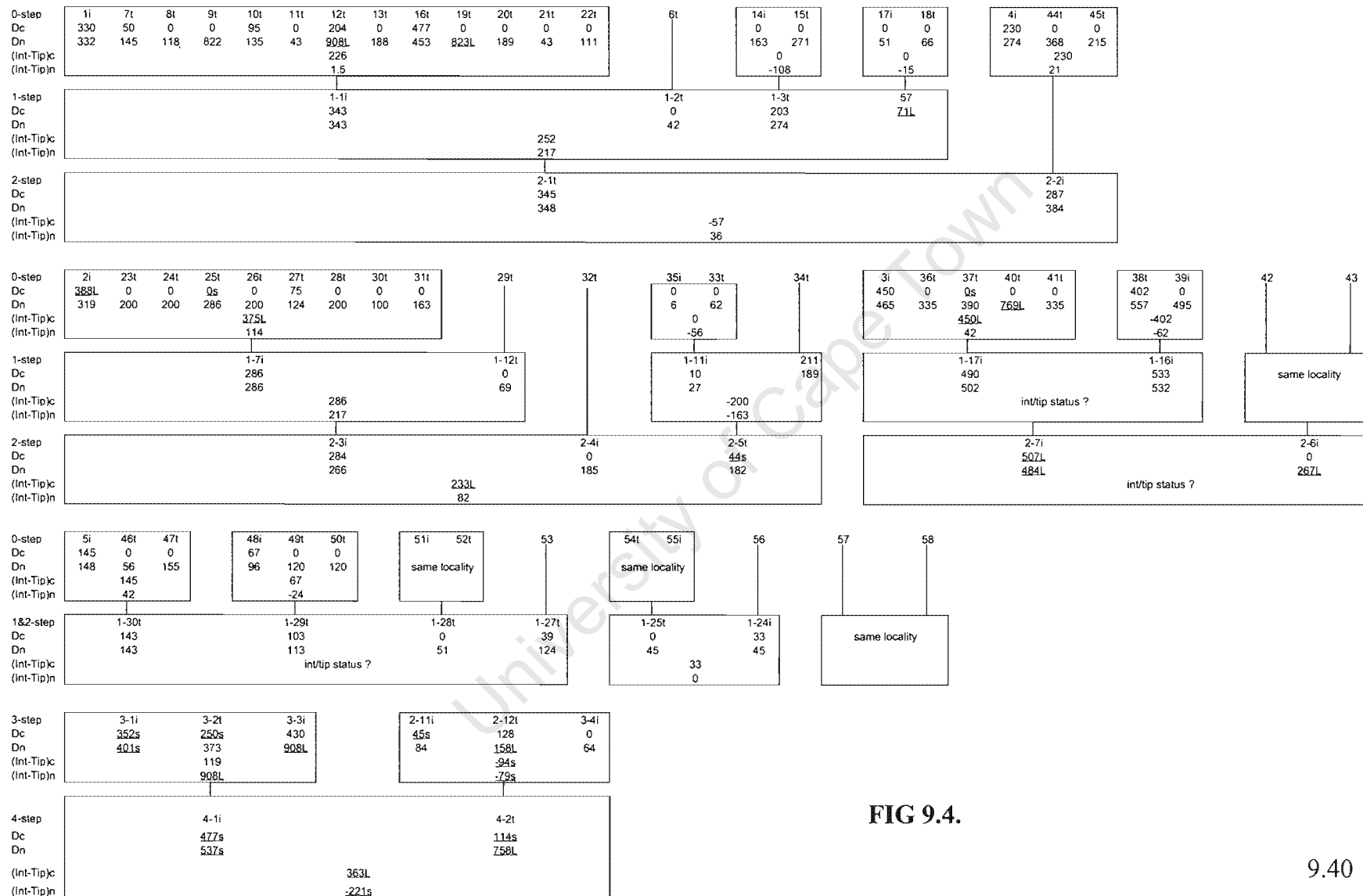


FIG 9.4.

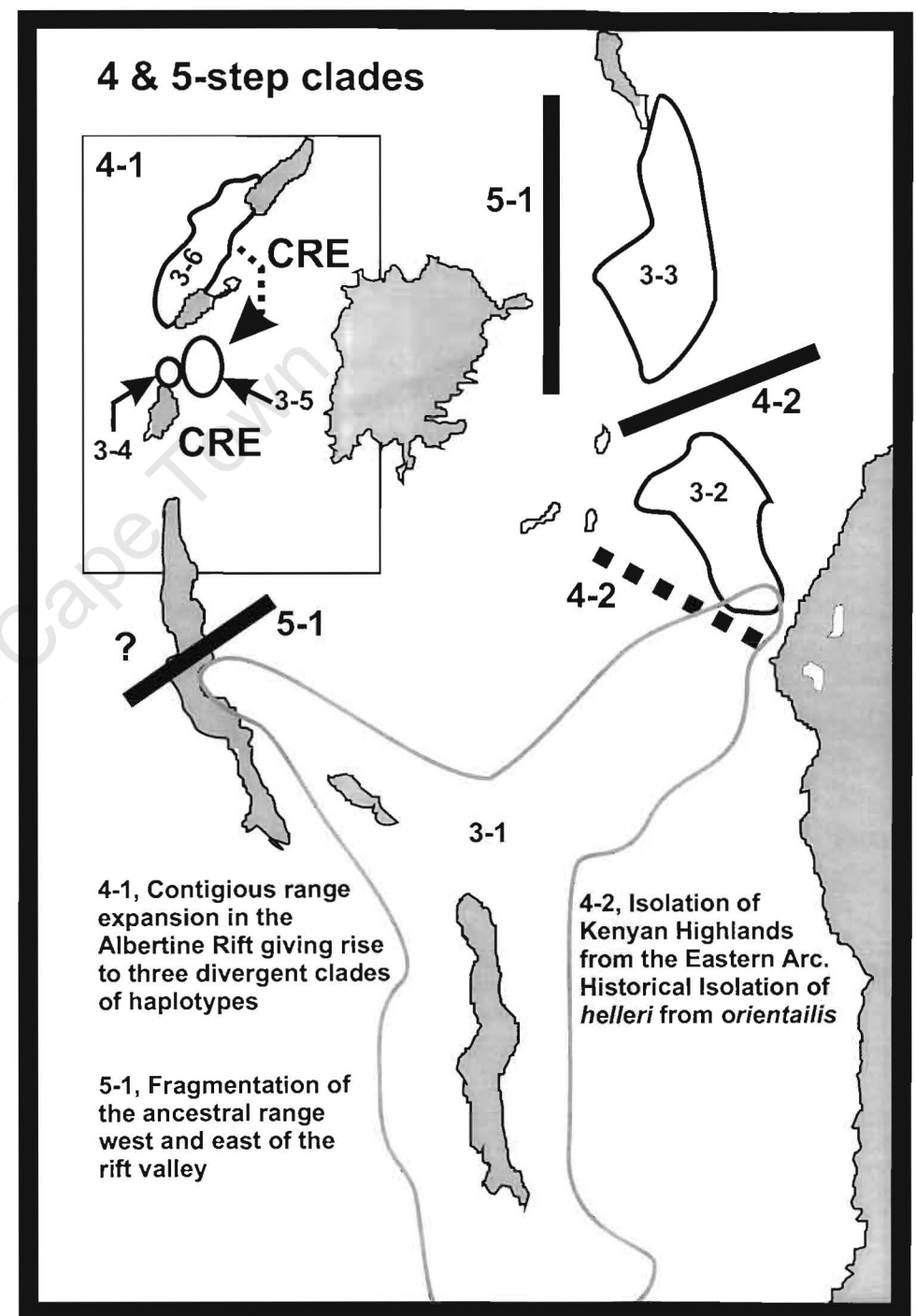
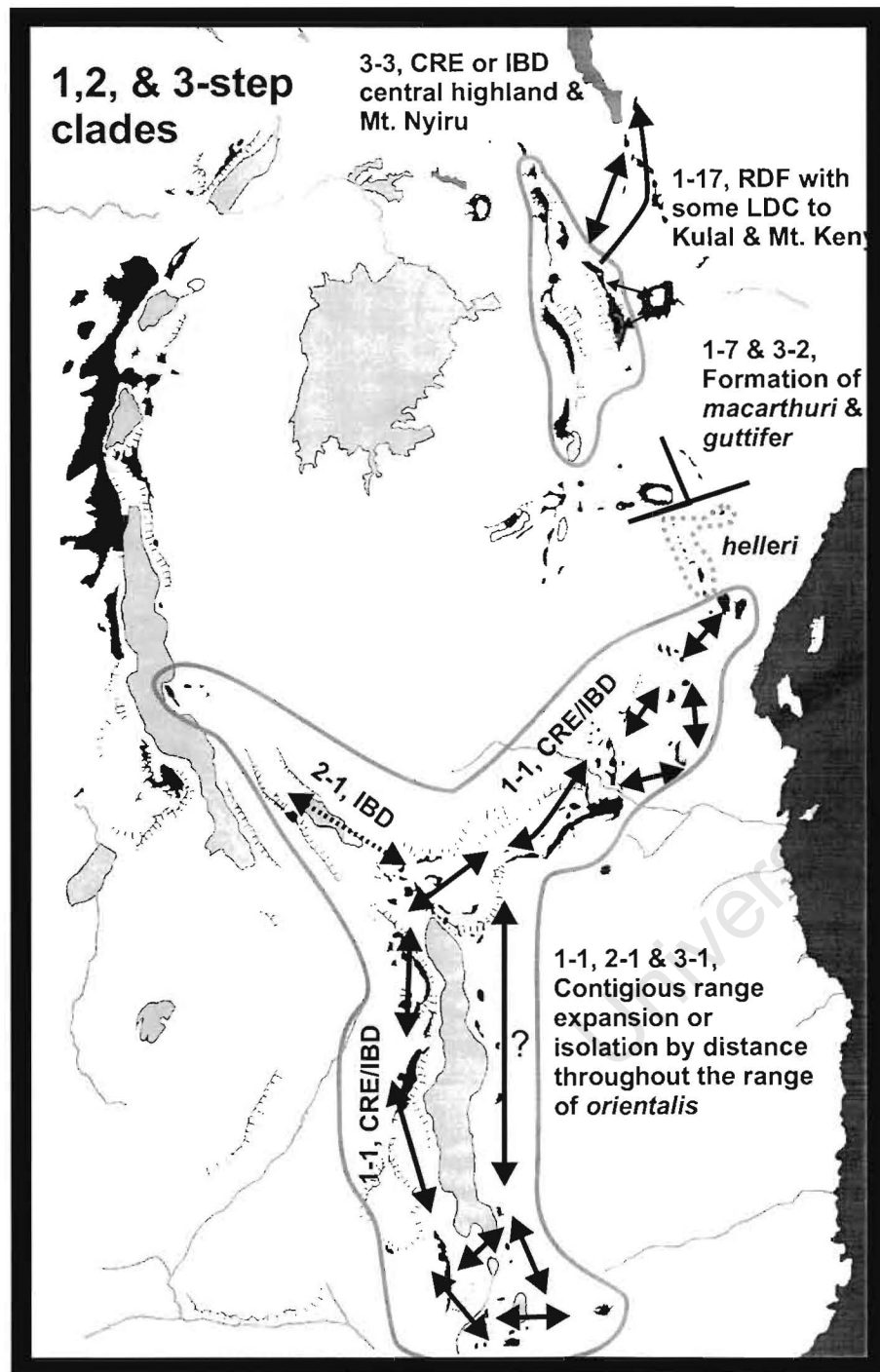


FIG 9.5



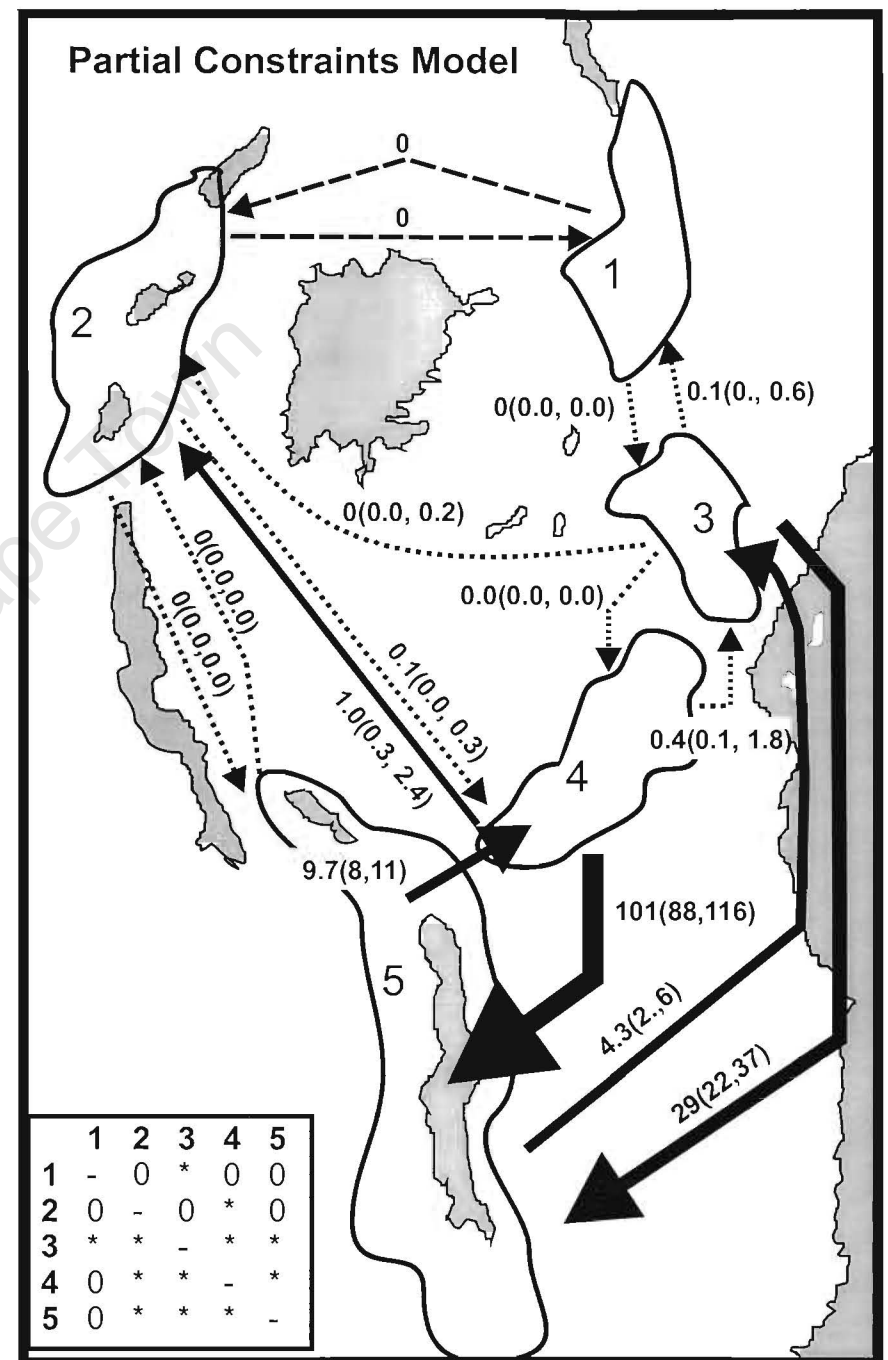
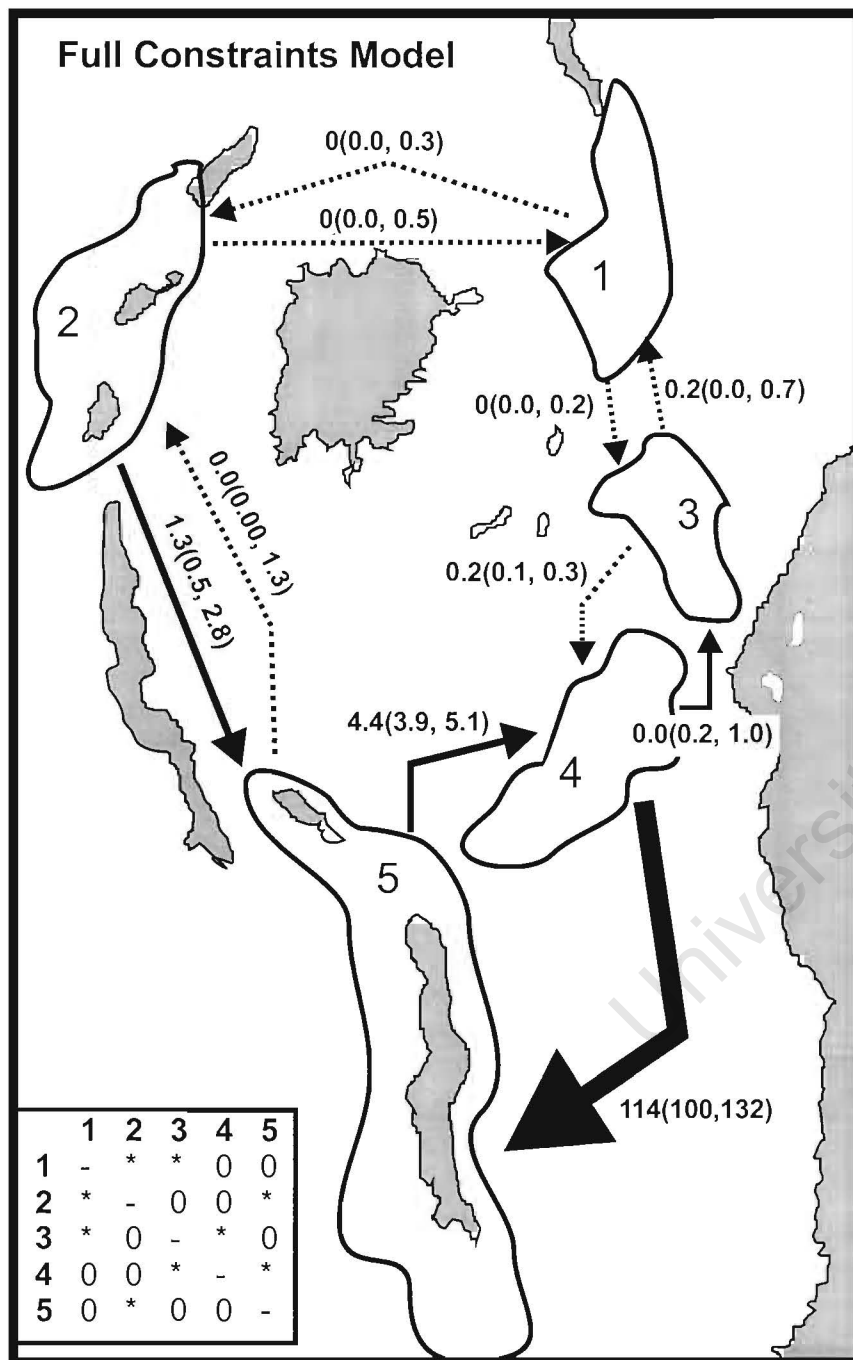


FIG 9.6

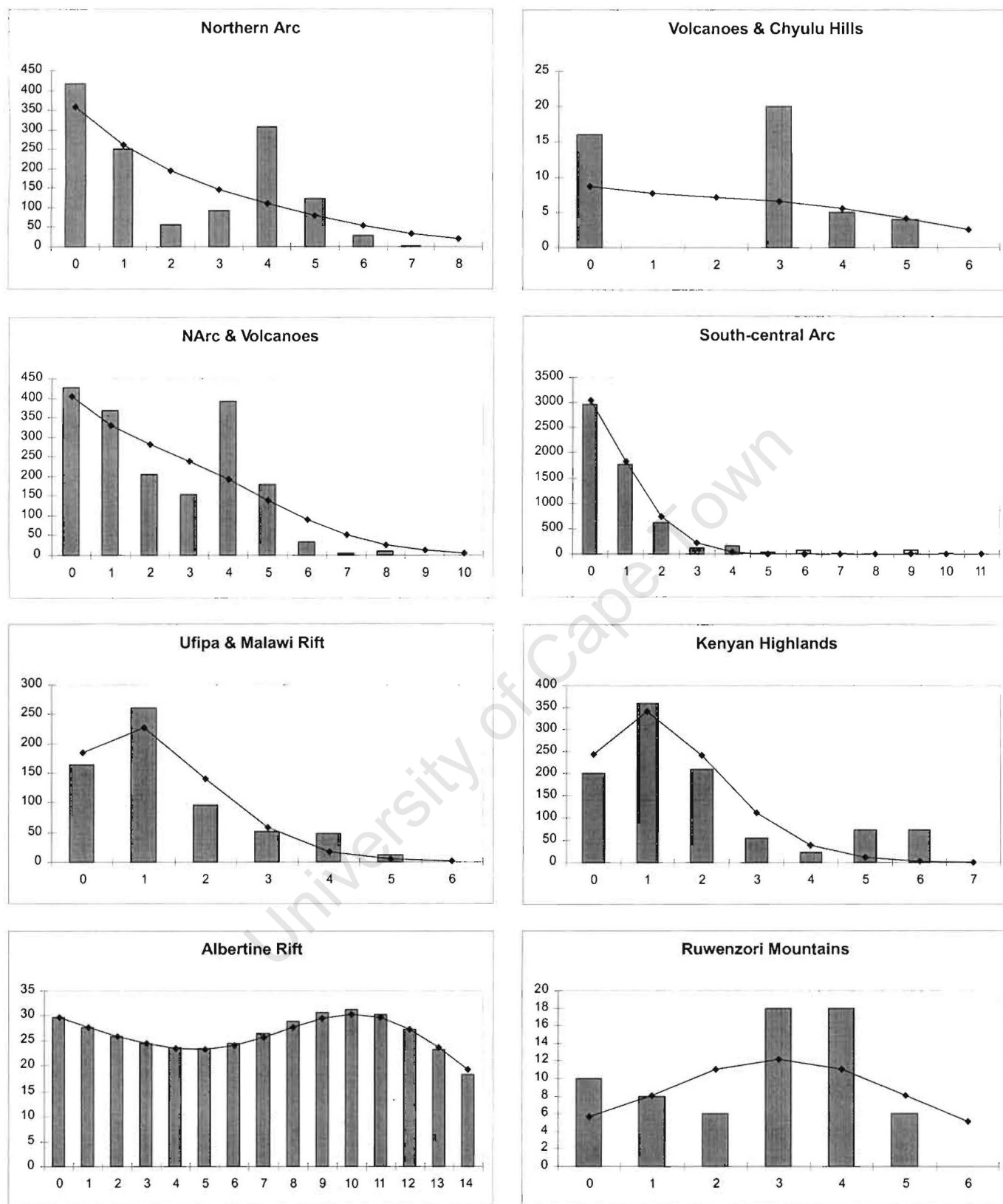


FIG 9.7

## Chapter 10

### **Synthesis: Climatic cycling and its putative influence on speciation among African montane birds**

#### **Space and speciation**

One of the fundamental tenets of systematic biology is centered on gaining an understanding of how spatial distributions of populations relate to the process of speciation. Addressing this question is not easy, as exemplified by the debate on how divergence takes place in isolation (allopatry), a mechanism widely thought to account for current levels of faunal biodiversity (Mayr 1942). Two models, vicariance and dispersal have been proposed to explain how populations and, ultimately, species may form in allopatry. In recent years, the vicariance model has become the preferred null hypothesis, with most biologists agreeing that it is necessary to first reject vicariance before invoking dispersal (Zink *et al.* 2000). The major objection to dispersal theories is centred on the idea that, if enough dispersal events are inferred, then any observed distributional pattern could be accommodated (Rosen 1978, Nelson & Platnick 1981). Consequently, the vicariance model has formed the cornerstone of modern historical biogeography and forms the foundation of a number of prominent speciation models, for example the Pleistocene Refuge Hypothesis (for Africa, Moreau 1966, Diamond & Hamilton 1980, Crowe & Crowe 1982) among others (see Haffer 1997 and Moritz *et al.* 2000 for reviews).

#### **Dispersal**

Yet, dispersal must take place, as exemplified by the formation of biotic assemblages on oceanic islands of volcanic origin. In addition, given the cyclical nature of many geological or climatological processes, accepting concordance in topologies between area-cladograms of two or more lineages as evidence that each lineage was temporally isolated by the same geographical or climatological barrier, i.e. vicariance, can be tenuous (Voelker 1999a, 2002). Indeed, whereas taxa have single histories, areas can have multiple histories with respect to the

component taxa of an area being considered (Cracraft 1988, Voelker 1999a). Thus, while there may be topological congruence in area-cladograms among several lineages, that suggests a common, shared history, the temporal origins of these patterns may be different (Cunningham & Collins 1994 concept of pseudo-congruence, see also Voelker 1999a).

All three of the above concepts, vicariance, dispersal and pseudo-congruence have been used to explain the origins underlying avian evolution on Africa's tallest mountains. If we assume that the degree of morphological divergence of two isolated sister taxa is correlated with the length of the isolation, how can allospecies, subspecies and morphologically similar allopatric populations 'co-occur within the same montane block (montane area of endemism, see Fig. 1.4)?

### **A role for 'refugia'**

Currently, in view of mounting evidence (reviewed by deMenocal 1995, Partridge *et al.* 1995), it is broadly accepted that, during peaks of glaciation, the tropics in Africa became more arid. During the dry and cold glacial periods, montane forests were reduced, whereas lowland forests mostly disappeared, except for small remnant patches that formed refugia. The reduction in montane forest would have isolated assemblages of montane taxa to specific mountain ranges, which would have then been free to drift genetically in isolation, eventually leading to the formation of species. Until recently, most authorities placed the above climatological mechanism within a vicariance framework, via the addition of an explicit temporal component leading to the suggestion that Pleistocene climatic changes drove speciation among African forest birds (Livingston 1975, Hamilton 1976, Diamond & Hamilton 1980, Crowe & Crowe 1982, Mayr & O'Hare 1986, Meadows 1996, Hamilton *et al.* 2001). Although variations in Pleistocene refugia may explain the origins of range-restricted taxa, they do not explain the high number of avian taxa that are shared between isolated montane groups.

### **The problem**

Diamond and Hamilton (1980) developed a dispersal-based hypothesis to accommodate this problem. They concluded that afromontane bird species with

disjunct populations “have probably either flown from one area to the other or else once occurred in the intervening lowland forest”. A central tenant to Diamond and Hamilton’s (1980) explanation for montane disjunctions is centred on lowland forest penetrations by montane species when competition was reduced. This could have happened during the short period at the beginning of an interglacial when lowland forest, and by extension associated species, would have been expanding rapidly from refugia. Accepting this interpretation to explain the discontinuous distribution patterns necessitates montane birds to have been very mobile or to have previously shown a much wider tolerance of altitudinal range (Dowsett 1986). Additionally, Diamond and Hamilton’s (1980) competitive exclusion theory seems inadequate, as many of the important montane refugia (e.g. Albertine Rift, Cameroon-Gabon, see Prigogine 1987) also included lowland forest. Thus, there is no reason to assume that lowland species would not be present to first exploit available niches that appeared with the expansion of the lowland forest. Consequently, rapid dispersal, possibly across huge distances, seems the more likely of Diamond and Hamilton’s (1980) hypotheses. This presents one of the greatest paradoxes of African biogeography, as it seems extremely unlikely when we consider that nearly all studies of montane birds suggest they have limited dispersal capabilities, and then mostly altitudinal, as well as natal philopatry (e.g. Dowsett 1982; 1985, Dowsett & Dowsett-Lemaire 1984, Dowsett-Lemaire 1983, 1988, 1989).

Prigogine (1987) suggested an alternative hypothesis; that during wet periods, montane forest would have occurred at lower altitudes and gradually expanded to cover the tops of ancient fault lines or uplifted escarpments of lower lying hills 600 to 900m above sea level, which connect a number of montane isolates. The premise for this hypothesis is based on the observation that on the East Usambara Mountains montane birds occur as low as 900m (Moreau 1952), while on the southeastern face of Mt. Cameroon, where temperatures fall even lower, montane birds extend down to 600m (Prigogine 1987). Thus, following expansion of montane forest, characteristic montane species could have dispersed in a stepping-stone fashion. Eventually, connections could be developed for instance between the Albertine Rift and the Cameroon Highlands via a series of populations occupying the hill-corridor running along the northern Congo basin.

Later, with the onset of glacial conditions, the increased aridity would have caused the fragmentation and eventual disappearance of the forest corridors. Thus, previously widespread taxa became isolated within the different montane blocks they had reached.

Prigogine's (1987) essentially vicariance model, although without an explicit temporal framework, does well to explain connectivity between montane blocks. However, it still does not provide a plausible explanation for the spatial distribution of morphologically similar and divergent taxa among different montane blocks. If a purely vicariance-based explanation were accepted to account for the distributional patterns of afromontane birds, then it would be necessary to accept that morphological divergence among taxa is not correlated with geological time. This may be true for some lineages, but it is unlikely to explain the highly structured patterns of taxa shared among, as well as endemic to, montane areas of endemism in Africa. In contrast, dispersal also seems to be a woefully inadequate explanation given the apparent limited dispersal abilities of afromontane birds. Prigogine (1987) extended his montane connectivity model described above to provide a simple solution couched within a pseudo-congruence (Cunningham & Collins 1994) framework. He suggested that allospecies isolated on different mountain ranges, dispersed by diffusion along corridors, and that subsequent isolation occurred further back in time than for subspecies, which in turn were isolated less recently than morphologically similar but allopatric populations (Fig. 1.7).

The central theme of Prigogine's model (1987) is that climatic fluctuations, especially recurrent glaciation periods over the last 3 million years, have played an important role in the repeated fragmentation of the afromontane biomes. Thus, the biotypes of different mountains are likely to have experienced a complex pattern of fragmentation. This ranges from being in contact with neighbours on a number of occasions, to never having been directly in contact with other montane forest or afro-alpine communities (e.g. Mt. Kulal and Mt. Marsabit in northern Kenya).

### **A role for molecular evidence**

The rapid development of molecular biology as a scientific discipline over the past 30 years has provided a new data source and a diversity of analytical techniques that have enriched biogeographical analyses. Perhaps the most significant contribution is the ability to reconstruct molecular phylogenies using nucleotide models of evolution, which enable estimation of branch-lengths and therefore speciation events to be tentatively dated (Riddle 1996, Voelker 1999a). If the molecular clock hypothesis is accepted, that is, for example in mitochondrial DNA (mtDNA) divergence accumulates at a roughly uniform and time-dependent rate, then we would expect sister-taxa in different lineages separated by the same biological barrier to exhibit similar mtDNA divergences (if they have similar population sizes). Thus, depending on the concordance between relative ages of species divergence and hypothesised vicariance events, assessment can be made as to whether vicariance (concordance between age of barrier and species divergence) or dispersal (lack of concordance between age of barrier and species divergence) based hypotheses better explain the observed distributional patterns (Voelker 1999a, Zink *et al.* 2000). Testing for pseudo-congruence poses more of a problem as demonstrating either concordance or lack thereof is insufficient, rather a nested pattern of concordant divergences among lineages at different points in time is predicted. This is as opposed to general concordance in time of divergence among lineages under a vicariance model, or a random temporal pattern associated with dispersal theories. However, one major caveat in being able to detect a pseudo-congruence pattern is that the area from which historical biogeographical patterns are being inferred needs to have remained relatively stable, and the associated community should not be prone to excessive levels of extinction. Otherwise the 'pile-up' (nested) pattern of repeated temporal congruence among sister-lineages could not be recovered.

### **Areas of endemism**

The montane circle of African mountains incorporates four of seven recognized African montane areas of endemism, (1) the Eastern Arc, (2) Albertine Rift, (3) Kenyan Highlands and (4) the tip of the southeastern block, which stretches from Malawi to South Africa (Fig. 1.4). This circle of mountains in Eastern and central Africa provides an interesting study area with which to evaluate alternate

models of montane bird evolution in Africa. For example, the Eastern-Arc Mountains exhibit high species endemism, a feature that has been attributed to persistent humidity facilitating the maintenance of forest on some mountain escarpments facing the Indian Ocean since the Tertiary (Fjeldså & Lovett 1997; Burgess *et al.* 1998). Consequently, it is not surprising that some endemic species appear to be relicts of a Tertiary/Miocene forest corridor that linked Africa with Asia (Cox & Moore 1993, Juste *et al.* 1999). For example the genera *Xenoperdix*, *Arcanator*, and *Modulatrix* are all monotypic with uncertain affinities (Sibley & Monroe 1990, Burgess *et al.* 1998). However, the Eastern Arc and montane circle in general is also an area of recent diversification as isolation has alternated with opportunities for dispersal and (re)colonisation (Fjeldså & Lovett 1997). The montane circle of Africa and specifically the mountains of the Eastern Arc, provide an ideal departure point from which to investigate the relative roles that dispersal and vicariance have played in shaping African montane bird communities.

## **VICARIANCE, DISPERSAL AND PSEUDO-CONGRUENCE: FIRST INSIGHTS**

### **Molecular ‘clocks’**

Species-level phylogenies for the Eastern Double-collared Sunbird complex (Chapter 3), Greater Double-collared Sunbird complex (Chapters 4 & 5), Olive Thrush species complex (Chapter 6 & 7), and two sister lineages of African Greenbuls (genus *Andropadus*, Roy 1997, Roy *et al.* 1998) are summarized in figures 10.1 to 10.4. For each of these lineages Kimura 2-parameter distances (Kimura 1980) were calculated and these distances were scaled into approximate times of divergence among taxa using the 1.6% sequence divergence per million years calibration estimated by Fleischer *et al.* (1998). Whereas it would be ideal to use passerine taxa with a good fossil record to calibrate a specific clock for each of the above lineages, as done for some non-passerine lineages (e.g. Krajewski & King 1996, Friesen & Anderson 1997), nearly all of these taxa lack a fossil record suitable for calibrating a clock. Consequently a proxy for divergence, such as the model proposed by Fleischer *et al.* (1998) had to be used. While this approach is adopted in this study, it was important to first test for rate heterogeneity across lineages (Voelker 1999a). None of the lineages



summarized exhibited significant departures from rate heterogeneity (see individual chapters and Roy 1997) consequently divergence dates are assigned to nodes. One important caveat to bear in mind with respect to the discussion below is that molecular evolution can also vary between taxonomic groups and if so, this may invalidate the general application of the rate of 1.6% per myrs calibration used in this study. However, this is unlikely given that clock values at or near 1.6-2% have been inferred for multiple studies from various avian orders (e.g. Shields & Wilson 1987, Tarr & Fleischer 1993, Wood & Krajewski 1996, Friesen & Anderson 1997, Fleischer *et al.* 1998).

Four montane areas of endemism occur within the montane circle: the Eastern Arc Mountains, the Southern Eastern block, represented in the montane circle by the Malawi Rift, the Albertine Rift and the Kenyan Highlands (Fig. 1.4). The validity of recognizing the Eastern Arc as a single area of endemism must be questioned given the significant genetic structure uncovered among disparate lineages of birds (Chapters 3 & 7, and Roy 1997, Roy *et al.* 1998, Roy *et al.* 2000). Consequently, the Eastern Arc is divided into four smaller areas, the northern Arc (Taita Hills, Pare and Usambara Mnts), the central Arc (Rubeho, Nguu and Nguru Mnts), the Uluguru Mnts and the southern Arc (Udzungwa Highlands), each of which has two or more endemic species restricted to them. The estimated times of divergence between taxa inhabiting adjacent areas of endemism are summarized in Table 10.1. It is immediately apparent that for at least five of the six comparisons there is little agreement between the times of divergence among sister taxa in adjacent areas of endemism. The only possible exception is between the Kenyan Highlands and the Albertine Rift, which given the limited divergence of *Turdus abyssinicus baraka* and *Turdus a. bambusicola* from *Turdus a. abyssinicus* (0.4 myrs) and the co-occurrence of *Andropadus nigriceps kikuyensis* and *Andropadus musukuensis kakamegae* in the Albertine Rift and Kenyan Highlands suggests that these two areas have recently been connected. As recently as the early Holocene a continuous forest corridor existed north of Lake Victoria during periods of high humidity and precipitation, which would have facilitated dispersal between the Albertine Rift and the Kenyan Highlands (Diamond & Hamilton 1980, Roy *et al.* 1998).

If a single temporal vicariance event appears to be implausible, then does random dispersal provide an answer despite behavioural evidence which suggests that forest birds tend to be sedentary as well philopatric to their natal site (e.g. Dowsett 1982; 1985, Dowsett & Dowsett-Lemaire 1984, Dowsett-Lemaire 1983, 1988, 1989)? Alternatively, does an overlay of multiple vicariance events at different times in the past (pseudo-congruence, Cunningham & Collins 1994) provide a better explanation as suggested by Prigogine (1987, see Fig 1.7 for model)? This is a difficult question to answer, but a number of splits among taxa have resulted in congruent spatial distributional patterns if not temporal patterns (Table 10.1). For example, the Central Eastern Arc, given the data summarized within this study, appears to have been connected on at least two occasions to the Uluguru Mountains: (1) an ancient connection *ca.* 6.7 myrs BP which lead to the isolation of *Andropadus fusciceps chlorigula* from either *Andropadus fusciceps neumanni* by long distance dispersal, or fragmentation of an ancestral species which was more widely distributed, and (2) a more recent (*ca.* 3 myrs BP) vicariant isolation of a widespread ancestral species lead to the isolation of *N. loveridgei* in the Uluguru Mnts and *N. moreaui* within the Central Eastern Arc (and *N. fuelleborni* in the Southern Arc and Malawi Rift, see Chapter 3). A series of hills connects the Central Eastern Arc to the Uluguru Mnts, which during favourable climatic conditions (wet interglacial periods) would have supported forest providing a dispersal corridor connecting the two areas. As aridity increased, for example in response to climatic forcing from the Northern Hemisphere associated with higher latitude glacial cycles, forest would have gradually disappeared ultimately isolating the Uluguru Mnts from the rest of the Eastern Arc.

A similar pattern of spatial concordance but temporal variability is recovered among other lineages. The Central Eastern Arc shares with the Udzungwa Highlands (Southern Eastern Arc) and the Malawi Rift, three species pairs which all show similar leaves of divergence, *N. moreaui/loveridgei* vs. *N. fuelleborni* (3.0 myrs BP), *Andropadus fusciceps chlorigula/neumanni* vs. *Andropadus fusciceps fusciceps* (3.7 myrs BP) and *Andropadus masukuensis roehli* vs. *Andropadus masukuensis masukuensis* (3.2 myrs BP). If one allows for some variation in the exact timing of lineage divergence and individual dispersal

ability, this suggests that these taxa may have been isolated during the same time period of global cooling. This could possibly be due to the same vicariance event, for instance the marked increase in aridity at the end of Pliocene 2.8 myrs BP (deMenocal 1995). However, as for the Uluguru Mnts, the Central Eastern Arc vs. the Udzungwa Highlands comparison also shows different patterns of temporal isolation, *N. skyei/whytei* show a much more recent connection (0.1-0.3 myrs BP), again suggesting that areas of endemism have been repeatedly connected in the past. A similar pattern is recovered if sister taxa restricted to the Udzungwa Highlands/Malawi Rift and the Albertine Rift are contrasted, or if sister taxa in the Kenyan Highlands are contrasted with the Northern Eastern Arc (Table 10.1).

### **Back to the key question**

Returning to our key question: Do the above studies support a pseudo-congruence pattern or is random dispersal driving avian montane community structure in Africa? I would argue that the above examples (discussed in more detail in preceding chapters), and the work by Roy and co-authors on Greenbuls (Roy 1997, Roy *et al.* 1998) and Akalats (Roy *et al.* 2000) support a pattern of multiple temporal connections between montane areas of endemism, many which have occurred before the Pleistocene. However, it should be acknowledged that this is a working hypothesis. Clearly not all taxa share concordant histories and dispersal ability must have been important in determining when and if a species utilized a corridor linking any two montane areas during climatic conditions favourable for forest expansion. This 'random element' may help account for why species cladograms are not completely concordant with area cladograms, both spatially and temporally.

### **IN THE ABSENCE OF RECIPROCAL MONOPHYLY: *POGONOCICHLA* AND *NECTARINIA OLIVACEA***

If climatic cycling can really explain how allospecies, subspecies and morphological similar but allopatrically distributed taxa can accumulate in montane communities as implied by Prigogine (1987, Fig. 1.7), then the temporal pattern of connection and subsequent spatial isolation between montane areas of endemism should not only be restricted to deeper (pre-Pleistocene as discussed in

the preceding section) nodes. It should also be recovered in the geographical structuring of widespread montane species (the subspecies and allopatric population level). However, one of the major differences in investigating geographical structuring within species is that in many cases reciprocal monophyly of putatively geographically structured clades has not yet been established, either as a consequence of incomplete lineage sorting, or in response to secondary contact (Fig. 10.5). Therefore, alternative analytical methods to phylogenetic tree building algorithms often need to be employed to resolve spatial patterns among closely related lineages. Indeed, many of the underlying assumptions of standard parsimony and maximum likelihood methods are often violated when analysing datasets for intraspecific taxa or structured populations (see Crandall *et al.* 1994, Crandall & Templeton 1996 for reviews). Consequently, in Chapters 8 and 9 the Templeton, Crandall and Sing parsimony algorithm (TCS - nested clade analysis, Templeton *et al.* 1992) was used together with mismatch analyses (Rogers & Harpending 1992, Harpending *et al.* 1998) to investigate phylogeography and demographic structure, and finally, coalescent modelling was used to estimate directional gene flow among regions in Chapter 9 (Beerli & Felsenstein 1999, 2001).

### **The Starred Robin**

The Starred Robin (*Pogonocichla stellata*) is a small brightly coloured forest robin, which typically breeds in montane forest between 2500 and 3300m (Oatley & Arnott 1998). The species is distributed in montane evergreen forest extending from the Imatong Mountains in southern Sudan and Mt. Kulal in Kenya, southwards across the eastern and central parts of the African continent. Altitudinal migration by this species is widespread, but in many areas this is probably partial. Mark-recapture studies on Starred Robins from Nyika Plateau in northern Malawi (Dowsett 1982) have revealed that females preferentially move away from the Plateau during the coldest months of the year (April to August), whereas males tend to remain at the breeding territory. Thus, altitudinal migration may occur to a greater or lesser extent depending on geographical location. Despite these movements, the Starred Robin is discontinuously distributed in the highlands of Africa and appears to be highly genetically structured with some 15 subspecies having been recognized.

Investigation of genetic structure among 283 individuals suggested that a protracted history of isolation has led to the geographical structuring of races observed today. Given the possibility of natal philopatry and recognition of extensive plumage and vocal variation by the description of a relatively large number of subspecies, it is not surprising that the most ancient demographic event detected by the nested-clade analysis is one of historical fragmentation (vicariance) of the ancestral range into at least three broad geographical regions, 1) Kenyan Highlands, 2) Albertine Rift and 3) the Eastern Arc. This was probably followed relatively quickly by isolation of the northern Eastern Arc from the south-central Arc, although because of secondary contact it is not possible to determine exactly where the barrier formed, or for how long it persisted.

Although a maximum of *ca.* 6% sequence divergence was detected among the 58 sampled haplotypes, due to lineage sorting it may be more appropriate to use average sequence divergence values among these three regions to infer the putative age of the fragmentation of the ancestral range of the Starred Robin. Using a calibrated rate of 1.6% divergence per million years (Fleischer *et al.* 1998) suggests that fragmentation of the ancestral range of the Starred Robin took place between 2.7 and 1.8 myrs before present (BP). This would have led to the isolation of present day *ruwenzorii* in the Albertine Rift, *keniensis* within the Kenyan Highlands, *orientalis* in the south-central Eastern Arc and Malawi Rifts, and *helleri* in the northern Eastern Arc. These dates are noteworthy as they correspond to the ending of a relatively stable Pliocene in Africa when montane forest was thought to have been well established and the onset of a period of increased aridity in Africa (deMenocal 1995).

### **The Olive Sunbird**

The Olive Sunbird is a relatively large polytypic sunbird widely distributed throughout evergreen, montane and coastal forests in Africa. Thus, it is something of a surprise that an analysis of geographical structure among 282 individuals within this species recovered the same basic areas as recovered for *Pogonocichla* (Chapter 9), as well as for the Eastern Double-collared Sunbird

(Chapter 3), Olive Thrush (Chapter 7) and in montane Greenbuls of the genus *Andropadus* (Roy 1997, Roy *et al.* 1998), two distinct evolutionary lineages, one in the (1) north and the other in the (2) central-south of the Eastern Arc, (3) the Kenyan Highlands, and (4) Albertine Rift were recovered.

The splitting of the Eastern Arc in to northern and south-central components suggests that the 100 km of low-lying arid savannah between the Usambara and Nguru Mountains is an old barrier to gene flow. In a broad analysis of distributional patterns of 28 forest species most of which are endemic to the Eastern Arc, Cordeiro (1998) identified the Nguru, Nguu and Rubeho Mountains as being among the most impoverished and distinctly nested (*sensu* Patterson 1987) montane communities within the Eastern Arc. When placed in context with geographical structuring in other lineages this suggest that even for fairly mobile species such as the Olive Sunbird, crossing the gap between the Nguru and Usambara Mountains is difficult, effectively restricting gene flow.

#### **Other taxa**

In *Nectarinia olivacea* there is evidence for an historical connection between Mt. Namuli in northern Mozambique and the Kenyan Highlands, and results from the nested clade analyses and mismatch analyses suggest that this may be a result of an old vicariance event. The Long-billed Apalis '*Apalis*' *moreaui*, which has uncertain evolutionary affinities and whose placement in *Apalis* is controversial (Sibley & Monroe 1990), has two relictual populations, one within the East Usambara Mountains and one on the Njesi Plateau in Northern Mozambique. Similarly the Dapplethroat (*Arcanator orostruthus*) and Swynnerton's Robin (*Swynnertonia swynnertonii*) have widely sundered populations, with *Arcanator* occupying forest on the East Usambara, Udzungwa Scarp and Mt. Namuli, and *Swynnertonia* occurring in understorey forest of the East Usambara, Udzungwa Highlands, Zimbabwe highlands and central Mozambique. These widely separated populations of apparently highly sedentary species suggest a complex pattern of origin, also reflected within the higher (and therefore older) nested clades of phylogeographic structure in *N. olivacea*. Whether these disjunct populations have a common vicariant origin remains to be tested.

### Population-level phenomena

The results of the population-level analyses suggest that the ancestral ranges of the Starred Robin and Olive Sunbird were fragmentation in response to aridification of Africa following the cooling of the Northern Hemisphere from about 2.8 myrs BP. With the retraction of the ice in the northern hemisphere, Africa entered a wetter phase in response to the greater influence of low-latitude insolation forcing of the west and east African monsoons in relation to the Earth's Orbital precession. Increased precipitation may have provided the impetus for the more recently observed secondary contact between populations in the northern and south-central Eastern Arc, and between the Albertine Rift and Eastern Arc. Thus, even within species, there appears to be evidence of lineages being isolated in the same areas of endemism as described in the preceding section, but within a more recent temporal (Plio-Pleistocene) framework.

### THE LAST STRAW: *CRYPTOSPIZA*

Crimsonwings (genus *Cryptospiza*) are a group of four species of mostly olive-green and red finches that are restricted to the undergrowth of montane rainforest. Based on knowledge about the understorey habits of these species, apparent limited dispersal ability and close association with montane rainforest, a highly resolved genetic structure was predicted. However, a study of nearly 200 individuals from the four species revealed a pattern inconsistent with the above hypotheses. Whereas *Cryptospiza shelleyi* and *C. jacksoni* both endemic to the Albertine Rift were basal relative to the other taxa, there was only a single mutational difference between *C. reichenovii* and *C. salvadorii* from the 383 bp sequenced (Bowie unpublished data). Worse still, not one of the four montane circle areas of endemism were recovered, rather from a 163 *C. reichenovii* and *C. salvadorii* individuals sequenced, only 17 haplotypes were identified (Fig. 10.6). No geographical structure was apparent throughout the species range, and no evidence of hybridization is apparent between the two taxa where their ranges contact in the northern Albertine Rift, on Mt. Meru and possibly in the Uluguru Mountains. This pattern of complete lack of geographical structure appears to contradict the general pattern described in the preceding sections suggesting that dispersal is extensive despite behavioural evidence to the contrary. An alternative explanation may be that these taxa have only recently expanded,

possibly within the last 0.2 myrs, and that not sufficient time has passed for mutations to accumulated within the mtDNA to be able to detect geographic structure. An analysis using microsatellite markers should help separate the above hypotheses.

### **A PULSED SPECIATION MODEL**

In summary, there appears to be deep genetic divergence between many clades (8-12%) of afromontane passerine birds, with some shallow divergence towards the tips (4-6%). For widespread species reciprocal monophyly has not been reached in some instances, but generally there is some support for the refuge idea, that isolation (fragmentation) of montane forests has facilitated speciation (species in the context of Zink & McKittrick 1995). However, most speciation events happened well before the Pleistocene and therefore the Pleistocene Refugia Model is not appropriate as a model with which to explain patterns of afromontane bird distribution. Rather, both dispersal and vicariance have played important roles in shaping montane bird communities. Thus, a refugium type model does work, but only within the context of pulsed or cyclic expansion and contraction of montane forests. This is supported in this study by the consistent recovery of spatially structured areas of endemism (except for the very recent putative expansion in *Cryptospiza*), despite varying temporal dynamics. The main features of this pulsed speciation model conforms the model outlined by Prigogine (1987) although the temporal dimension is wider than he hypothesized. Similar patterns of climatic cycling with repeated vicariance have also recently been postulated to occur in the Amazon lowlands (Bates in press) and may underlie community assemblage patterns in many different landscapes (see Jansson & Dynesius 2002). However, as stressed earlier, the notion of a pulsed speciation model as an explanation, which underlies the evolution of African montane communities' is a working hypothesis, as there are still too few phylogenies to determine the extent to which species cladograms agree with area-cladograms. However, it is hoped that the data presented within this thesis, together with the work of Roy and co-authors (Roy 1997, Roy *et al.* 1998, Roy *et al.* 2000) will form a foundation on which better evolutionary models can be built.



**Table 10.1.** Summary of times of divergence for sister taxa distributed in adjacent areas of endemism. This Table summarizes patterns of temporal divergence among lineages presented in Figures 10.1 to 10.4. Abbreviations are: EDC – Eastern Double-collared Sunbird complex, GDC – Greater Double-collared Sunbird complex, Turdus – the *Turdus olivaceus/abyssinicus* complex, and Greenbul A and B refers to the two groups of taxa in Figs 10.4a and b, respectively. An X designates a node that is not applicable to the two areas of endemism being compared.

Node	Group <sup>1</sup>	Taxa	Divergence Time (Mya BP)	Sister Taxa
Central Eastern Arc vs. Northern Eastern Arc	EDC	<i>moreaui</i> vs. <i>usambaricus</i>	6.0	No
	GDC	X	X	X
	Turdus	<i>roehli</i> vs. <i>nyikae</i>	1.9	
	Greenbul A	<i>usambare</i> vs. <i>chlorigula</i>	6.6	No
	Greenbul B	X	X	X
Central Eastern Arc vs. Uluguru Mnts	EDC	<i>moreui</i> vs. <i>loveridgei</i>	3.0	Yes
	GDC	X	X	X
	Turdus	X	X	X
	Greenbul A	<i>neumanni</i> vs. <i>chlorigula</i>	6.7	Yes
	Greenbul B	X	X	X
Central Eastern Arc vs. South Arc & Malawi Rift	EDC	( <i>moreaui</i> + <i>loveridgei</i> ) vs. <i>fuellborni</i>	3.0	Yes
	GDC	<i>skyei</i> vs. <i>whytei</i>	0.1-0.3	Yes
	Turdus	X	X	X

SE Arc + Malawi Rift vs. Albertine Rift	Greenbul A	<i>(chlorigula + neumanni) vs. fusciceps</i>	3.7	Yes
	Greenbul B	<i>roehli vs. masukuensis.</i>	3.2	Yes
	EDC	X	X	X
Albertine Rift vs. Kenyan Highlands	GDC	<i>(skyei + whytei) vs. stuhlmanni</i>	4.4	Yes
	Turdus	<i>nyikae vs. (baraka + bambusicola)</i>	1.6	Yes
	Greenbul A	<i>milanjensis vs. kikuyensis</i>	8.1	No
	Greenbul B	<i>(masukuensis vs. roehli) vs. kakamegae</i>	6.0	Yes
	EDC	X	X	X
	GDC	X	X	X
	Turdus	<i>(baraka + bambusicola) vs. abyssinicus</i>	X	X
Kenyan Highlands vs. NE Arc	Greenbul A	<i>kakamegae</i>	X	X
	Greenbul B	<i>kikuyensis</i>	0.4	Yes
	EDC	<i>mediocris vs. usambaricus</i>	6.0	Yes
	GDC	X	X	X
	Turdus	<i>abyssinicus (helleri + roehli)</i>	1.9-2.5	NO
	Greenbul A	<i>kikuyensis vs. (nigriceps + usambare)</i>	6.2	Yes
	Greenbul B	X	X	X

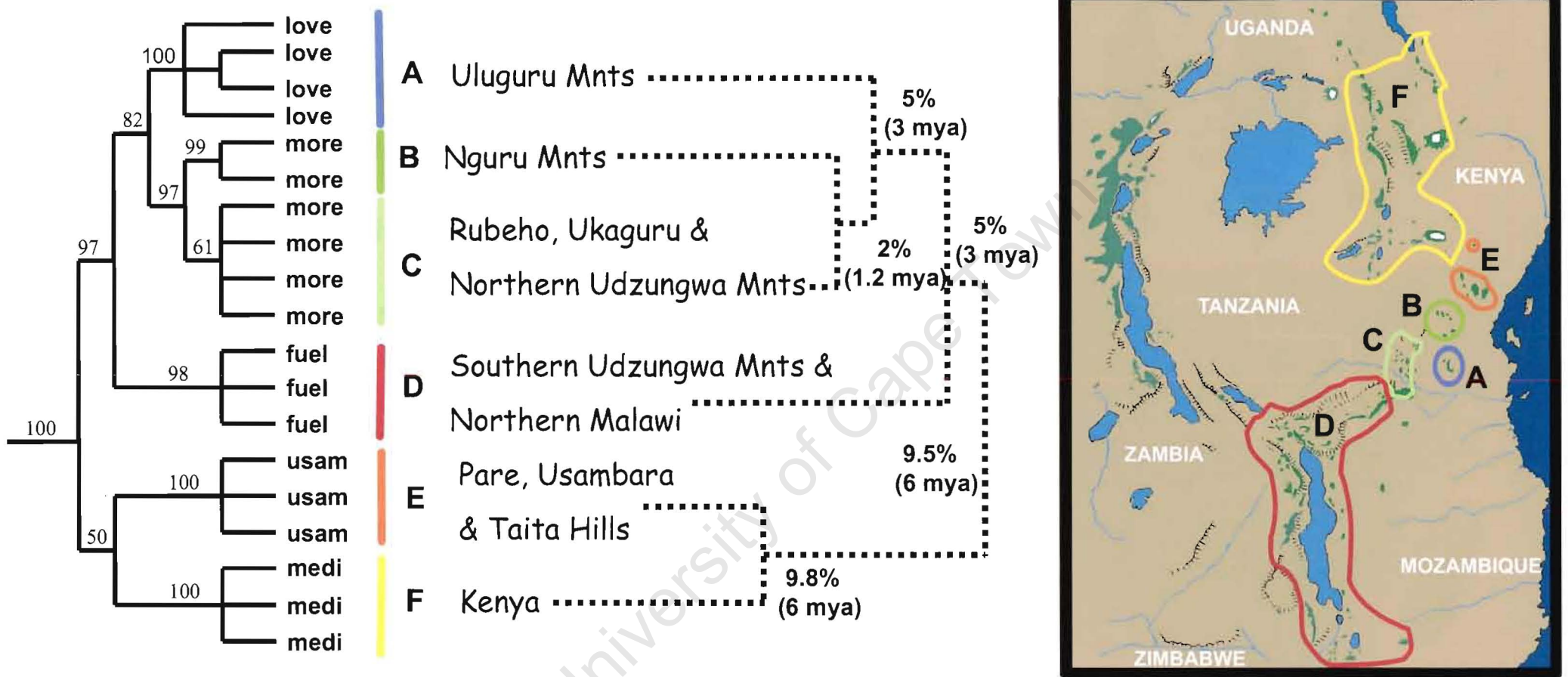


**FIG 10.1.** Relationships, area-cladogram, sequence divergence and estimated time of divergence for lineages within the Eastern Double-collared Sunbird complex (*Nectarinia mediocris* complex). Values above nodes on the cladogram on the left are bootstrap support values from 1000 random addition replicates. To the right is an area-cladogram for the species complex, Kimura-2-parameter sequence divergence values and estimated time of divergence using a rate of 1.6% per million years (after Fleischer *et al.* 1998). The map portrays present species distributions. Abbreviations for taxa are as follows: love - *Nectarinia loveridgei*, more - *N. moreau*, fuel - *N. Fuelleborni*, usam - *N. usambaricus* and medi - *N. mediocris*. See Chapter 3 for greater detail.

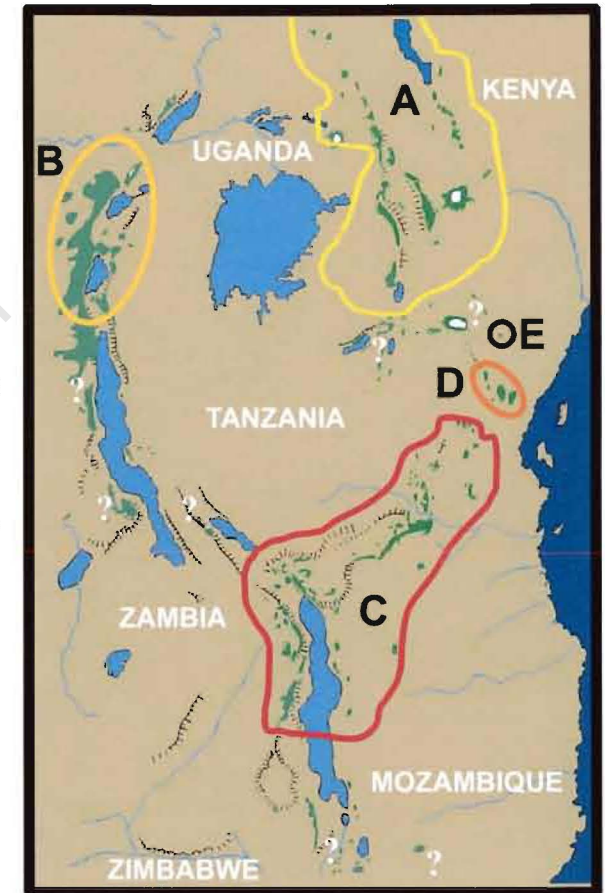
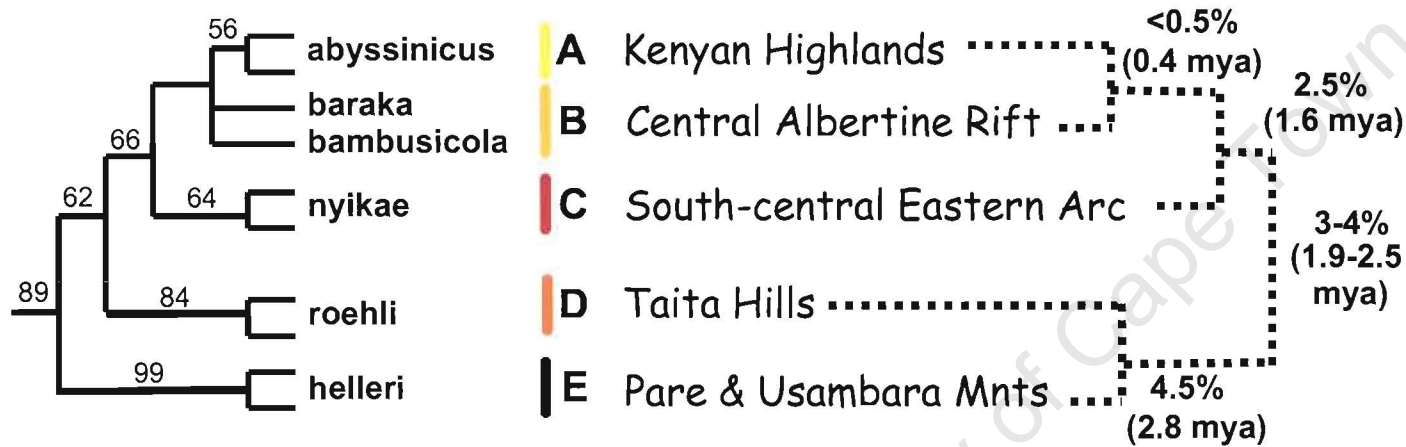


**FIG 10.3.** Relationships, area-cladogram, sequence divergence and estimated time of divergence for lineages within northern populations of the Olive Thrush complex (*Turdus olivaceus/abyssinicus* complex). Values above nodes on the cladogram on the left are bootstrap support values from 1000 random addition replicates. To the right is an area-cladogram for the species complex, Kimura-2-parameter sequence divergence values and estimated time of divergence using a rate of 1.6% per million years (after Fleischer *et al.* 1998). The map portrays present species distributions. See Chapters 6 & 7 for additional detail. ? - Represent taxa of uncertain affinities for which samples were not available for the present study.

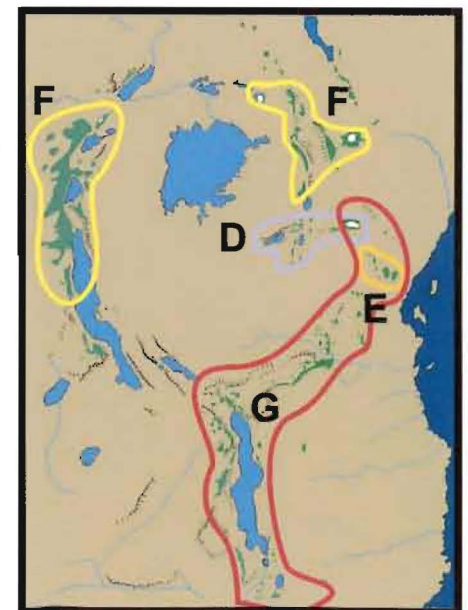
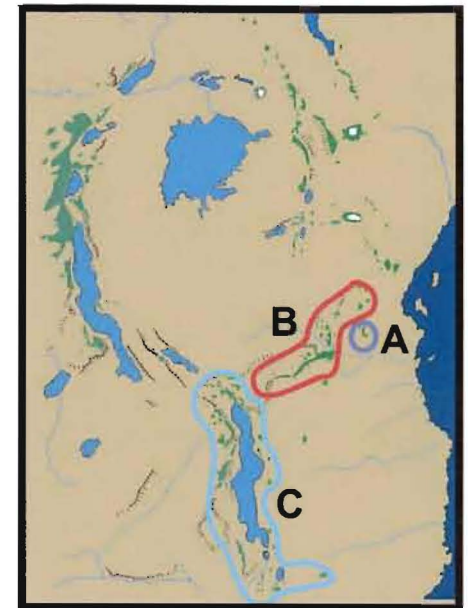
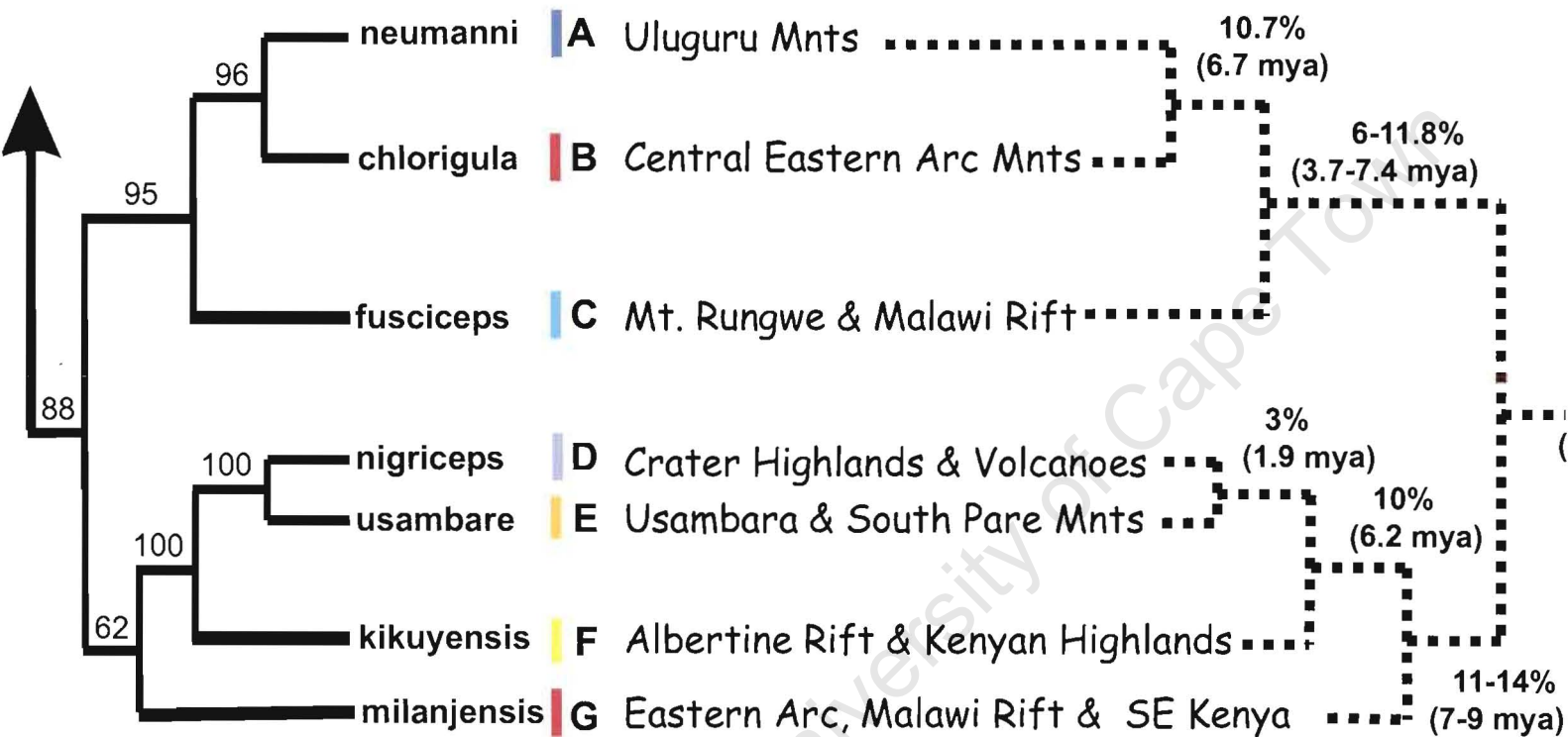


**FIG 10.4a.** Relationships, area-cladogram, sequence divergence and estimated time of divergence for lineages within montane greenbuls (Genus *Andropadus*). The arrow in the cladogram indicates that the taxa in this figure are sister to those in Figure 10.4b. Values above nodes on the cladogram on the left are bootstrap support values from 1000 random addition replicates. To the right is an area-cladogram for the species complex, Kimura-2-parameter sequence divergence values and estimated time of divergence using a rate of 1.6% per million years (after Fleischer *et al.* 1998). The map portrays present species distributions. See Roy (1997) and Roy *et al.* (1998) for additional detail.



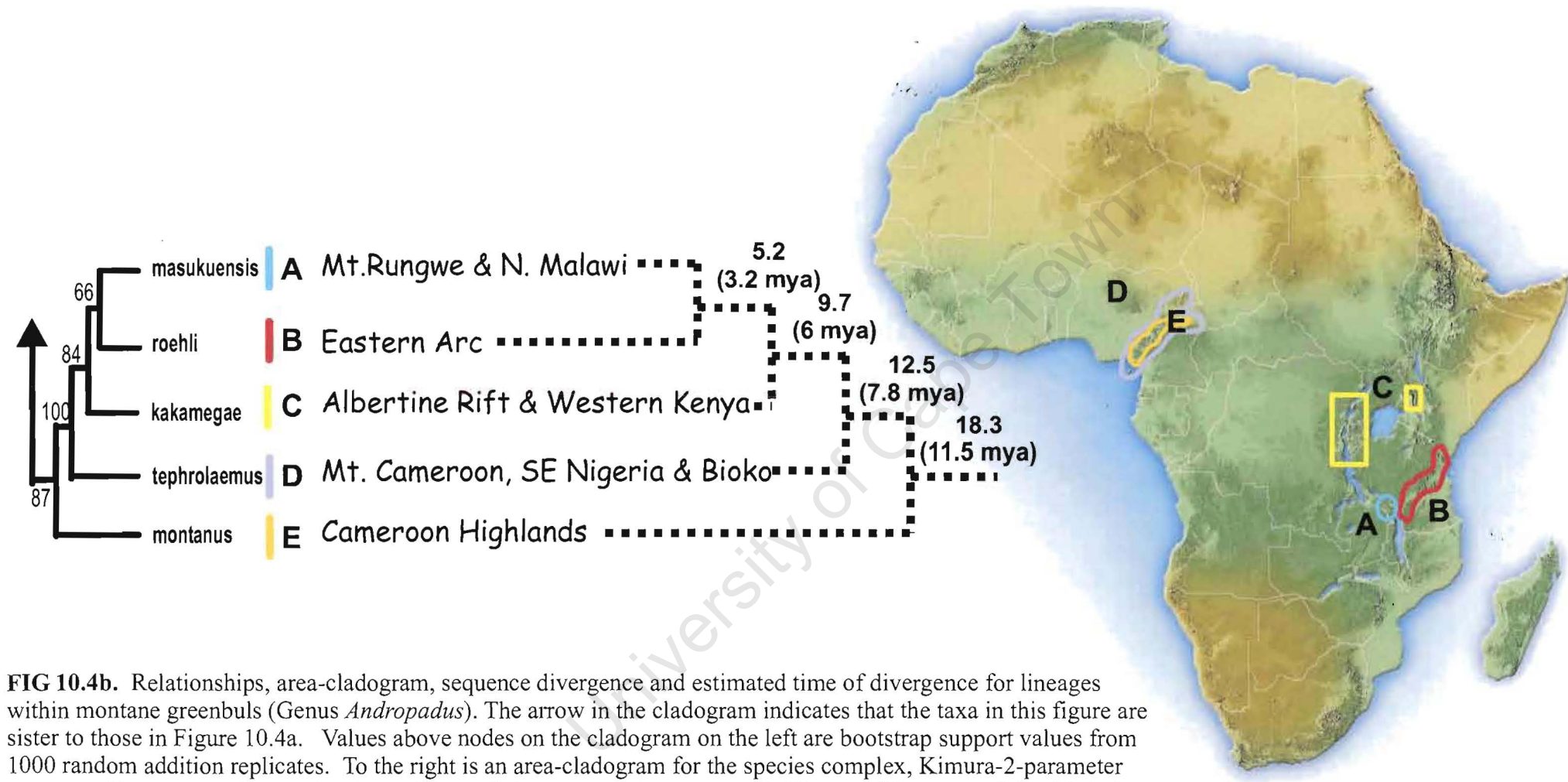


**FIG 10.4b.** Relationships, area-cladogram, sequence divergence and estimated time of divergence for lineages within montane greenbuls (Genus *Andropadus*). The arrow in the cladogram indicates that the taxa in this figure are sister to those in Figure 10.4a. Values above nodes on the cladogram on the left are bootstrap support values from 1000 random addition replicates. To the right is an area-cladogram for the species complex, Kimura-2-parameter sequence divergence values and estimated time of divergence using a rate of 1.6% per million years (after Fleischer *et al.* 1998). The map portrays present species distributions. See Roy (1997) and Roy *et al.* (1998) for additional detail.

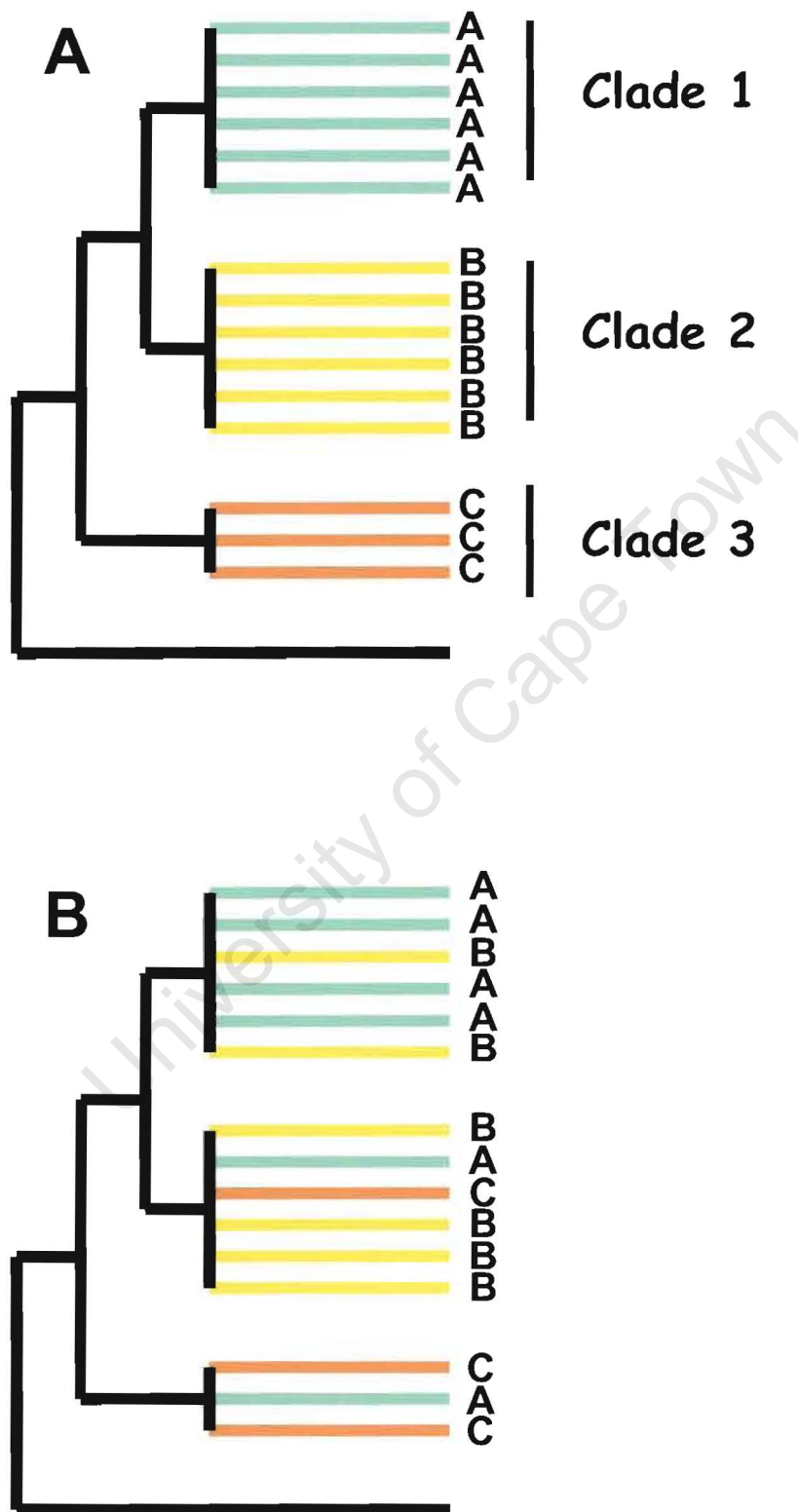


**FIG 10.5.** In A, clades are reciprocally monophyletic. In B, whereas there are differences in haplotype frequencies, lineage sorting has not been completed or else gene flow is still taking place, i.e. there is a lack of reciprocal monophyly.

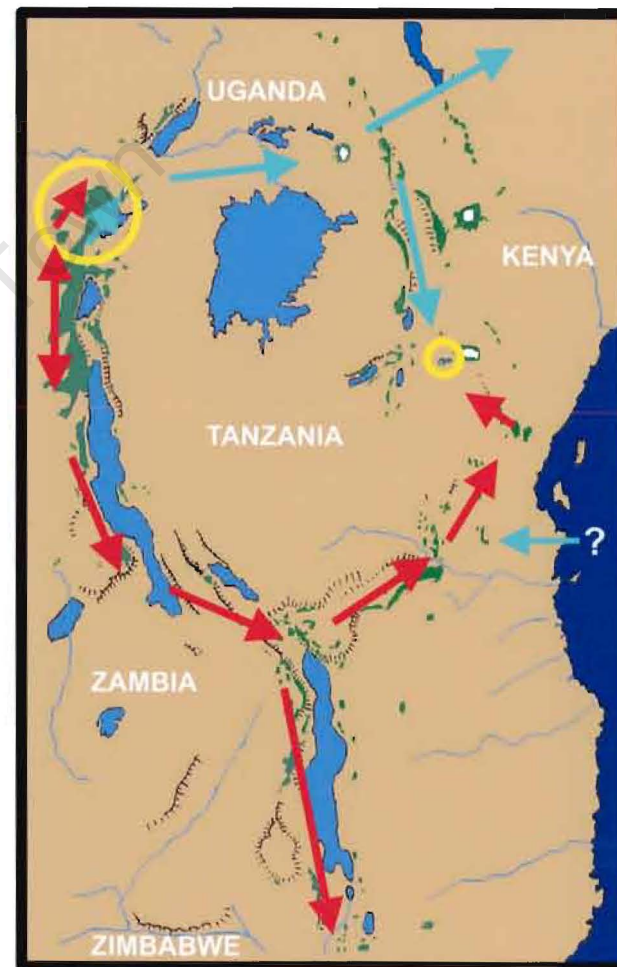
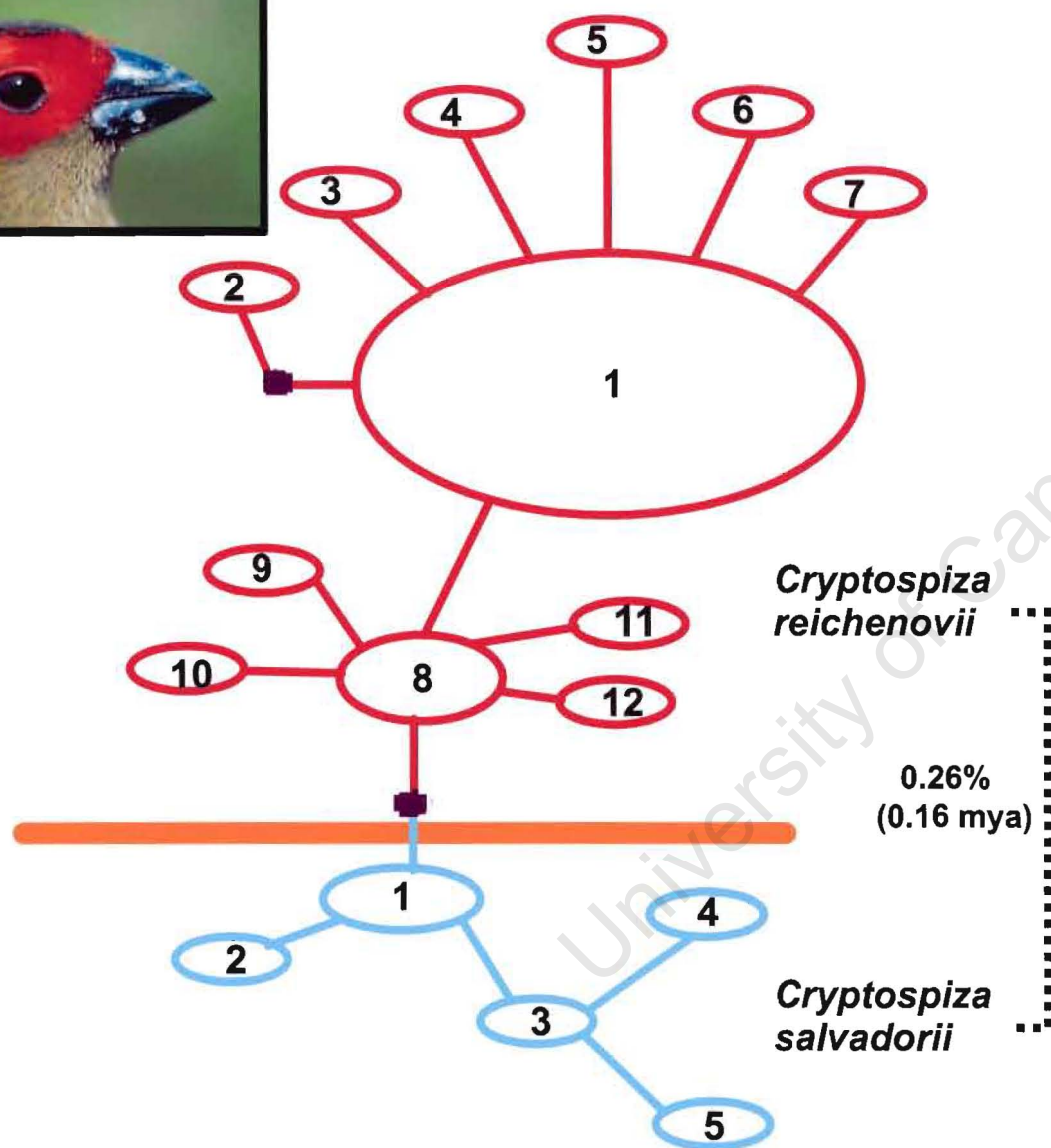
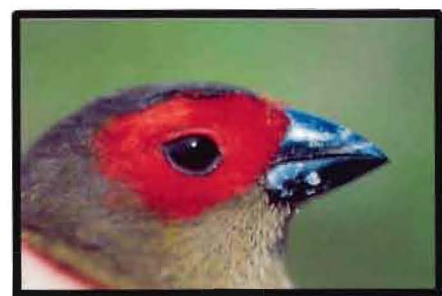


**FIG 10.6.** Genetic structure between two closely related species of crimsonwings (genus *Cryptospiza*). The two taxa differed in on a single mutation among the 383 bp sequenced, and a total of only 17 haplotypes were identified from 163 individuals for which mtDNA sequence data was collected (Bowie, Unpublished data). Kimura-2-parameter sequence divergence values and estimated time of divergence using a rate of 1.6% per million years (after Fleischer *et al.* 1998) were estimated. The picture insert is a male *Cryptospiza reichenovii*.



## Chapter 11

### LITERATURE CITED

- Akaike H. (1973).** Information theory and an extension of the maximum likelihood principle. In: Petrov B.N. & Csaki (eds), *Proceedings of the 2<sup>nd</sup> International Symposium on Information Theory*. Pp. 267-281. Akadémia Kiado, Budapest.
- Amadon D. (1951).** Le pseudo-souimanga de Madagascar. *Oiseau et R.F.O.* 21: 59-63.
- Amundsen T. (2000).** Why are female birds ornamented? *Trends in Ecology & Evolution*. 15: 149-155.
- Arbogast B.S., Edwards S.V., Wakeley J., Beerli P. & Slowinski J.B. (2002).** Estimating divergence times from molecular data on phylogenetic and population genetic timescales. *Annual Review of Ecology & Systematics*. 33: 707-740.
- Arctander P. (1995).** Comparison of a mitochondrial gene and a corresponding nuclear pseudogene. *Proceedings of the Royal Society of London, Series B*. 262: 13-19.
- Arctander P., Johansen C. & Coutellec-Vreto M.A. (1999).** Phylogeography of three closely related African bovids (tribe Alcelaphini). *Molecular Phylogenetics & Evolution*. 16: 1724-1739.
- Avise J.C. (2000).** *Phylogeography: the history and formation of species*. Harvard Univ. Press. Cambridge, MA. Pp447.
- Avise J.C. & Walker D. (1998).** Pleistocene phylogeographic effects on avian populations and the speciation process. *Proceedings of the Royal Society of London, Series B*. 265: 457-463.
- Avise J.C., Walker D. & Jones G.C. (1998).** Speciation durations and Pleistocene effects on vertebrate phylogeography. *Proceedings of the Royal Society of London, Series B*. 265: 1707-1712.
- Avise J.C., Nelson W.S. & Sibley C.S. 1994.** DNA support for a close phylogenetic relationship between some storks and New World Vultures.

*Proceedings of the National Academy of Sciences of the USA*. 91: 5173-5177.

**Baker A.J. & Marshall H.D. (1997).** Mitochondrial control region sequences as tools for understanding evolution. pp. 51-79. In Mindell D. P. (ed.) *Avian molecular evolution and systematics*. Academic Press, New York.

**Baker A.J., Piersma T. & Rosenmeier L. (1994).** Unraveling the intraspecific phylogeography of knots *Calidris canutus*: a progress report on the search for genetic markers. *Journal for Ornithology*. 135: 599-608.

**Barker F.K., Barrowclough G.F. & Groth J.G. (2002).** A phylogenetic hypothesis for passerine birds: taxonomic and biogeographic implications of an analysis of nuclear DNA sequence data. *Proceedings of the Royal Society of London, Series B*. 269: 295-308.

**Balmford A., Moore J.L., Brooks T., Burgess N., Hansen L.A., Williams P. & Rahbek C. (2001).** Conservation conflicts across Africa. *Science*. 291: 2616-2619.

**Bates J. M. (in press).** Avian diversification in Amazonia: evidence for historical complexity and a vicariance model for a basic diversification pattern. Pp. 119-138, in *Diversidade Biológica e Cultural da Amazônia*. (eds.) I. Viera, M.A. S'Incae, J. M. Cardoso da Silva and D. Oren. Museu Paraense Emilio Goeldi, Belém, Pará, Brazil.

**Beerli P. & Felsenstein J. (2001).** Maximum likelihood estimation of a migration matrix and effective population sizes in n subpopulations by using a coalescent approach. *Proceedings of the National Academy of Sciences of the USA*. 98: 4563-4568.

**Beerli P. & Felsenstein J. (1999).** Maximum likelihood estimation of a migration matrix and effective population sizes in two populations using a coalescent approach. *Genetics*. 152: 763-773.

**Bennun L. & Njoroge G. (1999).** *Important Bird areas of Kenya*. Birdlife International, Cambridge, Uk.

**Benson C.W. (1954).** The identity of *Cinnyris afer whytei* Benson. *Bulletin of the British Ornithology Club*. LXXIV: 95-96.

- Benson C.W. (1984).** Origins of Seychelles land birds. Pp. 469-486. In Stoddart D.R. (ed.). Junk Publishers, The Hague.
- Benson C.W. (1949).** A new race of sunbird from Nyasaland. *Bulletin of the British Ornithologists Club.* 69: 19-20.
- Beresford P. (2002).** *Molecular systematics and biogeography of certain Guineo-Congolian passerines.* Unpublished PhD thesis, The City University of New York, New York.
- Beresford P. & Cracraft J. (1999).** Speciation in African forest robins (*Stiphornis*): species limits, phylogenetic relationships, and molecular biogeography. *American Museum Novitates.* 3270: 1-22.
- Birdlife International (2000).** *Threatened birds of the world.* Barcelona and Cambridge, UK. Lynx Edicions and Birdlife International.
- Bock W.J. & Farrand J. Jr. (1980).** The number of species and genera of recent birds: a contribution to comparative systematics. *American Museum Novitates.* No. 2703: 1-19.
- Buckley T.R., Simon C., Shimodaira H. & Chambers G.K. (2001).** Evaluating hypotheses on the origin and evolution of the New Zealand alpine Cicadas (Maoricicada) using multiple-comparison tests of tree topology. *Molecular Biology & Evolution.* 18: 223-234.
- Bossuyt F. & Milinkovitch C. (2001).** Amphibians as indicators of early Tertiary "Out of India" dispersal of vertebrates. *Science.* 292: 93-95.
- Bossart J.L. & Prowell D.P. (1998).** Genetic estimates of population structure and gene flow: limitation, lessons, and new directions. *Trends in Ecology & Evolution.* 13: 202-206.
- Branco M., Monnerot M., Ferrand N. & Templeton A.R. (2002).** Postglacial dispersal of the European Rabbit (*Oryctolagus cuniculus*) on the Iberian Peninsula reconstructed from nested clade and mismatch analyses of mitochondrial DNA genetic variation. *Evolution.* 56: 792-803.
- Brooks T., Balmford A., Burgess N., Fjelds  J., Hansen L.A., Moore J., Rahbek C & Williams P. (2001).** Towards a blueprint for conservation in Africa. *Bioscience.* 51: 613-624.

- Brooks T, Lens L., De Meyer M., Waiyaki E. & Wilder C. (1998).** Avian biogeography of the Taita Hills. *Journal of the East African Natural History Society*. 87: 189-194.
- Brown W.M. Jr., George M., & Wilson A.C. (1979).** Rapid evolution of animal mitochondrial DNA. *Proceedings of the National Academy of Sciences of the USA*. 76: 1967-1971.
- Burbrink F.T, Lawson R. & Slowinski J.B. (2000).** Mitochondrial DNA phylogeography of the polytypic north American rate snake (*Elaphe obsoleta*): a critique of the subspecies concept. *Evolution*. 54: 2107-2118.
- Burgess N.C., de Klerk H., Fjelds  J., Crowe T.M. & Rahbek C. (2000).** A preliminary assessment of congruence of biodiversity patterns in Afrotropical forest birds and mammals. *Ostrich*. 71: 286-290.
- Burgess N.C., Fjelds  J. & Botterweg R. (1998).** Faunal importance of the Eastern Arc Mountains of Kenya and Tanzania. *Journal of the East African Natural History Society*. 87: 37-58.
- Burgess N.D., Nummelin M., Fjelds  J., Howell K.M., Lukumbyzya K., Mhando L., Phillipson P. & Vanden Berghe E. (1998).** Biodiversity and conservation of the Eastern Arc Mountains of Tanzania and Kenya. *Journal of the East African Natural History Society*. Special issue, 87: 367 pp.
- Carcasson R.H. (1964).** A preliminary survey of the zoogeography of African butterflies. *East African Wildlife Journal*. 2: 122-157.
- Castelloe J. & Templeton A.R. (1994).** Root probabilities for intraspecific gene trees under neutral coalescent theory. *Molecular Phylogenetics & Evolution*. 3: 102-113.
- Chapin J.P. (1954).** The birds of the Belgian Congo. Part 4. *Bulletin of the American Museum of Natural History*. 75b.
- Chapin J.P. (1932).** The birds of the Belgian Congo. Part 1. *Bulletin of the American Museum of Natural History*. 65: 1-756.
- Chapin J.P. (1923).** Ecological aspects of bird distribution in tropical Africa. *American Naturalist*. 77: 106-125.

- Cheke R.A., Mann C.F. & Allen R. (2001).** *Sunbirds: a guide to the sunbirds, flowerpeckers, spiderhunters and sugarbirds of the world*. Christopher Helm, London.
- Chesser R.T. (2000).** Evolution in the High Andes: the phylogenetics of *Muscisaxicola* Ground-Tyrants. *Molecular Phylogenetics & Evolution*. 15: 369-380.
- Chesser R.T. (1999).** Molecular systematics of the rhinocryptid genus *Pteroptochos*. *Condor*. 101: 439-446.
- Clancey P.A. (1992-1993).** The status of *Nectarinia olivacea* (Smith), 1840; a unitary species or two polytypic allospecies? *Le Gerfaut*. 82-83: 25-29.
- Clancey P.A. (1982).** Miscellaneous taxonomic notes on African birds LXII: the Olive Thrush *Turdus olivaceus* Linnaeus In Southern Africa. *Durban Museum Novitates*. 13: 65-70.
- Clancey P.A. (1972).** Miscellaneous taxonomic notes on African birds #34. *Durban Museum Novitates*. 9: 145-162.
- Clancey P.A. & Irwin M.P.S. (1978).** Species limits in the *Nectarinia afra* / *N. chalybea* complex of African Double-collared sunbirds. *Durban Museum Novitates*. 11:331-351.
- Clancey P.A. (1970).** A new isolate subspecies of *Nectarinia afra* (Linnaeus) from Mozambique. *Durban Museum Novitates*. 9: 25-28.
- Clancey P.A. (1962).** On the status of the taxon *Nectarinia afra afra* (Linnaeus). *Durban Museum Novitates*. 6: 187-189.
- Clement M., Posada D. & Crandall K.A. (2000).** TCS: a computer program to estimate gene genealogies. *Molecular Ecology*. 9: 1657-1660.
- Clement P. & Hathway R. (2000).** *Thrushes*. Helm identification guides. Christopher Helm, London.
- Coates B.J. & Bishop K.D. (1997).** *A guide to the birds of Wallacea*. Dove Publications, Alderley.
- Coe M.J. & Skinner J.D. (1993).** Connections, disjunctions and endemism in the eastern and southern African mammal faunas. *Transactions of the Royal Society of South Africa*. 233-255.

- Collar N. J. & Andrew P. (1988).** *Birds to watch: ICBP world checklist of threatened birds*. International Council for Bird Preservation, Cambridge.
- Collar N. J. & Stuart S. N. (1988).** *Key forests for threatened birds in Africa*. International Council for Bird Preservation, Cambridge.
- Collar N.J. & Stuart S.N. (1985).** *Threatened birds of Africa and related islands: the ICBP/IUCN red data book*. International Council for Bird Preservation and International Union for Conservation of Nature and Natural Resources, Cambridge, U.K.
- Collins T.M., Wimberger P.H. & Naylor J.P. (1994).** Compositional bias, character-state bias, and character-state reconstruction using parsimony. *Systematic Biology*. 43: 482-496.
- Cooper A., Lalueza-Fox C., Anderson S., Rambaut A., Austin J. & Ward R. (2001).** Complete mitochondrial genome sequences of two extinct moas clarify ratite evolution. *Nature*. 409: 704-707.
- Cooper A. & Pennny D. (1997).** Mass survival of birds across the Cretaceous-Tertiary boundary: molecular evidence. *Science*. 275: 1109-1113.
- Cordeiro N. (1998).** Preliminary analysis of nested patterns of montane forest birds of the Eastern Arc Mountains. *Journal of the East African Natural History Society*. 87: 101-118.
- Cox C.B. & Moore P.D. (1993).** *Biogeography: an ecological and evolutionary approach*. Blackwell Science, Oxford.
- Cracraft J. (2001).** Avian evolution, Gondwana biogeography and the Cretaceous-Tertiary mass extinction event. *Proceedings of the Royal Society, London, Series B*. 268: 459-469.
- Cracraft J. (1988).** Deep-history biogeography: retrieving the historical pattern of evolving continental biota. *Systematic Zoology*. 37: 221-236.
- Cracraft J. (1983).** Species concepts and speciation analysis. *Current Ornithology*. 1: 159-187.
- Cracraft J. (1973).** Continental drift, palaeoclimatology, and the evolution and biogeography of birds. *Journal of Zoology*. 169: 455-545.

- Crandall K.A. (1996).** Multiple interspecies transmissions of human and simian T-cell Leukemia/Lymphoma virus Type I sequences. *Molecular Biology & Evolution*. 13: 115-131.
- Crandall K.A., Templeton A.R. & Sing C.F. (1994).** Intraspecific phylogenetics: problems and solutions. Pp. 273-297. In Scotland R.W., Siebert D.J. & Williams D.M. (eds.) *Models in phylogeny reconstruction*. Clarendon Press, Oxford.
- Crandall K.A. & Templeton A.R. (1993).** Empirical tests of some predictions from coalescent theory with application to intraspecific phylogeny reconstruction. *Genetics*. 134: 959-969.
- Crowe T.M. & Crowe A.A. (1982).** Patterns of distribution, diversity and endemism in Afrotropical birds. *Journal of Zoology, London*. 198: 417-442.
- Cunningham C.W. (1997).** Can three incongruence tests predict when data should be combined? *Molecular Biology & Evolution*. 14: 733-740.
- Cunningham C.W. & Collins T.M. (1994).** Developing model systems for molecular biogeography: vicariance and interchange in marine invertebrates. Pp. 405-433, In B. Schierwater, B. Streit, G.P. Wagner & R. DeSalle (eds.). *Molecular ecology and evolution: approaches and applications*. Birkhäuser Verlag, Basel, Switzerland.
- deMenocal P.B. (1995).** Plio-Pleistocene African climate. *Science*. 270: 53-59.
- Davis A, Scholtz C. & Harrison J. (2001).** Cladistic, phenetic and biogeographical analysis of the flightless dung beetle genus, *Gyronotus* van Lansberge (Scarabaeidae), in the threatened eastern Afrotropical forests. *Journal of Natural History*. 35: 1607-1625.
- Delacour J. (1944).** A revision of the family Nectariniidae (Sunbirds). *Zoologica*. 29: 17-38.
- Desjardins P. & Morais R. (1990).** Sequence and gene organisation of the chicken mitochondrial genome. A novel gene order in higher vertebrates. *Journal of Molecular Evolution*. 212: 599-634.

- Diamond A.W. & Hamilton A.C. (1980).** The distribution of forest passerine birds and Quaternary climatic change in Africa. *Journal of Zoology*. (London.) 191: 379-402.
- Diamond A.W. & Keith G.S. (1980).** Avifaunas of Kenya Forest islands. 1- Mt. Kulal. *Scopus* 4: 49-55.
- Dinesen L., Lehmborg T., Rahner M.C. & Fjeldså J. (2001).** Conservation priorities for the forests of the Udzungwa Mountains, Tanzania, based on primates, duikers and birds. *Biological Conservation*. 99:223-236.
- Dinesen L., Lehmborg T., Svendsen J.O., Hansen L.A. & Fjeldså J. (1994).** A new genus and species of perdicine bird (Phasianidae: Perdicini) from Tanzania: a relict form with Indo-Malayan affinities. *Ibis*. 136: 3-11.
- Dowsett R.J. (1986).** Origins of the high-altitude avifaunas of tropical Africa. pp. 557-585. In Vuilleumier F. & Monastieu M. (eds) *High altitude tropical biogeography*. Oxford University Press, New York.
- Dowsett R.J. (1985)** Site-fidelity and survival rates of some montane forest birds in Malawi, south-central Africa. *Biotropica*. 17: 145-154.
- Dowsett R.J. (1982).** *The population dynamics and seasonal dispersal of the Starred Robin (Pogonochla stellata)*. Unpublished MSc Thesis, University of Natal, South Africa.
- Dowsett R.J. & Dowsett-Lemaire F. (1993).** *A contribution to the distribution and taxonomy of Afrotropical and Malagasy birds*. Tauraco Press, Liege, Belgium.
- Dowsett R.J. & Dowsett-Lemaire F. (1984).** Breeding and moult cycles of some montane forest birds in south-central Africa. *Review Ecology (Terre et Vie)*. 39: 89-111.
- Dowsett-Lemaire F. (1989).** Food plants and the annual cycle in a montane community of sunbirds (*Nectarinia* spp.) in northern Malawi. *Tauraco*. 1: 167-185.
- Dowsett-Lemaire F. (1988).** On the breeding behaviour of three montane sunbirds *Nectarinia* spp. in northern Malawi. *Scopus*. 11: 79-86.



- Dowsett-Lemaire F. (1983).** Ecological and territorial requirements of montane forest birds on the Nyika Plateau, south-central Africa. *Gerfaut*. 73: 345-378.
- Dowsett-Lemaire, F. & R.J. Dowsett. (2001).** African forest birds: patterns of endemism and species richness. Pp233-262, in Weber, W. et al. (eds). *African rain forest ecology and conservation: an interdisciplinary perspective*. Yale University Press, New Haven.
- Dupont L. & Hoogheimstra H. (1989).** The Saharan-Sahelian boundary during the Brunhes chron. *Acta Botanica Neerlandica*. 38: 405-415.
- Ericson P.G.P., Christidis L., Cooper A., Irestedt M., Jackson J., Johansson U.S. & Norman J.A. (2002).** A Gondwanan origin of passerine birds supported by DNA sequences of the endemic New Zealand wrens. *Proceedings of the Royal Society of London, Series B*. 269: 235-241.
- Edwards, S.V., Arctander, P. & Wilson, A.C. (1991).** Mitochondrial resolution of a deep branch in the genealogical tree for perching birds. *Proceedings of the Royal Society of London, Series B* 243: 99-107.
- Evans T.D. & Anderson G.Q.A. (1993).** Notes on Moreau's Sunbird *Nectarinia moreaui*. *Scopus*. 17: 63-64.
- Farquhar M.R., Lorenz M., Rayner J.L. & Graig A.J.F.K. (1996).** Feather ultrastructure and skeletal morphology as taxonomic characters in African sunbirds (Nectariniidae) and sugarbirds (Promeropidae). *Journal of African Zoology*. 110: 321-331.
- Farris J.S., Albert V.A., Källersjö M., Lipscomb D. & Kluge A.G. (1996).** Parsimony jackknifing outperforms neighbour-joining. *Cladistics*. 12: 99-124.
- Farris J.S., Källersjö M., Kluge A.G. & Bult C. (1995).** Constructing a significance test for incongruence. *Systematic Biology*. 44: 570-472.
- Feduccia A. (1996).** *The origin and evolution of birds*. Yale University Press, New Haven.
- Felsenstein, J. (1985).** Confidence limits of phylogenies: an approach using the bootstrap. *Evolution*. 39: 783-791.

- Fjeldså J. (1999).** The impact of human forest disturbance on the endemic avifauna of the Udzungwa mountains, Tanzania. *Bird Conservation International*. 9: 47-62.
- Fjeldså J. (1995).** Have ornithologists "slept during class"? On the response of ornithology to the "Biodiversity Crisis" and the "Biodiversity Convention". *Journal of Avian Biology*. 26: 89-93
- Fjeldså J. (1994).** Geographical patterns of relict and young species of birds in Africa and South America and implications for conservation priorities. *Biodiversity & Conservation*. 3: 107-126.
- Fjeldså J. & Kiure J. (in press).** A new population of the Udzungwa Forest Partridge. *Bulletin of the British Ornithologists Club*.
- Fjeldså J. & Lovett J.C. (1997).** Geographical patterns of old and young species in African forest biota: the significance of specific montane areas as evolutionary centres. *Biodiversity & Conservation* 6: 325-346.
- Fjeldså J. & Rabøl J. (1995).** Variation in avian communities between isolated units of the Eastern Arc montane forests, Tanzania. *Le Gerfaut*. 85: 3-18.
- Fleischer R.C., McIntosh C.E. & Tarr C.L. (1998).** Evolution on a volcanic conveyor belt: using phylogenetic reconstructions and K-Ar-based ages of the Hawaiian Islands to estimate molecular evolutionary rates. *Molecular Ecology*. 7: 533-545.
- Friedmann H. & Stager K.E. (1969).** Results of the 1964 Cheney Tanganyikan Expedition. Ornithology. *Contributions to Science* (Los Angeles). 84: 1-50.
- Friesen V.L. & Anderson D.J. (1997).** Phylogeny and evolution of the Sulidae (Aves: Pelecaniformes): a test of alternative modes of speciation. *Molecular Phylogenetics & Evolution*. 7: 252-260.
- Freitag S. & Robinson T.J. (1993).** Phylogeographic patterns in mitochondrial DNA of the Ostrich (*Struthio camelus*). *Auk*. 110: 614-622.
- Frost D.R. & Hillis D.M. (1990).** Species in concept and practice: Herpetological considerations. *Herpetologica*. 46: 87-104.
- Fry C.H. (2000).** The genus *Cinnyris*. In: C.H. Fry, S. Keith & E.K. Urban (Eds) *The Birds of Africa*. Vol VI. Academic Press, London.

- Fry C.H. & Keith S. (2000).** *The Birds of Africa*. Vol VI. London: Academic Press.
- Fu Y.X. (1997).** Statistical tests of neutrality of mutations against population growth, hitchhiking and background selection. *Genetics*. 147: 915-925.
- Galbusera P., Lens L., Schenck T., Waiyaki E. & Matthysen E. (2000).** Genetic Variability and gene flow in the globally, critically-endangered Taita thrush. *Conservation Genetics*. 1: 45-55.
- García-Moreno J. & Fjeldså J. (1999).** Re-evaluation of species limits in the genus *Atapetes* based on mtDNA sequence data. *Ibis*. 141: 199-207.
- Gill F.B. (1971).** Tongue structure of the sunbird *Hypogramma hypogrammicum*. *Condor*. 73: 485-486.
- Goldman N., Anderson J.P. & Rodrigo A.G. (2000).** Likelihood-based tests of topologies in phylogenetics. *Systematic Biology*. 49: 652-670.
- Goloboff P. (1999).** NONA ver. 2 Published by the author, Tucumán, Argentina
- Grant C.H.B. & Mackworth-Praed C.W. (1943).** On the racial status of *Cinnyris stuhlmanni* Reichenow and *Cinnyris ludovicensis* (Bocage). *Bulletin of the British Ornithologists Club*. LXIV. 9-10.
- Grant P.R. & Grant B.R. (1997).** Genetics and the origin of bird species. *Proceeding of the National Academy of Sciences of the United States*. 94: 7768-7775.
- Griffiths C.J. (1993).** The geological evolution of East Africa. Pp 9-21 in Lovett J.C. & Wasser S.K (eds). *Biogeography and Ecology of the Rain Forests of Eastern Africa*. Cambridge University Press, Cambridge, UK.
- Griswold C.E. (1991).** Cladistic biogeography of afro-montane spiders. *Australian Systematic Biology*. 4: 73-89.
- Haffer J. (1997).** Alternative models of vertebrate speciation in Amazonia: an overview. *Biodiversity & Conservation*. 6: 451-476.
- Hall B.P. & Moreau R.E. (1970).** *An atlas of speciation in African passerine birds*. London: British Museum of Natural History.
- Hamilton A., Taylor D. & Howard P. (2001).** Hotspots in African forest as Quaternary refugia. . Pp233-262, in Weber, W. et al. (eds.). *African rain*

*forest ecology and conservation: an interdisciplinary perspective*. Yale University Press, New Haven.

- Hamilton A.C. (1976).** The significance of patterns of distribution shown by forest plants and animals in tropical Africa for the reconstruction of upper Pleistocene paleoenvironments: a review. *Paleoecology of Africa*. 9: 63-97.
- Harpending H.C., Batzer M.A., Gurven M., Jorde L.B., Rogers A.R. & Sherry S.T. (1998).** Genetic traces of ancient demography. *Proceedings of the National Academy of Sciences of the USA*. 95: 1961-1967.
- Hasegawa M., Kishino H. & Yano T. (1985).** Dating of the human-ape splitting by a molecular clock of mitochondrial DNA. *Journal of Molecular Evolution*. 21: 160-174.
- Hedberg O. (1986).** Origins of the Afroalpine flora. pp. 443-465. In Vuilleumier F. & Monasteuio M. (eds) *High altitude tropical biogeography*. Oxford University Press, New York
- Hedges S.B., Parker P.H., Sibley C.G. & Kumar S. (1996).** Continental breakup and the ordinal diversification of birds and mammals. *Nature*. 381: 226-229.
- Hewitt G.M. (2000).** The genetic legacy of the Quaternary ice-ages. *Nature*. 405: 907-913.
- Hewitt G.M. (1996).** Some genetic consequences of ice ages, and their role in divergence and speciation. *Biological Journal of the Linnaean Society*. 58: 247-276.
- Hockey P.A.R., Underhill L.G., Neatherwag M. & Ryan P.G. (1989).** *Atlas of the birds of the southwestern Cape*. Cape Town: Cape Bird Club.
- Hubbard J.P. (1973).** Avian evolution in the aridlands of North America. *Living Bird*. 12: 155-196.
- Huelsenbeck, J.P. & Ronquist (2001).** Mr Bayes: a program for the Bayesian inference of phylogeny. Available at: [morphbank.ebc.uu.se/MrBayes/](http://morphbank.ebc.uu.se/MrBayes/)
- Huelsenbeck J.P., Larget B., Miller R.E. & Ronquist F. (2002).** Potential applications and pitfalls of Bayesian Inference of phylogeny. *Systematic Biology*. 51: 673-688.

- Huelsenbeck J.P., Hillis D.M. & Nielsen R. (1996).** A likelihood ratio test of monophyly. *Systematic Biology*. 45: 546-558.
- Hunt J.S., Bermingham E. & Ricklefs R.E. (2001).** Molecular systematics and biogeography of Antillean Thrashers, Tremblers, and Mockingbirds (Aves: Mimidae). *Auk*. 118: 35-55.
- Inger R.F. & Voris H.K. (2001).** The biogeographical relationships of the frogs and snakes of Sundaland. *Journal of Biogeography*. 28: 863-891.
- Irwin M.P.S. (1999).** The genus *Nectarinia* and the evolution and diversification of sunbirds: an Afrotropical perspective. *Honeyguide*. 45: 45-58.
- Irwin M.P.S. (1993).** What sunbirds belong to the genus *Anthreptes*. *Honeyguide* 39: 211-216.
- Irwin M.P.S. (1971).** The Starred Bush Robin *Pogonocichla stellata* in eastern Rhodesia and adjacent Mozambique. *Bulletin of the British Ornithologists Club*. 91: 14-18.
- Irwin M.P.S. & Clancey P.A. (1974).** A re-appraisal of the generic relationships of some African forest-dwelling robins (Aves: Turdidae). *Arnoldia* (Rhodesia). 6: 1-19.
- Jansson R. & Dynesius M. (2002).** The fate of clades in a world of recurrent climatic change: Milankovitch oscillations and evolution. *Annual Review of Ecology & Systematics*. 33: 741-777.
- Jensen F. P. (1983).** A new species of sunbird from Tanzania. *Ibis*. 125: 447-449.
- Johnson K.P. & Clayton D.H. (2000).** Nuclear and mitochondrial genes contain similar phylogenetic signal for Pigeons and Doves (Aves: Columbiformes). *Molecular Phylogenetics & Evolution*. 14: 141-151.
- Juste J.B., Álvarez Y., Tabarés E., Garrido-Pertierra A., Ibáñez C. & Bautista J.M. (1999).** Phylogeography of African Fruitbats (Megachiroptera). *Molecular Phylogenetics & Evolution*. 13: 596-604.
- Keast A. (1981).** Origins and relationships of the Australasian biota. In *Monographiae biologicae*, vol. 41: Ecological biogeography of Australia. Pp. 1999-2050. In Keast A. (ed). Dr W. Junk bv Publishers, The Hague.

- Keith S., Urban E.K. & Fry C.H. (1992).** *The Birds of Africa*. Vol IV. London: Academic Press.
- Kemp M.I., Kemp A.C. & Tarboton W.R. (1985).** *Catalogue of the birds of the Transvaal*. Pretoria: Transvaal Museum.
- Kennedy R.S., Gonzales P.C. & Miranda H.C. (1997).** New *Aethopyga* sunbirds (Aves: Nectariniidae) from the island of Mindanao, Phillipines. *Auk*. 114: 1-10.
- Kennett J.P. (1995).** A review of polar climatic evolution during the Neogene, based on the marine sediment record. Pp 49-64 in Vrba E.S., Denton G.H., Partridge T.C. & Buckle (eds). *Paleoclimate and evolution with emphasis on human origins*. Yale University Press., New Haven and London.
- de Klerk H.M. (1998).** *Biogeography and conservation of terrestrial birds*. Unpublished PhD Thesis, University of Cape Town, South Africa
- de Klerk H.M., Crowe T.M., Fjelds  J. & Burgess N.D. (2002a).** Patterns of species richness and narrow endemism of terrestrial bird species in the Afro-tropical region. *Journal of Zoology, London*. 256: 327-342.
- de Klerk H.M., Crowe T.M., Fjelds  J. & Burgess N.D. (2002b).** Biogeographical patterns of endemic terrestrial Afrotropical birds. *Diversity & Distributions*. 8: 147-162.
- Kimura M. (1980).** A simple model for estimating evolutionary rates of base substitutions through comparative studies of nucleotide sequences. *Journal of Molecular Evolution*. 16:111-120.
- Kingdon J. (1997).** *The Kingdon field guide to African mammals*. Academic Press, New York
- Kingdon J. (1989).** *Island Africa*. Princeton University Press, New Jersey.
- Kingman J. (1982).** The coalescent. *Stochastic Processes and Their Applications*. 13: 235-248.
- Kirchman J.J., Hackett S.J., Goodman S.M. & Bates J.M. (2001).** Phylogeny and systematics of Ground Rollers (Brachypteraciidae) of Madagascar. *Auk*: 849-863.

- Kishino H. & Hasegawa M. (1989).** Evaluation of the maximum likelihood estimate of the evolutionary tree topologies from DNA sequence data, and the branching order in Hominoidea. *Journal of Molecular Evolution*. 29: 170-179.
- Klicka J. & Zink R.M. (1999).** Pleistocene effects on North American songbird evolution. *Proceedings of the Royal Society of London, Series B*. 166: 695-700.
- Klicka J. & Zink R.M. (1997).** The importance of recent ice ages in speciation: a failed paradigm. *Science*. 277: 1666-1669.
- Klicka J., Zink R.M., Barlow J.C., McGillivray W.B., Doyle T.J. (1999).** Evidence supporting the recent origin and species status of the Timberline Sparrow. *Condor*. 101: 577-588.
- Knowles L.L. & Maddison W.P. (2002).** Statistical phylogeography. *Molecular Ecology*. 11: 2623-2635.
- Kocher T.D., Thomas W.K., Meyer A. Edwards S.V., Pääb, S., Villablanca F.X. & Wilson A.C. (1989).** Dynamics of mitochondrial DNA evolution in animals: amplification and sequencing with conserved primers. *Proceedings of the National Academy of Sciences of the USA*. 86: 6196-6200.
- Krajewski C. & King D.G. (1996).** Molecular divergence and phylogeny: rates and patterns of Cytochrome *b* evolution in cranes. *Molecular Biology & Evolution*. 13: 21-30.
- Lens L., Van Dongen S., Norris K., Githiru M. & Matthysen E. (2002).** Avian persistence in fragmented rainforest. *Science*. 298: 1238.
- Lewis A. & Pomeroy D. (1989).** *A bird atlas of Kenya*. A.A. Balkema, Rotterdam. Pp620.
- Lewis P.O. (2001).** Phylogenetic systematics turns over a new leaf. *Trends in Ecology & Evolution*. 16: 30-37.
- Li W.H. & Graur D. (1991).** *Fundamentals of molecular evolution*. Sinauer, Associates, Sunderland, MA.

- Liebers D., Helbig A.J. & de Knijff P. (2001).** Genetic differentiation and phylogeography of gulls in the *Larus cachinnans-fuscus* group (Aves: Charadriiformes). *Molecular Ecology*. 10: 2447-2462.
- Livingstone D.A. (1975).** Late Quaternary climatic change in Africa. *Annual Review of Ecology & Systematics*. 6: 249-280.
- Livingstone D.A. (1993).** *Evolution of African Climate*. Pp. 455-472. In P. Goldblatt (ed). *Biological relationships between Africa and South America*. Yale University Press, New Haven
- Lönnberg E. (1929).** The development and distribution of the African fauna in connection with and depending upon climatic changes. *Arkives för Zoologie*. 21A: 1-33.
- Louette M. (1992a).** Barriers, contact zones and subspeciation in central equatorial Africa. *Bulletin of the British Ornithology Club*. 112A: 209-216.
- Louette M. (1992b).** The origin and evolution of Comoro land birds. Pp. 207-215. In L. Bennun (ed.). *Proceedings of the Seventh Pan-African Ornithological Congress*. Nairobi, Kenya.
- Louette M. (1991).** Geographical morphometric variation in birds of the lowland equatorial forest of Africa. Pp 475-482. *Acta XX, International Ornithological Congress*, Wellington, New Zealand.
- Louette M. (1984).** Apparent range gaps in African forest birds. Pp275-286. *Proceedings of the fifth Pan-African Ornithological Congress*.
- Lovett J.C. & Pócs T. (1993).** *Assessment of the Condition of the Catchment Forest Reserves, a Botanical Appraisal*. Catchment Forestry Project, Forest and Beekeeping Division, Ministry of Lands, Natural Resources and Tourism and NORAD.
- Lovett J.C. & Wasser S.K. (1993).** *Biogeography and Ecology of the Rain Forests of Eastern Africa*. Cambridge University Press. UK.
- Lovett J.C. & Congdon T.C.E. (1990).** Some notes on a visit to Selegu mountain, Tanzania. *East Africa Natural History Society Bulletin*. 20: 4-5.



- Lovett J.C. & Congdon T.C.E. (1989).** Some notes on a visit to Magalisa mountain, Tanzania. *East African Natural History Society Bulletin*. 19: 25-26.
- Lovett J.C. & Minja T.R.A. 1990.** Notes on a visit to Ukwiva forest, Tanzania. *East Africa Natural History Society Bulletin*. 20: 3-4.
- Macdonald J.D. (1958).** Note on *Cinnyris manoensis* Reichenow. *Bulletin of the British Ornithology Club*. LXXVIII. 7-9.
- Macdonald J.D. (1957).** *Contribution to the ornithology of the western South Africa, results of the British Museum (Natural History), Southwest Africa expedition, 1949-1950*. British Museum of Natural History, London.
- Maclean G.L. (1985).** *Roberts' Birds of Southern Africa*. Cape Town: John Voelcker Bird book Fund.
- Maddison D.R. (1991).** The discovery and importance of multiple islands of most parsimonious trees. *Systematic Biology*. 40: 315-328.
- Marjoram P. & Donnelly P. (1994).** Pairwise comparisons of mitochondrial DNA sequences in subdivided populations and implications for early human evolution. *Genetics*. 136: 673-683.
- Maley J. (2001).** The impact of arid phases on the African rain forest through geological history. Pp68-87. in Weber W. et al. (eds). *African rain forest ecology and conservation: an interdisciplinary perspective*. Yale University Press, New Haven.
- Maley J. (1996).** The African rain forest – main characteristics of changes in vegetation and climate from the Upper Cretaceous to the Quaternary. *Proceedings of the Royal Society of Edinburgh*. 104B: 31-73.
- Mann C.F. (2002).** Taxonomic comments on some south and south-east Asian members of the family Nectariniidae. *Zoologische Verhandelingen*, Leiden. 340: 179:189.
- Mayr E. & O'Hara R. J. (1986).** The biogeographic evidence supporting the Pleistocene Forest Refuge Hypothesis. *Evolution*. 40: 55-66.
- Mayr E. (1944).** Timor and the colonization of Australia by birds. *Emu*. 44: 113-130.

- Mayr E. (1942).** *Systematics and the Origin of Species*. Columbia University Press, New York.
- McKittrick M.C. & Zink R.M. (1988).** Species concepts in Ornithology. *Condor*. 90: 1-14.
- Mengel R.M. (1970).** *The North American Central Plains as an isolating agent in bird speciation*. University of Kansas. Department of Geology. Pp. 279-340. Special Publication No. 3.
- Mindell D. P, Sorenson M.D. & Dimcheff D.E. (1998).** An extra nucleotide is not translated in mitochondrial ND3 of some birds and turtles. *Molecular Biology & Evolution*. 15: 1568-1571.
- Moore W. S. & DeFilippis V. R. (1997).** The window of taxonomic resolution for phylogenies based on Mitochondrial Cytochrome b. pp. 84-115. In Mindell D. P. (ed.) *Avian molecular evolution and systematics*. Academic Press, New York.
- Moreau R.E. (1966).** *The bird faunas of Africa and its islands*. Academic Press, London.
- Moreau R.E. (1963).** Vicissitudes of the African biomes in the Late Pleistocene. *Proceedings of the Zoological Society of London*. 141: 395-421.
- Moreau R.E. (1952).** Africa since the Mesozoic: with particular reference to certain biological problems. *Proceedings of the Zoological Society of London*. 121: 869-913.
- Moreau R.E. (1951).** Geographical variation and plumage sequence in *Pogonocichla*. *Ibis*. 93: 383-401.
- Moritz C., Patton J.L., Schneider C.J. & Smith T.B. (2000).** Diversification of rainforest faunas: an integrated molecular approach. *Annual Review of Ecology & Systematics*. 31: 533-563.
- Morrone J.J. & Crisci J.V. (1995).** Historical biogeography: introduction to methods. *Annual Review of Ecology & Systematics*. 26: 373-401.
- Nelson G. & Platnick N. (1981).** *Systematics and Biogeography*. Columbia University Press, New York.

- Nersting L.G. & Arctander P. (2001).** Phylogeography and conservation of impala and greater kudu. *Molecular Ecology*. 10: 711-719.
- Nixon K. C. (1999-2002).** WinClada ver. 1.0000 Published by the author, Ithaca, NY, USA
- Nixon K. C. (1999).** The parsimony ratchet, a new method for rapid parsimony analysis. *Cladistics* 15: 407-414
- Oatley T.B. (1982a).** The Starred Robin in Natal, Part1: Behaviour, territory and habitat. *Ostrich*. 53: 135-146.
- Oatley T.B. (1982b).** The Starred Robin in Natal, Part 2: Annual cycles and feeding ecology. *Ostrich*. 53: 193-205.
- Oatley T.B. (1982c).** The Starred Robin in Natal, Part 3: Breeding, populations and plumages. *Ostrich*. 53: 206-221.
- Oatley T.B. & Arnott G. (1998).** *Robins of Africa*. Acorn Books, Randberg, South Africa.
- Oatley T.B. & Tinley K.L. (1987).** The forest avifauna of Gorongosa Mountain, Mozambique. *Ostrich* suppl. 14: 57-61.
- Palkovacs E.P., Gerlach J. & Caccone A. (2002).** The evolutionary origin of Indian Ocean tortoises (*Dipsochelys*). *Molecular Phylogenetics & Evolution*. 216-227.
- Partridge T.C., Wood B.A. & deMenocal P.B. (1995).** The influence of global climatic change and regional uplift in large-mammalian evolution in East and Southern Africa. Chapter 24, pp. 331-355. In Vrba E.S., Denton G.H., Partridge T.C., Burckle L.H. (eds.) *Paleoclimate and evolution, with emphasis on Human origins*. Yale University Press, New Haven.
- Paterson B.D. (1987).** The principle of nested subsets and its implications for biological conservation. *Conservation Biology*. 1: 323-334.
- Paterson M. (1954).** The identity of *Cinnyris afer whytei* Benson. *Bulletin of the British Ornithologists Club*. LXXIV. 35-36.
- Pfenninger M. & Posada D. (2002).** Phylogeographic history of the land snail *Candidula unifasciata* (Helicellinae, Stylommatophora): fragmentation, corridor migration and secondary contact. *Evolution*. 56: 1776-1788.

- Posada D. & Crandall K.A. (2001).** Intraspecific gene genealogies: tree grafting into cladograms. *Trends in Ecology & Evolution*. 16: 37-45.
- Posada D. & Crandall K.A. (1998).** Modeltest: testing the model of DNA substitution. *Bioinformatics*. 14: 817-818.
- Posada D., Crandall K.A. & Templeton A.R. (2000).** GeoDis: a program for the cladistic nested analysis of the geographical distribution of genetic haplotypes. *Molecular Ecology*. 9: 487-488.
- Price J.J. & Lanyon S.M. (2002).** A robust phylogeny of the oropendolas: polyphyly revealed by mitochondrial sequence data. *Auk*. 119: 335-348.
- Prigogine A. (1987).** Disjunctions of montane birds in the Afrotropical region. *Bonner Zoologische Beiträge*. 38: S195-207.
- Prigogine A. (1979).** Subspecific variation of Stuhlmann's Double-collared Sunbird, *Nectarinia stuhlmanni* around the Albertine Rift. *Le Gerfaut*. 69: 225-238.
- Prigogine A. (1952).** Quatre nouveaux oiseaux du Congo belge. *Rev. Zool. Bot. Afr. XLIV*. 407-415.
- Prychitko T. M. & Moore W. S. (1997).** The utility of a nuclear encoded intron from the  $\beta$ -fibrinogen gene in phylogenetic analysis of woodpeckers (Aves: Picidae). *Molecular Phylogenetics & Evolution*. 8: 193-204.
- Quéroutil S., Hutterer R., Barrière P., Colyn M., Kerbis-Peterhans J.C. & Verheyen E. (2001).** Phylogeography and evolution of African shrews (Mammalia: Soricidae) inferred from 16s rRNA sequences. *Molecular Phylogenetics & Evolution*. 20: 185-195.
- Quinn T.W. (1997).** Molecular evolution of the mitochondrial genome. Pp. 4-29. In D.P. Mindell (ed.). *Avian Molecular Evolution and Systematics*. Academic Press, New York.
- Quinn T.W. (1992).** The genetic legacy of Mother Goose – phylogenetic patterns of lesser snow goose *Chen caerulescens caerulescens* maternal lineages. *Molecular Ecology*. 1: 105-118.

- Rand A.L. (1967).** Family Nectariniidae. In 'Checklist of the Birds of the World' Vol 12. Ed. Paynter R.A. Museum of Comparative Zoology, Cambridge, MA.
- Räsänen M.E., Linna A.M., Santos J.C.R. & Negri F.R. (1995).** Late Miocene tidal deposits in the Amazonian foreland basin. *Science*. 269: 386-390.
- Riddle B.R. (1996).** The molecular phylogeographic bridge between deep and shallow history in continental biotas. *Trends in Ecology & Evolution*. 11: 207-211.
- Ridgway R. (1912).** *Colour standards and nomenclature*. United States National Museum, Washington DC.
- Robinson T.J. & Matthee C.A. (1999).** Molecular genetic relationships of the extinct ostrich, *Struthio camelus syriacus*: consequences for ostrich introductions into Saudi Arabia. *Animal Conservation*. 2: 165-171.
- Rogers A.R. & Harpending H. (1992).** Population growth makes waves in the distribution of pairwise genetic differences. *Molecular Biology & Evolution*. 9: 552-569.
- Roff D.A. & Bentzen P. (1989).** The statistical analysis of mitochondrial DNA polymorphisms : Chi-squared and the problem of small sample sizes. *Molecular Biology & Evolution*. 6: 539-545.
- Ronquist F. (1997).** Dispersal-vicariance analysis: a new approach to the quantification of historical biogeography. *Systematic Biology*. 46: 195-203.
- Ronquist F. (1996).** DIVA version 1.1. Available from ftp.uu.se or ftp.systbot.uu.se.
- Rosen D.E. (1978).** Vicariant patterns and historical explanations in biogeography. *Systematic Zoology*. 27: 159-188.
- Roy M.S., Sponer R. & Fjeldså J. (2000).** Molecular systematics and evolutionary history of Akalats (Genus *Sheppardia*): a pre-Pleistocene radiation in a group of African forest birds. *Molecular Phylogenetics & Evolution*. 18: 74-83.

- Roy M.S., Arctander P. & Fjeldså J. (1998).** Speciation and taxonomy of montane greenbuls of the genus *Andropadus* (Aves: Pycnonotidae). *Steenstrupia*. 24: 51-66.
- Roy M.S. (1997).** Recent diversification in African greenbuls (Pycnonotidae: *Andropadus*) supports a montane speciation model. *Proceedings of the Royal Society of London, Series B*. 264: 1337-1344.
- Ruffo C.K. (1991).** *A report on the identification of species for Image Forest Inventory, Iringa Region*. Tanzania Forestry Institute.
- Rutherford S. & D'Hondt S. (2000).** Early onset and tropical forcing of 100,000-year Pleistocene glacial cycles. *Nature*. 408: 72-75.
- Ryan P.G. & Bloomer P. (1999).** The Long-Billed Lark complex: a species mosaic in southwestern Africa. *Auk*. 116: 194-208.
- Ryan P.G., Hood I., Bloomer P., Komen J. & Crowe T.M. (1998).** Barlow's Lark: a new species in the Karoo Lark *Certhilauda albescens* complex of southwest Africa. *Ibis*. 140: 605-619.
- Scharnke H. (1932).** Über den Bau Zunge der Nectariniidae, Promeropidae und Drepanididae. *Journal Für Ornithologie*. 80: 114-123.
- Schneider S, Roessli D, Excoffier L. (2000).** *Arlequin: a software for population genetics data analysis*. Ver. 2.0, genetics and Biometry Laboratory, University of Geneva, Switzerland.
- Sclater W.L. (1930).** *System Avium Aethiopicarum*. Part II. Taylor and Francis, London.
- Seehausen O. (2002).** Patterns in fish radiation are compatible with Pleistocene desiccation of Lake Victoria and 14 600 year history for its cichlid species flock. *Proceedings of the Royal Society of London, Series B*. 269: 491-497.
- Servat E., Hughes D., Fritsch J.M. & Hulme M. (1998)** *Water resources variability in Africa during the 20<sup>th</sup> Century*. IAHS Publication No. 252, Wallingford, U.K.
- Shelley G.E. (1900).** *The Birds of Africa*. Volume 2. Published by the author, London.

- Shelley G.E. (1876-1880).** *Monography of the Nectariniidae*. Published by the author, London.
- Shields G.F. & Wilson A.C. (1987).** Calibration of mitochondrial DNA evolution in geese. *Journal of Molecular Evolution*. 24: 212-217.
- Shimodaira H. & Hasegawa M. (1999).** Multiple comparisons of log-likelihoods with application to phylogenetic inference. *Molecular Biology & Evolution*. 16: 1114-1116.
- Sibley C.G. & Ahlquist J.E. (1990).** *Phylogeny and classification of birds*. Yale University Press, New Haven.
- Sibley C.G. & Monroe B.L. Jr. (1990).** *Distribution and taxonomy of birds of the world*. Yale University Press, New Haven.
- Simpson G. G. (1960).** Notes on the measurement of faunal resemblance. *American Journal of Science*. 258: 300-311.
- Slatkin M. & Hudson R.R. (1991).** Pairwise comparisons of mitochondrial DNA sequences in stable and exponentially growing populations. *Genetics*. 129: 555-562.
- Smith T. B., Wayne R. K., Girman D. J. & Bruford M. W. (1997).** A role for ecotones in generating rainforest biodiversity. *Science*. 276: 1855-1857.
- Snow D. W. (ed.) (1978).** *An atlas of speciation in Africa non-passerine birds*. British Museum of Natural History. London.
- Sorenson M.D. & Fleischer R.C. (1996).** Multiple independent transpositions of mitochondrial DNA control region sequences to the nucleus. *Proceeding of the National Academy of Sciences of the USA*. 93: 15239-15243.
- Steininger F.F., Rabeder G. & Rögl F. (1985).** Land mammal distribution in the Mediterranean Neogene: A consequence of geokinematic and climatic events. In Stanley D.J. & Wezel F.C. (eds). *Geological evolution of the Mediterranean Basin*. Pp. 48-138. Springer-Verlag, New York.
- Stevenson T. & Fanshawe J. (2002).** *Field Guide to the Birds of East Africa: Kenya, Tanzania, Uganda, Rwanda and Burundi*. T & A D Poyser, London.
- Strimmer K. & von Haeseler A. (1996).** Accuracy of neighbour-joining for *n*-taxon trees. *Systematic Biology*. 45: 516-523.

- Stuart S.N., Jensen F.P., Brøgger-Jensen S. & Miller R.I. (1993).** The zoogeography of the montane forest avifauna of eastern Tanzania. Pp. 203-28 in Lovett J.C & Wasser S.K. (eds.) *Biogeography and ecology of the rain forests of eastern Africa*. Cambridge Univ. Press, Cambridge, U.K.
- Stuart S.N., Jensen F.P. & Brøgger-Jensen S. (1987).** Altitudinal zonation of the avifauna in the Mwanihana and Magombera forests, eastern Tanzania. *Le Gerfaut*. 77: 165-186.
- Stuart S.N. & van der Willigen T. (1980).** Is Moreau's Sunbird *Nectarinia moreaui* a hybrid species. *Scopus*. 4: 56-58.
- Suzuki Y., Glazko G.V. & Nei M. (2002).** Overcredibility of molecular phylogenies obtained by Bayesian phylogenetics. *Proceedings of the National Academy of Sciences of the USA*. 99: 16138-16143.
- Swofford D.L. (2002).** PAUP\*: *Phylogeny analysis using parsimony (\*and other methods)*, version 4.0b10. Sutherland, MA: Sinauer Association, Inc.
- Swofford D.L., Olsen G.J., Waddell P.J. & Hillis D.M. (1996).** Phylogenetic inference. Pp. 407-514. In D.M. Hillis, C. Moritz & B.K. Mable (eds). *Molecular Systematics*. Sinauer Associates, Sunderland, MA.
- Taberlet P., Fumagalli L., Wust-saucy A.G. & Cosson J.F. (1998).** Comparative phylogeography and postglacial colonisation routes in Europe. *Molecular Ecology*. 7: 453-464.
- Tajima F. (1989).** Statistical method for testing the neutral mutation hypothesis by DNA polymorphism. *Genetics*. 123: 585-595.
- Tarr C.L. & Fleischer (1993).** Mitochondrial DNA variation and evolutionary relationships in the 'Amakihi complex. *Auk*. 110: 825-831.
- Templeton A.R. (2002).** Out of Africa again and again. *Nature*. 416: 45-51.
- Templeton A.R. (1998).** Nested clade analyses of phylogeographic data: testing hypotheses about gene flow and population history. *Molecular Ecology*. 4: 381-398.
- Templeton A.R., Routman E. & Phillips C.A. (1995).** Separating population structure from population history: a cladistic analysis of the geographical



distribution of mitochondrial DNA haplotypes in the Tiger Salamander, *Ambystoma tigrinum*. *Genetics*. 140: 767-782.

**Templeton A.R. & Sing C.F. (1993).** A cladistic analysis of phenotypic associations with haplotypes inferred from restriction endonuclease mapping. IV. Nested analyses with cladogram uncertainty and recombination. *Genetics*. 134: 659-669.

**Templeton A.R., Crandall K.A. & Sing C.F. (1992).** A cladistic analysis of phenotypic associations with haplotypes inferred from restriction endonuclease mapping and DNA sequence data. III. Cladogram estimation. *Genetics* 132: 619-633).

**Templeton A.R., Boerwinkle E. & Sing C.F. (1987).** A cladistic analysis of phenotypic associations with haplotypes inferred from restriction endonuclease mapping and DNA sequence data. I. Basic theory and an analysis of alcohol dehydrogenase activity in *Drosophila*. *Genetics*. 117: 343-351.

**Thompson J.D., Higgins D.G. & Gibson T.J. (1994).** CLUSTAL W: improving the sensitivity of progressive multiple sequence alignment through sequence weighting, position specific gap penalties and weight matrix choice. *Nucleic Acids Research*. 22:4673-4680

**Tolley K.A., Vikingsson G.A. & Rosel P.E. (2001).** Mitochondrial DNA sequence variation and phylogeographic patterns in harbour porpoises (*Phocoena phocoena*) from the North Atlantic. *Conservation Genetics*. 2: 349-361.

**Van Tuinen M. & Hedges S.B. (2001).** Calibration of avian molecular clocks. *Molecular Biology & Evolution*. 18: 206-213.

**Verdcourt B. (1969).** The arid-corridor between the north-eastern and south-west areas of Africa. *Paleoecology of Africa*. 4: 140-144.

**Voelker G. (2002).** Systematics and historical biogeography of wagtails: dispersal versus vicariance revisited. *Condor*. 104: 725-739.

**Voelker G. (1999a).** Dispersal, vicariance and clocks: historical biogeography and speciation in a cosmopolitan passerine genus (*Anthus*: Motacillidae). *Evolution*. 53: 1536-1552.

- Voelker G. (1999b).** Molecular evolutionary relationships in the avian genus *Anthus* (Pipits: Motacillidae). *Molecular Phylogenetics & Evolution*. 11: 84-94.
- Voris H.K. (2000).** Maps of Pleistocene sea levels in SE Asia: shorelines, river systems and time durations. *Journal of Biogeography*. 27: 1153-1168.
- Vrba E.S. (1999).** Habitat theory in relation to the evolution in African Neogene biota and Hominids. Pp. 19-34. In Bromage T.G. & Schrenk S. (eds). *African biogeography, climate change & human evolution*. Oxford University press, Oxford.
- Vrba E.S. (1985).** African Bovidae: Evolutionary events since the Miocene. *South African Journal of Science*. 81: 263-266.
- Wallace A.R. (1860).** On the zoological geography of the Malay archipelago. *Zoological Journal of the Linnaean Society, London*. 4: 172-184.
- Warren B.H., Bermingham E., Bowie RCK, Prys-Jones R.P. & Thébaud C. (in press).** Molecular phylogeography reveals island colonization history and diversification of western Indian Ocean sunbirds (*Nectarinia*: Nectariniidae). *Molecular Phylogenetics & Evolution*.
- Weibel A.C. & Moore W.S. (2002).** A test of a mitochondrial gene-based phylogeny of Woodpeckers (Genus *Picoides*) using an independent nuclear gene,  $\beta$ -Fibrinogen Intron 7. *Molecular Phylogenetics & Evolution*. 22: 247-257.
- Wetmore A. (1960).** A classification for the birds of the world. *Smithsonian Miscellaneous Collection*. 139: 1-37.
- White C.M.N. & Bruce M.D. (1986).** *The birds of Wallacea (Sulawesi, The Moluccas and Lesser Sunda Islands, Indonesian): an annotated check-list*. British Ornithological Union, London.
- White F. (1983).** *The vegetation of Africa*. UNESCO, Paris.
- Wilcox T.P., Zwickl D.J., Heath T.A. & Hillis D.M. (2002).** Phylogenetic relationships of the dwarf boas and a comparison of Bayesian and bootstrap measures of phylogenetic support. *Molecular Phylogenetics & Evolution*. 25: 361-371.

- Wilkinson J.A., Drewes R.C. & Tatum O.L. (2002).** A molecular phylogenetic analysis of the family Rhacophoridae with an emphasis on the Asian and African genera. *Molecular Phylogenetics & Evolution*. 24: 265-273.
- Williams P.H., de Klerk H.M. & Crowe T.M. (1999).** Interpreting biogeographical boundaries among Afrotropical birds: spatial patterns in richness gradients and species replacement, in Afrotropical birds. *Journal of biogeography*. 26: 459-474.
- Wolters H.E. (1977).** Die Gattungen der Nectariniidae (Aves: Passeriformes). *Bonn Zoological Bulletin*. 28: 82-101.
- Wood T.C. & Krajewski C. (1996).** Mitochondrial DNA sequence variation among subspecies of Sarus crane (*Grus antigone*). *Auk*. 113: 655-663.
- Zar J.H. (1996).** *Biostatistical Analysis*, 3<sup>rd</sup> ed. Englewood Cliffs, N.J., Prentice-Hall.
- Zink R.M., Blackwell-Rago R.C. & Ronquist F. (2000).** The shifting roles of dispersal and vicariance in biogeography. *Proceedings of the Royal Society of London, Series B*. 267: 497-503.
- Zink R.M. & Slowinski J.B. (1995).** Evidence from molecular systematics for decreased avian diversification in the Pleistocene Epoch. *Proceedings of the National Academy of Sciences of the USA*. 92: 5832-5835.
- Zimmerman D.A., Turner D.A. & Pearson D.J. (1999).** *Birds of Kenya and Northern Tanzania*. Helm Field Guides, Christopher Helm, London.